Computational and Chemical Proteomic Strategies for Deconvoluting Inhibitor and Drug Mode of Action

Adam Louis Borne

Vail, Colorado

B. Sc. Cell and Molecular Biology, University of South Florida, 2016

A Dissertation presented to the Graduate Faculty of the University of Virginia in Candidacy for the Degree of Doctor of Philosophy

Department of Pharmacology

University of Virginia

August 2021

Abstract

The analysis of proteomes using mass spectrometry has enabled the direct measure of the abundance for thousands of protein gene products from a single sample. Small molecule covalent probes can survey the activity of these proteins and through competition assays identify their ligands. This activity-based protein profiling (ABPP) provides the means to probe and potentially drug protein targets that may be otherwise inaccessible. Given that the development of new covalent probes enables the study of different subsections of the proteome, advances in proteomic and computational strategies are needed to optimize coverage and utility of probe modified proteomes.

This dissertation uses three different chemical proteomics strategies to 1) identify the targets of an inhibitor, 2) profile tyrosines across the proteome and 3) screen fragment electrophiles across the proteome. In addition, we present a computational tool kit built for the analysis of chemical proteomics datasets. **Chapter 1** provides background on proteomics with mass spectrometry, ABPP, and the relevant computational strategies. In **Chapter 2** we identify that repurposed serotonin receptor antagonist ritanserin, is cytotoxic in small cell and non-small cell lung cancer cell lines. Based on this finding we used a kinase specific chemical probe to identify c-Raf as an important ritanserin target in these cell lines. **Chapter 3** details the development of SuTEx probes as an *in vitro* and live cell tyrosine selective probe. We use this probe to identify tyrosines that readily react with the SuTEx scaffold and monitor changes in phosphorylation state of tyrosines. **Chapter 4** presents a computational platform for analysis of probe modified site-specific mass spectrometry datasets. Using this platform, we profile several probes, competitive ABPP data, and perform an *in silico* screen of covalent fragment electrophiles. **Chapter 5**

summarizes the findings and discusses future direction for these strategies.

Acknowledgements

I would like to thank all the members of my lab that I worked with on the projects presented. The field of Chemical Biology requires a multi-disciplinary team, since most member of the lab were graduate students everyone was learning what they contribute as the projects developed. Dr. Jeffery Brulet and I worked on several projects together and he was one of the hardest workers I have ever met. Dr. Caroline Franks and Dr. Mark Ross taught me activity-based protein profiling and mass spectrometry when I first joined the lab. Kun Yuan, Anthony Ciancone, Andy Heindel and Dr. Rebecca McCloud were always a reliable resources and great coworkers. Heindel was the second Pharmacology PhD candidate in the Hsu lab and provided much-needed perspective on being part of two departments. I joined the lab of Dr. Ku-Lung (Ken) Hsu because of his enthusiasm for his work which never waned even when times were difficult. He always made time for his students and helped many graduate students find their eventual post-doctoral positions.

My parents have both been supportive of me throughout this process and have always tried their best to help me through some of the tougher moments. My father would always be there to lend a helping hand and my mom would be there to listen to me complain about whatever ailed me. My grandparents always told me they were proud of me, and I fear my discomfort with compliments meant they never understood how much it meant to me. All three of my siblings were always there to help me; playing video games with Aaron or going to Disney with Tess and Spencer no matter what the occasion they always brought some joy and levity to tougher times. In addition, I need to give a special thanks to my Aunt Lynette, Uncle Rob and Uncle Steven for being so supportive during my candidacy.

Table of Contents

Chapter 1: Introduction

1.1 Tandem Mass Spectrometry and Proteomics

1.1.1. Tandem Mass Spectrometry

Mass Spectrometry (MS) is any technique that identifies the mass to charge (m/z) of a molecule through ionization, subjecting the ion to a magnetic field and detecting the effect on the ion or magnetic field[1]. Ionized molecules can be separated using a quadrupole mass filter which selects ions based on their m/z by subjecting them to an electromagnetic field destabilizes other ions. In a mass spectrometry instrument, this quadrupole will isolate ions from a complex mixture to perform focused quantitation of the ion or inject the ion into a collision chamber to break the precursor ion into fragment ions[1,2]. Tandem MS analyzes a complex mixture of ions, identifies the m/z of the precursor ion, selects specific ions from initial analysis, fragments the selected ions and analyzes the fragment ions[2]. This technique produces a MS1 spectra of all the precursor ions as well as an MS2 spectra of all the fragment ions for each selected precursor. Fragmentation can be accomplished in many ways but the most common is Collision Induced Dissociation (CID) where ions are accelerated into inert gas ions (He, N_2)[3,4]. The common variant of this technique is Higher-energy C-trap Dissociation (HCD) which will collide the ions in ion trap to produce more fragmentation[5]. Mass analyzers can be used to quantify the abundance of the precursor and fragment ions relative to other ions being analyzed in the complex mixture[1].

When performing tandem MS the spectra can be acquired spatially by aligning a linear ion detector for MS1 spectra followed by a collision chamber then another linear ion detector for the MS2 spectra[2]. Temporal separation requires that ions be continuously

injected into the mass spectrometer long enough for both scans to be conducted. The precursor ions are first injected directly into detector to create the MS1 spectra and then the MS2 is generated by selecting ions from the MS1 in the continuously inject ion stream isolating them, inducing fragmentation, and injecting the fragments into the same ion detector (Fig. 1.1)[1,6].

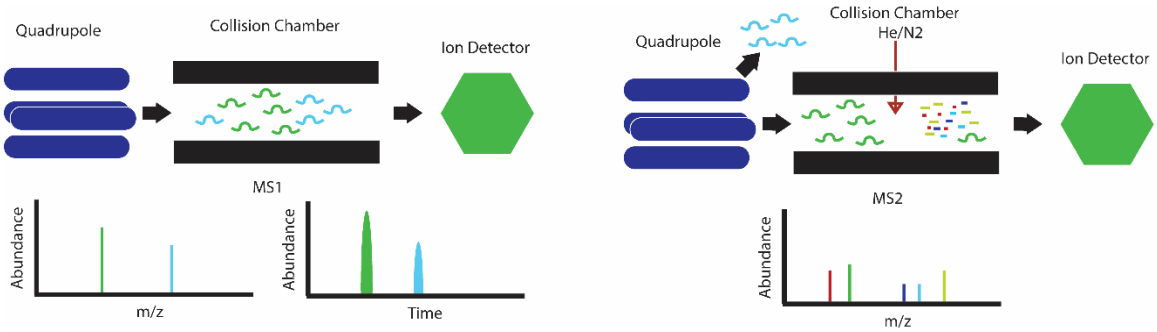

Figure 1.1. Temporally separated tandem MS using collision induced dissociation (CID) and the resulting spectra. The MS1 scan is complete scan of all charged precursor ions within the m/z window. Integrating these scans over time, the relative ion abundance can be measured. The MS2 spectra consists of the fragment ions produced by selecting a single precursor inducing and performing CID[3].

This technique is particularly useful when identifying complex molecules as the fragment ions can be used to determine which component of a molecule are attached to each other[1]. As ionization techniques made Nobel prize winning advances larger biomolecules could be effectively analyzed using tandem MS which included the analysis of peptides derived from proteins digested with proteolytic enzymes such as trypsin[2,7]. The

MS1 spectra can be used to measure relative abundance of a complex mixture of peptides and under specific collision conditions these peptides can be broken across the peptide backbone to produce MS2 spectra containing ions representing the different possible peptide bifurcations (b and y ions)[5]. These ions combined with other predictable fragment ions can be used to determine the peptide sequence.

1.1.2. Liquid Chromatography and Shotgun Proteomics

In a complex sample of unknown peptides, the highly abundant ions will suppress other ions. Liquid chromatography mass spectrometry (LC-MS) increases peptide coverage of samples by separating the complex mixture across a gradient such that a small numbers of peptides are injected into the instrument at a time[8]. Various methods exist for separating peptides across a gradient but the most common is reverse phase chromatography where peptides are loaded onto a hydrophobic stationary phase and slowly eluted off across a gradient of increasingly organic solvent[8]. This enables the evaluation of a peptide mixture over a long period of time and improvements in flow rates that has further improved coverage as decreased flow rate will produce discrete peaks that will have a higher relative abundance at a specific time in the gradient[8,9]. Combining LC and MS enables shotgun proteomics where an entire proteome is analyzed across a long gradient[10]. This technique will produce thousands of MS2 spectra from single sample that can be matched to theoretical spectra and assigned to a protein using database search algorithms[10,11]. These techniques have been expanded upon to identify up to 10,000 proteins in a single analysis[12].

1.1.3. Proteomics Database Searching

The ability to identify large numbers of peptides from proteins was made possible by the human genome project. A complete genome for a species enables the alignment of proteins from open reading frames[13]. A major challenge in shotgun proteomics is matching the large number usable spectra to peptides[14]. To address this several approaches to database search algorithm have been developed. Descriptive search algorithms (SEQUEST) do this by comparing theoretical spectra to a particular spectrum[11,15,16]. Interpretive strategies (Byonic) depend on predicted features of a fragmented peptide to narrow the search space before performing comparisons[17]. Stochastic search algorithms will build a model for peptide spectra matching based on many previously matched spectra[16,17].

While database searching is the most common approach to matching spectra to peptides in mass, *de novo* sequencing is still used and frequently needed to identify certain peptides[18]. A database search algorithm is unlikely to identify peptides created from splicing events or unique proteolytic activity inside the cell. Assigning a peptide to a protein can pose an additional challenge as many peptides are not unique to protein of interest[15,16]. The most likely protein for a peptide that belong to several proteins is usually determined by selecting the protein with the most other peptides found in the sample[15,16].

1.2 Design of Activity-Based Probes

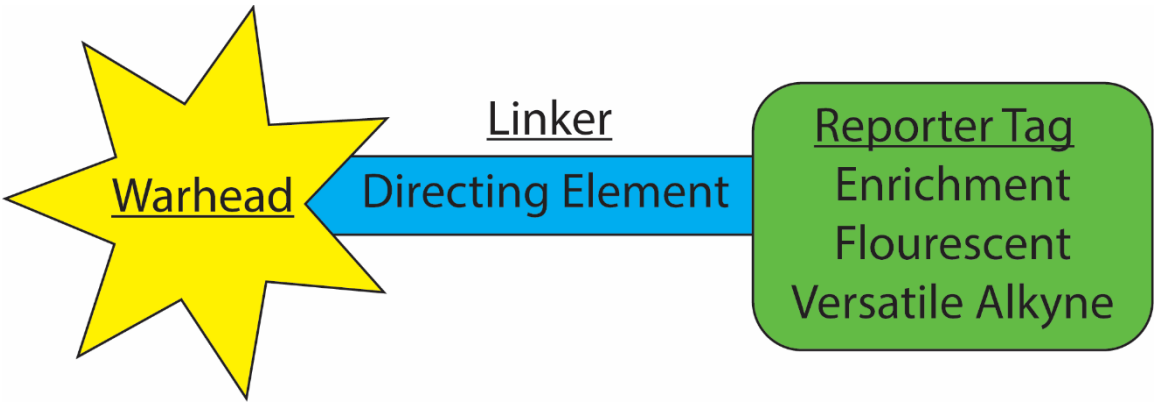

Figure 1.2. Three core components of an Activity-based probe (ABP) and their role.

Any compound that can be used to study a biological system could be described as a chemical probe. Activity-based probes (ABPs) report on a protein's activity through the use of a covalent small molecule that modifies proteins of interest[19–21]. These probes are made up of a warhead, linker and reporter tag (Fig. 1.2 [19]. The warhead used can determine the specificity and targets of the probe. The flourophosphanates (FP) and the adenosine tri-phosphate (ATP)-acyl phosphate covalently modify catalytic serines of serine hydrolases and ATP hydrolyzing proteins respectively[22–24]. In addition, covalent moieties (azetidine, acrylamide, or vinylsulfones) can be added to known inhibitors to potentially create a specific warhead[25].

Broadly reactive warheads like the NHS-esters that target lysines or iodoacetamide which targets cysteines can be used in profiling reactivity across a proteome[26–29] as well as report on post-translational modifications (PTM, expanded in chapters 3 and 4)[27,30].

The linker is frequently designed to limit its impact on the probe's warhead with an alkyl or polyethylene glycol (PEG) group[31]. The linker length can be optimized to prevent the handle from effecting the warhead's activity or to increase affinity for a protein[31]. This is accomplished by installing a chemical moiety on the linker that can function as directing element. These can be known ligands for the target of interest, developed through structure activity relationship (SAR) optimization, or a combination of these options[32]. If using a more complicated moiety it is important to balance membrane permeability with the size of the probe if the goal is to study the target in a live cells[32].

The handle enables most uses of an ABP as it provides the ability to either visualize or enrich probe modified protein. The alkyne group is an extremely reliable and versatile handle when combined with copper(I)-catalyzed azide-alkyne [3+2] cycloaddition (CuAAC) click-chemistry[33,34]. This bioorthogonal reaction efficiently forms a triazole ring from azido group and the alkyne connecting the two components[33]. Flourescent tags can be attached to the azido group, clicked onto a probe and used to visualize the probe when subjected to the absorption wavelength of the fluorophore[33]. Enrichment can be achieved by attaching biotin or desthiobiotin to the azido group and enriching the probe using avidin or streptavidin[21]. The biotin avidin interaction is particularly strong and require strong denaturing conditions to elute the probe modified peptide. Replacing the component with dethio- or strept- alternatives weaken this interaction to the point they can be eluted with organic solvents[35,36]. Alternative enrichment tags include TEV-sequence biotin, which can be eluted through the cleacage of enrichment tag with TEV-protease[27]. While versatile the alkyne handle requires click-chemistry for use. In cases where the small profile of the

handle is not needed, a handle that is simply the fluorescent or enrichment tag may be preferable[29]. Removing this step can produce task specific probe but could result in a loss of membrane permeability.

1.3 Activity Based Protein Profiling

1.3.1. ABPP Techniques

Using this basic framework one can build an ABP that will covalently modify proteins of interest and be used in a variety of biological assays. Activity based protein profiling uses ABPs to interrogate the activity of proteins in biology systems[19,21]. The most direct use is the visualization of targets separated by sodium dodecyl sulphate-polyacrylamide gel electrophoresis (SDS-PAGE)[36–38]. SDS-PAGE separates proteins by mass and charge as different size proteins will migrate through the cross-linked acrylamide matrix when subjected to a constant electrical field. SDS is used the charge the proteins to ensure they move towards one pole of the electrical field. This method combined with a family specific warhead and a fluorescent handle (clicked or prebuilt) can visualize and provide a relative abundance for the ABPs targets[22,36]. If using a broad probe, a protein can be visualized this way if it is overexpressed such that signal of the overexpressed protein can be discerned from a mock overexpression[36]. This provides a way to survey one to a family of proteins in a single gel lane. A higher throughput but lower coverage technique is to use a probe with purified protein in anisotropy based screen[39]. This is usually used for competitive ABPP discussed in section 1.3.2.

Fluorescence Microscopy is the fixing cells or tissues to a glass slide and subjecting

the slide to specific wavelengths of light that excite fluorophores in the sample. Most flourophores are introduced to the sample through use of fluorophore conjugated antibodies that recognize a specific epitope on a protein or group of proteins[40]. When paired with fluorescent microscopy an ABP with protein specific warhead and a clicked fluorescent tag can be used to visualize subcellular location[41]. Further, when using the acidic organelle specific 3-(2,4-dinitroanilino)-3'-amino-N-methyldipropylamine (DAMP) directing element with a cathepsin specific warhead a family of proteins can be visualized in a specific organelle. An ABP with a fluorophosphonate (FP) warhead and a TAMRA fluorescent tag have been used to identify serine hydrolase activity hotspots in fluorescent microscopy of tissue samples[41].

Pairing ABPP with tandem LC-MS (as described in section 1.1) the targets of any ABP warhead linker combination can be determined through use of an enrichment tag[36–38]. There are two major ways to identify the targets of an ABP. The first is to treat to a live cell or proteome, enrich the proteins on beads (i.e. biotin-avidin chromatography), digest the proteins and analyze the digested peptides[37,42]. This approach is like shotgun proteomics in that all peptide from the target proteins will be in the sample. Digesting the proteins prior to enrichment followed by eluting the probe modified peptide produces a sample where only the probe modified peptides are enriched in the sample[27,36]. This site-specific proteome profiling is major focus of all chapters and elaborated on in section 1.6.

1.3.2. Competitive ABPP

The major advantage of the ABP is the ability to be competed out by potential ligands in a dose-dependent manner[19,24,36]. Treating a cell lysate with a non-covalent or covalent compound followed by treatment with an ABP will report on the inhibition of the proteins targeted by the probe. It is possible to perform competitive ABPP with live cell compound treatment, but is very difficult unless using a covalent ligand or a membrane permeable ABP[24]. This methodology has been used to identify inhibitors for serine hydrolases, kinases, transcription factors and much more[37,43,44]. It can also be used to identify previously unknown targets for drugs at all steps of the drug discovery pipeline[45,46].

High-throughput screening with ABPs can be accomplished using an anisotropy-based screen with a purified protein[39]. This is done by treating the proteins with a compound library followed by the ABP with a fluorescent tag. The ABP will rotate in the solution and will be slowed by the additional mass of the protein, if the compound blocks probe labeling the rate of spinning remain high[47]. Moving down in throughput from thousands of molecules to hundreds gel-based screening can conducted by pre-treating cells or a lysate with an inhibitor then the ABP and performing SDS-PAGE, as described in section 1.3.1. This will lead to decreased gel band signal intensity for a protein inhibited by the compound[36–38]. The trade-off for lower throughput is the ability to use a family specific probe to test a probe across a protein family in a single gel lane.

LC-MS based competitive ABPP is lowest throughput version but is the best way to take advantage of a broad ABP as it can quantify thousands of proteins across the proteome[26,30]. Pre-treatment with a compound followed by ABPP LC-MS, as described in

section 1.3.1, will lead to decreased MS1 signal intensity for peptides that belong to the protein targets of the compound when compared to a vehicle control. If performing site-specific proteome profiling the site of protein-probe can be detected providing information on the compound binding site[36].

The major throttle for LC-MS competitive ABPP is the time needed to run a sufficiently long chromatographic gradient to get the proteome coverage needed. In addition, running lysates separated temporally means the relative abundance of the peptides are subject to the conditions of the run. There are several ways to address these issues, but the best is to analyze several compounds at same the same time. This is accomplished using multi-plexing where the m/z of ions produced by peptides are systematically changed through incorporation of isotopes into the amino acid itself or a reporter tag[48–50]. Multi-plexing at the MS1 level can be done by growing cell in media containing isotopically unique versions of essential amino acid such as lysine or arginine. The stable isotope labeling of amino acids in cell culture (SILAC) can use different levels of carbon or nitrogen replacement to create light (no replacement), medium (partial replacement) and heavy (complete replacement) channels[48]. Mixing the proteomes from cells grown in these different isotopically labeled amino acids will produce MS1 ions that all can discerned from each other using high-resolution MS. Recently this type of multi-plexing has been integrated into the design of a chemical probe by using isotopically unique version of a chemical probe on different samples[51].

The other techniques modify the peptides with different mass tags usually though addition to the N-terminus of the peptide generated by proteolytic digestion by trypsin.

Tandem mass tags (TMT)[49] and isobaric tags for relative and absolute quantitation (iTRAQ)[50] both modify the N-terminus of peptides but produce isotopically unique ions upon fragmentation of modified peptide. The different tags all have the same mass but have distributed isotopic carbons or nitrogen differently across each tag. Just as the peptide produces predictable ions through fragmentation the tag is fragmented at a particular bond that produces different ions in a MS2 scan based on how many of the isotopic carbons and nitrogens were on each part of the fragment. Mixing proteomes treated with different tags one can analyze the abundance of up to 16 treatments simultaneously[49]. Combining this multi-plexing strategy with a competitive ABPP has recently enabled a 265-molecule screen across a large portion of the proteome[29].

1.3.3. Surveying Serine Hydrolases with ABPP

Serine hydrolases are a group of hydrolyzing proteins that feature a conserved serine in the active site needed for catalytic activity. The roles of serine hydrolases include hydrolysis of lipids, esters, thioesters, amides, and peptides[52,53]. Given the broad array of hydrolysis targets it is unsurprising that they have been implicated in several diseases including cancer, inflammation and cardiovascular disease[52,53]. The FP warhead previously discussed (section 1.3.1) specifically labels this group of proteins and is one of the foundational family specific warheads for the development of ABPP[22].

A combination of gel and LC-MS based ABPP was used to identify inhibitors for the serine hydrolase Diacylglycerol Lipase β (DAGLβ)[37]. This enzyme mediates the production of 2-arachidonoylglycerol (2-AG) which regulated inflammation and is a major

cannabinoid receptor agonist. Inhibition has been shown to mitigate lipopolysaccharide induced inflammatory pain[54]. The same approach was used to identify inhibitors of α/β-Hydrolase Domain Containing 6 (ABHD6) which hydrolyzes 2-AG[38]. The inhibitors identified in both cases featured the 1,2 ,3-triazole urea which was key to the development of new probes discussed in Chapter 4.

1.3.4. Surveying Kinases Inhibitors with ABPP

Kinases are an important class of proteins that catalyze the addition of a phosphate from a molecule of (ATP) to another molecule[55]. They usually add the phosphate to a hydroxyl on a tyrosine, serine, threonine, sugar or lipid headgroup. These kinases are incredibly important to a functioning cell and when acting abnormally can lead to various disease states[45]. Cancer treatments frequently target kinases as they are often the location of oncogenic (cancer driving) mutations[56]. Given their importance several methods for surveying kinase inhibitors have been developed to identify their targets.

One approach uses kinases inhibitors immobilized on Sepharose beads to enrich kinases from a lysate[57,58]. The kinases from a lysate will interact with the inhibitors and non-interacting proteins can be removed by washing the beads. Then the proteins can be proteolytically digested on or off bead and analyzed by LC-MS/MS. The beads can be tailored to system of interest by immobilizing inhibitors that have higher affinities to the expected targets[59]. A different approach immobilizes the inhibitor of interest onto a bead, but this can only be done if the inhibitor is amenable to the coupling chemistry used to create the beads[60]. All versions can be performed competitively by treating the lysate with

an inhibitor of interest then subjecting the lysate to the immobilized inhibitors[57–60]. The targets are identified by the loss of peptide signal from proteins that were competed by the inhibitor treatment when compared to a vehicle or analog control. This technique dramatically increases kinase coverage when analyzed with LC-MS/MS but does not provide site-specific information[57,59,60].

The comparable ABP based technique, that is used in Chapters 2 and 5, replaces the beads with an ATP-acyl phosphate probe. This probe catalytically modified a lysine in the binding pocket of kinase[24]. This ABP can be competed out by pretreating the lysate with an inhibitor molecule to perform a competitive ABPP experiment[36]. The probe modified proteins or digested peptides are enriched with desthiobiotin-avidin enrichment described in Section 1.2 and analyzed by LC-MS. The targets are determined by loss of overall peptide signal or loss of probe modified peptide signal. The latter option provides site-specific data which have previous been used to describe the catalytic pocket of the lipid kinase diacylglycerol kinase α (DGKα)[36].

1.3.5. Broad Activity Based Probes

Broad or global ABPs include a warhead that hit a larger number of protein targets[27,30]. This include photoreactive warheads like diazirine and benzophenones which modify any nearby amino acid when subjected to ultraviolet light[61]. Both warheads can be provided specificity by integrating them into larger molecule or adding directing agent to a linker. Several of these warheads have amino acid specificity such are NHS-ester and iodoacetamide probes for modifying lysine and cysteine, respectively[29,62].

These warheads can be used to perform competitive ABPP across the proteome and when using site-specific profiling they can annotate the location of competition[36,62]. In addition, they can be used to determine hyper-reactive and ligandable amino acids across the proteome[27,29]. Hyper-reactive amino acids are identified comparing a lower and higher concentrations of an ABP. A site on the protein that reacts as readily with the lower concentration as it does with the higher concentration is considered hyper-reactive. These hyper-reactive sites likely reflect a combination of protein-ABP affinity, site accessibility, and amino acid reactivity. Ligandable amino acids are those inhibited by pretreating a lysate with a covalent compound. A ligandable site has the proper compound-protein affinity, accessibility, and reactivity to be targeted by a covalent pharmacophore. Identifying how ligand structural changes effect ligandability can provide a map of sites that can be access with different chemical moeities[27]. Hyper-reactivity and ligandability are discussed further in Chapters 3 and 4.

1.4 Applications of ABPP in Drug Development

1.4.1. The Undrugged Proteome

The human proteome contains at least 20,000 different proteins and it is estimated that only 3 percent of those proteins are targeted by a clinical drug. Only a further 7 percent have ligands with an IC50 less than 50 nM. The remaining 90 percent (~18,000 proteins) do not have known ligands capable of modulating a protein at biologically relevant doses. Among the proteins inhibited there is bias towards G-protein coupled receptors (GPCRs), ion channels, and kinases[63]. These three groups make up 44 percent of all clinical targets

with other enzymes making up an additional 31 percent[63,64]. This bias toward these targets is driven in part by their relevance in various disease state and by the tools available to assay these protein classes. One such tool, biochemical assays can be used with modern instrumentation to screen hundreds of thousands of compounds against a purified protein target[65]. This approach requires some way to measure the proteins activity or binding of compound to the protein. Enzymes can be screened relatively easily when the protein catalyzes a product that can be detected. Protein targets that do not catalyze a detectable target must depend on some form of chemical or protein probe that can report out the relevant change in activity or binding. This first step to finding an inhibitor, often fail to produce useful ligands as the lead compound may not show the same activity in a more complex biological system[32,66].

Phenotypic assays start with a biological system and screen molecules for changes in the behavior of the system. This technique can reach similar throughput as biochemical techniques depending on the complexity of the system needed to elicit the phenotype and method of measuring the change in behavior[67]. The phenotypic screen can suggest the protein targeted relevant to the change in behavior through a knock-down or out of a potential target to recover the phenotype. While powerful the phenotypic screen is rarely able to identify the relevant off-targets that may be contributing to the phenotype[67]. This may seem like a minor issue but more expansive targets coverage has illustrated that many clinical compounds work in part or completely through off-target effects[60,68].

The ability to interrogate as much of the proteome as possible is important in both understanding drug effects as well as bringing better treatments to the clinic[32]. We are

scratching the surface of what can be done with these techniques but there is still a need to bring new approaches to the table to expedite and enable the targeting of this undrugged proteome.

1.4.2. The Case for Covalent Inhibitors

The ABPP techniques previously discussed are optimal for identifying and discovering new covalent inhibitors. In addition, discovery of new ABP warheads introduce the possibility of generating new covalent pharmacophores for drug development[69]. While not nearly as common as their non-covalent counterparts, covalent inhibitors are receiving renewed interest[25]. Covalent small molecule inhibitors will bind to a protein of interest based on affinity and modifies the protein. The FDA has approved 13 covalent inhibitors in the past decade to make 32 total approved covalent inhibitors[45,70]. The covalent modification can be reversible or irreversible, but an irreversible covalent inhibitor will inhibit the protein until it is turned over by the cell[25]. This increased inhibition time may lower the effective dosage needed to get the response desire, depending on the rate of turnover of the target in the cell. In addition, the inhibitor does not need to directly compete with a substrate to influence activity on the protein as the addition of a properly positioned adduct could destabilize the protein or allosterically modulate the proteins activity[25,71]. This has the potential to provide new inhibitor modalities and lowering needed dose.

A covalent inhibitor once it has modified a protein cannot be used again so while it may not need the affinity to compete out an endogenous substrate it does need the

specificity to ensure it is delivered to its target[72]. This can be aided using liposomal delivery systems or through understanding the mechanics of a covalent pharmacophore to decrease its reactivity to forcibly rely on affinity to provide sufficient residence time for a covalent reaction[72,73]. The covalent molecule also has the possibility of producing increased toxicity as many inhibitors feature a leaving group generated as by product of a substitution reaction[74]. The only way to address this concern is understand the toxicity of covalent inhibitor leaving groups. These concerns however have not kept irreversible covalent inhibitors from seeing use in the clinic[70].

In cancer, carfilzomib is a second generation proteosome inhibitor with highly specific irreversible covalent modification of a catalytic threonine on 20S subunit[70,75]. The proteosome degrades unfolded an ubiquitinated proteins and if inhibited these species accumulate and lead the death of fast dividing cells[75]. Epithelial growth factor receptor (EGFR) is a receptor tyrosine kinase that regulates cell growth and is frequently mutated in lung and breast cancer[76]. Currently there are four FDA approved drugs that irreversibly modify this protein (Afatinib, Dacomitinib, Neratinib, and Osimertinib)[70]. Burton's tyrosine kinase is a non-receptor tyrosine kinase important in the proliferation of lymphomas and currently has three FDA approved covalent irreversible inhibitors (Acalabrutinib, Ibrutinib, and Zanubrutinib)[70].

The K-Ras G12C has long been considered a primary target in various cancers has been historically difficult to drug[77]. It functions through binding to key kinases when bound to guanosine triphosphate (GTP) activating them and this signal is removed by hydrolysis of the GTP to guanosine diphospohate (GDP). The G12C mutation increase the time K-

Ras is bound to GTP and increases binding to downstream kinases[77]. Sotorasib (AMG510) is a recent FDA approved irreversible covalent inhibitors that locks the protein in a GDP bound state[78,79]. It does this by binding to a cryptic grove on K-Ras and does not compete with GTP or GDP for the catalytic site[78]. This inhibitor serves as a good example of a new modality for targeting a difficult protein using a non-competitive covalent inhibitor.

Covalent molecules also provide solutions to the rise of acquired bacterial antibiotic resistance. The β-lactam class of antibiotics inhibit penicillin binding proteins (PBPs) and prevent the final step to the creation of the bacterial cell wall[80]. The most common resistance mechanism is the production of β-lactamase which metabolizes the β-lactam ring in the antibiotic. Avabactum inhibits the β-lactamase through a covalent mechanism and can be used to restore the efficiency of the β-lactam[80].

1.5 Sulfur-Fluoride Exchange (SuFEx) Chemistry

A promising new warhead for the development of ABPs and inhibitors, the Sulfur (VI) fluoride exchange (SuFEx) chemistry powered warhead has been shown to react with tyrosine, lysine, threonine and serine[81–84]. The sulfonyl fluorides are very stable in biological systems given their resistance to reduction and thermostability when compared to other sulfur-halide bonds[81]. In addition, the sulfonyl-fluoride core needs to be stabilized in order to react, meaning it will not react without a microenvironment suitable for the substitution reaction. Important for use with site-specific mass spectrometry, it does not have side-reactions meaning it will form a single adduct on these unique amino acids[81]. This dramatically narrows the possible changes in m/z on a probe modified peptide making

the resulting precursor ion predictable.

Based on these features SuFEx ABPs are already being used to study reactivity of previously difficult to assay amino acids such as tyrosine. Using XO-44, a kinase specific inhibitor, as directing agent SuFEx ABPs have been able to profile kinases in live cells[85]. Competitive ABPP experiments using the XO-44 enabled live cell profiling of dasatinib kinase targets.

SuFEx is poised to be a new warhead for accessing previously undrugged targets since they can react with serine, threonine and tyrosine and can be directed to a collection of targets[81–83,85]. Though they are unlikely to be the scaffold for the creation of new covalent inhibitors as it features a fluoride that is toxic to cells as discussed in section 1.4.3[74]. This chemistry is a key component to the development of SuTEx molecules discussed in Chapter 3.

1.6 Computational Strategies for ABPP

Computational tools for ABPP are usually taken from tools initially designed for other proteomics applications. Skyline a key component for the analysis throughout this this dissertation is designed for targeted proteomics but boasts features useful in quality control and ion quantification[86]. The major place where computational techniques needed are in an ABPP workflow peptide identification, quantification of peptide or proteins abundance, target prioritization and identifying new bioactive covalent molecules.

As previously mentioned, a database search algorithm is a key step in most proteomics analysis pipeline (section 1.1.3)[15,16]. When performing analysis of digested

peptides in a ABPP experiments the use of a basic search algorithm like SEQUEST is appropriate as the sample includes several tryptic peptides form the same protein[11]. This is not the case with site-specific ABPP as the identity of site is dependent on one to three peptides for identification. The same is true when dealing with PTMs and they can be identified with a standard search, but dedicated PTM search algorithms have been shown to outperform standard searches in both accuracy and coverage[87]. In addition, the use of synthetic standards databases enables direct comparisons to spectra belonging to the PTMed peptide of interest[88]. Another tool can use the MS1 spectra to develop custom databases of peptide elution time and precursor ion features that when compared to new analysis increase confidence in peptide spectra matches[89]. The same approaches could be applied to probe modified peptide spectra.

There are few computational tools dedicated to prioritizing of targets from ABPP experiments and even fewer take advantage of site-specific nature of ABPs. One recent example integrates genetic pathogenicity scores with combined annotation dependent depletion (CADD) scoring to prioritize targets from ABPP experiments[90]. A common technique for prioritizing of targets and characterizing ABPs is the use of gene ontology enrichment analysis[27,29,91]. This identifies over or underrepresented molecular function, cellular compartment or biological process annotations among the targets identified but this technique is primarily built around changes in mRNA sequence levels. The third technique usually involves interaction mapping of targets to find proteins that are central to a system or connected to important proteins or metabolites[92].

Virtual screening has been used to identify new covalent molecules through

covalent docking screening. These work by simulating the binding of a ligand to a 3D protein structure and compare the lowest energy conformations acquired. This approach can be facilitated by dedicated covalent docking programs. As an example, DOCKTITE identifies electrophilic warheads and docks the compounds with a focus on the electrophilic warhead and nucleophilic side chain interaction[93]. This technique was used to identify an irreversible inhibitor for FMS-like Tyrosine Kinase 3 (FLT3)[94]. AutoDock assigns the region near the site of attachment as gaussian well for the atom on the ligand that forms the covalent bond. This technique is used in Chapter 4 for ligand screening[95]. These approaches require that the site of modification be known which as discussed can be identified with ABPP.

1.7 Challenges in ABP Development

The development of new ABPs depends on mass spectrometry and computational tools to identify the targets of the probe. Current techniques vary among groups using these techniques and most approaches only use proteins identification information. Most techniques are built for the analysis of mRNA-seq or total protein mass spectrometry analysis techniques. Several of the methods discussed in Section 1.3 identify the amino acid modified and depending on traditional analysis approaches neglects the additional information in the identification and prioritization of protein targets. Combined the computational techniques used for ABP-MS experiments vary across the field, limit their utility and do not take full advantage of the information is the resulting spectral datasets. The work presented in this thesis provide ways to address these limitations.

In Chapter 2, a toolkit was developed to integrate quality control metrics as well as handle challenging singlets generated by complete competition in ABPP studies. Chapter 3 includes software to identify the specific amino acid modified, enables quantification of specific sites and introduces tools that uses domain annotation to analyze site. In addition, this Chapter introduces a first in class tyrosine selective broad probe for use with proteome profiling. Chapter 4 combines all this work to create a reproducible platform for the analysis of known and novel probes. Further, this Chapter introduces a number of analysis techniques that use more information gained form site-specific mass spectrometry and uses the technique to perform competitive ABPP guided docking. The work presented aim to advance ABPP through the generation of new computational tools as well as new ABPs.

Chapter 2: Chemoproteomic Discovery of a Ritanserin-Targeted Kinase Network Mediating Apoptotic Cell Death of Lung Tumor Cells

Adapted from: Sean T. Campbell‡, Caroline E. Franks‡, Adam L. Borne‡, Myungsun Shin, Liuzhi Zhang, and Ku-Lung Hsu. Molecular Pharmacology 94, 1246-1255 (2018).
‡ These authors contributed equally.

2.1 Abstract

Ritanserin was tested in the clinic as a serotonin receptor inverse agonist but recently emerged as a novel kinase inhibitor with potential applications in cancer. Here, we discovered that ritanserin induced apoptotic cell death of non-small cell and small cell lung cancer (NSCLC, SCLC) cells via a serotonin-independent mechanism. We used quantitative chemical proteomics to reveal a ritanserin-dependent kinase network that includes key mediators of lipid (DGKα, PI4KB) and protein signaling (FER, RAF), metabolism (EF2K, E2AK4), and DNA damage response (TLK2) to broadly kill lung tumor cell types. While ritanserin exhibits polypharmacology in NSCLC proteomes, this compound shows unexpected specificity for c-RAF in the SCLC subtype with negligible activity against other kinases mediating MAPK signaling. We show ritanserin blocks c-RAF but not B-RAF activation of established oncogenic signaling pathways in live cells, providing evidence in support of c-RAF as a key target mediating its anticancer activity. Given the role of c-RAF activation in RAS-mutated cancers resistant to clinical B-RAF inhibitors, our findings may have implications in overcoming resistance mechanisms associated with c-RAF biology. The unique target landscape, combined with acceptable safety profiles in humans, provides new opportunities for repositioning ritanserin in cancer.

2.2 Introduction

Ritanserin is a serotonin (5-hydroxytryptamine, 5-HT) receptor inverse agonist with specificity for the 5-HT2 subtype[96]. As a drug candidate, ritanserin was tested for treatment of several neuropsychiatric disorders but never received approval for clinical use[97]. The oral bioavailability and lack of adverse side effects in humans have since prompted studies to explore ritanserin for clinical applications beyond serotonin signaling[98]. Comparison of ritanserin with existing lipid kinase inhibitors revealed structural similarities that led to its discovery as an inhibitor of diacylglycerol kinase-alpha (DGKα)[98,99](Figure 2.1.a). We recently used quantitative chemical proteomics to discover ritanserin as an active-site inhibitor of DGKα and the non- receptor tyrosine protein kinase FER[36,100]. While distinct in substrate preference, DGKα[101] and FER[102]are kinases related by their role in coupling receptor activation with intracellular signaling important for cell survival and proliferation. Thus, ritanserin is capable of perturbing cellular signaling through serotonin-independent mechanisms. We and others have proposed that ritanserin may have potential applications in oncology by disrupting regulatory pathways through its largely unexplored action against the kinase superfamily.

In this study, we set out to define the target spectrum of ritanserin in order to better understand its mode of action in tumor cells. Previous reports demonstrated that ritanserin is cytotoxic against glioblastoma and melanoma through putative downstream targets of DGKα including mTOR[103], HIF-1a[103], and GGTase I[104]. We hypothesize that ritanserin's cellular activity is mediated through blockade of kinase networks to explain its broad action against diverse tumor cell types. An advantage of multi-targeted strategies is to minimize

the potential for development of resistance mechanisms[68]. We conducted cell viability assays to determine the impact of ritanserin treatments on survival of different lung cancer subtypes. We used quantitative chemoproteomics to determine the kinase targets of ritanserin in both non-small cell lung cancer (NSCLC) and small cell lung cancer (SCLC) proteomes. Our findings reveal that ritanserin shows novel activity against c-RAF in SCLC proteomes. The lack of activity against other kinases involved in MAPK signaling suggests that ritanserin mediates its cellular activity in SCLC cells at least in part through blockade of c-RAF.

2.3 Materials and Methods

Materials. pDONR223-DGKK was a gift from William Hahn & David Root (Addgene plasmid # 23487). pCSF107mT-GATEWAY-3'-FLAG was a gift from Todd Stukenberg (Addgene plasmid # 67619). pCSF107mT-DGKK-FLAG construct was generated by recombination of the Addgene plasmids using the Gateway cloning system (Invitrogen). Desthiobiotin ATP acyl phosphate nucleotide probe was obtained from ThermoFisher Scientific (PI88311). Ritanserin and ketanserin tartrate were purchased from Tocris Bioscience. WST-1 reagent kits were purchased from Cayman Chemical. Trypan Blue was purchased from ThermoFisher Scientific. CaspaseGlo Assay kits were purchased from Promega. PMA was purchased from Cayman Chemicals.

WST-1 Cell Proliferation Assays. Tumor cells were plated in transparent tissue-culture treated 96-well plates at a density of 100,000 cells/mL (A549, H1650) or 200,000 cells/mL

(H82) in a volume of 100 µL per well. Cells were treated with dimethyl sulfoxide (DMSO) vehicle or inhibitors dissolved in DMSO at the indicated concentrations (final DMSO concentration of 0.5%). Cells were allowed to grow for indicated times at 37 °C under 5% CO2, equal parts of WST-1 developer reagent and electron mediator solution were mixed, and 10 µL of the resulting solution ('WST-1 reagent') were added to each well. Plates were shaken in an orbital shaker for 60 s and then returned to the incubator for two hrs. Plates were again shaken followed measurement of absorbance at 450 nm. Data were normalized to DMSO- treated wells and significance values determined with one-way ANOVA.

Cell Counts. Tumor cells were plated in 60 mm plates at a density of 100,000 cells/mL (A549, H1650) or 200,000 cells/mL (H82) at a volume of 3.5 mL/plate. Cells were treated with inhibitors at the indicated concentrations (final DMSO concentration of 0.5%) for 48 hrs at 37 °C, adherent cells were washed and detached with trypsin, and all cells were collected and concentrated by spinning at 400 x g for 3 min followed by aspiration of media. Cells were resuspended in 10 nM Trypan Blue and 10 µL of this solution was counted via a hemocytometer. Dead cells were excluded from all counts. Data were normalized to DMSO-treated wells and significance values determined with one-way ANOVA.

Caspase Glo Assays. Assays were performed as directed by the manufacturer (Promega). Briefly, tumor cells were plated in black tissue culture treated transparent-bottom 96 well plates at a density of 200,000 cells/mL (A549, H1650) or 400,000 cells/mL (H82) in a

volume of 50 µL/well. Cells were treated with inhibitors at the indicated concentrations (final DMSO oncentration of 0.5%) for 24 hrs. Afterwards, 50 µL of the prepared CaspaseGlo reagent was added to each well. The reaction was allowed to proceed for 1 hr, at which point the cells were shaken in an orbital shaker at 500 rpm for 60 s and then luminescence was read for each well. Data were normalized to DMSO-treated wells and significance values determined with one-way ANOVA.

Sample preparation for quantitative LC-MS analysis using ATP acyl phosphates. Proteomes were diluted to 2 mg/mL in kinase buffer. The light and heavy proteomes (0.5 mg, 250 µL total reaction volume) were pre-treated with vehicle or compound, respectively (5 µL, DMSO (light) or 50X stock in DMSO (heavy)), mixed gently, and incubated at 25 °C for 30 min. Desthiobiotin ATP acyl phosphate nucleotide probe (0.5 mM in ddH2O) was then added to each sample (5 µL, 10 µM final), mixed gently, and allowed to incubate at 25 °C for 30 min. After incubation, matched light and heavy proteomes were transferred and mixed in a 1:1 ratio in a two-dram vial containing 4:1:3 MeOH/CHCl3/H2O (2 mL MeOH, 500 µL CHCl3, 1.5 mL H2O) for extraction of proteins to remove excess probe, quickly vortexed, and centrifuged at 1,400 x g for 3 min to pellet protein. Organic and aqueous layers were removed using a Pasteur pipette, and the protein pellet was transferred to a screw-top tube in 600 µL MeOH. A second extraction was performed by adding CHCl3 (150 µL) and H2O (600 µL) to each sample, vortexed, and centrifuged at 1,400 x g for 3 min to pellet protein. Organic and aqueous layers were removed by pipetting, MeOH added to pellet (600 µL) and pellets were re-suspended by sonication (3 x 1 sec pulse, 20%

amplitude) for a final extraction. Samples were then centrifuged at 17,000 x g for 5 min to pellet protein and MeOH was removed by pipetting. The pellets were re-suspended in 10 M urea/25 mM ammonium bicarbonate (500 mL), brought to a final volume of 1 mL with 25 mM ammonium bicarbonate, reduced with 10 mM DTT for 15 min at 65 °C, allowed to cool, and then alkylated with 40 mM iodoacetamide for 30 min at 25°C in the dark. To desalt the samples, each was transferred to a two-dram glass vial, and to the vial 4:1:2 MeOH/CHCl3/H2O (2 mL MeOH, 500 µL CHCl3, 1 mL H2O) was added. The vials were vortexed quickly, spun at 1,400 x g for 3 min to pellet protein, and aqueous and organic layers were removed using a Pasteur pipette. The resulting protein pellet was transferred to a screw-top tube in 600 µL MeOH, and then CHCl3 (150 µL) and H2O (600 µL) were added to extract protein a second time. The samples were vortexed quickly, centrifuged at 1,400 x g to pellet protein, and the aqueous and organic layers were removed by pipetting. Resulting protein pellet was suspended in MeOH (600 µL) via sonication (3 x 1sec pulse, 20% amplitude), centrifuged at 17,000 x g for 5 min to pellet protein, and MeOH removed by pipetting. Protein pellets were then re-suspended in 25 mM ammonium bicarbonate (500 µL) and digested with 7.5 µg Trypsin/Lys-C (Promega, 15 µL, 0.5 µg/µL) for 3 h at 37 °C. Avidin-agarose beads (Thermo Scientific Pierce, 100 µL aliquot per sample) were washed three times by adding 10 mL DPBS, centrifuged at 1,400 x g for 1 min, and decanting. This wash step was repeated for a total of 3 times. Digested protein samples were mixed with washed avidin beads (100 µL) and brought to a volume of 5.5 mL with DPBS in a 15 mL conical and rotated for 1 h to enrich samples for the covalent desthiobiotin modification. The beads were washed with 25 mM ammonium bicarbonate

(3X with 10 mL, centrifuge at 1,400 x g for 3 min, decant) and then H2O (3X with 10 mL, centrifuge at 1,400 x g for 3 min, decant). Washed beads were then transferred to a low-bind microfuge tube, centrifuged at 1,400 x g for 3 min, allowed to rest for 1 min to settle beads, and then excess H2O was removed carefully using a gel-loading pipette tip. To elute peptides, 100 µL of elution buffer (50% acetonitrile, ACN; 0.1% formic acid) was added to each sample and incubated for 3 min. Beads were spun down at 1,400 x g for 3 min, allowed to rest for 1 min to settle beads, and then 75 µL of peptide-containing supernatant was removed carefully using a gel-loading pipette tip and transferred to a new low bind centrifuge tube. This step was repeated two more times with 75 µL of elution buffer and all eluent were collected into the same centrifuge tube (~225 µL total). Peptides were dried on a speed vacuum, resulting peptide samples acidified in 5% (v/v) formic acid, and stored at -80 °C until analysis.

LC-MS/MS analysis of SILAC samples. The peptide samples were analyzed by liquid chromatography-mass spectrometry. An integrated autosampler-LC (Ultimate 3000 RSLC nanoSystem, Dionex) was used to load the peptides onto a trap column (Nano- Trap, Thermo Scientific, 2 cm, 5 µm C18) and washed for 2 minutes with 1% B (80% ACN, 1% formic acid). The peptides were eluted from the trap column and through a homemade nanocapillary analytical column (20 cm, 5 µm C18 packed in 360 µm o.d. x 75 µm i.d. fused silica), with an integrated electrospray tip, using a 180 min 1-95% reverse-phase LC gradient (A: 0.1% formic acid; B: 80% ACN, 0.1% formic acid) with the following parameters: 0-2 min 1% B, 400 nL/min; 2-144 min to 95% B, 300 nL/min; 144.1-180 min

1% B, 400 nL/min. The eluting peptides were electrosprayed into an Orbitrap Q Exactive Plus mass spectrometer (Thermo Scientific), which was operated with a top 10 data-dependent acquisition method that consisted of one full MS1 scan (375 - 1,500 m/z) followed by 10 MS2 scans of the most abundant ions recorded in the MS1 scan. Data analysis was accomplished using the IP2 (Integrated Proteomics Applications) software package, in which RawConverter was used to generate searchable MS1 and MS2 data from the .raw file followed by using the ProLuCID algorithm (publicly available at http://fields.scripps.edu/downloads.php) to search the data against a modified human protein database (UniProt human protein databaseangiotensin I and vasoactive intestinal peptide standards; 40,660 proteins) with the following parameters: static carbamidomethyl modification of cysteine (+57.0142 Da), differential modifications of oxidized methionine (+15.9949 Da) and desthiobiotin- labeled lysine residues (+196.1212 Da), added masses of the SILAC "heavy"-labeled amino acids (+10.0083 Da for R, +8.0142 Da for K), and trypsin enzyme specificity with 2 missed cleavages. The resulting MS2 spectra matches were assembled into protein identifications and filtered using DTASelect 2.0 using the --mass, --modstat, and --trypstat options with a 1% peptide FDR. mzIdent files corresponding to searches were generated in IP2-Integrated Proteomics Pipeline, mzXML spectra data was extracted from the raw file using RawConverter and uploaded into Skyline-daily[105] to determine SILAC ratios (SR) of light/heavy (vehicle/compound treated) peptides. Peptides used for analysis were assessed for quality in Skyline by the following criteria: isotope dot-product (iDOTP) $\geq$ 0.8, ratio dot-product (rDOTP) $\geq$ 0.8, and singletons defined by L/H ratios > 20 were set to 20. Dot-product values are measures of

similarity between the precursor peak area and expected isotope distribution (iDOTP) and between the light and heavy peak area (rDOTP) as calculated in Skyline and described by Schilling et al[104]. Probe-modified peptides that met these criteria were manually inspected and integrated. Peptide ratios reported were normalized to DMSO/DMSO peptide ratios to account for potential variations in mixing and sample preparations.

Transient Transfection. Recombinant B-RAF and c-RAF proteins were produced by transient transfection of HEK293T cells. HEK293T cells were plated at a concentration of 1 x 10^6 cells per 10 cm plate and grown to ~70% confluence. A polyethyleneimine (PEI) stock solution was prepared (1mg/mL, pH 7.4) and filter sterilized. Serum-free DMEM (600 µL) was mixed gently with 2.6 µg DNA and 20 µL of sterile PEI (1 mg/mL, pH 7.4) in a sterile microfuge tube. Mixtures were incubated for 30 min at 25 °C. The mixture was then added drop-wise to each 10 cm plate, rocked back and forth to mix, and placed back in the incubator. Cell pellets were harvested after two full days of growth, snap- frozen in liquid N2, and stored at -80°C until use. c-RAF plasmid (pCSF107mT-cRAF-FLAG) was generated by recombination of the Addgene plasmids using the Gateway cloning system (Invitrogen).

Phospho-MEK assay of RAF activity. Recombinant RAF- HEK293T cells were pretreated with DMSO vehicle or inhibitors at the indicated concentrations for 1 hr, followed by addition of PMA (20 ng/mL) for an additional 20 min at 37 °C. Cells were harvested for western blots and phospho-MEK detected using rabbit anti-phospho-MEK

antibody (S217/S221; Cell Signaling Technology) followed by goat anti-rabbit Dylight 550 secondary antibody (Thermo Scientific) for fluorescence detection. Western blot measurement of MEK (rabbit anti-MEK1/2, Cell Signaling Technology) was included to evaluate protein loading between samples.

Computational Methods. Data for A549 and H82 cell lines were searched with IP2 and manually validated using the methods previously described (Chapter 2.3). Data for desthiobiotin-tagged ATP acyl-phosphate probes and ATP competitive peptides were compared and clustered. Ritanserin and ketanserin inhibition profiles were compared using SILAC ratios and normalized to DMSO. The kinase profiles were displayed as a heatmap and clustered with hierarchical clustering using R package d3heatmaps (https://blog.rstudio.org/2015/06/24/d3heatmap/).

Lipid kinase phylogenetic tree. Phylogenetic tree of human lipid kinases was generated using MUSCLE multiple sequence alignment[106] of annotated lipid kinases and a least squared distance method for determining evolutionary distance. Calculations were conducted using the EMBOSS software suite[107].

Statistical analysis and determination of IC50 values. For all cell viability measurements, results were normalized to values obtained from DMSO treated cells. For CaspaseGlo assays, raw luminescence values are reported. All significance values for Cell Viability and CaspaseGlo assays were calculated with one-way ANOVA and Dunnett's

multiple comparison test (post-hoc analysis). IC50 values were calculated using a four-parameter logistic model of the response curve. All data are shown as mean + S.E.M. All statistical analyses were performed using GraphPad Prism.

2.4 Results

2.4.1. Ritanserin Shows Serotonin-Independent Cytotoxic Activity in Lung Tumor Cells

We chose H1650 and A549 as our non-small cell lung cancer (NSCLC) cell models to evaluate sensitivity of cells with different genetic backgrounds to ritanserin exposure. H1650 cells express EGFR receptors containing activating mutations in the kinase domain (exon 19 deletion E746-A750) of this receptor tyrosine kinase. A549 cells express wild-type EGFR but harbor mutant KRAS (G12S). We also included H82 cells in our studies to evaluate ritanserin activity in small cell lung cancer (SCLC). The mutational backgrounds of cell lines used in this study are listed in Table 4.1. Ketanserin (Boroda et al., 2017; Franks et al., 2017) was used alongside ritanserin to control for potential 5-H2 receptor (5-HTR) inverse agonist activity and other nonspecific pharmacological effects in our cell biology (Fig. 2.1.a).

Cells were treated with varying ritanserin concentrations (5 – 50 μM) and cell viability measured using established WST-1 metabolic assays[108]. We observed concentration-dependent decreases in viability in cells exposed to ritanserin but not ketanserin treatments (Fig. 2.1.b and 2.2.a). At a moderate concentration of ritanserin (25 μM), we observed >70% blockade of cell proliferation across all NSCLC and SCLC lines tested (Fig. 2.1.a). At lower concentrations (5 μM), ritanserin showed enhanced

cytotoxicity against the SCLC H82 (~50% cell death) cells compared with NSCLC cells (~5-15% cell death for A549 and H1650 cells, Fig 2.1.b). Cell killing with ritanserin was rapid with >50% of cell death occurring after 1 day and near-maximal cytotoxicity after 2 days of treatment in all cell lines tested (25 μM dose, Fig. 2.1.c). The lack of activity using ketanserin under the same treatment conditions supports a serotonin- independent mechanism of cytotoxicity for ritanserin (Fig. 2.1.b and c, Fig. 2.1.a). In contrast to the pan-kinase inhibitor staurosporine, which showed general cytotoxicity across all cells tested (Fig. 2.1.c and 2.2.b), ritanserin demonstrated negligible cell killing against noncancerous primary cells at high concentrations (25 μM, Figure 4.2B).

We performed a separate cell biology assay comparing the effects of serotonin, ritanserin and ketanserin treatments on global protein kinase-C (PKC) and -A (PKA) activity in A549 and H82 cells (Fig. 2.3.a). PKC and PKA are downstream mediators of serotonin receptors (5-HTR) and global changes in substrate phosphorylation profiles of either enzyme would allow evaluation of compound activity on 5-HTR signaling. We observed negligible changes in PKC and PKA substrate phosphorylation between cell treatment conditions (serotonin, 10 μM; ritanserin and ketanserin, 25 μM; Fig. 2.2.b). In contrast, treatment with PMA, a known PKC activator, resulted in moderate increases in PKC substrate phosphorylation, which matches previous reports using this same assay[99]. The consistent lack of 5-HTR activity with equivalent doses of ritanserin and ketanserin further supports that ritanserin effects observed in cellular assays are serotonin independent. Collectively, our results show that ritanserin is not generally cytotoxic but displays potent cell killing of NSCLC and SCLC cells tested.

2.4.2. Ritanserin Activates Apoptotic Cell Death of Broad Lung Tumor Cell Types

Since changes in cell metabolism can occur from non-lethal perturbations[108], we also used live cell counts to further support cytotoxicity of lung cancer cells using ritanserin. Akin to results from cell viability assays, we observed substantial cell killing across all lung cancer cell lines exposed to ritanserin but not ketanserin (Fig. 2.4.a). We observed potent cell killing (~70%) even at the lower dose tested (10 μM, Fig. 2.4.a). Next, we measured caspase activity in treated cells to determine whether ritanserin mediates cell killing through activation of apoptosis. Cells treated with ritanserin showed statistically significant ($P < 0.05$) enhanced caspase 3/7 activity after 24 hours compared with vehicle controls (Fig. 2.4.b). Caspase activation by ritanserin was specific because ketanserin treatments under the same experimental conditions did not induce these effects (Fig. 2.4.b). We compared ritanserin effects directly with staurosporine, which served as a positive control based on previous reports of activating apoptosis in treated lung cancer cells[109,110]. In both H1650 and H82 cells, we observed comparable activation of caspase 3/7 activity compared with staurosporine (Fig. 2.4.b). While ritanserin treatment of A549 cells resulted in a lower degree of activation, the increase in caspase 3/7 activity was statistically significant compared with vehicle treated cells ($P = 0.01$, Figure 2.4.b). In summary, our cell viability and caspase activation data support ritanserin-mediated activation of apoptotic cell death in lung cancer cells that differ in mutation status (EGFR, KRAS) and subtype (NSCLC vs SCLC).

2.4.3. Chemoproteomic Kinome Profiling of Ritanserin Action in Lung Tumor Cell Proteomes

Based on previous chemical proteomic analyses[36,100], we hypothesized that ritanserin is functioning as a kinase inhibitor to mediate cytotoxicity in our lung cancer cell studies. Since A549 and H1650 displayed similar sensitivities to ritanserin in our cell viability assays, we selected A549 and H82 for chemical proteomic evaluation of ritanserin targets in NSCLC and SCLC proteomes, respectively. We used desthiobiotin- tagged, ATP acyl-phosphates[24,111,112] to measure selectivity of compounds against native kinases detected in lung cancer proteomes. ATP acyl-phosphate probes permit global profiling of kinase activities by covalent attachment of reporter tags to conserved lysines in the ATP binding site of protein/lipid kinases as well as other ATP-binding proteins[24,36,100,111,112]. For these studies, NSCLC and SCLC cells were cultured in media containing isotopically light and heavy amino acids to enable quantitative chemical proteomics[38,113,114] by stable isotope labeling with amino acids in cell culture (SILAC, Fig. 2.5). Light and heavy cell proteomes were treated with DMSO vehicle or compound, respectively, prior to addition of ATP acyl phosphate to label active site lysines. After probe labeling, light and heavy proteomes were combined, digested with trypsin protease, and desthiobiotin-modified peptides enriched by avidin affinity chromatography and analyzed by LC-MS/MS to identify and quantify isotopically tagged active-site peptides from native kinases as previously described[36,100] and depicted in Figure 4.5.

Using our quantitative chemical proteomics assay, we compared kinase activity profiles between A549 and H82 cell proteomes. Kinases included in our comparisons showed potent competition with free ATP (SILAC ratios (SR) > 5, Fig. 2.6.a). The latter criterion was important to distinguish specific probe binding at ATP-binding sites versus

non-specific labeling of surface lysines. We detected ~120 unique probe-modified peptides from ~110 distinct kinases. Using ATP competition profiles, we separated kinases into groups detected in both proteomes (shared) or detected in either A549 (NSCLC) or H82 samples (SCLC, Fig. 2.6.a). Specifically, we observed probe-dependent detection of several kinases (AKT1/2/3 and IKKA) in A549 proteomes that are associated with PI3K/AKT signaling[115] (Fig. 2.6.a). These findings are consistent with enhanced PI3K/AKT signaling in NSCLC subtypes containing KRAS mutations[116]. Finally, we detected native DGKα activity in A549 proteomes (Figure 2.7 shows MS1 data for DGKα peptide), which may indicate a potential role for DAG and PA metabolism/signaling in these NSCLC cells. A similar analysis of SCLC kinase profiles revealed enrichment of kinases involved in RAF signaling (A-RAF, B-RAF, and c-RAF[117] as well as DNA damage response (ATR, CHK2, PRKDC, and TLK2[118]; Fig. 2.6.a). These findings support previous reports that c-RAF is one of several proto-oncogenes that are highly expressed in SCLC cells and tumor tissues[119]. Collectively, our kinase profiling studies establish a global map of kinase activities detected in A549 and H82 proteomes, including discovery of kinases that appear enriched in NSCLC compared with SCLC subtypes.

2.4.4. Chemoproteomic Profiling Reveals c-RAF as a Principal Target of Ritanserin in SCLC Proteomes

Next, we used our competitive ATP probe assay to determine the kinase targets of ritanserin in A549 and H82 proteomes (Fig. 2.6.b). Ketanserin was included in our LC-MS studies to discern ritanserin-specific from general non-specific activity of 5-HTR inverse agonists against the kinome. We chose to test inhibitor concentrations (100 μM)

10-fold higher than required for potent cell killing (10 μM, Fig. 2.4.a) to account for potential shifts in potency of reversible inhibitors due to irreversible labeling kinetics of the ATP acyl phosphate probe[111]. Kinase targets of ritanserin were defined as those active-site peptides that showed SILAC ratios > 4. As expected based on previous findings[36], we detected potent inhibition of FER and DGKα in A549 proteomes with ritanserin treatments (FER, SR = 9; DGKα, SR = 6; Figure 2.7). We identified an additional lipid kinase target, PI4KB in A549 proteomes, which is involved in modulating lipid-mediated PI3K/AKT signaling in tumor cells[120]. In addition to signaling, ritanserin treatment perturbed kinases implicated in glycolysis (EF2K[121]), amino acid metabolism (E2AK4[122]), and DNA damage response (TLK2[123]).

In contrast to polypharmacology observed in A549 proteomes, we identified c-RAF as the primary target of ritanserin in H82 proteomes (Fig. 2.6.b and c; Fig. 2.8 shows MS1 and MS2 data for c-RAF peptide). Ketanserin treatments did not perturb activity of key kinases involved in metabolism and signaling (Fig. 2.6.c). Since c-RAF is a key regulator of the mitogen-activated protein kinase (MAPK) pathway, we also measured activity of ritanserin against other MAPK targets in H82 SCLC proteomes including B-RAF, MAPK (ERK1 and ERK2), and MAP2K (MEK1 and MEK2) kinases. We show that ritanserin shows selective perturbation of c-RAF compared with other MAPK mediators in H82 proteomes (Figure 2.9.a). Collectively, our findings reveal, for the first time, a ritanserin-targeted lipid/protein kinase network involved in signaling, metabolism, and stress responses that help explain its broad anti- proliferative activity in lung tumor cells. In addition, we demonstrate that ritanserin shows selective blockade of c-RAF when

compared with other MAPK kinases in H82 SCLC proteomes.

2.4.5. Ritanserin Block c-RAF But Not B-RAF Activation of MEK Signaling in Live Cells

Our chemoproteomic studies identified c-RAF as a potential target mediating ritanserin anti-tumor activity. Here, we sought to test whether ritanserin blocked c-RAF signaling pathways relevant for its anti-tumor activity. RAFs are part of the mitogen-activated protein kinase (MAPK) pathway involved in regulation of cellular responses to external signals[124–126]. Growth factors and mitogens trigger activation of receptor tyrosine kinases (RTKs) that mediate guanosine triphosphate (GTP) loading of the RAS GTPase[127]. GTP-loaded RAS activate RAFs (A-RAF, B-RAF, and c-RAF) via recruitment to the cell membrane. Activated RAFs phosphorylate and activate MEK (MEK1 and MEK2), which phosphorylates and activates ERK (ERK1 and ERK2) as part of a signaling cascade to modulate cell proliferation, differentiation, apoptosis, and migration in cancer[128].

To directly measure c-RAF-mediated MEK phosphorylation in live cells, we overexpressed recombinant c-RAF in HEK293T cells, activated cells with PMA[129], and measured the resulting levels of phosphorylated MEK1/2 (phospho-MEK) by western blots (Fig. 2.9.b). We also overexpressed recombinant B-RAF to directly compare specificity of ritanserin activity against the various RAF isoforms. Both c-RAF and B-RAF overexpression resulted in substantially enhanced phospho-MEK levels compared with non-overexpressed (mock) counterparts (Fig. 2.9.b). Pretreatment of cells with ritanserin (50 μM) resulted in substantial blockade of recombinant c-RAF but not B-RAF signaling activity as judged by reductions in phospho-MEK levels (Fig. 2.9.b). Ketanserin did not

produce the same effects as ritanserin, which supports ritanserin-specific effects in our assay. The RAF inhibitor sorafenib[130] was used as a positive control to demonstrate blockade of both recombinant c- RAF- and B-RAF- mediated increases in phospho-MEK levels. Taken together, our results demonstrate ritanserin specifically blocks c-RAF activity in MAPK signaling pathways known to be important for tumor cell biology[128].

2.5 Discussion

Here, we provide evidence that ritanserin functions as a lipid and protein kinase inhibitor with broad action against diverse lung cancer types that is serotonin- independent. Using quantitative chemical proteomics, we discovered that ritanserin targets a kinase network in A549 proteomes (Fig. 2.6.b), which suggests polypharmacology as a likely mode of action in A549 and potentially other NSCLC cells (including H1650). Despite promiscuous activity in the kinome, ritanserin was not cytotoxic in noncancerous primary cells (Fig. 2.2.b), which is likely due to differences in cell metabolism and signaling between tumor and noncancerous cells as previously reported for ritanserin in glioblastoma[103]; further investigations are needed to determine whether ritanserin can specifically kill lung tumor cells in vivo.

A surprising finding from our studies was the identification of c-RAF as the primary target for ritanserin in H82 SCLC proteomes (Fig. 2.6 and 2.9). Recent studies demonstrated that loss of c-RAF activity resulted in tumor regression of aggressive K- RAS driven cancers with reduced systemic toxicity because canonical MAPK signaling is unaffected[117]. Our chemoproteomic (Fig. 2.6) and cell biology (Fig. 2.9) studies show

ritanserin specificity for blockade of c-RAF versus B-RAF activity. Thus, our findings position ritanserin as a novel scaffold for future medicinal chemistry efforts to develop potent and selective c-RAF inhibitors. The utility of targeting c-RAF in the clinic extends beyond studies of lung cancers. For example, clinical efficacy of B-RAF inhibitors in RAS-mutated cancers is limited by resistance through paradoxical activation (164-166). Drugs that selectively block B-RAF drive B-RAF binding to c-RAF in a RAS dependent manner, c-RAF activation, and consequent elevations in MEK and ERK signaling. Future studies are needed to determine whether ritanserin can be used to overcome resistance mechanisms associated with c- RAF activation.

We recognize our selectivity profiling studies have been performed in lysates and development of new activity-based probes for live cell profiling will be critical to fully understand the mechanism of action of ritanserin in future studies. Nonetheless, we identify a novel anticancer activity for ritanserin along with clinically relevant kinase targets like c-RAF that, coupled with its safety profiles in humans, should prove valuable for potential drug repurposing in cancer.

2.6 Author Contributions and Pipeline Development

Campbell, Franks, Borne and Hsu designed, conducted, performed data analysis and wrote components of the resulting paper. The cell viability experiments were conducted by Campbell, kinome profiling experiments were conducted by Franks and Borne, and western blot assays were conducted by Borne and Campbell. See figure legends for more details.

This early version of ABPP computational analysis was a R shiny application developed to analyze the sites of modification. After searching with IP2 software the results were quantified using skyline, which also provided idotp and rdotp information. The application integrated the byonic and skyline information to identify sites of modification. The ATP and inhibitor competition studies created situation where peptides had not signal from the heavy lysate producing singlets. These singlets require further investigation as they can be the result of improper peak picking by skyline or a bad PSM. The software would initially cluster hierarchically all non-singlet data and provide a selectable list of singlets identified in the study. This enabled the user to verify the singlet and integrate the site into the heatmap.

Additionally, the R shiny application included quality control (QC) comparisons between replicates. This enabled the identification of experimental errors created preparing the lysate for and the acquisition of MS data. These QC included correlation plot of SR across different replicates, boxplots of site SRs for single sites, and a boxplot of DMSO treated lysates. These tools combined with the heatmap generation comprised the earliest version of the computational pipeline known as HsuLabAnalysis.

2.7 Tables and Figures

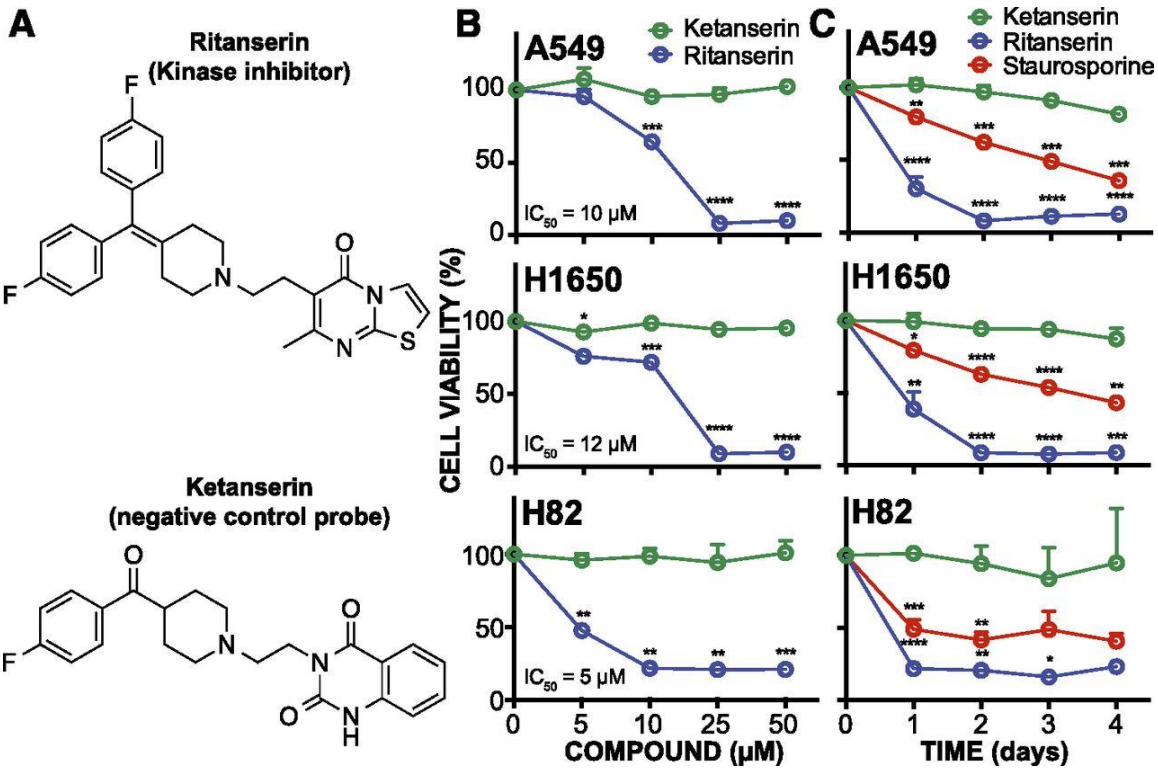

Figure 2.1. Ritanserin shows cytotoxic activity in lung tumor cells. (A) Ritanserin is a 5-HT2 receptor (5-HT2R) inverse agonist with known activity against lipid (DGKα) and protein (FER) kinases. Ketanserin is a 5-HT2 R inverse agonist that lacks DGKα/FER inhibitory activity and serves as a negative control. (B) Cell viability dose-response curves for NSCLC (A549, H1650) and SCLC (H82) tumor cells treated with ritanserin or ketanserin at the indicated concentrations for 2 days. (C) Time course of cell viability in tumor cells treated with 25 µM ritanserin, 25 µM ketanserin, or 1 µM staurosporine for 4 days. Staurosporine is a pan-kinase inhibitor and included as a positive control of tumor cell death. All experiments were performed in triplicate and data are from two independent

biological replicates performed on separate days (n = 6). Statistical significance was calculated with respect to ketanserin treatment. Data are shown as mean + S.E.M. *P ≤ 0.05, **P ≤ 0.01, *** P ≤ .001, and ****P ≤ 0.0001. Work conducted by Campbell.

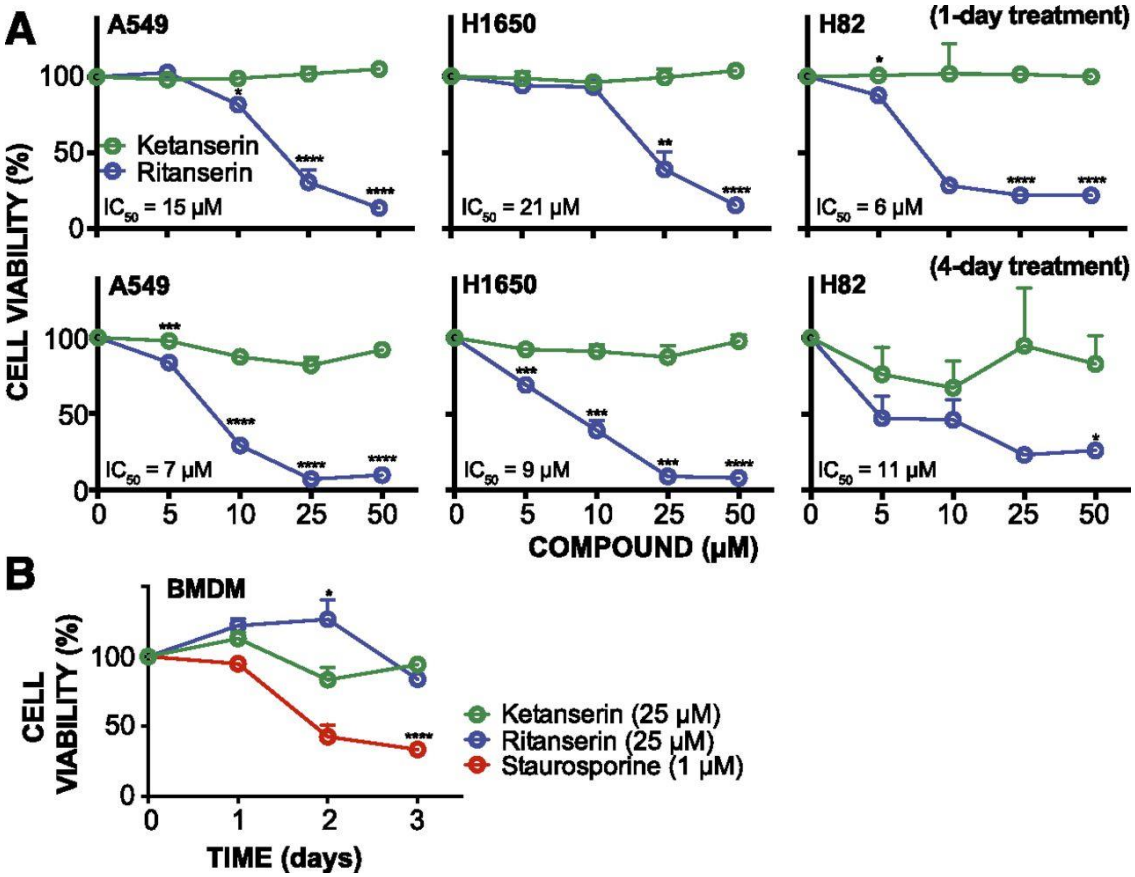

Figure 2.2. Ritanserin activity in lung tumor cells. (A) Lung cancer cell viability (%) at 1 and 4 days after treatment with compounds at the indicated concentrations as determined by the WST-1 metabolic assay. (B) Time course of cell metabolic activity (WST-1 assay) of primary bone marrow derived macrophages (BMDMs) treated with 1 μM staurosporine, 25 μM ritanserin, or 25 μM ketanserin. All experiments were performed in triplicate and

data are from two independent biological replicates performed on separate days (n = 6). Statistical significance was determined by comparison with ketanserin treatment (negative control) at the same concentration and treatment time. Cell viability shown is normalized to vehicle treated samples. Data are shown as mean +

S.E.M. * $P \leq 0.05$, ** $P \leq 0.01$, *** $P \leq .001$, and **** $P \leq 0.0001$. Work conducted by Campbell.

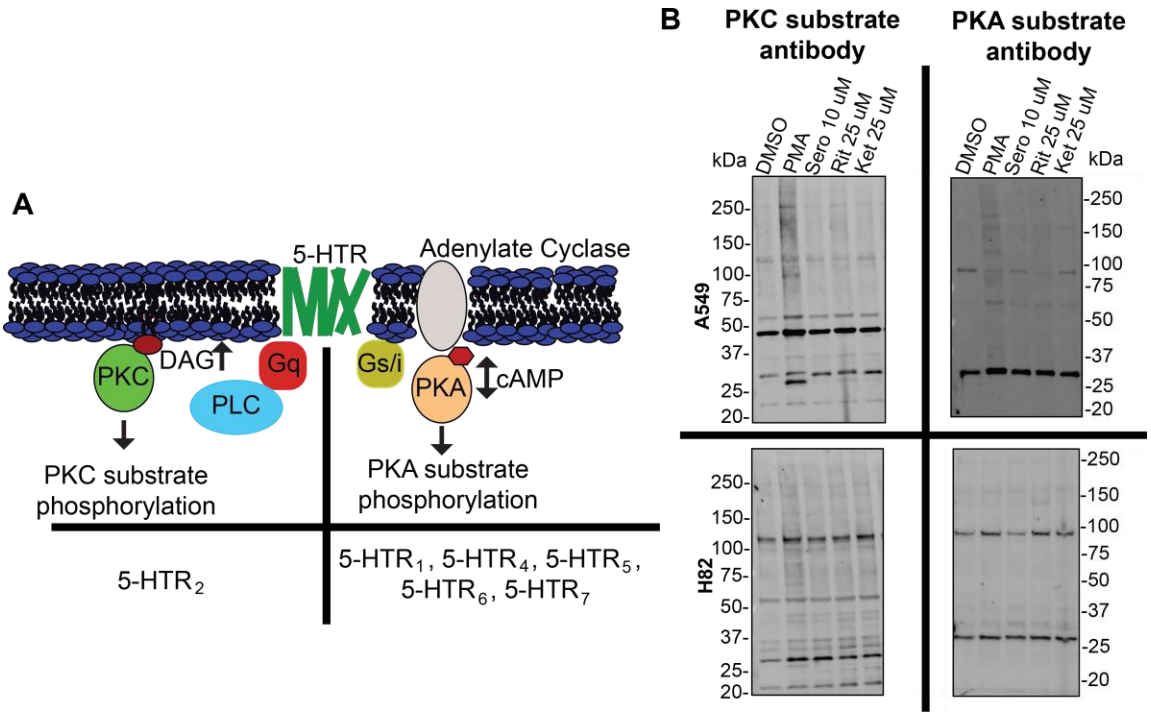

Figure 2.3. Ritanserin and ketanserin show negligible effects on 5-HTR signaling. (A) Schematic showing G-protein coupled receptor (GPCR) 5-HTR signaling. Activation of different members of the 5- HTR family leads to activation of Gq or Gs/i G-proteins, resulting in enhanced phospholipase C (PLC)- mediated diacylglycerol (DAG) activity or

changes in adenylate cyclase-mediated cyclic adenosine monophosphate (cAMP) signaling, respectively. DAG and cAMP activate protein kinase-C (PKC) or -A (PKA), respectively, and their activity (as measured by substrate phosphorylation) can be used to monitor potential 5-HTR signaling activity. (B) A549 or H82 cells were treated with DMSO vehicle, PMA (100 ng/µL), serotonin (Sero, 10 µM), ritanserin (Rit, 25 µM), or ketanserin (Ket, 25 µM) to determine effects of each compound on global PKC and PKA activity. We observed negligible changes in 5-HTR signaling activity across all conditions tested, except for a mild increase in PKC substrate phosphorylation using PMA as expected (PKC activator; positive control). Protein kinase substrate phosphorylation assays were performed as previously described[99]. Work conducted by Borne.

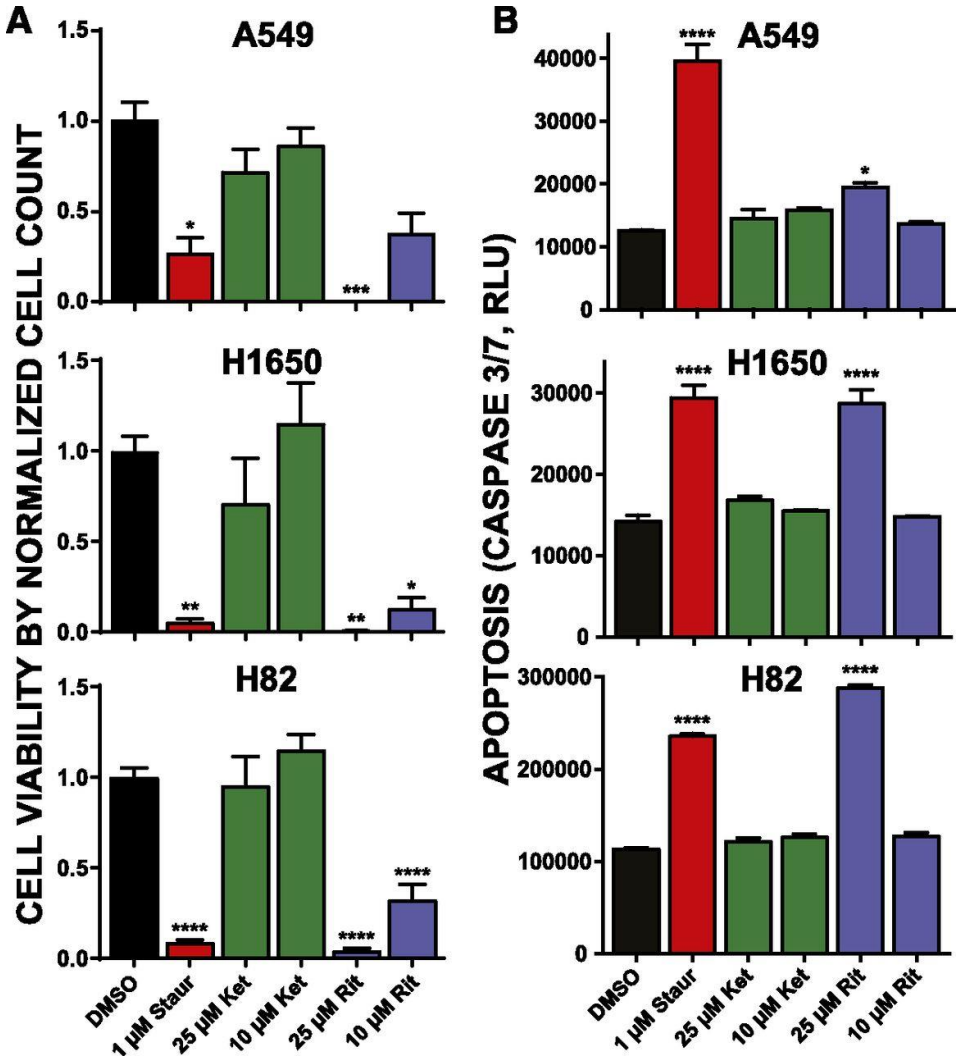

Figure 2.4. Ritanserin treatments activate apoptosis in NSCLC and SCLC tumor cells. (A) Cell viability as measured by Trypan blue cell counts after treatment with staurosporine (Staur), ketanserin (Ket), or ritanserin (Rit) at the indicated concentrations for 2 days. Cell counts were normalized to vehicle control (DMSO). Statistical significance was calculated by comparison with 10 µM ketanserin treatment. (B) Activation of apoptosis was determined by commercial CaspaseGlo 3/7 assay (see ESI for additional details). Cells were incubated with compounds at the concentrations given and allowed to grow for 1 day, at which point caspase activity was measured. Statistical significance was calculated by

comparison with vehicle control. All experiments were performed in triplicate and data are from two independent biological replicates performed on separate days (n = 6). Data are shown as mean + S.E.M. *P ≤ 0.05, **P ≤ 0.01, *** P ≤ .001, and ****P ≤ 0.0001. Work conducted by Campbell.

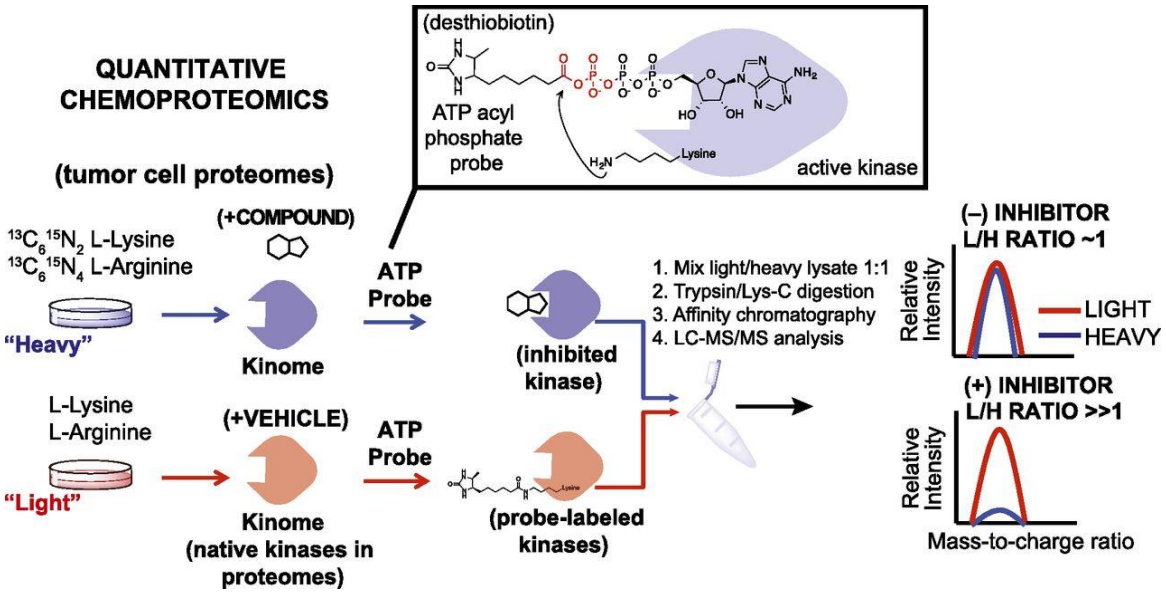

Figure 2.5. Quantitative chemoproteomics to define the target spectrum of ritanserin in tumor cell proteomes. Proteomes from lung tumor cells cultured in SILAC media are treated differentially with DMSO vehicle (light) or compound (heavy). Next, ATP acyl phosphate probe is added to both light and heavy proteomes to label active kinase via covalent modification of conserved lysines in kinase active sites. Proteomes are digested to tryptic peptides using proteases. Active-site probe-labeled peptides are enriched by avidin affinity chromatography and quantified by LC-MS/MS. SILAC (light/heavy) ratios are used to evaluate compound activity at individual kinase active sites. No inhibition

results in a SILAC ratio of ~1 while competition at respective kinase active sites blocks probe labeling and enrichment resulting in SILAC ratios >>1 to identify targets of small molecule inhibitors. Figure created by Franks and Hsu.

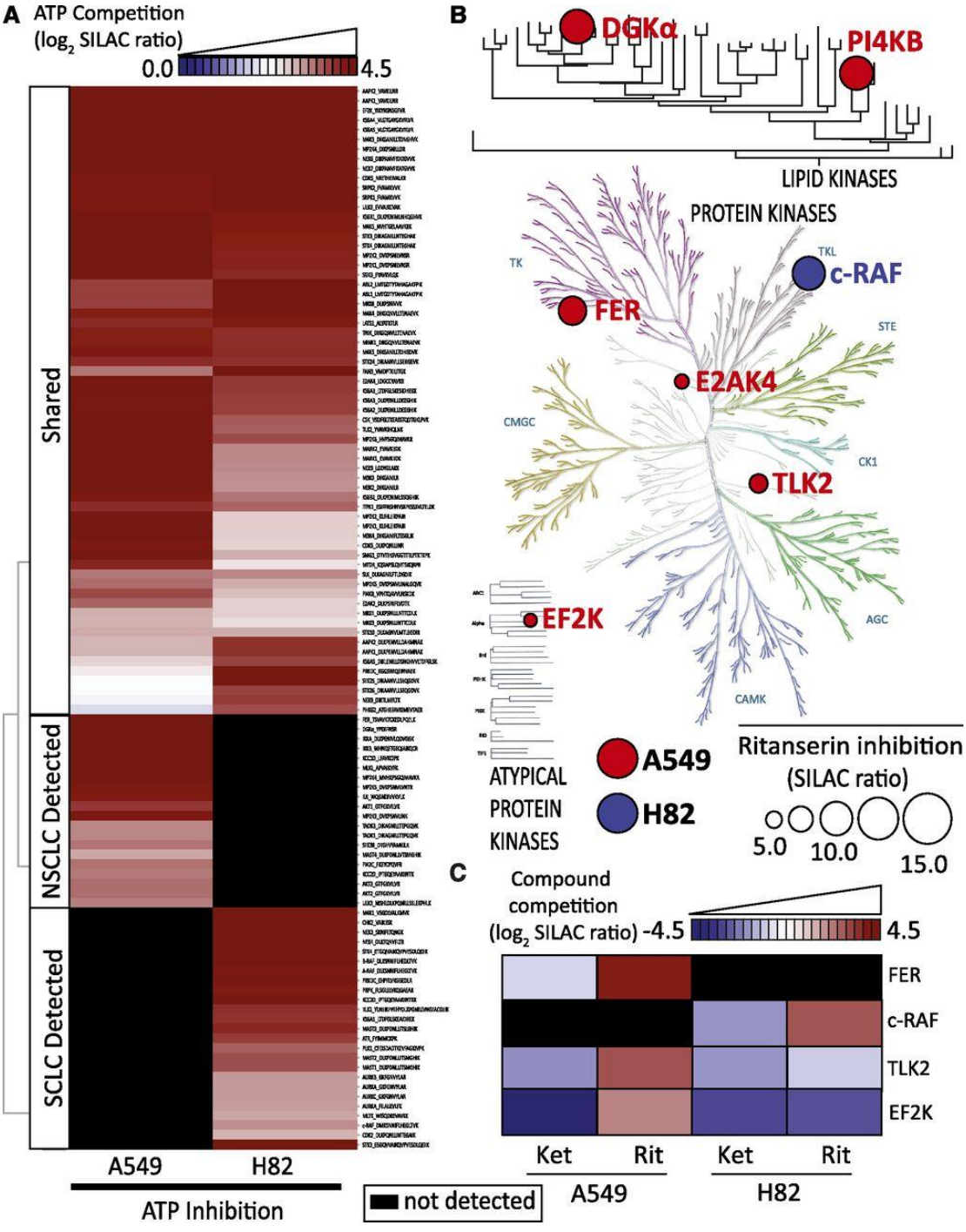

Figure 2.6. Target landscape of ritanserin in lung cancer kinomes. (A) Heatmap showing average log2 SILAC ratios of ATP competition at kinase active-sites detected in A549 and H82 cell proteomes. (B) Kinome tree showing proteins with SILAC ratios > 4 when treated

with ritanserin. The size of the circle is proportional to SILAC ratio measured. Background image for protein kinase tree used by permission of Cell Signaling Technology (http://www.cellsignal.com). The lipid kinase tree was generated in-house using least-squared distances of MUSCLE aligned sequences. (C) Heatmap showing log2 SILAC ratios for kinases inactivated by ritanserin but not ketanserin that have a minimum DMSO:ritanserin SILAC ratio > 4. All experiments were measured 2-3 times (technical replicates in LC- MS) using data from 2-3 independent biological replicates performed on separate days (n = 6-9). All values shown are normalized to DMSO control. Data acquired and analysis by Franks and Borne; figure created by Borne.

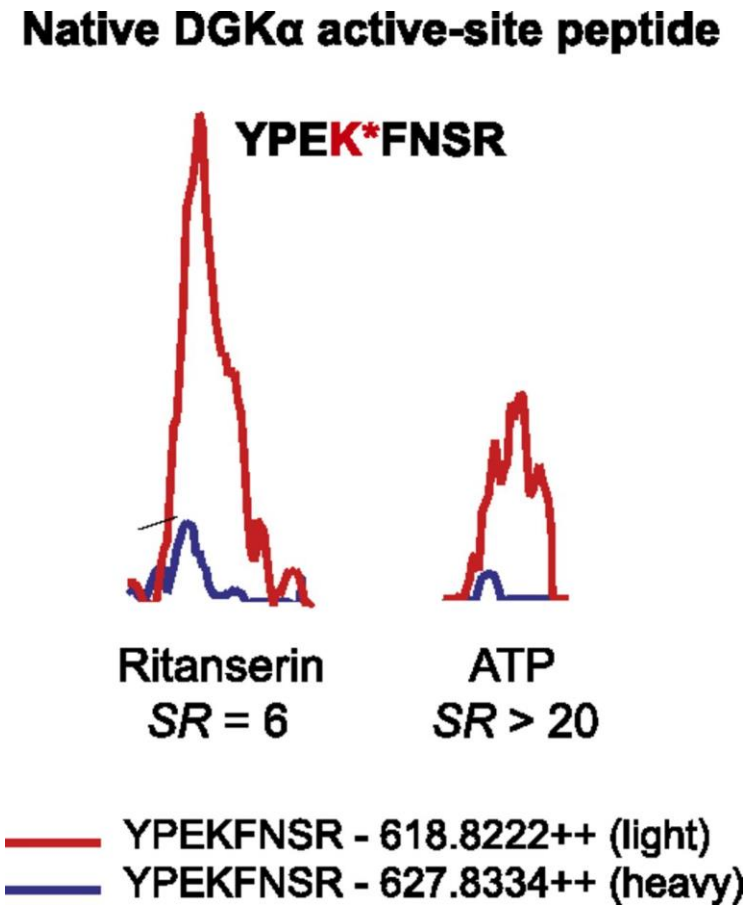

Figure 2.7. Detection and inhibition of native DGKα in A549 proteomes. MS1-extracted ion chromatograms of the probe labeled active-site peptide of DGKα. Pre-treatment of heavy A549 proteomes with ritanserin (100 μM) or ATP (1 mM) resulted in inhibition of DGKα active-site peptide probe labeling (ritanserin SR = 6; ATP SR > 20). All experiments were measured 3 times (technical replicates in LC-MS) using data from 3 independent biological replicates performed on separate days (n = 9). Peak images are a representative image from an individual injection. Data acquired by Franks.

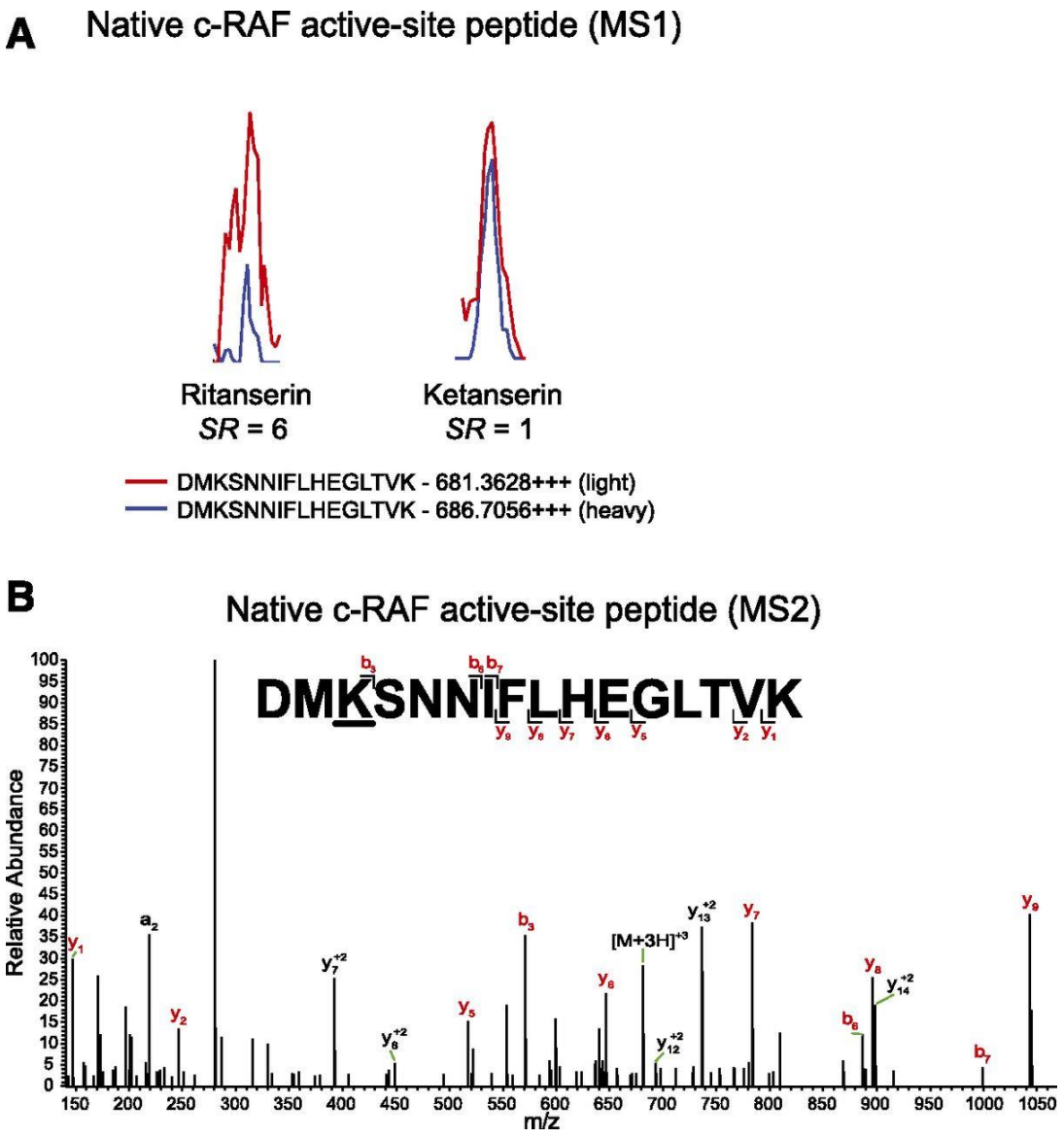

Figure 2.8. Native c-RAF active-site peptide detected in H82 proteomes. (A) MS1-extracted ion chromatograms of the probe labeled active-site peptide for c-RAF identified in H82 proteomes. Pre- treatment of heavy H82 proteomes with ritanserin (100 µM) results in blockade of c-RAF active-site probe labeling (SR > 6). Pre-treatment with ketanserin (100 µM) results in no inhibition (SR = 1). (B) MS2 spectra of probe-modified peptide corresponding to the active-site of c-RAF. Major b- and y-ion fragments derived from

neutral losses of the precursor (M) are shown in red in the spectrum. All experiments were measured 2-3 times (technical replicates in LC-MS) using data from 2 independent biological replicates performed on separate days (n = 6). A and B are representative images from a single measurement. Work conducted by Franks.

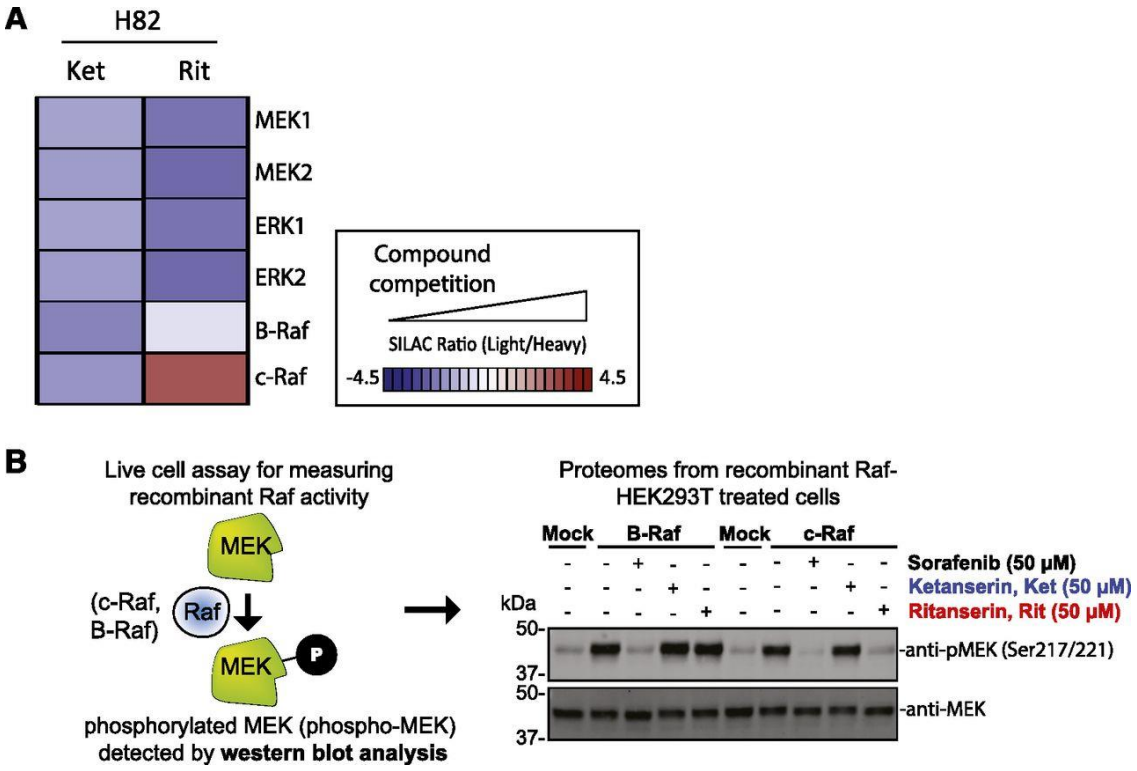

Figure 2.9. Activity of ritanserin against kinases involved in MAPK signaling. (A) Activity of ritanserin against native kinases involved in MAPK signaling as evaluated by quantitative chemoproteomics described in Fig. 4 and 5. The results show that in H82 SCLC proteomes, ritanserin shows selective blockade of c-RAF when compared with other MAPK kinases detected. Ketanserin show negligible activity, which supports serotonin-independent and ritanserin-specific effects. (B) Live cell activity assay to validate c-RAF

as a target of ritanserin. RAF kinases (c-RAF and B-RAF) phosphorylate MEK and phosphorylated MEK (phospho-MEK (S217/S221), ~40 kDa) can be used to measure RAF activity in live cells by western blot (anti-phospho-MEK antibody). Recombinant c-RAF and B-RAF were overexpressed in HEK293T cells, recombinant RAF-HEK293T cells pretreated with DMSO vehicle or inhibitors (50 μM), followed by activation of cells with PMA (20 ng/mL, 20 min). Cells were lysed and proteomes subjected to western blots to measure endogenous phospho-MEK. Overexpression of c- RAF and B-RAF resulted in enhanced phospho-MEK levels. Pretreatment with the pan- RAF inhibitor sorafenib blocked c-RAF- and B- RAF-mediated enhancement of phospho-MEK. In contrast, ritanserin showed inhibition of c-RAF but not B-RAF in overexpressing cells. Ketanserin was largely inactive in this assay. Blots shown are representative of 2 independent biological replicates (n = 2). Protein loading was comparable between sample conditions as evidenced by equivalent MEK levels measured (anti-MEK blot). Work conducted by Borne.

Table 2.1. Tumor cell line mutations.

Cell line	Subtype	Mutation
A549	NSCLC	KRAS (G12S)
H1650	NSCLC	EGFR (E746_A750del)

H82	SCLC	RB1

Chapter 3. Global targeting of functional tyrosines using sulfur triazole exchange chemistry

Adapted from: Heung Sik Hahm‡, Emmanuel K. Toroitich‡, Adam L. Borne‡, Jeffrey W. Brulet‡, Adam H. Libby, Kun Yuan, Timothy B. Ware, Rebecca L. McCloud, AnthonyM. Ciancone, and Ku-Lung Hsu. Nature Chemical Biology 16 150-159 (2020).
‡ These authors contributed equally.

3.1 Abstract

Covalent probes serve as valuable tools for global investigation of protein function and ligand binding capacity. Despite efforts to expand coverage of residues available for chemical proteomics (e.g. cysteine and lysine), a large fraction of the proteome remains inaccessible with current activity-based probes. Here, we introduce sulfur-triazole exchange (SuTEx) chemistry as a tunable platform for developing covalent probes with broad applications for chemical proteomics. We show modifications to the triazole leaving group can furnish sulfonyl probes with ~5-fold enhanced chemoselectivity for tyrosines over other nucleophilic amino acids to investigate, for the first time, more than 10,000 tyrosine sites in lysates and live cells. We discover tyrosines with enhanced nucleophilicity are enriched in enzymatic, protein-protein interaction, and nucleotide recognition domains. We apply SuTEx as a chemical phosphoproteomics strategy to monitor activation of phosphotyrosine sites. Collectively, we describe SuTEx as a biocompatible chemistry for chemical biology investigations of the human proteome.

3.2 Introduction

Chemical proteomics is a powerful technology for ascribing function to the vast number of uncharacterized proteins in the human proteome[19,131]. This proteomic method employs probes designed with reactive groups that exploit accessibility and reactivity of binding sites to covalently label active proteins with reporter tags for function assignment and inhibitor development[132]. Selective probes resulting from competitive screening efforts serve as enabling, and often first-in-class, tools for uncovering biochemical and cellular functions of proteins (e.g. serine hydrolases[53], proteases[133], kinases[24], phosphatases[134], and glycosidases[135]) and their roles in contributing to human physiology and disease. The basic and translational opportunities afforded by chemical proteomics has prompted exploration of new biocompatible chemistries for broader exploration of the proteome.

Covalent probes used for chemical proteomics range from highly chemoselective fluorophosphonates for catalytic serines[22] to general thiol alkylating agents and amine-reactive esters of cysteines[136] and lysines[27], respectively. The ability to globally measure protein functional states and selectively perturb proteins of interest has substantially augmented our basic understanding of protein function in cell and animal models[19,132]. Exploration of new redox-based oxaziridine chemistry, for example, identified a conserved hyper-reactive methionine residue (M169) in redox regulation of mammalian enolase[137]. Hydrazine probes revealed a novel N-terminal glyoxylyl post-translational modification on the poorly characterized protein SCRN3[138]. More recent exploration of photoaffinity probes facilitate global evaluation of reversible small molecule-protein interactions to expand the scope of proteins available for chemical proteomic profiling[139].

Sulfonyl-fluorides[140] (-SO2F) and fluorosulfates[141,142] (-OSO2F) have emerged as a promising scaffold for covalent probe development because of the wide range of amino acids (e.g. serine[143,144], tyrosine[145], lysine[85], histidine[146]) and diverse protein targets (proteases[143,144], kinases[85], GPCRs[147]) available for sulfur-fluoride exchange chemistry (SuFEx80). Reactivity of SuFEx is driven largely through stabilization of the fluorine leaving group (LG) at protein sites during covalent reaction[148]. The sensitivity of SuFEx to protein microenvironments allows, for example, the ability to target orthogonal nucleophilic residues in the same nucleotide-binding site of decapping enzymes[149]. The broad reactivity and context-dependent activation of SuFEx present opportunities for modulating the sulfur electrophile to target novel, and potentially functional, sites of proteins[82,85,148,150]. The reliance on fluorine, while key for activating SuFEx chemistry, is limiting in terms of LG modifications to modify reactivity, specificity, and binding affinity at protein sites across the proteome.

Here, we introduce sulfur-triazole exchange chemistry (dubbed SuTEx) for development of phenol-reactive probes that can be tuned for tyrosine chemoselectivity in proteomes (>10,000 distinct sites in ~3,700 proteins) through modifications to the triazole LG. We use these probes to discover a subset of tyrosines with enhanced reactivity that are localized to functional protein domains and to apply SuTEx for global phosphotyrosine profiling of pervanadate-activated cells. Our findings illustrate the broad potential for deploying SuTEx to globally investigate tyrosine reactivity, function, and post-translational modification state in proteomes and live cells.

3.3 Materials and Methods

HPLC assay for profiling solution reactivity and stability of sulfonyl probes. The following reagents were prepared and kept at 0 °C prior to use: 0.1 M solution of caffeine in acetonitrile (ACN), 1.0 M solution of n-butylamine, p-cresol, tetramethylguanidine (TMG), acetic acid in ACN, and 10 mM solution of the probes in a mixture of DMF-ACN (v/v=10:90) are made.

(i) p-Cresol reactivity against a probe mixture: A solution of p-cresol (16.5 µmol, 3.3 eq) was premixed with 1.1, 2.2, or 3.3 eq of TMG. To initiate the reaction, the p- cresol/TMG solution was added to a sulfonyl probe mixture of HHS-475/HHS-482/HHS- SF-1 (500 µL, 5 µmol, 1.0 eq each) and the reaction was kept at 0 °C. The reaction progress was monitored by taking out a 50.0 µL aliquot of the reaction mixture at various time points followed by addition of a 10 µL quenching solution of acetic acid (0.5 M final, 5.0 µmol) and the internal caffeine standard (0.05 M final, 0.5 µmol). Sample (1.0 µL) was injected and analyzed by reverse-phase HPLC on a Shimadzu 1100 Series spectrometer with UV detection at 254 nm. Reaction progress was evaluated by monitoring consumption of sulfonyl probes because all probes generate a shared p-cresol and n-butylamine product. Chromatographic separation was performed using a Phenomenex Kinetex C18 column (2.6 µm, 50 mm x 4.6 mm). Mobile phases A and B were composed of H2O (with 0.1% AcOH) and CH3CN (with 0.1% AcOH), respectively. Using a constant flow rate of 0.8 mL/min, the gradient was as follows: 0-0.5 min, 15% B; 0.5-6.5 min 15-85% B (linear gradient); 6.5-7 min 85-100% B (linear gradient); 7- 8.5 min 100% B; 8.5-9 min 100-15% B (linear gradient); 9-9.8 min 15% B.

(ii) n-Butylamine reactivity against a probe mixture: Reactivity of sulfonyl probes against n-butylamine (3.3 eq) was performed as described above except the amount of TMG was fixed at 3.3 eq.

(iii) Probe reactivity against a p-cresol/n-butylamine mixture: A solution of n- Butylamine (50.0 µL, 50.0 µmol, 5.0 eq), p-cresol (10.0 µL, 10.0 µmol, 1.0 eq), and TMG (5.0 µL, 5 µmol, 0.5 eq) were prepared. Probe reaction was initiated by addition of this solution to HHS-475, HHS-482, or HHS-SF-1 (10 µmol, 1.0 eq) at 0 °C. Reaction progress was monitored as described above. A control experiment was also performed where equal amounts of n-butylamine (1.0 eq) and p-cresol (1.0 eq) were mixed.

(iv) Probe stability studies: Each probe was dissolved in DMSO or a solution of DMF:ACN:PBS (4:6:1 (v/v)) at the following concentrations: 20 mM of HHS-475, 20 mM HHS-SF-1, and 10 mM of HHS-482 in a final volume of 50 µL. The internal caffeine standard (0.5 µmol) was spiked into each probe sample. Probe stability was monitored at room temperature by taking 1.0 µL of sample at three time points (0, 24, and 48 hours) and analyzing probe degradation by HPLC as described above.

Cell culture. Cell lines were cultured at 37 ˚C with 5% CO2 with manufacturer recommended media supplemented with 10% fetal bovine serum (FBS, U.S. Source, Omega Scientific) and 1% L-glutamine (Fisher Scientific): HEK293T: DMEM; DM93, A549, Jurkat, H82: RPMI. Cells were harvested for experimental use when they reached ~90% confluency. The media was aspirated, cells washed with cold PBS (2X) and scraped from plates. The cells were pelleted by centrifugation at 400 × g for 5 min, snap-frozen

using liquid nitrogen and stored at -80 ˚C until further use.

SILAC cell culture. SILAC HEK293T cells were cultured at 37 ˚C with 5% CO2 in either 'light' or 'heavy' media consisting of DMEM (Fisher Scientific) supplemented with 10% dialyzed FBS (Omega Scientific), 1% L-glutamine (Fisher Scientific), penicillin/streptomycin, and isotopically-labeled amino acids. Light media was supplemented with 100 μg/mL L- arginine and 100 μg/mL L-lysine. Heavy media was supplemented with 100 μg/mL [13C 15N] L-arginine and 100 μg/mL [13C 15N] L-lysine. The cells were grown for 6 passages before use in proteomics experiments. Cells were washed with PBS (2X), harvested, snap-frozen using liquid nitrogen and stored at -80 ˚C until further use.

Transient Transfection. Recombinant protein production by transient transfection of HEK293T cells was performed as previously described125. The following plasmid constructs (human proteins) were purchased from GenScript: pcDNA3.1-GSTP1-FLAG, pcDNA3.1-DPP3-FLAG, pcDNA3.1-PGAM1-FLAG, pcDNA3.1-EDC3-FLAG. Site-directed mutagenesis of wild- type constructs was used to generate mutant plasmids: pcDNA3.1-GSTP1 (Y8F)-FLAG, pcDNA3.1-DPP3 (Y417F)-FLAG, pcDNA3.1-PGAM1 (Y92F)-FLAG, pcDNA3.1-EDC3 (Y475F)-FLAG.

Pervanadate Activation. Pervanadate (100 mM) was prepared as previously described116 by mixing 100 μL of sodium orthovanadate (100 mM Na3VO4, New England BioLabs

#P0758S) with 1 µL of hydrogen peroxide (H2O2, 30% v/v in water) on ice. The mixture was incubated on ice for 15 min followed by immediate addition to cells (1:1000, 100 µM final) and incubation for 30 min at 37 ˚C with 5% CO2 for general inhibition of protein tyrosine phosphatases. After pervanadate treatment, cells were washed twice with cold PBS followed by harvest. Cell pellets were resuspended in PBS supplemented with protease and phosphatase inhibitor mini tablets (Thermo Scientific #A32959) and then lysed by sonication (3 x 1 sec pulse, 20% amplitude). For CTNND1 western blot studies, cell pellets were lysed in NP40 Cell Lysis Buffer (Invitrogen #FNN0021) supplemented with protease/phosphatase inhibitor tablets. Cell lysates were separated via centrifugation at 100,000 x g for 45 min at 4 ˚C for western blot or chemical proteomic studies. Note: pervanadate treatments are performed on live cells but SuTEx probe labeling occurs in proteomes in vitro.

Western blot analysis. Western blot analysis of recombinant protein expression was performed as previously described125. For analysis of tyrosine phosphorylation, the protocol used was the same except the nitrocellulose blot was blocked with 3% BSA instead of 5% milk in TBS-T. The following antibodies were purchased from Cell Signaling Technology (CST) for phosphotyrosine studies: Phospho-tyrosine (pY): P-Tyr-100 biotinylated, CST #9417S; pPKM: Phospho-PKM (Y105) Rabbit Ab, CST #3827S; PKM: PKM Rabbit Ab, CST #3198S; pSTAT3: Phospho-STAT3 (Y705) Rabbit mAb, CST #9145S; STAT3: STAT3 Mouse mAb, CST #9139S; pCTNND1: Phospho-Catenin δ-1 (Tyr228) Rabbit Ab, CST #2911; CTNND1: Catenin δ-1 Rabbit Ab, CST #4989;

GAPDH: GAPDH Rabbit mAb, CST #2118S. The following secondary antibodies were used for fluorescence detection: Goat Anti-Rabbit IgG DyLight 550 Conjugated, Thermo Scientific, #84541; Goat Anti- Mouse IgG DyLight 650 Conjugated, Invitrogen, #84545; Streptavidin DyLight 550 Conjugated, Thermo Scientific, #84542.

Gel-based chemical proteomic assay. Cell pellets were lysed in PBS by sonication and fractionated (100,000 × g, 45 min, 4 ˚C) to generate soluble and membrane fractions. Protein concentrations were determined using the Bio-Rad DC protein assay and adjusted to 1 mg/mL in PBS. Proteome samples (49 µL aliquots) were treated with sulfonyl-triazole or -fluoride probes at the indicated concentrations (1 µL, 50x stock in DMSO) for 1 hr at room temperature. Probe-labeled samples were conjugated by copper-catalyzed azide-alkyne cycloaddition (CuAAC) to rhodamine-azide (1 µL of 1.25 mM stock; final concentration of 25 µM) using tris(2- carboxyethyl)phosphine (TCEP; 1 µL of fresh 50 mM stock in water; final concentration of 1 mM), tris[(1-benzyl-1H-1,2,3-triazol-4-yl)methyl]amine (TBTA, 3 µL of a 1.7 mM 4:1 t-butanol/DMSO stock, final concentration of 100 µM), and copper sulfate (CuSO4, 1 µL of 50 mM stock, final concentration of 1 mM). Samples were reacted for 1 hr at room temperature, quenched with 17 µL of 4X SDS-PAGE loading buffer and beta-mercaptoethanol (βME), and quenched samples (30 µL) analyzed by SDS-PAGE gel and in-gel fluorescence scanning.

Live cell evaluation of sulfonyl-triazole probes. Cells grown to ~90% confluency in 10 cm plates were treated with DMSO vehicle or sulfonyl-triazole probe (10 µL of 1000X

DMSO stock) in serum-free media for the indicated concentrations and times at 37 ˚C with 5% CO2. After treatment, cells were washed with cold PBS twice before harvesting and preparation for gel-based chemical proteomic evaluation as described above. For LC-MS studies, protein concentrations were normalized to 2.3 mg/mL and 432 µL (for 1 mg final protein amount) were used for sample preparation as detailed below.

Preparation of proteomes for LC-MS/MS analysis. Proteomes were diluted to 2.3 mg/ mL in PBS and sample aliquots (432 µL) were treated with sulfonyl-triazole or -fluoride probes at the indicated concentrations (5 µL, 100X stock in DMSO), mixed gently and incubated for 1 h at room temperature. Probe-modified proteomes were subjected to CuAAC conjugation to desthiobiotin-PEG3-azide (10 µL of 10 mM stock in DMSO; final concentration of 200 µM) using TCEP (10 µL of fresh 50 mM stock in water; 1 mM final concentration), TBTA ligand (33 µL of a 1.7 mM 4:1 t-butanol/DMSO stock, 100 µM final concentration), and CuSO4 (10 µL of 50 mM stock, 1 mM final concentration). Samples were mixed by vortexing and then incubated for 1 h at room temperature. Excess reagents were removed by chloroform-methanol extraction as previously described[36]. Protein pellets were re-suspended in 500 µL of 6M urea/25 mM ammonium bicarbonate followed by DTT reduction and IAA alkylation as previously described[36]. Excess reagents were removed by chloroform/methanol extraction as described above, and the protein pellet was re-suspended in 500 µL of 25 mM ammonium bicarbonate and then digested to peptides using trypsin/Lys-C (7.5 µg in 15 µL of ammonium bicarbonate, sequencing grade from Promega) was added to the mixture and incubated for 3 hrs at 37 ˚C. Probe-modified

peptides were enriched by avidin affinity chromatography, eluted, and prepared for LC-MS analysis as previously described[36].

Preparation of SILAC proteomes for LC-MS/MS analysis. Heavy and light proteomes (432 µL of each) were diluted to 2.3 mg/mL in PBS. For 10:1 comparisons, heavy and light proteomes were treated with 250 µM and 25 µM of HHS465, respectively (5 µL, 100x stock in DMSO). In a control 1:1 comparison experiment both heavy and light proteome were treated with 25 µM of HHS465. Samples were mixed gently and incubated for 1 h at room temperature. Light and heavy samples were separately conjugated to desthiobiotin-PEG3-azide as described above. Light and heavy samples were mixed during the chloroform-methanol extraction step. Probe-modified peptides were prepared for LC-MS/MS analysis as described above.

LC-MS/MS analysis of samples. Nano-electrospray ionization-liquid chromatography-mass spectrometry analyses (LC- MS/MS) were performed using an Ultimate 3000 RSLC nanoSystem-Orbitrap Q Exactive Plus mass spectrometer (Thermo Scientific) as previously described125 except LC conditions were modified to use the following gradient (A: 0.1% formic acid/H2O; B: 80% ACN, 0.1% formic acid in H2O): 0-1:48 min 1% B, 400 nL/min; 1:48 – 2:00 min 1% B, 300 nL/min; 2-90 min 16% B; 90-146 25% B; 146-147 min 95% B; 147-153 min 95% B; 153-154 min 1% B; 154.0-154.1 min 1% B, 400 nL/min; 154.1-180 min 1% B, 400 nL/min. A top 10 data-dependent acquisition MS method was used.

LC-MS/MS data analysis. Identification of peptides and proteins from tandem mass spectrometry analyses was accomplished using the ByonicTM software package (Protein Metrics Inc.[17]). Data were searched against a modified human protein database (UniProt human protein database, angiotensin I and vasoactive intestinal peptide standards; 40,660 proteins) with the following parameters: up to 3 missed cleavages to account for a lysine probe modification, 10 ppm precursor mass tolerance, 20 ppm fragment mass tolerance, too high (narrow) "precursor isotope off by x", precursor and charge assignment computed from MS1, maximum of 1 precursor per MS2, 0.01 smoothing width, 1% protein false discovery rate, variable (common) methionine oxidation (+15.9949 Da) and fixed cysteine carbamidomethylation (+57.021464 Da). Sulfonyl-probe modifications of tyrosine, lysine, and other amino acids were included as a variable (common) modification of +635.27374 Da. Search results were imported into R and filtered for fully tryptic peptides (except N- and C-terminally modified), a Byonic score of >300 (unless otherwise specified), and a precursor mass error between -5 ppm and +5 ppm. A Byonic score of 300 was applied for a more inclusive initial evaluation of the search results and thereby consider more possible probe-modified sites. We manually verified the MS1 and MS2 spectra corresponding to the highest-scoring tyrosine- and lysine (internal or non-C terminal)-modified sequences (~50-100 peptides). The next most frequently matched and high-scored probe-modified amino acid residues were C-terminal lysines or arginines, which were determined to be false positive matches based on manual analysis of MS2 spectra (top ~50 highest Byonic scored-matches). These findings are consistent with the observation from previous studies

with other probes[27,36] that trypsin does not cleave after a modified lysine or arginine. Distinct peptides containing probe-modified amino acid residues (termed sites) were determined by identifying all unique razor protein and site combinations across all of the proteomes tested.

Analysis and comparison of sulfonyl probe modified amino acid sites. To compare amino acid residues modified by sulfonyl probes, protein and peptide identifications were accomplished as described above with variable (common) modification of +635.27374 Da on the following amino acid residues: cysteine, aspartic acid, glutamic acid, histidine, lysine, methionine, asparagine, glutamine, arginine, serine, threonine, tryptophan, and tyrosine. For these amino acid comparisons, carbamidomethylation (+57.021464 Da) of cysteines was searched as a variable/common modification to allow for the potential of probe modification on cysteines. Comparisons of probe-modified sites across all probes and cell lines tested were performed using the R package ggplot2 (https://ggplot2.tidyverse.org/). Venn diagrams for comparisons were generated using the VennDiagram R package[151]. For amino acid comparisons, a Byonic score cutoff of 600 was used to minimize false positive identifications of modified residues, which were confirmed by manual evaluation to be incorrect assignments.

Domain enrichment analysis. Probe-modified sites were compared to ProRule domain annotations (available on PROSITE, release 20.85127, http://prosite.expasy.org/) using the annotated human UniProt proteome (https://www.uniprot.org/) as a database for

identifying amino acid sequences that match ProRule domains. A probe-modified site that is within a ProRule domain is considered a “hit” and is counted as enrichment of a domain by the sulfonyl probe. Several sites within the same ProRule domain annotation are a considered a single hit. If a site had several annotations each one was considered a hit; for example, a modified site within the proton acceptor region of a kinase domain would be annotated as a hit for ProRules PRU10027 and PRU00159, respectively. The database count is determined by the number of non-overlapping occurrences of the domain such that calmodulin would account for 4 EF-hand domains (PRU00448). We find the probability of the domains P(D) in the reference UniProt human database to determine how frequently they exist in nature:

$$P(D) = n(D)/N$$

Where n(D) is the number of domain occurrences in the database and N is the total number of domains in the reference database. The p-values were calculated using a binomial test previously reported for GO statistical overrepresentation test 128.

$$P = \sum \binom{K}{k} P(D)^k (1 - P(D))^{K-k}$$

Binomial Test

Where K is number of domain annotation hits in the experimental data (sulfonyl probe). The p-value was then corrected for a 1% false discovery rate (FDR) using Benjamini- Hochberg correction for multiple hypothesis testing. From these statistical analyses, ProRule domains that show statistically significant overrepresentation (Q value < 0.01) are used to generate bar graphs and pie charts shown in figures. Note that a -log (Q

value) is used so that positive values are shown for simplicity. In order to verify that the binomial approximation to hypergeometric probability we ensured sum of all n(D) was less than 5 percent of N and verified that using a hypergeometric test did not alter the enriched domains. The enriched domains were grouped according to their function into four categories; nucleotide binding, enzyme, protein-protein interaction and undefined based on gene ontology molecular function annotation of the respective ProRule domain. Pie charts and bar graphs were generated using the ggplot2 package in R.

Classification of protein domains. The distinction between protein-protein interaction (PPI) and nucleotide binding domains was determined by whether the interacting partner of the domain is annotated as a peptide or a nucleotide sequence. The SH2 domain (PRU00191) which interacts with proteins featuring phosphorylated tyrosines is classified as a PPI domain, and a Homeobox DNA- binding domain (PRU00108) is classified as a nucleotide binding domain. An enzyme domain is the protein subunit that has been shown to catalyze the conversion of a substrate to a product. The Ribonuclease H domain (PRU00408) functions as an endonuclease which will interact with RNA but is classified as an enzyme domain because of its nuclease activity. We applied gene ontology (GO) molecular function annotations associated with the ProRule domains that inherit the annotation for catalytic activity (GO:0003824) to determine if proteins belong to the enzyme domain group. For example, the term Ribonuclease H domain (PRU00408) has the GO annotation for endonuclease activity (GO:0004519) which has catalytic activity (GO:0003824) in its ancestor chart and is therefore classified as an enzyme.

DrugBank analysis. Proteins labeled by sulfonyl probes in live cells were compared against protein targets of FDA approved and all drugs in the DrugBank databases[152] (version 5.1.1).

Phosphosite Plus analysis. Probe-labeled sites were searched for in the PhosphoSitePlus database[153] either unfiltered or filtered by a high-throughput reference score of 10 or greater where specified.

Nucleophilicity data analysis (SILAC). Peptide and protein identification was accomplished using Byonic as previously described above. SILAC samples were searched with added masses for heavy-labeled amino acids (+10.0083 Da for R, +8.0142 Da for K) and converted into mzXML (from raw data file) and mzid (exported from Byonic) format for export into Skyline-daily[154] to determine SILAC ratios (SR) of light/heavy peptides as previously described[36]. SILAC ratios from peptides with the same probe-modified site were averaged. The SILAC ratios were then plotted using the ggplot2 package in R. Nucleophilicity was defined as follows: hyper- reactive, SR <2; mild reactivity, 2 < SR <5; low reactivity, SR >5.

GSTP1 biochemical substrate assay. Recombinant GSTP1-HEK293T soluble cell proteomes were diluted to 1 mg/ml in assay buffer (100 mM NaH2PO4, pH 7.0). GSH stock solution (250 mM in water) was diluted to 4 mM in assay buffer and 25 µL of diluted

GSH solution was added to each sample. A substrate stock solution of 75 mM 1-bromo-2,4-dinitrobenzene (DBNB) in ethanol was diluted to 2 mM in assay buffer. Samples (25 µL) were aliquoted into a 96 well plate and spun briefly via centrifuge. 50 µl of 2 mM BDNB was added to each well and the reaction was monitored in kinetic mode by measuring absorbance at 340 nm for 10 min on a BMG Labtech CLARIOstar plate reader.

DPP3 biochemical substrate assay. Substrate assays were performed on recombinant DPP3-HEK293T soluble proteomes diluted to 1 mg/mL in assay. DPP3 sample (10 µL) was diluted to 85 µL with assay buffer and transferred to a black 96-well plate. A stock solution of DPP3 substrate (Arg-Arg β- naphthylamide trihydrochloride, 0.5 mM; Sigma-Aldrich) was diluted to 100 µM in assay buffer. Substrate solution (5 µL) was added to each sample. Samples were mixed briefly by shaking and reaction monitored in kinetic mode by measuring fluorescence at 450 nm for 10 min on a BMG Labtech CLARIOstar plate reader.

3.4 Results

3.4.1 Design and synthesis of sulfonyl-triazole probes

We reasoned that triazoles could serve as a suitable replacement for the fluorine LG used to promote SuFEx80. Previous studies demonstrated that triazoles activate ureas for covalent protein modification with a significant advantage of tunability[155], which is not possible with fluorine as a LG by comparison. We envisioned that a sulfonyl-triazole scaffold would permit evaluation, and potentially control, of reactivity and specificity of the sulfur electrophile through structural modifications to the triazole LG (Fig. 3.1.a). Our

hybrid probe strategy is further bolstered by the broad functional group tolerance of 1,2,3- and 1,2,4-triazoles as a LG for development of covalent serine hydrolase inhibitors[155,156].

3.4.2 Chemical proteomic evaluation of SuTEx chemistry

We established a chemical proteomic method to assess the reactivity of HHS-465 with amino acid residues in proteomes. HEK293T cell proteomes were treated with HHS-465 (100 µM, 1 hr, 25 °C) followed by copper-catalyzed azide-alkyne cycloaddition (CuAAC) coupling with a desthiobiotin-azide tag. Proteomes were digested with trypsin protease and desthiobiotin-modified peptides enriched by avidin affinity chromatography, released, and analyzed by high-resolution liquid chromatography-mass spectrometry (LC-MS, Fig. 3.1.c). Probe-modified peptide-spectrum matches (PSMs) that met our quality control confidence criteria of >300 Byonic score 106 and < 5 ppm mass accuracy were selected for further manual evaluation (see Methods for additional details).

We predicted, based on our proposed reaction mechanism, that amino acid residues modified by HHS-465 would be identified by differential modification with a sulfonyl-desthiobiotin adduct that is the product of SuTEx reaction (Fig. 3.1.c). We synthesized and included a 1,2,4-triazole counterpart, HHS-475, for testing to demonstrate SuTEx as a common mechanism among triazole regioisomers (Fig. 3.1.b and Fig. 3.3). Initial evaluation of our data assigned >60% of HHS-465- and HHS-475- labeled peptides as uniquely modified tyrosines (Fig. 3.4). Evaluation of MS2 spectra showed confident identification of all major y-ions and a large fraction of b-ions, including fragment ions (y and b) that allowed identification of the tyrosine site of HHS- 465 and HHS-475 binding

(mass adduct of 635.2737 Da, Fig. 3.1.d and Fig. 3.5-3.7). The remaining probe-modified peptides were assigned largely to lysines, which after removal of incorrect search algorithm matches to C-terminal modified peptides represented a minor fraction of total modified residues (<25%; Fig. 3.4, 3.8, and 3.9). We evaluated additional human cell proteomes to determine the number and type of tyrosines amenable to SuTEx reaction. On average, we reliably identified >2,800 tyrosines per data set and in aggregate, ~8,000 tyrosine sites from ~3,000 proteins with diverse enzymatic and non- catalytic functions across 5 cell proteomes evaluated with HHS-465- and -475 (Fig. 3.10.a and b). A large fraction of HHS-465/475-modified sites were also annotated as phosphorylation sites as reported in the PhosphoSitePlus database[153] (Fig. 3.10.c).

We next tested whether SuTEx probes exhibit sufficient stability and cell permeability to permit global tyrosine profiling in living systems. We observed robust proteome labeling that was concentration- and time-dependent in fluorescence gel-based analyses of proteomes from HEK293T cells treated with HHS-465 or HHS-475 (Fig. 3.11 and 3.12). Using a saturating probe labeling condition (100 µM, 2 hr, 37 °C) for our live cell studies, we consistently measured ~3,500 distinct tyrosine sites (corresponding to ~1,700 proteins), in total, across membrane and soluble fractions in each cell line tested (HEK293T, Jurkat). For comparison, recent reports using sulfonyl-fluorides showed probe modifications of ~70-130 protein targets in live cell studies[85,148]. HHS-465- and HHS-475-labeled proteins from live cell profiling were largely absent from the DrugBank database[152] (77%, Fig. 3.10.d). Evaluation of probe-enriched domains (Q-values < 0.01) from the non-DrugBank protein (non-DBP) group revealed highly enriched functions that include

proteins involved in RNA recognition (RRM domain[157]) and protein-protein interactions (PCI/PINT and SH3 domains[158], Fig. 3.10.d). By comparison, the DrugBank protein group (DBP) was largely overrepresented with domains found in enzymes (kinases and redox enzymes, Fig. 3.10.d).

3.4.3 Discovery of hyper-reactive tyrosines in human proteomes

Previous studies identified a subset of hyper-reactive cysteine and lysine residues that specify function and are susceptible to binding with electrophilic ligands30, 36. Whether tyrosines differ in intrinsic reactivity and the functional implications of heightened nucleophilicity remain largely underexplored on a proteome-wide scale. Here, we used HHS-465 and quantitative chemical proteomics to evaluate tyrosine reactivity directly in human cell proteomes derived from isotopically light and heavy amino acid-labeled HEK293T cells (i.e. stable isotope labeling with amino acids in cell culture; SILAC[112]). We measured concentration-dependent HHS-465 labeling where nucleophilic tyrosines are expected to exhibit comparable labeling intensity at low and high concentrations of HHS-465 while less nucleophilic tyrosines show concentration-dependent increases in probe labeling. We treated HEK293T proteomes with high versus low concentrations of HHS-465 (250 versus 25 µM; 10:1 comparison) for 1 hr (25 °C) and then analyzed samples by quantitative LC-MS (Fig. 3.13). Tyrosine nucleophilicity was segregated into low, medium, and high groups based on their respective SILAC ratios (SR >5, 2 < SR <5, SR < 2, respectively; Fig. 3.14.a). We also verified in a control experiment (25 vs 25 µM) that SR values were ~1 in a 1:1 comparison (Fig. 3.15).

3.4.4 Tuning the triazole LG for tyrosine chemoselectivity

A key advantage of SuTEx technology is the capacity for modifying the triazole LG to tune chemoselectivity of resulting probes. Here, we tested whether we could enhance the selectivity of HHS-465/475 for tyrosine modification through addition of functional groups to the triazole (Fig. 3.16.a). To globally evaluate probe reactivity and selectivity in parallel, we compared the total number of probe-modified sites (Y and K combined) as a function of the ratio of modified tyrosines to lysines (Y/K ratio), respectively, for each SuTEx analog. First, we synthesized a sulfonyl-fluoride counterpart to HHS-465/475, termed HHS-SF-1 (Fig. 3.16a), to directly compare fluoro- and triazole-LGs with respect to proteome specificity and reactivity. HHS-SF-1 exhibited a ~4-fold reduction in the total number of modified sites and lower selectivity for tyrosine compared with HHS-465 and HHS-475 (Y/K of 2.3 versus 2.5 and 2.8, respectively; Fig. 3.16.a and Fig. 3.17).

In light of the improved tyrosine selectivity of HHS-475, we synthesized and evaluated a series of 1,2,4-triazole analogs bearing different substituents at the R2 position (Fig. 3.1.a and 3.16.a). Addition of a phenyl group improved both tyrosine selectivity (Y/K = 3.5) and overall proteome reactivity of the resulting HHS-481 probe (~4,000 total sites; Fig. 3.16.a). Modification of the phenyl-triazole resulted in further alterations in proteome activity of SuTEx probes. Addition of a para-fluoro substituent (HHS-483) resulted in comparable reactivity and slightly lowered tyrosine selectivity compared with HHS-481 (Fig. 3.16.a). In contrast, the para-methoxy probe HHS-482 showed the highest tyrosine selectivity (Y/K ratio of ~5) while maintaining good overall proteome reactivity (~3,000

probe-modified sites, HHS-482; Fig. 3.16.a). Evaluation of HHS-482 reactivity against other amino acids revealed high tyrosine selectivity with ~75% of probe-modified residues assigned to tyrosines (Fig. 3.16.b).

Comparison of tyrosine sites modified by HHS-SF-1 and HHS-482 revealed high overlap (>90%) indicating that substitution of fluorine for a triazole LG did not result in loss of tyrosine coverage (Fig. 3.16.c). In contrast, LG modifications to 1,2,4-SuTEx probes furnished analogs that each expanded tyrosine coverage via detection of unique-modified sites (HHS-475, 391 sites; HHS-482, 112 sites; HHS-483, 433 sites; HHS-481, 445 sites; Fig. 3.16.d). In summary, our studies highlight a key difference between sulfonyl-fluoride compared with -triazole chemistry; the latter reaction dramatically enhances overall reactivity and through LG modifications can be tuned for enhanced tyrosine chemoselectivity and coverage in proteomes (Fig. 3.16.b and d).

In total, we quantified ~2,400 tyrosine residues from >1,100 proteins in soluble proteomes from HEK293T cells that showed consistent SILAC ratios across replicate experiments (n = 4, Fig. 3.14.a). The majority of quantified tyrosines showed concentration- dependent increases in HHS-465 labeling, which is indicative of low intrinsic nucleophilicity (Fig. 3.14.a). Similar to cysteines and lysine residues, a subset of tyrosines (~5%, 127 sites in total; Fig. 3.14.a) demonstrated enhanced nucleophilicity (i.e. hyper- reactivity30, 36) as evidenced by SR < 2 for 10:1 conditions (Fig. 3.14.a). The majority of proteins contained a single hyper-reactive tyrosine among several tyrosines quantified (Fig. 3.18). Reactive tyrosines (SR < 5) were enriched in domains of enzymes while tyrosines with lower reactivity (SR > 5) were localized at small molecule binding

sites (Fig. 3.14.b). Comparison of tyrosine reactivity and evidence of phosphorylation revealed a marked inverse correlation. Specifically, tyrosines with low reactivity (SR > 5) were significantly overrepresented for phosphotyrosine sites compared with medium- and hyper-reactive groups (SR < 5, Fig. 3.14.c).

We verified our tyrosine reactivity annotations by comparing SuTEx probe labeling of recombinant wild-type (WT) and tyrosine-to-phenylalanine mutants of human proteins with tyrosine sites identified as high (Y8, GSTP1; Y475, EDC3), low/medium (Y417, DPP3), or low hyper-reactivity (Y92, PGAM1). Proteins like glutathione S- transferase Pi (GSTP1) with a single hyper-reactive tyrosine, among several modified tyrosines, showed robust HHS-475 labeling that was largely abolished in recombinant Y8F mutant (Fig. 2.14d). Mutation of the hyper-reactive tyrosine in the Yjef-N domain of enhancer of mRNA decapping protein 3 (EDC3) also resulted in near-complete loss of probe labeling (Y475F, Fig. 3.14.d). In contrast, mutation of a tyrosine with low nucleophilicity in PGAM1 resulted in negligible alterations in probe labeling (Y92F, Fig. 2.14d). A notable exception was dipeptidyl peptidase 3 (DPP3), which contains a single modified tyrosine (Y417) that, despite a low/medium nucleophilicity ratio (SR ~6), showed near-complete blockade of probe labeling in corresponding tyrosine mutants (Y417F, Fig. 3.14.d).

Finally, we confirmed the catalytic role of GSTP1 tyrosine 8, located in the GSH binding site (G-site), by mutating this residue (Y8F) and demonstrating abolished biochemical activity (Fig. 3.19.a and b, 3.20). In comparison, recombinant DPP3 WT- and Y417F mutant-overexpressed cell lysates showed comparable catalytic activity in a peptidase substrate assay, supporting a non-catalytic role for Y417 (Fig. 3.20.c and d, 3.21).

Future studies will focus on testing whether the moderate reactivity of the non- catalytic Y417 (Fig. 2.14.d) can be exploited for DPP3 inhibitor development.

3.4.5 Triazole LG enhances phenol reactivity of probes

Next, we compared solution reactivity of sulfonyl probes to evaluate whether the enhanced tyrosine reactivity of SuTEx is a function of the LG or protein microenvironment. We established an HPLC assay to test reactivity of SuTEx and SuFEx probes with nucleophiles that model side chain groups of tyrosine (p-cresol) and lysine (n-butylamine). We synthesized the predicted products from p-cresol (KY-2-48) and n- butylamine (KY-2-42) reaction with sulfonyl probes to establish HPLC conditions for monitoring this covalent reaction in solution (Fig. 3.22). We incubated p-cresol with a mixture of all three sulfonyl probes and monitored time-dependent reaction by depletion of respective SuTEx (HHS-475, HHS-482) and SuFEx (HHS-SF-1) probe signal. Our probe competition studies were performed with increasing tetramethylguanidine (TMG112) base to compare probe reactivity as a function of increasing phenol nucleophilicity. We also measured stability and found that all three sulfonyl probes showed negligible hydrolysis in aqueous and organic solvents even after incubation for 48 hours at room temperature (Fig. 3.23).

At lower TMG (1.1 equivalents), HHS-475 (peak 3) was the most reactive probe as evidenced by consumption by 30 minutes while unreacted HHS-SF-1 (peak 4) and HHS-482 (peak 7) was still detectable (Fig. 3.24.a). The difference in reactivity between SuTEx and SuFEx was apparent at higher TMG (2.2 equivalents) conditions. Both SuTEx probes (HHS-475 and HHS-482) were consumed by 10 minutes while HHS-SF-1 was still

detectable even after 90 minutes of reaction (Fig. 3.24.a); depletion of HHS-SF-1 signal was only observed at the highest TMG tested (3.3 equivalents, Fig. 3.24.a and Fig. 2.25). We also verified a similar trend in reactivity when p-cresol was incubated with individual sulfonyl probes. The reactivity of all three sulfonyl probes for n-butylamine was substantially reduced compared with p-cresol even at high TMG (3.3 equivalents) conditions (Fig. 3.24.b). Reaction of HHS-475 with n-butylamine required 6 hours to complete and HHS-482 and HHS-SF-1 were not consumed even after 24 hours (Fig. 3.24.b and Fig. 3.25). To investigate selectivity further, we incubated sulfonyl probes with n-butylamine and p-cresol mixed in a 5:1 ratio and demonstrated minimal n-butylamine- compared with p-cresol-probe adduct formation for HHS-475 as well as HHS-482 and HHS-SF-1 (Fig. 3.26).

Collectively, we show the triazole LG enhances intrinsic reactivity of sulfonyl probes for phenol without compromising stability in solvents commonly used for biological experiments (i.e. DMSO). While our solution findings agree with the enhanced reactivity of SuTEx compared with SuFEx observed by proteomics, the differences in tyrosine chemoselectivity between HHS-482 and HHS-475 are likely a function of the protein microenvironment and a feature of probe reactivity that has been reported for other electrophiles[159].

3.4.6 Chemoproteomic profiling of phosphotyrosine activation

Considering the overlap of SuTEx-modified tyrosines with reported phosphotyrosine sites (pY, Fig 3.2.c), we investigated whether we could apply this

methodology for a “chemical” phosphoproteomics approach. We hypothesized that tyrosine accessibility by SuTEx probes would be inversely correlated with modification status and could be used to identify changes in pY sites (Fig. 3.27). Given the low abundance of phospho-tyrosine (1%) compared with -serine (88%) and -threonine (11%) detected in cell[160] and tissue proteomes[161], we activated global phosphorylation using cell permeable tyrosine phosphatase inhibitors to increase pY signals for our LC-MS studies. Previous live cell studies demonstrated the high efficiency of pervanadate for global inhibition of tyrosine phosphatase activity116. We treated live A549 cells with pervanadate at varying concentrations (0 – 500 μM) and time (0 – 30 min) and measured global changes in tyrosine phosphorylation by western blot using a pY-specific antibody (P-Tyr-100117). We observed robust increases in global tyrosine phosphorylation as judged by a massive increase in pY-antibody signals that appeared to saturate at 100 μM and 30 min of pervanadate treatment (Fig. 3.28 and 3.29).

Proteomes from cells treated with our pervanadate activation conditions (100 μM, 30 min) were labeled with HHS-475 or HHS-482 (100 μM, 30 min) followed by CuAAC with desthiobiotin and quantitative LC-MS to evaluate how phosphorylation status affected SuTEx probe labeling. Pervanadate blockade of tyrosine phosphatases should activate endogenous phosphorylation and compete for SuTEx probe labeling at phosphorylated- but not unmodified-tyrosine sites that can be differentiated by SILAC ratios of vehicle- (light) versus pervanadate (heavy)-treated cells (Fig. 3.27 and Fig. 3.30.a). We detected in total ~2,200 probe-modified tyrosine sites across ~1,000 proteins using both HHS-475 and HHS-482 that were further separated into pervanadate-sensitive (PerS, SR > 2) and -

insensitive groups (PerI, SR < 2, Fig. 3.30b and Fig. 3.31). In support of our hypothesis, the probe-modified tyrosines found in the PerS group appeared to be enriched for annotated phosphotyrosine sites (HTP >10 in PhosphoSitePlus, Fig. 3.30.c and Supplementary Fig. 3.31) and represented only a small fraction of all unique HHS- 475- and HHS-482-modified tyrosines detected by chemical proteomics (~3%, 67 sites). The overall median SR of all probe-modified tyrosines was ~1 for both HHS-475 and HHS-482 datasets, which supports tyrosine phosphorylation as a rare post-translational event and the ability of our platform to capture subtle changes in the tyrosine phosphoproteome.

To further validate our chemical phosphoproteomics strategy, we tested whether tyrosine sites identified as pervanadate sensitive were also directly phosphorylated under the same treatment conditions. For our studies, we chose several proteins from the PerS group based on a high phosphotyrosine annotation score (HTP >100, PhosphoSitePlus) and evidence for a role in signaling in human cancer cells like A549. We identified signal transducer and activator of transcription 3 (STAT3) as a target protein with reduced SuTEx probe labeling at Y705 (SR = 2.3, Fig. 3.30.d) that corresponded with enhanced phosphorylation at this site upon pervanadate activation (Fig. 3.30.e). Our data are in agreement with previous findings reporting STAT3 Y705 as a phosphorylation site for activation by tyrosine kinases in human non-small cell lung cancer lines including A549[162]. We validated another tyrosine kinase-targeted site (Y228) on catenin δ-1 (CTNND1119) and showed blockade of SuTEx probe labeling (SR = 3.3, Fig. 2.30d) coincided with direct phosphorylation at this tyrosine site by western blot analysis (Fig. 3.30.e).

In contrast, we identified Y105 as a pervanadate insensitive site (SR = 1.1, Fig.

3.30.d) on pyruvate kinase (PKM) that showed negligible changes in phosphorylation at this tyrosine upon pervanadate activation (Fig. 3.30.e). Our proteomic findings support previous reports of substantial basal levels of phosphorylated-Y105 on PKM in A549 cells[163], which could explain why pervanadate activation did not further enhance pY levels. As a control, we showed that SuTEx probe treatment of pervanadate-activated cell proteomes did not result in non-specific displacement of phosphates from tyrosines (Fig. 3.32). In summary, we applied SuTEx technology as a chemical strategy that exploits probe labeling as a site-specific readout of changes in pY levels upon global activation of the phosphoproteome.

3.5 Discussion

We describe sulfur-triazole exchange chemistry for development of covalent probes that are compatible with biological systems, easily accessible via modern synthetic chemistry, and can be adapted for diverse chemical proteomic applications. We demonstrate, on a proteomic scale, that addition of a triazole LG introduces key capabilities to the sulfur electrophile including tunability for protein reaction, robust cellular activity, and capacity for directing amino acid selectivity. Compared with more widely used sulfonyl-fluorides, the triazole LG dramatically enhanced overall reactivity of sulfonyl probes in solution (Fig. 3.24) that can, through modest structural modifications, be optimized for high tyrosine chemoselectivity in proteomes (Fig. 3.16.a and b). Key to success is a general synthetic strategy for introducing a common mass spectrometry-stable enrichment tag (Fig. 3.1.d) and incorporating diverse triazole LGs to enable global

structure-activity relationship (SAR) studies of SuTEx probes directly in lysates and live cells (Fig. 3.10).

We exploit these features of SuTEx for functional studies of >10,000 unique tyrosine sites from ~3,700 protein targets detected in human cell proteomes. While previous chemical proteomic studies have shown promise for functional tyrosine profiling[145,148,150,164], the broad coverage of SuTEx permitted global tyrosine quantitation with unprecedented depth and breadth. A striking discovery from our studies was high enrichment of tyrosine sites in nucleotide-binding domains from in vitro and in situ probe-labeling experiments using HHS-465 and HHS-475 (Fig. 3.10.b and d). We identified prominent labeling of tyrosines localized in RNA-recognition motifs (RRMs) of serine/arginine-rich protein splice factors (SRSF1-12, ~70% coverage of members by SuTEx) involved in regulation of mRNA splicing, export, and translation121. Several probe-labeled tyrosines including Y13 of SRSF3 RRM have been shown through structural studies to directly mediate RNA binding122. Combined with prominent in situ labeling at domains mediating protein-protein interactions (e.g. PCI/PINT and SH3[158]), SuTEx offers a valuable resource for developing chemical probes against proteins that have been historically challenging to target with small molecules (Fig. 3.10.d).

Our functional profiling studies led to the discovery of intrinsically nucleophilic tyrosines that are enriched in enzyme sites but also prominent in domains mediating protein-small molecule and protein-protein interactions (SR < 5, Fig. 3.14.b). The rare nature of hyper-reactive tyrosines (~5% of all quantified sites) are in agreement with previous chemical proteomic studies that identified minor subsets of cysteine and lysine

residues that demonstrate enhanced reactivity[27,136]. We demonstrated that hyper-reactive residues like Y8 of GSTP1 are key for catalytic function and mutation of this site (Y8F) abolished biochemical activity (Fig. 3.19.a and b). We also identified a non-catalytic tyrosine near the zinc-binding region of DPP3 (Y417) that exhibited moderate nucleophilicity (SR ~6) and may offer future opportunities for developing site-selective ligands (Fig. 3.14.d and Fig. 3.19.d). We find it noteworthy that several arginines (R548 and R572, Fig. 3.19.c) are in close proximity to Y417 and these positively-charged residues may play a role in perturbing the pKa of neighboring tyrosine residues as previously reported for alanine racemase[165]. In contrast with GSTP1 and DPP3 enzymes, the discovery of a hyper-reactive tyrosine (Y475, Fig. 3.14.d) in the Yjef-N domain of the scaffolding protein EDC3 is intriguing given the role of this domain in assembly of cytoplasmic RNA–protein (RNP) granules known as P-bodies involved in post- transcriptional regulation[166]. Future studies will test whether the hyper-reactive nature of the Y475 site can be exploited for developing ligands to modulate EDC3 function.

We applied SuTEx for development of a chemical phosphoproteomics platform to identify and quantitatively measure tyrosine sites whose probe modification status is competed by activation of phosphorylation. As proof of concept, we studied global changes in the tyrosine phosphoproteome under pervanadate activation of A549 cells to identify pervanadate-sensitive (PerS) sites that represented putative phosphotyrosines (Fig. 3.30 and Fig. 3.31). Across >2,000 quantified sites, we identified a small subset of PerS sites (67 sites), which is in agreement with the low frequency of tyrosine phosphorylation (1%) compared with more abundant phospho-serines and -threonines[160,161]. We verified that

SuTEx probe labeling is anticorrelated with phosphorylation at Y705 and Y228 of STAT3 and CTNND1, respectively (Fig. 3.30.d and e). Both sites are highly annotated phosphotyrosines and reported substrates for tyrosine kinases in cancer cell signaling[167,168]. In contrast, the pervanadate-insensitive Y105 site of PKM did not show changes in phosphotyrosine signals with pervanadate activation and further supports the ability of SuTEx to differentiate probe labeling of tyrosines based on phosphorylation state (Fig. 3.30.d and e). Future studies will focus on further refinement, e.g. improvements to LC-MS method and use of SuTEx probe cocktails, to expand the number and type of phosphotyrosine sites quantified.

In summary, we deployed SuTEx for development of a quantitative chemical proteomics platform to globally profile tyrosine nucleophilicity and post-translational modification state in human cell proteomes. We believe our current findings serve as a blueprint for design of activity-based probes that can be synthetically modulated to meet the proteomic demands of chemical biology applications. Expansion of our chemical phosphoproteomics to other activation paradigms should afford additional opportunities for studying and potentially targeting tyrosine post-translational modifications in future studies (Fig. 3.10.c). The latter effort will be expedited by conversion of SuTEx probes into inhibitors or ligands to reveal the inventory of tyrosine (and potentially phospho-tyrosine) sites that are “druggable” in proteomes.

3.6 Author Contributions and Pipeline Development

Hahm., Toroitich, Borne, Brulet and Hsu conceived of the project, designed

experiments and analyzed data. Hahm and Toroitich performed mass spectrometry experiments and data analysis. Borne wrote software and performed bioinformatics analysis. Hahm, Brulet and Yuan synthesized compounds. Brulet expressed proteins, conducted inhibition studies and performed biochemical assays. Toroitich and Brulet conducted cellular studies. Libby assisted with compound design, synthesis and characterization. Ware, Ciancone and McCloud performed site-directed mutagenesis and assisted with cloning and expression of proteins. Hahm, Toroitich, Borne, Brulet and Hsu wrote the manuscript.

The R shiny application used in Chapter 2 could not be used to analyze the global proteome profiling experimental data given the amount of time manual verification would take for 10,000 sites. A collection of script written in R and python were developed to address the large amount of data and provide the highest confidence site identification. These scripts used same byonic and skyline quality control features as well as quantify the SR for sites seen in hyperreactivity and pY studies. The resulting lists were used to identify sites that were significantly changed that could then be manually verified in both studies.

Additionally, individual scripts were developed to perform nucleophilic amino acid comparisons, drug bank comparison, domain enrichment analysis, venn-diagram comparisons and phosphosite plus database comparison. The multi-layered analysis seen in Fig. 3.10.d was done by stitching together two different python scripts and an R visualization script. These tools solely existed as scripts that could be run from the command line but were limited to the analysis of SuTEx probes. This was due to the code base being built around the adduct formed by SuTEx modification of amino acids.

3.7 Tables and Figures

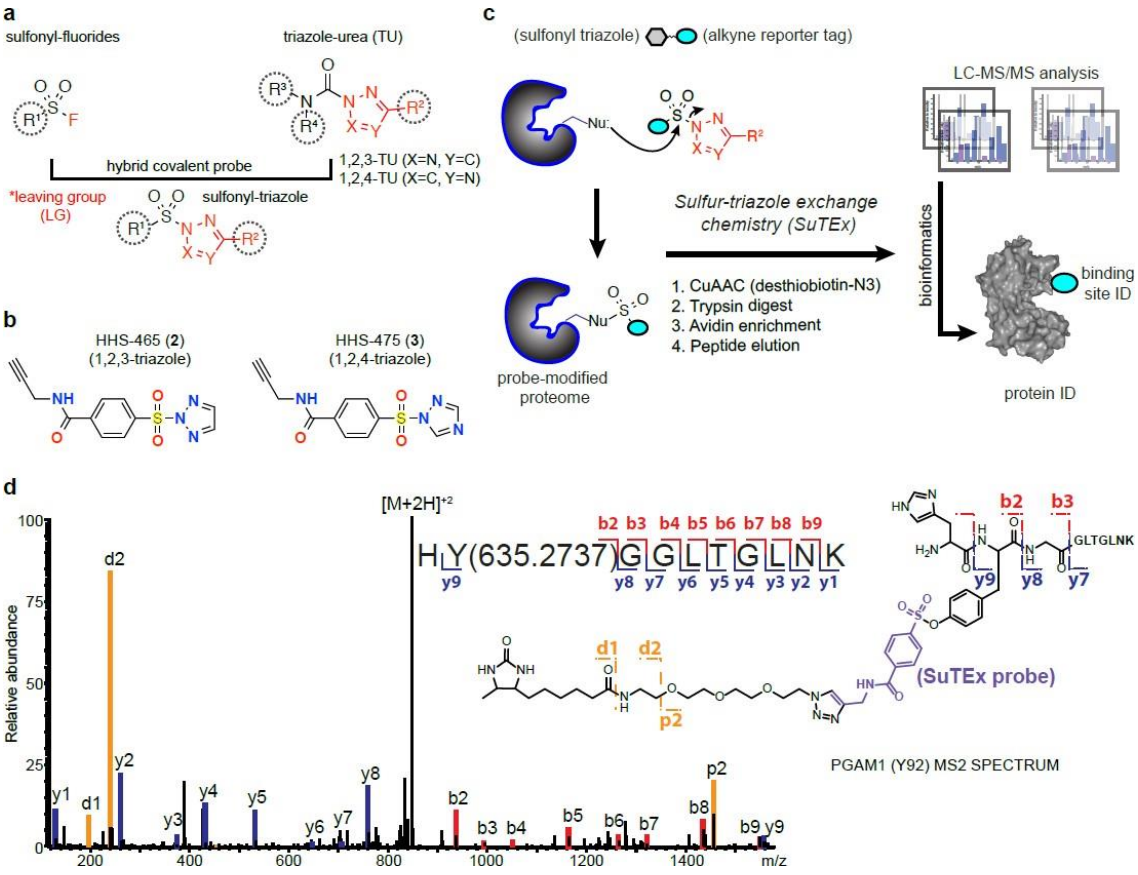

Figure 3.1. Development of sulfur-triazole exchange (SuTEx) chemistry for chemical proteomics. a) Sulfonyl-triazoles are a hybrid of sulfonyl-fluoride and triazole-ureas for developing covalent probes with reactivity that can be modulated through the triazole leaving group (LG). b) Chemical structures of 1,2,3- and 1,2,4-sulfonyl triazoles HHS- 465 and HHS-475, respectively. c) Proposed reaction mechanism of sulfur-triazole exchange (SuTEx) chemistry and LC-MS/MS workflow to identify proteins and corresponding binding sites from SuTEx reaction. See Methods for additional details. d) MS2 spectrum annotation of an HHS-475-modified tyrosine site (Y92) found in PGAM1. Covalent

reaction with HHS-465 and HHS-475 adds +635.2737 Da to the modified amino acid (Y92 from PGAM1 shown as a representative example) and supports the proposed SuTEx reaction mechanism. Data shown are representative of two experiments (n=2 biologically independent experiments). Scheme created by Hsu; data acquired by Hahm and Toroitich; spectra annotated by Hahm.

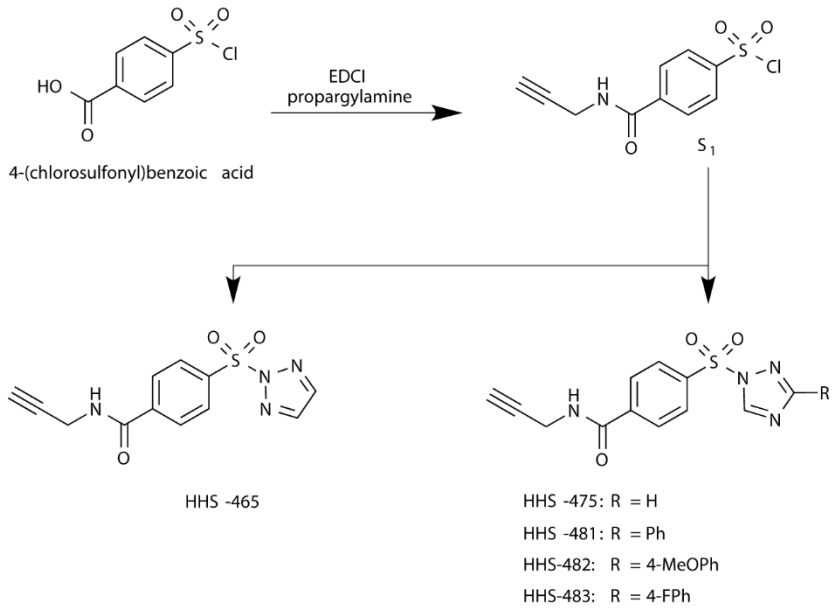

Figure 3.2. Synthetic scheme showing general strategy for developing alkyne-modified sulfonyl-triazole probes. Scheme created by Hsu.

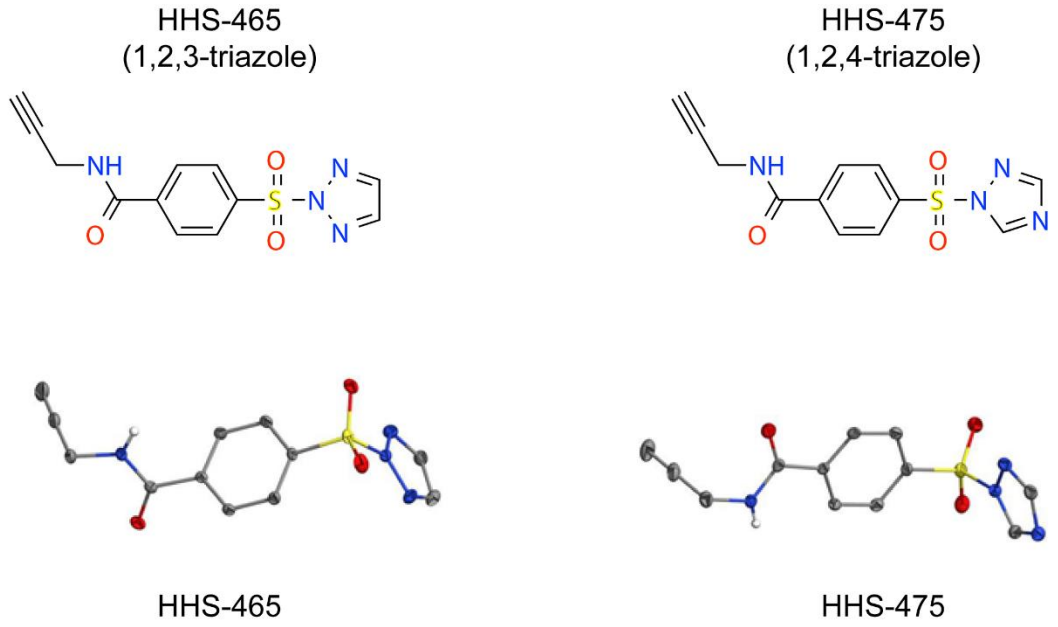

Figure 3.3. Crystal structures of HHS-465 and HHS-475. Crystal structure generated by Libby and D. Dickie.

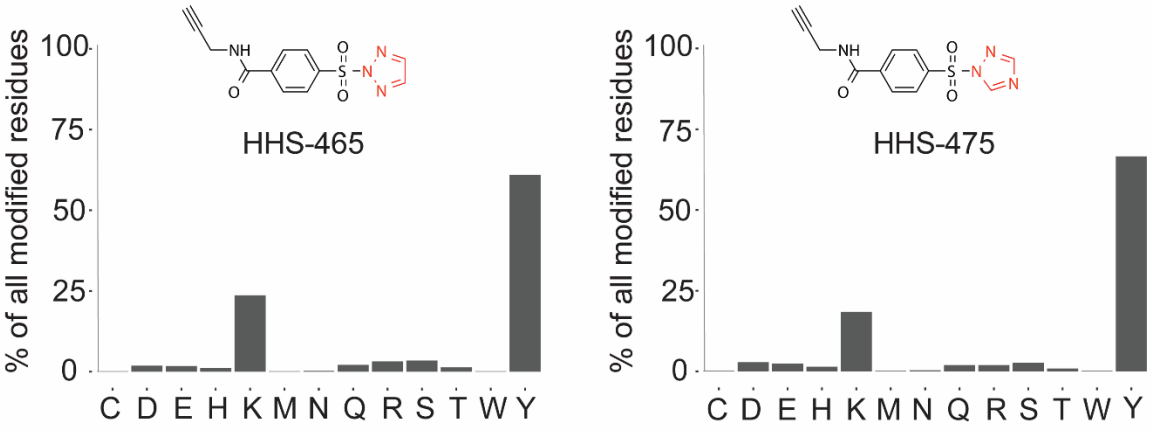

Figure 3.4. Bar plot showing distribution of HHS-465 and HHS-475-modified sites (high confidence sites; Byonic score > 600) against nucleophilic amino acid residues detected in proteomes. Data shown are representative of two experiments (n=2 biologically

independent experiments). Data acquired by Hahm and Toroitich; Analysis conducted by Borne.

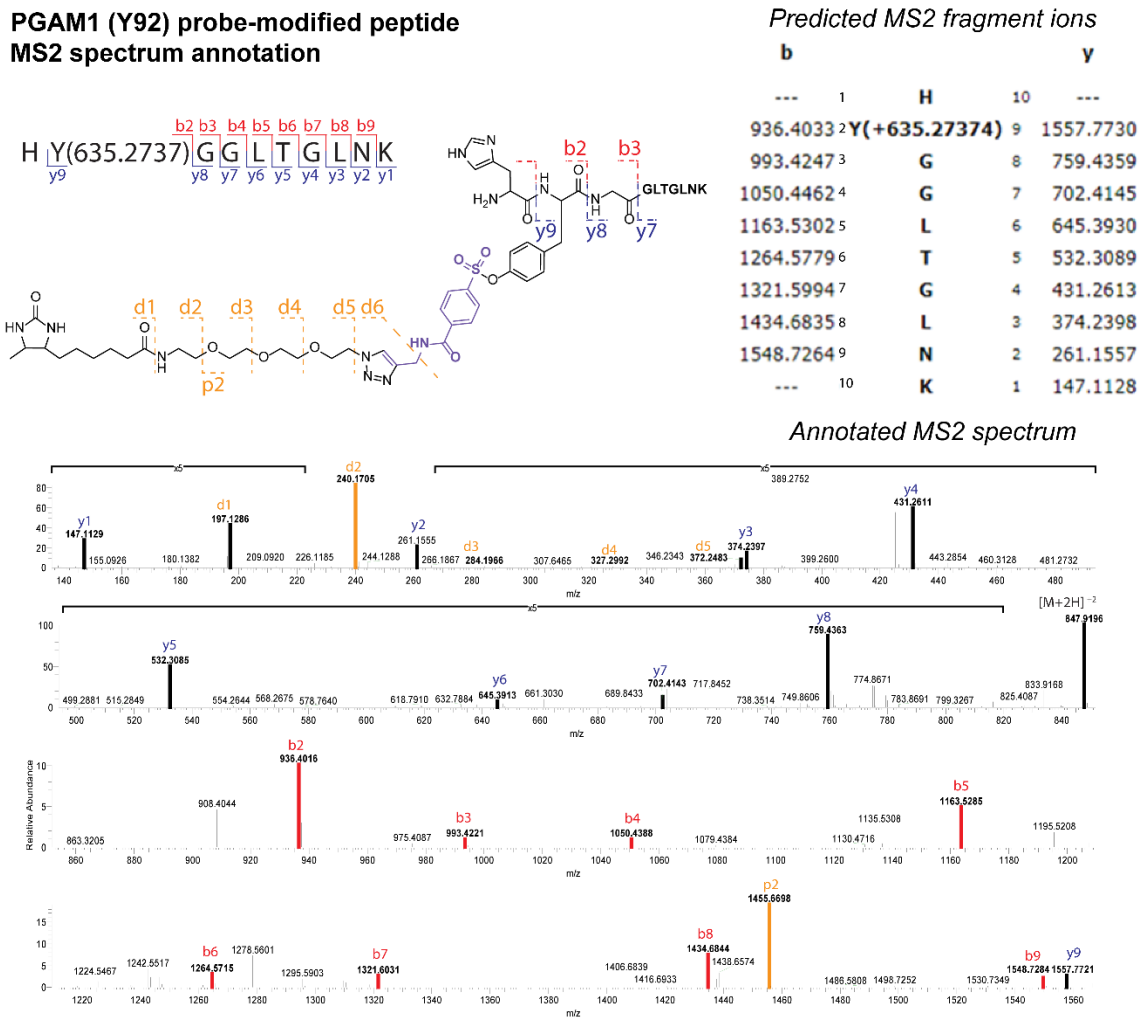

Figure 3.5. MS2 annotation of the PGAM1 (Y92) HHS-475-modified tryptic peptide. Left panel: Modified sequence and fragment ion notation of HY*GGLTGLNK (residue 91-100) peptide from PGAM1. Covalent reaction of HHS-475 with Y92 results in a modified tyrosine (Y*) with the addition of +635.2737 Da. Fragmentation of the desthiobiotin-

containing tag is also shown. Right panel: predicted MS2 b- and y-fragment ions from collision-induced dissociation (CID) as determined using Protein Prospector software (http://prospector.ucsf.edu/prospector/mshome.htm). Bottom panel: annotation of the MS2 spectrum for the HHS-475-modified PGAM1 Y92 tryptic peptide including fragment ions containing the probe binding site (modified tyrosine). Data shown are representative of two experiments (n=2 biologically independent experiments). Data acquired by Hahm and Toroitich; spectra annotated by Hahm.

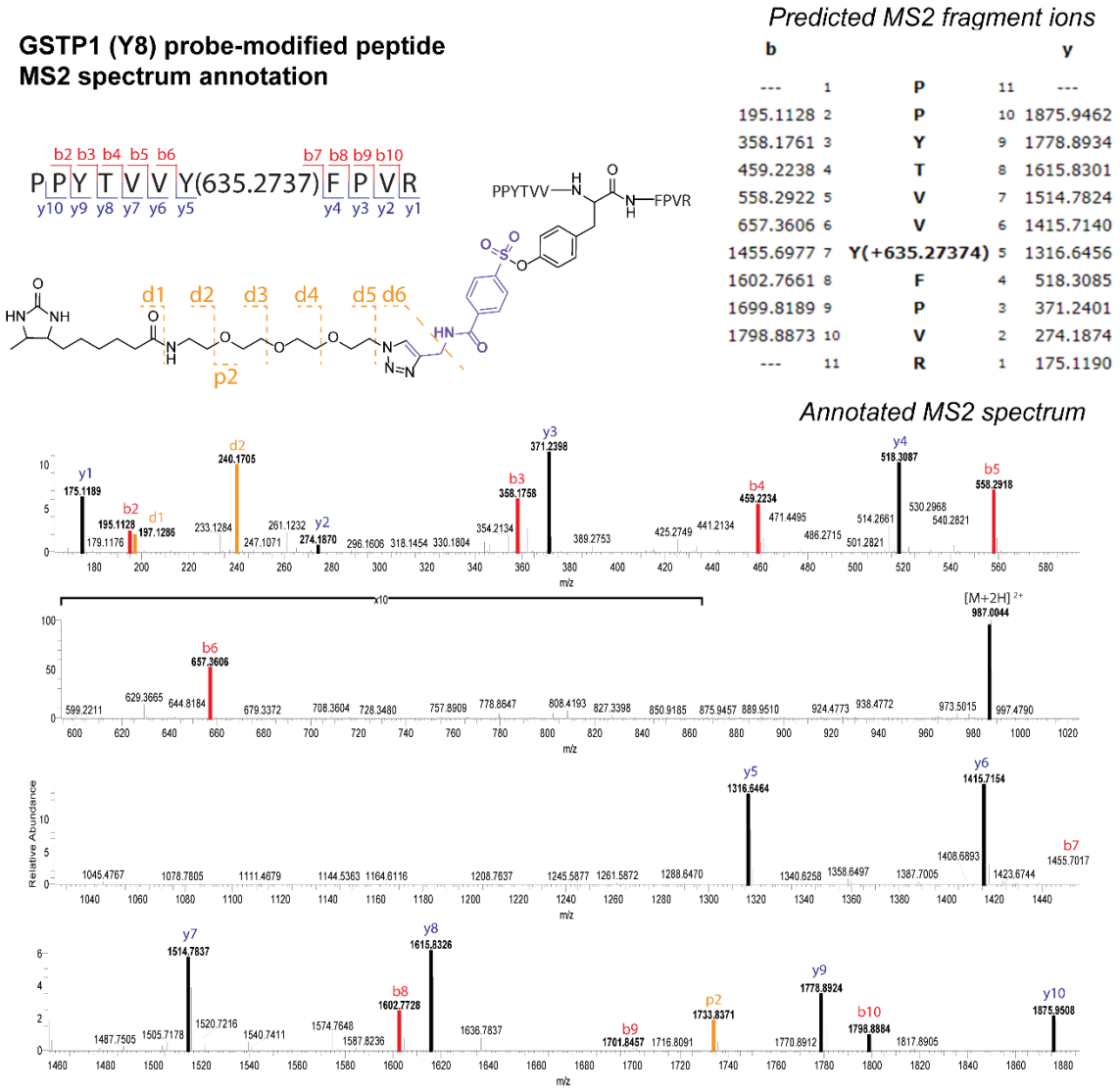

Figure 3.6. MS2 annotation of the GSTP1 (Y8) HHS-475-modified tryptic peptide. Left panel: Modified sequence and fragment ion annotation of PPYTVVY*FPVR (residue 2-12) peptide from PGAM1. Covalent reaction of HHS-475 with Y8 results in a modified tyrosine (Y*) with the addition of +635.2737 Da. Fragmentation of the desthiobiotin-containing tag is also shown. Right panel: predicted MS2 b- and y-fragment ions from CID as determined using Protein Prospector software. Bottom panel: annotation of the MS2 spectrum for the HHS-475-modified GSTP1 Y8 tryptic peptide including fragment ions

containing the probe binding site (modified tyrosine). Data shown are representative of two experiments (n=2 biologically independent experiments). Data acquired by Hahm and Toroitich; spectra annotated by Hahm.

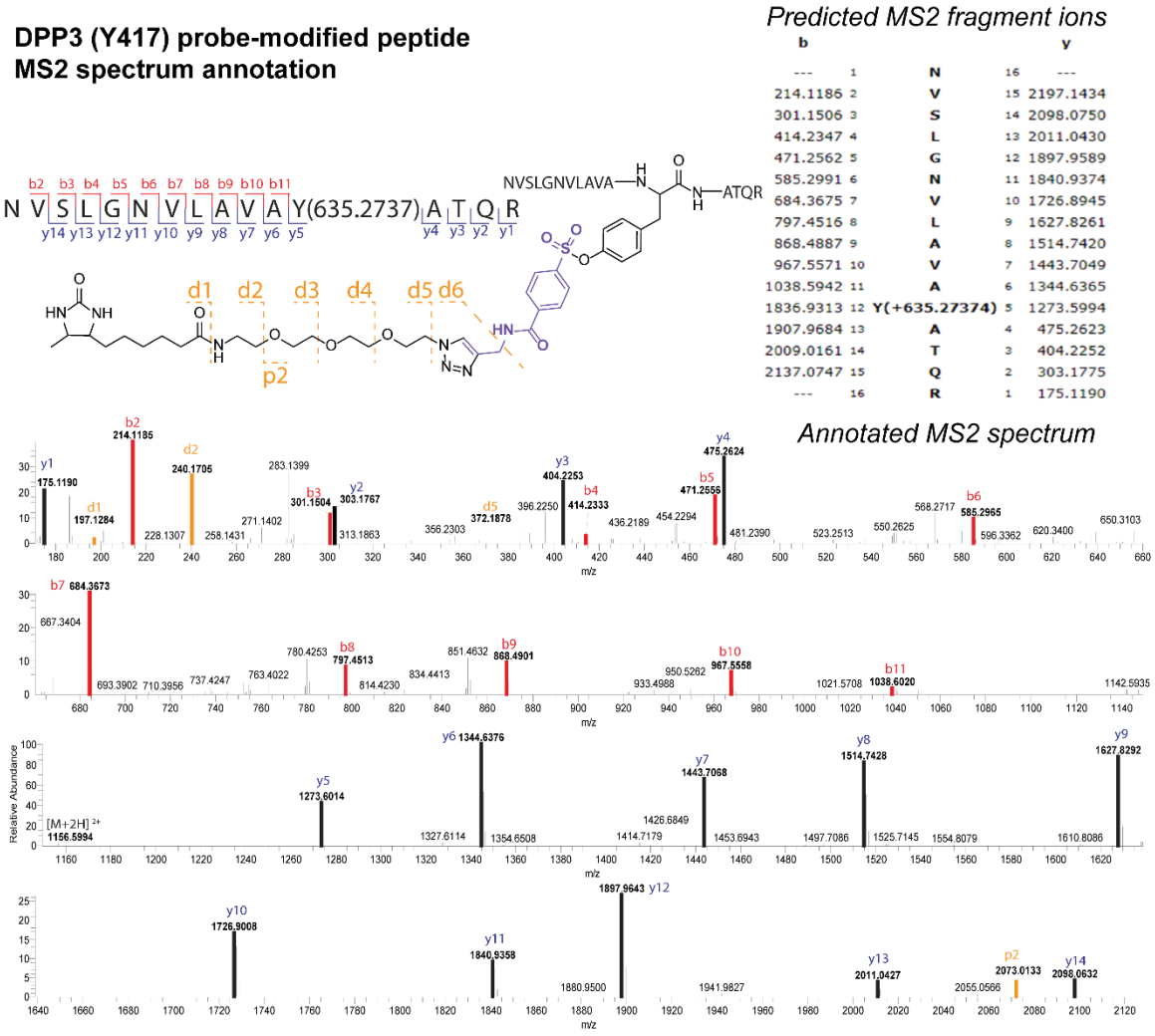

Figure 3.7. MS2 annotation of the DPP3 (Y417) HHS-475-modified tryptic peptide. Left panel: Modified sequence and fragment ion notation of NVSLGNVLAVAY*ATQR (residue 406-421) peptide from DPP3. Covalent reaction of HHS-475 with Y417 results in

a modified tyrosine (Y*) with the addition of +635.2737 Da. Fragmentation of the desthiobiotin-containing tag is also shown. Right panel: predicted MS2 b- and y-fragment ions from CID as determined using Protein Prospector software. Bottom panel: annotation of the MS2 spectrum for HHS-475-modified DPP3 Y417 tryptic peptide including fragment ions containing the probe binding site (modified tyrosine). Data shown are representative of two experiments (n=2 biologically independent experiments). Data acquired by Hahm and Toroitich; spectra annotated by Hahm.

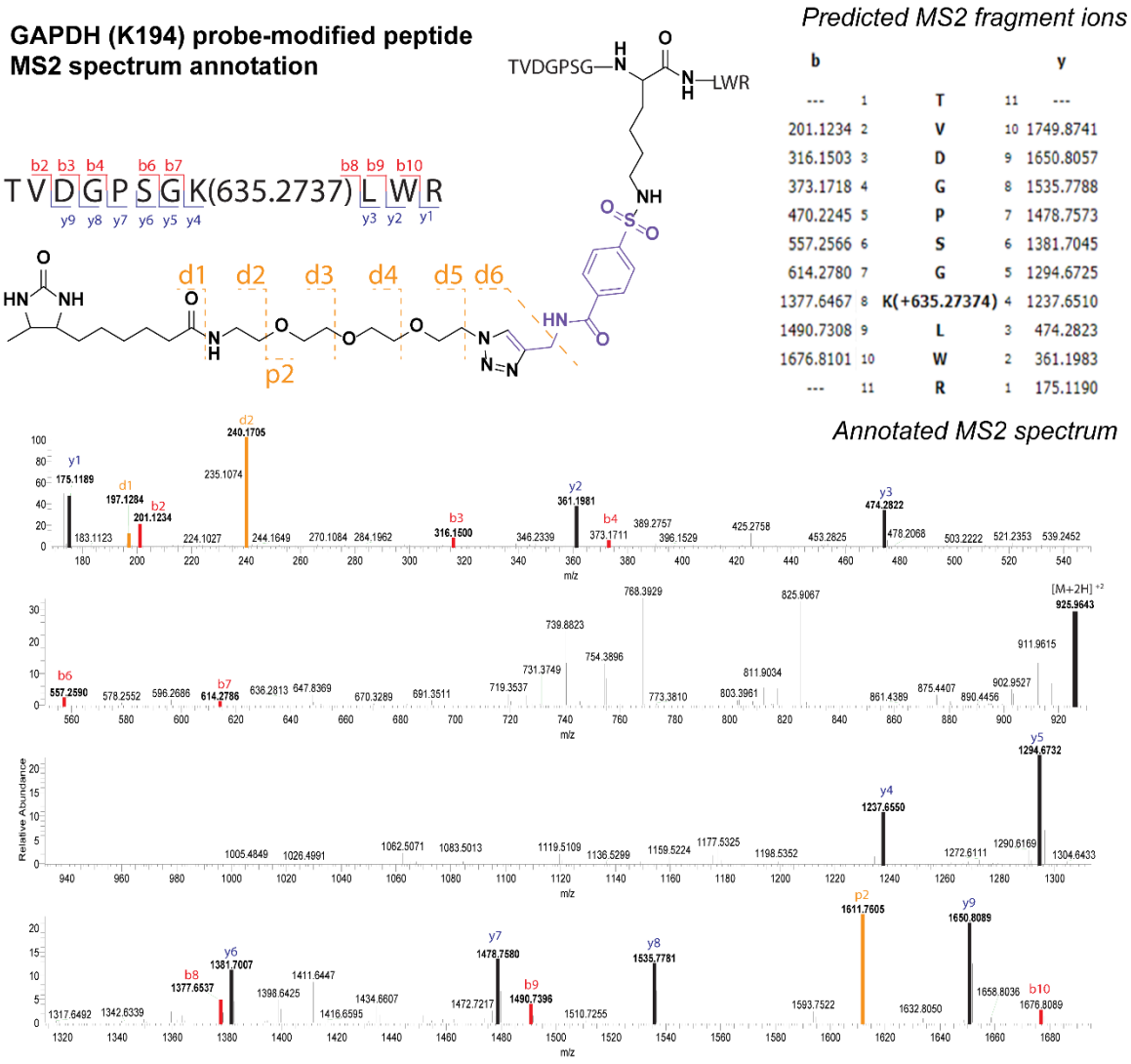

Figure 3.8. MS2 annotation of the GAPDH (K194) HHS-475-modified tryptic peptide. Left panel: Modified sequence and fragment ion notation of TVDGPSGK*LWR (residue 187-197) peptide from GAPDH. Covalent reaction of HHS-475 with K194 results in a modified lysine (K*) with the addition of +635.2737 Da. Fragmentation of the desthiobiotin-containing tag is also shown. Right panel: predicted MS2 b- and y-fragment ions from CID as determined using Protein Prospector software. Bottom panel: annotation of the MS2 spectrum for HHS-475-modified GAPDH K194 tryptic peptide including

fragment ions containing the probe binding site (modified lysine). Data shown are representative of two experiments (n=2 biologically independent experiments). Data acquired by Hahm and Toroitich; spectra annotated by Hahm.

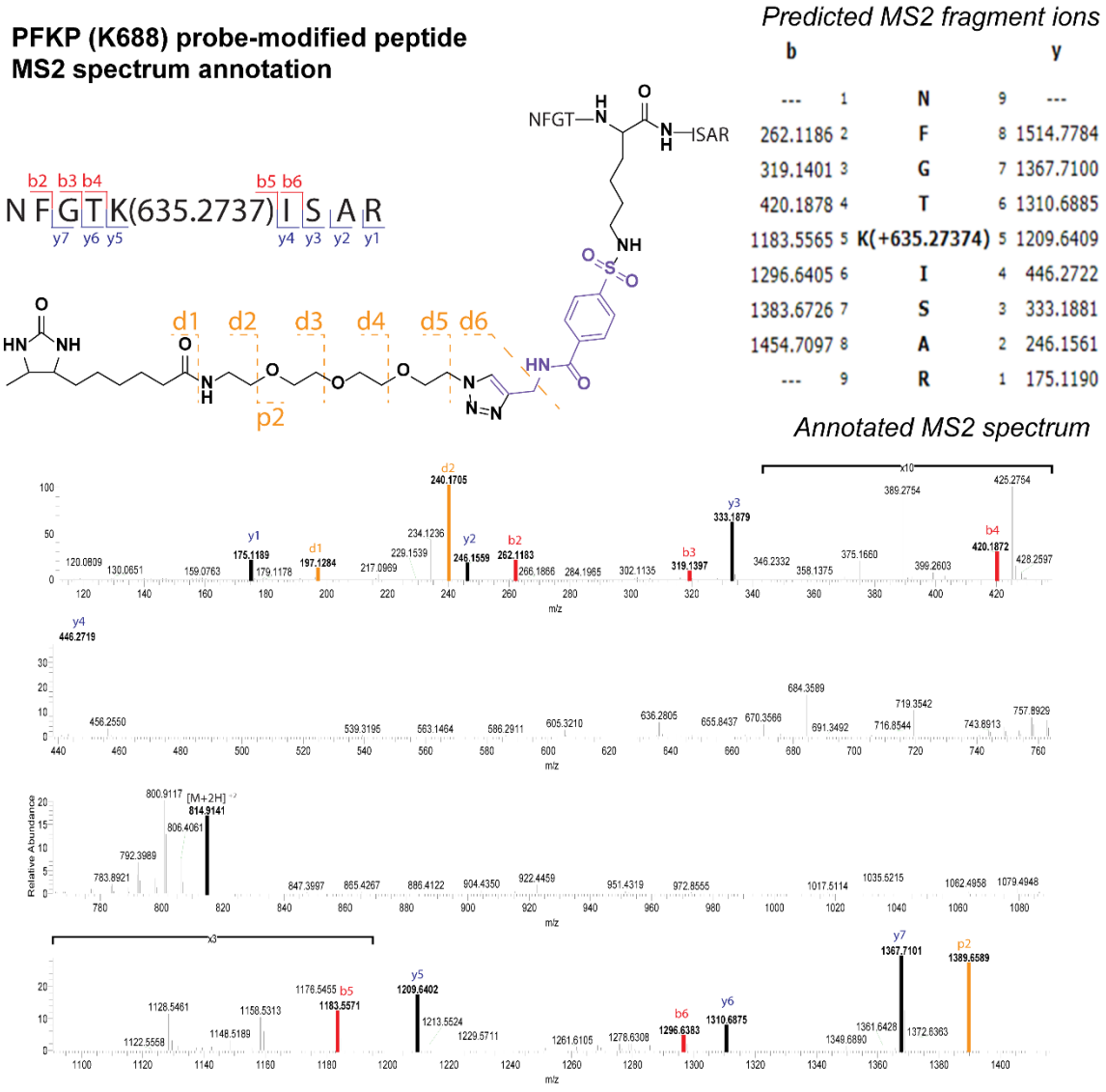

Figure 3.9. MS2 annotation of the PFKP (K688) HHS-475-modified tryptic peptide. Left panel: Modified sequence and fragment ion notation of NFGTK*ISAR (residue 684- 692)

peptide from PFKP. Covalent reaction of HHS-475 with K688 results in a modified lysine (K*) with the addition of +635.2737 Da. Fragmentation of the desthiobiotin- containing tag is also shown. Right panel: predicted MS2 b- and y-fragment ions from CID as determined using Protein Prospector software. Bottom panel: annotation of the MS2 spectrum for the HHS-475-modified PFKP K688 tryptic peptide including fragment ions containing the probe binding site (modified lysine). Data shown are representative of two experiments (n=2 biologically independent experiments). Data acquired by Hahm and Toroitich; spectra annotated by Hahm.

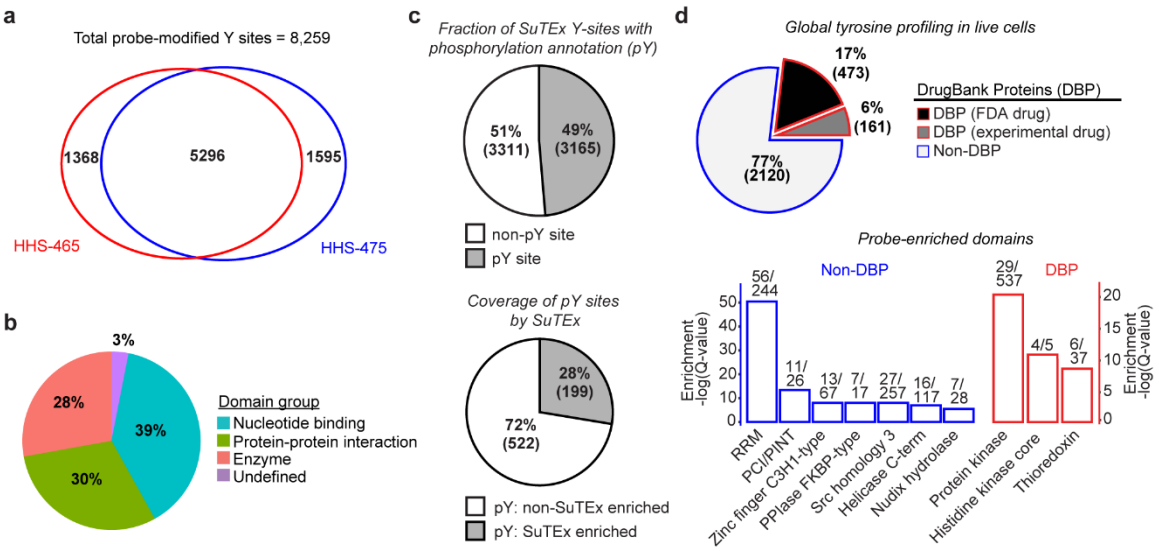

Figure 3.10. Functional tyrosine profiling in proteomes and live cells. a) Comparison of HHS-465- and HHS-475-tyrosine modified sites identified from human cell proteomes (HEK293T, A549, DM93, H82, and Jurkat cells) treated with SuTEx probes (100 µM, 1 hr, 25 °C). b) Distribution of protein domain groups that are significantly overrepresented

using probe-modified tyrosine sites from in situ chemical proteomic studies. Enriched domain annotations are those with a Q-value < 0.01 after Benjamini–Hochberg correction of a two-sided binomial test (see Methods for details). c) Top panel: Overlap between in situ HHS-465- and HHS-475-modified tyrosine sites that are also phosphorylation sites (number of phosphotyrosine high throughput annotation on PhosphoSitePlus (HTP score); HTP >1). Bottom panel: coverage of phospho-tyrosine sites (HTP >10) that were detected by in situ chemical proteomics of HEK293T and Jurkat cells (HHS-465 and - 475). d) Top panel: Comparison of HHS-465 and HHS-475 in situ probe-modified proteins with DrugBank proteins (DBP group). The Non-DBP group consists of proteins that did not match a DrugBank entry. Bottom panel: probe-enriched domains from DBP and non-DBP groups. Enriched domain annotations are those with a Q-value < 0.01 after Benjamini–Hochberg correction of a two-sided binomial test. All data shown are representative of two experiments (n=2 biologically independent experiments). Data acquired by Hahm and Toroitich; Analysis conducted by Borne.

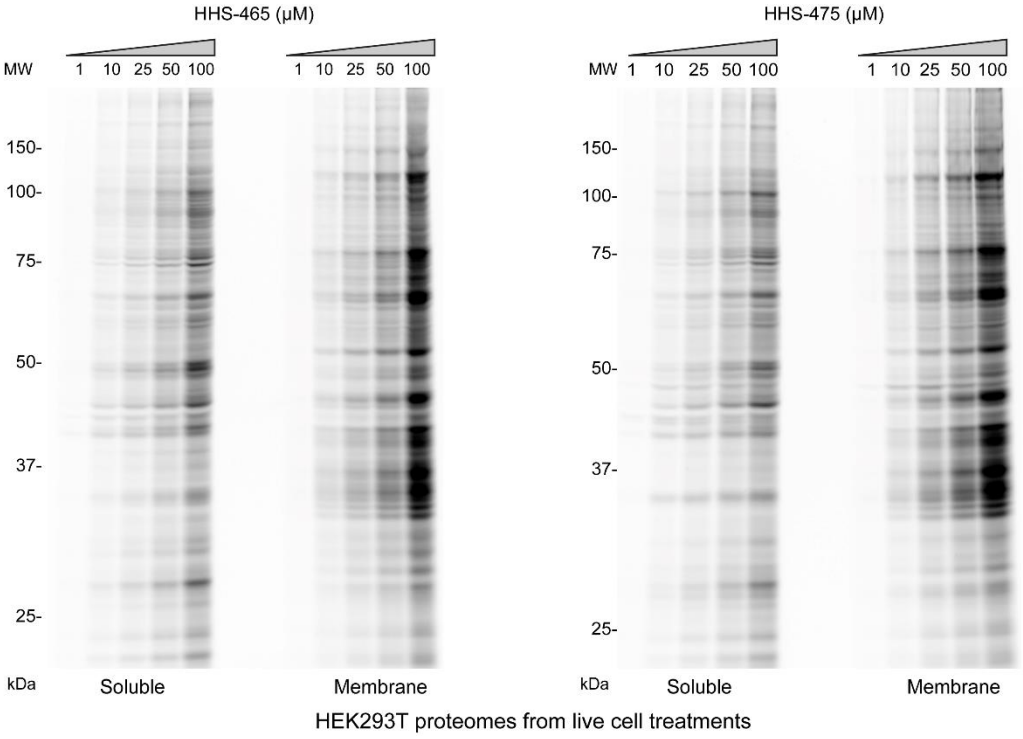

Figure 3.11. Concentration-dependent labeling of live HEK293T cells treated with SuTEx probes. HEK293T cells were treated with indicated concentrations of HHS-465 (left panel) or HHS-475 (right panel) for 2 h at 37 °C. After treatment, cells were lysed, probe-modified proteomes (1 mg/mL) subjected to CuAAC with rhodamine-azide followed by SDS-PAGE analysis and in-gel fluorescence scanning. Data shown are representative of two experiments (n=2 biologically independent experiments). Data acquired by Toroitich.

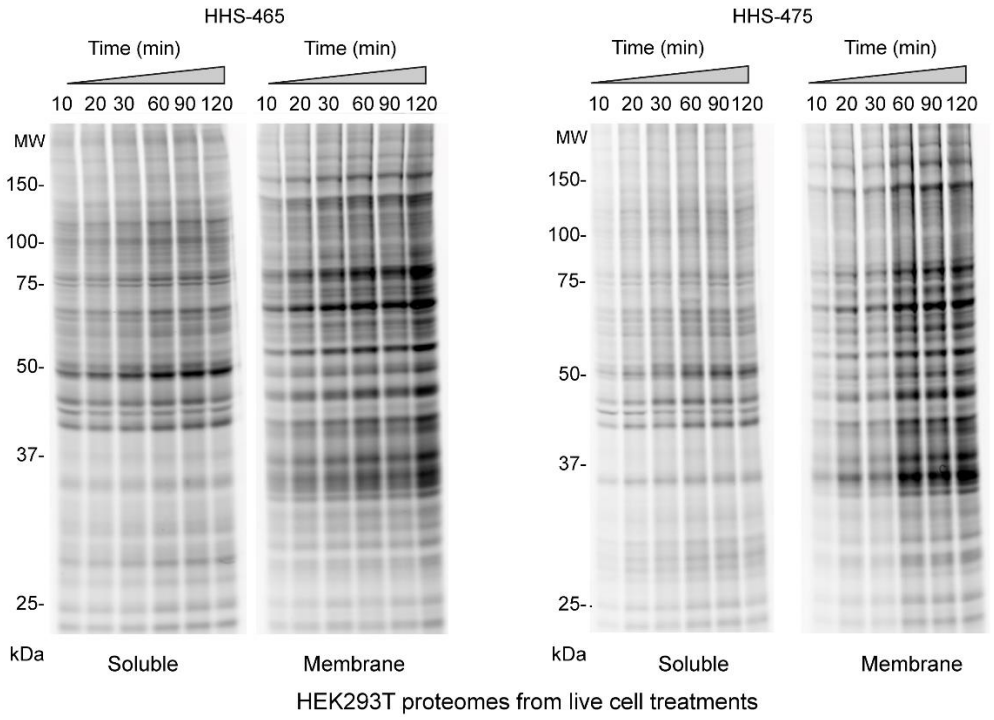

Figure 3.12. Time-dependent labeling of live HEK293T cells treated with SuTEx probes. HEK293T cells were treated with 25 µM of HHS-465 (left panel) or HHS-475 (right panel) for the indicated times at 37 °C. After treatment, cells were lysed, and the probe-modified proteomes (1 mg/mL) were subjected to CuAAC with rhodamine-azide followed by SDS-PAGE analysis and in-gel fluorescence scanning. Data shown are representative of two experiments (n=2 biologically independent experiments). Data acquired by Toroitich.

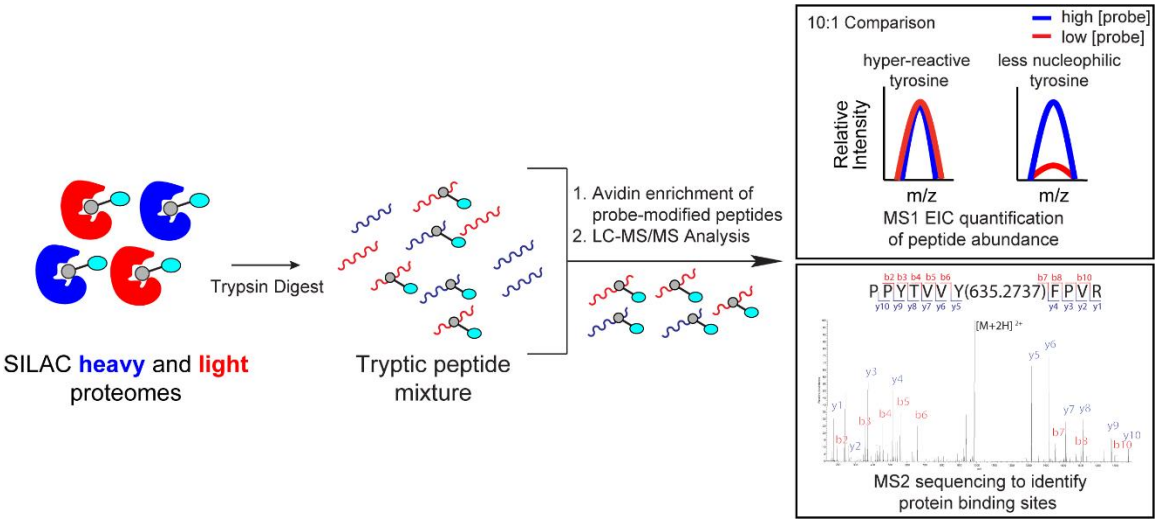

Figure 3.13. Quantitative chemical proteomics for profiling tyrosine reactivity. Experimental workflow for quantitative chemical proteomics to measure intrinsic tyrosine nucleophilicity (i.e. reactivity). HEK293T cells were cultured in SILAC media supplemented with either "light" 12C, 14N-labeled lysine and arginine (denoted in red) or "heavy" 13C, 15N-labeled lysine and arginine (denoted in blue). Heavy and light HEK293T proteomes were treated with 250 (high [probe]) or 25 μM (low [probe]) HHS-465, respectively (10:1 comparison). The resulting SILAC ratios (SR) were quantified using the area under the curve of MS1 extracted ion chromatograms. Hyper-reactive tyrosines are expected to show equivalent probe labeling intensity at high and low [probe] (left MS1, SR~1) while less nucleophilic tyrosines show concentration dependent probe labeling (right MS1, SR >>1). A separate experiment where heavy and light proteomes are treated with equivalent [probe] (1:1 comparison) is used as a control for potential false quantifications. Peptide sequencing and validation of the site of probe binding are determined using MS2 (fragmentation) spectra (bottom panel). Scheme generated by Hsu.

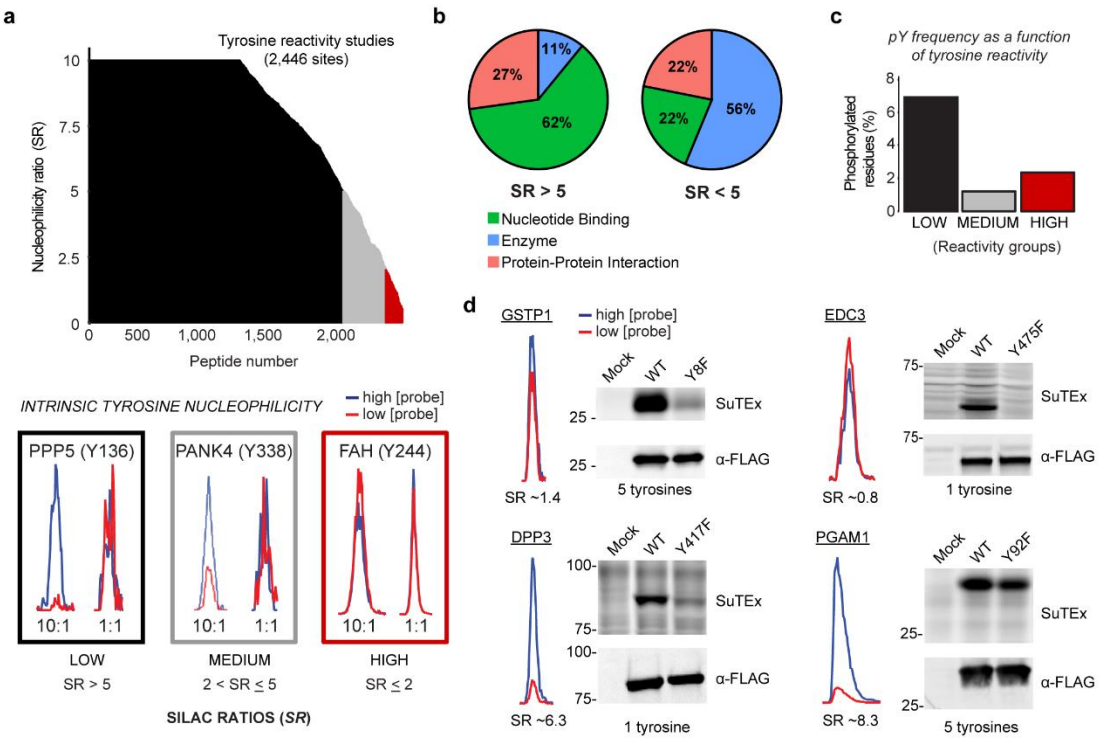

Figure 3.14. SuTEx-enabled discovery of intrinsically nucleophilic tyrosines in human cell proteomes. HEK293T SILAC heavy and light soluble proteomes were treated with 250 or 25 µM HHS-465 (10:1 comparison), respectively. The resulting SILAC ratios (SR) were quantified using the area under the curve of MS1 extracted ion chromatograms (EIC) to determine tyrosine nucleophilicity. a) A waterfall plot of nucleophilicity ratio (median SR values) as a function or probe-modified tyrosine sites to quantitate tyrosine reactivity across the proteome. A MS1 EIC is shown for SR values that represent each nucleophilicity group (low-black, medium-grey, and high-red). b) Distribution of protein domain groups that contain tyrosines quantified as low (SR >5) or medium/high (SR <5) reactivity.

Domain annotations shown were significantly enriched (Q-value < 0.01 after Benjamini–Hochberg correction of a two-sided binomial test) with HHS-465. c) Bar plot depicting tyrosines with medium to high nucleophilicity are less likely to be phosphorylated (HTP >10, PhosphoSitePlus) compared with less reactive tyrosines. d) Proteins containing a hyper-reactive tyrosine (GSTP1 Y8, EDC3 Y475) or single probe-modified tyrosine (DPP3 Y417) can be site-specifically labeled with SuTEx probes (50 μM, 30 min, 37 °C). Recombinant wild-type (WT) protein or corresponding tyrosine (Y)-to-phenylalanine (F) mutant HEK293T proteomes were treated with HHS- 475 (GSTP1, DPP3, PGAM1) or HHS-465 (EDC3) and analyzed by gel-based chemical proteomics. Proteins that contain less nucleophilic tyrosines (PGAM1 Y92) are labeled at multiple sites and show negligible differences in probe labeling between WT and tyrosine mutant. Western blots show equivalent expression of recombinant WT and mutant proteins. All data shown are representative of two experiments (n=2 biologically independent experiments). Data acquired by Hahm and Toroitich; Analysis conducted by Borne.

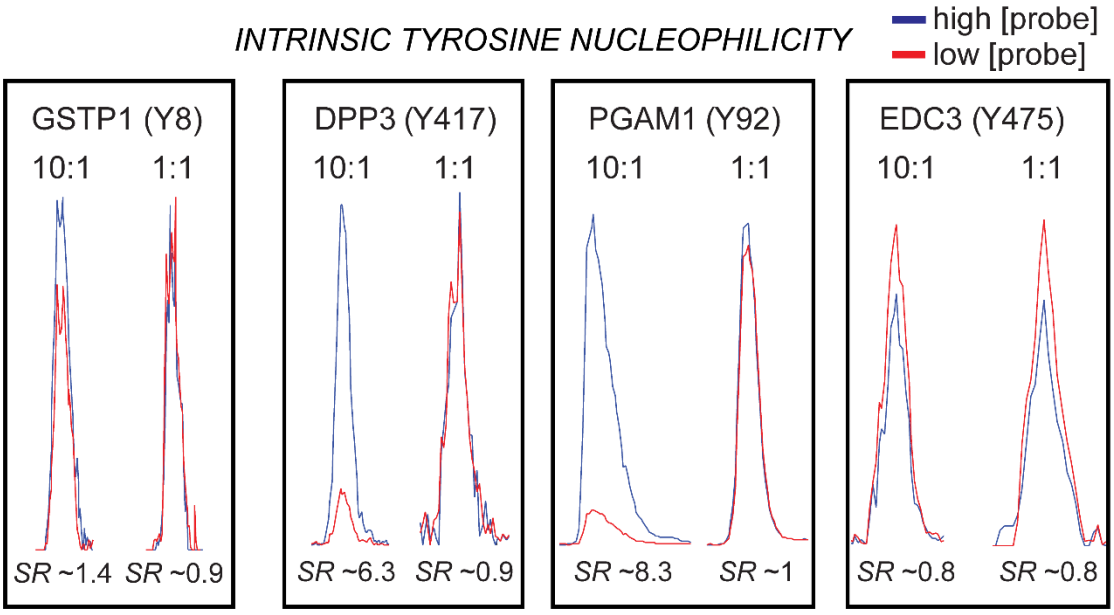

Figure 3.15. Quantitative analysis of tyrosine reactivity. Quantitative comparison of tyrosine nucleophilicity between sites detected in human GSTP1 (Y8), DPP3 (Y417), PGAM1 (Y92), and EDC3 (Y475). Heavy and light MS1 extracted ion chromatograms were used to calculate the SILAC ratio (SR) for 10:1 and 1:1 probe (HHS-465) comparisons. Data shown are representative of two experiments (n=2 biologically independent experiments). Data acquired by Hahm and Toroitich; Analysis conducted by Borne.

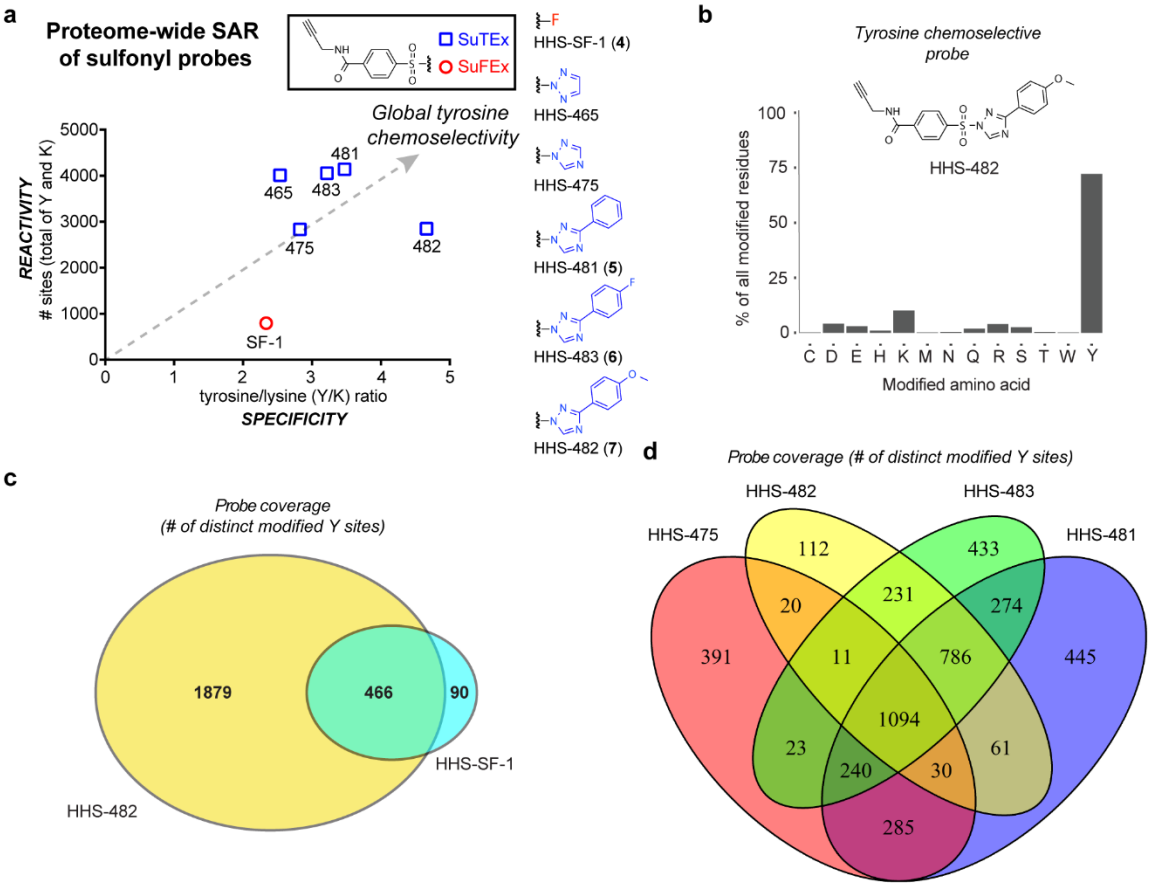

Figure 3.16. Tuning SuTEx probes for tyrosine chemoselectivity in cell proteomes. HEK293T soluble proteomes were treated with SuFEx and SuTEx probes. a) Global reactivity [total number of tyrosine (Y) and lysine (K) sites] and specificity (Y/K ratio) of probe-labeled sites from LC-MS chemical proteomic experiments. A bar graph depiction of reactivity and selectivity data can be found in Fig. 2.17b) Bar plot showing distribution of HHS-482-modified sites (high confidence sites; Byonic score > 600) against nucleophilic amino acid residues detected in proteomes. c) High overlap of tyrosine-modified sites from proteomes treated with sulfonyl-triazoles (HHS-482) compared with -fluorides (HHS-SF-1). d) Comparison of probe-modified tyrosine sites from LC-MS chemical proteomic studies using 1,2,4-sulfonyl-triazoles. Each 1,2,4-sulfonyl-triazole

probe was able to modify unique tyrosine sites to increase overall tyrosine coverage. All data shown are representative of two experiments (n=2 biologically independent experiments). Data acquired by Hahm and Toroitich; Analysis conducted by Borne and Hsu.

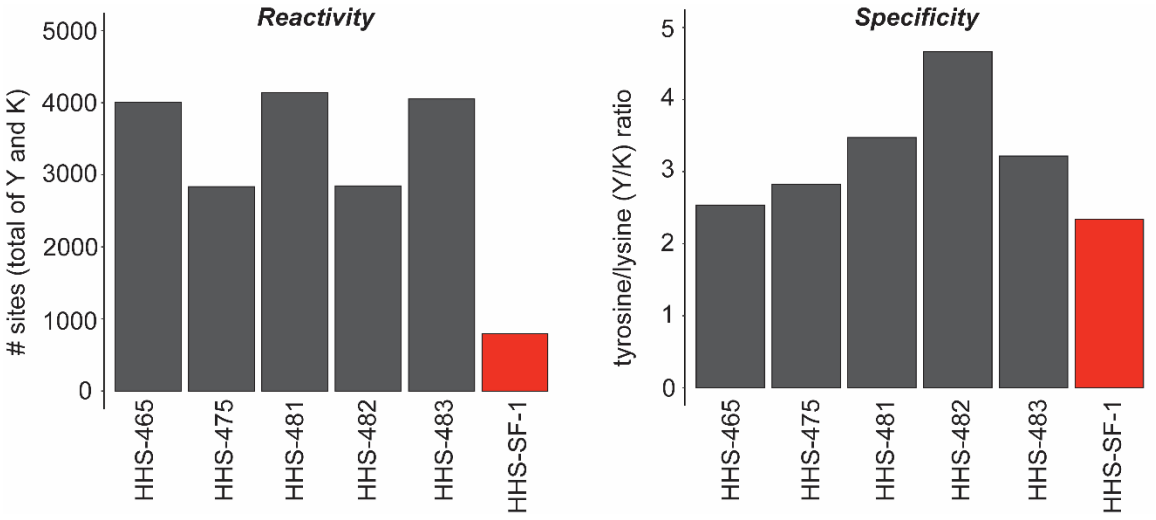

Figure 3.17. Bar plot depiction of global tyrosine reactivity and selectivity of SuTEx and SuFEx probes shown in Fig 3.16.a. Data acquired by Hahm and Toroitich; Analysis conducted by Borne and Hsu.

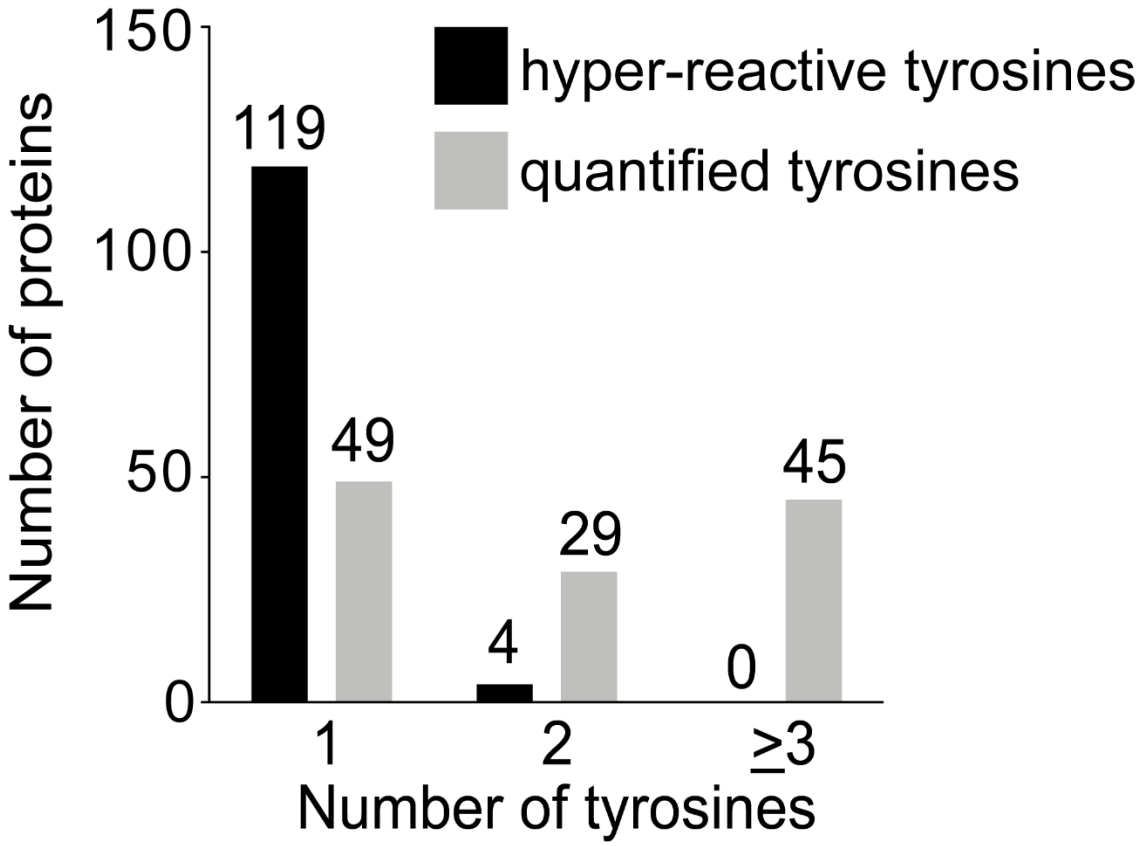

Figure 3.18. Bar plot of the number of hyper-reactive (high nucleophilicity) and quantified tyrosines per protein that contained at least a single hyper-reactive tyrosine. Data shown are representative of two experiments (n=2 biologically independent experiments). Data acquired by Hahm and Toroitich; Analysis conducted by Borne and Hsu.

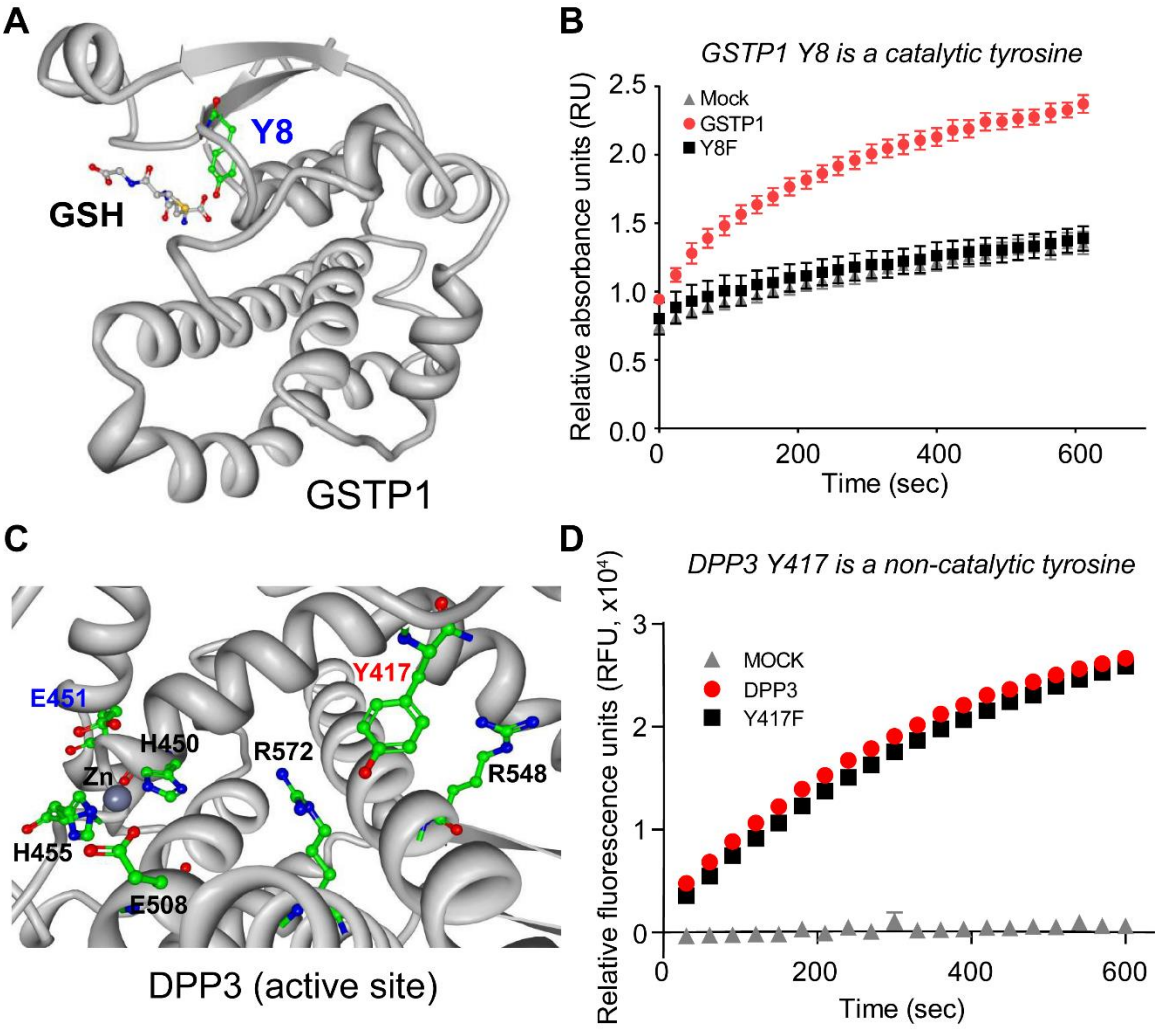

Figure 3.19. SuTEx probes target reactive catalytic and non-catalytic tyrosines of enzymes. A) Crystal structure of human GSTP1 (grey, PDB accession code 6GSS) shows tyrosine 8 (Y8) is located in the GSH binding site. B) Loss of biochemical activity in GSTP1 Y8F mutant supports tyrosine 8 as a catalytic residue. Biochemical activity of recombinant GSTP1-HEK293T proteomes (1 mg/mL) was assessed using a substrate assay measuring GSTP1-catalyzed conjugation of GSH to BDNB (10 min, 37 °C). See Fig. 3.20 for additional details. Data are shown as mean + s.e.m,; n=7 biologically independent experiments. C) Crystal structure of human DPP3 (grey, PDB accession code 3FVY)

showing location of residues involved in zinc metal binding (H450, H455, E508), the catalytic glutamate (E451), and a non-catalytic tyrosine 417 (Y417) identified by SuTEx. Positively-charged arginines (R548, R572) are found in close proximity to Y417. D) Recombinant DPP3- and Y417F mutant-HEK293T soluble proteomes (1 mg/mL) showed comparable activity in a peptidase substrate assay supporting Y417 as a non-catalytic tyrosine. Data are show as mean + s.e.m,; n=4 biologically independent experiments. Work conducted by Brulet.

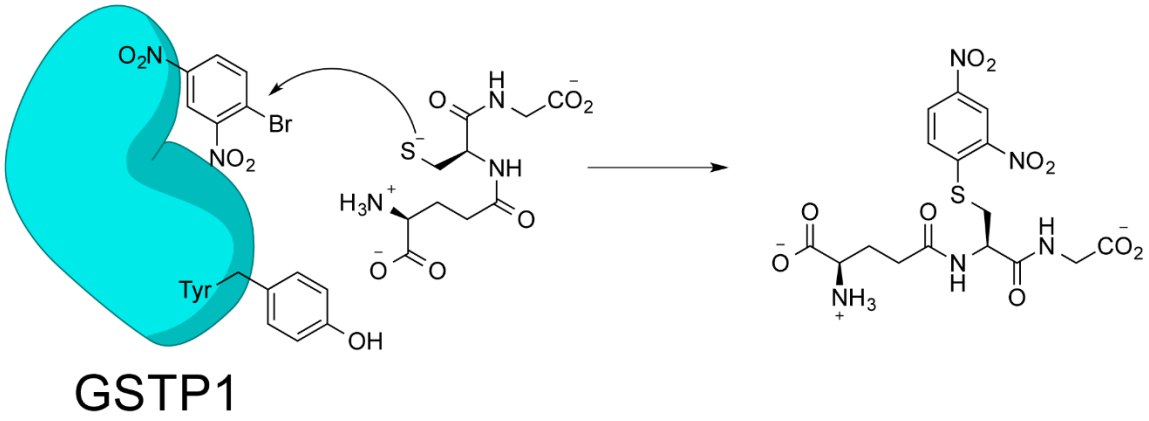

Figure 3.20. GSTP1 biochemical substrate assay. GSTP1 catalytic activity was evaluated by monitoring transfer of glutathione (GSH) to 1-bromo-2,4-dinitrobenzene (BDNB), which produces a dinitrophenyl thioether that can be detected spectrophotometrically by measuring absorbance at 340 nm. Scheme generated by Brulet and Hsu.

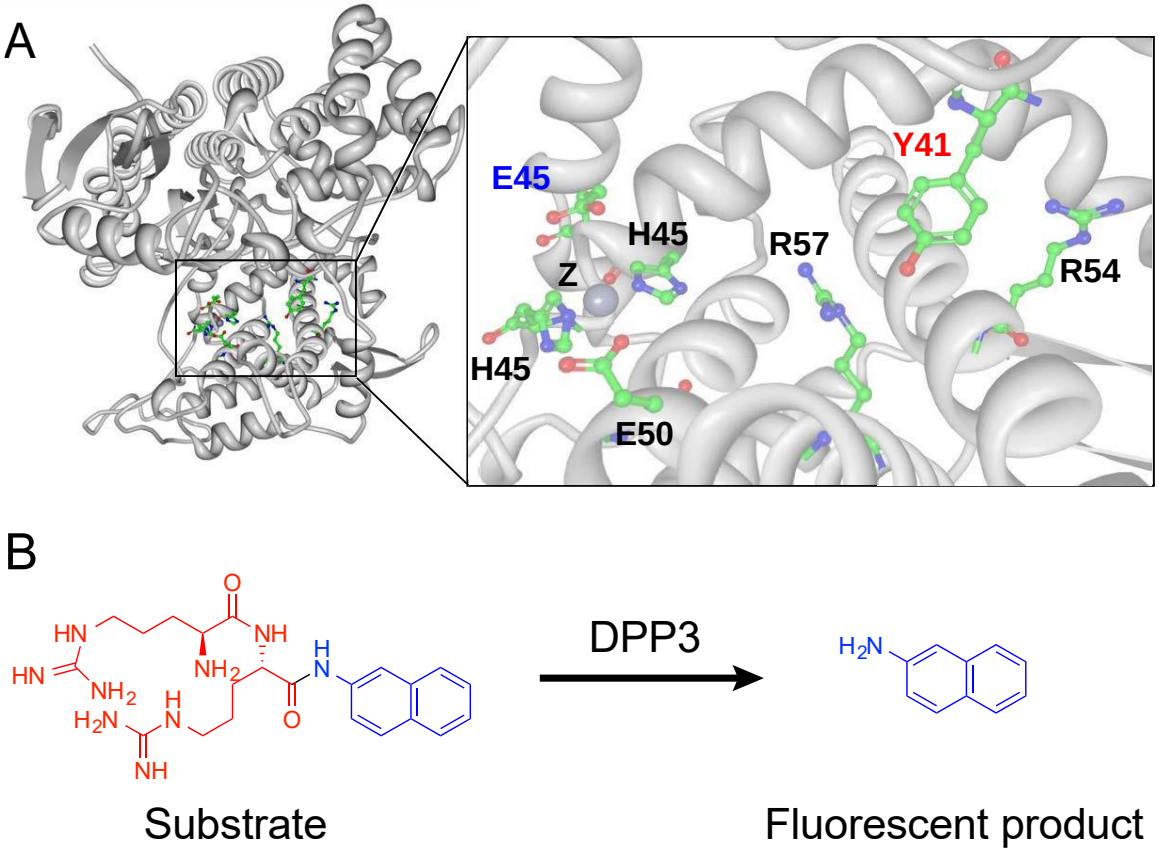

Figure 3.21. Substrate assay for evaluating DPP3 tyrosine 417 mutant. A) Crystal structure of human DPP3 (grey, PDB accession code 3FVY) showing location of residues involved in zinc metal binding (H450, H455, E508), the catalytic glutamate (E451), and a non-catalytic tyrosine 417 (Y417) identified by SuTEx. Positively-charged arginines (R548, R572) are found in close proximity to Y417. B) DPP3 cleaves Arg-Arg β- naphthylamide substrate to release the colored naphthylamide product that can be detected spectrophotometrically by measuring fluorescence at 450 nm. Work conducted by Hsu.

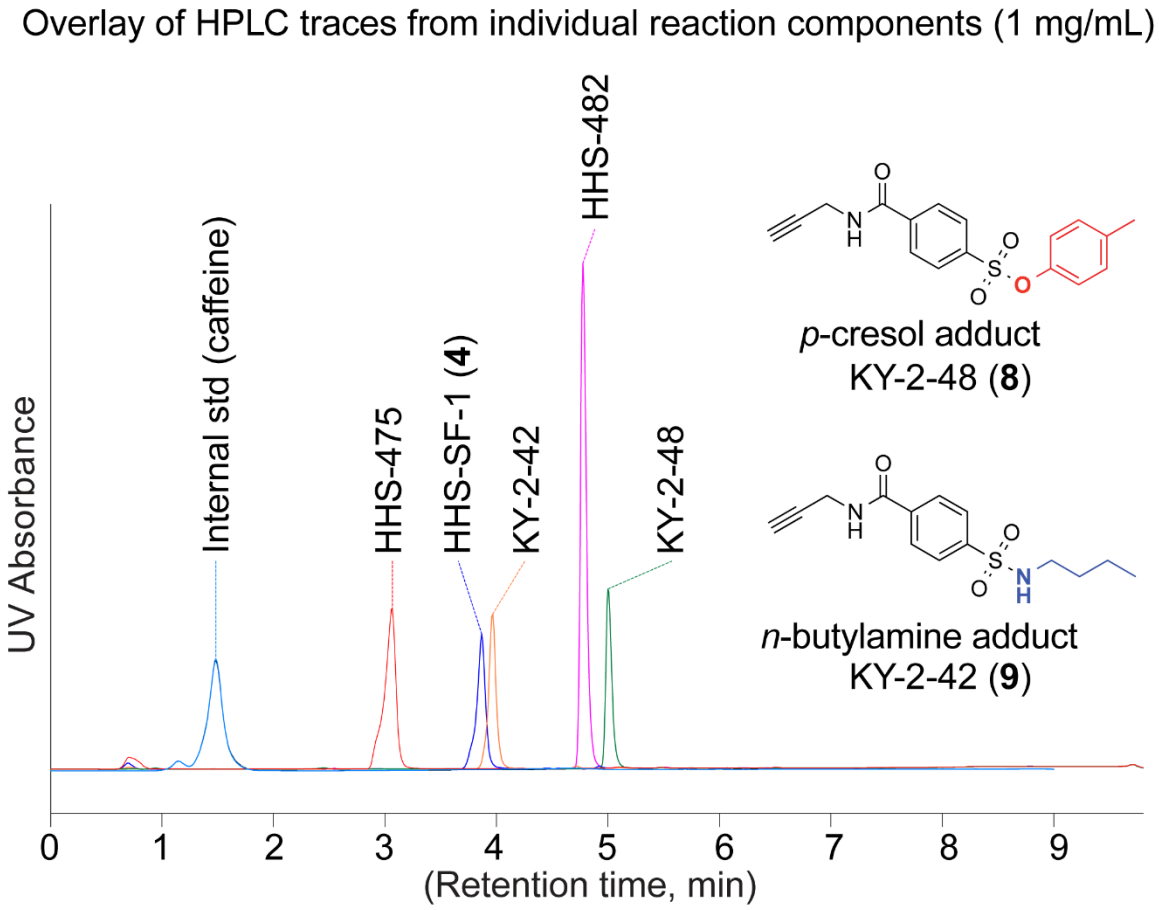

Figure 3.22. Overlay of individual HPLC traces at 1 mg/mL concentrations to show chromatographic resolution of reaction components: caffeine (sky blue), HHS-475 (red), HHS-SF-1 (blue), KY-2-42 (orange, n-butylamine-probe adduct), HHS-482 (pink), KY-2-48 (green, p-cresol-probe adduct). Caffeine was spiked into each sample as an internal standard to control for run-to-run variations in HPLC analysis (UV detection at 254 nm) of SuTEx and SuFEx reactions. Data shown are representative of two independent experiments (n=2). Work conducted by Hahm and Yuan.

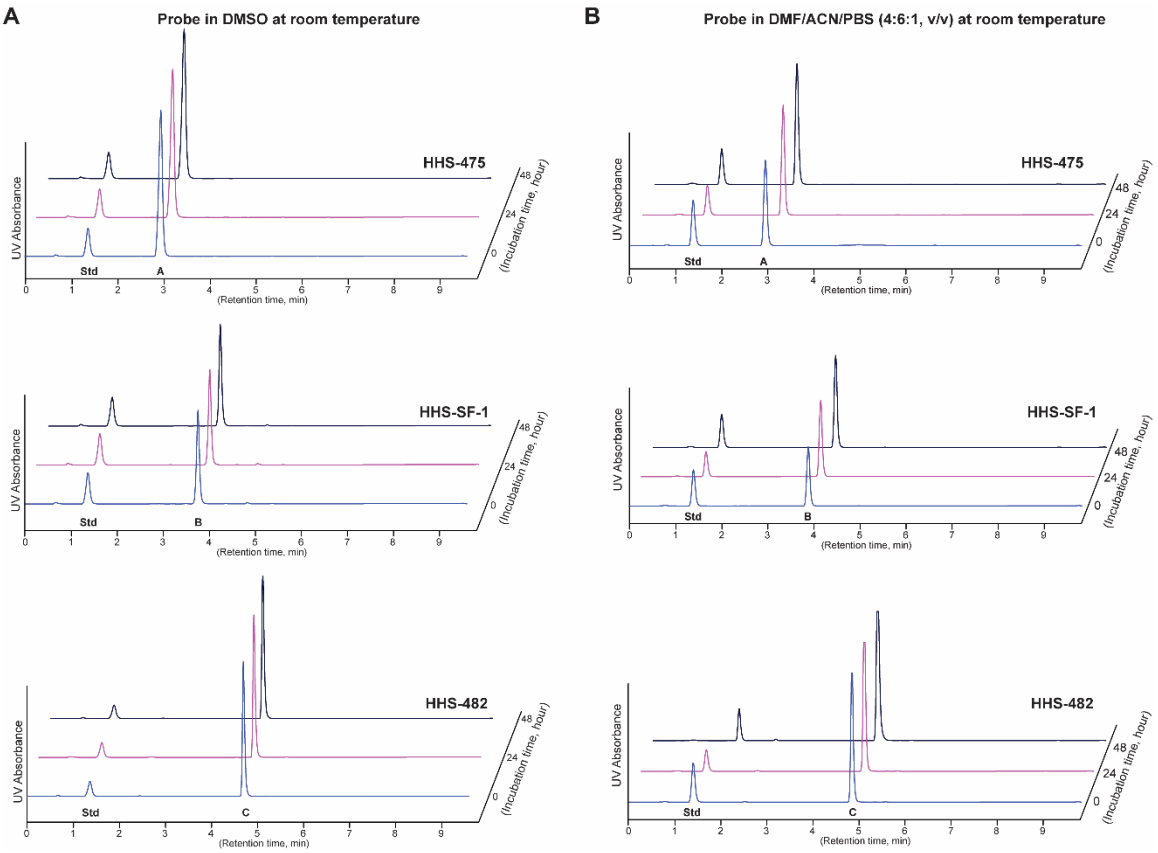

Figure 3.23. Stability of sulfonyl probes in DMSO and aqueous/solvent mixtures. DMSO solutions of HHS-475 (20 mM), HHS-SF-1 (20 mM), and HHS-482 (10 mM) were prepared and HPLC analysis of these probes measured at the indicated time points. Negligible degradation, as judged by reduction of probe signal, was observed after 24- and 48-hours incubation in DMSO or DMF:ACN:PBS (4:6:1, (v/v)) at room temperature. See Supplementary Methods for additional details of the stability assay. DMSO: dimethyl sulfoxide, DMF: dimethylformamide, ACN: acetonitrile, PBS: phosphate-buffered saline. Data shown are representative of three independent experiments (n=3). Work conducted by Hahm and Yuan.

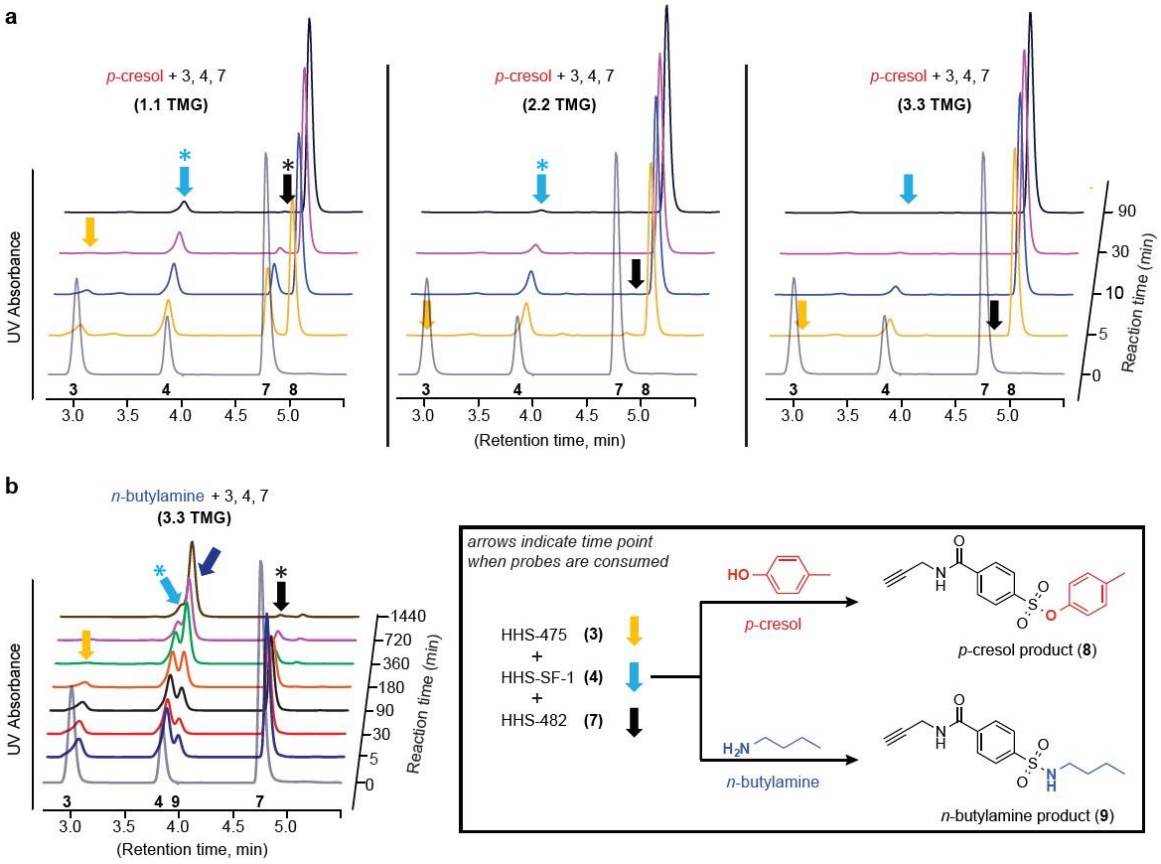

Figure 3.24. Triazole LG enhances phenol reactivity of sulfonyl probes in solution. a) A mixture of HHS-475 (peak 3), HHS-SF-1 (peak 4), and HHS-482 (peak 7) was incubated with p-cresol in the presence of increasing amounts of tetramethylguanidine (TMG) base and time dependent covalent reaction monitored by reduction of respective probe signal. Formation of the common p-cresol-probe adduct (peak 8) was confirmed by retention time that matched our synthetic standard KY-2-48 (Fig. 2.22). Colored arrows denote the time points when each respective probe was consumed, and the asterisks denote time points corresponding to substantial but not complete probe depletion. b) Reduced reactivity of n-butylamine against sulfonyl probes under high TMG conditions (3.3 equivalents). Formation of the n-butylamine-probe adduct (peak 9) was validated by retention time that

matched our KY-2-42 synthetic standard (Fig. 2.22). See Methods for additional details. Data shown are representative of three independent experiments (n=3). Work conducted by Hahm and Yuan.

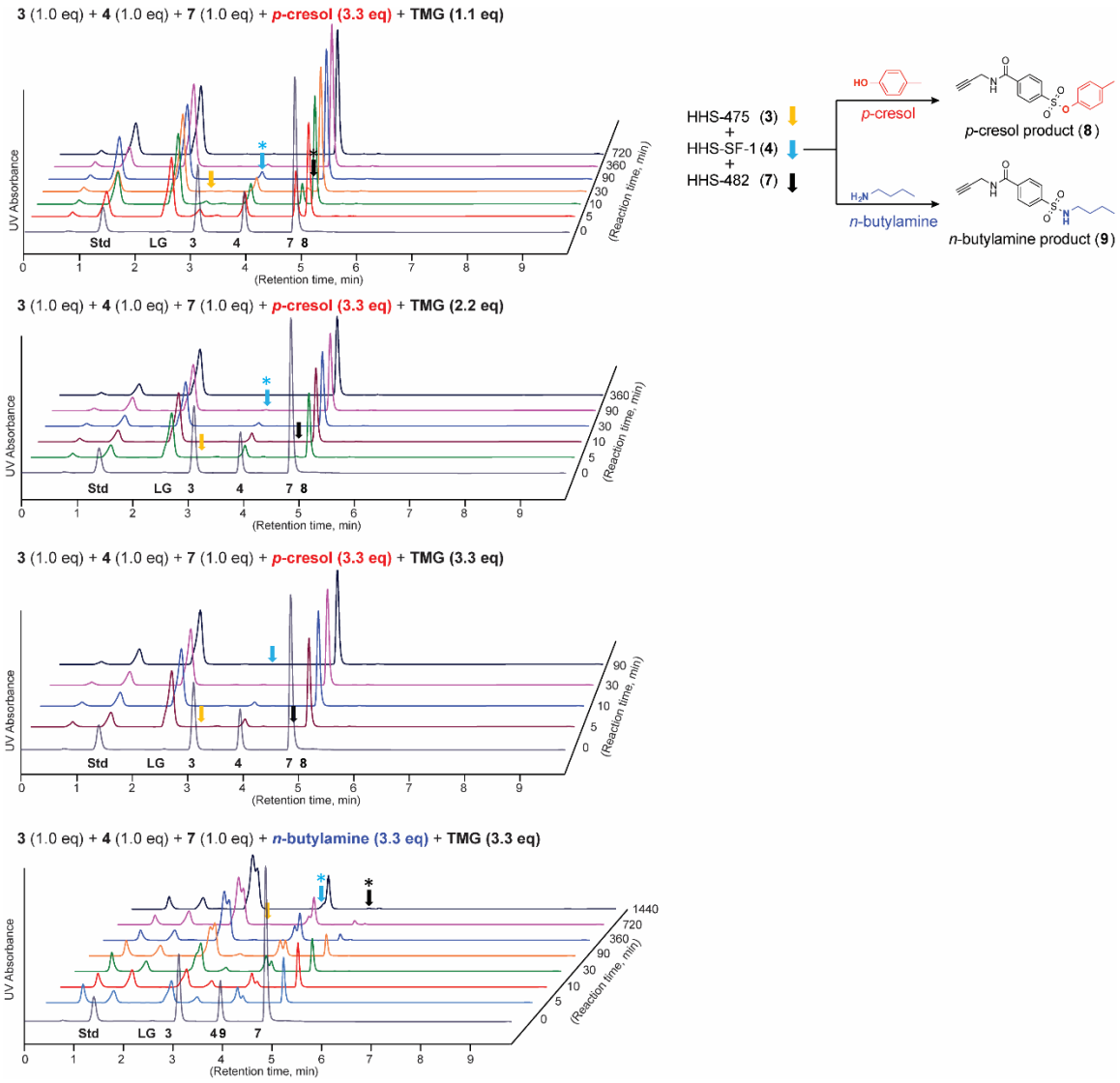

Figure 3.25. Comparison of SuTEx and SuFEx reactivity against nucleophiles in solution.

Time-dependent reactions between p-cresol or n-butylamine with a mixture of HHS-475 (peak 3), HHS-SF-1 (peak 4), and HHS-482 (peak 7) under increasing amounts of TMG base. Formation of the corresponding p-cresol-probe (peak 8) or n-butylamine-probe products (peak 9) was confirmed by retention times that matched the synthetic standards KY-2-48 and KY-2-42, respectively (Fig. 2.22). Std: internal standard, Caffeine, LG: leaving group of HHS-482 (3-(4-methoxy phenyl)-1,2,4-triazole) from covalent reaction, TMG: tetramethylguanidine. Data shown are representative of three independent experiments (n=3). Work conducted by Hahm and Yuan.

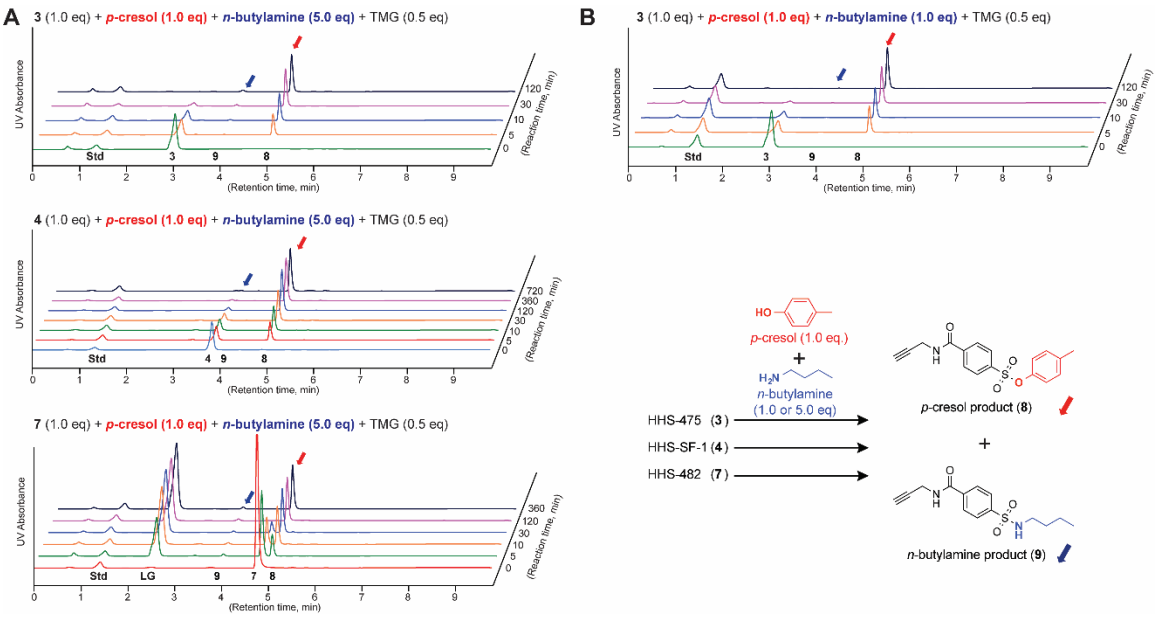

Figure 3.26. Chemoselectivity of sulfonyl probes against p-cresol and n-butylamine in solution. Reaction of individual sulfonyl probes against a mixture of n-butylamine and p-cresol mixture. Condition A shows the traces of a mixture of n-butylamine and p- cresol of 5:1 ratio under catalytic TMG (0.5 equivalents). Condition B entails the reaction of the

sulfonyl probes with a mixture of equivalent amounts of n-butylamine and p-cresol under catalytic amount of TMG (0.5 equivalents). Red arrows show formation of p- cresol-probe product (peak 8) and blue arrows show formation of n-butylamine-probe product (peak 9) under respective reaction conditions. Std: internal standard, caffeine, LG: leaving group of HHS-482 (3-(4-methoxy phenyl)-1,2,4-triazole) from covalent reaction, TMG: tetramethylguanidine. Data shown are representative of three independent experiments (n=3). Work conducted by Hahm and Yuan.

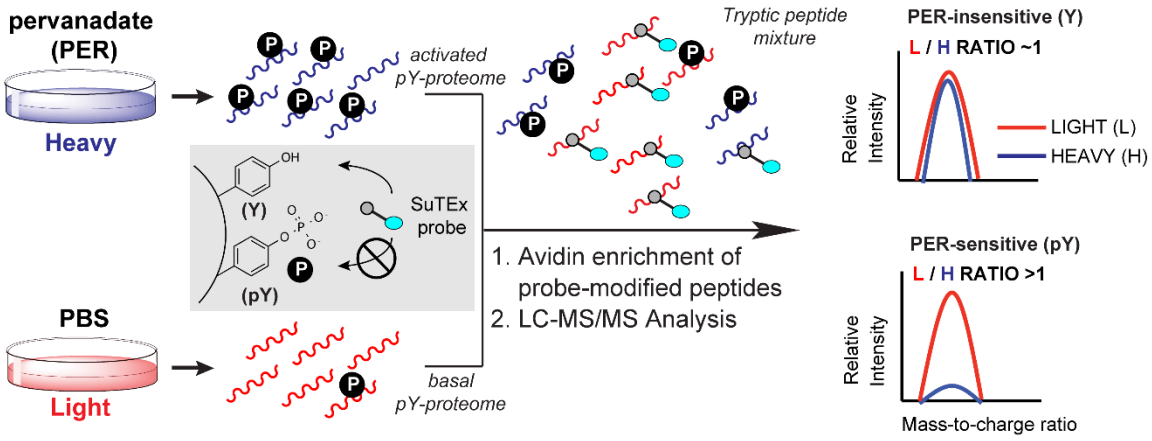

Figure 3.27. Schematic of a SuTEx platform for global tyrosine phosphoproteomic studies. Activation of tyrosine phosphorylation (pY) using a general tyrosine phosphatase inhibitor (pervanadate) will reduce availability of tyrosines (Y) for SuTEx probe labeling, which can be readout by quantitative chemical proteomics (SILAC). Scheme generated by Hsu.

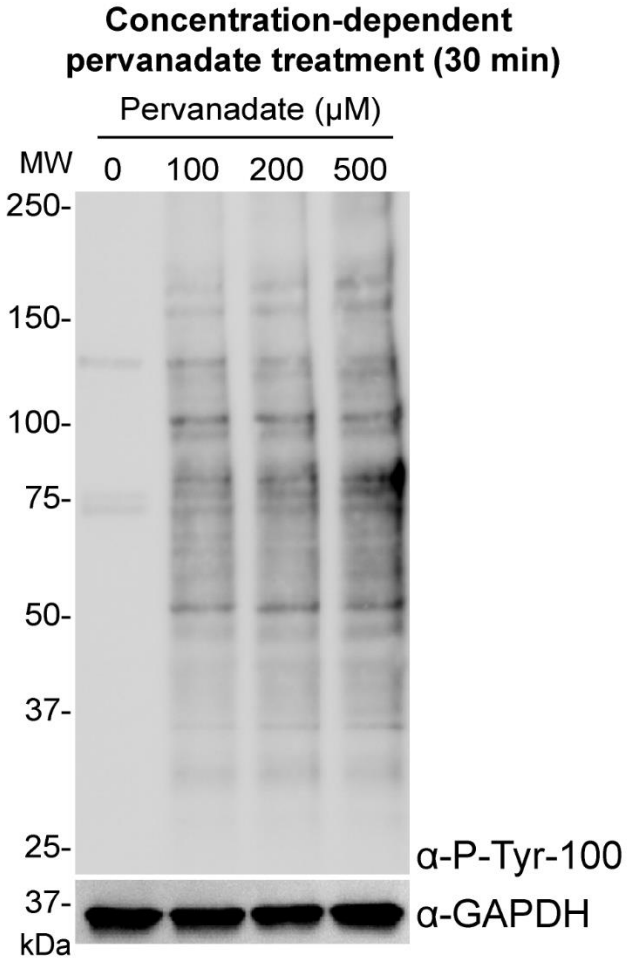

Figure 3.28. Concentration-dependent activation of global tyrosine phosphorylation. A549 cells were treated with vehicle (PBS) or pervanadate at the indicated concentrations for 30 min followed by cell lysis in PBS + protease and phosphatase inhibitors. Activation of global tyrosine phosphorylation was assessed by western blot analysis with a phospho-tyrosine monoclonal antibody (P-Tyr-100). Equivalent protein loading was confirmed using an antibody against GAPDH. Data shown are representative of two experiments (n=2 biologically independent experiments). Work conducted by Hahm.

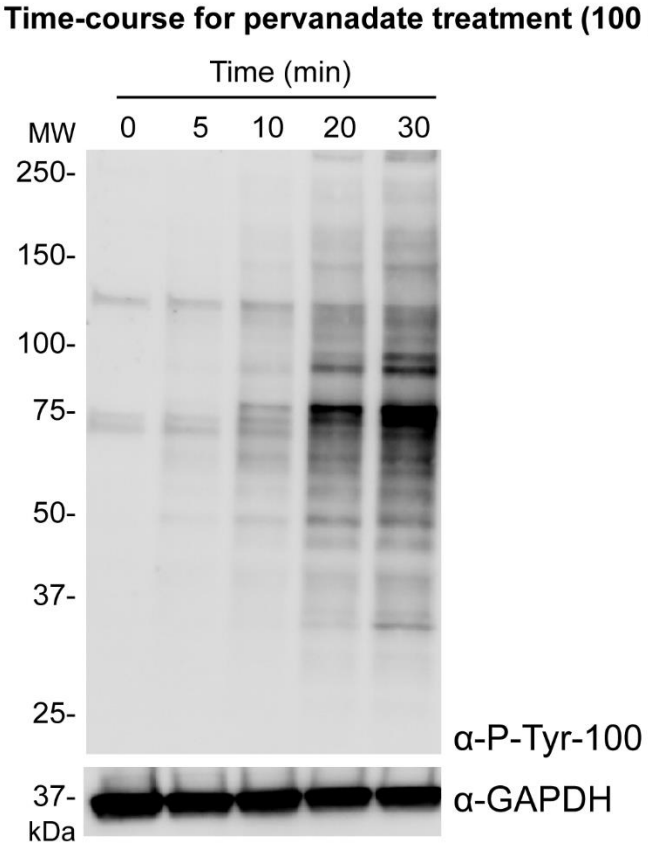

Figure 3.29. Time-dependent activation of global tyrosine phosphorylation. A549 cells were treated with vehicle (PBS) or pervanadate (100 µM) and lysed in PBS + protease and phosphatase inhibitors at the indicated time points. Global tyrosine phosphorylation activation measured by western blot analysis using a phospho-tyrosine monoclonal antibody (P-Tyr-100). Equivalent protein loading was confirmed using an antibody against GAPDH. Data shown are representative of two experiments (n=2 biologically independent experiments). Work conducted by Hahm.

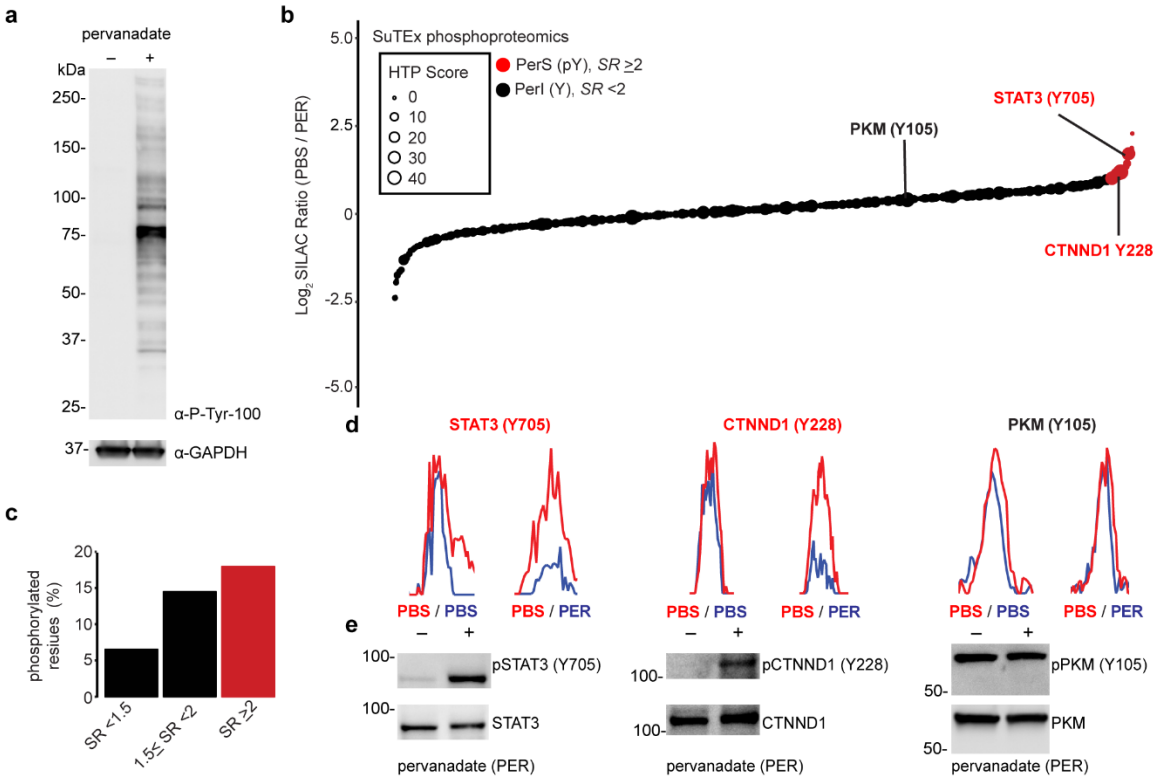

Figure 3.30. Chemical phosphotyrosine-proteomics by SuTEx. a) Western blot analysis confirming activation of global tyrosine phosphorylation (detected via a phospho-tyrosine monoclonal antibody, P-Tyr-100) with pervanadate treatment conditions of A549 cells (100 µM, 30 min) used for chemical proteomic studies. b) Plot of HHS-475-modified tyrosine sites (represented by individual circles) as a function of SILAC ratios (SR, light (PBS)/heavy (pervanadate or PER)). Size of circles reflect the HTP score (PhosphoSitePlus). Tyrosine sites were further segregated into pervanadate-insensitive (PerI) and -sensitive (PerS) groups based on SR <2 or >2, respectively. Soluble proteomes from pervanadate activated-A549 cells were labeled with HHS-475 (100 µM) for 30 min at 37 °C. c) Bar plot showing trend towards increased number of phosphotyrosine annotations (HTP >10) on tyrosine sites with enhanced pervanadate sensitivity. Validation

that blockade of HHS-475 labeling (d) of individual tyrosine sites on STAT3 (Y705), CTNND1 (Y228), and PKM (Y105) coincides with increased phosphorylation at respective sites with pervanadate activation (e). Equivalent protein loading was confirmed by western blot analysis of non-phosphorylated protein counterparts. See Methods for additional details of pervanadate activation and phosphotyrosine western blot procedures. All data shown are representative of two experiments (n=2 biologically independent experiments). Data acquired by Hahm and Toroitich; Analysis conducted by Borne; Gel work conducted by Hahm and Toroitich.

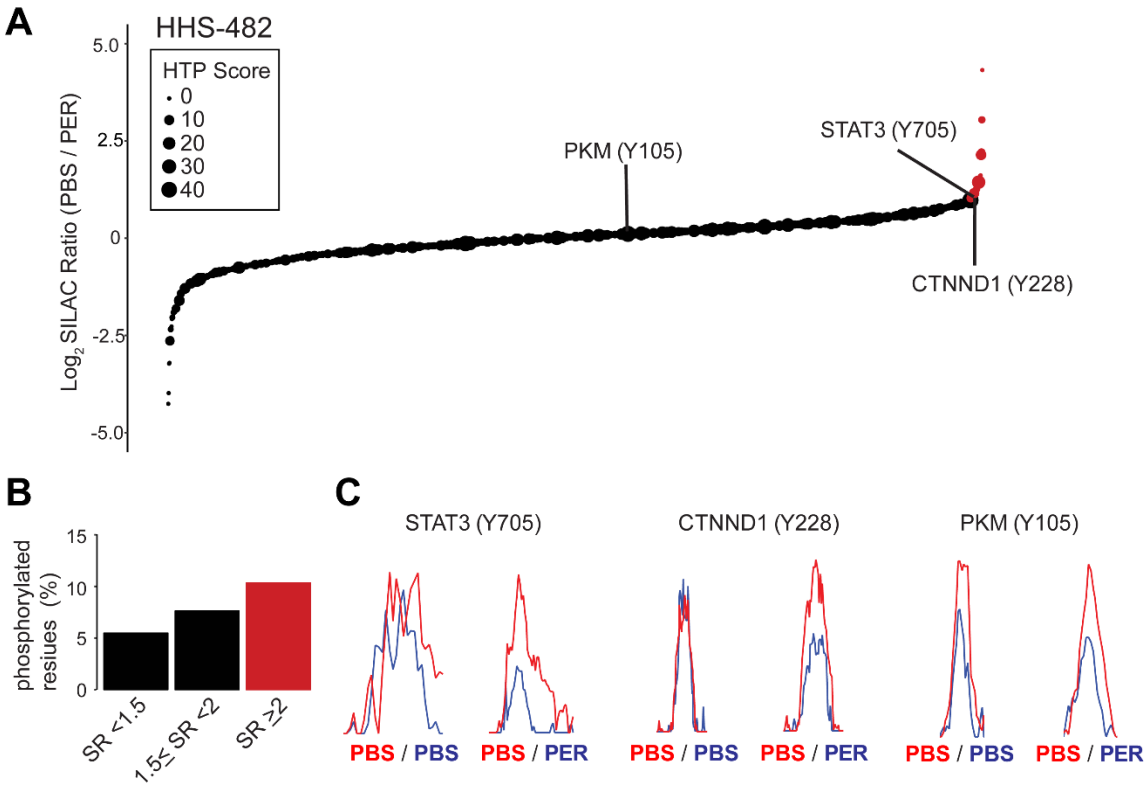

Figure 3.31. Chemical phosphotyrosine-proteomics by HHS-482. (A) Plot of HHS-482-modified tyrosine sites (represented by individual circles) as a function of SILAC ratios (SR, light (PBS)/heavy (pervanadate or PER)). Size of circles reflect the number of phosphotyrosine high throughput annotations on PhosphoSitePlus (HTP score). Tyrosine sites were further segregated into pervanadate-insensitive (black circles) and -sensitive (red circles) groups based on SR <2 or >2, respectively. Soluble proteomes from pervanadate activated-A549 cells were labeled with HHS-482 (100 µM) for 30 min at 37°C. (B) Bar plot showing trend towards increased phosphotyrosine annotation (HTP >10) in tyrosine sites with enhanced pervanadate sensitivity. (C) Validation that blockade of HHS-482 labeling of individual tyrosine sites on STAT3 (Y705), CTNND1 (Y228), and PKM (Y105) coincides with increased phosphorylation at respective sites with pervanadate activation (see Fig 7F). See Table S1 for SR values of tyrosines sites detected by chemical proteomics. Data shown are representative of two experiments (n=2 biologically independent experiments). Data acquired by Hahm and Toroitich; Analysis conducted by Borne; Gel work conducted by Hahm and Toroitich.

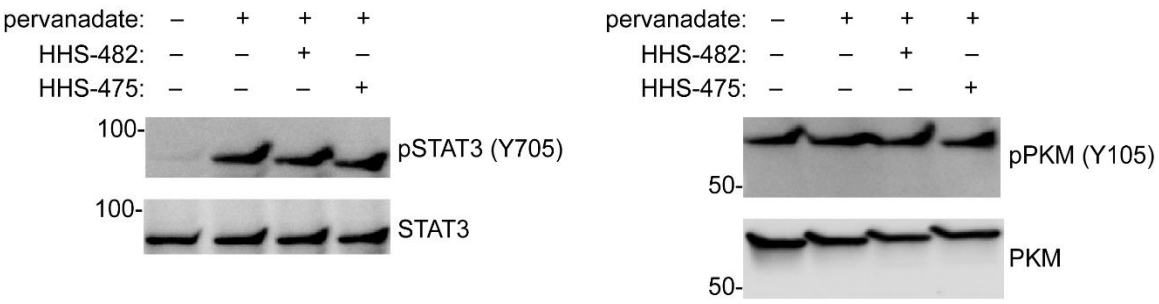

Figure 3.32. SuTEx probe treatment of proteomes from pervanadate-treated cells does not displace phospho-tyrosines. A549 cells were treated with vehicle (PBS) or pervanadate (100 µM, 30 min) followed by lysis in PBS + protease and phosphatase inhibitors. Proteomes from pervanadate-treated cells were treated with either HHS-482 or HHS-475 (100 µM of SuTEx probe) for 30 min at 37 °C followed by western blot analysis of individual tyrosine sites on STAT3 (Y705) and PKM (Y105). Treatment with either HHS-482 or HHS-475 did not affect phosphotyrosine signals indicating that SuTEx probes do not non-specifically displace phosphates from tyrosines. See Methods for additional details of western blot analyses. Data shown are representative of two experiments (n=2 biologically independent experiments). Work conducted by Hahm.

Chapter 4. Development of Computational Methods for Chemical Probe Mass Spectrometry Data

CPASS was developed and applied to datasets ultimately published in*: Jeffrey W. Brulet, Adam L. Borne, Kun Yuan, Adam H. Libby and Ku-Lung Hsu Journal of the American Chemical Society, 142(18), pp.8270-8280.*

4.1 Abstract

Performing effective site-specific activity-based protein profiling (ABPP) depends on the ability to confidently identify and quantify sites of probe modification and the availability of computational tools to interpret the results. Tools built using the amino acid level specificity of this approach have the potential to reveal new insights about the probe and probe targets. Chemical Probe Analysis Suite for Site-specific Mass Spectrometry (CPASS-MS) is versatile toolkit built in the galaxy framework to provide confidence in targets identified and analyze the targets based on the information gained by discerning the site of modification. Using this approach we show the specificity of ATP-acyl phosphate for the kinase domain, profile SuTEx lysine reactivity, illustrate the ability to change the proteome reactivity of SuTEx ligands, and screen SuTEx fragment electrophiles *in silico.*

4.2 Introduction

The ABPP techniques presented thus far have been used to identify targets of a known inhibitor, profile a global tyrosine probe across several proteomes, and monitor phosphotyrosine abundance. This work combined with work other on ABPP experimental strategies continue to expand the capabilities of chemical biology techniques[21,26,27]. Fragment electrophile competitive ABPP is another technique used to screen covalent small molecules to identify their targets across a proteome[27,28]. This technique enables the discovery of important ligands for difficult to access target as well as provide new modalities to study well known targets[21].

The analysis of the such data is complex even when compared to other ABPP strategies as it is usually paired with various multi-plexing techniques (SILAC, TMT) to semi-quantitatively compare peptide abundances[26,29,36]. This dataset does not rely on various tryptic peptides to identify a protein. Instead, it uses a probe modified MS2 or MS3 spectra from a few peptides to identify the site modified[19,29]. Gaining deeper insights into this type of data requires the optimization of coverage while minimizing false positives to produce reliable and verbose datasets.

Once the sites have been identified and quantified they can be used with a series of computational tools to identify important features in the data[27,91,164]. Tools like gene ontology and gene set enrichment have been used to find important protein groups targeted by the ABPs or fragment electrophiles[91,169]. Yet, these tools do not take advantage of the additional insights gained by knowing the site of modification. Recently a few tools have become available that do[90,170], but this is far from exhausting the potential of being able to

survey specific sites. Thus, to gain deeper insights new tools are needed that are built to harness the site-specific information gained using a chemical probe.

Collectively these issues represent a need in the chemical biology field for tools that can address the challenges of site-specific proteome profiling while leveraging it to make discoveries. To this end we created Chemical Probe Analysis Suite for Site-specific Mass Spectrometry (CPASS-MS) a galaxy[171] integrated tool kit for identifying probe modified sites and taking advantage of site-specific data (Fig. 4.1). Here we use this analysis suite to profile the ATP-acyl phosphate probe, profile the lysine reactivity of SuTEx probes, perform competitive ABPP experiments with SuTEx fragment electrophiles and conduct an *in silico* SuTEx fragment electrophile screen. The versatile nature of the toolkit provides the methods to perform all these tasks within as single framework as well as develop workflows to reproducible perform the analysis.

4.3 Materials and Methods

SILAC cell culture. SILAC cells were cultured at 37 °C with 5% CO2 in either 'light' or 'heavy' media supplemented with 10% dialyzed fetal bovine serum (Omega Scientific), 1% L-glutamine (Fisher Scientific), and isotopically labeled amino acids. Light media was supplemented with 100 μg ml−1 L-arginine and 100 μg ml−1 L-lysine. Heavy media was supplemented with 100 μg ml−1 [13C 15N] L-arginine and 100 μg ml−1 [13C 15N] L-lysine. Labelled amino acids were incorporated for at least five passages before utilizing SILAC cells for experiments. Media was aspirated and cells washed with cold PBS (2X) before scraping from plates. Cells were transferred to microfuge tubes and pelleted by

centrifugation at 500 x g for 5 min, and snap-frozen using liquid N2 and stored -80 °C until further use.

Gel-based chemical proteomic assay. Cell pellets were lysed in PBS and fractionated (100,000 x g, 45 min, 4 °C) to generate soluble and membrane fractions. Protein concentrations were determined using Bio-Rad DC protein assay and adjusted to 1 mgml-1 in PBS. Proteome samples (49 μL aliquots) were treated with DMSO vehicle or indicated concentration of SuTEx fragment (1 μL, 50X stock in DMSO) for 30 min at 37 °C. Samples were then treated with HHS-482 probe (1 μL, 2.5 mM stock in DMSO) for 30 min at 37 °C. Probe labeled samples were conjugated to rhodamine-azide (1 μL, 1.25 mM stock; final concentration of 25 μM) by copper-catalyzed azide-alkyne cycloadditions (CuAAC) for 1 hr at room temperature followed by SDS-PAGE and in-gel fluorescence scanning as previously described[172].

Live cell evaluation of sulfonyl-triazole fragments. Cells grown to ~90% confluency in 10 cm plates were treated with DMSO vehicle or SuTEx fragment (10 μl of 1,000X stock) in serum-free media for the indicated concentrations and times at 37 °C with 5% CO2. After treatment, cells were washed with cold PBS twice before collection and preparation for gel-based chemical proteomic evaluation as described above. For LC–MS studies, protein concentrations were normalized to 2.3 mg ml−1 and 432 μl (for 1 mg final protein amount) were used for sample preparation as detailed below.

Preparation of SILAC proteomes for liquid chromatography–tandem mass spectrometry (LC–MS/MS) analysis. Heavy and light proteomes (432 µl of each) were diluted to 2.3 mg ml−1 in PBS and sample aliquots (432 µl) were treated with SuTEx fragment at the indicated concentrations (5 µl, 100X stock in DMSO), mixed gently and incubated for 30 min at 37 °C. Samples were then treated with HHS-482 (5 µL, 5 mM stock in DMSO) for 30 min at 37 °C. Probe-modified proteomes were conjugated to desthiobiotin-PEG3-azide followed by enrichment of probe-modified peptides for nano-electrospray ionization– LC–MS/MS analyses as previously described[172]**.**

Software Design. The production server of CPASS-MS is built on a CentOS operating system. CPASS-MS uses SciPy, Statsmodels, Pandas and xlrd external python packages as well as the plyr, dplyr, readr, stringr, reticulate, ggplot2, htmlwidgets, d3heatmaps and cdgsr external R libraries.

Data Format. CPASS-MS accepts Byonic XLSX files as well as MZID files generated by other search software[17]. Additionally, skyline output can be used to incorporate Isotope Dot Products (IDOTP), Ratio Dot Products (RDOTP), as well as metabolic labeling ratio calculations[86]. Spectral files are provided as targeted Mascot Generic Format (MGF) files produced by Byonic searches. CPASS-MS works with Stable Isotope Labeling of Amino Acids in Cell Culture (SILAC) and Tandem Mass Tag (TMT) quantification methods[48,49].

Processing of Search Results into Probe Modified Sites. In order to access the rest of

the tools C peptide spectra matches (PSMs) are converted to sites. Since several peptides can be created from oxidation events, missed cleavages (particularly for lysine probes), and post-translational modifications (PTMs) a single probe modified amino acid on a protein can produce various peptides[16]. These various peptides are combined into sites to create the most complete representation of the quantitative value (SILAC ratio, or reporter ion abundance) for each probe modified amino acid. All probe modified peptides provided to CPASS-MS are converted to a UniprotID_Residue (i.e. P9999_10) format to represent the site. The specified quantitative value for each site will be determined by taking the median of all peptides that represent that site.

This tool allows for the use of specific filters from the various data sources. Some basic thresholds can be applied for all searches, this includes parts-per million (ppm) error of precursor ions, requiring specific cleavage, minimum and maximum peptide length, and uses the Byonic Score to filter based on quality of PSM[17]. If skyline is used it can also include filtering by IDOTP, and RDOTP (SILAC only)[105].

CPASS-MS can use the provided spectral information to ensure that spectra contain specific diagnostic adducts. Probes during High-Energy Induced Dissociation (HCD) are fragmented in predictable ways. This frequently produces highly abundant ions that can be used to ensure the peptide of interest is probe modified. Additionally, these ions are frequently ignored by the search algorithms. Using this as a filter can provide confidence when looking at peptides that produce few fragment ions (like shorter peptides) that have lower database search scores[15]. Diagnostic adducts are unique to the probe, and the process of Copper-Catalyzed Click Chemistry produces a 240.1704 ion that can be used with any

probe enriched using this technique (ion d2 Fig. 3.1.a, 3.5-3.9).

Replicates are specified using a format file that matches the search result mzid to an experimental design. The resulting data is in a tabular format usable by the rest of the tools in CPASS-MS and it includes the probe modified site, median or mean quantitative value across replicates, standard deviation, standard error, gene name, the treatment condition, all peptides attributed to the site, all scans that represent the site as well as the best scoring peptide spectra match for each peptide.

Basic Filtering of CPASS-MS Formatted Data and Cross Treatment Thresholds. CPASS-MS formatted data can then further be filtered by the treatment conditions, or the quantitative value. One treatment's quantitative value can be used to filter any number of the other treatments (i.e. In SILAC data a Light Probe treated, Heavy No Probe treated control can be filtered for a SILAC Ratio greater than 5 and the other treatments can be filtered by sites that meet this threshold in this control)[36]. This tool can also be used to separate treatment conditions into their own CPASS-MS formatted file.

Domain Enrichment Analysis. Since the CPASS-MS works with specific sites of modification it enables the identification of domains that are labeled. Identification of enriched domain is done as described in chapter 3, but CPASS-MS includes the ability to adjust the Q-value cutoff used to make the graph as well as use a hypergeometric test as well as a binomial test. This option was included as it is a more stringent option that more accurately represents the underlying distribution:

$$P = \frac{\binom{n(D)}{k}\binom{N-n(D)}{n-k}}{\binom{N}{n}}$$

Hypergeometric test

where n(D) is the number of domain occurrences in the database, N is the total number of domains in the reference database, k is the number of a specific domain in the dataset, and n is the total number of domains annotated in the dataset. P-values are corrected for a 1% false discovery rate using Benjmani-Hochberg correction for multiple comparisons. CPASS-MS will also produce a bar graph, a complete list of domain annotations, and the statistical test results.

Subcellular Location Decision Tree Analysis. Since chemical probes must penetrate cellular barriers to access certain proteins for modification CPASS-MS uses a decision tree algorithm to identify the most accessible subcellular location for the protein modification (Fig. 3.2). A protein that can be detected in various compartments would receive allocation assignment matching the most accessible location. For example, MAPK1 has been shown to translocate from the plasma membrane through the cytosol to the nucleus[173]. MAPK1 would be considered a plasma membrane protein using this subcellular location analysis algorithm. Membranes of organelles are grouped into respective organelles because a molecule can interact with membrane proteins without necessarily passing through membranes. A protein is excluded from the analysis if it does not have a CCGO annotation. The tool produces a bar graph with y-axis of annotated compartment in dataset as a percent of database entries and as a percent of overall dataset entries with the fill of each bar

representing the other, a count file, and a complete list of proteins with all CCGO terms and final designations.

pKa Analysis of Probe Modified Sites. The propka runner tool in CPASS-MS can analyze the pKa and Buried percent of a structure modified sites using propka[174]. The pka grapher combines this data with a CPASS-MS formatted file compares pKas of modified aimino acid to pKas of unmodified amino acids of the same species (i.e. SuTEx probes modify tyrosine thus it will be compared to other tyrosine). The statistical significance is determined using a Welch t-test as there are unequal sample sizes and the variance is unequal. It also compares Buried percent with statistical significance determined using a Wilcoxon rank-sum test. This method can be applied to a single protein structure or a group of structures. Note that not all proteins labeled will a have a crystal structure that can be used for this analysis. This tool will produce bar plot comparing the two groups for buried percent and propka, it will also produce a Manhattan plot of sites, and the propka output for every protein structure provided. Running a single file will produce a more detailed propka report for the structure. The get best structure tool can be used to aid in identifying optimal crystal structures but should be manually validated for site structure amino acid position matching and potential mutations that would produce changes in protein activity.

Post-Translation Modification Database Comparisons. Various probes will label amino acids that are also sites of PTMs (i.e. SuTEx modifies tyrosine, where phosphorylation occurs). This tool will compare the sites to the Phosphosite Plus[153] databases for

phosphorylation, ubiquitination, acetylation and methylation. Since several of these PTMs are on lysine tool can be rerun using different PTMs. The tool will produce a list of all sites that have the post-translational modification and pie chart showing what percent of sites have the PTM chosen.

DrugBank Database Comparison. Chemical probes are used to develop high throughput screening and activity-based screening approaches for targets that have been previously difficult to access. This tool aims to understand the current ligand and inhibitor landscape of the probe modified proteins by comparing the dataset to the DrugBank Databases[152]. This tool will provide the database entry information as well as provide a pie chart of the proteins with FDA approved and non-FDA approved ligands from DrugBank.

Interactive Heatmap Generator. This tool will generate a HTML and a static image heatmap for all the various treatments in the datasets. This tool has a hard maximum of 10.0 and will only show sites seen in all treatments. The heatmaps is clustered on the y and x axis using hierarchical clustering.

MEME File Formatter. Using a CPASS-MS formatted file a MEME formatted fasta file can be generated for the amino acid sequences flanking the probe modified sites[175]. The length of the sequences is specified by the user.

Site Specific Docking Screen. The tool takes a list of compounds and their SMILES

string[176] and converts them into 3D structures using open babel. The compounds are then docked to a user provide protein structure using AutoDock Vina[177]. The docking region is determined by the probe modified site provided by the user. The tool returns an excel with the binding affinity of all conformations for all structures docked and a zip file containing all the conformations for the compounds provided. These can be used with molecular visualization software (i.e. PyMOL[178]) for further investigation.

4.4 Results

4.4.1. Development of CPASS-MS

To take advantage of the site-specific features and perform reproducible analysis of probe modified mass spectrometry data we developed CPASS-MS (Fig. 4.1). It is written in R and Python and integrated into the Galaxy framework for data management and use of built-in workflows[171]. The software integrates peptide spectra matching (PSM) software results with skyline quality controls to identify probe modified sites and quantifies those sites using SILAC and TMT labeling strategies. This processing step produces a CPASS-MS formatted dataset that can be used with all tools in the analysis suite.

The tools include an integrated enrichment analysis tools for gene ontology and MEME motif analysis. In addition, there are custom tools to determine amino acid specificity and perform a domain enrichment analysis. These tools are designed for site-specific mass spectrometry datasets generated using chemical biology techniques. To investigate the component of the cell a probe or ligand reaches a subcellular location analysis for live cell treatments was developed that categorize protein targets based on their

most accessible subcellular compartment. The integration of propka tool performs pKa and depth calculations for structural data that is then compared to probe modified site data for identification of unique microenvironments of probe labeled peptides. When performing competitive ABPP experiments the quantitative values can be used to generate a clustered interactive heatmap for identification of patterns in inhibitor profiles. Finally, there is an integrated AutoDock Vina docking tool that screens series of compounds against a 3D protein structure with the docking region defined by the probe modified site of interest.

4.4.2. Analysis of ATP-acyl phosphate data

Results from previous studies have used a list of kinase sites aggregated from previously annotated MS2 spectra to filter results for only kinases. To identify sites independent of these lists we searched a selection of previously published datasets (Table 4.1) using byonic software as described in chapter 3 but using a lysine variable modification of (+196.1212 Da)[36,179]. Next sites are identified using CPASS-MS processing. This resulted in 89 high confidence ATP-acyl phosphate modified sites that had ATP competition SILAC Ratio (SR) > 5 across 83 proteins (Table 4.2).

Using this reanalyzed data, we performed a domain enrichment analysis (Q-value < 0.01) on the ATP competitive sites and found the protein kinase domain (PRU00159) to be the most enriched domain (Fig 4.3.a) with 24 sites from 23 proteins of a possible 512 annotated kinase domains. The kinase domain of CDK5 was labeled on both lysine 33 and 128. The only other enriched domain was the Stathim-like domain (SLD, PRU00998) with 3 sites from 3 proteins of a possible 5 annotated (Table 4.3)[180]. We performed

ubiquitination, methylation, and acetylation PTM database comparison (Fig. 4.3.b-d) and found that the sites were frequently ubiquitinated with 55 site and rarely methylated having only 1 site. Acetylation was in the middle with 25 sites.

4.4.3. HHS-465 and HHS-475 live cell lysine coverage

It was previously shown that lysine was the second most likely amino acid modified by HHS-465 and HHS-475 (Figure 3.4). We analyzed the live cell datasets from Chapter 3 changing our byonic search parameters to identify lysine sites by setting a variable modification of (+635.27374) on both tyrosine and lysine. Byonic frequently improperly annotated a c-terminal lysine modification on a peptide that had a tyrosine modified site so peptides that had an c-term lysine modification and a tyrosine modification in the same sequence was removed in R prior to use in CPASS-MS. We then performed CPASS-MS processing manually and identified ~4,100 distinct lysine sites (corresponding to ~1,200 proteins), in total, across membrane and soluble fractions in all cell lines tested (HEK293T and Jurkat, Table 4.4). HHS-465 had the most unique targets with ~40% of the targets being unique compared to ~20% for HHS-475 (Fig 4.4.a).

Domain enrichment analysis (Q-values < 0.01) of all sites found that RNA recognition motif (RRM, PRU00176) and thioredoxin domain (PRU00691) were highly enriched (Fig. 4.4.b, Table 4.5). Upon performing the drug bank comparison, we found 67% of HHS-465 and HHS-475 live cell lysine labeled proteins were absent from the DrugBank database (Table 4.6, Fig. 4.4.c) compared to 77% of the live cell profiled tyrosine sites (Fig. 3.10.d)[152]. Evaluation of probe-enriched domains from the DrugBank

protein group (DBP) was largely overrepresented with domains found in enzymes (thioredoxin and kinases, Table 4.8, Fig. 4.4.c)[85,181]. By comparison, the non-DrugBank protein (non-DBP) group revealed highly enriched domains including the nucleotide binding RRM and protein-protein interactions domains (PCI[182] and DZF[183] domains, PRU01185 and PRU01040, Table 4.7). These results largely matched the results seen in the tyrosine profiling of the same live cell data (Fig. 3.10.d).

The probe modified lysines could overlap with sites of ubiquitination, methylation, acetylation as well as other less annotated PTMs. To investigate this, we compared the live cell probe modified sites to respective Phosphosite plus database using the database comparison tool. We found that ~66% of the sites have been previously annotated as sites of ubiquitination (Fig. 4.5.a), few sites were previously annotated as methylation sites (Fig. 4.5.b), and ~33% of sites were sites of acetylation (Fig. 4.5.c). It has not previously been shown that the HHS-465 and HSS-475 probes are able to access all subcellular locations thus we analyzed the live cell sites to get a breakdown of proteins with modified lysines across different subcellular compartments. As expected, we identified proteins in all cellular compartment with ~13% of the proteins that could be modified in the mitochondria were modified. The most frequent subcellular location for the probe to modify was the cytoplasm as ~60% of the proteins that were modified were found in the cytoplasm (Fig. 4.5.d, Table 4.8).

4.4.4. Competitive ABPP using CPASS-MS

The common SuTEx electrophile core was structurally elaborated with diverse small molecule binding elements on both the adduct group (AG) and LG to create library

members with an average molecular weight of 336 Da (Fig 4.6). Fragments were created with structural elements bearing differing electron-withdrawing (EWG) or -donating (EDG) properties to test substituent effects on thr SuTEx reaction mechanism. Functional groups that are EWG by both resonance and polar interactions (cyano) as well as substituents (fluoro) with opposing effects from resonance (EDG) and polar (EWG) components were represented in our library[184]. We also included alkyl groups (cyclopropyl) for direct comparison with aryl substituents. Competitive ABPP was used to investigate AG/LG effects on SuTEx fragment reactivity in complex proteomes (Fig. 4.7). In brief, isotopically light and heavy soluble proteomes from DM93 melanoma cells cultured by stable isotopic labeling by amino acids in cell culture (SILAC144) media were used for quantitative liquid chromatography-mass spectrometry (LC-MS) studies. Light and heavy DM93 proteomes were treated with dimethyl sulfoxide (DMSO) vehicle or SuTEx fragment (50 μM, 30 min, 37 °C), respectively, followed by labeling with the tyrosine-reactive probe HHS-482[172] (50 μM, 30 min, 37 °C) and copper- catalyzed azide-alkyne cycloaddition (CuAAC) conjugation of a desthiobiotin-azide enrichment tag. Proteomes were digested with trypsin protease, HHS-482-modified peptides were enriched by avidin chromatography and analyzed by high-resolution LC-MS/MS. Analysis of the dataset was performted as described in section 3.3.

To evaluate substituent effects on proteome activity, we compared reactivity profiles of each respective SuTEx fragment across >1500 total distinct HHS-482 modified tyrosine sites from >650 detected proteins and in a heatmap from the interactive heatmap tool (Fig. 4.8). Fragments were screened across independent biological replicates (n = 2-3)

and high-quality tyrosine site annotations were identified by detection in at least a single biological replicate from each fragment dataset, probe-specific enrichment (HHS-482 probe/DMSO SILAC ratio (SR >5), and quality control confidence criteria of Byonic score > 300 106, 1% protein false discovery rate (FDR), and <5 ppm mass accuracy in order to minimize the potential for false positives. Database search results were filtered, converted to sites and quantified using skyline and CPASS-MS processing. SILAC ratios (SR) from competitive studies (Light – DMSO/Heavy- fragment) were used to identify fragment-competed tyrosine residues as sites showing >75% reduction in enrichment by HHS-482 compared with DMSO vehicle control (i.e. liganded tyrosines, SR >4; Fig. 4.9.a and b). In total, we identified 305 liganded tyrosines on 213 distinct proteins, which corresponded to ~30% and ~44% of total quantified tyrosines and proteins, respectively (Fig. 4.10.a); these percentages are comparable with ligandability measures reported for cysteines[185].

Liganded tyrosines showed clear structure-activity relationships (SAR) with the SuTEx fragment library (Fig. 4.9.a). Comparison of JWB150, JWB152, and JWB146 uncovered relative trends in proteomic reactivity that suggest EWGs on the AG as a common feature of SuTEx fragments with higher liganded tyrosine frequencies (Fig. 4.9.a and c). These data suggest that in addition to driving reactivity, structural modifications on the AG can contribute to binding events that enhance fragment-tyrosine interactions of compounds sharing a common LG. The differences in reactivity profiles of JWB198 and JWB202, which are differentiated by AG structure on a common LG scaffold, further support recognition as a contributor of SuTEx fragment interactions on proteins (Fig. 4.9.a). We also identified several fragments including JWB142 and JWB146 with a

reduced liganded tyrosine frequency while retaining high activity (SR >6) against tyrosine competed sites on YWHAE 148 (Y49) and PLD3 149 (Y437), respectively (Fig. 4.9.a and c). Finally, we discovered that the cyclopropyl-AG-modified fragment JWB131 was largely unreactive against the proteome (Fig. 4.9.a). The liganded sites had a relatively high previously drugged percent at 50% of targets having a known ligand (4.10.b).

Next, to compare the subcellular accessibility of the lignands we treated SILAC DM93 cells with JWB152 or JWB198 to determine whether these SuTEx fragments could ligand Y8 of endogenous GSTP1 in living systems (50 μM compound, 1.5 h, 37 °C). Cells were pretreated with DMSO vehicle or SuTEx fragments followed by cell lysis, HHS-482 labeling of proteomes, and quantitative chemical proteomics (Fig. 4.7). Database search results were filtered, converted to sites and quantified using skyline and CPASS-MS processing. Using the subcellular location tool, we found that JWB152 and JWB198 showed comparable ability to modify proteins found in intracellular compartments including the cytosol and nuclear lumen (Fig. 4.11).

In summary, our chemical proteomic studies highlight the advantage of modifying the AG and LG on SuTEx fragments for tuning reactivity and selectivity at tyrosine sites on proteins (Fig. 4.8 and 4.9.a). In contrast with previous efforts to develop globally reactive probes61, our current efforts identified SuTEx fragments with reduced proteome reactivity while retaining high efficiency for competing at tyrosine sites on select proteins (JWB202, and JWB198; Fig. 4.10.a and 4.9). In addition, we verified that the fragment electrophiles have the capacity to reach every subcellular compartment of live cells (Fig. 4.11).

4.4.5. Domain enrichment comparison of hyperreactive and liganded sites

Given that different probes and covalent libraries can access new targets for study and investigation we wanted to investigate the different domain enrichment profiles between another broad probe study and SuTEx. We took the Cravatt group's published hyper-reactivity results obtained by treating SILAC MDA-MB-231 proteomes with sulfotetrafluorophenyl (STP)-alkyne at 1 mM heavy and 0.1 mM light followed by copper-catalyzed azide-alkyne cycloaddition (CuAAC) conjugation of a TEV-cleavable biotin enrichment tag. Proteins were enriched by avidin chromatography digested on bead with trypsin protease, STP-alkyne-modified peptides were eluted using TEV protease and analyzed by high-resolution LC-MS/MS[27]. Using the ratios and sites provided by the study we performed a domain enrichment for lysines with a SR < 2.0 when treated with the two difference probe concentrations. This probe produces a different adduct +464.2491 or +470.26331, for light and heavy versions respectively[27] which can be compared to the other probe data using CPASS-MS. We then compared these results to the domain enrichment of hyper-reactive HHS-465 sites described in 3.4.3. While the hyper-reactive STP-alkyne sites enriched tRNA binding WHEP-TRS domain (PRU00531)[186] by modifying both possible domains in the database the SuTEx probe did not label this domain (Table 4.11-12, Fig. 4.12.a). In contrast the HHS-465 SuTEx hyper-reactivite sites enriched the structural Intermediate filament (IF) rod and Calponin-homology (CH) domains (PRU01188, PRU00044)[187,188]. The only shared enriched domain was the RRM domain (PRU00176, Table 4.12, Fig. 4.12.a).

Next, we performed on a domain enrichment for the liganded sites identified by screening ~30 activated ester fragment electrophiles. In brief, the light lysate was treated with DMSO while the heavy was treated with 50-100 uM fragment electrophile followed by 100 uM STP-alkyne treatment[27]. All other steps were performed as was done for the hyper-reactivity data. Liganded sites were determined using the ratios and sites from the publication[27]. Activated ester liganded sites enriched the membrane curvature mediating reticulon domain (PRU00170) and the SAM-dependent methyltransferase TRM10-type domain (PRU01012, Table 4.13, Fig. 4.12.b). In addition, the activated ester frequently liganded rare domain as all five of the top domains had less than 10 annotations in the human proteome (Table 4.13). 1,2,4 SuTEx liganded tyrosine sites were enriched for functional domains involved in nucleotide binding (PRU00267, PRU1059), protein-protein interactions (PRU00191, PRU00386), enzymatic reactions (PRU00691, PRU00277), and metal binding (PRU01163, PRU00472, Fig. 4.12.b, Table 4.14).

These data support the importance of molecular recognition for both molecular probes as well as fragment electrophiles. Further, it supports the use of the domain enrichment tool for identifying functionally unique protein components targeted by a covalent molecule.

4.4.6. Nucleophilicity and depth of SuTEx liganded sites

Knowing the exact amino acid modified on a protein enables the comparison of liganded to non-liganded amino acids of the same species (i.e. tyrosine). Using 3D structure information, we can predict both the pKa and depth of all amino acids of a species using

propka[174]. Using the get best structure tool followed by manual verification we were able to identify 89 structures that featured the liganded amino acid and lacked mutations known to induce conformational or activity changes. All ligands were removed from the structures, and then were analyzed with the pKa analysis tool. We found the liganded sites had a significantly significant decrease in pKa and buried percent (p-value = 0.014, 0.049 respectively, Fig. 4.13a-b, Table 4.15) when compared to other tyrosines on the same structures.

To better understand these features we wanted look specifically at DPP3 and GSTP1 both of which have been shown to lose activity in response to 1,2,4 SuTEx fragment electrophile treatment. DPP3 was not liganded in the initial screen[189] but a ligand was found with a IC50 of 17 μM[189] and showed mild inhibition at Y417 by mass spectrometry. We found the Y417 had both the features identified by the global propka analysis as it is found at the surface of the protein (0% buried, Table 4.15) with one of the lower pKas quantified (10.75, Fig. 4.13.c). This is likely due to the 3 nearby lysines and arginines identified by propka as contributing to the shift in pKa (Fig. 4.14.d)[174]. GSTP1 was liganded at Y7 but it does not show the features identified by the propka analysis. GSTP1 Y7 was one of the highest pKas (14.37) with maximum buried percent (100%, Figure 4.13.c-d, Table 4.15).

Collectively these results suggest that while these general trends might be interesting, they are not an effective threshold for excluding proteins from further consideration. As both proteins were inhibited by nucleophiles despite having opposing features.

4.4.7. In silico screen of SuTEx ligands

DPP3 and GSTP1 being inhibited by fragment electrophiles with greater specificity than the parent 1,2,4 triazole HHS-475 suggested that binding affinity of the ligands may play a role in determining effective ligands for a target of interest. Given the low proteome reactivity of these fragment electrophiles (Fig. 4.9.a and c) increased residence time at the site of binding through increased reactivity may enable covalent modification of a specific site. To look at affinity of molecules we screened all the ligands in the 1,2,4 SuTEx library using both the docking tool and gel based ABPP. We then compared the predicted binding affinity to loss of band intensity upon pre-treatment with a fragment (Fig. 4.14). In brief, HEK293T cell lysates were pre-treated with 100μM inhibitor for 30 minutes at 37° C followed by 50μM of HHS-482, a tyrosine selective 1,2,4-sulfonyl triazole probe, for 30 minutes. Samples underwent copper catalyzed azide-alkyne cycloaddition (CuAAC) with rhodamine azide and were resolved by SDS- PAGE (Fig 4.14). Gels were visualized and the total lane fluorescent intensity was normalized to DMSO and compared (Fig. 4.15-4.24, Table 4.16 and 4.17). Inhibitors that decreased lane intensity compared by greater than 30% were removed as they were likely to be broadly reacting molecules. The loss of band intensity and the AutoDock (see Materials and Methods, Table 4.16) calculated binding affinities were z-transformed and compared using a simple linear model in R. Correlation and p-value were calculated using a Pearson's product-moment correlation test.

The GSTP1 affinities showed a statistically significant correlation with the loss of gel band intensity (correlation = 0.40, p-value = 0.0096) while DPP3 screening showed no correlation (correlation = -0.02, p-value = 0.90, Fig. 4.25, Table 4.17). This suggests that

only certain sites can use affinity for predicting inhibition and combined with the results from the propka analysis of these structures it seems the approach performed better on with liganded sites that are buried with increased pKa.

4.4.8 Workflows for analysis in CPASS-MS

One of the major advantages of CPASS-MS on galaxy framework is ability to create workflows for reproducible analysis of datasets[171]. To this end we generated 3 custom pipelines to reproduce the analysis performed. To perform general profiling of the ATP acyl phosphate probe the process SILAC Probe Data tool was used to integrate the byonic and skyline results. The Filter Data tool performed the ATP cutoff (SR > 5) and the results were analyzed Get Domain Info tool and compared to the 3 PTM databases to produce Fig. 4.3 (Fig. 4.26.a). Another general profiling approach was used to analyze the SuTEx lysine data (Fig. 4.26.b). Since this data was label-free there was no quantification, and the initial dataset was manually CPASS-MS formatted. Get Domain info was run on all sites to produce Fig. 4.4.b while Drug Bank tool was used to produce part of Fig. 4.4.c and split the targets into DBP and non-DBP. The two group were rerun with Get Domain Info to produce the rest of the figure.

A pipeline for the analysis of competitive ABPP data was generated to reproducibly analyze new ligands (Fig. 4.27). After Process SILAC Probe Data a global heatmap was generated using the Heatmap Generator as seen in Fig. 4.8. Once Filtered a liganded only heatmap was generated as seen in Fig. 4.9.a. The Drug Bank Comparison tool and Get Domain Info tool were used to produce Fig. 4.10.b and 4.12.b respectively. As mentioned

previously the Get Best Structure tool was used identify structures of liganded protein but these structures were manually verified prior to use downstream. The structure data was manually downloaded and analyzed using the pKa Single/Multi File tools for use in the pKa graphing tool which produce the majority of Fig. 4.13 (a,b,c,e, and f).

These pipelines can be used regardless of the chemical probe used in the study as various parameters can be changed to address differences in the adduct produced from probe modification of amino acids (see Materials and Methods). There are other tools not directly integrated into the pipelines, but all of the tools can use information from the other tools to inform their use (i.e. AutoDock runner uses a Site to define binding region).

4.5 Discussion

The development of CPASS-MS has produced a tool kit with site-specific mass spectrometry at its core. Using approaches like diagnostic adduct and site identification the initial processing can turn a complex list of peptides, quantitative values and spectral data into an accessible format that can tie into various other tools. The custom tools either use the site modified (domain enrichment, pKa grapher, database comparisons, autodock runner and heatmap generator) or are built around the unique way covalent molecules interact with live cells (subcellular location). These tools can provide insight into various forms of ABPP data in reproducible and standardized manner using the workflows as shown. In addition, the plug and play nature of the tools and the CPASS-MS formatted data can be used to integrate new tools into ABPP data analysis workflows.

Using this workflow, we show that the ATP-acyl phosphate is very specific for

protein kinase domains (Fig. 4.3.a). While expected based off the probe design there has always been a lingering question about the possibility of large off-target effects caused by reactivity of the warhead or the various other ATP binding proteins. This result suggest that the catalytic activity of a kinase dramatically increases its chance to be labeled by this probe. The analysis of the different PTMs on lysine likely does not suggest that the ATP acyl phosphate enriches ubiquitinated sites as it is dependent on the frequency of each PTM in cellular system[190]. The primary utility of this analysis is ability to identify where a probe might be able to report on a PTM or ligand a PTM site that may be important for activity[27,189]. This also applies to the PTM analysis of SuTEx lysine sites.

The investigation into the SuTEx lysine sites did not show a great deal of variation when compared to the tyrosine profiling in Section 3.3 but did enrich a couple undrugged domains that were unique to the lysine data namely the DZF the WH1 domains (Fig. 4.4.b)[183,191]. Thus, if a target features one of these domains targeting a lysine with SuTEx molecule may be an effective strategy. In addition, we were able to show that HHS-465 and HHS-475 are not modifying just cytosolic proteins in live cells (Fig. 4.5.d) which can inform the decision to use a SuTEx warhead in designing an ABP that needs to reach certain targets (see Section 1.2). We also found that the choice of warhead, even among the broad options, enrich different domains at lower doses (hyper-reactivity) or when developing a small covalent inhibitor library (ligandability, Fig. 4.12).

Using CPASS-MS with competitive ABPP of SuTEx derived fragment electrophiles showed the ability to “tune” the warhead using SAR as probe with different adduct and leaving groups showed massive differences in proteome reactivity. This tuning

reveals the possibility of using less reactive SuTEx molecules for the liganding or probing of more a specific target or groups of targets. Doing so would require the use of directing elements and medicinal chemistry style elaboration to design molecules for specific targets but our current understanding of how the EDG and EWGs effect the warhead activity suggest that such targeting can be accomplished[72]. In addition, we have shown that the fragment electrophiles can reach any subcellular location in live cells. Another key step in understanding the utility of SuTEx chemistry in probe design and drug discovery.

Finally, we have taken steps to create a predictive model of liganding sites with fragment electrophiles. The revelation that *in silico* docking some probe modified sites with fragment electrophiles can be predictive of inhibition measured using gel-based screening can dramatically increase the throughput for screening of such targets (Fig. 4.24). Further, while far from conclusive the ligandability, pKa and depth analysis suggest that a previously liganded, less nucleophilic target buried in the protein are more accurately predicted using this approach. It follows that docking would only work on a target that require high affinity binding of less reactive fragment to require increase probe site interaction time to perform the covalent reaction[93].

4.6 Author Contributions and Pipeline Development

Analysis of previously published ATP acyl phosphate data was conducted by Borne and S. Brodowski. The reanalysis of the lysine data was conducted by Borne. The ligandability studies were conducted by Brulet and analyzed by Brulet and Borne. These results were published in Brulet et al. 2021. Analysis of SuTEx lysine data and Cravatt

published STP-alkyne data was performed by Borne. Analysis of depth, pKa, docking and subcellular location was performed by Borne. Gel screening was conducted by Brulet, Borne, R. Rumana, and K. Isbell. Analysis of gel screening conducted by Borne.

This final version of the CPASS-MS was reworked to function with any probe and was rebuilt to work with galaxy platform by Borne and S. Brodowski. This enabled the integration of other bioinformatics tools and workflows to conduct reproducible analysis of probe data. The toolkit was combined with new tools for competitive ABPP, subcellular location, site targeted docking, and global propka analysis tools. The reworked pipeline and all tools developed for the analysis of site-specific mass spectrometry make up CPASS-MS.

4.7 Figures

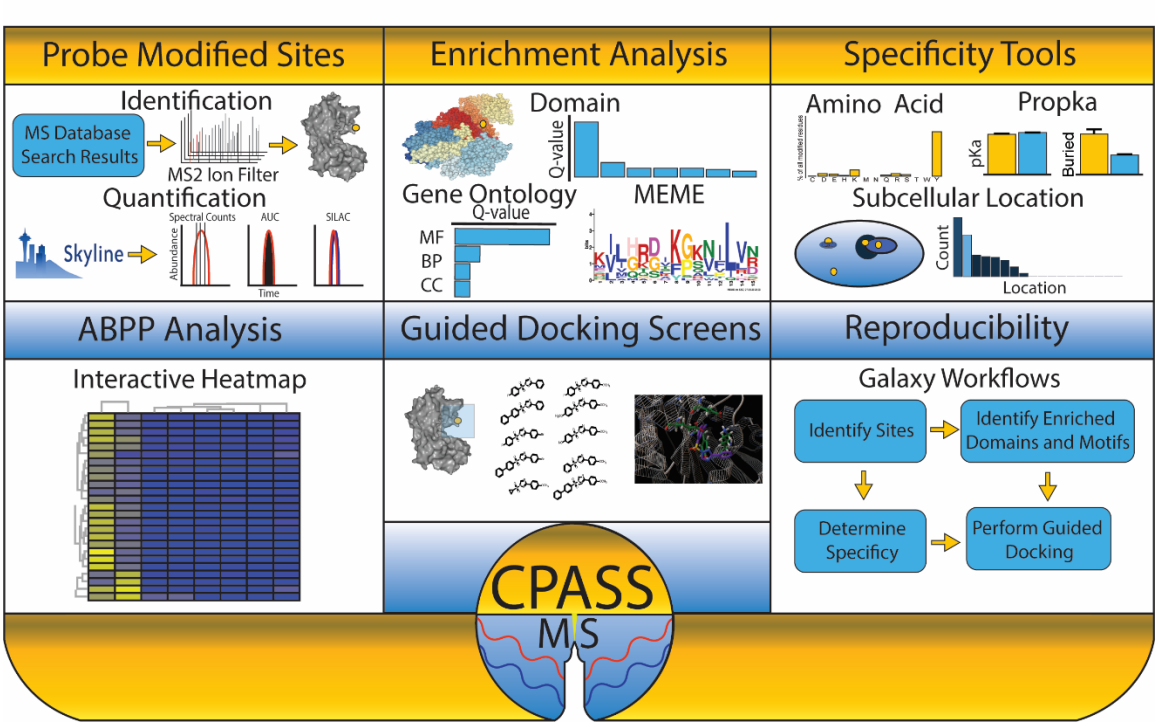

Figure 4.1. Overview of CPASS-MS. Scheme designed by Borne.

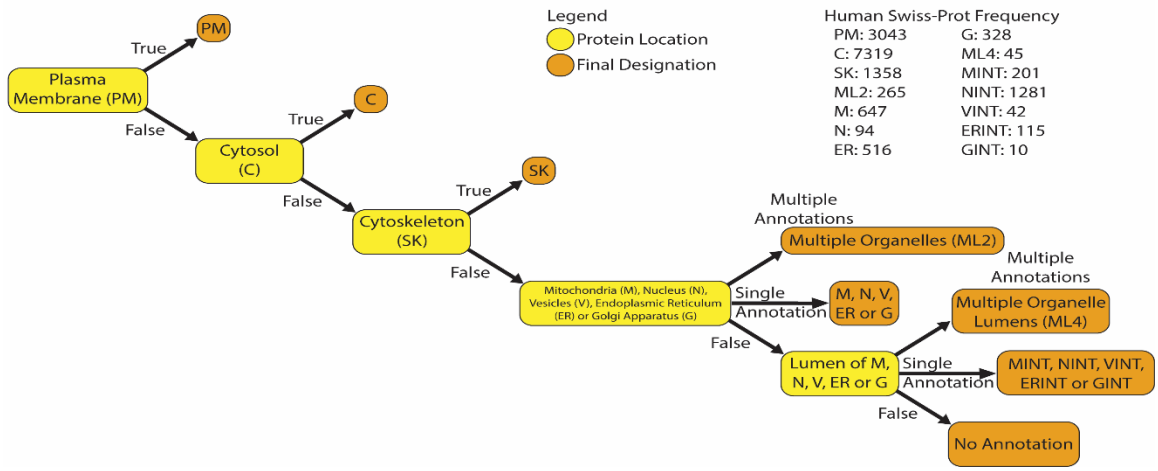

Figure 4.2. Subcellular location decision tree. Uses cell compart gene ontology annotations to determine the most accessible compartment. The subcellular compartments used for analyses are as follows: PM: Plasma Membrane, C: Cytosol, SK: Cytoskeleton, M: Mitochondria, N: Nucleus, V: Vesicle, ER: Endoplasmic Reticulum, G: Golgi Apparatus, ML2: Multiple Organelles, MINT: Mitochondrial Lumen, NINT: Nuclear Lumen, VINT: Vesicle Lumen, ERINT: Endoplasmic Reticulum Lumen, GINT: Golgi Apparatus Lumen, ML4: Multiple Organelle Lumens. Corner table shows all final designation for the human Swiss-Prot database using this decision tree. Missing protein had no usable cell compartment annotations. Scheme developed by Borne.

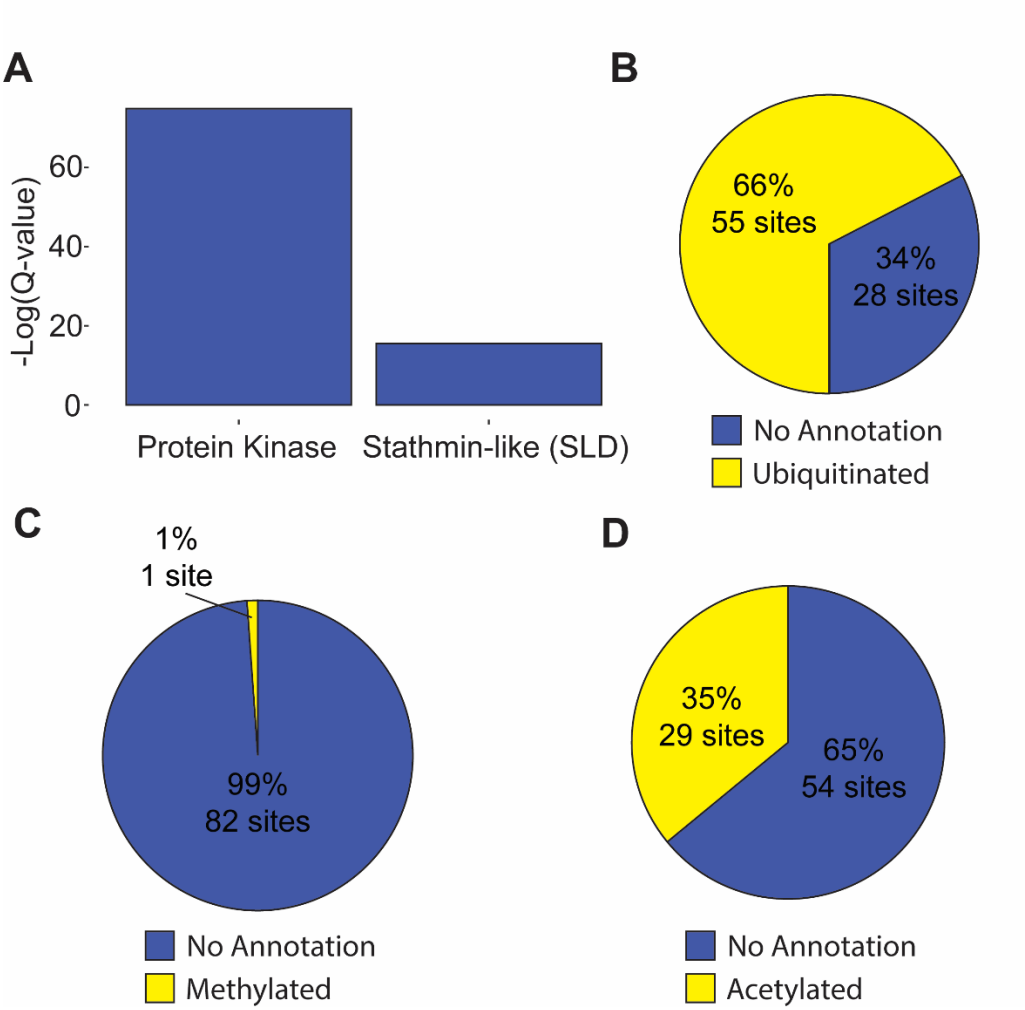

Figure 4.3. Analysis of ATP sensitive sites identified using the ATP-acyl phosphate and CPASS-MS. (A) Enriched domain annotations of ATP sensitive sites (SR > 5) as determined by Q < 0.01 after Benjamini–Hochberg correction of a two-sided binomial test. (B-D) Overlap between ATP sensitive sites that are also ubiquitination (B), methylation (C) and acetylation (D) sites in HEK293T, A549 and H82 cell lines. Original data published in Franks et al. 2017 and Campbell et al. 2018. Analysis conducted by S. Brodowski and Borne.

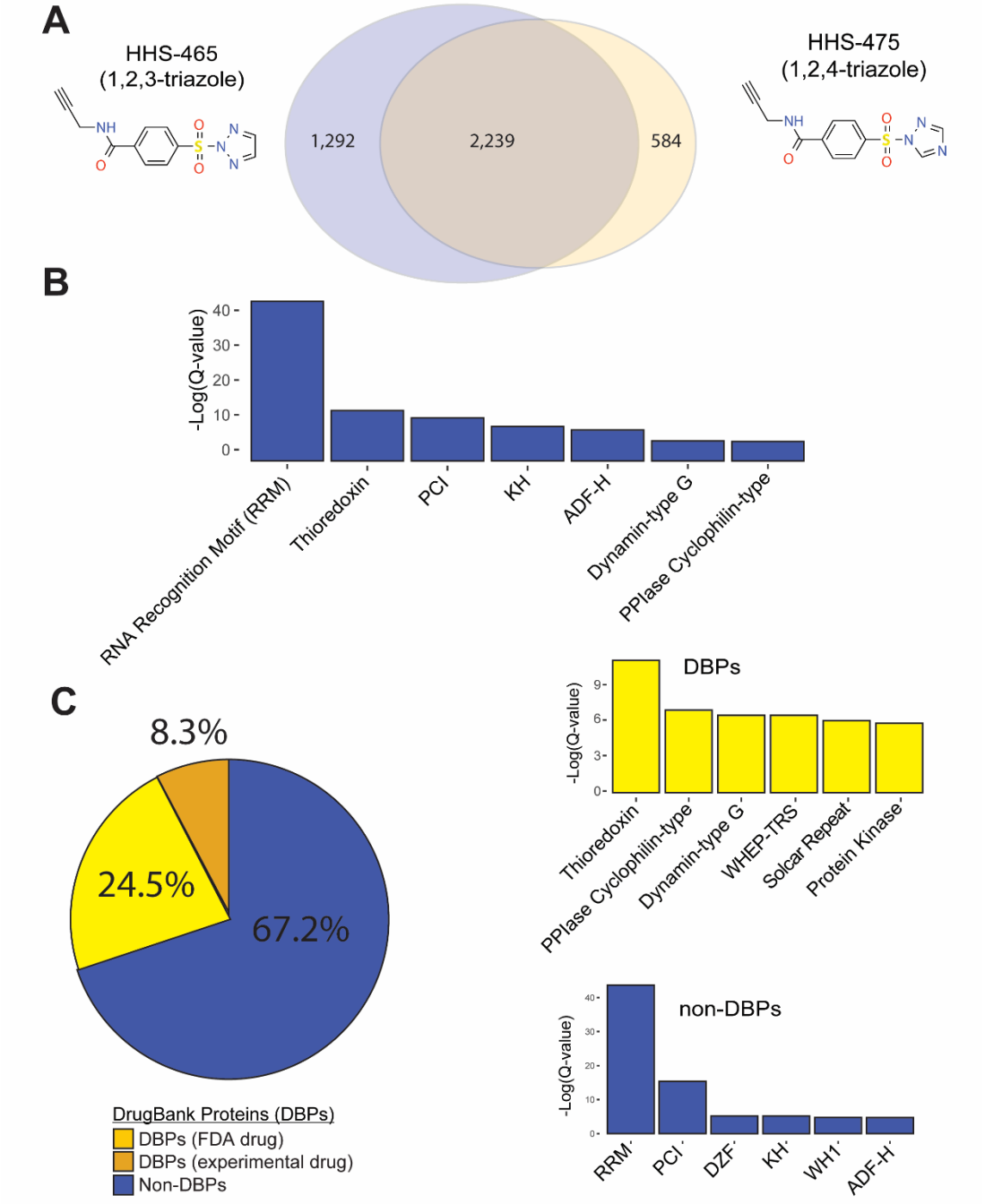

Figure 4.4. Profile of live cell SuTEx lysine sites (A) Comparison of HHS-465- and HHS-475-lysine-modified sites identified from in situ treatments. (B) Probe enriched domains for all lysine-modified sites detected in situ. (C) Left, comparison of HHS-465 and HHS-

475 in situ probe-modified proteins with DrugBank proteins (DBP group). The non-DBP group consists of proteins that did not match a DrugBank entry. Right, probe-enriched domains from DBP and non-DBP groups. Enriched domain annotations for (B) and (C) are those with a $Q < 0.01$ after Benjamini–Hochberg correction of a two-sided binomial test. All data shown are representative of two experiments (HEK293T and Jurkat treated with SuTEx probes (100 μM, 2 h, 37 °C, $n = 2$ biologically independent experiments). Data published in Hahm et al. 2020. Analysis performed by Borne.

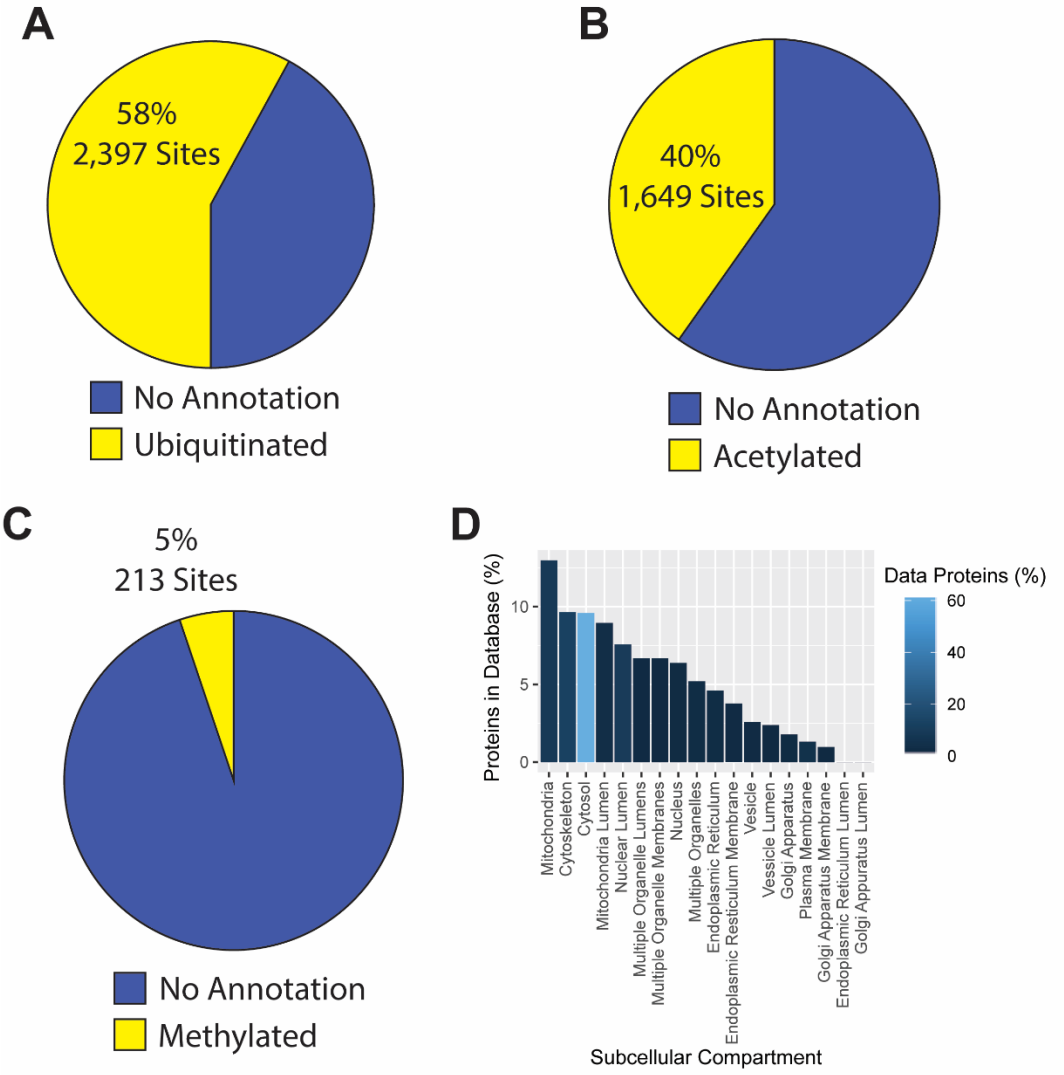

Figure 4.5. PTMs and subcellular location of lysine-modified sites. (A-C) Overlap between HHS-465 and HHS-475 modified lysine sites that are also ubiquitination (A), acetylation (B) and methylation (C) sites. (D) The number of SuTEx lysine-modified proteins compared with the number of proteins from the Swiss-Prot database for each subcellular compartment (x-axis) using SLA are shown (Proteins in Database, y-axis). The color bars depicts the percentage of SuTEx lysine-modified proteins from each subcellular compartment compared with all liganded proteins quantified in datasets. All data shown

are representative of two experiments (HEK293T and Jurkat treated with SuTEx probes (100 μM, 2 h, 37 °C, $n = 2$ biologically independent experiments). Analysis performed by Borne.

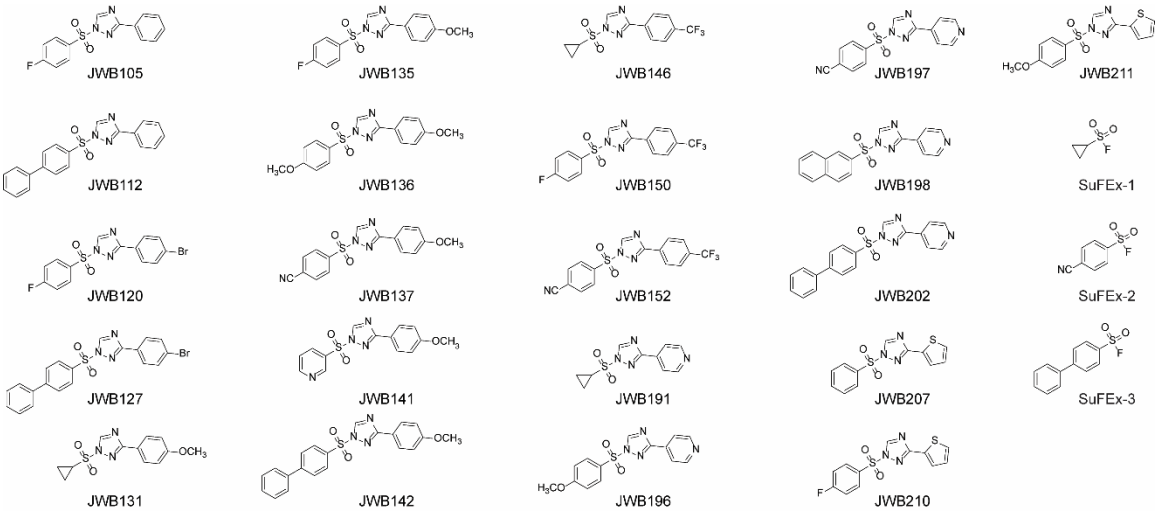

Figure 4.6. Chemical structures of a SuTEx fragment library displaying adduct- and leaving-group diversity. Compound synthesized by Bruletm published in Brulet et al. 2021.

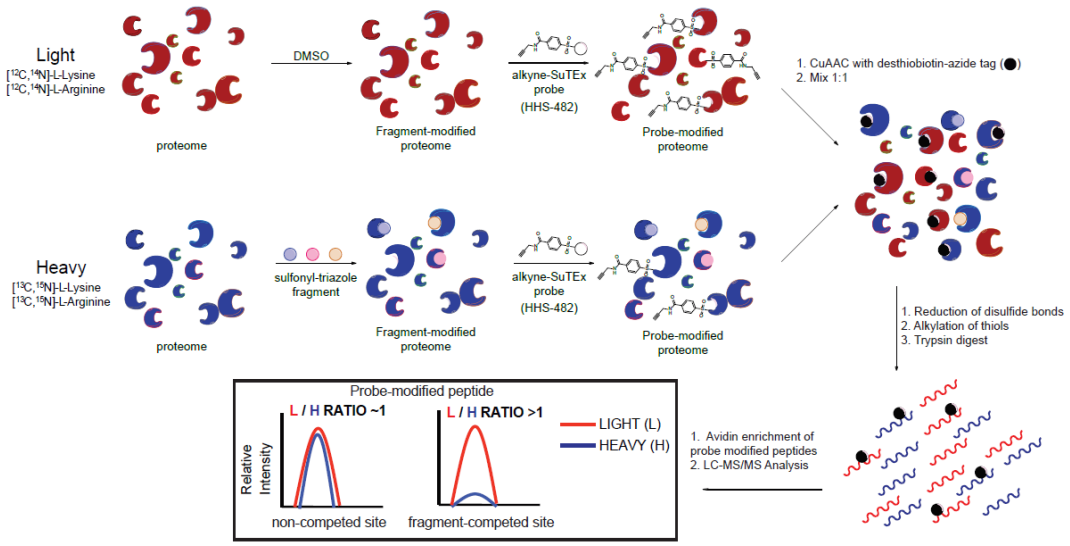

Figure 4.7. Quantitative chemical proteomics for evaluating proteome-wide activity of SuTEx fragments. Experimental workflow for quantitative chemical proteomics evaluate fragment reactivity and specificity in proteomes. DM93 cells were cultured in SILAC media supplemented with either “light” 12C, 14N-labeled lysine and arginine (denoted in red) or “heavy” 13C, 15N-labeled lysine and arginine (denoted in blue). Heavy and light DM93 proteomes were treated with DMSO vehicle or SuTEx fragment (50 µM, 37 °C, 30 min) followed by HHS-482 probe labeling using the same reaction conditions. The resulting SILAC ratios (SR) were quantified using the area under the curve of MS1 extracted ion chromatograms. Non-liganded tyrosines are expected to show equivalent probe labeling intensity in vehicle and fragment treated conditions (left MS1, SR~1). Fragment-competed tyrosines (i.e. liganded tyrosine) are identified by sites showing substantial reduction in enrichment by HHS-482 compared with DMSO vehicle control (right MS1, SR >>1). Scheme generated by Brulet and Hsu.

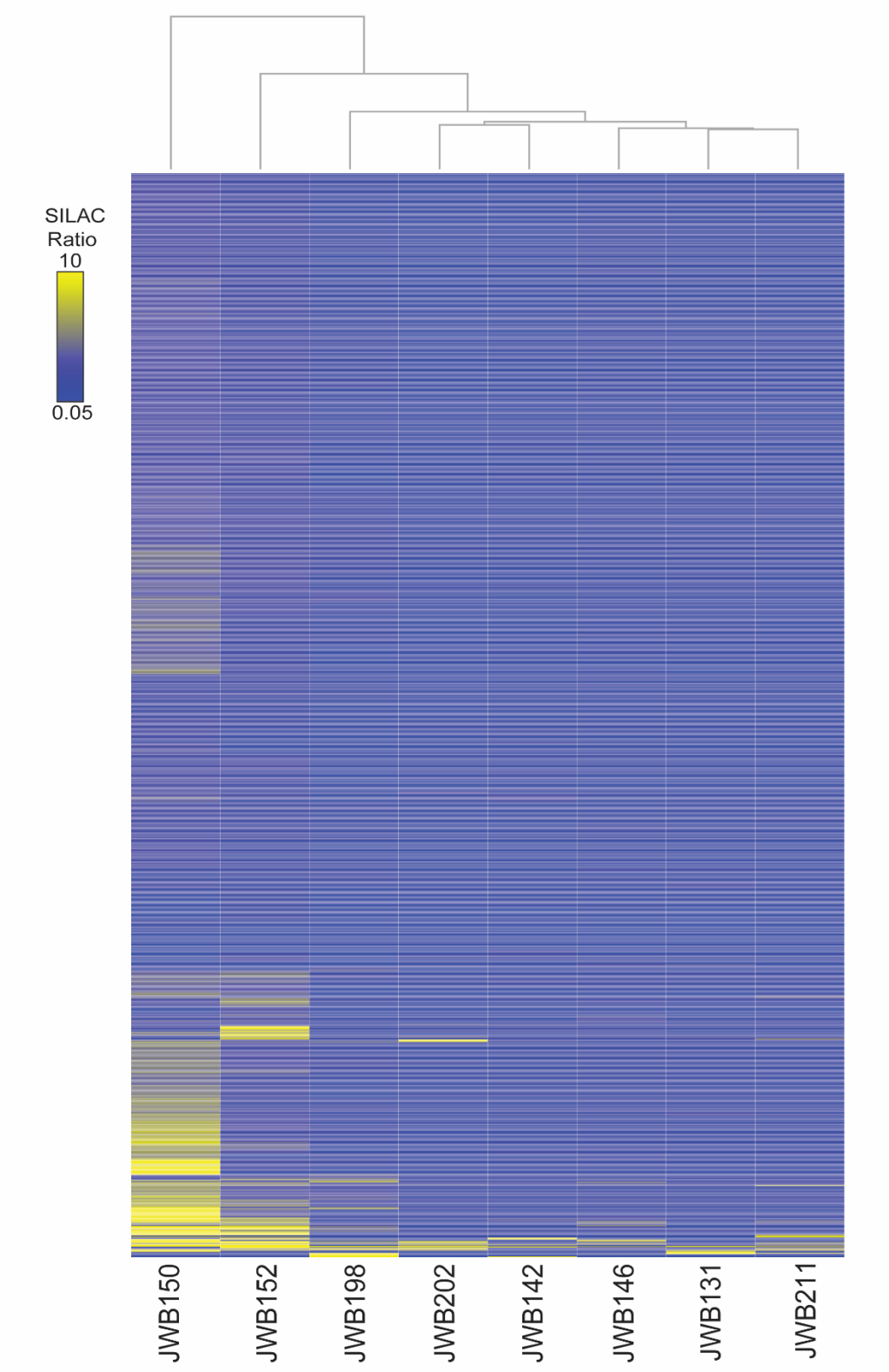
SILAC
Ratio
10
0.05
JWB150
JWB152
JWB198
JWB202
JWB142
JWB146
JWB131
JWB211

Figure 4.8. Fragment-based ligand discovery using SuTEx (all tyrosine sites). Heat map showing SILAC ratios (SR) of all quantified tyrosines in chemical proteomic studies configured for evaluating ligand competition. Fragments and liganded tyrosine sites are organized by hierarchical clustering. Data shown are representative of n = 2-3 biologically independent experiments. Data acquired by Brulet and analyzed by Borne.

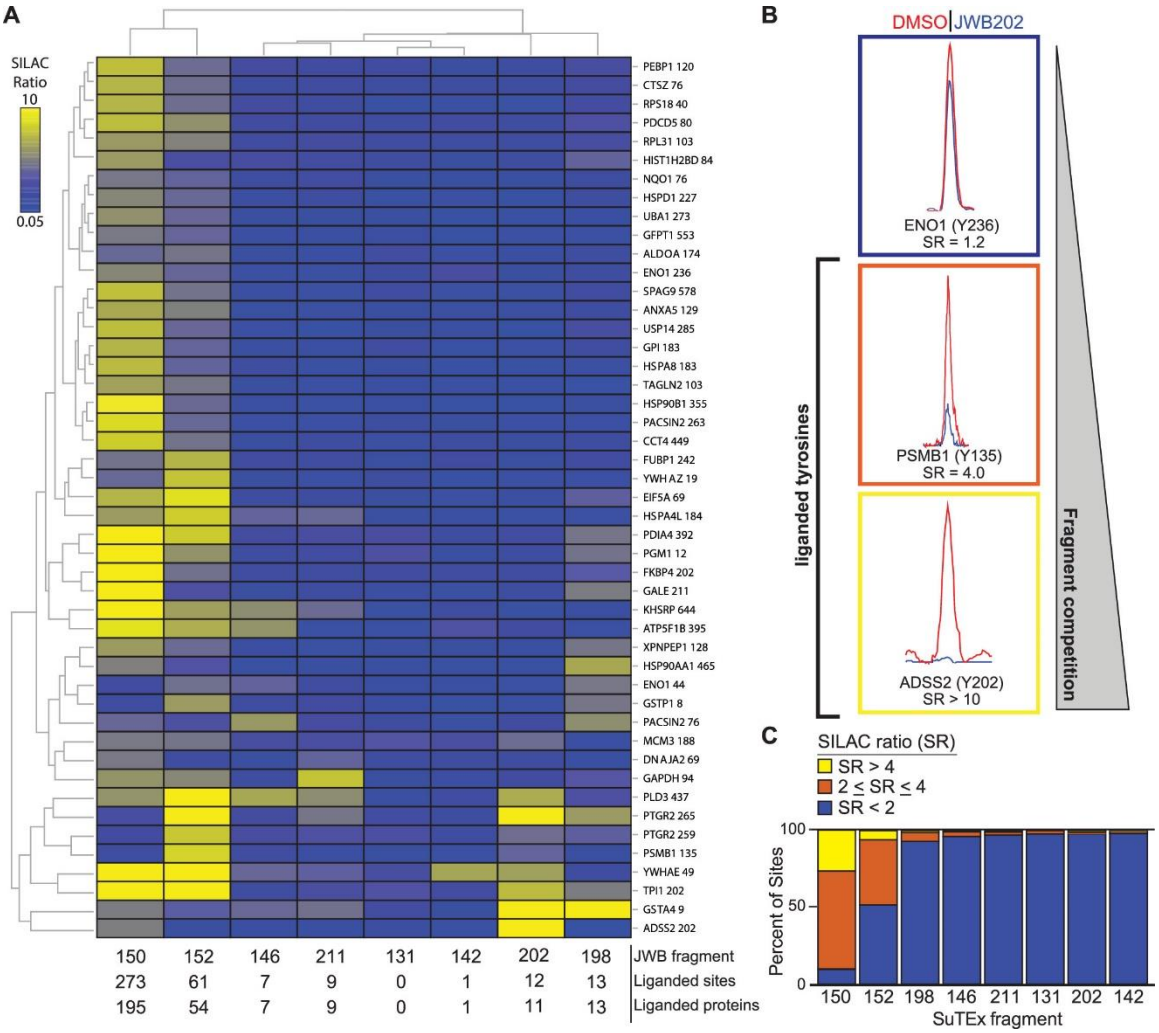

Figure 4.9. Fragment-based ligand discovery using SuTEx. (A) Heat map showing SILAC ratios (SR) of representative tyrosines competed by fragments and organized by hierarchical clustering. Fragment competition at tyrosine sites was quantified using the area under the curve of MS1 extracted ion chromatograms (EIC) from HHS-482-labeled peptides in DMSO (light, red) versus fragment-treated (heavy, blue) DM93 soluble proteomes. Competitive chemical proteomic studies were performed as shown in Figure S3. Tyrosine sites shown are liganded (SR > 4) by at least 2 fragments with the number of liganded sites and proteins listed for each molecule. The y-axis lists the protein name and

quantified tyrosine site. (B) Representative MS1 EICs of tyrosine sites from quantitative LC-MS chemical proteomics: nonliganded (blue, SR < 2), partially liganded (orange, 2≤ SR ≤ 4), and liganded (yellow, SR > 4). (C) Reactivity of fragments was assessed by comparing the fraction of tyrosine sites competed: nonliganded (blue, SR < 2), partially liganded (orange, 2≤ SR ≤ 4), and liganded (yellow, SR > 4). All data shown are representative of n = 2–3 biologically independent experiments. Data acquired by Brulet and analyzed by Borne.

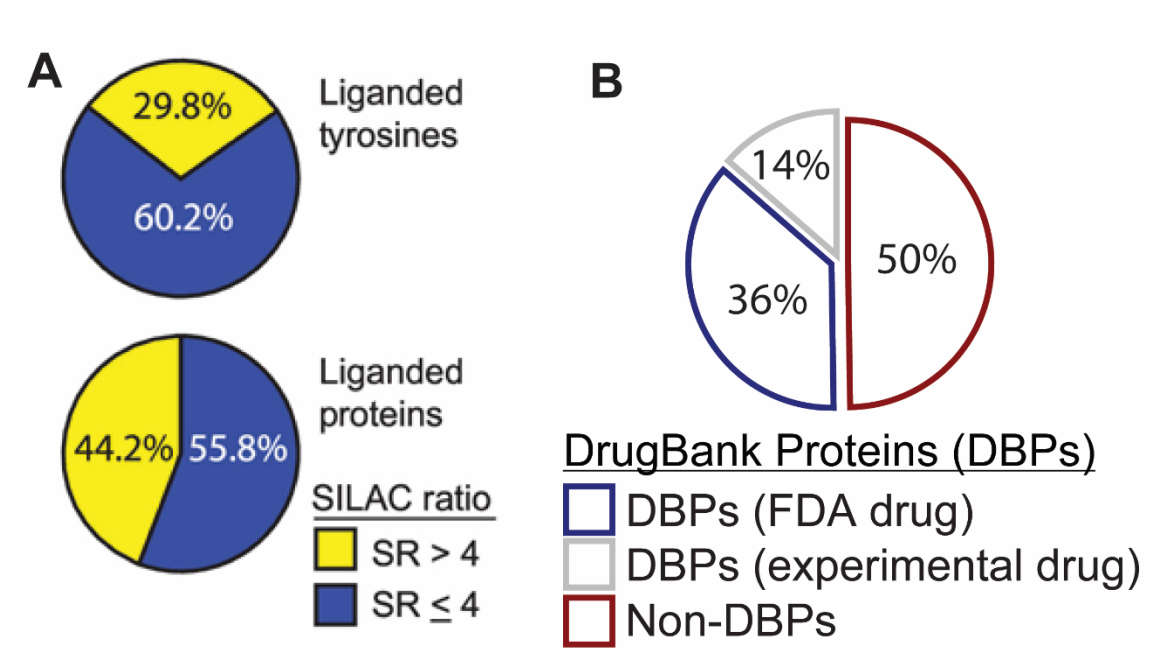

Figure 4.10. Analysis of tyrosines and proteins liganded by SuTEx fragments. (A) Distribution of liganded and nonliganded tyrosine sites and proteins from chemical

proteomic analyses of DM93 soluble proteomes. Data are shown for quantified tyrosines (top) and proteins (bottom) that were liganded (SR > 4) by at least 1 fragment. (B) Distribution of liganded proteins (SR > 4) found in DrugBank (DBP group) compared with proteins that did not match a DrugBank entry (non-DBP). All data shown are representative of n = 2–3 biologically independent experiments. Data acquired by Brulet and Analyzed by Borne.

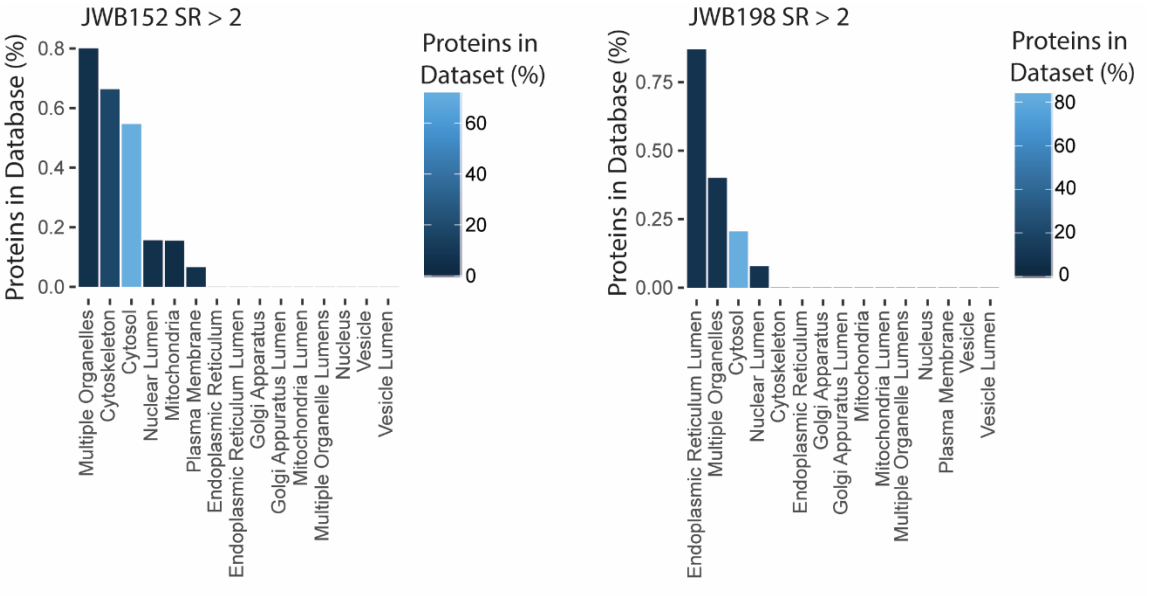

Figure 4.11. Subcellular location analysis of liganded proteins from DM93 live cell chemical proteomics. Proteins containing a liganded tyrosine site (SR>2) were grouped based on subcellular location using a subcellular location analysis (SLA) algorithm. Data shown are from DM93 cells treated with JWB152 (left panel) or JWB198 (right panel) SuTEx fragment at 50 μM for 30 min. The number of liganded proteins compared with the

number of proteins from the Swiss-Prot database for each subcellular compartment (x-axis) using SLA analyses are shown (Proteins in Database,y-axis).The colored bars depict the percentage of liganded proteins from each subcellular compartment compared with all liganded proteins quantified in datasets. See Methods section for detailed explanation of SLA algorithm. All data shown are representative of n = 2 biologically independent experiments. Data acquired by Brulet and Analyzed by Borne.

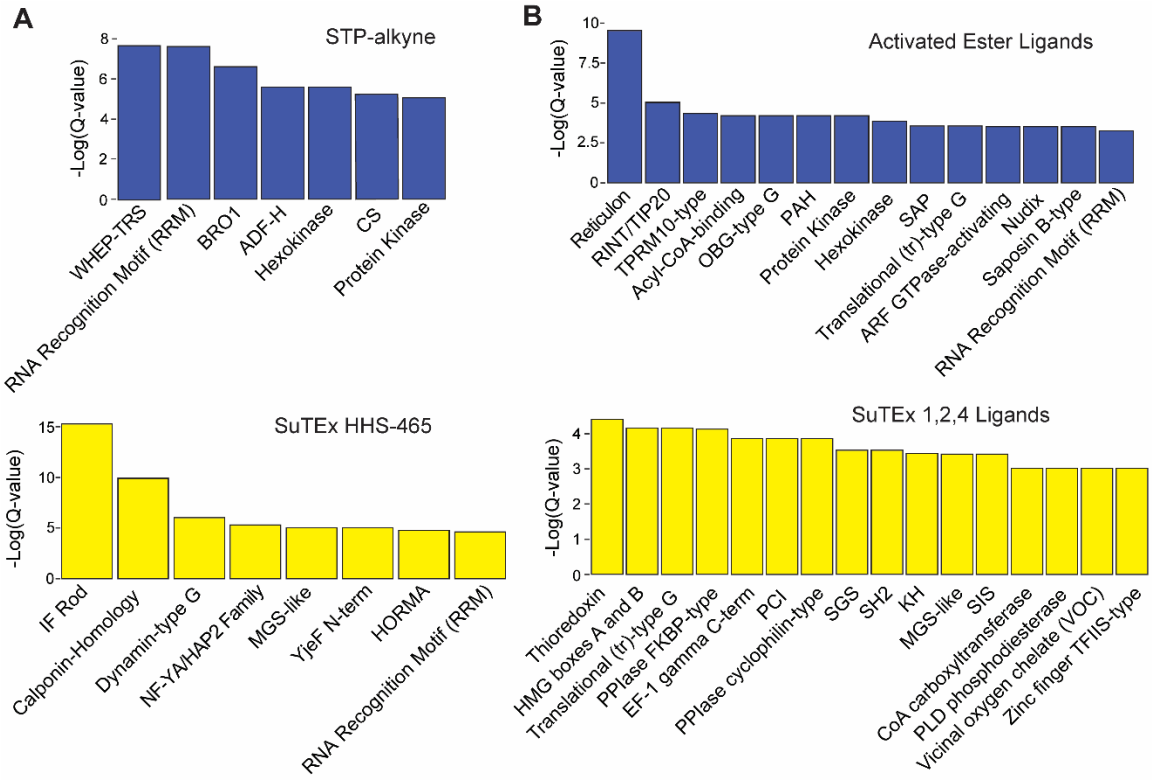

Figure 4.12. Domain enrichment of hyper-reactive and liganded sites between studies. (A) Top, domain enrichment of hyper-reactive STP-alkyne (0.1 mM vs. 1mM, MDA-MB-231,

Ramos and Jurkat) lysine sites. Bottom domain enrichment of hyper-reactive HHS-465 (250 uM vs 25 uM, HEK293T) tyrosine sites. Enriched domain annotations as determined by $Q < 0.01$ after Benjamini–Hochberg correction of a two-sided binomial test. (B) Top, domain enrichment of activated ester liganded sites (50-100 uM, HEK293T) lysine sites. Bottom, domain enrichment of liganded SuTEx 1,2,4 fragment electrophiles (50 uM, DM93) tyrosine sites Enriched domain annotations as determined by $Q < 0.05$ after Benjamini–Hochberg correction of a two-sided binomial test[27]. Data acquired by Brulet and Hacker et al. 2017; Analyzed by Borne.

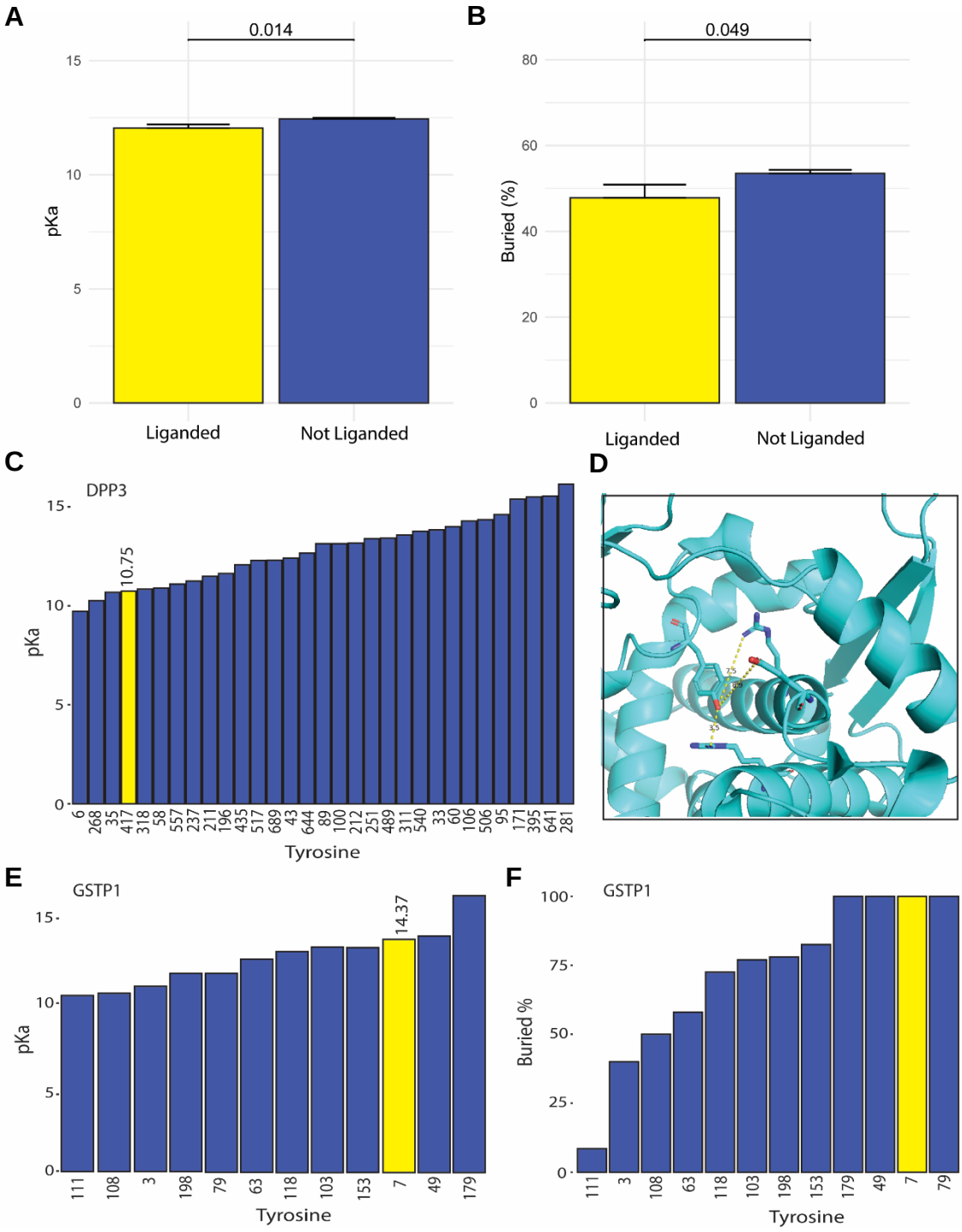

Figure 4.13. pKa and depth analysis of SuTEx modified targets. (A) pKa comparison of SuTEx fragment electrophile liganded tyrosine and non-liganded tyrosines from the same 3D structures. P-value is determined using a Welch t-test, error bars represent standard

deviation. (B) Buried percent comparison of SuTEx fragment electrophile liganded tyrosine and non-liganded tyrosines from the same 3D structures. P-value is determined using a Wilcoxon rank-sum test, error bars represent standard deviation. List of all 89 structures used in table 4.15. (C) pKa of labeled but not liganded Y417 compared to other tyrosines on DPP3. (D) Labeled Y417 and nearby positively charged amino acid predicted to alter pKa by propka analysis (PDB ID: 3FLY). (E) pKa of liganded Y7 compared to other tyrosines on GSTP1. (E) Buried percent of liganded Y7 compared to other tyrosines on GSTP1 (PDB ID: 5GSS). Work conducted by Borne.

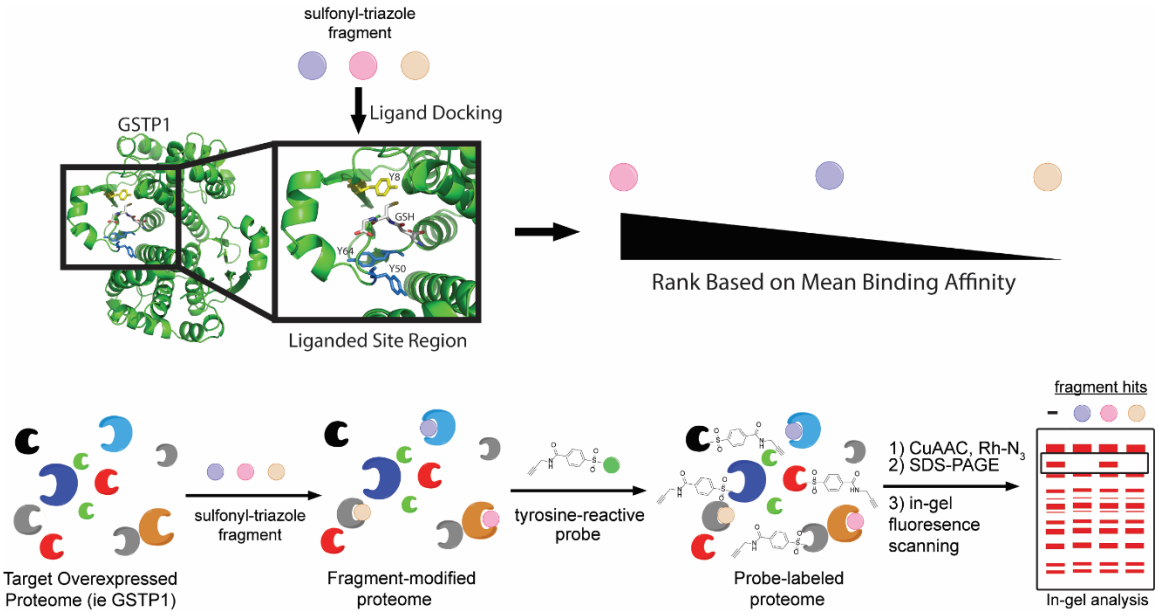

Figure 4.14. Schematic for comparison of *in silico* and gel-based ABPP screen of 1, 2, 4 SuTEx fragment electrophiles. Fragments will be docked using CPASS-MS AutoDock screen tool and ranked using mean binding affinity of conformations identified. Lysate s expressing the target protein are pre-treated with SuTEx fragment before probe labeling with

HHS-482. Cell lysates undergo click chemistry and are resolved by SDS-PAGE, before visualization using a rhodamine. Scheme generated by Borne and Brulet.

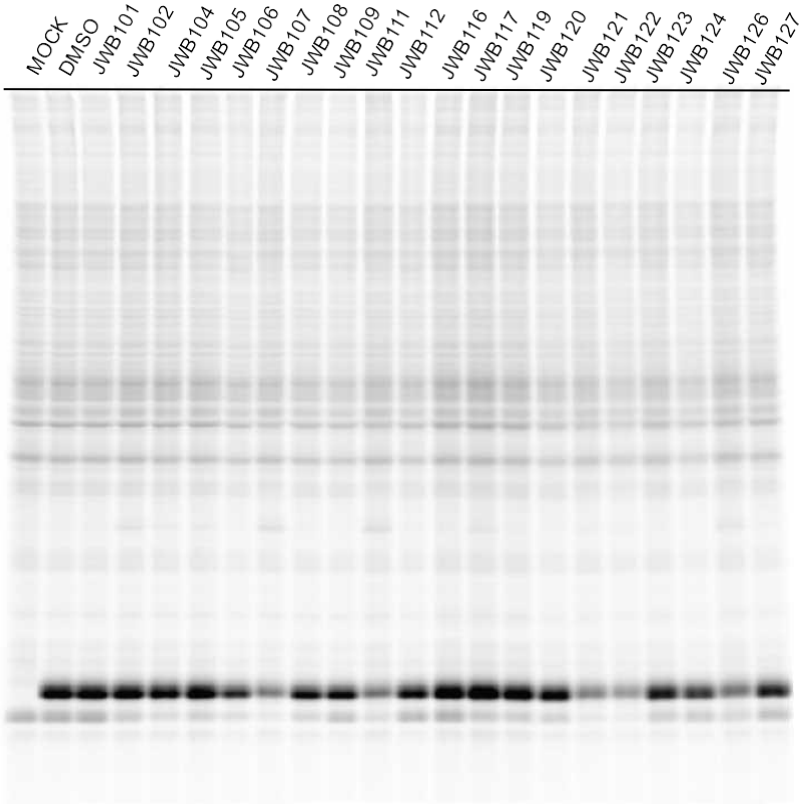

Figure 4.15. competitive ABPP gel results of HEK293T cells expressing recombinant GSTP1 treated with SuTEx fragments JWB101-JWB127. Gel screening was conducted by Brulet, R. Rumana, and K. Isbell. Analysis of gel screening conducted by Borne.

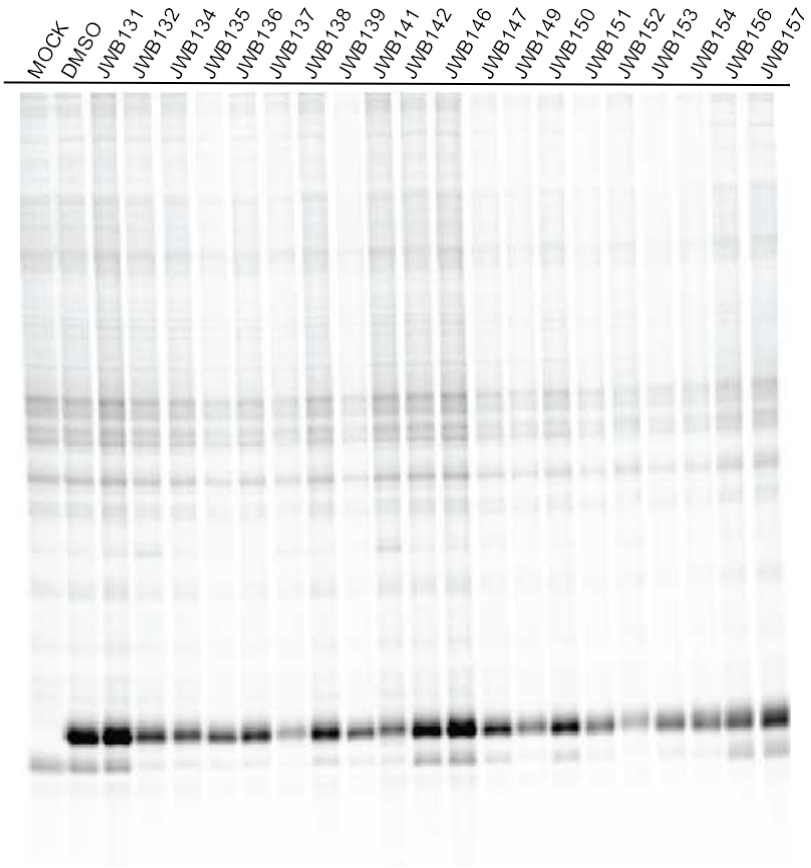

Figure 4.16. competitive ABPP gel results of HEK293T cells expressing recombinant GSTP1 treated with SuTEx fragments JWB131-JWB157. .Gel screening was conducted by Brulet, R. Rumana, and K. Isbell. Analysis of gel screening conducted by Borne.

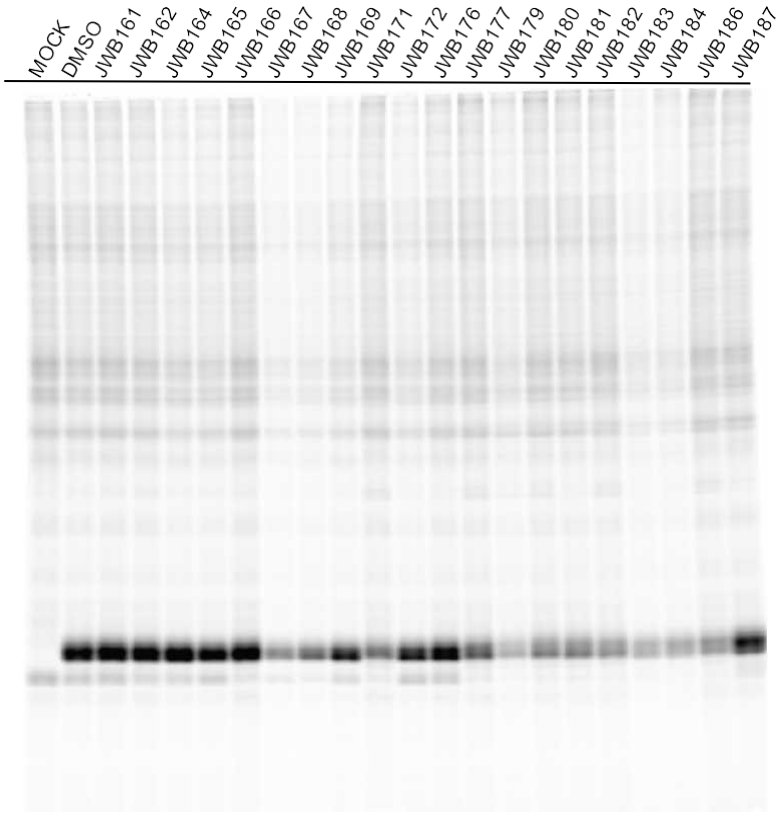

Figure 4.17. competitive ABPP gel results of HEK293T cells expressing recombinant GSTP1 treated with SuTEx fragments JWB161-JWB187. . Gel screening was conducted by Brulet, R. Rumana, and K. Isbell. Analysis of gel screening conducted by Borne.

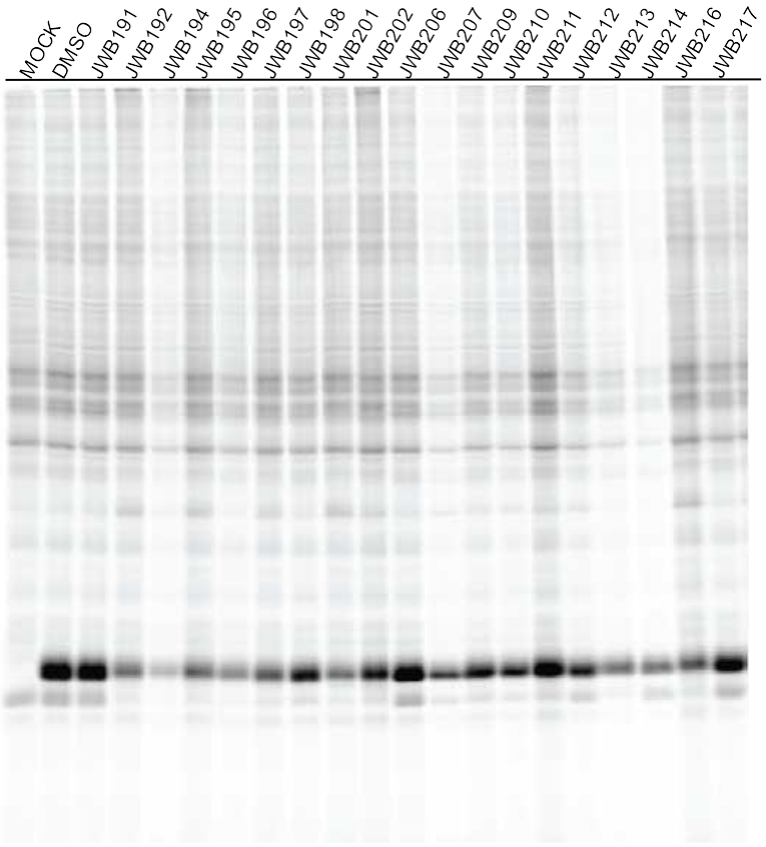

Figure 4.18. competitive ABPP gel results of HEK293T cells expressing recombinant GSTP1 treated with SuTEx fragments JWB191-JWB217. Gel screening was conducted by Brulet, R. Rumana, and K. Isbell. Analysis of gel screening conducted by Borne.

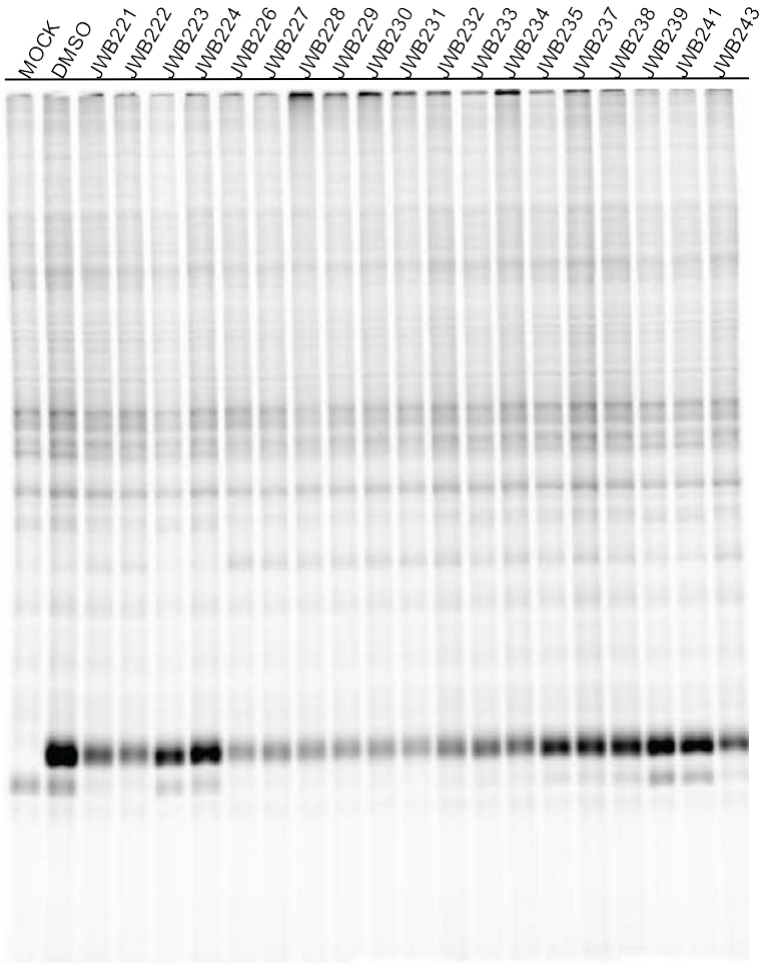

Figure 4.19. competitive ABPP gel results of HEK293T cells expressing recombinant GSTP1 treated with SuTEx fragments JWB221-JWB243. Gel screening was conducted by Brulet, R. Rumana, and K. Isbell. Analysis of gel screening conducted by Borne.

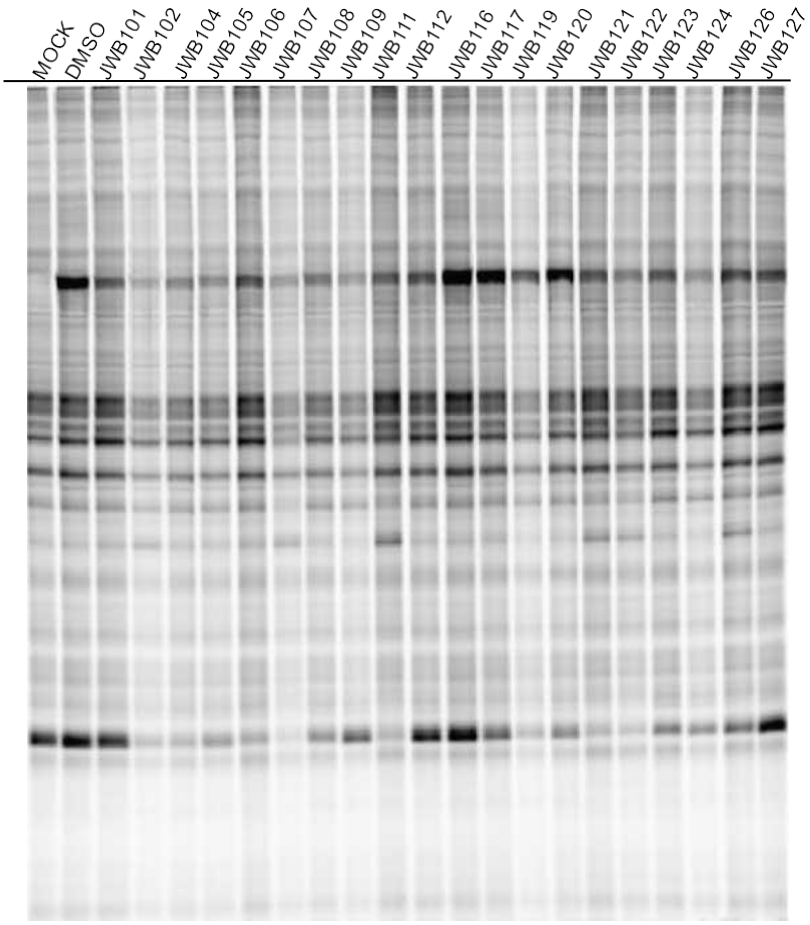

Figure 4.20. competitive ABPP gel results of HEK293T cells expressing recombinant DPP3 treated with SuTEx fragments JWB101-JWB127. Gel screening was conducted by Brulet , R. Rumana, and K. Isbell. Analysis of gel screening conducted by Borne.

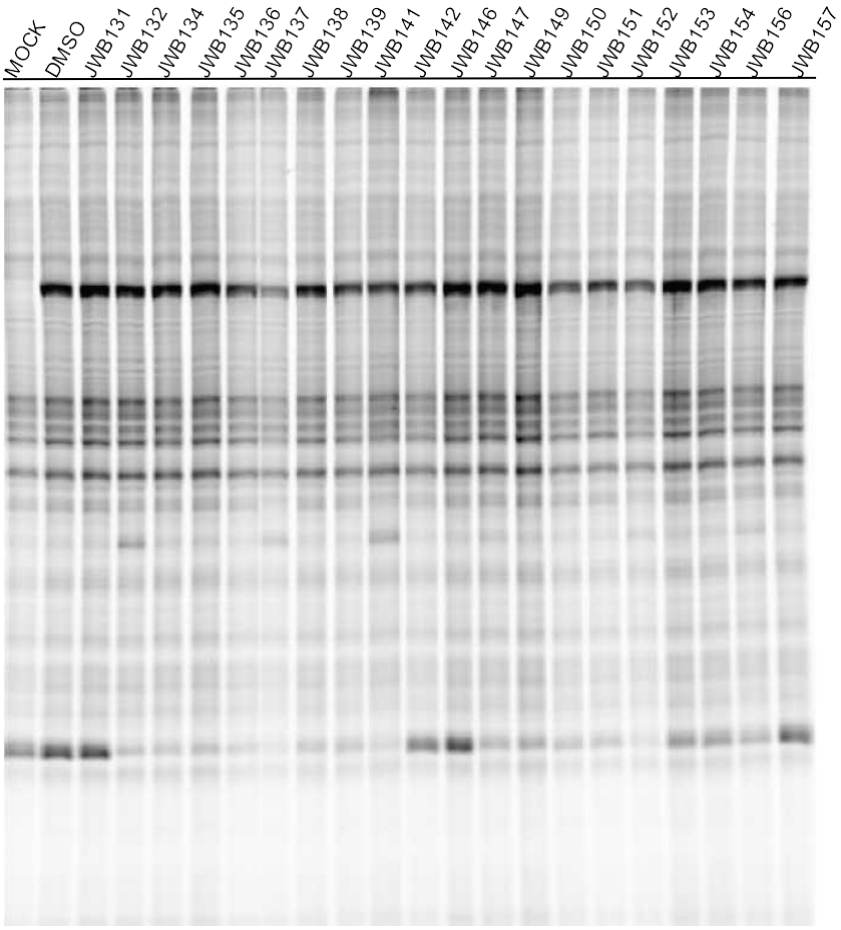

Figure 4.21. competitive ABPP gel results of HEK293T cells expressing recombinant DPP3 treated with SuTEx fragments JWB131-JWB157. Gel screening was conducted by Brulet , R. Rumana, and K. Isbell. Analysis of gel screening conducted by Borne.

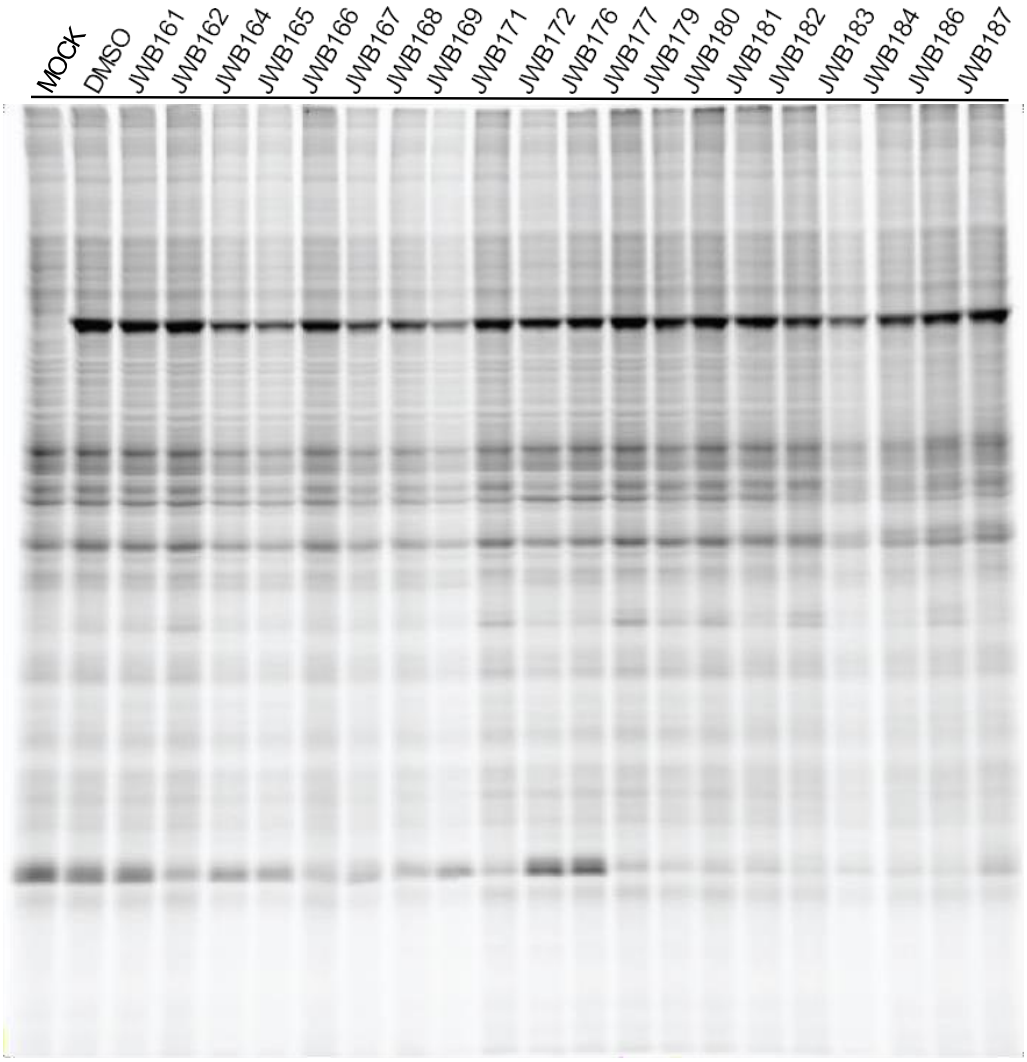

Figure 4.22. competitive ABPP gel results of HEK293T cells expressing recombinant DPP3 treated with SuTEx fragments JWB161-JWB187. Gel screening was conducted by Brulet , R. Rumana, and K. Isbell. Analysis of gel screening conducted by Borne.

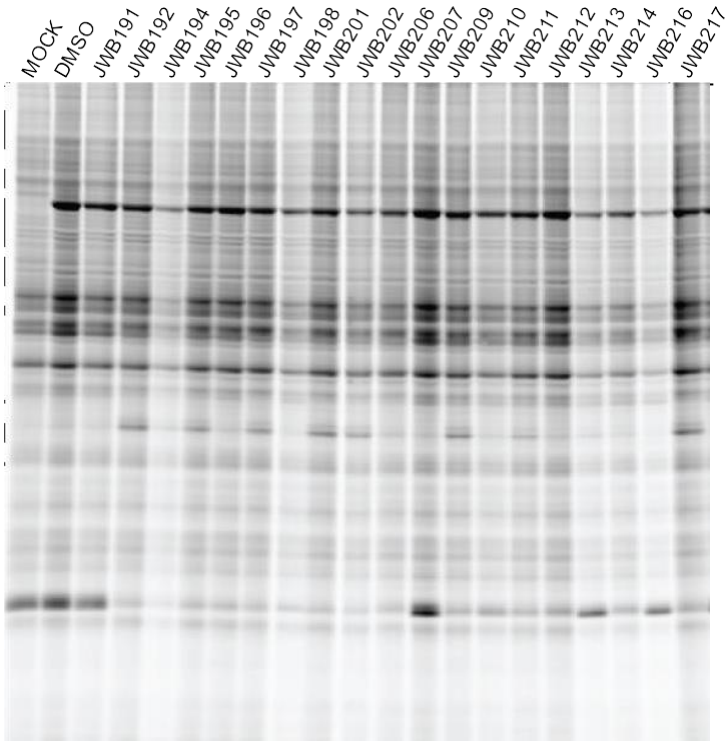

Figure 4.23. competitive ABPP gel results of HEK293T cells expressing recombinant DPP3 treated with SuTEx fragments JWB191-JWB217. Gel screening was conducted by Brulet, R. Rumana, and K. Isbell. Analysis of gel screening conducted by Borne.

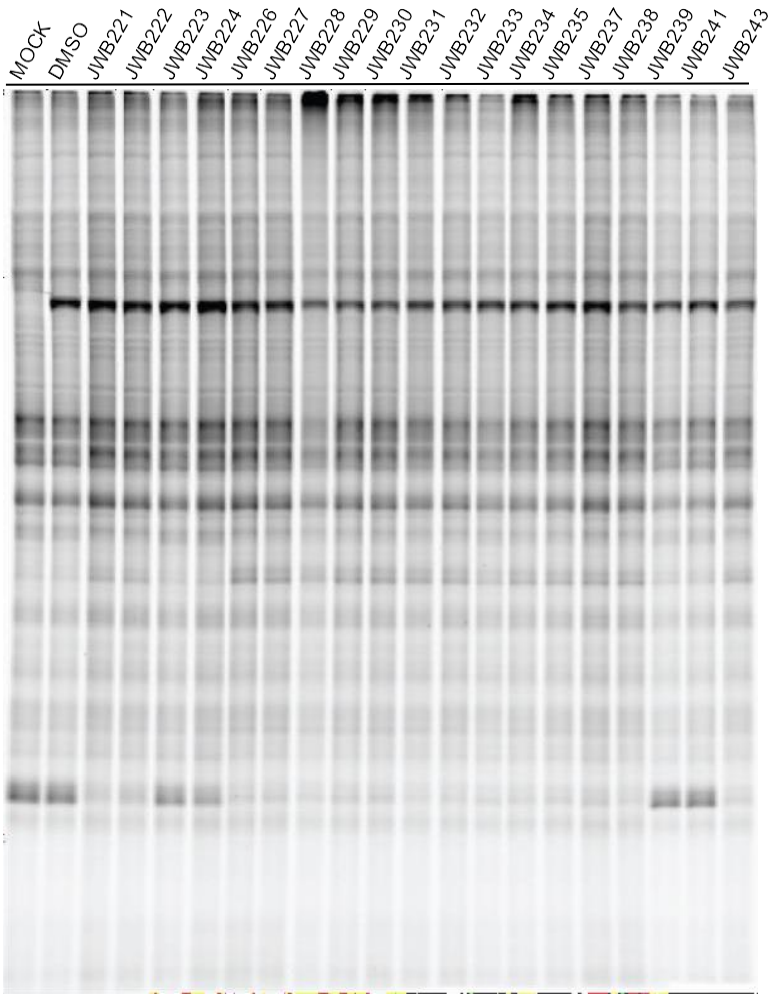

Figure 4.24. competitive ABPP gel results of HEK293T cells expressing recombinant DPP3 treated with SuTEx fragments JWB221-JWB243. Gel screening was conducted by Brulet, R. Rumana, and K. Isbell. Analysis of gel screening conducted by Borne.

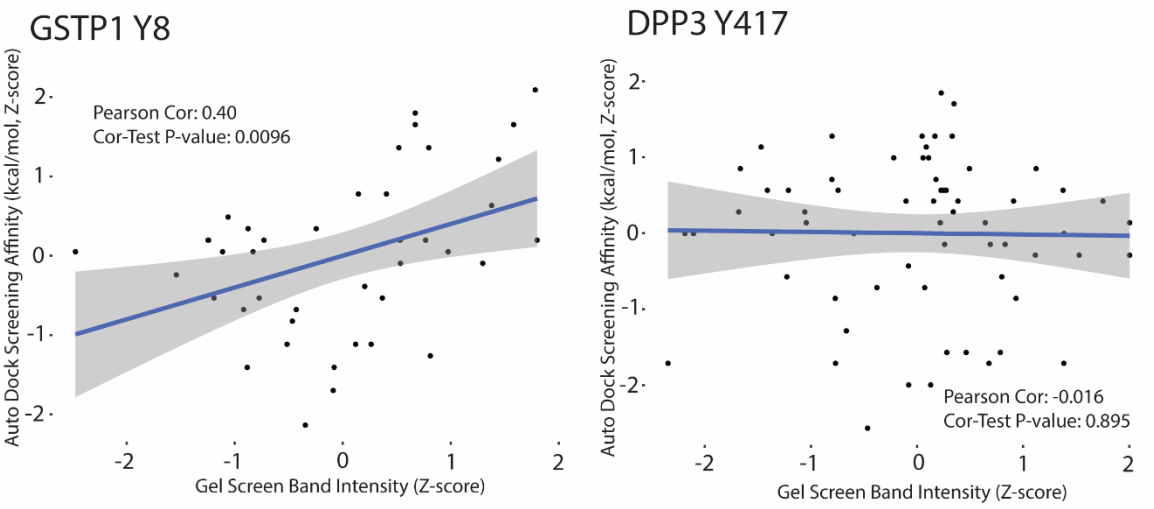

Figure 4.25. Comparison of gel and *in silico* screen. Comparison of z-transformed AutoDock and mock normalized gel band intensities. Docking was performed on structure within 15 Angstroms cube centered on GSTP1 Y7 (Y8 with n-terminal methionine in structure) or DPP3 Y417. Blue line represents simple linear model with grey area representing standard error for the model. Correlation and p-value were calculated using a Pearson's product-moment correlation test. Gel screening was conducted by Brulet, R. Rumana, and K. Isbell. Docking and analysis of gel screening conducted by Borne.

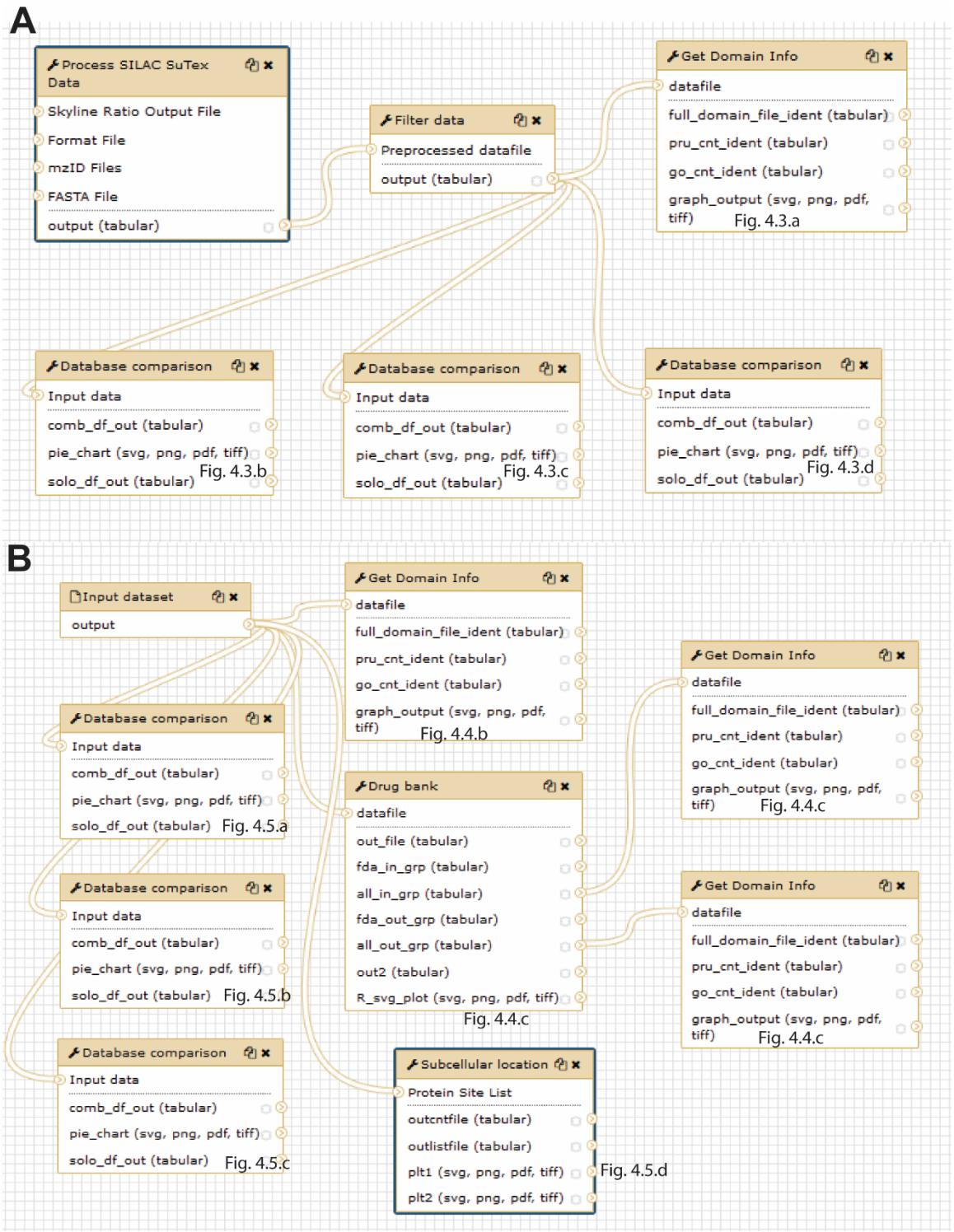

Figure 4.26. Galaxy workflows for global profiling analysis. (A) Workflow for ATP-acyl phosphate analysis. (B) Workflow for HHS-465 and HHS-475 lysine analysis. Figure

numbers denotes where the figure was used. Workflows created by Borne.

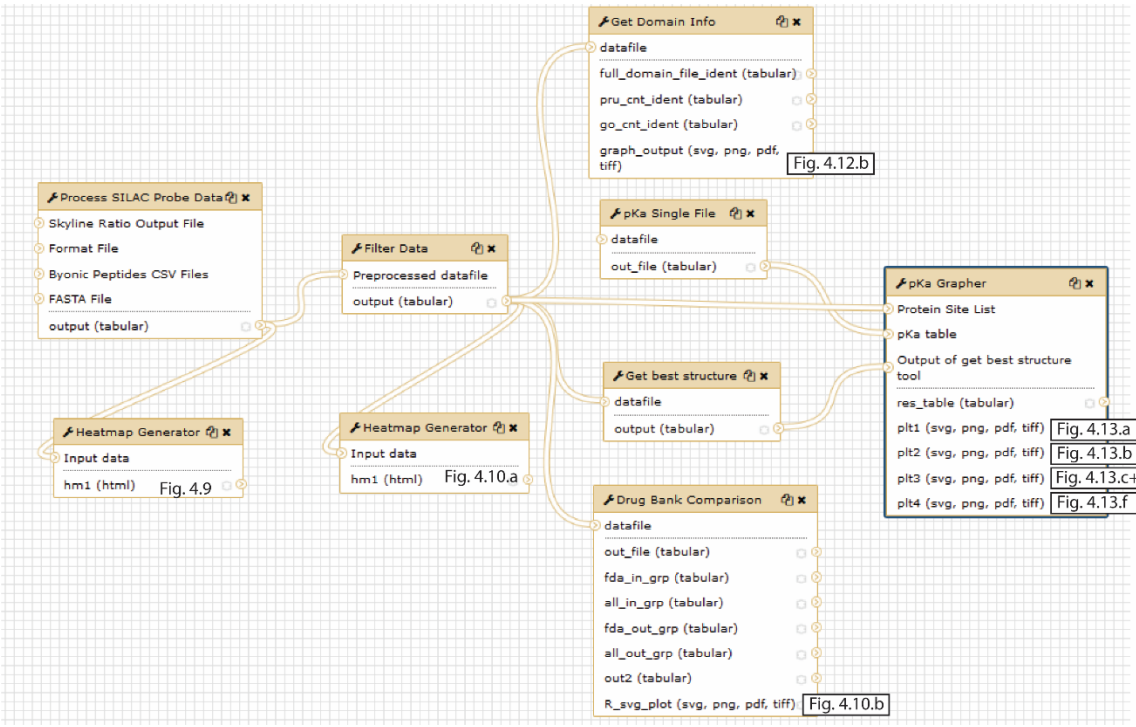

Figure 4.27. Galaxy workflows for competitive ABPP of SuTEx fragment electrophiles. Figure numbers denotes where the figure was used, options for all tools not shown. Workflow created by Borne.

Chapter 5: Discussion

5.1 Summary and Significance

Chapter 2 largely focused on using a known probe to identify previously unknown targets of Ritanserin for the potential repurposing of that compound in cancer. Previously work suggested this compound had the potential to go from a 5'-HT receptor antagonist to a cancer therapeutic. This was supported by the discovery that it inhibited DGKα which is key regulator of signaling pathways that regulate growth, survival and metabolism[103,104]. The study in Chapter 2 provided evidence that more targets (c-Raf in particular) play a role in the cytotoxic effect of Ritanserin in SCLC and NSCLC cell lines. This finding combined with other work using similar approaches has revealed that targeted cancer therapeutics may work best through polypharmacology which is reinforced by the increased use dual-therapies in the treatment of various cancers[60,68]. This also illustrates how the use of an ABP and ABPP can be used to better understand the mechanism of action for kinase inhibitors. This ATP-acyl phosphate, used in this study, has been used to identify off-targets for various clinical and pre-clinical kinase inhibitors[24]. This study adds to the effort to understand mechanisms of action for these molecules by showing that Ritanserin can be added to list of inhibitors that have several relevant kinase targets.

Chapter 3 focuses on the development of a new chemical probe that can perform broad profiling of tyrosine across the proteome. The development of SuTEx chemistry for use as a small molecule covalent probe is a step forward in the development of molecular probing methods for more of the human proteome (Section 1.4). It is the broadest tyrosine selective probe identified to date and many of the targets identified are in the undrugged

proteome. Using this new probe, we were able to draw the first map of SuTEx chemistry hyper-reactive tyrosine sites across the proteome which serves as strong starting point for identifying targets amenable to selective probing and eventual inhibition. Further, we show that the SuTEx molecule has the potential to study phophotyrosine sites across the proteome. Given this PTMs rarity and importance in eukaryotic cell signaling, this probe could be used to improve our understanding of cell signaling[162].

Chapter 4 focuses on developing computational strategies to work with ABPP. This is accomplished by building a platform to improve confidence in site identification as well as leverage the information gained through site-specific MS. Using this platform, we performed a domain enrichment analysis of ATP-acyl phosphate targets and profiled the lysine reactivity of SuTEx probes. The analysis of a small library of fragment electrophiles synthesized in the Hsu lab revealed that SuTEx ligands can be tuned to have lower proteome reactivity. These datasets provide the first map of SuTEx liganded tyrosine sites across the proteome. Further, we were able to use this map to inform an *in silico* docking screen of SuTEx fragment electrophiles. The major contribution of this work is the ability to perform all these tasks in a pipeline that can be used to advance the use of any covalent chemical probe.

This work combined, advances ABPP strategies by contributing to the tools available and applying those tools to biological systems. Similar work has been used to contribute to drug discovery and the creation of clinical tools[69]. While still in the early stages this work has the potential to contribute to the treatment of various human diseases.

5.2 Future Directions

5.2.1. ATP-acyl phosphate and Ritanserin

The ATP-acyl phosphate has already been used in large scale inhibitor profiling and will likely continue to be used to survey protein kinases inhibitors. An interesting application of this probe is using it to define ATP binding pockets on proteins that lack a crystal structure. The probe modified several lysine sites that were sensitive to ATP competition in several domains suggesting these regions are involved in ATP binding[23,36]. Using CPASS-MS to perform an unfiltered screen of targets has the potential to identify more opportunities to perform this type of analysis. Within the targets identified here 16 target that do not have structure in PDB. Combining this information with structures of homologs and mutagenesis could provide key insights into the activity and catalytic mechanisms of kinases as was done with DGKα[36]. In addition, improved probe modified site identification (section 5.2.3) could produce more coverage and targets.

In our group, ritanserin has already been broken into fragments and screened across the kinome[36,100]. We have also combined one of the fragments with SuTEx chemistry and found many kinases are labeled[192]. The results of those studies combined with information presented here suggest ritanserin has some level of binding affinity for several kinases. While on its own it does not bind as many targets as staurosporine or XO-44 it could be elaborated to increase its reach[111]. This late-stage functionalization using RF-01 fragment as directing element has proven a good starting point for the development of live cell kinase probe. Future studies could take advantage of the proteome reactivity changes caused by changing the adduct group seen in Chapter 4 (Fig. 4.9) to increase specificity for targets

that have increased affinity for ABP.

5.2.2. Development of SuTEx Chemical Platform

The ability to tune the reactivity of the SuTEx warhead by appending different EWG and EDG provides a path to create family specific probes and higher affinity ligands. Combined with the information of a domain enrichment analysis directing elements can be selected to create a protein family targeting probe. As an example, combining the probe with a nucleotide like molecule could better enrich RRMs. This may come with the loss of membrane permeability but will still be useful to increase the coverage of these domains *in vitro.* This can be combined with covalent inhibitor screening of live cells can be used to find inhibitors for this generally undrugged class of proteins. This molecule could as be used to target P-glycoproteins (P-gp) which are highly expressed in cancer cells to pump out toxins produced by chemotherapeutics increasing resistance to drug induced cell death[193,194]. There are efforts to develop covalent nucleotide-based inhibitors for this target and a less reactive SuTEx warhead could aid in the development of these inhibitors.

The other major direction for the platform is increased chemical diversity in fragment electrophiles to expand the map and target profile of SuTEx ligands. Thus far only 6 1,2,4 triazole fragments have been screened across a proteome and all of them using limited synthetic chemistry methods. The screening 1,2,3 ligands could identify new targets on lysine as HHS-465 had the greatest lysine reactivity among the original probes (Fig. 3.6.a and 4.4.a). The LC-MS screening of more fragments that include more complex elaboration of the leaving and staying groups combined with the CPASS-MS platform

would enable the identification of structure activity relationships across the proteome.

5.2.3. Advancing Computational Tools for ABPP

CPASS-MS is a useful staging ground for the integration and development of new tools but operates after the acquisition of data and identification of peptide spectra matches. As mentioned in the introduction database search algorithms built with PTMs in mind can outperform standard methods[87]. Through the work presented we have identified unique features of probe modified peptides that could be the basis of dedicated site-specific ABPP database search algorithm. Such an algorithm could be built using these ions or built based on the validated PSMs from previous studies.

Recently, an onboard search algorithm was used to identify peptides from MS2 spectra while the ion is still being injected which is then reanalyzed using an MS3 with different fragmentation conditions to better quantify TMT reporter ions[29]. This is an extension of MS/MS/MS techniques that perform an MS3 scan of an ion based on the presence of a few fragment ions in an MS2 spectra. Either approach could be used to increase the probability that spectra collected can identified by the database search algorithm. Thus, both approaches have the potential to increase SuTEx proteome coverage.

Despite the limited scope of the tools, targets and ligands used the covalent docking screening with SuTEx ligands has shown some promise. Addressing the limited tools can be done by performing the analysis with different docking approaches and comparing them (i.e. DOCKTITE[93]). The second can be done though a focused approach to validating the docking screen where a larger library is screened *in silico* then molecules are selected from across the predicted binding affinities for validation by gel. In addition, any information

gained from the screening of additional ligands can help in the identification of features that make target sites amenable to docking and liganding.

Appendices

Appendix A: Semi-quantitative Profiling of SuTEx Sites with Deuterated Desthiobiotin

A.1 Introduction

The use of SILAC limits the ability to use certain cell lines as not all cell lines can grow in limited culture media. In addition, working with mice requires large amounts of isotopically labelled food to generate a SILAC mouse line. There are several techniques that have aimed to address this such as TMT and iTRAQ which create labeling through covalently modifying the free anime produced by trypsin digestion with mass tag. This study aims to use the desthiobiotin that is attached to the alkyne handle of an ABP to create a mass tag on the probe. This was done by replace eight hydrogens with deuterium in the PEG chain to change the mass of the probe modified by eight Daltons.

A.2 Materials and Methods

SILAC cell culture. DM93 SILAC cells were cultured at 37 °C with 5% CO2 in either ‘light’ or ‘heavy’ media supplemented with 10% dialyzed fetal bovine serum (Omega Scientific), 1% L-glutamine (Fisher Scientific), and isotopically labeled amino acids. Light media was supplemented with 100 μg ml−1 L-arginine and 100 μg ml−1 L-lysine. Heavy media was supplemented with 100 μg ml−1 [13C 15N] L-arginine and 100 μg ml−1 [13C 15N] L-lysine. Labelled amino acids were incorporated for at least five passages before utilizing SILAC cells for experiments. Media was aspirated and cells washed with cold

PBS (2X) before scraping from plates. Cells were transferred to microfuge tubes and pelleted by centrifugation at 500 x g for 5 min, and snap-frozen using liquid N2 and stored -80 °C until further use.

Preparation of SILAC proteomes for liquid chromatography–tandem mass spectrometry (LC–MS/MS) analysis. Heavy and light proteomes (432 µl of each) were diluted to 2.3 mg ml−1 in PBS and sample aliquots (432 µl) were treated with HHS-482 (5 µL, 10mM stock in DMSO) for 1hr at 37 °C. Probe-modified proteomes were conjugated to desthiobiotin-PEG3-azide followed by enrichment of probe-modified peptides for nano-electrospray ionization– LC–MS/MS analyses as previously described[172]**.**

Preparation of d0/d8 proteomes for liquid chromatography–tandem mass spectrometry (LC–MS/MS) analysis. Separate light proteomes (432 µl of each) were diluted to 2.3 mg ml−1 in PBS and sample aliquots (432 µl) Samples were treated with HHS-482 (5 µL, 10mM stock in DMSO) for 1 hr at 37 °C. Probe-modified proteomes were conjugated to d0-desthiobiotin-PEG3-azide or d8-desthiobiotin-PEG3-azide followed by enrichment of probe-modified peptides for nano-electrospray ionization– LC–MS/MS analyses as previously described[172]**.**

LC-MS/MS analysis of samples. Acquisition of spectral data was performed as previously described.

Analysis of LC-MS/MS Spectral Data. Analysis of spectral data performed using Byonic[17], Skyline[86] and CPASS-MS as previously described.

A.3 Results

In order to directly compare the ability of the d0/d8 strategy to quantify site to SILAC, SILAC light and heavy DM93 cell lysates or 2 separate light lysates were treated with 100 uM HHS-475. The SILAC lysates had d0-Desthiobiotin attached via copper catalyzed click chemistry. While the 2 separate light lysates were treated with either d0 or d8-desthiobiotin prepared and analyzed by LC-MS/MS. The resulting MS1 spectra should have d0/d8 and SILAC ratios at ~1 (Fig. Ap.A.1).

The resulting ratios for SILAC were largely consistent but the d0/d8 was shifted up (Fig. Ap.A.2.a). While the means of both samples were near one (SILAC: 1.02, d0/d8: 1.11) there were several sites that reported higher ratios resulting in high standard deviation (Fig. Ap.A.2.b). This shift is not a reflection of the preparation but rather the difficulty in applying the same computational threshold and peak picking for peptide co-eluting versus those that elute at earlier due to the increased acidity of the deuterium on the PEG linker (Fig. Ap.A.3.a-b).

A.4 Discussion

The use of deuterated desthiobiotin has the potential to replace SILAC when it is difficult to use. The computational strategy could be improved to deal with increased ratios resulting from changes in chromatography or deuterium could be replaced with heavy

carbon. This second strategy has already been used to perform such an analysis in E. Coli using iodoacetamide alkyne. In addition, the use of TMT in tandem with probe modified peptides has largely been used to perform multi-plexing for up to 16 probe modified lysates. While there is a benefit of having the mass tag on the probe it removes the additional step in mass spectrometry prep. The obvious next steps have been performed in other publications.

A.5 Author Contributions

The d0/d8 desthiobiotin was synthesized by A. Libby. All other work was performed by Borne.

A.6 Figures

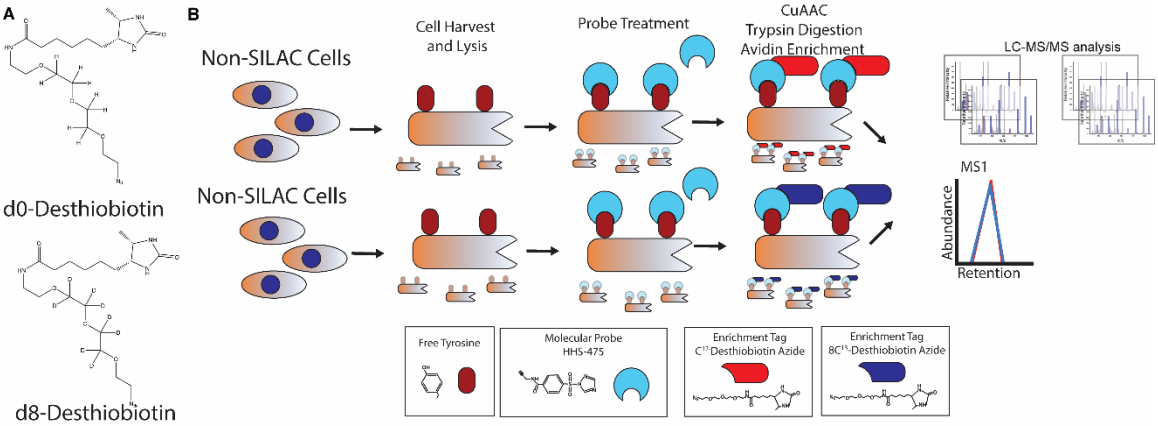

Figure Ap.A.1: (A) Chemical structures of d0 and d8 desthiobiotin with deuterium located on the PEG linker. (B) Schematic of a SuTEx d0/d8 platform. DM93 cells were cultured in SILAC media supplemented with “light” 12C, 14N-labeled lysine and arginine. Heavy and light DM93 lysates were treated with HHS-475 probe. Then the d0 or d8 desthiobiotin was clicked on to the proteins using copper catalyzed click chemistry. The resulting d0/d8

ratios were quantified using the area under the curve of MS1 extracted ion chromatograms. Resulting ratios are expected to be 1. Schematic generated by Borne.

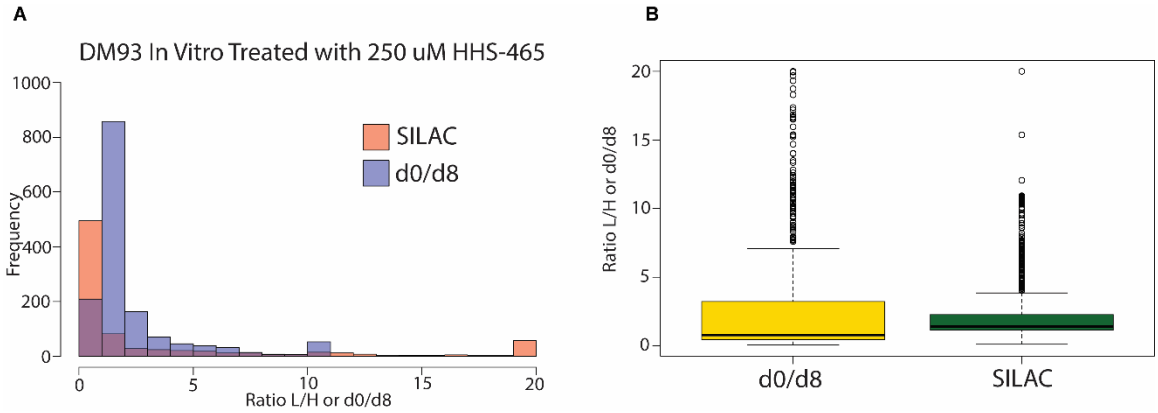

Figure Ap.A.2: (A) Histogram of SILAC and d0/d8 ratios. (B) Box and whisker plot of d0/d8 and SILAC ratios data acquired in DM93 lysates. All work conducted by Borne.

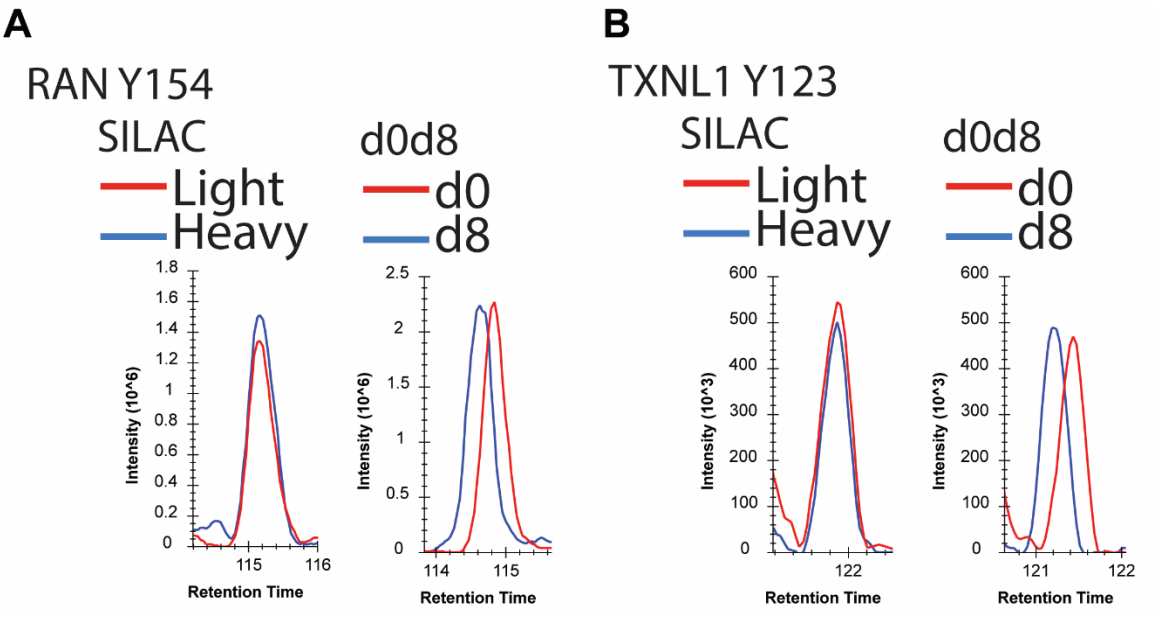

Figure Ap.A.3: EICs for SILAC and d0d8 for RAN Y158 (A) and TXNL1 Y123 (B)

showing differences in retention time for d8 and d0 that is not seen with heavy SILAC. All work conducted by Borne.

Appendix B: Monitoring of DUSP6 Dephosphorylation of ERK1 with SuTEx Probes

B.1 Introduction

The data presented in chapter 3 suggested that SuTEx molecules could be used to measure the level of phosphotyrosine (pY) as in response to treatment in tyrosine phosphatase inhibitor pervanadate several previously annotated pY sites saw decrease abundance. The sites were termed pervanadate sensitive and correlated with increases in pY levels as measures by phospho-blot[172]. It had not yet been shown that the decreased abundance as of probe modified peptide was a direct product of pY blocking probe modification. This study aimed to use approach to determine the targets of phosphatases by treating a lysate with phosphatase and identifying the sites that had increased probe labeling. In order to work with a well annotated pY site and a phosphatase we designed a study to show that Dual Specificity Protein Phosphatase 6 (DUSP6) dephosphorylation of Extracellular signal-regulated kinase 2 (ERK2) Y187 could be measured using SuTEx probes and MS.

B.2 Materials and Methods

SILAC cell culture. DM93 SILAC cells were cultured at 37 °C with 5% CO2 in either ‘light’ or ‘heavy’ media supplemented with 10% dialyzed fetal bovine serum (Omega Scientific), 1% L-glutamine (Fisher Scientific), and isotopically labeled amino acids. Light media was supplemented with 100 μg ml−1 L-arginine and 100 μg ml−1 L-lysine. Heavy

media was supplemented with 100 μg ml−1 [13C 15N] L-arginine and 100 μg ml−1 [13C 15N] L-lysine. Labelled amino acids were incorporated for at least five passages before utilizing SILAC cells for experiments. Media was aspirated and cells washed with cold PBS (2X) before scraping from plates. Cells were transferred to microfuge tubes and pelleted by centrifugation at 500 x g for 5 min, and snap-frozen using liquid N2 and stored -80 °C until further use.

Gel-based chemical proteomic assay. Cell pellets were lysed in PBS and fractionated (100,000 x g, 45 min, 4 °C) to generate soluble and membrane fractions. Protein concentrations were determined using Bio-Rad DC protein assay and adjusted to 1 mgml-1 in PBS. Proteome samples (49 μL aliquots) were treated with DMSO vehicle or indicated concentration of caping molecule (1 μL, 50X stock in DMSO) for 30 min at 37 °C. Samples were then treated with HHS-482 probe (1 μL, 2.5 mM stock in DMSO) for 30 min at 37 °C. Probe labeled samples were conjugated to rhodamine-azide (1 μL, 1.25 mM stock; final concentration of 25 μM) by copper-catalyzed azide-alkyne cycloadditions (CuAAC) for 1 hr at room temperature followed by SDS-PAGE and in-gel fluorescence scanning as previously described[172].

Preparation of SILAC proteomes for liquid chromatography–tandem mass spectrometry (LC–MS/MS) analysis. Heavy and light proteomes (432 μl of each) were diluted to 2.3 mg ml−1 in PBS with protease and phosphatase inhibitor (432 μl). The capped samples were then treated with JWB-150 (5 μL, 10mM stock in DMSO). The

heavy samples were then treated with 10 uL of 5 mg/mL (20 ug/mL final) DUSP6 for 30 minutes. Samples were treated with HHS-482 or HHS-475 as indicated (5 μL, 10mM stock in DMSO) for 30 min at 37 °C. Probe-modified proteomes were conjugated to desthiobiotin-PEG3-azide followed by enrichment of probe-modified peptides for nano-electrospray ionization– LC–MS/MS analyses as previously described[172]**.**

LC-MS/MS analysis of samples. Acquisition of spectral data was performed as previously described.

Analysis of LC-MS/MS Spectral Data. Analysis of spectral data performed using Byonic[17], Skyline[86] and CPASS-MS as previously described.

B.3 Results

Testing the ability to detect DUSP6 mediated changes in pY 187 on ERK2 was done by taking SILAC heavy and light cells lysing them and treating the light cells with DUSP6. This was followed by the 100 uM HHS-482 treatment, addition of destiobiotin, enrichment, elution and analysis by LC-MS. The expectation would be that sites of DUSP6 dephosphorylation would have an increase light to heavy ratio (Fig Ap.B.1.a). We validated the loss of ERK2 Y187 with by taking a portion of the lysate and performing a western blot for pY187 and overall ERK (Fig. Ap.B.1.b). Despite the decrease in pY as measured by gel we saw no change in the SILAC ratio for ERK2 187 site (Fig. Ap.B.1.b-c).

In order to remove more free tyrosine from the system prior to treatment with DUSP6 we attempted to generate a capping molecule that would remove covalently modify the free tyrosine leaving only the phosphorylated version. Initially we created two non-clickable HHS-482 analogs that replaced the alkyne handle with an alkene (ALB-001) and an alkane (ALB-002). We compared these analogs to the most reactive molecule identified in chapter 4, JWB-150 in a gel based competitive screen as previously described. Despite ALB-001/2 being direct analogs JWB-150 showed the greatest level of inhibition by gel (Fig. Ap.B.2).

Using 100 uM JWB-150 as a capping agent we performed the same LC-MS assay as previously described but with 1 hr 37 °C capping step prior to DUSP6 treatment (Fig. Ap.B.3.a). We used the phosphobotting assay to show that we could still see dephosphorylation of ERK2 Y187 by DUSP6 in the presence of JWB-150 and HHS-482 (Fig. Ap.B.3.b). Once again we saw no change in the SILAC ratio for ERK 187 using both HHS-482 and HHS-475 as probes (Fig. Ap.B.3.c).

B.4 Discussion

These results suggest that the probe is not able to measure the abundance of ERK2 Y187 despite being able to report the probe modified site by MS. The first possible explanation for this is that the portion pY to free tyrosine is very low despite being in B-RAF driven melanoma cell line. The B-RAF V600E mutation would increase the amount phosphorylated ERK through the increased MAPK signaling activity[126]. The capping agent was attempted to remove some of the free tyrosine from the lysate through covalent modification with non-clickable SuTEx probe. Despite this change there was no detectable

change in probe modified ERK2 Y187 after DUSP6 dephosphorylation.

There are several possible explanations for the lack of change in SILAC ratio. First, despite capping there is still mostly free tyrosine on ERK Y187. Larger concentrations of cap are likely to cause additional issues as it has 200 uM combined SuTEx electrophile pushes the limit of solubility in PBS, thus lower protein concentrations should be used to attempt to lower overall free tyrosine. Second, pervanadate sensitivity reflects changes in protein or peptide availability from sources other than phosphorylation. The two proteins shown as pervanadate sensitive STAT3 and CTNND1 are both transcription factors that associate with DNA when activated by phosphorylation[167,168]. Given that the previous assay does not include a resuspension step the protein could be lost in the membrane fraction. This can be rectified by performing the same experiment with a resuspension step.

B.5 Author Contributions

ALB-001/2 was synthesized by A. Libby. All data was generated and analyzed by Borne.

B.6 Figures

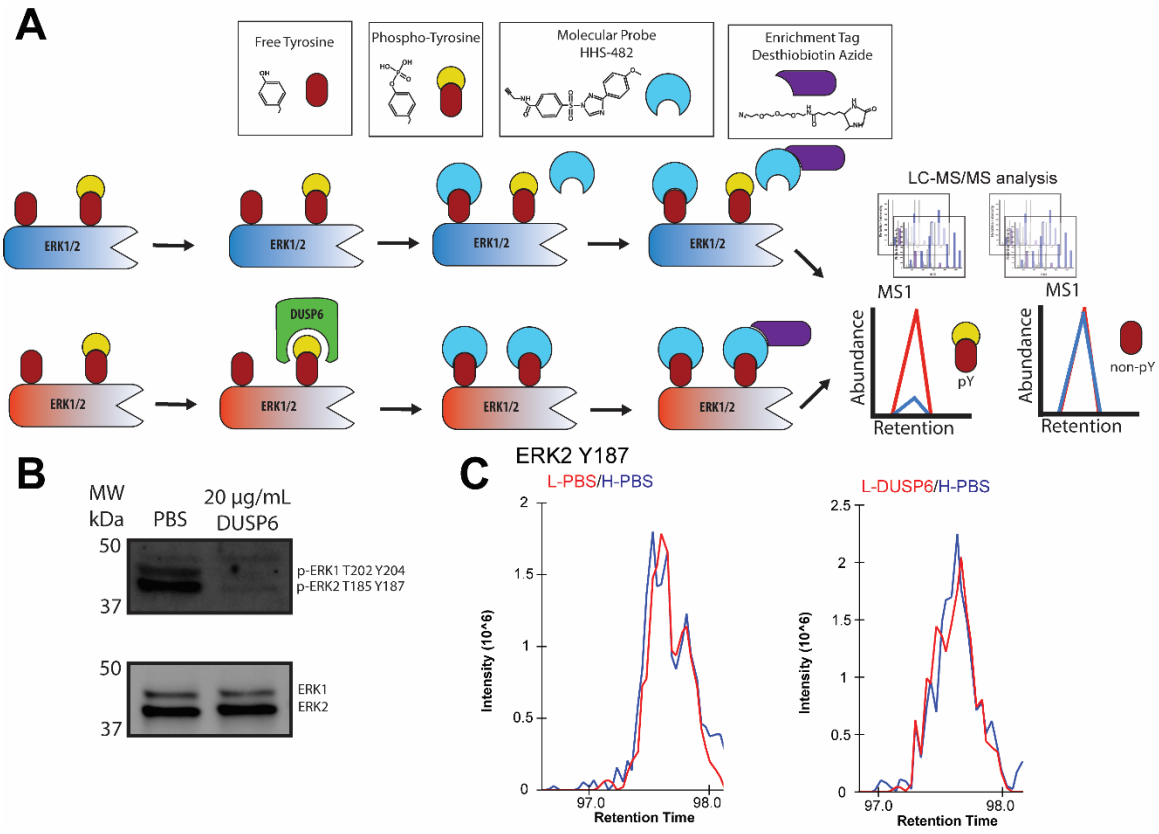

Figure Ap.B.1: (A) Schematic of a SuTEx platform for monitoring DUSP6 phosphotyrosine sites. DM93 cells were cultured in SILAC media supplemented with either "light" 12C, 14N-labeled lysine and arginine (denoted in red) or "heavy" 13C, 15N-labeled lysine and arginine (denoted in blue). Heavy and light DM93 proteomes were treated with PBS vehicle or DUSP6 20 ug/mL, 37 °C, 30 min) followed by HHS-482 probe labeling using the same reaction conditions. The resulting SILAC ratios (SR) were quantified using the area under the curve of MS1 extracted ion chromatograms. Dephosphorylated tyrosines are expected to show increased probe labeling intensity in the light (left MS1, SR~1). (B) Validation of ERK2 dephosphorylation by DUSP6 using western blot for p-ERK2 and overall ERK. (C) MS1 EICs of ERK2 Y187 tyrosine sites from quantitative LC-MS chemical proteomics. Data shown are representative of n = 2

biologically independent experiments. Data acquired and analyzed by Borne.

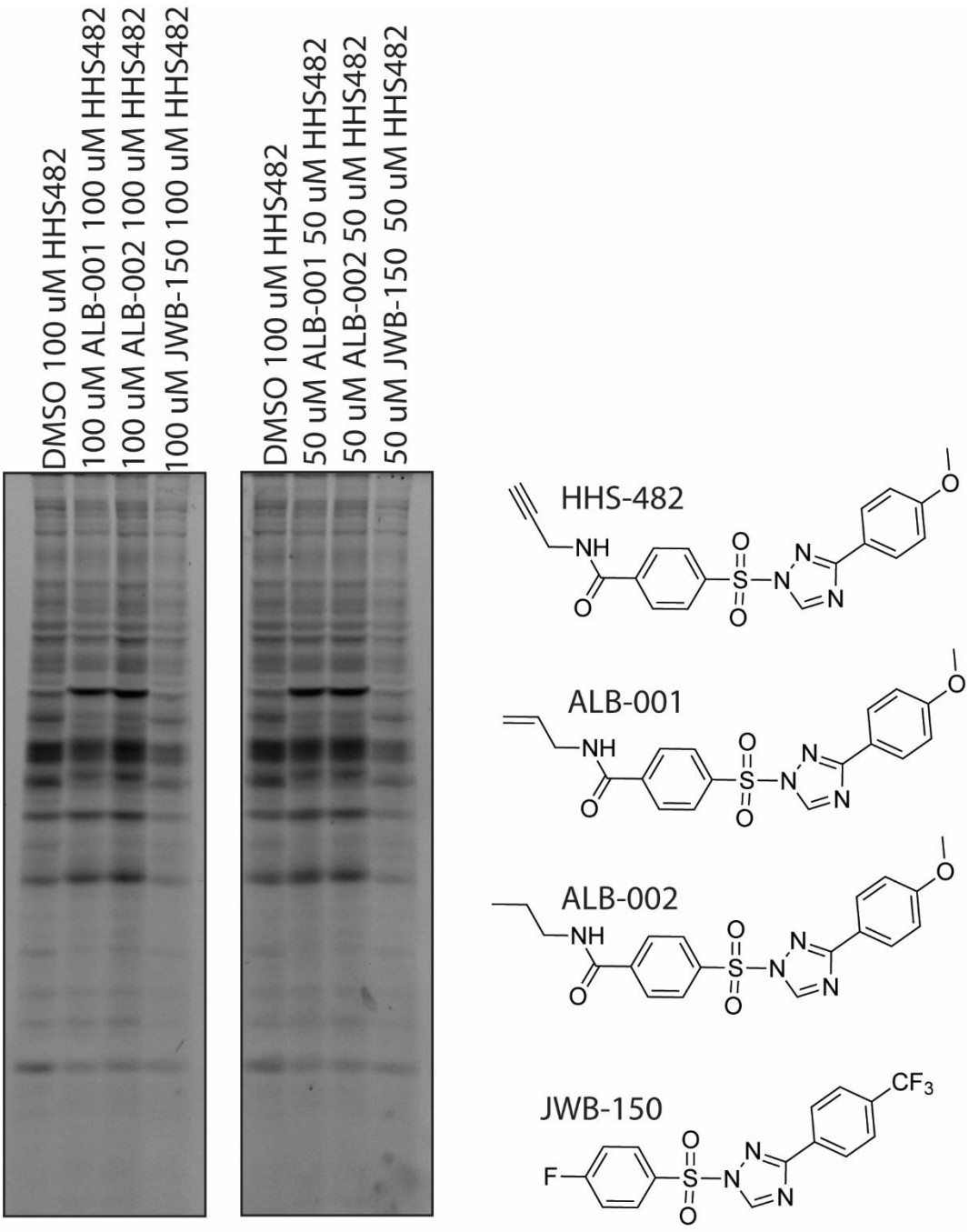

Figure Ap.B.2: Competitive capping molecule screen. Lysates were treated with indicated

concentration of cap followed by HHS-482. Rhodamine was appended using copper-catalyzed click chemistry and lysates run on SDS-PAGE gel. All work conducted by Borne.

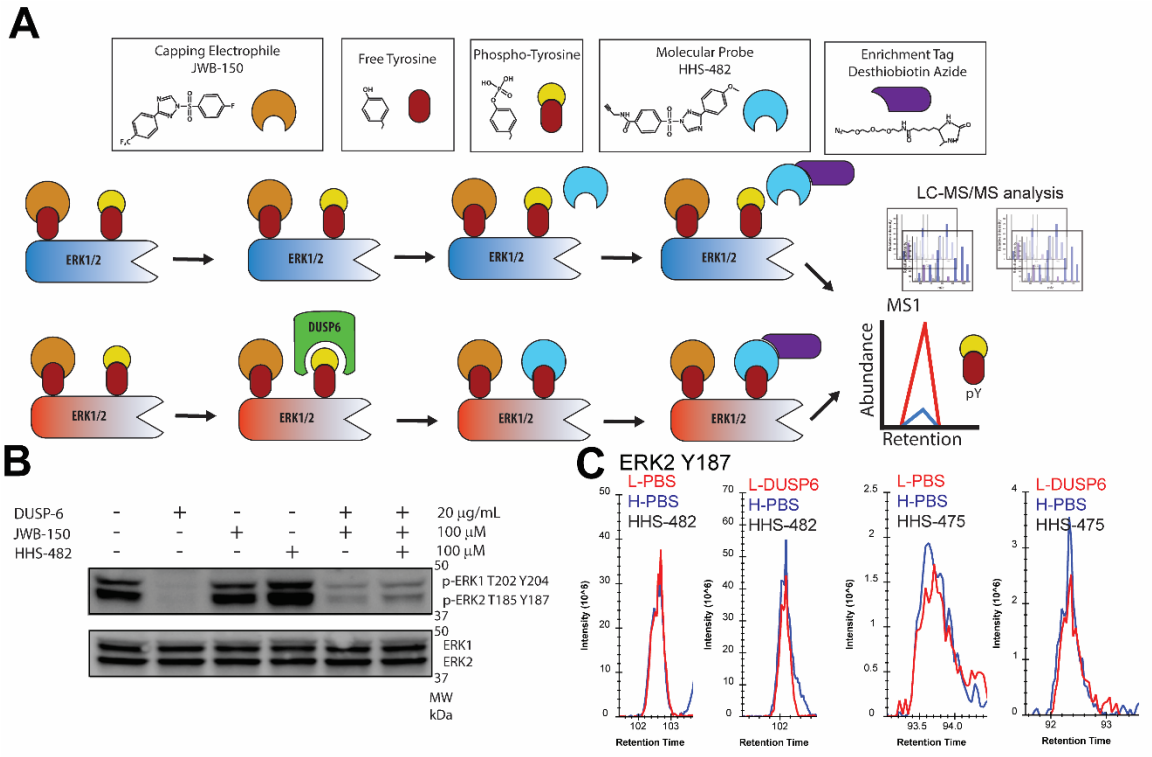

Figure Ap.B.3: (A) Schematic of a SuTEx platform for monitoring DUSP6 phosphotyrosine sites with cappuing. DM93 cells were cultured in SILAC media supplemented with either “light” 12C, 14N-labeled lysine and arginine (denoted in red) or “heavy” 13C, 15N-labeled lysine and arginine (denoted in blue). Heavy and light DM93 proteomes were treated withJWB-150 (100uM, 1hr at 37 °C) then PBS vehicle or DUSP6 (20 ug/mL, 37 °C, 30 min) followed by HHS-482 probe labeling using the same reaction conditions. The resulting SILAC ratios (SR) were quantified using the area under the curve of MS1 extracted ion chromatograms. Dephosphorylated tyrosines are expected to show

increased probe labeling intensity in the light (left MS1, SR~1). (B) Validation of ERK2 dephosphorylation by DUSP6 in the presence of JWB-150, HHS-482 and the combination using western blot for p-ERK2 and overall ERK. (C) MS1 EICs of ERK2 Y187 tyrosine sites from quantitative LC-MS chemical proteomics using HHS-482 and HHS-475. Data shown are representative of n = 2 biologically independent experiments. Data acquired and analyzed by Borne.

Appendix C: Investigation of SHMT1 Inhibition by SuTEx ligands

C.1 Introduction

In addition to gel-based screening SuTEx ligands against DPP3 and GSTP1 discussed in chapter 4 Serine Hydroxymethyltransferase 1 (SHMT1) was also screened. The same docking comparison was also performed, and four molecules were selected for MS screening.

C.2 Materials and Methods

SILAC cell culture. DM93 SILAC cells were cultured at 37 °C with 5% CO2 in either 'light' or 'heavy' media supplemented with 10% dialyzed fetal bovine serum (Omega Scientific), 1% L-glutamine (Fisher Scientific), and isotopically labeled amino acids. Light media was supplemented with 100 μg ml−1 L-arginine and 100 μg ml−1 L-lysine. Heavy media was supplemented with 100 μg ml−1 [13C 15N] L-arginine and 100 μg ml−1 [13C 15N] L-lysine. Labelled amino acids were incorporated for at least five passages before utilizing SILAC cells for experiments. Media was aspirated and cells washed with cold

PBS (2X) before scraping from plates. Cells were transferred to microfuge tubes and pelleted by centrifugation at 500 x g for 5 min, and snap-frozen using liquid N2 and stored -80 °C until further use.

Preparation of SILAC proteomes for liquid chromatography–tandem mass spectrometry (LC–MS/MS) analysis. Heavy and light proteomes (432 µl of each) were diluted to 2.3 mg ml−1 in PBS and sample aliquots (432 µl) were treated with SuTEx fragment at the indicated concentrations (5 µl, 100X stock in DMSO), mixed gently and incubated for 30 min at 37 °C. Samples were then treated with HHS-482 (5 µL, 10mM stock in DMSO) for 30 min at 37 °C. Probe-modified proteomes were conjugated to desthiobiotin-PEG3-azide followed by enrichment of probe-modified peptides for nano-electrospray ionization– LC–MS/MS analyses as previously described[172]**.**

C.3 Results

To look at affinity of molecules we screened all the ligands in the 1,2,4 SuTEx library using both the docking tool and gel based ABPP. We then compared the predicted binding affinity to loss of band intensity upon pre-treatment with a fragment. In brief, HEK293T cell lysates were pre-treated with 100µM inhibitor for 30 minutes at 37° C followed by 50µM of HHS-482, a tyrosine selective 1,2,4-sulfonyl triazole probe, for 30 minutes. Samples underwent copper catalyzed azide-alkyne cycloaddition (CuAAC) with rhodamine azide and were resolved by SDS- PAGE. Gels were visualized and the total lane fluorescent intensity was normalized to DMSO and compared (Fig. Ap.C.1- Ap.C.5.

Inhibitors that decreased lane intensity compared by greater than 30% were removed as they were likely to be broadly reacting molecules. The loss of band intensity and the AutoDock (see Materials and Methods, Table 4.16) calculated binding affinities were z-transformed and compared using a simple linear model in R. Correlation and p-value were calculated using a Pearson's product-moment correlation test. A strong correlation was seen between docking results and gel data (0.6, Fig. A).

JWB-101, 112, 147 and 157 were selected for further validation by MS competitive ABPP as described in Chapter 4. We quantified 1,385 sites from 700 proteins (Fig. Ap.C.7). Among which only a few had SRs greater than 2 and even less with ratios greater than 4 (Fig.Ap.C.7). This is likely due to the filtering out of generally reactive molecules in the gel-based screening (Section 4.6) resulting in the selection of less reactive electrophiles. This low reactivity is also reflected in gel-based dose response experiments (Fig.Ap.C.8). In addition, we were unable to detect SHMT1 Y34 among the 1,385 sites quantified making the LC-MS data unable to provide inhibition information for the target screened by gel.

C.4 Discussion

While the gel-based screening showed promise but the inability to determine compound activity against SHMT1 means the docking results could not be verified by MS. The SHMT1 study is incomplete and could be attempted in another cell line with higher endogenous levels of SHMT1 or overexpressing the protein. In addition, the results could be used to expand the chemoproteomic profiling dataset used to determine important

proteome structure activity relationships[192].

C.5 Author Contributions

Gel screening was conducted by Brulet, Borne, R. Rumana, and K. Isbell. Everything else conducted by Borne.

C.6 Figures

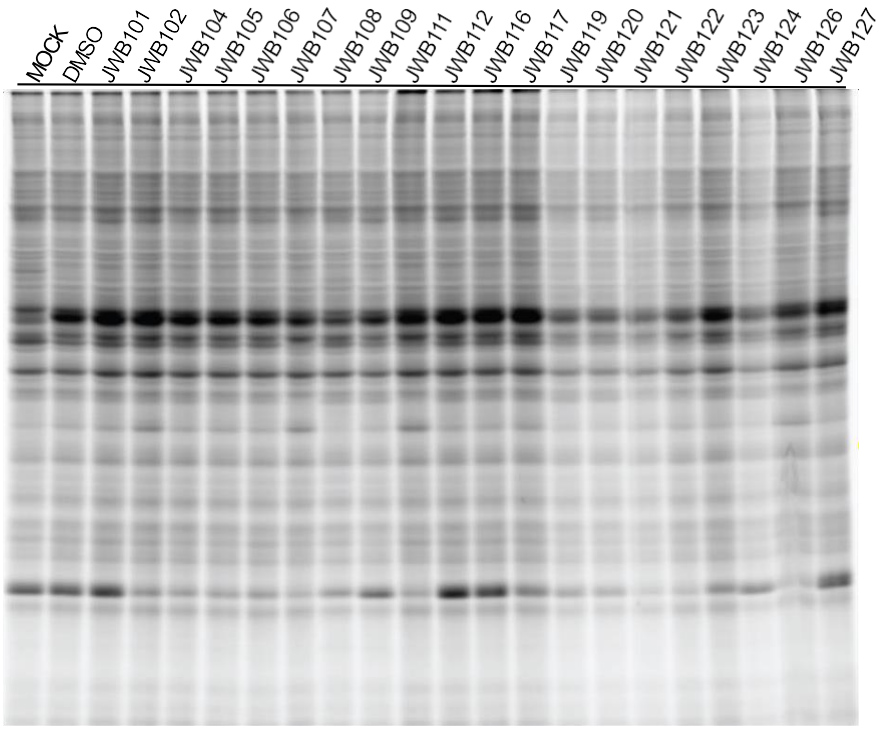

Figure Ap.C.1: competitive ABPP gel results of HEK293T cells expressing recombinant SHMT1 treated with SuTEx fragments JWB101-JWB127. Gel screening was conducted by Brulet, R. Rumana, and K. Isbell. Analysis of gel screening conducted by Borne.

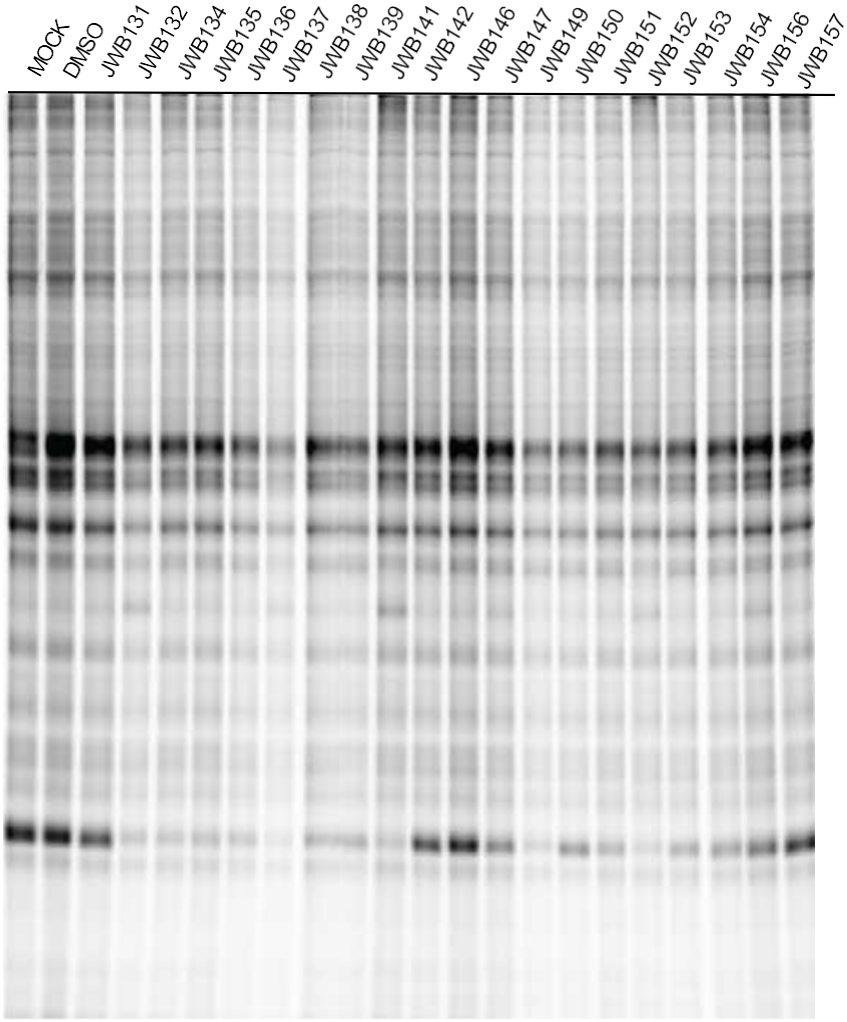

Figure Ap.C.2: competitive ABPP gel results of HEK293T cells expressing recombinant SHMT1 treated with SuTEx fragments JWB131-JWB157. Gel screening was conducted by Brulet, R. Rumana, and K. Isbell. Analysis of gel screening conducted by Borne.

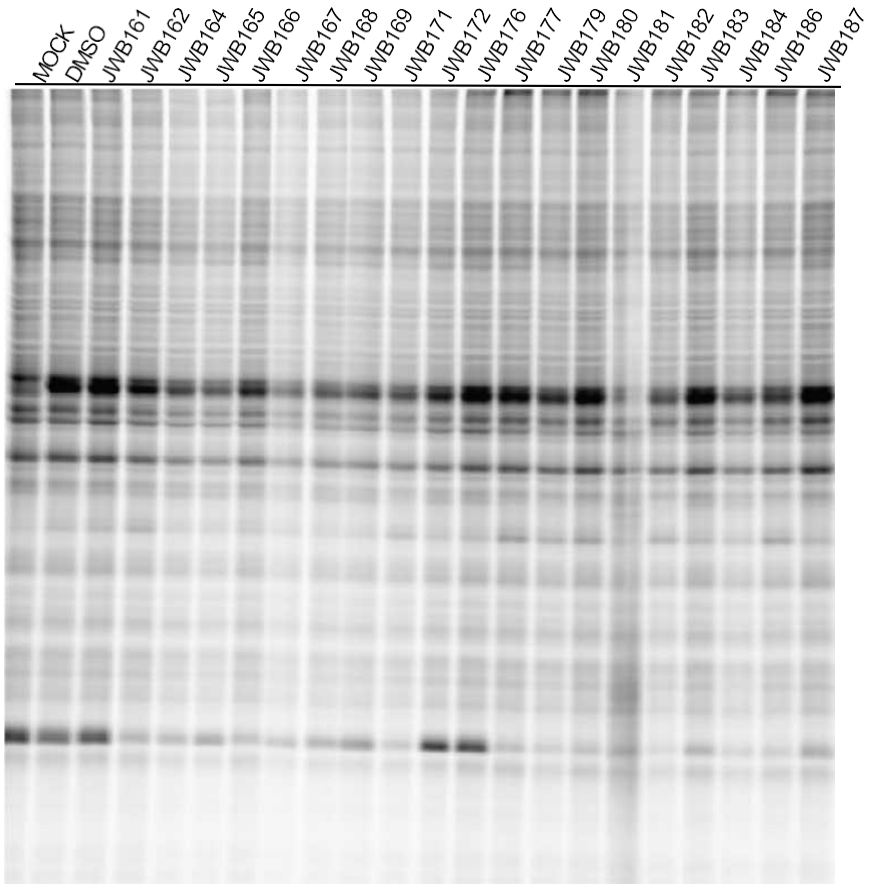

Figure Ap.C.3: competitive ABPP gel results of HEK293T cells expressing recombinant SHMT1 treated with SuTEx fragments JWB161-JWB187. Gel screening was conducted by Brulet, R. Rumana, and K. Isbell. Analysis of gel screening conducted by Borne.

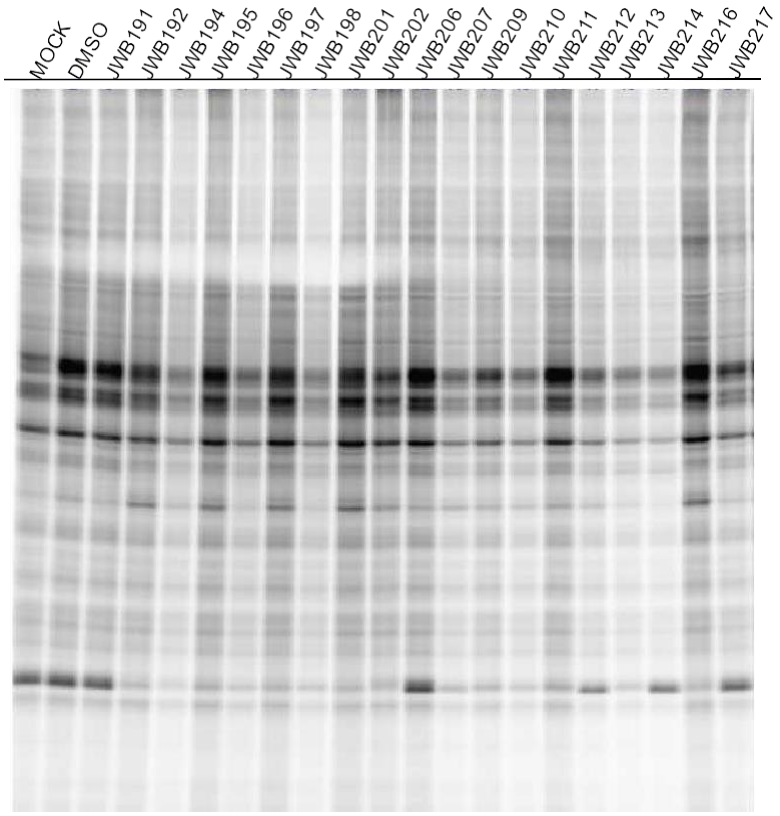

Figure Ap.C.4: competitive ABPP gel results of HEK293T cells expressing recombinant SHMT1 treated with SuTEx fragments JWB191-JWB243. Gel screening was conducted by Brulet, R. Rumana, and K. Isbell. Analysis of gel screening conducted by Borne.

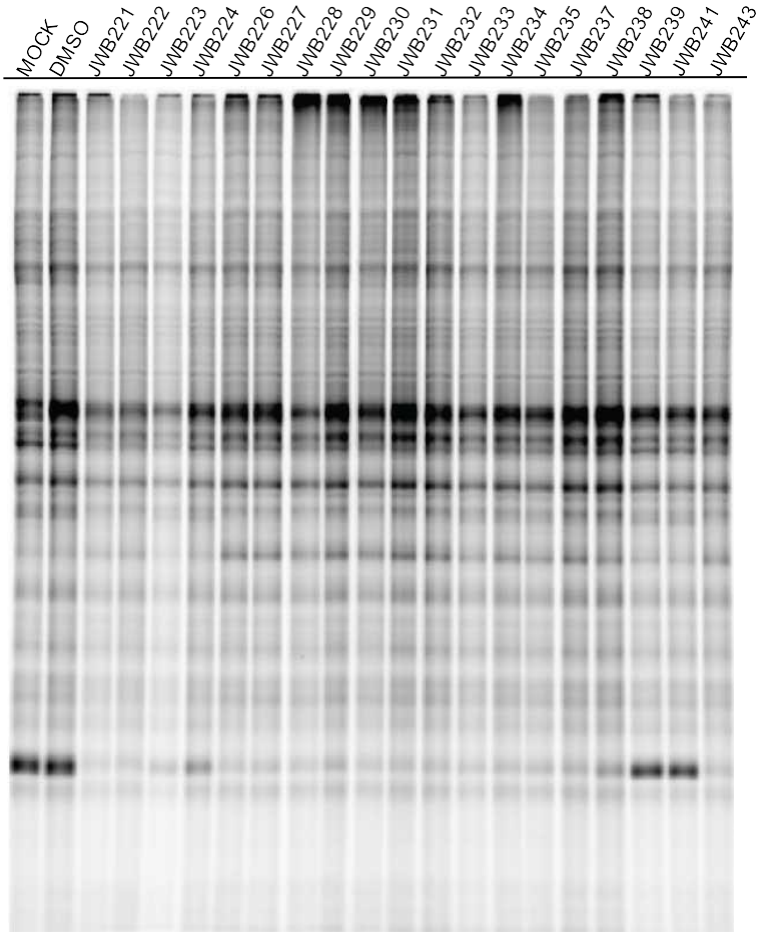

Figure Ap.C.5: competitive ABPP gel results of HEK293T cells expressing recombinant SHMT1 treated with SuTEx fragments JWB221-JWB243. Gel screening was conducted by Brulet, R. Rumana, and K. Isbell. Analysis of gel screening conducted by Borne.

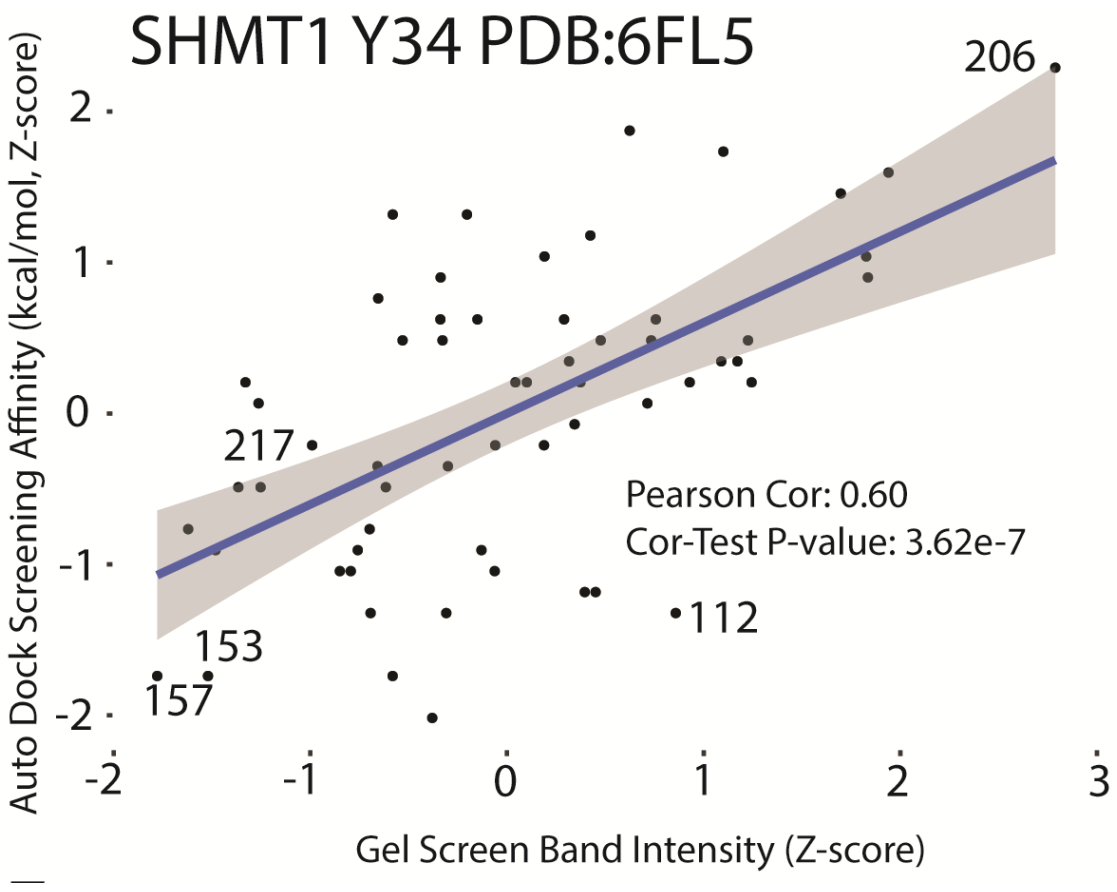

Figure Ap.C.6: Comparison of gel and *in silico* screen. Comparison of z-transformed AutoDock and mock normalized gel band intensities. Docking was performed on structure within 15 Angstroms cube centered on SHMT1 Y34. Blue line represents simple linear model with grey area representing standard error for the model. Correlation and p-value were calculated using a Pearson's product-moment correlation test (PDB: 6FL5). Gel screening was conducted by Brulet, R. Rumana, and K. Isbell. Docking and analysis of gel screening conducted by Borne.

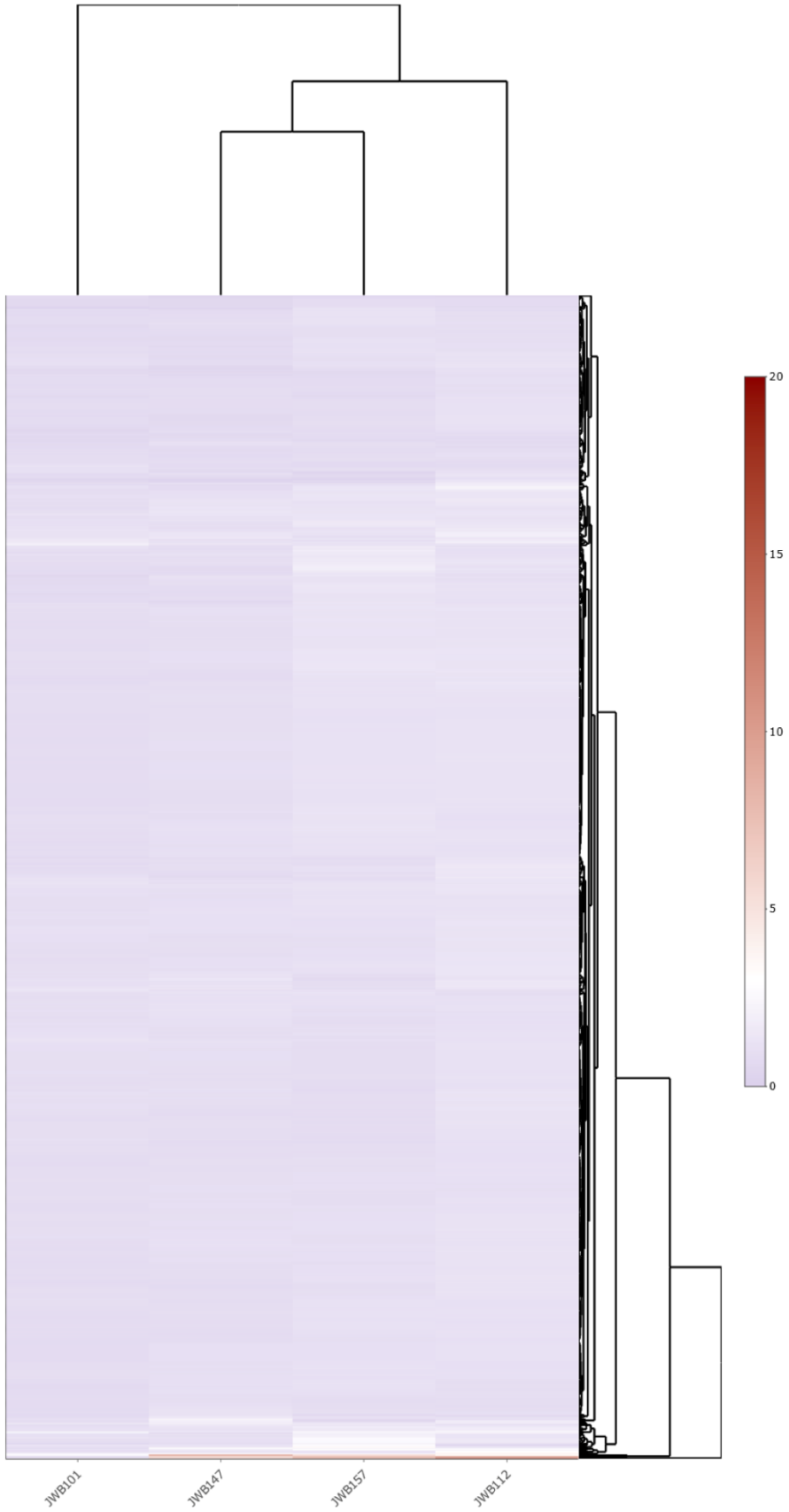
20
15
10
5
0
JWB101
JWB147
JWB157
JWB112

Figure Ap.C.7: Fragment-based ligand discovery using SuTEx (all tyrosine sites). Heat map showing SILAC ratios (SR) of all quantified tyrosines in chemical proteomic studies configured for evaluating ligand competition. Fragments and liganded tyrosine sites are organized by hierarchical clustering. Data shown are representative of n = 3 biologically independent experiments. Data acquired and analyzed by Borne.

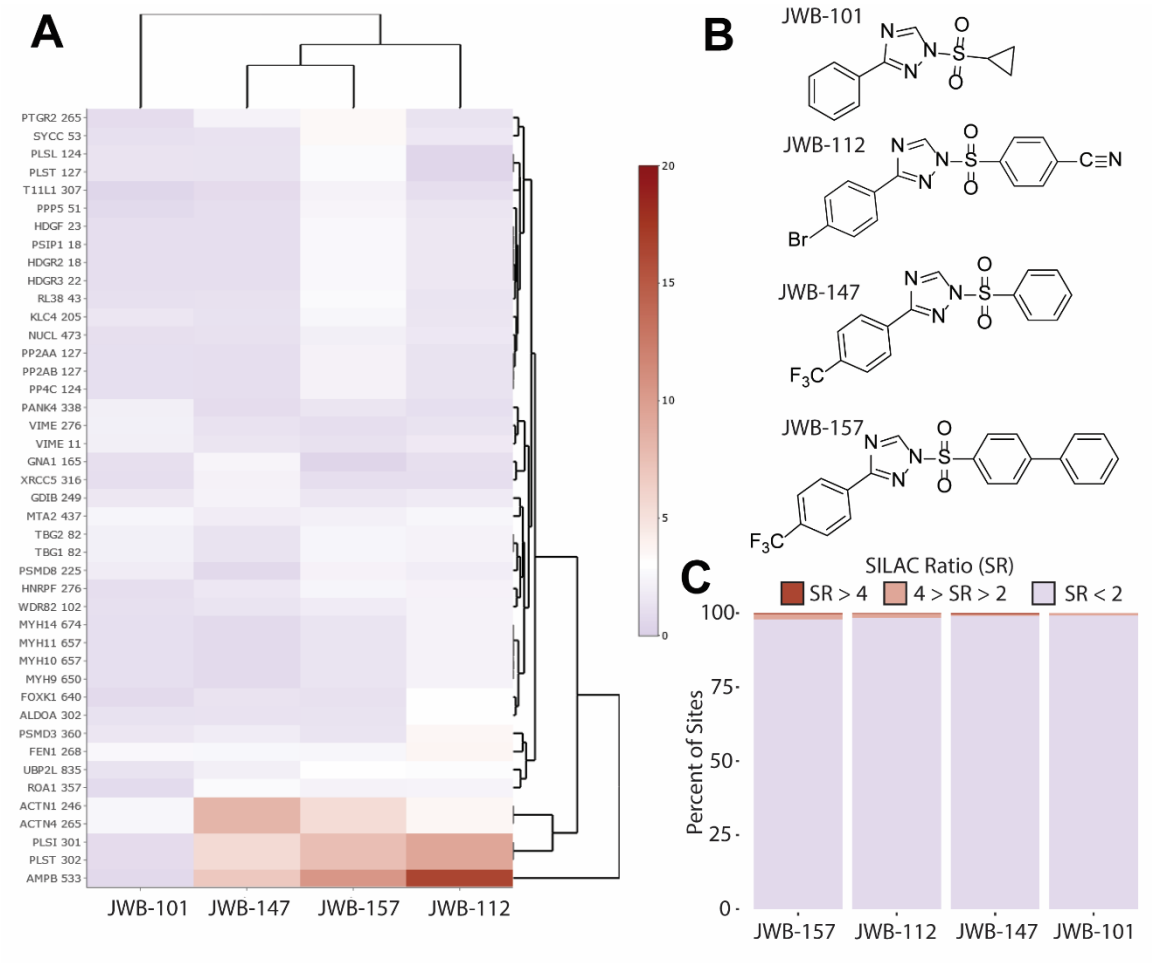

Figure Ap.C.8: Figure 4.9. Fragment-based ligand discovery using SuTEx. (A) Heat map

showing SILAC ratios (SR) of representative tyrosines competed by fragments and organized by hierarchical clustering. Fragment competition at tyrosine sites was quantified using the area under the curve of MS1 extracted ion chromatograms (EIC) from HHS-482-labeled peptides in DMSO (light, red) versus fragment-treated (heavy, blue) DM93 soluble proteomes. Competitive chemical proteomic studies were performed as shown in Figure S3. Tyrosine sites shown are liganded (SR > 4) by at least 2 fragments with the number of liganded sites and proteins listed for each molecule. The y-axis lists the protein name and quantified tyrosine site. (B) Chemical structures of JWB-101/112/147 and 157. (C) Reactivity of fragments was assessed by comparing the fraction of tyrosine sites competed: nonliganded (blue, SR < 2), partially liganded (orange, 2≤ SR ≤ 4), and liganded (yellow, SR > 4). All data shown are representative of n = 3 biologically independent experiments. Data acquired and analyzed by Borne.

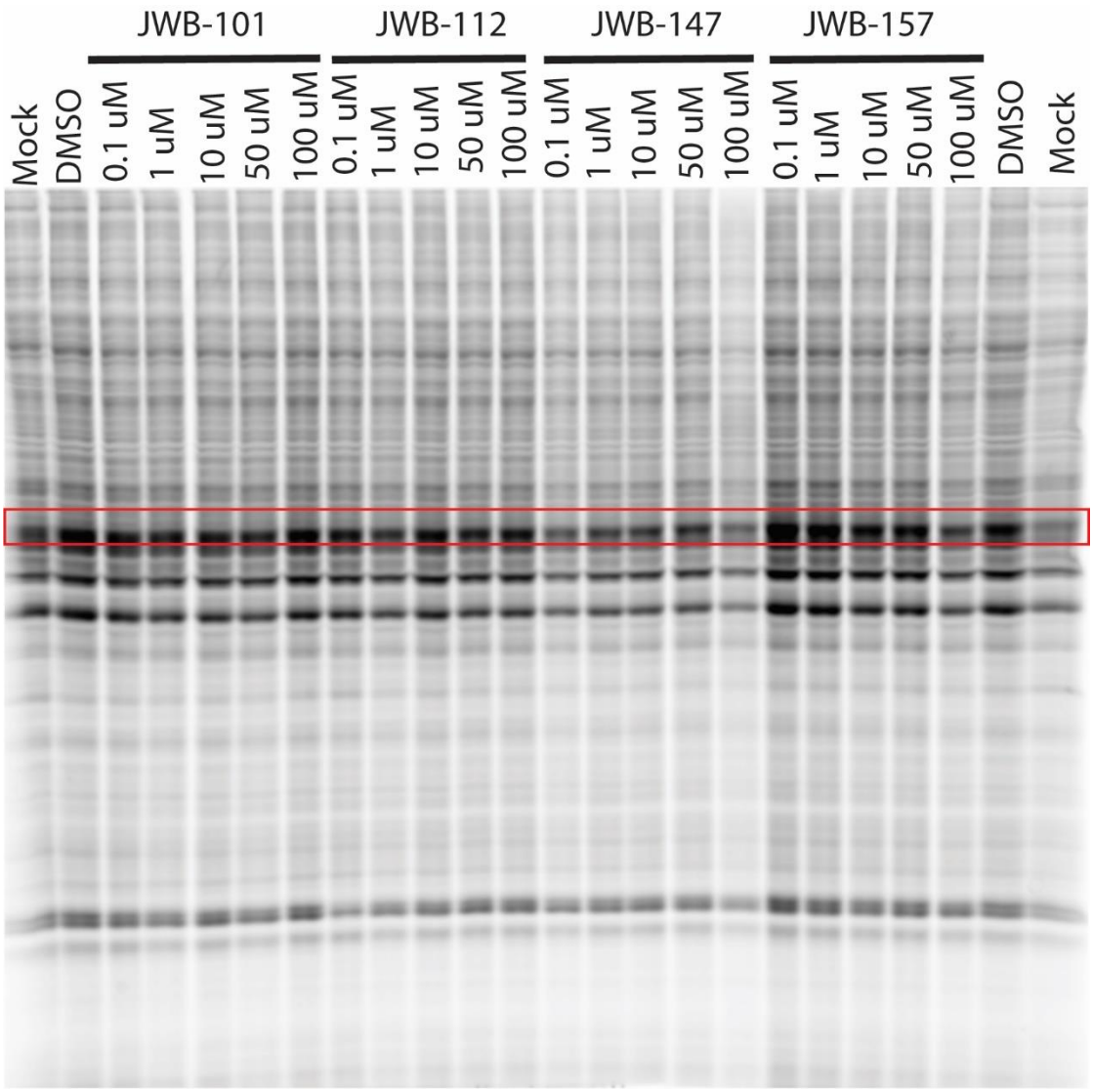

Figure Ap.C.9: Competitive dose-response gels for SHMT1. HEK293T cells were transfected with a Mock control of SHMT1 overexpression plasmid. Lysates were treated with DMSO, or concentration of fragment electrophile shown. All work done by Borne.

Appendix D: Chapter 4 Tables

Table 4.1. Datafiles used in ATP-acyl phosphate analysis.

Raw File	Source	Treatment
20161101_CEF_SILAC_DGKA_HEK293T_S_LDMSO_HATP_LYSC_3hr_21.mzXML	Franks et al. 2017	HEK ATP
20161101_CEF_SILAC_DGKA_HEK293T_S_LDMSO_HDMSO_LYSC_3hr_21.mzXML	Franks et al. 2017	HEK DMSO
20161102_CEF_SILAC_DGKA_HEK293T_S_LDMSO_HATP_LYSC_3hr_21.mzXML	Franks et al. 2017	HEK ATP
20161102_CEF_SILAC_DGKA_HEK293T_S_LDMSO_HDMSO_LYSC_3hr_21.mzXML	Franks et al. 2017	HEK DMSO
20161109_CEF_SILAC_DGKZ_HEK293T_S_LDMSO_HATP_LYSC_3hr_21.mzXML	Franks et al. 2017	HEK ATP
20161109_CEF_SILAC_DGKZ_HEK293T_S_LDMSO_HATP_LYSC_3hr_22.mzXML	Franks et al. 2017	HEK ATP
20161109_CEF_SILAC_DGKZ_HEK293T_S_LDMSO_HDMSO_LYSC_3hr_21.mzXML	Franks et al. 2017	HEK DMSO
20161109_CEF_SILAC_DGKZ_HEK293T_S_LDMSO_HDMSO_LYSC_3hr_22.mzXML	Franks et al. 2017	HEK DMSO
20161117_CEF_SILAC_DGKI_HEK293T_S_LDMSO_HATP_LYSC_3hr_21.mzXML	Franks et al. 2017	HEK ATP
20161117_CEF_SILAC_DGKI_HEK293T_S_LDMSO_HDMSO_LYSC_3hr_21.mzXML	Franks et al. 2017	HEK DMSO
20170118_CEF_SILAC_DGKA_HEK293T_S_LDMSO_HATP_LYSC_3hr_21.mzXML	Franks et al. 2017	HEK ATP
20170118_CEF_SILAC_DGKA_HEK293T_S_LDMSO_HATP_LYSC_3hr_22.mzXML	Franks et al. 2017	HEK ATP
20170118_CEF_SILAC_DGKA_HEK293T_S_LDMSO_HDMSO_LYSC_3hr_21.mzXML	Franks et al. 2017	HEK DMSO
20170118_CEF_SILAC_DGKA_HEK293T_S_LDMSO_HDMSO_LYSC_3hr_22.mzXML	Franks et al. 2017	HEK DMSO
20170227_CEF_SILAC_HEK293T_DGKE_M_LDMSO_HATP_LYSC_3hr_21.mzXML	Franks et al. 2017	HEK ATP
20170227_CEF_SILAC_HEK293T_DGKE_M_LDMSO_HDMSO_LYSC_3hr_21.mzXML	Franks et al. 2017	HEK DMSO
20170419_CEF_A549_S_LDMSO_HATP_LYSC_3hr_21.raw	Campbell et al. 2018	A549 ATP
20170419_CEF_A549_S_LDMSO_HATP_LYSC_3hr_22.raw	Campbell et al. 2018	A549 ATP
20170419_CEF_A549_S_LDMSO_HDMSO_LYSC_3hr_21.raw	Campbell et al. 2018	A549 DMSO
20170419_CEF_A549_S_LDMSO_HDMSO_LYSC_3hr_22.raw	Campbell et al. 2018	A549 DMSO
20170610_CEF_SILAC_H82_S_LDMSO_HATP_LYSC_3hr_BR4_21.raw	Campbell et al. 2018	H82 ATP
20170610_CEF_SILAC_H82_S_LDMSO_HATP_LYSC_3hr_BR4_22.raw	Campbell et al. 2018	H82 ATP
20170610_CEF_SILAC_H82_S_LDMSO_HDMSO_LYSC_3hr_BR4_21.raw	Campbell et al. 2018	H82 DMSO

20170610_CEF_SILAC_H82_S_LDMSO_HDMSO_LYSC_3hr_BR4_22.raw	Campbell et al. 2018	H82 DMSO
20170612_CEF_SILAC_A549_S_LDMSO_HATP_LYSC_3hr_BR3_21.raw	Campbell et al. 2018	A549 DMSO
20170612_CEF_SILAC_A549_S_LDMSO_HDMSO_LYSC_3hr_BR3_21_170612120000.raw	Campbell et al. 2018	A549 ATP

Table 4.2. ATP sensitive sites (SR >5)

Site	Gene_ID	Uniprot_ID	QuantitativeValue	Treatment
O00418_238	EF2K	O00418	20	H82ATP
O08560_5	DGKZ	O08560	20	HEK293TATP
O75912_553	DGKI	O75912	20	HEK293TATP
O95835_734	LATS1	O95835	20	HEK293TATP
P15735_364	PHKG2	P15735	20	HEK293TATP
P22102_219	PUR2	P22102	20	HEK293TATP
P23919_19	KTHY	P23919	20	A549ATP
P23919_19	KTHY	P23919	20	HEK293TATP
P36507_196	MP2K2	P36507	20	A549ATP
P36507_196	MP2K2	P36507	20	HEK293TATP
P45985_231	MP2K4	P45985	20	A549ATP
P45985_231	MP2K4	P45985	20	HEK293TATP
P46734_93	MP2K3	P46734	20	HEK293TATP
P51812_81	KS6A3	P51812	20	HEK293TATP
P52564_82	MP2K6	P52564	20	A549ATP
P54646_45	AAPK2	P54646	20	HEK293TATP
P54819_28	KAD2	P54819	20	HEK293TATP
P55072_336	TERA	P55072	20	A549ATP
Q02750_192	MP2K1	Q02750	20	A549ATP
Q02750_192	MP2K1	Q02750	20	HEK293TATP
Q12905_228	ILF2	Q12905	20	HEK293TATP
Q12931_324	TRAP1	Q12931	20	HEK293TATP
Q13131_56	AAPK1	Q13131	20	HEK293TATP
Q13574_662	DGKZ	Q13574	20	HEK293TATP
Q15418_75	KS6A1	Q15418	20	HEK293TATP
Q2M389_868	WASH7	Q2M389	20	HEK293TATP
Q8IZ83_564	A16A1	Q8IZ83	20	A549ATP
Q99759_491	M3K3	Q99759	20	A549ATP
Q99986_5	VRK1	Q99986	20	HEK293TATP
Q9BTW9_299	TBCD	Q9BTW9	20	HEK293TATP
Q9UK32_86	KS6A6	Q9UK32	20	HEK293TATP
Q9Y2U5_485	M3K2	Q9Y2U5	20	A549ATP
O14965_143	AURKA	O14965	19.44132	HEK293TATP
Q96GD4_87	AURKB	Q96GD4	19.44132	HEK293TATP
Q9UQB9_53	AURKC	Q9UQB9	19.44132	HEK293TATP
P22102_219	PUR2	P22102	18.8114	H82ATP
P55072_336	TERA	P55072	18.30731	HEK293TATP
O95835_734	LATS1	O95835	18.0738	A549ATP

Q99759_491	M3K3	Q99759	17.68801	HEK293TATP
Q9Y2U5_485	M3K2	Q9Y2U5	17.68801	HEK293TATP
Q8IZ83_564	A16A1	Q8IZ83	17.28536	HEK293TATP
P43155_245	CACP	P43155	16.94135	H82ATP
P23368_156	MAOM	P23368	16.61946	H82ATP
P12268_208	IMDH2	P12268	16.56918	H82ATP
P07900_585	HS90A	P07900	16.19542	A549ATP
Q99759_491	M3K3	Q99759	16.08953	H82ATP
Q9Y2U5_485	M3K2	Q9Y2U5	16.08953	H82ATP
P78527_3753	PRKDC	P78527	15.97752	H82ATP
P23919_19	KTHY	P23919	15.94403	H82ATP
Q96J92_328	WNK4	Q96J92	15.70905	HEK293TATP
Q9H4A3_375	WNK1	Q9H4A3	15.70905	HEK293TATP
Q9Y3S1_349	WNK2	Q9Y3S1	15.70905	HEK293TATP
P23743_547	DGKA	P23743	15.69557	HEK293TATP
P51556_3	DGKA	P51556	15.69557	HEK293TATP
P54819_28	KAD2	P54819	15.44264	H82ATP
P55072_336	TERA	P55072	15.02316	H82ATP
P52564_82	MP2K6	P52564	14.61583	H82ATP
P36959_325	GMPR1	P36959	13.85757	HEK293TATP
Q9P2T1_325	GMPR2	Q9P2T1	13.85757	HEK293TATP
O75385_140	ULK1	O75385	13.7045	HEK293TATP
P23368_156	MAOM	P23368	13.45212	HEK293TATP
Q13418_341	ILK	Q13418	13.32629	HEK293TATP
P53396_836	ACLY	P53396	12.94504	HEK293TATP
P23526_188	SAHH	P23526	12.90413	HEK293TATP
Q14166_419	TTL12	Q14166	12.82891	HEK293TATP
P60891_194	PRPS1	P60891	12.39342	HEK293TATP
P54819_28	KAD2	P54819	12.30128	A549ATP
P46734_93	MP2K3	P46734	12.1995	A549ATP
Q00535_128	CDK5	Q00535	12.02202	HEK293TATP
P78527_3753	PRKDC	P78527	11.98977	HEK293TATP
P55072_236	TERA	P55072	11.64623	HEK293TATP
P23368_156	MAOM	P23368	11.42615	A549ATP
P40306_101	PSB10	P40306	10.87086	A549ATP
Q15126_22	PMVK	Q15126	10.81531	HEK293TATP
P36507_196	MP2K2	P36507	10.7826	H82ATP
Q02750_192	MP2K1	Q02750	10.7826	H82ATP
P30837_383	AL1B1	P30837	10.58033	A549ATP
Q00535_128	CDK5	Q00535	9.641793	A549ATP
P52564_82	MP2K6	P52564	8.925375	HEK293TATP
Q00535_33	CDK5	Q00535	8.785498	HEK293TATP
P30837_383	AL1B1	P30837	8.718923	HEK293TATP
Q00535_128	CDK5	Q00535	8.691988	H82ATP
P54646_45	AAPK2	P54646	8.648296	A549ATP
Q13131_56	AAPK1	Q13131	8.648296	A549ATP
Q9BTW9_299	TBCD	Q9BTW9	8.519497	A549ATP
Q00535_33	CDK5	Q00535	8.497057	A549ATP

O94804_159	STK10	O94804	8.054743	HEK293TATP
P42345_2166	MTOR	P42345	7.530975	A549ATP
Q9NVE7_171	PANK4	Q9NVE7	6.890847	HEK293TATP
Q00535_33	CDK5	Q00535	6.788359	H82ATP
P23528_144	COF1	P23528	6.629744	A549ATP
P22102_219	PUR2	P22102	6.574142	A549ATP
P60709_328	ACTB	P60709	6.536011	A549ATP
P62736_330	ACTA	P62736	6.536011	A549ATP
P63261_328	ACTG	P63261	6.536011	A549ATP
P63267_329	ACTH	P63267	6.536011	A549ATP
P68032_330	ACTC	P68032	6.536011	A549ATP
P68133_330	ACTS	P68133	6.536011	A549ATP
Q562R1_329	ACTBL	Q562R1	6.536011	A549ATP
P16949_53	STMN1	P16949	6.282388	HEK293TATP
Q93045_87	STMN2	Q93045	6.282388	HEK293TATP
Q9H169_97	STMN4	Q9H169	6.282388	HEK293TATP
Q6P2I7_38	EBLN2	Q6P2I7	6.045202	HEK293TATP
P51812_81	KS6A3	P51812	6.01306	H82ATP
Q15418_75	KS6A1	Q15418	6.01306	H82ATP
Q9UK32_86	KS6A6	Q9UK32	6.01306	H82ATP
Q9HB71_146	CYBP	Q9HB71	5.82521	H82ATP
Q6L8Q7_377	PDE12	Q6L8Q7	5.810859	HEK293TATP
P48643_176	TCPE	P48643	5.669828	HEK293TATP
Q8TBX8_101	PI42C	Q8TBX8	5.616329	HEK293TATP
P12268_422	IMDH2	P12268	5.594532	H82ATP
Q8N4P3_97	MESH1	Q8N4P3	5.566254	HEK293TATP
P60709_113	ACTB	P60709	5.513931	A549ATP
P63261_113	ACTG	P63261	5.513931	A549ATP
O00479_18	HMGN4	O00479	5.489477	HEK293TATP
P05204_18	HMGN2	P05204	5.489477	HEK293TATP
P04083_166	ANXA1	P04083	5.416856	A549ATP
P50502_153	F10A1	P50502	5.33632	HEK293TATP
Q8IZP2_149	ST134	Q8IZP2	5.33632	HEK293TATP
Q8NFI4_153	F10A5	Q8NFI4	5.33632	HEK293TATP
P62937_155	PPIA	P62937	5.201141	H82ATP
O15530_465	PDPK1	O15530	5.160405	A549ATP
P07737_116	PROF1	P07737	5.138126	HEK293TATP
Q15208_118	STK38	Q15208	5.094903	HEK293TATP
P60709_113	ACTB	P60709	5.08162	HEK293TATP
P63261_113	ACTG	P63261	5.08162	HEK293TATP
Q13574_1025	DGKZ	Q13574	5.029271	HEK293TATP

Table 4.3. Domain enrichment of ATP sensitive sites.

ProRule Domain	Number Liganded	Number in Database	Database Frequency	P-Value	Description	BH Corrected Q-Value

PRU00159	24	512	0.01684377	2.80E-34	Protein kinase domain	3.08E-33
PRU00998	3	5	0.00016449	3.16E-08	Stathmin-like (SLD) domain	1.74E-07
PRU01175	1	3	9.87E-05	0.003547	HD domain	0.0130051
PRU01040	1	5	0.00016449	0.005905	DZF domain	0.0155792
PRU00501	1	6	0.00019739	0.007081	Alpha-type protein kinase	0.0155792
PRU00781	1	9	0.00029608	0.010604	Phosphatidylinositol phosphate kinase (PIPK) domain	0.0194405
PRU00599	1	12	0.00039478	0.014114	ADF-H domain	0.0219315
PRU00568	1	14	0.00046057	0.016448	TTL domain	0.0219315
PRU00547	1	17	0.00055927	0.019938	CS domain	0.0219315
PRU00269	1	17	0.00055927	0.019938	PI3K/PI4K domain	0.0219315
PRU00156	1	24	0.00078955	0.028035	PPIase cyclophilin-type domain	0.0280346

Table 4.4. Identified HHS-465 and HHS-475 lysine sites.

Combined Lysine Sites	465 Sites	475 Sites
P60709_50	P10809_31	P10809_387
P60709_61	P10809_58	P13010_265
P60709_113	P10809_72	P09429_30
P60709_191	P10809_75	Q9BWD1_235
P60709_213	P10809_89	P10809_133
P60709_284	P10809_91	P10809_269
P60709_291	P10809_125	P10809_473
P60709_315	P10809_130	P0DMV8_108
P60709_326	P10809_156	P0DMV8_159
P60709_328	P10809_202	P0DMV8_328
P10809_31	P10809_205	P0DMV8_345
P10809_58	P10809_233	P63261_61
P10809_72	P10809_236	P63261_113
P10809_75	P10809_249	P63261_326
P10809_82	P10809_269	P13639_337
P10809_89	P10809_292	P09874_249
P10809_87	P10809_352	P22626_59
P10809_91	P10809_359	P68104_146
P10809_96	P10809_387	P68104_172
P10809_125	P10809_389	P68104_215
P10809_130	P10809_473	P68104_273

P10809_133	P68104_41	P11142_159
P10809_156	P68104_44	A0A024RB53_8
P10809_160	P68104_146	A0A024RB53_298
P10809_180	P68104_219	Q00839_265
P10809_191	P68104_255	Q00839_635
P10809_196	P68104_273	P62805_92
P10809_202	P68104_392	P38646_206
P10809_205	P68104_395	P06748_54
P10809_233	P68104_408	P06748_248
P10809_236	P68104_439	P06748_250
P10809_249	P68104_444	P06748_257
P10809_250	P68104_450	P06748_273
P10809_269	P68104_453	P61978_405
P10809_292	P68104_457	P61978_456
P10809_301	P0DMV8_77	P14625_561
P10809_310	P0DMV8_88	P68363_96
P10809_352	P0DMV8_102	P58876_109
P10809_359	P0DMV8_108	P19338_333
P10809_361	P0DMV8_159	P19338_513
P10809_364	P0DMV8_251	P06733_281
P10809_387	P0DMV8_328	P17844_470
P10809_389	P0DMV8_345	P06576_432
P10809_396	P0DMV8_348	P13010_291
P10809_469	P0DMV8_524	P12956_189
P10809_473	P0DMV8_569	P43243_798
P10809_481	P0DMV8_597	P14866_418
P07437_19	P11142_108	P78527_1407
P07437_58	P11142_159	P52272_381
P07437_122	P11142_187	P40926_165
P07437_154	P11142_251	P63241_39
P07437_216	P11142_328	P63241_67
P07437_252	P11142_345	P05141_23
P07437_297	P11142_524	Q14103_129
P07437_324	P11142_539	Q14103_197
P07437_336	P09874_23	P62937_28
P07437_350	P09874_97	P62937_31
P07437_379	P09874_108	P62937_49
P68363_40	P09874_196	O00571_581
P68363_60	P09874_192	D6RBZ0_102
P68363_96	P09874_249	Q92945_291
P68363_112	P09874_621	Q92945_646
P68363_163	P09874_683	Q12931_560
P68363_280	P08238_107	P34897_409
P68363_304	P08238_624	P34897_469
P68363_311	P08238_685	P13797_52
P68363_326	P60709_50	P15880_257
P68363_336	P60709_61	P26641_147
P68363_352	P60709_113	P54819_93

P68363_370	P60709_326	Q07955_38
P68363_394	P60709_328	P62826_60
P68363_401	P62807_12	P18621_49
P08238_53	P62807_109	P62277_43
P08238_107	P62807_121	P00558_75
P08238_180	P61978_52	Q07020_119
P08238_186	P61978_60	P24534_185
P08238_204	P61978_103	P31930_134
P08238_275	P61978_219	P61604_80
P08238_284	P61978_405	P50502_17
P08238_286	P61978_422	P30042_141
P08238_350	P61978_456	A0A024RBE8_233
P08238_399	P06748_27	P05198_141
P08238_406	P06748_32	Q99459_466
P08238_435	P06748_54	O15347_30
P08238_477	P06748_141	P60900_102
P08238_481	P06748_223	Q13242_36
P08238_526	P06748_230	P30041_209
P08238_550	P06748_236	P26583_30
P08238_577	P06748_239	P61221_431
P08238_607	P06748_248	P83881_27
P08238_624	P06748_250	P48444_38
P08238_641	P06748_257	Q9BZJ0_224
P08238_646	P06748_263	Q9NVS9_100
P68104_41	P06748_267	Q9HC36_237
P68104_44	P06748_273	Q96P70_865
P68104_146	Q00839_265	Q10570_99
P68104_179	Q00839_464	O15318_49
P68104_215	Q00839_516	Q86U86_416
P68104_219	Q00839_551	P35914_179
P68104_255	Q00839_565	Q96M27_253
P68104_273	Q00839_626	O75431_206
P68104_386	Q00839_635	Q9BRT2_69
P68104_392	P06733_54	Q562M3_30
P68104_395	P06733_71	P10809_72
P68104_408	P06733_81	P10809_389
P68104_439	P06733_80	P60709_61
P68104_444	P06733_193	P60709_113
P68104_450	P06733_281	P60709_326
P68104_453	P06733_326	P68104_255
P68104_457	P62805_92	Q5CAQ5_561
P11142_108	P22626_17	P78527_963
P11142_112	P22626_59	P52272_388
P11142_137	P22626_104	Q6FHZ0_165
P11142_159	P22626_173	P40227_377
P11142_187	P13639_283	P62906_91
P11142_246	P13639_337	O14979_180
P11142_251	P13639_445	P48047_84

P11142_257	P13639_439	Q9Y3U8_62
P11142_319	P08670_129	Q969Q0_27
P11142_328	P08670_439	P84090_84
P11142_345	A0A024RB53_8	P08238_53
P11142_348	A0A024RB53_52	P08238_69
P11142_497	A0A024RB53_87	P08238_107
P11142_507	A0A024RB53_298	P08238_180
P11142_512	P38646_138	P08238_186
P11142_524	P38646_206	P08238_204
P11142_526	P38646_288	P08238_275
P11142_539	P38646_368	P08238_284
P11142_601	P38646_377	P08238_354
P48735_45	P38646_394	P08238_399
P48735_48	P38646_468	P08238_402
P48735_69	P38646_653	P08238_406
P48735_80	P68363_60	P08238_410
P48735_106	P68363_96	P08238_428
P48735_130	P68363_370	P08238_435
P48735_133	Q08211_14	P08238_477
P48735_155	Q08211_146	P08238_531
P48735_166	P19338_324	P08238_550
P48735_180	P19338_333	P08238_557
P48735_193	P19338_398	P08238_565
P48735_199	P19338_513	P08238_574
P48735_272	P14866_97	P08238_577
P48735_275	P14866_418	P08238_607
P48735_280	P36578_364	P08238_623
P48735_282	P23246_279	P08238_624
P48735_384	P23246_330	P08238_641
P48735_413	P23246_338	P08238_646
P48735_426	P23246_421	P08238_685
P08133_75	P23246_472	P68104_5
P08133_81	Q5CAQ5_561	P68104_41
P08133_102	Q5CAQ5_671	P68104_44
P08133_299	Q5CAQ5_682	P68104_179
P08133_314	P52272_381	P68104_180
P08133_315	P52272_388	P68104_219
P08133_354	P52272_698	P68104_386
P08133_370	P43243_798	P68104_392
P08133_377	P17844_391	P68104_395
P08133_406	P17844_470	P68104_408
P08133_418	Q6FI13_120	P68104_439
P08133_442	P62937_28	P68104_444
P08133_446	P62937_31	P68104_450
P08133_478	P62937_44	P68104_453
P08133_613	P62937_49	P68104_457
P04406_107	P62937_76	P06733_28
P04406_117	P62937_82	P06733_54

P04406_139	P62937_125	P06733_60
P04406_145	P40926_78	P06733_64
P04406_194	P40926_91	P06733_71
P04406_215	P40926_301	P06733_80
P04406_219	P40926_307	P06733_81
P04406_227	P40926_314	P06733_89
P04406_254	P04075_13	P06733_92
P04406_263	P04075_28	P06733_105
P04406_271	P04075_111	P06733_193
P06733_54	P04075_322	P06733_197
P06733_64	P14618_66	P06733_199
P06733_71	P14618_206	P06733_202
P06733_80	P39023_312	P06733_221
P06733_81	Q5VU21_300	P06733_228
P06733_89	Q5VU21_306	P06733_233
P06733_92	P06576_133	P06733_256
P06733_193	P06576_480	P06733_326
P06733_197	P63241_27	P06733_330
P06733_199	P63241_39	P06733_335
P06733_202	P63241_67	P06733_358
P06733_221	P63241_68	P06733_420
P06733_233	P63241_85	P06733_434
P06733_256	P11021_185	P11142_25
P06733_281	P60842_54	P11142_108
P06733_326	P60842_193	P11142_112
P06733_330	P62979_48	P11142_137
P06733_335	P62979_107	P11142_187
P06733_358	P62979_152	P11142_251
P06733_420	Q00610_246	P11142_319
P06733_434	Q00610_637	P11142_328
P06576_124	Q00610_1441	P11142_345
P06576_133	P07910_89	P11142_348
P06576_161	P07910_157	P11142_497
P06576_159	P11940_78	P11142_507
P06576_259	P11940_104	P11142_512
P06576_350	P11940_312	P11142_524
P06576_351	P11940_361	P11142_526
P06576_480	P50990_16	P11142_535
P06576_485	P50990_20	P11142_539
P06576_522	P50990_400	P11142_583
P19338_223	D6RBZ0_83	P0DMV8_77
P19338_288	D6RBZ0_87	P0DMV8_88
P19338_294	D6RBZ0_102	P0DMV8_102
P19338_295	D6RBZ0_215	P0DMV8_112
P19338_324	D6RBZ0_232	P0DMV8_246
P19338_333	Q15233_203	P0DMV8_251
P19338_348	Q15233_249	P0DMV8_257
P19338_370	Q15233_371	P0DMV8_319

P19338_377	Q15233_467	P0DMV8_348
P19338_382	Q12906_342	P0DMV8_451
P19338_398	P62241_157	P0DMV8_497
P19338_403	P62241_170	P0DMV8_500
P19338_410	P27824_170	P0DMV8_512
P19338_424	P48643_160	P0DMV8_524
P19338_429	P48643_170	P0DMV8_526
P19338_477	P48643_483	P0DMV8_539
P19338_513	A0A024RDF4_114	P0DMV8_550
P19338_521	A0A024RDF4_129	P0DMV8_569
P19338_523	A0A024RDF4_178	P0DMV8_597
P19338_545	A0A024RDF4_182	P68363_60
P19338_572	A0A024RDF4_197	P68363_112
P19338_577	A0A024RDF4_242	P68363_326
P19338_624	A0A024RDF4_243	P68363_336
P19338_646	A0A024RDF4_251	P68363_370
P38646_76	P78527_1407	P07900_414
P38646_135	P78527_2683	P07900_418
P38646_138	P49327_436	P07900_443
P38646_159	P49327_673	P07900_458
P38646_175	P09429_29	P07900_478
P38646_187	P09429_30	P07900_485
P38646_206	P09429_59	P07900_489
P38646_234	P09429_88	P07900_539
P38646_288	P09429_114	P07900_546
P38646_300	P09429_128	P07900_559
P38646_394	Q6NXR8_34	P07900_576
P38646_467	P51991_73	P07900_585
P38646_625	P62753_14	P07900_631
P38646_646	P12268_511	P13639_42
P38646_653	Q06830_109	P13639_252
P09429_29	Q06830_178	P13639_259
P09429_30	P63244_183	P13639_283
P09429_55	P62277_27	P13639_318
P09429_59	P62277_39	P13639_391
P09429_88	P62277_43	P13639_426
P09429_114	P05141_23	P13639_445
P09429_127	P05141_147	P13639_439
P09429_128	P00338_14	P13639_512
P09429_157	Q07021_104	P13639_594
P09429_165	P42704_750	P13639_605
P09429_167	P62826_60	P13639_629
P09429_172	P26641_220	P13639_648
P09429_177	P15880_257	P13639_845
P14866_97	P15880_263	P60709_50
P14866_229	O75390_76	P60709_328
P14866_269	O75390_103	P07437_58
P14866_493	O75390_382	P07437_216

P14866_533	O75390_459	P07437_324
P14625_95	P07737_38	P07437_336
P14625_269	P07737_54	P04075_13
P14625_340	P07737_108	P04075_14
P14625_404	P30101_129	P04075_28
P14625_458	P26599_428	P04075_42
P14625_534	P26373_209	P04075_87
P14625_547	P12277_304	P04075_99
P14625_561	P38159_22	P04075_111
P14625_593	P38159_63	P04075_200
P14625_597	P62906_91	P04075_294
P14625_630	P62906_92	P04075_312
P14625_633	P62906_106	P04075_318
P14625_663	P62081_49	P04075_322
P14625_671	P49368_248	P04075_330
P14625_682	P49368_381	P04075_342
P13010_265	P54819_93	P00338_14
P13010_291	P62280_144	P00338_59
P13010_307	P23396_197	P00338_76
P13010_532	P62847_83	P00338_81
P13010_534	Q07666_175	P00338_90
P13010_544	Q07666_432	P00338_118
P13010_648	P34897_181	P00338_126
P13010_660	P34897_409	P00338_149
P13010_703	P34897_469	P00338_222
P34897_103	P34897_474	P00338_318
P34897_181	P23528_144	P04406_61
P34897_200	Q99832_292	P04406_107
P34897_269	Q92945_627	P04406_145
P34897_297	Q92945_628	P04406_194
P34897_302	Q92945_653	P04406_215
P34897_356	O00571_335	P04406_219
P34897_409	P63104_49	P04406_227
P34897_459	O14979_180	P04406_259
P34897_464	O14979_302	P04406_263
P34897_469	P42167_346	P19338_79
P34897_474	P17987_484	P19338_110
P40926_74	P17987_494	P19338_223
P40926_78	P78371_46	P19338_228
P40926_91	P18621_49	P19338_288
P40926_157	P30050_40	P19338_324
P40926_165	P30050_130	P19338_370
P40926_185	P14174_78	P19338_382
P40926_203	Q7KZF4_116	P19338_398
P40926_215	Q13283_357	P19338_429
P40926_239	Q13283_413	P19338_577
P40926_297	Q07020_119	P19338_624
P40926_301	P25398_93	P49327_436

P40926_307	P25398_116	P49327_673
P40926_314	O15371_53	P49327_1116
P40926_324	P39748_267	P49327_1151
P40926_329	P26368_462	P49327_1878
P62807_6	Q02543_11	P18669_39
P62807_12	P35579_910	P18669_100
P62807_17	P24534_176	P18669_106
P62807_21	P24534_185	P18669_113
P62807_47	P31948_252	P18669_157
P62807_109	P31948_434	P18669_176
P62807_117	P31948_513	P18669_251
P62807_121	P22392_100	P14618_62
P00338_14	P52292_459	P14618_66
P00338_76	O15347_30	P14618_115
P00338_81	P18669_106	P14618_135
P00338_222	P46783_139	P14618_141
P00338_243	P11177_336	P14618_186
P00338_318	P04181_405	P14618_206
P25705_123	P43487_111	P14618_305
P25705_126	Q15029_64	P07195_7
P25705_161	P38919_198	P07195_82
P25705_167	Q13151_176	P07195_119
P25705_230	Q04837_122	P07195_156
P25705_305	Q9UMS4_179	P07195_308
P25705_427	Q96PK6_593	P07195_310
P25705_506	Q9Y2W1_481	P07195_318
P25705_531	Q9Y2W1_876	P07195_319
P61978_52	P83731_12	P12277_101
P61978_60	Q9Y265_453	P12277_265
P61978_163	P07814_513	P12277_298
P61978_179	P07814_512	P12277_304
P61978_219	A0A024RBE8_233	P12277_313
P61978_405	Q12931_382	P62258_50
P61978_456	Q12931_560	P62258_73
A0A024RB53_8	Q12849_242	P62258_69
A0A024RB53_52	P61254_136	P62258_118
A0A024RB53_78	P62857_16	P62258_215
A0A024RB53_87	Q96AE4_248	P31948_13
A0A024RB53_105	Q99459_219	P31948_50
A0A024RB53_106	P00558_75	P31948_63
A0A024RB53_166	P84098_190	P31948_73
A0A024RB53_179	P62851_52	P31948_109
A0A024RB53_298	P62851_66	P31948_123
B4DLR3_193	P26583_29	P31948_169
B4DLR3_197	P26583_30	P31948_252
B4DLR3_224	P26583_147	P31948_434
B4DLR3_423	P63173_9	P31948_453
B4DLR3_475	O75947_63	P31948_462

B4DLR3_510	O75947_85	P31948_486
B4DLR3_524	O75947_109	P31948_513
B4DLR3_585	P52597_224	P62937_44
B4DLR3_594	Q92804_306	P62937_76
B4DLR3_633	P62333_206	P62937_82
B4DLR3_773	Q13242_36	P62937_91
P62937_28	Q02790_163	P62937_125
P62937_31	Q02790_222	P62937_131
P62937_44	Q04760_88	P62937_151
P62937_49	P05198_141	P62937_155
P62937_76	P14927_96	P60842_54
P62937_82	P50502_118	P60842_68
P62937_91	P23526_389	P60842_174
P62937_118	P30405_91	P60842_193
P62937_125	P30041_209	P60842_226
P62937_131	Q9BWD1_235	P60842_291
P62937_133	P30084_128	P60842_369
P10412_46	P55786_222	P07737_38
P10412_52	P55786_853	P07737_54
P10412_63	P00367_480	P07737_70
P10412_64	P62899_70	P07737_105
P10412_85	Q9H583_1675	P07737_108
P10412_90	Q8NBS9_140	P07737_116
P10412_97	P20674_72	P07737_126
P10412_106	P50213_77	Q06830_16
P10412_110	P30040_99	Q06830_27
P10412_117	Q9Y262_403	Q06830_35
P10412_119	Q9NY12_94	Q06830_67
P10412_127	P08559_385	Q06830_93
P10412_136	O94925_164	Q06830_109
P10412_148	E5KS55_205	Q06830_136
P10412_156	P30042_141	Q06830_185
P10412_168	O75521_92	Q06830_178
P10412_186	Q5SY16_670	Q06830_190
P10412_197	P61221_169	Q06830_192
P10412_213	P61221_191	Q06830_197
P06748_27	P61221_431	P60174_92
P06748_32	Q96I24_525	P60174_106
P06748_54	O15318_49	P60174_122
P06748_141	Q13526_63	P60174_193
P06748_154	P17858_677	P60174_212
P06748_155	Q9BZJ0_224	P60174_225
P06748_202	Q9HB71_178	P60174_231
P06748_212	P41227_148	P60174_275
P06748_215	Q01813_688	P00558_11
P06748_223	Q9HC36_237	P00558_30
P06748_229	Q9NSE4_500	P00558_41
P06748_230	P10606_57	P00558_91

P06748_236	P08758_309	P00558_131
P06748_239	Q10570_99	P00558_133
P06748_248	Q8N5C6_852	P00558_141
P06748_250	Q99986_98	P00558_156
P06748_257	P07954_292	P00558_191
P06748_263	P50570_598	P00558_199
P06748_273	P32322_307	P00558_264
P00558_41	O00231_417	P00558_279
P00558_75	Q15459_419	P00558_291
P00558_91	P55084_72	P00558_323
P00558_131	P17980_125	P63104_9
P00558_139	B4DZJ6_890	P63104_11
P00558_141	Q03701_195	P63104_49
P00558_156	Q9UJX3_306	P63104_68
P00558_191	P08237_678	P63104_115
P00558_199	Q9UDR5_584	P63104_120
P00558_267	O15460_57	P63104_138
P00558_279	Q14671_718	P63104_158
P00558_291	Q7Z7F7_104	P63104_212
P00558_323	Q02218_970	Q6IBN1_219
P62805_9	Q9Y617_323	P23528_19
P62805_13	P35606_336	P23528_22
P62805_92	Q9NVS9_100	P23528_30
P23396_18	Q14258_320	P23528_44
P23396_90	Q8N5F7_305	P23528_45
P23396_108	P54709_182	P23528_92
P23396_132	O95071_28	P23528_112
P23396_197	Q13085_323	P23528_114
P23396_201	Q93034_492	P23528_127
P23396_202	Q14181_232	P23528_132
A0A024RDF4_72	P35914_179	P23528_144
A0A024RDF4_110	P38432_496	P22314_627
A0A024RDF4_114	Q9BSJ2_426	P22314_802
A0A024RDF4_119	Q14203_397	P22314_806
A0A024RDF4_129	Q8WVM8_515	P53396_948
A0A024RDF4_158	Q86U86_416	P53396_962
A0A024RDF4_161	Q8IZX4_1610	P53396_1077
A0A024RDF4_176	O00186_197	P14625_95
A0A024RDF4_182	P08133_314	P14625_458
A0A024RDF4_178	O14727_142	P09429_55
A0A024RDF4_231	Q9BRT2_69	P09429_59
A0A024RDF4_237	P10809_96	P09429_88
A0A024RDF4_238	P10809_469	P09429_114
A0A024RDF4_243	P0DMV8_539	P09429_128
A0A024RDF4_251	P68104_215	P09429_146
A0A024RDF4_255	Q00839_543	P09429_147
P05141_23	P08238_284	P09429_150
P05141_33	P61978_102	P09429_154

P05141_43	P61978_179	P09429_157
P05141_63	P58876_12	P09429_165
P05141_92	P58876_109	P09429_167
P05141_147	P58876_117	P09429_177
P05141_166	P58876_121	P34932_185
P05141_245	P06748_202	P34932_388
P05141_272	P07437_58	P34932_430
Q02878_5	P06733_92	P34932_674
Q02878_8	P06733_330	P26641_132
Q02878_26	P06733_434	P26641_220
Q02878_41	P38646_159	P26641_277
Q02878_77	P68363_336	P26641_401
Q02878_87	P52272_672	P26641_434
Q02878_100	P23246_314	Q32Q12_74
Q02878_210	P12956_582	Q32Q12_125
Q02878_237	P13010_265	Q32Q12_189
P31946_13	P43243_146	Q32Q12_240
P31946_51	P40926_185	Q32Q12_264
P31946_122	P17844_236	Q32Q12_268
P31946_160	Q5CAQ5_663	Q9HB71_134
P62826_38	G3V4C1_89	Q9HB71_197
P62826_60	G3V4C1_144	Q02790_88
P62826_71	P48643_261	Q02790_222
P62826_134	P48643_439	P62826_71
P62826_142	Q8NC51_321	P62826_127
P62826_152	Q8NC51_327	P62826_134
P62826_159	Q15233_198	P62826_142
P04075_13	Q15233_239	P62826_159
P04075_14	P61247_34	P63241_27
P04075_28	Q06830_93	P63241_68
P04075_42	P05141_92	P00918_39
P04075_87	P62277_78	P00918_45
P04075_99	P26641_277	P00918_76
P04075_111	P26641_434	P00918_167
P04075_200	P23396_202	P00918_256
P04075_322	Q6P2Q9_1840	P35579_29
P07737_38	P62826_142	P35579_102
P07737_54	O75390_43	P35579_909
P07737_70	Q92945_203	P35579_910
P07737_91	P00338_318	P35579_1445
P07737_105	P23528_22	P35579_1477
P07737_108	O14979_142	P13797_126
P07737_116	F8VY04_51	P13797_582
P07737_126	P46782_191	P29401_232
P07737_127	P17987_515	P29401_319
B2RB06_81	P49411_286	P11586_10
B2RB06_179	P24534_147	P11586_262
B2RB06_185	Q9NZI8_465	P11586_878

B2RB06_192	O15347_29	Q15366_23
B2RB06_202	Q9NYF8_842	Q15366_185
B2RB06_206	Q9NYF8_891	P11940_104
B2RB06_271	P25205_177	P11940_196
P07900_414	P25205_194	P11940_299
P07900_631	O00264_105	P11940_512
P07900_632	P25786_115	P49321_530
P13639_15	P62851_94	P49321_636
P13639_283	P46781_30	P49321_643
P13639_337	P49792_983	P49321_652
P13639_445	Q9Y265_201	Q01105_132
P13639_439	P41091_275	Q01105_150
P13639_498	A8KAP3_64	Q01105_167
P13639_512	P10599_94	Q01105_172
P13639_598	O75821_172	P14174_78
P13639_605	P60866_8	P24534_74
P39023_39	P12236_23	P24534_129
P39023_103	P63167_36	P24534_133
P39023_294	P41252_410	P24534_139
P39023_300	P41252_844	P24534_176
P39023_312	Q00341_883	P25205_177
P39023_366	O60832_80	P61221_126
Q00610_96	P54577_310	P61221_191
Q00610_246	Q9HAV7_100	P50990_138
Q00610_367	P50570_206	P50990_400
Q00610_619	O95470_155	P06744_142
Q00610_637	Q8N183_108	P06744_234
Q00610_737	Q8TCG1_252	P06744_366
Q00610_1441	A2NX49_323	P06744_447
P14618_62	Q9Y4W2_540	P06744_454
P14618_66	Q5SRE5_51	P23526_20
P14618_115	Q14C86_1035	P23526_389
P14618_247	O75899_196	O75369_2342
P14618_261	P04075_14	F5GWF6_46
P14618_305	Q14103_129	P27348_9
P22626_17	Q5U071_30	P27348_49
P22626_22	V9HW62_88	P27348_158
P22626_59	P08238_64	P27348_212
P22626_104	P08238_69	Q9Y490_685
P22626_112	P08238_180	Q9Y490_1314
P22626_113	P08238_186	Q9Y490_1544
P22626_173	P08238_204	Q9Y490_1947
P62277_27	P08238_275	Q9Y490_2133
P62277_39	P08238_286	Q99832_292
P62277_43	P08238_347	Q99832_366
P62277_78	P08238_350	Q16576_21
P62277_93	P08238_354	Q16576_119
P23528_19	P08238_399	Q92598_275

P23528_30	P08238_402	P09211_55
P23528_44	P08238_406	P09211_128
P23528_45	P08238_410	P09211_191
P23528_73	P08238_411	P40925_110
P23528_92	P08238_428	P40925_220
P23528_112	P08238_435	P40925_236
P23528_114	P08238_477	P40925_298
P23528_127	P08238_481	Q14247_144
P23528_144	P08238_491	P27694_489
P12268_109	P08238_526	Q96AE4_248
P12268_450	P08238_531	Q96AE4_591
P12268_511	P08238_538	P50991_126
P62847_32	P08238_552	P22234_30
P62847_43	P08238_550	P22234_47
P62847_46	P08238_557	P22234_226
P62847_68	P08238_559	P22234_235
P62847_83	P08238_565	P22234_304
P62847_129	P08238_568	P52209_154
P13796_88	P08238_573	P12268_450
P13796_294	P08238_574	P55209_87
P13796_579	P08238_577	P55209_271
P62258_69	P08238_607	P31939_266
P62258_215	P08238_623	O75131_208
P49411_79	P08238_641	P31946_11
P49411_88	P08238_646	P31946_70
P49411_91	P08238_649	P31946_160
P49411_234	P68104_5	P31946_214
P49411_238	P68104_172	P43487_150
P49411_286	P68104_179	P43487_179
P49411_342	P68104_180	P43487_190
P49411_361	P68104_244	Q14974_376
P49411_447	P68104_330	P50395_103
Q12906_454	P68104_386	P50395_269
P00505_59	P68104_460	P62979_6
P00505_82	P06733_28	P62979_11
P00505_90	P06733_60	P62979_48
P00505_159	P06733_64	P32119_16
P00505_309	P06733_89	P32119_26
P00505_338	P06733_105	P32119_92
P00505_363	P06733_197	P32119_177
P27824_118	P06733_199	P18206_352
P27824_127	P06733_202	P18206_366
P27824_170	P06733_221	P68371_58
P27824_182	P06733_228	O14980_686
P27824_398	P06733_233	O14980_693
P27824_515	P06733_239	Q00610_246
P62424_11	P06733_256	P09874_621
P62424_20	P06733_335	O43719_26

P62424_34	P06733_358	O43719_303
P62424_97	P06733_420	P08758_101
P62424_125	P0DMV8_25	P55060_848
P62424_212	P0DMV8_112	O43175_394
P62424_217	P0DMV8_128	P48643_170
P62424_255	P0DMV8_190	P48643_226
P12956_189	P0DMV8_246	P48643_275
P12956_287	P0DMV8_257	P10599_94
P12956_463	P0DMV8_319	P54577_310
P12956_516	P0DMV8_325	P54577_319
P12956_526	P0DMV8_451	P49773_21
P12956_553	P0DMV8_497	P49773_82
P12956_570	P0DMV8_500	O75347_21
P12956_575	P0DMV8_507	P06493_20
P12956_582	P0DMV8_512	P06493_33
P12956_596	P0DMV8_526	P20618_164
P50990_16	P0DMV8_550	O00299_119
P50990_20	P0DMV8_573	O00299_183
P50990_138	P0DMV8_589	P62633_103
P50990_225	P0DMV8_628	Q9NTK5_294
P50990_260	P11142_25	P55786_712
P50990_326	P11142_88	P08133_75
P50990_400	P11142_112	P31689_37
P51991_29	P11142_137	P06454_21
P51991_36	P11142_246	O95373_429
P51991_73	P11142_257	P38606_580
P51991_134	P11142_319	Q07866_384
P51991_199	P11142_348	Q9BRA2_35
P48643_170	P11142_361	P35580_1869
P48643_259	P11142_423	P15170_490
P48643_261	P11142_497	P07814_693
P48643_265	P11142_500	P07814_861
P48643_439	P11142_512	P07814_951
P48643_483	P11142_526	P04080_39
P62081_49	P11142_535	P04080_44
P62081_58	P11142_583	P04080_78
P62081_142	P11142_601	Q14166_510
P62081_155	P07900_74	P15121_12
P62081_160	P07900_84	P15121_22
P62081_178	P07900_209	P84077_142
P62081_179	P07900_414	Q86VP6_586
P62906_47	P07900_418	P50502_14
P62906_92	P07900_436	P50502_118
P62906_91	P07900_443	Q15181_233
P62906_95	P07900_458	Q04760_88
P62906_106	P07900_478	Q04760_157
P62906_118	P07900_485	Q9NVS9_186
P62906_130	P07900_489	Q9Y617_116

P62241_128	P07900_513	Q9Y617_127
P62241_139	P07900_534	Q9Y617_323
P62241_157	P07900_539	P41250_82
P62241_170	P07900_546	P41250_108
P62701_94	P07900_559	P05455_37
P62701_211	P07900_576	O75083_256
P62701_230	P07900_585	P06737_29
P62701_233	P07900_631	P06737_295
P52566_114	P07900_632	P06737_819
P52566_124	P07900_657	Q9Y266_315
P52566_135	P07900_693	Q99497_130
P52566_138	P19338_15	Q99497_182
P52566_175	P19338_71	P30520_164
P52566_196	P19338_79	P30520_173
Q06830_16	P19338_80	P30520_203
Q06830_93	P19338_87	Q14C86_87
Q06830_109	P19338_95	Q14C86_1035
Q06830_178	P19338_96	P37837_269
P26583_29	P19338_102	P37837_307
P26583_30	P19338_109	P12004_80
P26583_59	P19338_110	P13693_89
P26583_127	P19338_116	P13693_93
P26583_128	P19338_124	P13693_100
P26583_147	P19338_125	P13693_112
P26583_167	P19338_132	Q13765_113
P26583_173	P19338_223	Q13765_142
P61604_28	P19338_228	P46108_189
P61604_40	P19338_282	P40227_129
P61604_80	P19338_288	P40227_251
P11940_78	P19338_294	P40227_424
P11940_104	P19338_318	Q13526_63
P11940_157	P19338_348	Q16543_276
P11940_196	P19338_370	A0A087X1X7_483
P11940_312	P19338_382	P33993_89
P11940_348	P19338_403	Q13564_381
P11940_361	P19338_410	P63167_36
Q3ZCM7_122	P19338_424	P22102_156
Q3ZCM7_154	P19338_429	P22102_350
P26038_64	P19338_477	O60271_714
P26038_151	P19338_523	P14735_364
P26038_253	P19338_545	P23381_27
P26038_254	P19338_572	P09960_573
P26038_391	P19338_577	O76003_151
P26038_400	P19338_624	O76003_294
P26038_538	P19338_646	Q9BTE3_61
P15880_211	P13639_15	B2RDE1_13
P15880_212	P13639_42	B2RDE1_215
P15880_257	P13639_235	B2RDE1_228

P15880_263	P13639_252	Q15185_48
P15880_275	P13639_259	P61956_33
Q96KK5_37	P13639_272	P61956_45
Q96KK5_120	P13639_275	Q8WUM4_23
Q96KK5_126	P13639_314	Q8WUM4_501
P40939_60	P13639_318	Q06203_349
P40939_214	P13639_328	Q06203_371
P40939_255	P13639_333	Q09028_212
P40939_259	P13639_391	P33316_155
P40939_289	P13639_407	P10768_186
P40939_295	P13639_426	P10768_200
P40939_303	P13639_512	P15311_254
P40939_415	P13639_571	P68032_70
P40939_460	P13639_594	P0DN79_269
P40939_728	P13639_598	P26583_147
P27797_41	P13639_605	O14929_15
P27797_48	P13639_619	P31150_269
P27797_62	P13639_629	Q9UHD1_198
P27797_151	P13639_648	P26640_903
P27797_153	P13639_676	A6NHG4_33
P78371_46	P13639_845	Q92688_101
P78371_154	P04075_42	Q9Y237_75
P78371_248	P04075_87	P39687_101
P78371_272	P04075_99	Q9UHB9_277
P78371_441	P04075_108	O95721_191
P68371_58	P04075_140	Q9UJU6_164
P24752_66	P04075_153	Q15029_64
P24752_174	P04075_200	Q8TCG1_252
P24752_190	P04075_294	Q9Y2L1_107
P24752_230	P04075_330	Q7Z4S6_1058
P24752_251	P04075_342	Q9Y696_130
P23246_314	P68363_112	P41252_410
P23246_338	P68363_163	P41252_844
P23246_421	P68363_304	P52701_537
P23246_518	P68363_394	Q9Y3F4_104
P52272_145	P00338_59	Q8NCW5_144
P52272_388	P00338_76	P68036_73
P52272_651	P00338_81	P68036_96
P52272_698	P00338_118	Q99615_41
O75947_5	P00338_126	O14737_66
O75947_63	P00338_155	Q96AC1_55
O75947_85	P00338_224	Q13617_728
O75947_109	P00338_222	Q8IV38_265
O75947_117	P00338_228	Q99729_101
O75947_144	P00338_232	P17858_677
O75947_149	P00338_243	Q96G03_586
P61247_27	P49327_235	Q93034_492
P61247_34	P49327_786	A5PL36_1161

P61247_144	P49327_787	Q9UKK9_218
P61247_222	P49327_1116	Q96HC4_127
P61247_240	P49327_1142	Q9HC38_305
P61247_249	P49327_1151	P52565_178
O75390_76	P49327_1158	P49720_77
O75390_103	P49327_1239	P23588_223
O75390_382	P49327_1591	O94903_47
P62851_14	P49327_1866	P25325_164
P62851_20	P49327_1878	P41236_67
P62851_25	P49327_1911	P18754_335
P62851_52	P07437_19	P49643_65
P62851_57	P07437_216	Q9BRX5_207
P62851_60	P07437_324	Q7Z4Q2_46
P62851_66	P07437_336	O75886_376
P62851_94	P07437_379	Q16204_81
P62851_98	P60709_191	Q96KB5_121
Q13423_394	P07195_7	P13984_154
Q13423_1059	P07195_60	P46459_586
P62979_6	P07195_77	Q12802_1765
P62979_11	P07195_82	Q5TBB1_25
P62979_48	P07195_119	Q5TBB1_259
P62979_63	P07195_156	Q13045_39
P62979_107	P07195_244	Q6P996_680
P62979_152	P07195_308	P17987_515
O00299_119	P07195_310	Q9NR45_61
Q08211_14	P07195_318	P30101_129
Q08211_236	P07195_319	Q9UHY7_111
Q08211_235	P04406_61	Q9Y6G9_310
Q08211_943	P04406_107	P40763_177
P40227_10	P04406_145	P40424_74
P40227_388	P04406_186	O43242_315
P40227_426	P04406_194	P78417_110
P40227_424	P04406_215	P78417_143
Q99729_82	P04406_219	Q9HC35_228
Q99729_86	P04406_227	Q9BPX3_924
Q99729_101	P04406_259	O43847_325
Q99729_118	P04406_263	Q00534_26
Q99729_149	P04406_271	Q01469_61
Q99729_153	P14618_62	Q9BXJ9_262
Q99729_210	P14618_115	P08237_678
Q99729_214	P14618_125	Q01813_688
Q99729_215	P14618_135	Q96C23_101
Q99729_223	P14618_141	E5RJR5_130
Q99729_232	P14618_162	Q13616_759
Q01813_139	P14618_166	Q9HAV4_1147
Q01813_688	P14618_186	Q7Z4V5_39
P63244_12	P14618_188	Q9UIA9_395
P63244_185	P14618_261	P25786_115

P63244_264	P14618_305	P33992_396
P63244_271	P14618_336	Q13325_218
P36578_29	P14618_367	Q13404_87
P36578_364	Q06830_16	Q9NQW7_130
P36578_368	Q06830_27	Q9BSJ2_87
P36578_374	Q06830_35	Q96CW1_400
P36578_375	Q06830_67	P12081_22
P36578_380	Q06830_68	Q14185_1469
P36578_399	Q06830_136	Q9UJX3_435
P36578_412	Q06830_168	Q00013_329
P09874_23	Q06830_185	P14324_295
P09874_196	Q06830_190	P61758_114
P09874_621	Q06830_192	Q9P260_633
Q8NC51_39	Q06830_197	Q9UK45_63
Q8NC51_299	P60842_68	P35219_192
Q8NC51_320	P60842_146	Q8TDX7_281
Q8NC51_321	P60842_174	P43490_189
Q8NC51_327	P60842_226	Q9UBQ0_73
P07954_94	P60842_238	O75821_71
P07954_115	P60842_291	Q13257_200
P07954_292	P60842_309	Q96EK6_166
P07954_470	P60842_369	P31153_303
P07954_477	P00558_11	P60981_19
P78527_310	P00558_30	P17980_125
P78527_1407	P00558_41	Q9UQ13_134
P78527_2683	P00558_91	P35221_178
P78527_2829	P00558_97	O43447_153
P78527_3260	P00558_106	Q9NVG8_287
P62913_38	P00558_131	P48739_104
P62913_52	P00558_139	P61970_55
P62913_67	P00558_141	P09972_111
Q16891_270	P00558_156	Q16763_63
Q16891_282	P00558_191	Q14181_232
Q16891_315	P00558_199	Q5VYK3_1456
Q16891_427	P00558_264	Q9GZN8_105
Q16891_436	P00558_267	P51617_397
Q16891_640	P00558_279	P40426_77
Q99832_67	P00558_291	P57737_103
Q99832_109	P00558_323	Q12874_92
Q99832_157	P00558_361	P61077_128
Q99832_292	P09429_12	Q7L5N1_102
Q99832_463	P09429_55	P20700_123
P07814_512	P09429_65	Q99961_171
P07814_788	P09429_82	Q86V21_633
P07814_841	P09429_150	Q9NXF7_167
P07814_861	P09429_154	Q96F45_180
P07814_951	P09429_157	Q96F45_607
P84243_5	P09429_165	Q9UBF2_313

P84243_19	P09429_167	Q53FA7_257
P84243_24	P09429_172	Q15126_69
P84243_57	P09429_177	Q9NXR1_263
P84243_65	P31948_13	P08238_491
P84243_123	P31948_50	P08238_568
Q99798_144	P31948_63	P13639_272
Q99798_409	P31948_73	P13639_275
Q99798_605	P31948_109	P13639_333
Q99798_730	P31948_123	P13639_571
Q92688_101	P31948_169	P60709_191
P06744_366	P31948_207	P60709_213
P06744_454	P31948_227	P07900_74
P35579_30	P31948_317	P07900_513
P35579_29	P31948_347	P04075_140
P35579_910	P31948_364	P04075_153
P35579_1129	P31948_381	P00338_155
P35579_1445	P31948_442	P00338_224
P35579_1862	P31948_486	P00338_243
P16401_35	P26641_132	P04406_186
P16401_49	P26641_147	P14618_256
P16401_132	P26641_212	P14618_367
P16401_133	P26641_219	P19338_95
P16401_140	P26641_227	P19338_348
P16401_168	P26641_228	P19338_410
P16401_188	P26641_249	P49327_235
P16401_209	P26641_253	P49327_1142
P16401_214	P26641_401	P49327_1523
P17987_484	P18669_39	P49327_1591
P17987_494	P18669_100	P18669_241
P17987_515	P18669_113	P31948_347
P55809_176	P18669_157	P00558_97
P55809_185	P18669_176	P00558_267
P55809_296	P18669_225	P60174_179
P55809_418	P18669_228	Q06830_68
P55809_421	P18669_241	Q13263_296
P55809_481	P18669_251	P62258_123
P25205_177	P23528_19	P62258_125
Q68D11_798	P23528_30	P62258_142
Q04837_81	P23528_44	Q6IBN1_405
Q04837_103	P23528_45	P22314_671
Q04837_113	P23528_73	P09429_44
Q04837_122	P23528_78	P14625_663
P31948_50	P23528_92	Q02790_163
P31948_123	P23528_112	P34932_754
P31948_252	P23528_114	A0A024R895_59
P31948_434	P23528_121	A0A024R895_62
P31948_486	P23528_127	A0A024R895_119
P31948_513	P23528_132	A0A024R895_137

P27348_9	P23528_152	A0A024R895_154
P27348_49	P62937_91	A0A024R895_159
P42677_16	P62937_118	Q32Q12_196
P60842_54	P62937_131	P11586_543
P60842_146	P62937_133	P11586_553
P60842_174	P62937_151	P35579_30
P60842_193	P62937_155	P29401_16
P60842_291	P34932_53	P50990_260
P60842_369	P34932_185	Q15366_322
P46782_191	P34932_332	P46821_2240
P46782_201	P34932_388	P78371_46
P27635_82	P34932_430	P61221_121
P27635_121	P34932_437	Q92598_430
P27635_145	P34932_668	P09211_189
P27635_170	P34932_679	P27694_410
P27635_188	P34932_754	Q14974_867
P60866_8	P34932_766	P08758_97
P21796_20	P60174_43	P22234_116
P21796_109	P60174_92	P62979_63
P21796_201	P60174_106	P55786_293
P21796_236	P60174_122	P10599_39
P46783_139	P60174_179	P20618_184
O75083_90	P60174_193	Q96FW1_59
O75083_104	P60174_212	P37802_17
O75083_223	P60174_225	P05455_229
O75083_256	P60174_231	P52209_147
P48047_54	P60174_275	Q14204_692
P48047_70	P63104_9	P50502_5
P48047_73	P63104_11	P08133_377
P48047_162	P63104_68	Q9H0B6_369
P00367_183	P63104_115	P31689_221
P00367_258	P63104_120	B4DZJ6_890
P00367_365	P63104_138	P12004_168
P00367_480	P63104_139	Q13526_82
P18669_106	P63104_158	E9PAV3_1976
P18669_176	P63104_212	E9PAV3_2005
P62917_93	Q32Q12_74	P26639_222
P62917_144	Q32Q12_81	P11021_185
P62917_155	Q32Q12_125	P39748_200
P26641_277	Q32Q12_189	Q04760_44
P07195_7	Q32Q12_196	Q04760_140
P07195_156	Q32Q12_264	O76003_253
P38159_22	Q32Q12_275	B2RDE1_76
P38159_63	Q32Q12_268	Q15185_91
P38159_86	P61978_163	P15311_427
P38159_150	P12277_101	Q969T7_98
P38159_217	P12277_242	O43865_487
B3KX96_29	P12277_267	P38646_653

B3KX96_39	P12277_298	O15347_112
B3KX96_42	P12277_307	O15347_145
B3KX96_89	P12277_313	P16152_148
B3KX96_144	P62826_38	O95433_212
B3KX96_163	P62826_71	Q14683_146
O43390_114	P62826_99	Q01469_55
Q9Y277_15	P62826_134	Q9Y5A7_128
Q9Y277_20	P62826_159	O00231_252
Q9Y277_109	Q13263_188	P19623_96
Q99714_99	Q13263_296	Q8WVJ2_147
Q99714_104	Q13263_319	P47813_56
O43837_96	Q13263_377	Q9BUJ2_731
O43837_146	Q13263_469	Q9Y312_131
O43837_354	Q13263_774	P51580_32
A0A0D9SF54_969	Q13263_779	P32321_131
A0A0D9SF54_1560	P07737_70	O14617_684
A0A0D9SF54_2411	P07737_105	Q9BSH5_15
Q86V81_81	P07737_116	Q9Y3Z3_312
Q86V81_86	P07737_126	Q6ZMR3_155
Q86V81_156	P62258_50	Q07002_158
Q86V81_164	P62258_69	Q5TCZ1_321
Q13838_384	P62258_73	O75330_589
Q00325_209	P62258_118	Q96ST8_588
Q00325_214	P62258_123	Q13206_768
Q00325_234	P62258_142	Q16352_215
Q00325_247	P62258_153	P08238_481
P55084_72	P62258_215	P08238_526
P55084_181	P35579_30	P08238_573
P55084_188	P35579_29	P0DMV8_25
P55084_272	P35579_63	P0DMV8_325
Q02543_11	P35579_102	P0DMV8_507
P20700_261	P35579_355	P07900_436
P20700_457	P35579_1240	P07900_560
P20618_164	P35579_1445	P07900_632
P20618_184	P35579_1477	P13639_15
P05388_77	P35579_1802	P13639_235
P05388_106	P35579_1862	P13639_572
P05388_264	P22314_627	P19338_96
Q12931_369	P22314_671	P19338_102
Q12931_382	P22314_802	P19338_282
Q12931_560	P22314_806	P19338_318
P62753_14	P22314_838	P19338_477
P62753_64	P00918_24	P19338_523
P62753_203	P00918_39	P49327_1993
P62753_211	P00918_45	P18669_228
P46781_30	P00918_76	Q13263_319
P46781_91	P00918_167	Q13263_774
P46781_121	Q02790_88	P53396_469

P46781_139	Q02790_108	P53396_732
P46781_155	Q02790_254	P60842_146
B4DRW8_907	Q02790_287	P62937_118
P31146_233	Q02790_390	P62937_133
Q9BWD1_180	P11586_10	P12277_242
Q9BWD1_235	P11586_66	P34932_679
P69905_17	P11586_246	P23528_73
P69905_41	P11586_245	P23528_152
Q92945_627	P11586_262	Q9HB71_178
Q92945_628	P11586_543	P11940_78
Q92945_653	P11586_878	Q32Q12_275
B4DIZ3_66	P06744_12	P61221_64
B4DIZ3_213	P06744_142	O75131_523
Q9Y262_101	P06744_234	P50395_112
Q9Y262_393	P06744_252	P50395_137
Q9Y262_403	P06744_366	P63241_85
Q9Y262_549	P06744_447	F5GWF6_272
P63241_27	P06744_454	P06744_252
P63241_34	P06744_523	P27348_68
P63241_39	P06744_524	Q14974_73
P63241_67	P53396_469	P17812_109
P63241_68	P53396_468	Q92945_281
P61221_126	P53396_471	P22234_36
P61221_169	P53396_732	P43487_76
P61221_191	P53396_780	P68371_379
P61221_431	P53396_948	Q14204_748
P08575_641	P53396_962	P55786_853
P08575_664	P53396_968	Q01105_72
P08575_780	P53396_1077	Q01105_75
P08575_1145	P54577_146	Q86VP6_577
P08575_1149	P54577_247	A0A024RB53_15
P50213_77	P54577_319	P22102_852
P50213_116	P54577_334	P05455_105
Q14697_472	P54577_348	P05455_185
P08865_89	P54577_391	O75347_52
P08865_212	P54577_474	P40227_426
P09211_55	P29401_232	P84085_36
P09211_128	P29401_260	A0A0S2Z4I4_13
P09211_189	P29401_254	A0A0S2Z4I4_76
P17844_91	P29401_319	A0A0S2Z4I4_215
P17844_284	Q92598_185	A0A0S2Z4I4_228
P17844_391	Q92598_221	P62987_6
P27694_458	Q92598_272	P62987_11
P13073_53	Q92598_275	P62987_48
P13073_60	Q92598_430	P37802_153
Q2TU64_78	Q92598_772	Q53GN4_256
Q2TU64_248	Q92598_790	P63167_5
Q2TU64_427	A0A024R895_59	P63167_9

Q71UI9_116	A0A024R895_119	P52292_459
P41252_410	A0A024R895_137	Q9BTE3_37
P41252_844	A0A024R895_154	P09936_123
P31943_349	A0A024R895_159	P61160_217
Q92608_437	A0A024R895_164	Q9Y266_93
Q92608_1474	A0A024R895_176	Q9UNS2_418
P61254_136	P55786_279	Q15181_253
P26599_410	P55786_712	Q13085_323
P26599_428	P55786_753	O94966_993
P12236_23	P55786_821	P07954_292
P12236_147	P10809_87	O15347_161
P12236_166	Q16576_21	Q15813_463
P83731_12	Q16576_119	P52565_141
P83731_27	Q16576_155	P41236_61
P83731_119	Q9HB71_19	P0DN79_83
P83731_144	Q9HB71_41	O94903_49
P49458_41	Q9HB71_134	P35244_33
P49458_52	Q9HB71_197	O00154_168
Q96EY1_152	P50990_138	Q9UQE7_743
Q96EY1_299	P50990_459	Q96DG6_159
P07237_271	P11940_196	Q8TEX9_801
P07237_328	P11940_299	Q9BV20_259
Q9NZ45_55	P63241_121	Q96A72_50
Q9NZ45_68	P13797_52	Q13625_773
P26368_462	P13797_452	Q13033_755
Q9HB71_178	P13797_545	Q9NRV9_140
Q9HB71_197	P13797_582	P55263_224
P45880_247	P32119_16	P40425_84
P67809_64	P32119_26	Q969Q4_31
P67809_92	P32119_92	P48507_90
P67809_170	P32119_135	Q9Y678_313
Q9P0L0_52	P32119_177	Q6ZU80_659
Q9P0L0_125	O00299_119	Q93045_87
Q9P0L0_205	O00299_183	P08238_350
Q9P0L0_211	Q15366_23	P08238_552
P29401_319	Q15366_31	P68104_378
P62841_58	Q15366_115	P11142_257
P62841_65	Q15366_185	P07900_558
P62841_108	Q15366_309	P07437_379
P84098_146	Q15366_322	P19338_80
P84098_153	P40925_107	P19338_87
P84098_190	P40925_110	P19338_109
O75521_92	P40925_205	P19338_116
Q9BXW7_69	P40925_214	P19338_124
Q9BXW7_279	P40925_220	P19338_294
P31930_111	P40925_236	P19338_572
Q14152_694	P40925_298	P04406_251
A0A0S2Z5H3_158	P14625_404	Q13263_337

P30519_168	P14625_458	Q13263_377
P30519_199	P14625_561	P14618_125
Q6P2Q9_1840	P14625_663	P60842_309
Q92841_547	P27348_9	P34932_766
P22234_47	P27348_49	P23528_121
P00813_23	P27348_68	P35579_299
P00813_273	P27348_115	P35579_1793
P42704_103	P27348_212	P11940_324
P42704_1332	P43487_50	Q92598_185
P49257_87	P43487_68	P06744_524
P49257_346	P43487_150	P31939_199
P35637_316	P43487_179	F5GWF6_248
P31040_182	P43487_190	P23526_46
P31040_335	P15121_12	Q9Y490_841
P31040_538	P15121_173	P08758_70
P26373_118	P15121_179	P54577_391
P26373_145	P15121_222	P09874_196
P26373_200	O15347_112	P49773_83
P26373_209	O15347_126	P15170_72
P16403_119	O15347_145	P55209_197
P16403_168	P18206_170	P15121_173
P16403_172	P18206_276	O14744_227
P16403_181	P18206_352	Q7Z6Z7_1147
P32969_21	P18206_366	Q8TCG1_647
P32969_28	P18206_464	P14735_303
Q15233_249	Q15181_41	Q13098_349
Q15233_371	Q15181_199	A0A0S2Z4I4_212
P30042_141	Q15181_233	Q09028_102
P62899_6	Q15181_253	Q06203_442
P62899_55	P15170_72	O14737_98
P62899_70	P15170_103	P09936_15
P46778_120	P15170_138	Q15056_80
O94925_164	P15170_208	A8KAP3_64
P09622_430	P15170_247	Q9C0C9_132
O43143_760	P15170_254	O75832_30
P18621_49	P15170_490	O60610_133
P18621_55	O43175_21	P28340_278
P18621_96	O43175_289	O75150_943
P18621_169	O43175_351	P78417_198
P11586_245	O43175_394	P62333_206
P11586_262	P09211_55	Q9H4A4_162
Q01082_842	P09211_128	P19623_135
Q01082_1354	P09211_191	Q13085_1564
Q9NSE4_241	P09211_209	O43592_634
Q9NSE4_500	P22234_30	Q12802_1773
P39748_200	P22234_36	Q92973_81
P39748_267	P22234_47	P53004_253
Q13151_99	P22234_110	Q9UJX3_379

Q13151_176	P22234_116	Q8N4J0_163
P15153_133	P22234_226	Q9NZW5_388
P61313_83	P22234_235	Q7L1Q6_255
Q2VIR3_275	P08133_75	E7ETY4_391
Q9UMS4_179	P08133_377	P22061_206
Q9UMS4_244	Q9Y617_116	Q7Z6K5_101
P35606_336	Q9Y617_127	O14776_820
P68032_70	P84077_142	B4DWT1_114
Q92804_277	P62979_6	O95817_460
Q92804_306	P62979_11	Q8IZX4_1610
Q9P2J5_464	P62979_63	P16949_53
Q9P2J5_719	P24534_60	P62837_128
Q9UDR5_584	P24534_64	Q2M2Z5_39
P18124_48	P24534_74	P19525_385
P18124_88	P24534_129	A0PK00_55
P47914_79	P24534_132	P10809_31
P47914_82	P24534_133	P10809_75
P47914_149	P30520_157	P10809_87
Q9BZJ0_224	P30520_164	P10809_89
Q9Y4L1_537	P30520_173	P10809_91
O43242_76	P30520_403	P10809_96
O43242_315	P30520_419	P10809_125
Q4G176_421	P06737_29	P10809_130
P39019_23	P06737_295	P10809_196
P39019_29	P06737_804	P10809_202
P39019_143	P06737_819	P10809_233
P22307_438	P30041_56	P10809_236
P22307_534	P30041_63	P10809_249
O15372_269	P30041_97	P10809_250
O15372_274	P09960_127	P10809_292
Q96AE4_248	P09960_573	P10809_301
P63167_36	Q92945_473	P10809_310
Q969G3_123	P09936_4	P10809_352
P60953_133	P09936_65	P10809_359
P32322_215	P09936_71	P10809_364
P32322_307	P09936_123	P10809_369
P55265_494	P09936_221	P10809_396
P55265_1115	Q99832_109	P68363_163
Q07021_91	Q99832_157	P68363_304
Q07021_104	Q99832_172	P68363_311
Q07021_123	P08758_97	P68363_394
P36542_39	P08758_101	P68363_401
P36542_115	P08758_290	P07437_122
P30084_128	P08758_301	P07437_252
P50914_85	P23526_20	P60709_291
P50914_164	P23526_43	P11142_246
P50914_165	P46821_1176	P11142_325
P50914_171	P48643_265	P11142_531

P30101_129	P68371_58	P38646_135
P30101_218	P68371_379	P38646_175
P30050_40	P27694_458	P38646_187
P30050_130	P27694_588	P38646_288
P50995_255	P50502_14	P38646_300
P50995_282	P50502_17	P38646_314
P04843_413	P50502_153	P38646_345
P31939_14	P50502_160	P38646_394
Q9BPW8_51	P50502_353	P38646_467
Q9BPW8_56	P50502_360	P38646_625
Q9BPW8_80	Q9Y266_93	P38646_675
P62263_63	Q9Y266_123	P38646_671
P62263_86	Q9Y266_160	P68104_443
P27695_125	Q9Y266_297	P08133_314
Q9Y265_453	Q9Y266_315	P08133_354
P04083_90	P22102_598	P08133_370
Q15366_31	P31939_199	P08133_406
Q15366_185	P31939_266	P08133_478
Q15366_322	P31939_389	P08133_613
P61353_27	P05455_37	P08238_286
P30048_149	P05455_105	P14625_137
P06239_130	P05455_229	P14625_168
P52597_224	P05455_276	P14625_404
Q14566_256	P05455_280	P14625_467
Q09028_212	P05455_344	P14625_534
A4D1M6_176	P05455_352	P14625_630
A4D1M6_185	P61221_64	P14625_671
Q7KZF4_515	P61221_121	P14625_682
P62280_30	P61221_478	P14625_683
P62280_45	O43719_56	P40926_78
P62280_144	O43719_303	P40926_91
Q13310_104	P49321_530	P40926_105
Q13310_361	P49321_626	P40926_185
Q9NSD9_560	P49321_636	P40926_203
P30040_99	P49321_643	P40926_239
P25398_93	P49321_652	P40926_301
P25398_116	O75131_149	P40926_324
P25787_92	O75131_167	P40926_329
Q9UII2_49	O75131_208	P40926_335
Q9UII2_72	P26583_59	P05141_33
Q9UII2_82	P26583_114	P05141_43
Q9UII2_83	P26583_128	P05141_63
Q9UII2_100	Q09028_102	P05141_92
P62249_60	Q09028_212	P05141_147
P35268_52	Q04760_44	P05141_166
P35268_69	Q04760_140	P05141_199
P33993_89	Q04760_157	P05141_245
P21912_126	P50991_55	P05141_272

P21912_261	P50991_126	P19338_286
P42766_71	P50991_213	P19338_377
P42766_79	P50991_288	P19338_384
P42766_118	P50991_319	P19338_424
P46779_127	P17812_557	P19338_521
Q12905_186	P49773_21	P19338_545
Q12905_328	P49773_30	P19338_646
P09972_13	P49773_83	P48735_45
P09972_111	P49773_82	P48735_48
P14174_78	P49368_138	P48735_127
A8K1X9_274	P55209_271	P48735_130
P10515_362	A6NHG4_21	P48735_155
P10515_368	A6NHG4_33	P48735_166
P10515_386	A6NHG4_87	P48735_180
P14324_295	P04080_39	P48735_193
O95202_284	P04080_44	P48735_272
O15347_30	P04080_78	P48735_275
Q9NX58_50	Q9Y265_372	P48735_280
P62942_53	P29692_117	P48735_360
O15382_156	P07814_861	P48735_384
O15382_377	P07814_951	A0A024RB53_87
Q9H2W6_216	P10599_39	A0A024RB53_105
P62750_7	O00410_437	A0A024RB53_106
P62750_14	O00410_705	A0A024RB53_166
P62750_26	A0A024R321_373	P25705_126
P62750_36	Q9NTK5_248	P25705_161
P14927_96	Q9NTK5_253	P25705_230
O43719_303	Q9NTK5_294	P25705_427
Q05D08_174	Q9NTK5_326	P25705_531
Q05D08_188	Q8TCG1_647	P09429_7
P14868_9	Q8TCG1_783	P09429_68
P11310_175	O14980_686	P09429_172
P11310_212	Q99497_130	P09429_180
P11310_271	Q99497_182	P14866_97
Q8N183_58	P40227_10	P14866_493
Q8N183_108	O76003_92	B4DLR3_193
P50991_21	O76003_151	B4DLR3_197
P50991_55	O76003_253	B4DLR3_475
P50991_489	O76003_294	B4DLR3_502
P62888_44	Q14204_748	B4DLR3_510
Q14204_1649	Q14204_754	B4DLR3_524
Q9UJV9_416	Q14204_1649	B4DLR3_568
P56192_860	Q14204_4204	B4DLR3_573
Q14683_146	Q14103_197	B4DLR3_594
Q14683_766	P52565_105	B4DLR3_629
Q00688_170	P52565_127	B4DLR3_653
O75643_1294	P52565_141	B4DLR3_773
O75643_1603	P52565_167	P12268_109

Q9NYF8_842	P52565_178	P12268_436
Q9NYF8_891	P06493_20	P12268_511
P83111_199	P06493_33	P06576_124
P83111_231	Q13098_183	P06576_133
P17858_677	P13693_19	P06576_159
Q9GZR7_808	P13693_89	P06576_264
P0DMV8_108	P13693_93	P06576_350
P0DMV8_159	P13693_112	P06576_351
Q13601_264	P62942_53	P06576_485
P62191_24	P41250_108	P06576_522
P62191_217	P41250_219	P34897_181
Q10570_99	P41250_501	P34897_297
Q92621_1150	P68036_9	P34897_302
Q9NTJ3_170	P68036_73	P34897_474
Q13247_143	P68036_96	P62805_9
P53007_97	P68036_146	P62805_13
O15318_49	P31946_11	P62807_6
P09012_60	P31946_70	P62807_12
P09012_80	P31946_214	P62807_17
P09012_114	Q14C86_233	P62807_21
P83881_22	O15067_25	P62807_47
P83881_27	P52209_147	P62807_86
P33991_549	P52209_154	P62807_109
P62333_206	Q15365_115	P62807_117
Q9HC36_237	P30086_47	P62807_121
P37108_55	P30086_80	P10412_52
P62873_209	Q96P70_865	P10412_63
Q8N163_97	Q96FW1_59	P10412_81
P03928_45	Q92688_99	P10412_85
P03928_49	Q92688_101	P10412_90
Q15046_492	E7EVH7_481	P10412_97
P16402_123	E7EVH7_556	P10412_106
O00231_252	Q9Y696_130	P10412_110
P38919_198	Q9Y696_194	P10412_117
P31689_37	Q9Y696_199	P10412_119
P69849_170	P31153_234	P10412_122
P69849_927	P31153_303	P10412_127
Q16778_35	Q9UHD1_38	P10412_148
P62269_91	Q9UHD1_101	P10412_153
P62269_150	Q9UHD1_198	P10412_180
P62861_1	A0A0S2Z4I4_76	P10412_186
P62861_51	A0A0S2Z4I4_100	P10412_190
Q02790_163	A0A0S2Z4I4_212	P10412_195
Q9HAV7_186	A0A0S2Z4I4_215	P10412_197
Q15459_419	A0A0S2Z4I4_228	P10412_200
Q14554_219	P21333_2417	P10412_210
Q99613_643	P21333_2513	P10412_213
Q99613_712	P15311_3	P27824_99

P29144_1216	P15311_60	P27824_118
Q04760_88	P15311_254	P27824_127
P46777_242	P15311_344	P27824_170
P20674_72	P33991_549	P27824_182
P55884_209	Q8WUM4_339	P27824_199
P55884_529	Q8WUM4_486	P27824_210
O95470_155	Q8WUM4_501	P27824_398
P49207_36	Q8WUM4_627	P27824_515
Q92930_58	P55060_848	P22626_17
Q96I99_338	Q9Y3F4_104	P22626_104
Q1KMD3_626	Q9Y3F4_122	P22626_113
P63173_9	Q9Y3F4_246	P22626_151
P63173_67	P31689_37	P22626_173
P40429_114	P31689_221	Q02878_5
Q96F07_1234	P33316_155	Q02878_8
Q9P2R7_205	P33316_179	Q02878_20
H0Y2W2_200	P12004_77	Q02878_66
H0Y2W2_481	P12004_80	Q02878_77
H0Y2W2_554	P12004_168	Q02878_79
Q15067_260	Q9UNS2_254	Q02878_100
Q9Y2W1_711	Q9UNS2_418	P06748_27
P05198_141	P35580_865	P06748_154
O75746_406	P35580_1869	P06748_193
Q9H9P8_104	P39748_200	P06748_202
Q9UBQ0_30	O75347_21	P06748_206
Q9UJZ1_233	O75347_36	P06748_212
P12235_23	O75347_51	P06748_215
Q00013_329	P10768_186	P06748_223
P56381_37	P10768_200	P06748_229
P61981_69	P61981_69	P06748_230
P48556_324	P61981_88	P06748_233
Q92522_146	P27797_62	P06748_236
D3DTY9_112	Q9Y490_685	P06748_239
P30405_67	Q9Y490_2133	P06748_263
P30405_91	Q9BRA2_35	A0A024RDF4_110
Q9BSJ2_426	P50395_103	A0A024RDF4_114
P30626_68	P50395_142	A0A024RDF4_129
O95453_335	P50395_253	A0A024RDF4_158
Q96G03_586	P50395_269	A0A024RDF4_161
Q96IX5_16	Q15185_7	A0A024RDF4_176
Q8NBS9_140	Q15185_48	A0A024RDF4_178
Q96AG4_73	Q15185_91	A0A024RDF4_182
Q96AG4_138	P11766_120	A0A024RDF4_197
P10606_57	P11766_357	A0A024RDF4_231
P14735_364	P11766_366	A0A024RDF4_238
Q8N5C6_852	P39687_86	A0A024RDF4_243
Q9Y3U8_62	P39687_99	A0A024RDF4_251
Q8NEV1_102	P39687_101	P26583_44

P22695_21	P46109_265	P26583_55
P22695_42	P78371_154	P26583_114
P41227_148	Q14566_256	P26583_128
Q02218_970	Q14974_376	P26583_150
Q01844_644	Q14974_859	P26583_154
Q96CS3_167	Q14974_867	P26583_157
Q13283_357	O43143_143	P26583_167
P52565_141	O43143_760	P13010_195
P62834_128	Q06203_442	P13010_532
Q86SR1_379	Q9Y450_657	P13010_603
O14979_302	P61956_11	P13010_660
P46776_94	P61956_33	P13010_702
P49406_129	P61956_45	P61604_28
O95347_177	O75436_116	P61604_56
Q86U86_416	Q01469_40	Q12906_214
Q13526_63	Q01469_55	Q12906_389
Q9NYU2_596	Q01469_61	Q12906_454
Q96CW1_400	Q93034_455	Q12906_742
Q7Z4V5_39	Q9BTE3_61	P49411_88
Q96PK6_135	Q9BTE3_328	P49411_91
P28331_467	Q16543_154	P49411_286
P31937_297	Q16543_273	P49411_342
Q5SRE5_51	Q16543_276	P61978_52
O14737_98	P27695_125	P61978_60
Q01469_61	P08243_379	P61978_166
O60832_80	O75832_30	P62424_20
P62857_10	Q13765_142	P62424_21
P62857_16	Q01813_139	P62424_97
P23368_26	Q14697_472	P62424_121
Q13243_60	P37802_17	P62424_125
Q93034_492	P37802_153	P62424_150
P22830_118	Q00341_494	P62424_255
Q9BTE3_61	O00151_192	P23246_338
P48444_38	Q9NRX4_48	P62847_32
Q53HG1_102	Q9NRX4_87	P62847_43
Q9NVP1_645	Q99615_32	P62847_46
Q9H1K4_82	P14735_303	P62847_83
C7DJS2_60	P14735_364	P62847_84
Q99986_98	P55072_754	P62847_88
P25789_210	P35606_199	P62847_129
P35580_1869	Q96G03_586	P78527_700
Q8TDX7_281	P61158_317	P78527_2366
P62316_118	O95757_185	P78527_2683
Q96CT7_40	Q9BTT0_101	P78527_2829
Q99460_146	P37837_269	P78527_3260
P62304_12	Q7Z6Z7_1147	P78527_3550
P30044_86	Q53GN4_256	P13639_598
P30044_142	Q86VP6_577	P26038_64

P16615_400	Q86VP6_586	P26038_151
P09496_242	P63167_9	P26038_162
P27708_964	Q9NTJ3_170	P26038_253
Q96H79_185	Q9NTJ3_607	P26038_254
Q8TCG1_252	P18754_335	P26038_262
P15170_247	P49588_366	P26038_313
Q00059_95	P49588_766	P26038_391
E5KS55_205	Q9H773_140	P26038_400
P53999_101	P11021_447	P26038_538
Q8NBU5_165	P68032_70	P11940_167
P62829_113	P31150_253	P11940_348
C9JVQ0_10	P31150_269	P11940_361
P60228_82	P00491_265	Q00610_367
Q9UFN0_166	Q9Y6Y8_931	Q00610_619
Q9P2K5_85	P49591_12	Q00610_637
P22033_621	P0DN79_269	P50990_20
Q9NTJ5_456	P23381_27	P27797_62
P50502_118	P23381_47	P62701_233
Q496E4_233	P09651_15	B2RB06_81
P84103_23	P09651_350	B2RB06_192
P23284_89	O14737_66	B2RB06_206
Q9NZ01_12	O14737_98	B2RB06_212
Q9UQ35_169	Q9UHY7_106	B2RB06_295
Q8IYB3_54	Q9UHY7_111	B2RB06_301
Q14008_1859	Q9H8S9_210	P30048_149
Q9NVS9_100	Q00013_329	P30048_217
O14656_76	Q9UHV9_18	P60866_8
Q99536_372	Q14320_305	P60866_30
P09110_198	Q9BXJ9_262	P60866_44
Q9H0D6_641	Q15691_148	P60866_46
Q93009_841	O00193_75	P48047_54
P35754_20	Q9UHB9_277	P48047_60
P35573_1303	Q9H3K6_47	P48047_70
Q14964_63	Q9Y237_75	P48047_73
Q9H082_83	Q5TBB1_259	P48047_162
Q9NUI1_230	O43765_137	P62906_56
Q7Z7F7_104	P46940_939	P62906_95
P51572_204	Q13526_82	P62906_106
Q9H300_75	O00154_157	P62906_118
Q8N5K1_81	O00154_168	P62906_130
O43707_108	Q6FI81_48	P23396_108
Q8WU39_111	Q6FI81_297	P23396_197
P61769_111	O43592_634	P23396_201
P30041_209	Q7L1Q6_223	Q8NC51_102
P17980_125	P48444_38	Q8NC51_140
P00846_51	P13984_154	Q8NC51_299
P19784_103	P52701_1013	Q8NC51_320
Q9HAN9_56	C7DJS2_60	Q8NC51_321

P08574_315	Q99729_101	Q8NC51_327
P08574_325	Q9P289_233	P0C0S8_6
O95071_28	P26640_243	P0C0S8_37
O60884_226	Q04917_69	P0C0S8_96
P39687_101	Q32MZ4_593	P0C0S8_120
Q9BSH5_15	Q13085_2127	P0C0S8_126
P08708_72	Q9UKK9_210	P62277_27
Q99623_89	Q9UKK9_218	P62277_34
P14678_50	O14744_227	P62277_39
Q5JTV8_556	P26639_273	P62277_100
Q6DD88_375	P26639_319	P62277_130
O14950_151	P40763_177	O75947_5
O14950_164	P15927_231	O75947_63
P55786_222	P53990_38	O75947_85
P55327_137	P53990_48	O75947_109
Q9H0A0_823	O75937_127	O75947_117
P78406_154	O75937_168	O75947_149
P49189_366	Q9NR45_61	P12956_249
P08559_385	Q7Z4V5_39	P12956_287
Q15555_165	Q15003_424	P12956_317
O00186_197	Q9BZZ5_51	P12956_338
P46459_586	Q9BZZ5_84	P12956_463
Q9HBD4_835	P46459_586	P12956_468
O95831_593	Q8NEV1_102	P12956_516
Q9UNF1_311	Q13310_361	P12956_553
P49720_77	P53611_34	P12956_570
P47985_168	P50995_255	P12956_575
Q15052_722	Q9NY27_84	P62081_49
Q15029_244	Q13404_87	P62081_86
Q06203_442	Q16658_43	P62081_155
Q9UJA5_145	P47813_56	P62081_160
P52815_142	P47813_94	P62081_179
Q13435_570	Q5VW32_141	P11021_122
O43447_153	P09972_111	P11021_125
O00182_88	Q93009_841	P11021_340
Q14161_135	P33993_89	P11021_370
P49841_292	P35244_33	P11021_447
O75347_51	Q92621_1150	Q3ZCM7_122
O75323_53	Q14683_146	A0A0D9SF54_1314
Q15031_79	Q15029_244	A0A0D9SF54_1635
Q9BUT1_48	Q9NYL9_13	P07737_127
Q9H4G4_53	O43865_487	P09622_146
Q03001_1114	P49189_366	P09622_155
O60814_121	Q14008_1761	P09622_159
Q93079_6	Q14008_1859	P09622_166
P15927_231	Q96C23_101	P09622_430
P12814_89	O14929_364	P39023_294
Q6IPU0_241	O95163_1042	P39023_300

Q9Y520_1160	P51580_32	P61247_34
Q6UXB8_80	Q13616_759	P61247_46
P36551_404	Q69YN2_505	P61247_219
Q8WXX5_107	O00232_368	P61247_240
Q01130_36	P62633_103	P61247_249
Q8WYP5_2050	Q8NFC6_81	P27635_82
Q9UBF2_313	Q9C0B1_216	P27635_141
P10599_94	O00231_252	P27635_145
P98171_460	P62191_217	P27635_170
Q9Y512_248	O43847_325	P14618_247
Q56VL3_41	P78417_198	P04406_117
O43488_242	O15541_126	P35579_821
Q96C36_47	Q96AC1_55	P35579_1129
Q9UKM9_146	P49458_52	P35579_1249
O75489_260	P35611_406	P35579_1775
P57737_103	Q9UBQ0_73	P35579_1862
Q14103_111	P16152_148	Q13423_70
Q5K651_1495	O94776_341	Q13423_394
P05408_166	P61970_55	Q13423_1059
Q9BQE5_54	Q02750_84	P52272_145
Q6ZQQ6_2341	P53621_1028	P13796_456
Q13011_327	P51151_112	P13796_579
Q9UPV0_936	P22061_206	Q14152_68
P60709_336	P22061_219	Q14152_632
P04406_61	Q15056_80	P21796_109
P04406_251	P48739_50	P21796_252
P04406_259	P16949_53	Q9P0L0_52
P08238_69	O95149_144	Q9P0L0_161
P08238_402	O43242_315	Q9P0L0_180
P08238_410	Q8TB03_84	Q9P0L0_205
P08238_428	Q9NVE7_590	Q9P0L0_211
P08238_531	S4R435_252	P46778_120
P08238_538	Q7Z4S6_1058	O75390_76
P08238_557	P20073_199	O75390_103
P08238_568	Q99961_171	O75390_352
P08238_623	P00390_401	O75390_459
P08238_649	P56192_860	P30042_233
P00338_59	P63279_49	P42766_43
P00338_126	P32321_78	P42766_74
P00338_155	P14324_295	P42766_79
P00338_224	Q9UNH7_291	P42766_118
P00338_228	P61077_8	P36578_364
P06733_28	Q96PU8_91	P36578_368
P06733_60	P47756_95	P36578_374
P14618_89	Q9NXG2_56	P36578_375
P14618_135	Q04446_39	P36578_399
P14618_141	P25325_164	P36578_412
P14618_188	Q15785_100	P36578_411

P13796_76	P60983_119	P36578_423
P13796_82	O15355_367	P45880_120
P13796_92	Q7KZ85_381	P45880_247
P13796_97	O43447_153	Q08211_235
P13796_297	P12081_22	Q08211_943
P13796_444	A0AVT1_168	P78371_272
P13796_449	P62304_12	P51991_118
P13796_456	P19623_135	P51991_134
P13796_468	A0A024RA19_251	P51991_199
P13796_472	Q9BUT1_48	O43390_584
P13796_542	Q9H1E3_9	P07954_115
P04075_312	Q9UPN3_6160	P07954_122
P04075_318	P06454_21	P07954_263
P04075_330	Q16763_63	P07954_470
P07900_418	O95347_177	P07954_473
P07900_443	Q8N8S7_22	P07954_477
P07900_489	P49840_355	Q02543_11
P07900_539	Q13573_456	P67809_64
P07900_585	P61088_92	P67809_81
P00558_11	P49593_334	P67809_92
P00558_15	P63208_130	P67809_93
P00558_30	O95456_65	P67809_170
P00558_48	Q16531_897	Q02218_561
P00558_56	Q8NFH4_114	Q02218_970
P00558_133	O00160_194	P62241_157
P00558_146	P61758_114	P62241_170
P00558_192	P49643_65	Q16891_211
P00558_353	Q7Z6K5_101	Q16891_270
P00558_361	Q6P4I2_55	Q16891_314
P35579_403	Q9HAV4_1147	Q16891_344
P35579_909	A6NDG6_72	Q16891_427
P35579_1024	P49720_77	Q13838_156
P35579_1212	Q9Y2T4_91	Q13838_163
P35579_1240	P35754_20	Q13838_188
P35579_1249	Q6ZMR3_155	P62979_107
P35579_1775	O75794_168	P62979_152
P35579_1793	Q9Y2A7_16	P62851_10
P35579_1806	Q9UNF1_311	P62851_14
P35579_1918	O15144_295	P62851_20
P68104_5	Q4VCS5_596	P62851_18
P29401_232	O00244_25	P62851_25
P06744_142	Q92925_312	P62851_37
P06744_234	P60520_24	P62851_52
P06744_447	Q9Y678_313	P62851_66
Q06830_35	P19784_103	P62851_98
Q06830_67	P61024_11	Q99714_99
Q06830_68	Q9UJX3_435	Q99714_105
Q06830_168	P23588_223	O75521_51

Q06830_185	P62837_8	O75521_62
Q06830_190	Q5W0Q7_56	O75521_92
Q06830_192	Q709C8_2092	O75521_335
Q06830_197	Q96H79_185	Q96EY1_152
O75083_95	P57737_103	P09874_653
O75083_182	P15924_2317	Q04837_81
O75083_569	Q6ZSG2_124	Q04837_103
P07195_82	Q13126_241	Q04837_122
P07195_319	Q9NXR1_263	Q9Y277_115
P13639_318	Q2VJ45_324	P41252_382
P62826_99	O14950_164	P51659_184
P62826_127	Q13206_768	P51659_415
P11142_535	Q9NQ75_589	Q4G176_563
P11142_583	P08238_53	P42677_16
P09429_12	P06733_422	P61313_83
P09429_43	P13639_239	Q7KZF4_497
P09429_65	P13639_322	Q7KZF4_513
P09429_82	P13639_330	P31040_182
P09429_90	P13639_438	P31040_335
P09429_154	P13639_572	P31040_538
P09429_180	P0DMV8_100	P31040_608
P50990_466	P0DMV8_415	Q92945_627
P09211_116	P04406_5	Q92945_653
P63104_9	P04406_66	P27694_458
P63104_11	P04406_86	P27695_125
P63104_49	P04406_139	P52566_114
P63104_68	P04406_251	P52566_124
P63104_120	P04406_254	P52566_135
P63104_138	P11142_507	P52566_138
P63104_158	P07900_204	P26373_118
P63104_212	P07900_208	P26373_200
P26038_262	P07900_314	P26373_209
P26038_306	P07900_419	P50213_116
P26038_313	P19338_62	Q01082_1878
P53396_732	P19338_70	P62917_144
P53396_978	P19338_297	P46783_31
P26641_132	P19338_437	P46783_139
P26641_227	P19338_589	P31689_59
P26641_434	P19338_708	P31689_66
Q01518_63	P49327_1993	P84243_5
Q01518_298	P60709_284	P84243_19
P52566_25	P00558_48	P84243_24
P52566_33	P00558_133	P84243_80
P52566_63	P00558_146	P84243_123
P52566_96	Q32Q12_240	P49257_346
P52566_197	P26641_208	P36542_39
P18669_39	P09429_43	P36542_43
P18669_100	P09429_127	P36542_46

P18669_113	P09429_180	P36542_49
P18669_228	P62826_127	P36542_64
P18669_241	P62826_141	P36542_115
P18669_251	P62826_152	Q9NX63_45
P50991_126	P63104_75	P61254_41
P62937_151	P23528_95	P61254_134
P62937_155	P31948_210	P61254_136
Q02790_222	P31948_250	P50914_85
P31146_20	P31948_337	P50914_128
P31146_207	P31948_453	P50914_141
P31146_449	P22314_68	P50914_142
P23528_22	P22314_604	P50914_164
P23528_78	P22314_884	P50914_165
P23528_121	P62258_78	P50914_171
Q01082_2269	P53396_64	P47914_82
Q32Q12_125	P29401_310	P47914_84
Q32Q12_240	P29401_497	P47914_149
Q32Q12_264	P00918_80	P16401_132
P31939_266	Q02790_250	P16401_140
P22234_116	P11586_553	P16401_149
P22234_226	P61978_411	P16401_178
P22234_304	P34932_353	P16401_188
P62258_123	P34932_356	P16401_192
P00813_170	P34932_477	P16401_194
P31948_63	P34932_719	P16401_209
P31948_73	Q59HH3_192	P55084_181
P31948_109	Q59HH3_285	P55084_188
P31948_169	Q59HH3_488	P55084_253
P31948_207	Q59HH3_888	P07814_788
P31948_250	Q13263_275	P07814_841
P31948_337	Q13263_337	P40939_129
P31948_347	Q9HB71_212	P40939_214
P31948_364	P35579_1441	P40939_255
P41250_82	Q92598_316	P40939_295
P41250_219	O43175_58	P40939_411
P41250_646	O43175_384	P40939_631
Q99832_153	P54577_231	P31943_173
Q01813_736	P54577_412	P31943_349
O14818_115	Q15365_23	Q99729_70
P50395_253	Q15365_31	Q99729_153
P50395_269	P50990_466	Q99729_149
Q86VP6_577	P55786_293	Q99729_210
Q86VP6_586	Q9Y617_333	Q99729_215
P10768_64	P14625_597	P08865_89
P10768_186	P14625_682	P07910_29
P10768_200	P32119_10	P07910_42
P34932_185	P32119_34	P46782_191
P34932_332	P09211_189	P46782_201

P34932_674	P22234_80	P04843_517
P34932_719	P23526_46	P04843_579
P40925_110	Q04760_151	P20700_261
P40925_236	P0CG47_48	P62269_91
Q9HB71_134	P0CG47_87	P62269_150
P46940_368	P0CG47_200	Q9NTJ3_170
O75369_2342	P0CG47_215	B4DRW8_456
B1AK87_83	P09936_15	P26599_428
P31153_303	P09936_78	P61513_28
P78417_11	P10599_8	P83731_12
P78417_136	P10599_96	P83731_113
P78417_143	Q92945_281	P83731_119
P78417_198	O15347_161	P83731_139
P78417_220	Q9NTK5_79	P62753_14
P27348_68	O15318_61	P62753_203
P49368_248	P24534_66	Q15233_203
Q14141_353	P41250_204	Q15233_249
Q14141_379	P49321_637	P43243_478
P60900_102	Q9BRA2_78	P46777_242
P48643_226	Q9BRA2_89	P48643_282
A0A0D9SF54_39	O75369_373	P48643_439
A0A0D9SF54_602	P26583_127	P12236_147
A0A0D9SF54_1314	D3DPU2_327	P12236_166
A0A0D9SF54_1635	P21333_771	Q9Y265_453
P68032_86	O15067_279	P62899_70
P52209_147	P55209_87	P62829_113
P26583_3	Q9Y490_1544	P62829_123
P26583_114	P27694_489	P15880_71
P26583_172	P15311_64	P40227_261
O00154_286	P68036_82	P40227_388
P25789_64	P68036_145	Q96HS1_144
Q06323_13	P13693_100	Q00325_234
Q06323_190	P30086_132	P04083_90
O75533_1086	O95433_212	P04083_245
Q92688_99	O95433_328	P26368_462
P12814_157	Q9BWD1_180	P50991_55
P12814_682	P50502_5	P50991_489
Q14974_376	P07814_841	P08575_448
P21333_865	P30520_163	P08575_1149
P21333_1538	P37837_277	O95202_150
P60174_92	P26639_222	Q8WWV3_102
P60174_225	P61088_24	P38919_60
P60174_231	A0A0S2Z4I4_13	P38919_152
P49736_216	Q96AE4_400	P38919_198
Q9Y617_116	P63167_5	Q99798_409
Q9UL46_180	P61956_42	Q99798_520
O95433_189	Q9H4A4_162	Q9BPW8_51
P26639_279	Q07866_384	Q9BPW8_56

P49773_21	O14737_63	Q9BPW8_80
P49773_83	O75347_52	Q92841_269
P23526_389	O75832_221	Q92841_547
Q96P70_865	Q8WUM4_11	P55809_271
Q92598_185	O95757_788	P55809_296
P33316_155	O43143_17	P55809_421
P27707_88	P37802_171	Q92900_318
P15170_103	D6RBW1_220	P84098_146
P24534_139	Q15691_174	P84098_190
P24534_176	Q9UBT2_86	Q92608_145
P24534_185	P60953_133	Q92608_1474
Q9Y490_875	O75937_105	P39019_29
Q9Y490_2133	Q06203_372	P39019_122
Q99426_188	Q9BRX5_207	P39019_143
P49321_530	P09651_8	P13073_60
P49321_636	P30566_295	Q9NQC3_1174
P49321_652	P52907_226	Q9Y3U8_16
P49321_657	P52907_273	Q86V81_134
P30566_295	Q9NZZ3_100	Q86V81_156
P50570_629	P61158_240	Q86V81_161
Q13907_180	O95347_187	Q13151_99
P61221_478	O60841_1195	Q13151_176
P62942_45	P14324_123	O43837_354
Q8NCW5_144	P16949_100	P11310_279
Q8NCW5_148	P62633_85	P62750_7
P31946_11	P19623_96	P62750_14
P31946_77	P36507_88	P62750_23
P51784_766	P53004_147	P62750_26
Q8N163_791	O60271_655	Q9P2J5_464
O60234_35	Q14185_1469	P25398_116
O60234_119	P25789_64	P62280_144
P67936_13	Q9NRN7_74	Q12931_369
P67936_76	Q9BZD4_275	Q12931_432
P67936_113	Q9H074_337	Q9Y4W6_508
P67936_116	P52272_145	P16403_119
P67936_212	Q9Y2L1_107	P16403_172
A0A024R5M9_1610	Q92905_194	P16403_191
Q16181_349	P46063_70	P16403_207
Q16181_368	Q9H444_17	P16403_211
Q7L5N1_102	P30626_68	O94925_164
Q7Z6Z7_1147	P63279_74	P00505_82
Q9NTK5_79	Q9UBU8_240	P00505_309
Q12874_92	P52888_220	P00505_363
P09960_573	Q96A72_50	A0A087X2I1_220
P60520_24	Q99471_47	P00367_365
Q709C8_2356	O95817_460	P00367_480
P18754_335	Q15631_219	O15372_269
P52907_278	P55327_137	O15372_274

Q04446_39	Q9HBG6_392	Q9H936_80
Q16576_119	P55160_14	Q9H936_83
Q07866_314	P63151_95	P53007_97
P53621_607	P57076_7	Q96FJ2_5
P55160_326	P21675_1591	Q8WU39_70
Q99497_130	Q8WXH0_6754	Q8WU39_111
Q9H9T3_414	Q8NE71_545	P51572_149
O14929_364	P51532_835	Q9H9P8_104
Q15181_41	Q86VS8_324	P63173_52
A8K8F0_290	Q9UHX1_267	Q2TU64_21
P05455_37	Q02878_29	P32969_28
P05455_185	Q12849_337	P55072_663
P31150_253	Q7Z4S6_963	Q13310_361
P39687_99	Q2M2Z5_39	O75533_1086
Q01469_34	O43502_328	P56192_860
P50502_17	Q6ZU80_659	P16615_120
P51532_835	Q96DT5_3875	P16615_510
Q15428_57	Q14765_88	P39748_267
Q9BXJ9_262	P08238_273	P83111_199
P68036_73	P68104_64	P83111_231
P68036_96	P13639_638	P35232_202
O94903_47	P04406_84	P25685_37
Q9NRX4_87	P11142_597	Q15046_88
Q92888_214	P19338_521	Q92499_702
P49593_334	P19338_610	Q9Y262_393
Q14019_98	P14618_230	Q9Y262_549
O60306_1045	P07737_127	P55265_494
P32321_78	P29401_314	P55265_591
P32321_131	P32119_67	P31146_233
P06400_791	A0A024R895_62	P13995_50
Q9Y678_313	P63241_34	P62191_24
P09651_350	P22102_156	P62191_217
O95865_51	P22102_249	P46781_30
P52565_178	P22102_852	P46781_91
O15355_367	P54577_346	O75431_95
Q8N1F7_387	P35579_1129	Q9NZ45_55
P25788_174	P35579_1132	P42704_103
B7Z738_456	P50990_225	P42704_760
P50851_251	P31939_137	P37108_32
V5YQL4_1126	P31939_357	P37108_38
O75821_172	P0CG47_11	Q92930_58
Q9UHY7_111	P0CG47_63	A8K228_45
Q9Y2L1_107	P0CG47_124	Q7Z7H5_172
Q00839_814	P0CG47_163	Q7L014_793
Q04760_157	P27694_167	P35268_16
O76003_294	P05455_204	Q15067_260
Q07666_214	P05455_208	P23284_89
O75663_106	P05455_354	P48556_324

Q15185_48	P05455_397	P17987_494
Q9NZZ3_51	Q99832_153	P17987_538
Q6ZMR3_155	P09936_131	P16402_111
Q14847_17	P09936_157	P16402_123
Q16763_63	Q9Y266_53	P16402_169
Q5VU61_187	Q9Y266_96	P16402_209
Q5VU61_203	P21333_865	O15382_111
Q01844_404	P21333_1538	O15382_377
Q86U86_553	Q9NTK5_394	Q99613_332
P63208_130	Q92945_448	P22830_133
Q00535_237	P15170_238	P60953_131
Q14258_320	P43487_76	P60953_133
Q6ZUM4_426	P40227_251	Q93084_120
P43487_179	Q9UHD1_190	P13667_528
Q15813_451	P49321_657	Q5SRE5_51
O95260_64	P61221_126	P62841_65
Q92785_207	P78371_248	Q14008_1859
Q7KZ85_381	Q14103_178	P61221_169
Q9NY27_84	Q14103_243	Q15269_127
O43847_325	Q14103_255	Q92804_277
Q96ST2_666	Q09028_215	Q15084_150
P14921_138	Q96AE4_233	Q86U86_553
Q9Y2Z0_41	Q15181_228	Q86U86_1025
Q86VS8_324	Q15181_282	Q16778_35
O14776_820	B4DPD5_96	Q92621_66
Q6S8J3_1036	P31689_24	P41227_148
P13984_236	P31689_32	P46940_1558
O14497_1230	P62942_45	Q9NYU2_596
P23588_223	P62942_48	Q9NYU2_1208
Q86V21_633	P68036_64	P03928_45
P53990_48	P50570_562	P03928_49
Q13094_38	P37837_307	P49748_276
Q3LXA3_487	P49588_625	P62873_209
P50552_21	P39687_111	P27708_964
Q96KB5_50	E7EVH7_486	Q14151_437
O60563_33	Q9UBT2_409	Q99832_153
Q9UN37_356	P78417_136	Q99832_231
P48426_140	P78417_220	Q96RE9_435
Q13362_418	P37802_79	P26641_249
P26640_903	O00267_143	P53597_308
P07951_149	O00267_199	Q9UII2_49
P08238_354	P61088_10	Q9UII2_72
P06733_228	Q00013_299	Q9UII2_82
P14618_136	Q9Y2L1_627	Q9UII2_83
P14618_256	Q9Y2L1_654	O60884_39
P00558_382	B4DQ80_34	P30050_40
V9HWJ7_76	B4DQ80_146	P30050_41
V9HWJ7_82	B4DQ80_149	Q13283_413

V9HWJ7_88	B4DQ80_162	Q15555_165
V9HWJ7_92	B4DEA6_137	P30405_67
V9HWJ7_294	O95347_320	P30405_183
V9HWJ7_444	P62316_71	P56378_49
V9HWJ7_449	P20618_184	P11387_148
V9HWJ7_456	P25789_210	P18621_46
V9HWJ7_468	P51858_19	P18621_169
V9HWJ7_472	Q13451_155	Q9NY12_94
V9HWJ7_542	Q9UBQ0_30	C7DJS2_60
V9HWJ7_579	Q6P1N4_368	O95831_593
P04075_140	Q96KB5_50	Q8N183_108
P07900_576	P16949_43	Q96IX5_16
P35579_1802	P16949_80	P30038_487
P29401_260	P08243_385	O14949_82
P09429_7	Q9UHV9_136	P49406_205
P09429_50	Q9BXJ9_312	Q9BX67_287
P26641_401	P35080_116	Q9BX67_283
P63104_74	Q15056_120	Q9Y487_240
P63104_75	Q562M3_30	O95573_58
P52566_40	Q53GN4_104	O95573_706
P52566_47	Q53GN4_182	O60762_136
D3DPU2_63	Q96A72_16	P56381_37
P22314_671	Q9H3P7_117	P56381_44
P00813_164	P14314_438	Q6UB98_868
P00813_225	Q8N6H7_359	Q6UB98_1105
O00299_183	Q99714_99	Q9NSE4_241
P22234_235	P61077_128	H0Y2W2_80
O43143_132	Q7L1Q6_255	H0Y2W2_200
P31948_388	P62993_76	H0Y2W2_481
P34932_430	P48637_172	Q00059_186
P31939_199	Q13257_200	Q9Y2W1_711
P49588_766	H0YC42_137	P62857_10
P48643_232	Q8WUA2_82	P62857_16
P60174_106	A0A0F7NGI8_537	Q7Z7F7_104
P60174_212	P09884_829	Q6DD88_375
P26583_43	Q96DG6_227	Q01844_404
O00154_168	Q12965_196	P30101_218
P27348_85	O43707_108	P30101_332
P63241_85	Q9UJA5_145	P22033_621
O60610_786	P23284_89	Q96A72_16
P22102_156	Q9GZM8_262	Q6UB99_1345
P49368_78	Q05209_65	Q6UB99_1531
Q96G03_565	Q96ST8_588	Q6UB99_1621
P62942_35	P60981_19	B4DVV3_332
Q96A72_50	Q8WWS9_693	Q9UJS0_408
A0A024RDF4_197	Q9Y6K9_309	P10606_57
Q14980_715	P78316_334	Q03701_195
Q14980_1624	P60709_213	O60306_1045

P40121_137	P60709_291	P62861_1
P40121_341	P60709_315	P62861_18
O14744_343	P10809_82	P09110_198
P52907_268	P10809_133	P55327_137
P24534_133	P10809_160	P10515_368
Q15027_302	P10809_180	O75964_54
P06400_427	P10809_191	Q9Y512_248
P49589_49	P10809_196	Q14964_63
P14550_127	P10809_250	Q9H082_83
D4YW74_2318	P10809_301	P55160_326
Q8NFH4_114	P10809_310	P52815_142
Q99459_219	P10809_361	P09012_80
Q16543_154	P10809_364	Q9UQ35_169
Q9UNS2_418	P10809_396	P33992_196
P41567_56	P10809_481	Q8NBU5_165
Q96SN8_865	P07437_122	Q9Y2R9_63
P23743_260	P07437_154	Q14571_1662
O75351_363	P07437_252	Q96EY7_517
P37802_17	P07437_297	Q9H845_456
Q99996_2015	P07437_350	Q9UJX3_306
Q7RTS9_312	P68363_40	C9JVQ0_16
P04406_84	P68363_280	Q5JTV8_556
P08238_64	P68363_311	O95347_177
P08238_552	P68363_326	P30049_165
P08238_559	P68363_352	P18124_48
P08238_565	P68363_401	Q96AG4_138
P08238_573	P48735_45	O75190_60
P08238_574	P48735_48	P49711_405
P08238_685	P48735_69	Q8WXF1_257
P14618_125	P48735_80	P35754_20
P14618_206	P48735_106	Q99623_89
P14618_224	P48735_130	O00186_197
P14618_336	P48735_133	P49841_292
P14618_504	P48735_155	Q93079_6
P00558_97	P48735_166	Q96DI7_275
P00558_106	P48735_180	Q8NI27_158
P00558_264	P48735_193	O14874_233
P00558_297	P48735_199	Q9Y2X7_135
P00558_388	P48735_272	Q9H300_75
P07900_74	P48735_275	Q15031_79
P07900_84	P48735_280	Q9UJZ1_222
P07900_208	P48735_282	P17252_35
P07900_436	P48735_384	O75821_172
P07900_458	P48735_413	P08754_67
P07900_513	P48735_426	Q9HBD4_835
P07900_534	P08133_81	O00182_88
P07900_546	P08133_102	O15320_500
P07900_559	P08133_299	Q00839_215

V9HWJ7_97	P08133_315	Q96PK6_167
V9HWJ7_132	P08133_354	Q9UIF9_748
V9HWJ7_297	P08133_370	Q8NBS9_407
V9HWJ7_328	P08133_406	Q9UNL2_103
P04075_153	P08133_418	Q9UJA5_145
P04075_342	P08133_442	Q709C8_2092
P35579_79	P08133_446	Q9C0D2_389
P35579_299	P08133_478	Q8TDB6_593
P35579_637	P08133_613	O75347_51
P35579_682	P04406_117	Q14651_94
P35579_860	P06576_124	Q8NB50_475
P35579_938	P06576_161	Q9H4G4_53
P35579_1132	P06576_159	O60814_121
P35579_1404	P06576_259	P53990_48
P35579_1441	P06576_350	B4DZB4_636
P35579_1477	P06576_351	Q9BSJ2_426
P35579_1716	P06576_485	O43488_242
P35579_1754	P06576_522	Q02880_1327
Q06830_27	P19338_295	P84090_41
P13639_239	P19338_377	Q9Y520_1160
P13639_272	P38646_76	P98171_460
P13639_275	P38646_135	P04844_311
P13639_594	P38646_175	Q9Y655_32
P13639_629	P38646_187	P62913_67
P07195_308	P38646_234	Q86XL3_447
P29401_254	P38646_300	Q9UPV0_936
P06744_252	P38646_467	O60488_49
P09429_146	P38646_625	Q9Y6N5_260
P09211_191	P38646_646	P48426_140
P62826_37	P14866_229	Q6ZQQ6_2341
P11142_451	P14866_269	Q07021_123
O75083_362	P14866_493	O60508_380
P26038_35	P14866_533	O75489_260
P50990_459	P14625_95	P08574_325
P52566_102	P14625_269	H3BUE4_21
P52566_110	P14625_340	Q09161_342
P18669_138	P14625_534	P05408_166
P18669_225	P14625_547	P05114_42
P31948_32	P14625_593	Q13011_327
P31948_210	P14625_630	Q52LJ0_256
P31948_317	P14625_633	Q03001_1114
P31948_453	P14625_671	Q9Y3A2_114
P26641_212	P13010_291	Q4LE39_647
P23528_132	P13010_307	O43283_498
P31146_439	P13010_532	P30044_142
Q01082_1312	P13010_534	Q9H3S7_600
Q01082_1878	P13010_544	Q96LB3_197
Q01082_1991	P13010_648	Q9BXT5_1381

Q01082_2054	P13010_660	A0A024R856_2276
D3DPU2_71	P13010_703	Q7Z333_1290
D3DPU2_81	P34897_103	Q9UIG0_576
D3DPU2_287	P34897_200	Q2KHM9_377
D3DPU2_298	P34897_269	E5RHP9_40
D3DPU2_304	P34897_297	P10809_469
P62258_50	P34897_302	P07437_154
P62258_73	P34897_356	P11142_451
P62258_142	P34897_459	P38646_368
P00813_232	P34897_464	P38646_612
P00813_323	P40926_74	Q5VTE0_41
P00813_331	P40926_157	Q5VTE0_44
P53396_64	P40926_165	Q5VTE0_179
P53396_968	P40926_203	Q5VTE0_215
O00299_131	P40926_215	Q5VTE0_255
O00299_192	P40926_239	Q5VTE0_273
P31939_66	P40926_297	Q5VTE0_392
Q32Q12_189	P40926_324	Q5VTE0_408
Q32Q12_196	P40926_329	Q5VTE0_439
Q32Q12_268	P62807_6	Q5VTE0_444
P40227_199	P62807_17	Q5VTE0_450
P40227_430	P62807_21	Q5VTE0_453
P15121_173	P62807_47	Q5VTE0_457
P22234_110	P62807_117	P08133_9
P22234_286	P25705_123	P08133_315
P26583_65	P25705_126	P14625_269
P26583_90	P25705_161	P48735_106
P26583_139	P25705_167	P25705_132
P41250_99	P25705_230	P25705_167
P41250_108	P25705_305	P25705_539
P34932_53	P25705_427	P62807_13
P34932_679	P25705_506	P06576_259
P34932_754	P25705_531	Q02878_87
P34932_766	A0A024RB53_78	Q02878_237
P10768_10	A0A024RB53_105	P06748_32
P14324_123	A0A024RB53_106	B4DLR3_224
P14324_413	A0A024RB53_166	P34897_103
P50395_103	A0A024RB53_179	A0A024RDF4_237
P50395_142	B4DLR3_193	P10412_136
P50395_221	B4DLR3_197	P23396_132
P11586_10	B4DLR3_224	P23396_202
P11586_66	B4DLR3_423	P22626_112
P11586_543	B4DLR3_475	P11940_157
P11586_553	B4DLR3_510	P11940_312
O75369_681	B4DLR3_524	P13010_334
O75369_1979	B4DLR3_585	B3KTT6_72
P60174_122	B4DLR3_594	B3KTT6_85
A0A0D9SF54_613	B4DLR3_633	B3KTT6_189

A0A0D9SF54_1573	B4DLR3_773	B3KTT6_196
A0A0D9SF54_2063	P10412_46	B3KTT6_210
Q9BWD1_136	P10412_52	B3KTT6_299
P52209_154	P10412_63	B3KTT6_305
P52209_375	P10412_64	P62701_230
Q92688_110	P10412_85	P39023_366
B1AK87_211	P10412_90	P13796_294
B1AK87_223	P10412_97	P13796_449
B1AK87_240	P10412_106	P78527_3603
P61158_317	P10412_110	P78527_4019
Q14141_327	P10412_117	P13639_438
Q14141_351	P10412_119	P27797_153
Q14141_400	P10412_127	P27797_207
P54578_49	P10412_136	P27797_209
P54578_214	P10412_148	Q13813_1334
O00154_157	P10412_156	Q13813_1650
P15311_3	P10412_168	P09622_277
P49368_21	P10412_186	D3DQ69_203
P49368_222	P10412_197	D3DQ69_341
P49368_381	P10412_213	D3DQ69_362
P32119_10	P06748_154	D3DQ69_363
P32119_26	P06748_155	Q93077_6
P32119_177	P06748_212	Q93077_37
P21333_1071	P06748_215	Q93077_120
P21333_1294	P06748_229	Q93077_126
P21333_2513	P62805_9	Q14152_278
P00491_265	P62805_13	P35579_992
P27348_11	P23396_18	Q04837_113
Q9Y490_685	P23396_90	O43390_120
Q9Y490_1933	P23396_108	P62081_147
P23526_20	P23396_132	P26373_210
O60610_771	P23396_201	Q99798_605
Q06323_35	A0A024RDF4_72	Q99798_730
P41091_275	A0A024RDF4_110	P50213_77
P25789_239	A0A024RDF4_119	P21796_201
P09972_42	A0A024RDF4_158	P00558_15
P13010_603	A0A024RDF4_161	P40939_415
Q13263_469	A0A024RDF4_176	P00367_258
P50570_206	A0A024RDF4_231	P35637_312
P50570_562	A0A024RDF4_237	Q3ZCM7_154
P33992_196	A0A024RDF4_238	P00505_73
Q9BRA2_35	A0A024RDF4_255	P00505_94
Q15366_23	P05141_33	P55084_44
P63167_5	P05141_43	Q02543_136
Q9Y617_323	P05141_63	O75521_177
Q9Y266_53	P05141_166	P47914_87
Q9Y266_93	P05141_245	P47914_134
Q9Y266_268	P05141_272	P09874_87

P52272_672	Q02878_5	Q99729_223
P24534_60	Q02878_8	Q99729_330
P24534_74	Q02878_26	Q16891_122
P24534_132	Q02878_41	Q16891_306
Q13098_183	Q02878_77	P62241_37
Q04917_69	Q02878_87	P62241_128
Q9Y696_199	Q02878_100	O43837_199
P39748_80	Q02878_210	P36578_348
P68036_9	Q02878_237	P36578_390
P68036_146	P31946_13	P50914_79
Q9UI08_21	P31946_51	P50914_177
Q9UI08_22	P31946_122	P46779_127
Q9UI08_70	P31946_160	P13073_53
Q01105_167	P07737_91	P13073_65
P12004_80	B2RB06_81	P46777_220
P52907_97	B2RB06_179	P16401_27
P52907_103	B2RB06_185	P16401_35
P52907_273	B2RB06_192	P16401_133
P67936_100	B2RB06_202	P16401_161
Q13303_274	B2RB06_206	P16401_172
P25787_53	B2RB06_271	P16401_217
Q96AE4_591	P13639_498	P15880_275
Q8N163_839	P39023_39	Q01082_1981
P17252_197	P39023_103	P30101_226
P17252_209	P39023_294	P84098_196
B3KTT6_85	P39023_300	P61513_87
P06493_33	P39023_366	Q9Y262_403
Q16181_239	Q00610_96	Q9Y262_558
Q16181_326	Q00610_367	P24539_233
Q16181_333	Q00610_619	Q00325_209
B7Z217_1013	Q00610_737	Q00325_214
Q5TBB1_145	P14618_247	A0A0S2Z5H3_471
P29692_117	P22626_22	Q08257_116
P40121_300	P22626_112	P69905_17
P54577_146	P22626_113	P11310_175
P31946_70	P62277_93	P62750_18
P26639_273	P12268_109	P62263_86
O76003_151	P12268_450	P62263_106
P50502_14	P62847_32	P49207_62
P50502_153	P62847_43	Q9Y4W6_785
Q01469_55	P62847_46	Q9NY12_140
Q9UBT2_447	P62847_68	P25787_92
Q00013_299	P62847_129	P78406_131
P09651_8	P13796_88	P78406_154
P09651_15	P13796_294	P07237_328
P63279_18	P13796_579	Q9NX63_86
P63279_49	P49411_79	P49458_52
P63279_76	P49411_88	Q9H1K4_79

Q99879_109	P49411_91	Q9H1K4_82
Q99879_117	P49411_234	P14314_83
Q99879_121	P49411_238	P08621_138
O43175_289	P49411_342	P07910_94
O43175_394	P49411_361	Q99832_77
P52565_105	P49411_447	P62841_58
Q92945_281	Q12906_454	P62841_72
Q9Y450_657	P00505_59	O15372_221
P39687_110	P00505_82	P40227_199
P39687_111	P00505_90	Q00688_96
O94776_492	P00505_159	Q00688_170
P48739_50	P00505_309	Q2TU64_248
Q9BTE3_328	P00505_338	P50995_495
Q02750_84	P00505_363	P62913_38
O75396_38	P27824_118	Q9UII2_100
P49591_12	P27824_127	Q86U86_225
Q93034_455	P27824_182	P14735_896
O75347_52	P27824_398	Q4GUF2_45
Q9UHY7_106	P27824_515	Q4GUF2_49
B4DW52_56	P62424_11	Q7L2H7_177
Q9NZZ3_100	P62424_20	P61026_136
P55786_712	P62424_34	Q6NZ52_92
P36507_88	P62424_97	P11387_669
Q13177_136	P62424_125	P24752_230
Q13177_246	P62424_212	P24752_266
Q9UQE7_143	P62424_217	P26196_482
P13693_89	P62424_255	O60841_393
Q14008_1761	P12956_189	P28062_133
Q15365_115	P12956_287	Q8IYB8_404
A0AVT1_168	P12956_463	B4DEB0_290
F6WQW2_227	P12956_516	Q8NFH4_114
F6WQW2_256	P12956_526	Q8N0V3_70
Q9C0B1_216	P12956_553	P18077_66
Q9H444_17	P12956_570	Q13505_190
O00232_368	P12956_575	Q96RE9_491
P08758_309	P12956_596	O14832_120
Q9HC35_228	P50990_260	P30044_86
Q9UBQ0_73	P50990_326	Q9HAV7_100
Q16775_229	P51991_29	O76021_116
O95149_144	P51991_36	Q13442_132
Q9NR45_61	P51991_134	P47813_104
Q8WVM8_515	P51991_199	Q9HAN9_56
O43865_487	P48643_259	Q9NVP1_542
Q14019_93	P62081_58	Q8WVM8_515
A6NDG6_72	P62081_142	O14979_142
Q8WXF1_257	P62081_155	Q8WXF1_380
P11021_185	P62081_160	Q14161_135
A0A0S2Z4I7_21	P62081_178	O14617_189

Q9Y2X7_135	P62081_179	P49840_355
Q13085_323	P62906_47	Q6UB35_880
A8MWD9_10	P62906_95	P22307_453
Q15056_80	P62906_118	Q15031_81
P13929_60	P62906_130	P01130_830
H3BVE0_79	P62241_128	Q8WZ42_3065
Q5THR3_563	P62241_139	Q8WZ42_29371
Q5W0Q7_56	P62701_94	Q13129_618
Q9HBG6_392	P62701_211	O75489_259
Q14790_250	P62701_230	Q99996_2015
Q9BZH6_223	P62701_233	Q6ZN06_297
Q96ST8_588	P52566_114	Q8N532_316
Q02224_1444	P52566_124	Q10713_478
P08238_347	P52566_135	P55786_222
P14618_166	P52566_138	Q96PK6_593
P07900_204	P52566_175	Q8WXH0_4586
P07900_485	P52566_196	P26440_146
P35579_102	P26583_167	Q15024_178
P35579_186	P26583_173	P27701_263
P35579_560	P61604_28	Q3L8U1_2507
P35579_1081	P61604_40	P22695_21
P35579_1193	P61604_80	P13984_236
P35579_1234	P11940_157	P36957_145
P06744_423	P11940_348	P12814_89
P06744_523	Q3ZCM7_122	P47985_168
P09429_112	Q3ZCM7_154	A0A0A6YYL4_103
P13639_259	P26038_64	Q86WX3_110
P26038_263	P26038_151	P10809_481
P26038_448	P26038_253	P25705_305
O75083_7	P26038_254	A0A0S2Z377_81
O75083_480	P26038_391	A0A0S2Z377_265
P31948_13	P26038_400	A0A0S2Z377_314
P31948_162	P26038_538	A0A0S2Z377_354
P31948_429	P15880_211	A0A0S2Z377_370
P31948_523	P15880_212	A0A0S2Z377_406
P26641_249	P15880_275	A0A0S2Z377_442
D3DPU2_327	Q96KK5_37	A0A0S2Z377_478
O43143_384	Q96KK5_120	A0A0S2Z377_607
P31939_137	Q96KK5_126	A0A024RB53_78
P49588_625	P40939_60	P14625_532
P60174_193	P40939_214	P14625_633
B1AK87_66	P40939_255	B4DLR3_561
O75369_142	P40939_259	P13010_566
O75369_838	P40939_289	P61978_219
P34932_356	P40939_295	P14866_269
P46940_1445	P40939_303	Q00610_96
O60610_377	P40939_415	Q02878_247
P52209_51	P40939_460	P06748_141

P61158_240	P40939_728	P06748_155
P33316_179	P27797_41	P40926_307
P15170_208	P27797_48	P62424_11
P15170_490	P27797_151	P62424_217
P11766_366	P27797_153	P05141_96
P27348_139	P78371_272	P23396_148
P15311_60	P78371_441	P39023_66
Q15366_115	P24752_66	P61247_56
P49915_182	P24752_174	P36578_405
P26639_222	P24752_190	P26583_3
P07814_513	P24752_230	P63244_271
P31946_214	P24752_251	Q9UQ80_158
P25787_70	P23246_518	P78527_2746
A0A0S2Z4I4_76	P52272_651	Q5VU21_102
A0A0S2Z4I4_116	O75947_5	Q5VU21_140
A0A0S2Z4I4_212	O75947_117	Q5VU21_278
A0A0S2Z4I4_228	O75947_144	Q5VU21_299
P58876_12	O75947_149	Q5VU21_300
P58876_109	P61247_27	P49411_447
P58876_121	P61247_144	A0A0D9SF54_602
Q9UHD8_262	P61247_222	A0A0D9SF54_1560
P31150_269	P61247_240	P21796_236
Q07666_175	P61247_249	Q16891_436
P61163_200	P62851_14	P62263_63
A8KAP3_244	P62851_20	P23246_208
Q16543_110	P62851_25	P08865_212
Q14019_110	P62851_57	P62753_30
A6NHG4_87	P62851_60	P07237_326
P14735_303	P62851_98	P62851_60
Q9UHD1_198	Q13423_394	P35637_448
P35241_3	Q13423_1059	P00505_159
Q9UHX1_201	Q08211_236	P00505_234
Q9UHX1_267	Q08211_235	P42766_77
P00390_401	Q08211_943	P39019_111
Q9P016_60	P40227_388	Q7KZF4_541
P25685_242	P40227_426	P62917_149
P62633_103	P40227_424	P62917_155
P63151_95	Q99729_82	P08708_72
P61088_92	Q99729_86	Q01082_1824
Q9C0C9_132	Q99729_118	P62888_44
O75044_245	Q99729_149	Q86V81_86
P29350_257	Q99729_153	P07910_89
Q15631_219	Q99729_210	D6RBZ0_150
Q99961_171	Q99729_214	D6RBZ0_210
O75935_59	Q99729_215	D6RBZ0_215
Q9HAV4_1147	Q99729_223	P17987_484
Q08AE8_288	Q99729_232	P41252_1042
P0DMV8_77	P63244_12	Q9NX63_37

P0DMV8_88	P63244_185	Q92522_143
P0DMV8_102	P63244_264	P62249_26
P0DMV8_251	P63244_271	Q96A26_150
P0DMV8_328	P36578_29	P61353_93
P0DMV8_345	P36578_368	P61513_7
P0DMV8_348	P36578_374	E9M4D4_17
P0DMV8_524	P36578_375	P24752_223
P0DMV8_569	P36578_380	P31948_250
P0DMV8_597	P36578_399	O75746_406
P09874_97	P36578_412	P22307_534
P09874_108	Q8NC51_39	P84095_130
P09874_192	Q8NC51_299	P63220_74
P09874_249	Q8NC51_320	P46940_939
P09874_683	P07954_94	Q9GZR7_808
P61978_103	P07954_115	Q5T3I4_144
P61978_422	P07954_470	Q9UJV9_416
P06748_267	P07954_477	P35606_199
Q00839_265	P78527_310	O60610_377
Q00839_464	P78527_2829	Q9UNX3_136
Q00839_516	P78527_3260	P09496_242
Q00839_551	P62913_38	Q15555_156
Q00839_565	P62913_52	P38117_53
Q00839_626	P62913_67	P06730_184
Q00839_635	Q16891_270	P46977_340
P08670_129	Q16891_282	Q86SR1_379
P08670_439	Q16891_315	Q04446_39
P38646_368	Q16891_427	Q8N254_280
P38646_377	Q16891_436	Q15052_722
P38646_468	Q16891_640	Q96SI9_75
Q08211_146	Q99832_67	P13804_226
P14866_418	Q99832_463	Q9UNF1_311
P23246_279	P07814_788	Q9NRX4_87
P23246_330	P84243_5	P08686_232
P23246_472	P84243_19	P20338_173
Q5CAQ5_561	P84243_24	O94913_354
Q5CAQ5_671	P84243_57	P78344_187
Q5CAQ5_682	P84243_65	P13612_189
P52272_381	P84243_123	Q14103_111
P43243_798	Q99798_144	Q9P2K5_85
P17844_470	Q99798_409	Q8N3U4_53
Q6FI13_120	Q99798_605	Q96QR8_251
Q5VU21_300	Q99798_730	Q8NFC6_365
Q5VU21_306	P16401_35	P11142_500
P07910_89	P16401_49	P08238_649
P07910_157	P16401_132	A0A0S2Z377_9
D6RBZ0_83	P16401_133	A0A0S2Z377_102
D6RBZ0_87	P16401_140	P14625_628
D6RBZ0_102	P16401_168	P38646_654

D6RBZ0_215	P16401_188	B4DLR3_503
D6RBZ0_232	P16401_209	B4DLR3_647
Q15233_203	P16401_214	P48735_199
Q15233_467	P55809_176	Q00610_189
Q12906_342	P55809_185	Q02878_12
P48643_160	P55809_296	Q02878_15
A0A024RDF4_242	P55809_418	B4DUQ1_52
P49327_436	P55809_421	B4DUQ1_60
P49327_673	P55809_481	B4DUQ1_381
Q6NXR8_34	Q68D11_798	P06733_422
P63244_183	Q04837_81	P27797_276
P42704_750	Q04837_103	P12956_262
P26641_220	Q04837_113	P12956_582
O75390_459	P42677_16	P26583_59
P12277_304	P46782_201	P26583_127
P54819_93	P27635_82	P10412_129
Q07666_432	P27635_121	P10412_130
O00571_335	P27635_145	P10412_168
O14979_180	P27635_170	P63244_185
P42167_346	P27635_188	P62753_211
Q7KZF4_116	P21796_20	B2RB06_185
Q13283_413	P21796_109	P27635_121
Q07020_119	P21796_201	P08575_967
O15371_53	P21796_236	P42766_71
P22392_100	O75083_90	P36542_36
P52292_459	O75083_104	Q99798_689
P11177_336	O75083_223	P46782_44
P04181_405	O75083_256	P16401_184
P43487_111	P48047_54	P16401_214
Q15029_64	P48047_70	P47914_63
Q96PK6_593	P48047_73	P47914_103
Q9Y2W1_481	P48047_162	P47914_130
Q9Y2W1_876	P00367_183	D6RBZ0_154
A0A024RBE8_233	P00367_258	D6RBZ0_232
Q12849_242	P00367_365	D6RBZ0_325
Q13242_36	P62917_93	P62750_30
P55786_853	P62917_144	P62750_114
Q9H583_1675	P62917_155	P12236_23
Q9NY12_94	P38159_86	P61353_126
Q5SY16_670	P38159_150	O75083_104
Q96I24_525	P38159_217	B3KS98_283
P50570_598	B3KX96_29	B3KS98_288
O00231_417	B3KX96_39	Q12931_629
B4DZJ6_890	B3KX96_42	P35268_6
Q03701_195	B3KX96_89	Q99623_216
Q9UJX3_306	B3KX96_144	P46776_92
P08237_678	B3KX96_163	Q9Y3U8_35
O15460_57	O43390_114	P30405_91

Q14671_718	Q9Y277_15	P62316_88
Q8N5F7_305	Q9Y277_20	Q9Y4L1_883
P54709_182	Q9Y277_109	Q9UII2_71
Q14181_232	Q99714_104	Q9UII2_96
P35914_179	O43837_96	P63218_36
P38432_496	O43837_146	P30626_68
Q14203_397	O43837_354	Q96C36_291
Q8IZX4_1610	A0A0D9SF54_969	P18077_15
O14727_142	A0A0D9SF54_1560	P11387_174
Q9BRT2_69	A0A0D9SF54_2411	P34932_332
P0DMV8_539	Q86V81_81	Q14204_1649
Q00839_543	Q86V81_86	Q3KP31_298
P61978_102	Q86V81_156	Q96BR6_416
P58876_117	Q86V81_164	Q9UIF9_660
P43243_146	Q13838_384	Q9UIF9_758
P17844_236	Q00325_209	Q99986_98
Q5CAQ5_663	Q00325_214	O75477_205
G3V4C1_89	Q00325_234	Q9Y4W2_540
G3V4C1_144	Q00325_247	Q15027_302
Q15233_198	P55084_181	P10515_363
Q15233_239	P55084_188	Q9UK58_307
O75390_43	P55084_272	Q14694_780
Q92945_203	P20700_261	B4DLN1_183
O14979_142	P20700_457	P53804_1571
F8VY04_51	P20618_164	Q9HCL3_254
P24534_147	P05388_77	P60709_284
Q9NZI8_465	P05388_106	P60709_315
O15347_29	P05388_264	P68363_40
P25205_194	Q12931_369	P68363_280
O00264_105	P62753_64	P68363_352
P25786_115	P62753_203	P07437_19
P49792_983	P62753_211	P07437_103
Q9Y265_201	P46781_91	P07437_297
A8KAP3_64	P46781_121	P07437_350
Q00341_883	P46781_139	P10809_58
P54577_310	P46781_155	P10809_191
Q9HAV7_100	B4DRW8_907	P10809_205
A2NX49_323	P31146_233	P04406_271
Q9Y4W2_540	P69905_17	P11142_601
Q14C86_1035	P69905_41	P08133_81
O75899_196	B4DIZ3_66	P08133_102
Q14103_129	B4DIZ3_213	P08133_442
Q5U071_30	Q9Y262_101	P08133_446
V9HW62_88	Q9Y262_393	P14625_593
P08238_411	Q9Y262_549	P14625_597
P08238_491	P08575_641	P14625_623
P68104_172	P08575_664	P48735_69
P68104_180	P08575_780	P48735_80

P68104_244	P08575_1145	P48735_133
P68104_330	P08575_1149	P48735_243
P68104_460	P50213_116	P48735_256
P06733_105	P08865_89	P48735_282
P06733_239	P08865_212	P48735_426
P0DMV8_25	P17844_91	P38646_138
P0DMV8_112	P17844_284	P38646_159
P0DMV8_128	P13073_53	P38646_234
P0DMV8_190	P13073_60	P38646_646
P0DMV8_246	Q2TU64_78	P06576_161
P0DMV8_257	Q2TU64_248	P06576_480
P0DMV8_319	Q2TU64_427	P25705_506
P0DMV8_325	Q71UI9_116	P40926_74
P0DMV8_451	P31943_349	P40926_157
P0DMV8_497	Q92608_437	P40926_215
P0DMV8_500	Q92608_1474	P40926_297
P0DMV8_507	P26599_410	P40926_314
P0DMV8_512	P12236_147	P40926_328
P0DMV8_526	P12236_166	P13010_307
P0DMV8_550	P83731_27	P13010_534
P0DMV8_573	P83731_119	P13010_544
P0DMV8_589	P83731_144	P13010_545
P0DMV8_628	P49458_41	P13010_703
P11142_25	Q96EY1_152	P09429_29
P11142_88	Q96EY1_299	P61978_163
P11142_361	P07237_271	P61978_179
P11142_423	P07237_328	A0A024RB53_52
P11142_500	Q9NZ45_55	A0A024RB53_179
P07900_209	Q9NZ45_68	P34897_200
P07900_478	P45880_247	P34897_269
P07900_657	P67809_64	P34897_464
P07900_693	P67809_92	Q00610_1441
P19338_15	P67809_170	Q00610_1443
P19338_71	Q9P0L0_52	P13639_498
P19338_79	Q9P0L0_125	B4DLR3_423
P19338_80	Q9P0L0_205	B4DLR3_585
P19338_87	Q9P0L0_211	Q02878_210
P19338_95	P62841_58	Q93079_12
P19338_96	P62841_65	Q93079_17
P19338_102	P62841_108	Q93079_21
P19338_109	P84098_146	Q93079_47
P19338_110	P84098_153	Q93079_109
P19338_116	Q9BXW7_69	Q93079_117
P19338_124	Q9BXW7_279	Q93079_121
P19338_125	P31930_111	P23396_18
P19338_132	Q14152_694	P23396_214
P19338_228	A0A0S2Z5H3_158	P31946_13
P19338_282	P30519_168	P31946_51

P19338_318	P30519_199	P31946_122
P13639_42	Q92841_547	P39023_103
P13639_235	P00813_23	P39023_312
P13639_252	P00813_273	P22626_22
P13639_314	P42704_103	P10412_46
P13639_328	P42704_1332	P48643_259
P13639_333	P49257_87	P48643_261
P13639_391	P49257_346	P48643_265
P13639_407	P35637_316	P48643_483
P13639_426	P31040_182	P48643_496
P13639_571	P31040_335	P62277_78
P13639_619	P31040_538	P27797_41
P13639_648	P26373_118	P27797_48
P13639_676	P26373_145	P00505_59
P13639_845	P26373_200	P00505_227
P04075_108	P16403_119	P07737_91
P04075_294	P16403_168	P62701_94
P00338_118	P16403_172	P62701_211
P00338_232	P16403_181	P00558_139
P49327_235	P32969_21	P50990_16
P49327_786	P32969_28	P50990_326
P49327_787	P62899_6	P50990_459
P49327_1116	P62899_55	P62424_34
P49327_1142	P46778_120	Q08211_14
P49327_1151	P09622_430	Q08211_220
P49327_1158	P18621_55	P15880_212
P49327_1239	P18621_96	P15880_263
P49327_1591	P18621_169	P12268_422
P49327_1866	Q01082_842	P12956_596
P49327_1878	Q01082_1354	P62906_152
P49327_1911	Q9NSE4_241	B2RB06_202
P07195_60	Q13151_99	A0A024RBE8_208
P07195_77	P15153_133	A0A024RBE8_213
P07195_119	P61313_83	A0A024RBE8_246
P07195_244	Q2VIR3_275	A0A024RBE8_303
P07195_310	Q9UMS4_244	P05388_77
P07195_318	Q92804_277	P05388_106
P04406_186	Q9P2J5_464	P05388_246
P14618_162	Q9P2J5_719	P05388_264
P14618_186	P18124_48	P62241_139
P14618_367	P18124_88	O75390_43
Q06830_136	P47914_79	O75390_215
P60842_68	P47914_82	O75390_321
P60842_226	P47914_149	O75390_382
P60842_238	Q9Y4L1_537	P21796_266
P60842_309	O43242_76	P36578_29
P09429_150	Q4G176_421	P36578_380
P31948_227	P39019_23	P11021_113

P31948_381	P39019_29	P11021_213
P31948_442	P39019_143	P62979_113
P26641_147	P22307_438	P63244_12
P26641_219	P22307_534	P63244_264
P26641_228	O15372_269	P78527_357
P26641_253	O15372_274	P78527_3264
P18669_157	Q969G3_123	P40939_60
P23528_152	P32322_215	P40939_303
P34932_388	P55265_494	P40939_334
P34932_437	P55265_1115	P27635_188
P34932_668	Q07021_91	Q96KK5_6
P60174_43	Q07021_123	Q96KK5_120
P60174_179	P36542_39	Q96KK5_126
P60174_275	P36542_115	P49411_238
P63104_115	P50914_85	P52566_175
P63104_139	P50914_164	P52566_197
Q32Q12_74	P50914_165	Q99798_144
Q32Q12_81	P50914_171	Q99798_739
Q32Q12_275	P30101_218	Q8NC51_39
P12277_101	P50995_282	Q14697_472
P12277_242	P04843_413	P26373_136
P12277_267	P31939_14	P26373_145
P12277_298	Q9BPW8_51	P51991_36
P12277_307	Q9BPW8_56	P51991_73
P12277_313	Q9BPW8_80	P07814_512
Q13263_188	P62263_63	Q01813_139
Q13263_296	P62263_86	P08575_641
Q13263_319	P04083_90	P08575_664
Q13263_377	P61353_27	P08575_759
Q13263_774	P30048_149	P08575_1145
Q13263_779	P06239_130	P09874_23
P62258_118	A4D1M6_176	P09874_940
P62258_153	A4D1M6_185	P61247_20
P35579_63	Q7KZF4_515	P61247_27
P35579_355	P62280_30	P61247_144
P22314_627	P62280_45	P61247_222
P22314_802	Q13310_104	P62851_94
P22314_806	Q9NSD9_560	P62913_52
P22314_838	P25787_92	P78371_154
P00918_24	Q9UII2_49	P78371_248
P00918_39	Q9UII2_72	Q04837_51
P00918_45	Q9UII2_82	P46781_121
P00918_76	Q9UII2_83	P46781_139
P00918_167	Q9UII2_100	P46781_155
Q02790_88	P62249_60	Q9Y277_15
Q02790_108	P35268_52	Q9Y277_20
Q02790_254	P35268_69	Q99714_104
Q02790_287	P21912_126	Q9Y262_101

Q02790_390	P21912_261	Q9Y262_437
P11586_246	P42766_71	P25205_656
P11586_878	P42766_79	P07954_502
P06744_12	P42766_118	P23246_421
P06744_524	P46779_127	P23246_518
P53396_469	Q12905_186	P52272_698
P53396_468	Q12905_328	P00367_183
P53396_471	P09972_13	P12236_105
P53396_780	A8K1X9_274	P55084_72
P53396_948	P10515_362	P55084_272
P53396_962	P10515_368	Q99832_109
P53396_1077	P10515_386	Q99832_157
P54577_247	O95202_284	P39019_23
P54577_319	Q9NX58_50	P35268_10
P54577_334	O15382_156	P35268_52
P54577_348	O15382_377	Q9NZ45_68
P54577_391	Q9H2W6_216	Q14152_694
P54577_474	P62750_7	P69905_41
Q92598_221	P62750_14	Q9NUJ1_70
Q92598_272	P62750_26	P84098_144
Q92598_275	P62750_36	P84098_153
Q92598_430	Q05D08_174	Q16891_640
Q92598_772	Q05D08_188	P68032_86
Q92598_790	P14868_9	O43837_146
A0A024R895_59	P11310_175	P24752_174
A0A024R895_119	P11310_212	P83731_131
A0A024R895_137	P11310_271	P62249_4
A0A024R895_154	Q8N183_58	P62249_60
A0A024R895_159	P50991_21	P62249_105
A0A024R895_164	P50991_489	Q9P0L0_125
A0A024R895_176	P62888_44	P26599_410
P55786_279	Q9UJV9_416	Q9UQ80_144
P55786_753	Q14683_766	Q9P2J5_350
P55786_821	Q00688_170	P83881_22
Q16576_21	O75643_1294	P55809_176
Q16576_155	O75643_1603	P55809_481
Q9HB71_19	P83111_199	Q86V81_164
Q9HB71_41	P83111_231	Q68D11_798
P11940_299	Q9GZR7_808	P11310_212
P63241_121	Q13601_264	P11310_271
P13797_52	P62191_24	P11310_301
P13797_452	Q13247_143	Q9NSD9_560
P13797_545	P53007_97	P16401_168
P13797_582	P09012_60	P16401_204
P32119_16	P09012_80	P62899_55
P32119_92	P09012_114	P25398_84
P32119_135	P83881_22	P25398_93
Q15366_309	P83881_27	Q96EY1_299

P40925_107	P37108_55	B4DRW8_907
P40925_205	P62873_209	P04083_214
P40925_214	Q8N163_97	P00813_23
P40925_220	P03928_45	P00813_273
P40925_298	P03928_49	P68431_19
P27348_115	Q15046_492	P68431_123
P27348_212	P16402_123	P18124_88
P43487_50	P69849_170	A0A0D9SF54_969
P43487_68	P69849_927	Q9Y285_315
P43487_150	Q16778_35	Q9Y285_342
P43487_190	P62269_91	P17844_391
P15121_12	P62269_150	P55072_754
P15121_179	P62861_1	P62753_218
P15121_222	P62861_51	P63173_9
O15347_112	Q9HAV7_186	P63173_67
O15347_126	Q14554_219	P61353_27
O15347_145	Q99613_643	Q92608_1435
P18206_170	Q99613_712	P47914_77
P18206_276	P29144_1216	P49257_87
P18206_352	P46777_242	Q01082_1354
P18206_366	P55884_209	Q01082_2269
P18206_464	P55884_529	P18621_55
Q15181_199	P49207_36	P18621_96
Q15181_233	Q92930_58	Q9UDR5_584
Q15181_253	Q96I99_338	Q2TU64_78
P15170_72	Q1KMD3_626	Q2TU64_381
P15170_138	P63173_67	P42704_224
P15170_254	P40429_114	Q12931_382
O43175_21	Q96F07_1234	Q99613_643
O43175_351	Q9P2R7_205	P37268_318
P09211_209	H0Y2W2_200	P21912_126
P22234_30	H0Y2W2_481	P21912_261
P22234_36	H0Y2W2_554	P06239_130
Q9Y617_127	Q15067_260	P30050_130
P84077_142	Q9Y2W1_711	P30084_128
P24534_64	O75746_406	Q9NSE4_500
P24534_129	Q9H9P8_104	Q15029_244
P30520_157	Q9UJZ1_233	Q9BXJ9_848
P30520_164	P12235_23	P50995_255
P30520_173	P56381_37	P50995_282
P30520_403	P48556_324	Q12905_186
P30520_419	Q92522_146	O95202_284
P06737_29	D3DTY9_112	P30519_199
P06737_295	P30405_67	P41091_275
P06737_804	O95453_335	O15382_156
P06737_819	Q96IX5_16	O43143_760
P30041_56	Q96AG4_73	P40429_114
P30041_63	Q96AG4_138	P25789_210

P30041_97	Q9Y3U8_62	P09972_13
P09960_127	P22695_21	B2R5W2_39
Q92945_473	P22695_42	B2R5W2_42
P09936_4	Q01844_644	B2R5W2_144
P09936_65	Q96CS3_167	P22695_42
P09936_71	P62834_128	P52597_224
P09936_123	Q86SR1_379	Q96AG4_73
P09936_221	P46776_94	Q96AG4_108
Q99832_172	P49406_129	P61026_59
P08758_97	Q9NYU2_596	Q06323_13
P08758_101	Q96CW1_400	P30040_99
P08758_290	Q96PK6_135	Q8N183_58
P08758_301	P28331_467	O43242_76
P23526_43	P31937_297	P16615_502
P46821_1176	P62857_10	O15371_53
P68371_379	P23368_26	P55884_529
P27694_588	Q13243_60	H0Y2W2_554
P50502_160	P22830_118	Q99460_429
P50502_353	Q53HG1_102	P10515_376
P50502_360	Q9NVP1_645	P10515_396
Q9Y266_123	Q9H1K4_82	Q96C36_307
Q9Y266_160	Q8TDX7_281	Q53HG1_102
Q9Y266_297	P62316_118	Q53HG1_146
Q9Y266_315	Q96CT7_40	P33991_549
P22102_598	Q99460_146	P29144_1216
P31939_389	P30044_86	Q8TCC3_152
P05455_105	P30044_142	P62861_51
P05455_229	P16615_400	O95470_155
P05455_276	P09496_242	P07384_84
P05455_280	P27708_964	P07384_86
P05455_344	Q00059_95	Q9UJZ1_233
P05455_352	P53999_101	P07766_158
P61221_64	Q8NBU5_165	O14979_302
P61221_121	P62829_113	Q9H0X9_402
O43719_56	C9JVQ0_10	P20674_72
P49321_626	P60228_82	Q8NBS9_140
P49321_643	Q9UFN0_166	P35606_336
O75131_149	Q9P2K5_85	P50395_253
O75131_167	P22033_621	Q96I99_338
O75131_208	Q9NTJ5_456	Q9HAV7_186
Q09028_102	Q496E4_233	P61224_128
Q04760_44	P84103_23	D3DTY9_112
Q04760_140	Q9NZ01_12	P46776_94
P50991_213	Q9UQ35_169	P12235_23
P50991_288	Q8IYB3_54	P32322_215
P50991_319	O14656_76	Q8N5C6_852
P17812_557	Q99536_372	P22830_118
P49773_30	P09110_198	P62308_10

P49773_82	Q9H0D6_641	O95347_523
P49368_138	P35573_1303	P54819_147
P55209_271	Q14964_63	Q96CS3_167
A6NHG4_21	Q9H082_83	P62820_140
A6NHG4_33	Q9NUI1_230	Q07021_104
P04080_39	P51572_204	Q96CT7_40
P04080_44	Q9H300_75	P38159_150
P04080_78	Q8N5K1_81	Q9NZ01_12
Q9Y265_372	Q8WU39_111	Q8IZP2_114
P10599_39	P61769_111	Q9P035_72
O00410_437	P00846_51	P23368_26
O00410_705	Q9HAN9_56	Q06787_425
A0A024R321_373	P08574_315	E5KS55_205
Q9NTK5_248	P08574_325	P23743_671
Q9NTK5_253	O60884_226	Q15269_801
Q9NTK5_294	Q9BSH5_15	Q8N5K1_81
Q9NTK5_326	P08708_72	P49748_556
Q8TCG1_647	Q99623_89	Q96A33_374
Q8TCG1_783	P14678_50	O14656_76
O14980_686	Q5JTV8_556	P62304_12
Q99497_182	Q6DD88_375	P49189_366
O76003_92	O14950_151	P35573_1303
O76003_253	Q9H0A0_823	P05023_487
Q14204_748	P78406_154	A0A024RAP0_197
Q14204_754	Q15555_165	O95071_28
Q14204_4204	Q9HBD4_835	Q8IYB3_54
Q14103_197	O95831_593	P36551_404
P52565_127	P47985_168	P08559_385
P52565_167	Q15052_722	O75323_53
P06493_20	P52815_142	Q6FI58_135
P13693_19	Q13435_570	P08574_315
P13693_93	O00182_88	O95865_51
P13693_112	Q14161_135	Q56VL3_41
P41250_501	P49841_292	O43707_108
Q14C86_233	O75323_53	Q5TCQ9_439
O15067_25	Q15031_79	Q9Y2R5_41
P30086_47	Q9H4G4_53	Q5K651_1495
P30086_80	Q03001_1114	E9PI68_81
Q96FW1_59	O60814_121	Q9NYZ3_294
E7EVH7_481	Q93079_6	P08183_290
E7EVH7_556	P12814_89	P60709_336
Q9Y696_130	Q6IPU0_241	P08238_538
Q9Y696_194	Q9Y520_1160	P00338_228
P31153_234	Q6UXB8_80	P13796_76
Q9UHD1_38	P36551_404	P13796_82
Q9UHD1_101	Q8WXX5_107	P13796_88
A0A0S2Z4I4_100	Q01130_36	P13796_92
A0A0S2Z4I4_215	Q8WYP5_2050	P13796_97

P21333_2417	Q9UBF2_313	P13796_297
P15311_254	P98171_460	P13796_444
P15311_344	Q9Y512_248	P13796_468
Q8WUM4_339	Q56VL3_41	P13796_472
Q8WUM4_486	O43488_242	P13796_542
Q8WUM4_501	Q96C36_47	P14618_261
Q8WUM4_627	Q9UKM9_146	P00558_48
P55060_848	O75489_260	P00558_56
Q9Y3F4_104	Q14103_111	P00558_106
Q9Y3F4_122	Q5K651_1495	P00558_146
Q9Y3F4_246	P05408_166	P00558_192
P31689_221	Q9BQE5_54	P00558_361
P12004_77	Q6ZQQ6_2341	P35579_403
P12004_168	Q13011_327	P35579_1024
Q9UNS2_254	Q9UPV0_936	Q06830_168
P35580_865	P60709_336	P09429_43
O75347_21	P14618_89	P09429_65
O75347_36	P13796_76	P09429_82
P61981_88	P13796_82	P09429_90
Q15185_7	P13796_92	P09429_127
Q15185_91	P13796_97	O75083_90
P11766_120	P13796_297	O75083_95
P11766_357	P13796_444	O75083_569
P39687_86	P13796_449	P09211_116
P46109_265	P13796_456	P62826_38
Q14974_859	P13796_468	P50990_466
Q14974_867	P13796_472	P63104_75
O43143_143	P13796_542	P52566_25
P61956_11	P04075_312	P52566_33
P61956_33	P04075_318	P52566_63
P61956_45	P00558_15	P52566_196
O75436_116	P00558_56	P31146_20
Q01469_40	P00558_192	P31146_207
Q16543_273	P00558_353	P31146_449
Q16543_276	P35579_403	P26641_227
P08243_379	P35579_909	Q01518_63
O75832_30	P35579_1024	P53396_978
Q13765_142	P35579_1212	O43143_132
P37802_153	P35579_1249	P22234_110
Q00341_494	P35579_1775	P31939_66
O00151_192	P35579_1793	P31948_207
Q9NRX4_48	P35579_1806	P31948_337
Q99615_32	P35579_1918	P31948_366
P55072_754	O75083_95	P00813_170
P35606_199	O75083_182	P00813_232
O95757_185	O75083_569	P41250_646
Q9BTT0_101	P09429_90	P78417_11
P37837_269	P09211_116	P78417_220

Q53GN4_256	P26038_262	P49588_766
P63167_9	P26038_306	P11586_245
Q9NTJ3_607	P26038_313	P61158_317
P49588_366	P53396_978	Q9BWD1_180
Q9H773_140	Q01518_63	Q14141_379
P11021_447	Q01518_298	P21333_1538
Q9Y6Y8_931	P52566_25	P34932_719
P0DN79_269	P52566_33	P50570_629
P23381_27	P52566_63	P26583_173
P23381_47	P52566_96	O00154_286
O14737_66	P52566_197	P12814_682
Q9H8S9_210	P31146_20	P61981_120
Q9UHV9_18	P31146_207	P25205_194
Q14320_305	P31146_449	Q13263_469
Q15691_148	Q01082_2269	Q9Y490_875
O00193_75	P22234_304	Q99426_188
Q9UHB9_277	P00813_170	P27707_88
Q9H3K6_47	P41250_82	O75533_866
Q9Y237_75	P41250_646	P15170_103
Q5TBB1_259	Q01813_736	Q8N163_791
O43765_137	O14818_115	P49368_78
P46940_939	P10768_64	P49368_248
Q13526_82	P34932_674	A8K8F0_290
Q6FI81_48	P46940_368	P52907_278
Q6FI81_297	O75369_2342	Q709C8_2356
O43592_634	B1AK87_83	Q16181_326
Q7L1Q6_223	P78417_11	Q16181_349
P13984_154	P78417_143	Q969G3_123
P52701_1013	Q14141_353	Q9Y450_657
Q9P289_233	Q14141_379	Q9BUT1_48
P26640_243	P60900_102	Q01469_34
Q32MZ4_593	P48643_226	B4DQ80_50
Q13085_2127	A0A0D9SF54_39	B4DQ80_162
Q9UKK9_210	A0A0D9SF54_602	Q15459_419
Q9UKK9_218	A0A0D9SF54_1314	Q00013_299
O14744_227	A0A0D9SF54_1635	Q9H2P0_118
P26639_319	P68032_86	O75663_106
P40763_177	P26583_3	P51532_835
P53990_38	P26583_172	Q14019_98
O75937_127	O00154_286	P32321_78
O75937_168	Q06323_13	P39687_99
Q15003_424	Q06323_190	Q9UHY7_106
Q9BZZ5_51	O75533_1086	F6RFD5_19
Q9BZZ5_84	P12814_157	P50851_251
P53611_34	P12814_682	O14929_364
Q13404_87	P49736_216	P41567_56
Q16658_43	Q9UL46_180	P14550_127
P47813_56	O95433_189	Q14258_320

P47813_94	P26639_279	P49593_334
Q5VW32_141	P27707_88	P09651_87
P35244_33	P24534_139	P09651_350
Q9NYL9_13	Q9Y490_875	Q96H79_185
Q96C23_101	Q99426_188	Q14847_17
O95163_1042	P50570_629	Q96ST2_666
P51580_32	Q13907_180	O15355_367
Q13616_759	Q8NCW5_144	P63208_130
Q69YN2_505	Q8NCW5_148	Q9Y2Z0_41
Q8NFC6_81	P31946_77	Q6ZUM4_426
O15541_126	P51784_766	Q16775_229
Q96AC1_55	Q8N163_791	Q14790_250
P35611_406	O60234_35	O14497_1230
P16152_148	O60234_119	Q86VS8_324
O94776_341	P67936_13	Q8TAQ2_326
P61970_55	P67936_76	Q13362_418
P53621_1028	P67936_113	O75351_363
P51151_112	P67936_116	O60563_33
P22061_206	P67936_212	P67936_212
P22061_219	A0A024R5M9_1610	Q02878_29
P16949_53	Q16181_349	Q9BZH6_223
Q8TB03_84	Q16181_368	P04406_254
Q9NVE7_590	Q7L5N1_102	V9HWJ7_76
S4R435_252	Q12874_92	V9HWJ7_82
Q7Z4S6_1058	Q709C8_2356	V9HWJ7_88
P20073_199	P52907_278	V9HWJ7_92
Q9UNH7_291	Q07866_314	V9HWJ7_294
P61077_8	P53621_607	V9HWJ7_328
Q96PU8_91	P55160_326	V9HWJ7_444
P47756_95	Q9H9T3_414	V9HWJ7_449
Q9NXG2_56	A8K8F0_290	V9HWJ7_456
P25325_164	P05455_185	V9HWJ7_468
Q15785_100	Q01469_34	V9HWJ7_472
P60983_119	Q15428_57	V9HWJ7_542
P12081_22	O94903_47	V9HWJ7_579
P19623_135	Q92888_214	P07900_58
A0A024RA19_251	Q14019_98	P07900_534
Q9H1E3_9	O60306_1045	P04075_108
Q9UPN3_6160	P32321_131	P35579_1802
P06454_21	P06400_791	P68104_244
Q8N8S7_22	O95865_51	P06744_523
P49840_355	Q8N1F7_387	O75083_223
Q13573_456	P25788_174	P62826_99
O95456_65	B7Z738_456	P09429_12
Q16531_897	P50851_251	P52566_40
O00160_194	V5YQL4_1126	P52566_47
P61758_114	Q00839_814	P52566_96
P49643_65	Q07666_214	Q01518_81

Q7Z6K5_101	O75663_106	Q01518_298
Q6P4I2_55	Q9NZZ3_51	Q01518_304
Q9Y2T4_91	Q14847_17	P23528_78
O75794_168	Q5VU61_187	P00813_164
Q9Y2A7_16	Q5VU61_203	P00813_331
O15144_295	Q01844_404	P41250_219
Q4VCS5_596	Q86U86_553	P31948_364
O00244_25	Q00535_237	V9HW33_185
Q92925_312	Q6ZUM4_426	V9HW33_332
P61024_11	Q15813_451	V9HW33_430
Q9UJX3_435	O95260_64	V9HW33_674
P62837_8	Q92785_207	V9HW33_719
Q709C8_2092	Q96ST2_666	Q9BWD1_136
P15924_2317	P14921_138	A0A0D9SF54_2063
Q6ZSG2_124	Q9Y2Z0_41	P25789_64
Q13126_241	O14776_820	P61978_168
Q9NXR1_263	Q6S8J3_1036	Q14141_327
Q2VJ45_324	P13984_236	Q14141_351
Q13206_768	O14497_1230	Q14141_353
Q9NQ75_589	Q86V21_633	Q92688_99
P06733_422	Q13094_38	Q06323_190
P13639_322	Q3LXA3_487	P62942_35
P13639_330	P50552_21	P62942_53
P13639_438	O60563_33	Q9UI08_22
P13639_572	Q9UN37_356	P67936_13
P0DMV8_100	P48426_140	P67936_76
P0DMV8_415	Q13362_418	P67936_116
P04406_5	P26640_903	P60520_24
P04406_66	P07951_149	P31150_253
P04406_86	P14618_136	O60234_35
P07900_314	P14618_256	A0A024R5M9_1610
P07900_419	P00558_382	V5YQL4_1126
P19338_62	V9HWJ7_76	Q8WXH0_3093
P19338_70	V9HWJ7_82	Q9NY27_84
P19338_297	V9HWJ7_88	P55735_143
P19338_437	V9HWJ7_92	O95260_64
P19338_589	V9HWJ7_294	Q15813_451
P19338_708	V9HWJ7_444	O75396_38
P49327_1993	V9HWJ7_449	Q2TAY7_509
P26641_208	V9HWJ7_456	P62333_27
P62826_141	V9HWJ7_468	Q7KZ85_381
P23528_95	V9HWJ7_472	O60664_262
P22314_68	V9HWJ7_542	P06400_427
P22314_604	V9HWJ7_579	P06400_791
P22314_884	P09429_7	P50552_21
P62258_78	P09429_50	Q15257_331
P29401_310	P63104_74	P23743_260
P29401_497	P52566_40	Q9UN37_356

P00918_80	P52566_47	Q9UHX1_267
Q02790_250	D3DPU2_63	Q13094_38
P61978_411	P00813_164	Q8N1F7_387
P34932_353	P00813_225	P49454_2972
P34932_477	O43143_132	Q7RTS9_312
Q59HH3_192	P31948_388	Q9NQ75_589
Q59HH3_285	P48643_232	O95747_42
Q59HH3_488	P26583_43	
Q59HH3_888	P27348_85	
Q13263_275	O60610_786	
Q13263_337	P49368_78	
Q9HB71_212	Q96G03_565	
Q92598_316	P62942_35	
O43175_58	Q14980_715	
O43175_384	Q14980_1624	
P54577_231	P40121_137	
P54577_412	P40121_341	
Q15365_23	O14744_343	
Q15365_31	P52907_268	
P55786_293	Q15027_302	
Q9Y617_333	P06400_427	
P32119_34	P49589_49	
P22234_80	P14550_127	
P23526_46	D4YW74_2318	
Q04760_151	P41567_56	
P0CG47_48	Q96SN8_865	
P0CG47_87	P23743_260	
P0CG47_200	O75351_363	
P0CG47_215	Q99996_2015	
P09936_15	Q7RTS9_312	
P09936_78	P14618_224	
P10599_8	P14618_504	
P10599_96	P00558_297	
O15347_161	P00558_388	
O15318_61	V9HWJ7_97	
P24534_66	V9HWJ7_132	
P41250_204	V9HWJ7_297	
P49321_637	V9HWJ7_328	
Q9BRA2_78	P35579_79	
Q9BRA2_89	P35579_299	
O75369_373	P35579_637	
P21333_771	P35579_682	
O15067_279	P35579_860	
P55209_87	P35579_938	
Q9Y490_1544	P35579_1404	
P27694_489	P35579_1716	
P15311_64	P35579_1754	
P68036_82	P09429_146	

P68036_145	P62826_37	
P13693_100	P11142_451	
P30086_132	O75083_362	
O95433_212	P26038_35	
O95433_328	P52566_102	
P50502_5	P52566_110	
P30520_163	P18669_138	
P37837_277	P31948_32	
P61088_24	P31146_439	
A0A0S2Z4I4_13	Q01082_1312	
Q96AE4_400	Q01082_1878	
P61956_42	Q01082_1991	
Q9H4A4_162	Q01082_2054	
Q07866_384	D3DPU2_71	
O14737_63	D3DPU2_81	
O75832_221	D3DPU2_287	
Q8WUM4_11	D3DPU2_298	
O95757_788	D3DPU2_304	
O43143_17	P00813_232	
P37802_171	P00813_323	
D6RBW1_220	P00813_331	
Q15691_174	O00299_131	
Q9UBT2_86	O00299_192	
O75937_105	P31939_66	
Q06203_372	P40227_199	
Q9BRX5_207	P40227_430	
P52907_226	P22234_286	
O95347_187	P26583_65	
O60841_1195	P26583_90	
P16949_100	P26583_139	
P62633_85	P41250_99	
P19623_96	P10768_10	
P53004_147	P14324_413	
O60271_655	P50395_221	
Q14185_1469	O75369_681	
Q9NRN7_74	O75369_1979	
Q9BZD4_275	A0A0D9SF54_613	
Q9H074_337	A0A0D9SF54_1573	
Q92905_194	A0A0D9SF54_2063	
P46063_70	Q9BWD1_136	
P63279_74	P52209_375	
Q9UBU8_240	Q92688_110	
P52888_220	B1AK87_211	
Q99471_47	B1AK87_223	
O95817_460	B1AK87_240	
P55160_14	Q14141_327	
P57076_7	Q14141_351	
P21675_1591	Q14141_400	

Q8WXH0_6754	P54578_49	
Q8NE71_545	P54578_214	
Q02878_29	P49368_21	
Q12849_337	P49368_222	
Q7Z4S6_963	P21333_1071	
Q2M2Z5_39	P21333_1294	
O43502_328	P27348_11	
Q6ZU80_659	Q9Y490_1933	
Q96DT5_3875	O60610_771	
Q14765_88	Q06323_35	
P08238_273	P25789_239	
P68104_64	P09972_42	
P13639_638	P13010_603	
P11142_597	P33992_196	
P19338_610	Q9Y266_268	
P14618_230	P39748_80	
P29401_314	Q9UI08_21	
P32119_67	Q9UI08_22	
A0A024R895_62	Q9UI08_70	
P22102_249	Q01105_167	
P22102_852	P52907_97	
P54577_346	P52907_103	
P31939_357	P67936_100	
P0CG47_11	Q13303_274	
P0CG47_63	P25787_53	
P0CG47_124	Q96AE4_591	
P0CG47_163	Q8N163_839	
P27694_167	P17252_197	
P05455_204	P17252_209	
P05455_208	B3KTT6_85	
P05455_354	Q16181_239	
P05455_397	Q16181_326	
P09936_131	Q16181_333	
P09936_157	B7Z217_1013	
Q9Y266_96	Q5TBB1_145	
Q9NTK5_394	P40121_300	
Q92945_448	Q9UBT2_447	
P15170_238	P63279_18	
P43487_76	P63279_76	
P40227_251	Q99879_109	
Q9UHD1_190	Q99879_117	
Q14103_178	Q99879_121	
Q14103_243	P39687_110	
Q14103_255	O94776_492	
Q09028_215	O75396_38	
Q96AE4_233	B4DW52_56	
Q15181_228	Q13177_136	
Q15181_282	Q13177_246	

B4DPD5_96	Q9UQE7_143	
P31689_24	F6WQW2_227	
P31689_32	F6WQW2_256	
P62942_48	Q9HC35_228	
P68036_64	Q16775_229	
P37837_307	Q14019_93	
E7EVH7_486	Q8WXF1_257	
Q9UBT2_409	A0A0S2Z4I7_21	
P37802_79	Q9Y2X7_135	
O00267_143	A8MWD9_10	
O00267_199	P13929_60	
P61088_10	H3BVE0_79	
Q9Y2L1_627	Q5THR3_563	
Q9Y2L1_654	Q14790_250	
B4DQ80_34	Q9BZH6_223	
B4DQ80_146	Q02224_1444	
B4DQ80_149	P35579_186	
B4DQ80_162	P35579_560	
B4DEA6_137	P35579_1081	
O95347_320	P35579_1193	
P62316_71	P35579_1234	
P51858_19	P06744_423	
Q13451_155	P09429_112	
Q6P1N4_368	P26038_263	
P16949_43	P26038_448	
P16949_80	O75083_7	
P08243_385	O75083_480	
Q9UHV9_136	P31948_162	
Q9BXJ9_312	P31948_429	
P35080_116	P31948_523	
Q15056_120	O43143_384	
Q562M3_30	B1AK87_66	
Q53GN4_104	O75369_142	
Q53GN4_182	O75369_838	
Q96A72_16	P46940_1445	
Q9H3P7_117	O60610_377	
P14314_438	P52209_51	
Q8N6H7_359	P27348_139	
P61077_128	P49915_182	
Q7L1Q6_255	P25787_70	
P62993_76	A0A0S2Z4I4_116	
P48637_172	Q9UHD8_262	
Q13257_200	P61163_200	
H0YC42_137	A8KAP3_244	
Q8WUA2_82	Q16543_110	
A0A0F7NGI8_537	Q14019_110	
P09884_829	P35241_3	
Q96DG6_227	Q9UHX1_201	

Q12965_196	Q9P016_60	
Q9GZM8_262	P25685_242	
Q05209_65	Q9C0C9_132	
P60981_19	O75044_245	
Q8WWS9_693	P29350_257	
Q9Y6K9_309	O75935_59	
P78316_334	Q08AE8_288	
P10809_369		
P11142_325		
P11142_531		
P38646_314		
P38646_345		
P38646_675		
P38646_671		
P68104_443		
P14625_137		
P14625_168		
P14625_467		
P14625_683		
P40926_105		
P40926_335		
P05141_199		
P19338_286		
P19338_384		
P48735_127		
P48735_360		
P09429_68		
B4DLR3_502		
B4DLR3_568		
B4DLR3_573		
B4DLR3_629		
B4DLR3_653		
P12268_436		
P06576_264		
P62807_86		
P10412_81		
P10412_122		
P10412_153		
P10412_180		
P10412_190		
P10412_195		
P10412_200		
P10412_210		
P27824_99		
P27824_199		
P27824_210		
P22626_151		
Q02878_20		

Q02878_66		
Q02878_79		
P06748_193		
P06748_206		
P06748_233		
P26583_44		
P26583_55		
P26583_150		
P26583_154		
P26583_157		
P13010_195		
P13010_702		
P61604_56		
Q12906_214		
Q12906_389		
Q12906_742		
P61978_166		
P62424_21		
P62424_121		
P62424_150		
P62847_84		
P62847_88		
P78527_700		
P78527_2366		
P78527_3550		
P26038_162		
P11940_167		
B2RB06_212		
B2RB06_295		
B2RB06_301		
P30048_217		
P60866_30		
P60866_44		
P60866_46		
P48047_60		
P62906_56		
Q8NC51_102		
Q8NC51_140		
P0C0S8_6		
P0C0S8_37		
P0C0S8_96		
P0C0S8_120		
P0C0S8_126		
P62277_34		
P62277_100		
P62277_130		
P12956_249		
P12956_317		

P12956_338		
P12956_468		
P62081_86		
P11021_122		
P11021_125		
P11021_340		
P11021_370		
P09622_146		
P09622_155		
P09622_159		
P09622_166		
P61247_46		
P61247_219		
P27635_141		
P35579_821		
Q13423_70		
Q14152_68		
Q14152_632		
P21796_252		
Q9P0L0_161		
Q9P0L0_180		
O75390_352		
P30042_233		
P42766_43		
P42766_74		
P36578_411		
P36578_423		
P45880_120		
P51991_118		
O43390_584		
P07954_122		
P07954_263		
P07954_473		
P67809_81		
P67809_93		
Q02218_561		
Q16891_211		
Q16891_314		
Q16891_344		
Q13838_156		
Q13838_163		
Q13838_188		
P62851_10		
P62851_18		
P62851_37		
Q99714_105		
O75521_51		
O75521_62		

O75521_335		
P09874_653		
Q9Y277_115		
P41252_382		
P51659_184		
P51659_415		
Q4G176_563		
Q7KZF4_497		
Q7KZF4_513		
P31040_608		
P46783_31		
P31689_59		
P31689_66		
P84243_80		
P36542_43		
P36542_46		
P36542_49		
P36542_64		
Q9NX63_45		
P61254_41		
P61254_134		
P50914_128		
P50914_141		
P50914_142		
P47914_84		
P16401_149		
P16401_178		
P16401_192		
P16401_194		
P55084_253		
P40939_129		
P40939_411		
P40939_631		
P31943_173		
Q99729_70		
P07910_29		
P07910_42		
P04843_517		
P04843_579		
B4DRW8_456		
P61513_28		
P83731_113		
P83731_139		
P43243_478		
P48643_282		
P62829_123		
P15880_71		
P40227_261		

P40227_377		
Q96HS1_144		
P04083_245		
P08575_448		
O95202_150		
Q8WWV3_102		
P38919_60		
P38919_152		
Q99798_520		
Q92841_269		
P55809_271		
Q92900_318		
Q92608_145		
P39019_122		
Q9NQC3_1174		
Q9Y3U8_16		
Q86V81_134		
Q86V81_161		
P11310_279		
P62750_23		
Q12931_432		
Q9Y4W6_508		
P16403_191		
P16403_207		
P16403_211		
A0A087X2I1_220		
Q9H936_80		
Q9H936_83		
Q96FJ2_5		
Q8WU39_70		
P51572_149		
P63173_52		
Q2TU64_21		
P55072_663		
P16615_120		
P16615_510		
P35232_202		
P25685_37		
Q15046_88		
Q92499_702		
P55265_591		
P13995_50		
O75431_95		
P42704_760		
P37108_32		
P37108_38		
A8K228_45		
Q7Z7H5_172		

Q7L014_793		
P35268_16		
P17987_538		
P16402_111		
P16402_169		
P16402_209		
O15382_111		
Q99613_332		
P22830_133		
P60953_131		
Q93084_120		
P13667_528		
Q15269_127		
Q15084_150		
Q86U86_1025		
Q92621_66		
P46940_1558		
Q9NYU2_1208		
P49748_276		
Q14151_437		
Q99832_231		
Q96RE9_435		
P53597_308		
O60884_39		
P30050_41		
P30405_183		
P56378_49		
P11387_148		
P18621_46		
P30038_487		
O14949_82		
P49406_205		
Q9BX67_287		
Q9BX67_283		
Q9Y487_240		
O95573_58		
O95573_706		
O60762_136		
P56381_44		
Q6UB98_868		
Q6UB98_1105		
H0Y2W2_80		
Q00059_186		
P30101_332		
Q6UB99_1345		
Q6UB99_1531		
Q6UB99_1621		
B4DVV3_332		

Q9UJS0_408		
P62861_18		
P22102_350		
O75964_54		
Q9Y2R9_63		
Q14571_1662		
Q96EY7_517		
Q9H845_456		
C9JVQ0_16		
P30049_165		
O75190_60		
P49711_405		
Q96DI7_275		
Q8NI27_158		
O14874_233		
Q9UJZ1_222		
P17252_35		
Q9HC38_305		
P08754_67		
O15320_500		
Q00839_215		
Q96PK6_167		
Q9UIF9_748		
Q8NBS9_407		
Q9UNL2_103		
Q9C0D2_389		
Q8TDB6_593		
Q14651_94		
Q8NB50_475		
B4DZB4_636		
Q02880_1327		
P84090_41		
P04844_311		
Q9Y655_32		
Q86XL3_447		
O60488_49		
Q9Y6N5_260		
O60508_380		
H3BUE4_21		
Q09161_342		
P05114_42		
Q52LJ0_256		
Q9Y3A2_114		
Q4LE39_647		
O43283_498		
Q9H3S7_600		
Q96LB3_197		
Q9BXT5_1381		

A0A024R856_2276		
Q7Z333_1290		
Q9UIG0_576		
Q2KHM9_377		
E5RHP9_40		
P38646_612		
Q5VTE0_41		
Q5VTE0_44		
Q5VTE0_179		
Q5VTE0_215		
Q5VTE0_255		
Q5VTE0_273		
Q5VTE0_392		
Q5VTE0_408		
Q5VTE0_439		
Q5VTE0_444		
Q5VTE0_450		
Q5VTE0_453		
Q5VTE0_457		
P08133_9		
P25705_132		
P25705_539		
P62807_13		
P13010_334		
B3KTT6_72		
B3KTT6_189		
B3KTT6_196		
B3KTT6_210		
B3KTT6_299		
B3KTT6_305		
P78527_3603		
P78527_4019		
P27797_207		
P27797_209		
Q13813_1334		
Q13813_1650		
P09622_277		
D3DQ69_203		
D3DQ69_341		
D3DQ69_362		
D3DQ69_363		
Q93077_6		
Q93077_37		
Q93077_120		
Q93077_126		
Q14152_278		
P35579_992		
O43390_120		

P62081_147		
P26373_210		
Q969Q0_27		
P35637_312		
P00505_73		
P00505_94		
P55084_44		
Q02543_136		
O75521_177		
P47914_87		
P47914_134		
P09874_87		
Q99729_330		
Q16891_122		
Q16891_306		
P62241_37		
O43837_199		
P36578_348		
P36578_390		
P50914_79		
P50914_177		
P13073_65		
P46777_220		
P16401_27		
P16401_161		
P16401_172		
P16401_217		
Q01082_1981		
P30101_226		
P84098_196		
P61513_87		
Q9Y262_558		
P24539_233		
A0A0S2Z5H3_471		
Q08257_116		
P62750_18		
P62263_106		
P49207_62		
Q9Y4W6_785		
Q9NY12_140		
P78406_131		
Q9NX63_86		
Q9H1K4_79		
P14314_83		
P08621_138		
P07910_94		
Q99832_77		
P62841_72		

O15372_221		
Q00688_96		
P50995_495		
Q86U86_225		
P14735_896		
Q4GUF2_45		
Q4GUF2_49		
Q7L2H7_177		
P61026_136		
Q6NZ52_92		
P11387_669		
P24752_266		
P26196_482		
O60841_393		
P28062_133		
Q8IYB8_404		
B4DEB0_290		
Q8N0V3_70		
P18077_66		
Q13505_190		
Q96RE9_491		
O14832_120		
O76021_116		
Q13442_132		
P47813_104		
Q9NVP1_542		
Q8WXF1_380		
O14617_189		
P55209_197		
Q6UB35_880		
P22307_453		
Q15031_81		
P01130_830		
Q8WZ42_3065		
Q8WZ42_29371		
Q13129_618		
O75489_259		
Q6ZN06_297		
Q8N532_316		
Q10713_478		
Q8WXH0_4586		
P26440_146		
Q15024_178		
P27701_263		
Q3L8U1_2507		
P36957_145		
A0A0A6YYL4_103		
Q86WX3_110		

A0A0S2Z377_81		
A0A0S2Z377_265		
A0A0S2Z377_314		
A0A0S2Z377_354		
A0A0S2Z377_370		
A0A0S2Z377_406		
A0A0S2Z377_442		
A0A0S2Z377_478		
A0A0S2Z377_607		
P14625_532		
B4DLR3_561		
P13010_566		
Q02878_247		
P05141_96		
P23396_148		
P39023_66		
P61247_56		
P36578_405		
Q9UQ80_158		
P78527_2746		
Q5VU21_102		
Q5VU21_140		
Q5VU21_278		
Q5VU21_299		
P23246_208		
P62753_30		
P07237_326		
P35637_448		
P00505_234		
P42766_77		
P39019_111		
Q7KZF4_541		
P62917_149		
Q01082_1824		
D6RBZ0_150		
D6RBZ0_210		
P41252_1042		
Q9NX63_37		
Q92522_143		
P62249_26		
Q96A26_150		
P61353_93		
P61513_7		
E9M4D4_17		
P24752_223		
P84095_130		
P63220_74		
Q5T3I4_144		

Q9UNX3_136		
Q15555_156		
P38117_53		
P06730_184		
P46977_340		
Q8N254_280		
Q96SI9_75		
P13804_226		
P08686_232		
P20338_173		
O94913_354		
P78344_187		
P13612_189		
Q8N3U4_53		
Q96QR8_251		
Q8NFC6_365		
A0A0S2Z377_9		
A0A0S2Z377_102		
P14625_628		
P38646_654		
B4DLR3_503		
B4DLR3_647		
Q00610_189		
Q02878_12		
Q02878_15		
B4DUQ1_52		
B4DUQ1_60		
B4DUQ1_381		
P27797_276		
P12956_262		
P10412_129		
P10412_130		
P08575_967		
P36542_36		
Q99798_689		
P46782_44		
P16401_184		
P47914_63		
P47914_103		
P47914_130		
D6RBZ0_154		
D6RBZ0_325		
P62750_30		
P62750_114		
P61353_126		
B3KS98_283		
B3KS98_288		
Q12931_629		

P35268_6		
Q99623_216		
P46776_92		
Q9Y3U8_35		
P62316_88		
Q9Y4L1_883		
Q9UII2_71		
Q9UII2_96		
P63218_36		
Q96C36_291		
P18077_15		
P11387_174		
Q3KP31_298		
Q96BR6_416		
Q13033_755		
Q9UIF9_660		
Q9UIF9_758		
O75477_205		
P10515_363		
Q9UK58_307		
Q14694_780		
B4DLN1_183		
P53804_1571		
Q9HCL3_254		
P07437_103		
P14625_623		
P48735_243		
P48735_256		
P40926_328		
P13010_545		
Q00610_1443		
Q93079_12		
Q93079_17		
Q93079_21		
Q93079_47		
Q93079_109		
Q93079_117		
Q93079_121		
P23396_214		
P48643_496		
P00505_227		
Q08211_220		
P12268_422		
P62906_152		
A0A024RBE8_208		
A0A024RBE8_213		
A0A024RBE8_246		
A0A024RBE8_303		

P05388_246		
O75390_215		
O75390_321		
P21796_266		
P11021_113		
P11021_213		
P62979_113		
P78527_357		
P78527_3264		
P40939_334		
Q96KK5_6		
Q99798_739		
P26373_136		
P08575_759		
P09874_940		
P61247_20		
Q04837_51		
Q9Y262_437		
P25205_656		
P07954_502		
P12236_105		
P35268_10		
Q9NUJ1_70		
P84098_144		
P83731_131		
P62249_4		
P62249_105		
Q9UQ80_144		
Q9P2J5_350		
P11310_301		
P16401_204		
P25398_84		
P04083_214		
P68431_19		
P68431_123		
Q9Y285_315		
Q9Y285_342		
P62753_218		
Q92608_1435		
P47914_77		
Q2TU64_381		
P42704_224		
P37268_318		
Q9BXJ9_848		
B2R5W2_39		
B2R5W2_42		
B2R5W2_144		
Q96AG4_108		

P61026_59		
P16615_502		
Q99460_429		
P10515_376		
P10515_396		
Q96C36_307		
Q53HG1_146		
Q8TCC3_152		
P07384_84		
P07384_86		
P07766_158		
Q9H0X9_402		
P61224_128		
P62308_10		
O95347_523		
P54819_147		
P62820_140		
Q9BSJ2_87		
Q8IZP2_114		
Q9P035_72		
Q06787_425		
P23743_671		
Q15269_801		
P49748_556		
Q96A33_374		
P05023_487		
A0A024RAP0_197		
Q6FI58_135		
Q5TCQ9_439		
Q9Y2R5_41		
E9PI68_81		
Q9NYZ3_294		
P08183_290		
P62258_125		
P31948_366		
P15121_22		
P61981_120		
P33992_396		
Q9Y490_1314		
O75533_866		
B4DQ80_50		
Q9H2P0_118		
F6RFD5_19		
P30520_203		
P09651_87		
Q8TAQ2_326		
P07900_58		
P07900_560		

Q01518_81		
Q01518_304		
V9HW33_185		
V9HW33_332		
V9HW33_430		
V9HW33_674		
V9HW33_719		
P61978_168		
Q8WXH0_3093		
P55735_143		
Q2TAY7_509		
P62333_27		
O60664_262		
Q15257_331		
P49454_2972		
O95747_42		
P63261_61		
P63261_113		
P63261_326		
P06576_432		
O00571_581		
Q92945_291		
Q92945_646		
Q07955_38		
P31930_134		
Q99459_466		
Q96M27_253		
O75431_206		
P78527_963		
Q6FHZ0_165		
P48047_84		
P84090_84		
P00338_90		
P00338_149		
P12277_265		
P31948_462		
Q6IBN1_219		
P09429_147		
P00918_256		
P13797_126		
P11940_512		
Q01105_132		
Q01105_150		
Q01105_172		
F5GWF6_46		
P27348_158		
Q9Y490_1947		
Q99832_366		

Q14247_144		
O14980_693		
O43719_26		
P48643_275		
O95373_429		
P38606_580		
P07814_693		
Q14166_510		
Q9NVS9_186		
Q14C86_87		
Q13765_113		
P46108_189		
P40227_129		
A0A087X1X7_483		
Q13564_381		
O60271_714		
B2RDE1_13		
B2RDE1_215		
B2RDE1_228		
Q8WUM4_23		
Q06203_349		
Q06203_371		
O14929_15		
O95721_191		
Q9UJU6_164		
P52701_537		
Q99615_41		
Q13617_728		
Q8IV38_265		
A5PL36_1161		
Q96HC4_127		
P41236_67		
Q7Z4Q2_46		
O75886_376		
Q16204_81		
Q96KB5_121		
Q12802_1765		
Q5TBB1_25		
Q13045_39		
Q6P996_680		
Q9Y6G9_310		
P40424_74		
P78417_110		
Q9BPX3_924		
Q00534_26		
E5RJR5_130		
Q9UIA9_395		
Q13325_218		

Q9NQW7_130		
Q9P260_633		
Q9UK45_63		
P35219_192		
P43490_189		
O75821_71		
Q96EK6_166		
Q9UQ13_134		
P35221_178		
Q9NVG8_287		
P48739_104		
Q5VYK3_1456		
Q9GZN8_105		
P51617_397		
P40426_77		
P20700_123		
Q9NXF7_167		
Q96F45_180		
Q96F45_607		
Q53FA7_257		
Q15126_69		
P49327_1523		
Q6IBN1_405		
P09429_44		
P29401_16		
P46821_2240		
P27694_410		
Q14204_692		
Q9H0B6_369		
E9PAV3_1976		
E9PAV3_2005		
B2RDE1_76		
P15311_427		
Q969T7_98		
Q9Y5A7_128		
Q8WVJ2_147		
Q9BUJ2_731		
Q9Y312_131		
O14617_684		
Q9Y3Z3_312		
Q07002_158		
Q5TCZ1_321		
O75330_589		
Q16352_215		
O75131_523		
P50395_112		
P50395_137		
F5GWF6_272		

Q14974_73		
P17812_109		
Q01105_72		
Q01105_75		
A0A024RB53_15		
P84085_36		
P62987_6		
P62987_11		
P62987_48		
Q9BTE3_37		
P61160_217		
O94966_993		
Q15813_463		
P41236_61		
P0DN79_83		
O94903_49		
Q9UQE7_743		
Q96DG6_159		
Q8TEX9_801		
Q9BV20_259		
Q13625_773		
Q9NRV9_140		
P55263_224		
P40425_84		
Q969Q4_31		
P48507_90		
Q93045_87		
P68104_378		
P07900_558		
P11940_324		
F5GWF6_248		
Q9Y490_841		
P08758_70		
Q13098_349		
O60610_133		
P28340_278		
O75150_943		
Q13085_1564		
Q12802_1773		
Q92973_81		
P53004_253		
Q9UJX3_379		
Q8N4J0_163		
Q9NZW5_388		
E7ETY4_391		
B4DWT1_114		
P62837_128		
P19525_385		

A0PK00_55		

Table 4.5. All lysine sites domain enrichment.

ProRule Domain	Number Liganded	Number in Database	Database Frequency	P-Value	Description	BH Corrected Q-Value
PRU00176	39	244	0.017097611	9.58E-23	RNA recognition motif (RRM) domain	1.29E-20
PRU00691	10	37	0.00259267	7.76E-09	thioredoxin domain	5.24E-07
PRU01185	8	26	0.001821877	9.37E-08	PCI domain	4.22E-06
PRU00042	1	811	0.056828533	1.52E-06	Zinc finger C2H2-type	5.12E-05
PRU00117	8	39	0.002732815	1.91E-06	KH domain	5.15E-05
PRU00599	5	12	0.000840866	5.98E-06	ADF-H domain	0.00013448
PRU01059	4	13	0.000910938	0.000168	Translational (tr)-type guanine nucleotide-binding (G) domain	0.00323913
PRU00156	5	26	0.001821877	0.000226	PPIase cyclophilin-type domain	0.00381309
PRU00542	9	117	0.008198444	0.000811	Helicase C-terminal domain	0.01103868
PRU00531	2	2	0.000140144	0.000818	WHEP-TRS domain	0.01103868
PRU01040	3	9	0.00063065	0.000908	DZF domain	0.01114262
PRU00410	3	11	0.000770794	0.001608	WH1 domain	0.01750219
PRU00278	2	3	0.000210217	0.001815	PpiC domain	0.01750219
PRU00282	2	3	0.000210217	0.001815	Solute carrier (Solcar) repeat	0.01750219
PRU00998	2	4	0.000280289	0.003183	Stathmin-like (SLD) domain	0.02865082
PRU00277	3	17	0.001191227	0.005425	PPIase FKBP-type domain	0.04577262
PRU00547	3	18	0.001261299	0.006344	CS domain	0.05037831
PRU00526	2	6	0.000420433	0.006972	BRO1 domain	0.05229121
PRU00044	7	109	0.007637867	0.007878	Calponin-homology (CH) domain	0.05326455

PRU00267	5	59	0.004134258	0.007891	HMG boxes A and B DNA-binding domains	0.05326455
PRU00507	2	7	0.000490505	0.009363	NAC-A/B (NAC-alpha/beta) domain	0.06019155
PRU00532	3	23	0.00161166	0.012283	Gcn5-related N-acetyltransferase (GNAT) domain	0.07537347
PRU00214	5	67	0.004694836	0.013079	Ubiquitin-like	0.0767698
PRU00541	7	123	0.008618877	0.014474	Helicase ATP-binding domain	0.08141673
PRU00573	2	10	0.000700722	0.018355	Acyl-CoA-binding (ACB) domain	0.08850131
PRU00813	1	1	7.01E-05	0.020323	DhaL domain	0.08850131
PRU01006	1	1	7.01E-05	0.020323	Clathrin heavy-chain (CHCR) repeat	0.08850131
PRU01145	1	1	7.01E-05	0.020323	Zinc finger C2HC LYAR-type	0.08850131
PRU00519	1	1	7.01E-05	0.020323	Elongation factor 1 (EF-1) gamma C-terminal domain	0.08850131
PRU00272	1	1	7.01E-05	0.020323	Thermonuclease domain	0.08850131
PRU00118	1	1	7.01E-05	0.020323	KH type-2 domain	0.08850131
PRU00686	2	11	0.000770794	0.021915	Glutaredoxin domain	0.09245571
PRU00984	2	14	0.00098101	0.03411	DHR-2 domain	0.1324759
PRU00175	1	298	0.020881508	0.036591	Zinc finger RING-type	0.1324759
PRU00209	1	2	0.000140144	0.040233	tRNA-binding domain	0.1324759
PRU01151	1	2	0.000140144	0.040233	Pyruvate carboxyltransferase domain	0.1324759
PRU00386	1	2	0.000140144	0.040233	SGS domain	0.1324759
PRU00666	1	2	0.000140144	0.040233	B12-binding domain	0.1324759
PRU00264	1	2	0.000140144	0.040233	Zinc finger PARP-type	0.1324759
PRU00182	1	2	0.000140144	0.040233	S4 RNA-binding	0.1324759
PRU00734	1	2	0.000140144	0.040233	CHORD domain	0.1324759
PRU00837	2	16	0.001121155	0.043387	Linker histone H1/H5 globular (H15) domain	0.1362136
PRU00115	2	16	0.001121155	0.043387	Importin N-terminal	0.1362136

PRU01134	2	17	0.001191227	0.048336	Alpha-carbonic anhydrase domain	0.14830462
PRU01133	1	3	0.000210217	0.059741	Translationally controlled tumor protein (TCTP) domain	0.16459257
PRU01175	1	3	0.000210217	0.059741	HD domain	0.16459257
PRU01170	1	3	0.000210217	0.059741	Peripheral subunit-binding (PSBD) domain	0.16459257
PRU00605	1	3	0.000210217	0.059741	Glutamine amidotransferase (GATase) type 1 domain	0.16459257
PRU01202	1	3	0.000210217	0.059741	MGS-like domain	0.16459257
PRU00160	3	44	0.003083176	0.063133	Protein-tyrosine phosphatase domain	0.17045859
PRU00782	3	46	0.00322332	0.070074	Myosin motor domain	0.18548903
PRU00286	3	47	0.003293392	0.073668	dnaJ domain	0.18675809
PRU01094	1	4	0.000280289	0.078853	Letm1 ribosome-binding (RBD) domain	0.18675809
PRU00398	1	4	0.000280289	0.078853	PARP alpha-helical domain	0.18675809
PRU00843	1	4	0.000280289	0.078853	Phosphagen kinase C-terminal domain	0.18675809
PRU00280	1	4	0.000280289	0.078853	Heavy-metal-associated domain	0.18675809
PRU00627	1	4	0.000280289	0.078853	PWI domain	0.18675809
PRU00159	17	539	0.037768902	0.088432	Protein kinase domain	0.20582993
PRU01138	1	5	0.000350361	0.097579	CoA carboxyltransferase domain	0.20582993
PRU00658	1	5	0.000350361	0.097579	L-type lectin-like (leguminous) domain	0.20582993
PRU00231	1	5	0.000350361	0.097579	Longin domain	0.20582993
PRU00972	1	5	0.000350361	0.097579	MRG domain	0.20582993
PRU00711	1	5	0.000350361	0.097579	4Fe-4S ferredoxin-type domain	0.20582993
PRU00107	1	5	0.000350361	0.097579	Histidine kinase core domain	0.20582993
PRU00266	2	27	0.001891949	0.106973	Double stranded RNA-binding domain	0.22041978
PRU00132	1	6	0.000420433	0.115924	MSP	0.22041978
PRU00369	1	6	0.000420433	0.115924	BAG domain	0.22041978

PRU01163	1	6	0.000420433	0.115924	Vicinal oxygen chelate (VOC) domain	0.22041978
PRU00170	1	6	0.000420433	0.115924	Reticulon	0.22041978
PRU00378	1	6	0.000420433	0.115924	DDHD domain	0.22041978
PRU01187	1	6	0.000420433	0.115924	Lamin-tail (LTD) domain	0.22041978
PRU00100	2	29	0.002032093	0.120255	Guanylate kinase-like domain	0.22547762
PRU00534	1	7	0.000490505	0.133899	FAT domain	0.23177675
PRU01047	1	7	0.000490505	0.133899	OBG-type guanine nucleotide-binding (G) domain	0.23177675
PRU00465	1	7	0.000490505	0.133899	2Fe-2S ferredoxin-type domain	0.23177675
PRU00464	1	7	0.000490505	0.133899	HIT	0.23177675
PRU01106	1	7	0.000490505	0.133899	HotDog acyl-CoA thioesterase (ACOT)-type domain	0.23177675
PRU00162	2	31	0.002172237	0.133915	PWWP	0.23177675
PRU00316	1	221	0.015485951	0.146008	FN3 domain	0.24642951
PRU00332	1	8	0.000560577	0.151509	La-type HTH domain	0.24642951
PRU00385	1	8	0.000560577	0.151509	KASH domain	0.24642951
PRU00698	1	8	0.000560577	0.151509	MI domain	0.24642951
PRU01228	1	8	0.000560577	0.151509	PRU01228	0.24642951
PRU00137	1	9	0.00063065	0.168762	NTF2	0.26491643
PRU00695	1	9	0.00063065	0.168762	W2 domain	0.26491643
PRU00240	1	9	0.00063065	0.168762	Adenosine to inosine editase domain	0.26491643
PRU00579	1	10	0.000700722	0.185665	Rho GTPase-binding/formin homology 3 (GBD/FH3) domain	0.28482697
PRU00781	1	10	0.000700722	0.185665	Phosphatidylinositol phosphate kinase (PIPK) domain	0.28482697
PRU00045	1	11	0.000770794	0.202226	CAP-Gly	0.29355361
PRU00130	1	11	0.000770794	0.202226	Zinc finger matrin-type	0.29355361
PRU01015	1	11	0.000770794	0.202226	SAM-dependent methyltransferase PRMT-	0.29355361

					type domain	
PRU00164	1	11	0.000770794	0.202226	RanBD1	0.29355361
PRU00409	1	11	0.000770794	0.202226	ATP-grasp domain	0.29355361
PRU00221	1	12	0.000840866	0.218451	WD repeat	0.31043034
PRU00370	1	12	0.000840866	0.218451	BAH domain	0.31043034
PRU01188	3	81	0.005675846	0.232796	Intermediate filament (IF) rod domain	0.3261534
PRU00649	1	13	0.000910938	0.234347	TFIIS N-terminal domain	0.3261534
PRU00774	1	14	0.00098101	0.249921	Formin homology-2 (FH2) domain	0.33405322
PRU00404	1	14	0.00098101	0.249921	Mu homology domain (MHD)	0.33405322
PRU00983	1	14	0.00098101	0.249921	DHR-1 domain	0.33405322
PRU01056	1	14	0.00098101	0.249921	Septin-type guanine nucleotide-binding (G) domain	0.33405322
PRU00568	1	15	0.001051083	0.26518	TTL domain	0.35097301
PRU01083	1	16	0.001121155	0.280129	Cytidine and deoxycytidylate deaminases domain	0.35687655
PRU00239	1	16	0.001121155	0.280129	Cysteine proteinase calpain-type catalytic domain	0.35687655
PRU00167	1	16	0.001121155	0.280129	Ras-GAP	0.35687655
PRU00143	1	177	0.012402775	0.280214	PDZ	0.35687655
PRU00434	2	52	0.003643753	0.289144	ABC transporter family domain	0.36480738
PRU00397	1	17	0.001191227	0.294774	PARP catalytic domain	0.36508758
PRU01055	1	17	0.001191227	0.294774	Dynamin-type guanine nucleotide-binding (G) domain	0.36508758
PRU00145	3	293	0.020531147	0.299291	PH	0.36731139
PRU00084	2	54	0.003783897	0.304223	FERM	0.3693066
PRU01082	1	18	0.001261299	0.309123	PPM-type phosphatase domain	0.3693066
PRU01182	1	18	0.001261299	0.309123	MPN (Mpr1 Pad1 N-terminal) domain	0.3693066
PRU00639	1	19	0.001331371	0.323181	Galactoside-binding lectin (galectin) domain	0.38271459

PRU00361	1	20	0.001401443	0.336954	BAR domain	0.39555472
PRU01190	1	22	0.001541588	0.363667	Myosin N-terminal SH3-like domain	0.4232335
PRU00803	1	23	0.00161166	0.376619	FG-GAP repeat	0.43456033
PRU00186	1	25	0.001751804	0.401739	SAP	0.45961708
PRU00794	1	28	0.001962021	0.437541	Nudix hydrolase domain	0.4963699
PRU00322	1	29	0.002032093	0.448994	Zinc finger RanBP2-type	0.50094339
PRU01077	1	29	0.002032093	0.448994	F-BAR domain	0.50094339
PRU00441	1	31	0.002172237	0.471207	ABC transporter integral membrane type-1 domain	0.52141736
PRU00047	1	33	0.002312382	0.492527	Zinc finger CCHC-type	0.54057877
PRU00192	3	258	0.018078621	0.504599	Src homology 3 (SH3) domain	0.54936158
PRU00127	1	36	0.002522598	0.522912	MAGE	0.56474537
PRU00124	1	44	0.003083176	0.595363	LDL-receptor class A	0.63788939
PRU00448	3	230	0.0161166	0.639043	EF-hand	0.67929812
PRU00548	1	108	0.007567795	0.7314	B30.2/SPRY domain	0.76541846
PRU00191	1	108	0.007567795	0.7314	SH2 domain	0.76541846
PRU00163	1	50	0.003503609	1	Rab-GAP TBC	1
PRU00224	1	68	0.004764908	1	WW/rsp5/WWP domain	1
PRU00041	2	139	0.009740032	1	C2 domain	1
PRU00125	1	87	0.006096279	1	LIM zinc-binding domain	1
PRU00035	1	54	0.003783897	1	Bromodomain	1
PRU00024	1	86	0.006026207	1	Zinc finger B-box-type	1

Table 4.6. DrugBank proteins with modified lysines.

Sites	Gene Name	DrugBank Entry

P54577_146|P54577_310|P54577_247|P54577_319|P54577_334|P54577_348|P54577_391|P54577_474|P54577_231|P54577_412|P54577_346|	YARS	DB00135; DB01766; DB02709; DB03978; DB07205; DB08371; DB08617
Q96I99_338|	SUCLG2	DB00139; DB12695
P68363_40|P68363_60|P68363_96|P68363_112|P68363_163|P68363_280|P68363_304|P68363_311|P68363_326|P68363_336|P68363_352|P68363_370|P68363_394|P68363_401|	TUBA1B	DB01873; DB03010; DB05147; DB07574
P13693_89|P13693_19|P13693_93|P13693_112|P13693_100|	TPT1	DB11093; DB11348
P63261_61|P63261_113|P63261_326|	ACTG1	DB09130; DB11638
P62753_14|P62753_64|P62753_203|P62753_211|P62753_30|P62753_218|	RPS6	DB11638
P62750_7|P62750_14|P62750_26|P62750_36|P62750_23|P62750_18|P62750_30|P62750_114|	RPL23A	DB02494; DB07374; DB08437; DB11638
P22392_100|	NME2	DB04315
P04075_13|P04075_14|P04075_28|P04075_42|P04075_87|P04075_99|P04075_111|P04075_200|P04075_322|P04075_312|P04075_318|P04075_330|P04075_140|P04075_153|P04075_342|P04075_108|P04075_294|	ALDOA	DB01593; DB02512; DB04326; DB04733; DB08240; DB11638
P61978_52|P61978_60|P61978_163|P61978_179|P61978_219|P61978_405|P61978_456|P61978_103|P61978_422|P61978_102|P61978_411|P61978_166|P61978_168|	HNRNPK	DB11638; DB12695
P08183_290|	ABCB1	DB00171; DB00482; DB00778; DB00813; DB04877; DB04881; DB04905; DB05449; DB06191; DB06240; DB09031; DB11635; DB14061; DB14062; DB14063; DB14064; DB14065; DB14066; DB14067; DB14068; DB14069; DB14070; DB14071; DB14072
P27707_88|	DCK	DB01073; DB02594; DB05494
P84077_142|	ARF1	DB02774; DB04121; DB04137; DB04315; DB07348; DB08231; DB09462
P13995_50|	MTHFD2	DB00116; DB00157
Q15428_57|	SF3A2	DB09130
P52209_147|P52209_154|P52209_375|P52209_51|	PGD	DB00789; DB00851; DB00920; DB02076; DB03962
Q00535_237|	CDK5	DB02052; DB02116; DB02950; DB03428; DB03496; DB04014; DB07364

P28062_133|	PSMB8	DB08889
O43283_498|	MAP3K13	DB12010
P30041_209|P30041_56|P30041_63|P30041_97|	PRDX6	DB02325; DB03814; DB09130
P41252_410|P41252_844|P41252_382|P41252_1042|	IARS	DB00167
P51580_32|	TPMT	DB01250
P30044_86|P30044_142|	PRDX5	DB00995; DB03608; DB03793
Q9Y678_313|	COPG1	DB03963
P40429_114|	RPL13A	DB02494; DB07374; DB08437
P51858_19|	HDGF	DB09130
Q13838_384|Q13838_156|Q13838_163|Q13838_188|	DDX39B	DB02325; DB11638
P08574_315|P08574_325|	CYC1	DB04141; DB04799; DB07401; DB07636; DB07763; DB07778; DB08330; DB08453; DB08690
Q14790_250|	CASP8	DB12651
Q6ZMR3_155|	LDHAL6A	DB00157
P53004_147|P53004_253|	BLVRA	DB00157
P15121_173|P15121_12|P15121_179|P15121_222|P15121_22|	AKR1B1	DB00143; DB00157; DB00605; DB01689; DB02007; DB02020; DB02021; DB02101; DB02132; DB02383; DB02518; DB02712; DB02834; DB02994; DB03461; DB04272; DB05327; DB05383; DB05533; DB06246; DB07028; DB07030; DB07063; DB07093; DB07139; DB07187; DB07450; DB07498; DB07999; DB08000; DB08084; DB08098; DB08449; DB08772
P20618_164|P20618_184|	PSMB1	DB00188; DB08515; DB08889
P25786_115|	PSMA1	DB08515
P25787_92|P25787_53|P25787_70|	PSMA2	DB08515

P25789_210|P25789_64|P25789_239|	PSMA4	DB08515
P07766_158|	CD3E	DB00075; DB06607
Q13362_418|	PPP2R5C	DB02506; DB06905
P29401_319|P29401_232|P29401_260|P29401_254|P29401_310|P29401_497|P29401_314|P29401_16|	TKT	DB09130
P14735_364|P14735_303|P14735_896|	IDE	DB00030; DB00071; DB00626
P39023_39|P39023_103|P39023_294|P39023_300|P39023_312|P39023_366|P39023_66|	RPL3	DB02494; DB04865; DB07374; DB08437; DB09092
P35241_3|	RDX	DB03401
O75533_1086|O75533_866|	SF3B1	DB14017
P61158_317|P61158_240|	ACTR3	DB08235; DB08236
P62807_6|P62807_12|P62807_17|P62807_21|P62807_47|P62807_109|P62807_117|P62807_121|P62807_86|P62807_13|	HIST1H2BC	DB09130
Q14103_111|Q14103_129|Q14103_197|Q14103_178|Q14103_243|Q14103_255|	HNRNPD	DB11638
P67936_13|P67936_76|P67936_113|P67936_116|P67936_212|P67936_100|	TPM4	DB12695

P68104_41|P68104_44|P68104_146|P68104_179|P68104_215|P68104_219|P68104_255|P68104_273|P68104_386|P68104_392|P68104_395|P68104_408|P68104_439|P68104_444|P68104_450|P68104_453|P68104_457|P68104_5|P68104_172|P68104_180|P68104_244|P68104_330|P68104_460|P68104_64|P68104_443|P68104_378|	EEF1A1	DB01593; DB04315; DB09130; DB11638
P27635_82|P27635_121|P27635_145|P27635_170|P27635_188|P27635_141|	RPL10	DB11638
Q9C0B1_216|	FTO	DB11638
P36542_39|P36542_115|P36542_43|P36542_46|P36542_49|P36542_64|P36542_36|	ATP5C1	DB04216; DB07384; DB07394; DB08399; DB08629
P19525_385|	EIF2AK2	DB12010

P11142_108|P11142_112|P11142_137|P11142_159|P11142_187|P11142_246|P11142_251|P11142_257|P11142_319|P11142_328|P11142_345|P11142_348|P11142_497|P11142_507|P11142_512|P11142_524|P11142_526|P11142_539|P11142_601|P11142_535|P11142_583|P11142_451|P11142_25|P11142_88|P11142_361|P11142_423|P11142_500|P11142_597|P11142_325|P11142_531|	HSPA8	DB01254; DB07045; DB09130; DB11638
O43837_96|O43837_146|O43837_354|O43837_199|	IDH3B	DB00157
Q92930_58|	RAB8B	DB02082; DB04315
P12268_109|P12268_450|P12268_511|P12268_436|P12268_422|	IMPDH2	DB00157; DB00688; DB00811; DB01024; DB03070; DB03948; DB04566; DB06103
P12268_109|P12268_450|P12268_511|P12268_436|P12268_422|	IMPDH2	DB01033

P34897_103|P34897_181|P34897_200|P34897_269|P34897_297|P34897_302|P34897_356|P34897_409|P34897_459|P34897_464|P34897_469|P34897_474|	SHMT2	DB00114; DB00116; DB00145; DB11638
O75899_196|	GABBR2	DB00181; DB00996; DB02530; DB05010; DB08891; DB08892
P06400_791|P06400_427|	RB1	DB00030; DB00071
Q07955_38|	SRSF1	DB09130
P37802_17|P37802_153|P37802_171|P37802_79|	TAGLN2	DB11638
P08686_232|	CYP21A2	DB01026
P00338_14|P00338_76|P00338_81|P00338_222|P00338_243|P00338_318|P00338_59|P00338_126|P00338_155|P00338_224|P00338_228|P00338_118|P00338_232|P00338_90|P00338_149|	LDHA	DB00157; DB02483; DB02701; DB03940; DB09118; DB09130; DB11638
Q15185_48|Q15185_7|Q15185_91|	PTGES3	DB05036; DB09130
P37268_318|	FDFT1	DB05317

P09960_573|P09960_127|	LTA4H	DB01197; DB02062; DB02352; DB03366; DB03424; DB05177; DB06828; DB06851; DB06917; DB07094; DB07099; DB07102; DB07104; DB07196; DB07237; DB07258; DB07259; DB07260; DB07292; DB08040; DB08466; DB11781
P17844_91|P17844_284|P17844_391|P17844_470|P17844_236|	DDX5	DB11638
Q9UNX3_136|	RPL26L1	DB02494; DB07374; DB08437
P07814_512|P07814_788|P07814_841|P07814_861|P07814_951|P07814_513|P07814_693|	EPRS	DB00142; DB00172; DB02510; DB02684; DB03376
P30084_128|	ECHS1	DB02563; DB02910; DB03059; DB04117; DB09568
O94903_47|O94903_49|	PROSC	DB00114; DB00172
P14550_127|	AKR1A1	DB02383; DB03461; DB09130
P22102_156|P22102_598|P22102_249|P22102_852|P22102_350|	GART	DB00642; DB02236; DB03546

P06744_366|P06744_454|P06744_142|P06744_234|P06744_447|P06744_252|P06744_423|P06744_523|P06744_12|P06744_524|	GPI	DB02007; DB02076; DB02093; DB02548; DB03042; DB03581; DB03937; DB04493; DB09130; DB11638
Q13126_241|	MTAP	DB00173; DB02158; DB02281; DB02282; DB02933
Q6P996_680|	PDXDC1	DB00114
P06748_27|P06748_32|P06748_54|P06748_141|P06748_154|P06748_155|P06748_202|P06748_212|P06748_215|P06748_223|P06748_229|P06748_230|P06748_236|P06748_239|P06748_248|P06748_250|P06748_257|P06748_263|P06748_273|P06748_267|P06748_193|P06748_206|P06748_233|	NPM1	DB11638
P32322_215|P32322_307|	PYCR1	DB00157; DB00172
Q13085_323|Q13085_2127|Q13085_1564|	ACACA	DB00121
P63151_95|	PPP2R2A	DB02506
Q96C36_47|Q96C36_291|Q96C36_307|	PYCR2	DB00157; DB00172
O00299_119|O00299_183|O00299_131|O00299_192|	CLIC1	DB09130; DB11638

P07195_7|P07195_156|P07195_82|P07195_319|P07195_308|P07195_60|P07195_77|P07195_119|P07195_244|P07195_310|P07195_318|	LDHB	DB00157; DB02401; DB03940; DB09118; DB11638
Q02750_84|	MAP2K1	DB02152; DB03115; DB05239; DB06616; DB06892; DB07046; DB07101; DB08130; DB08208; DB08911
O00244_25|	ATOX1	DB00515; DB02772; DB03127
P16152_148|	CBR1	DB01698; DB02709; DB03556; DB04216; DB04463; DB11672
P04080_39|P04080_44|P04080_78|	CSTB	DB09131
P60981_19|	DSTN	DB04147
P54578_49|P54578_214|	USP14	DB12695
Q15046_492|Q15046_88|	KARS	DB00123
P15924_2317|	DSP	DB01593; DB11638
P26640_903|P26640_243|	VARS	DB00161
P60709_50|P60709_61|P60709_113|P60709_191|P60709_213|P60709_284|P60709_291|P60709_315|P60709_326|P60709_328|P60709_336|	ACTB	DB04216; DB12695
Q12965_196|	MYO1E	DB03366
P49915_182|	GMPS	DB00142

P13639_15|P13639_283|P13639_337|P13639_445|P13639_439|P13639_498|P13639_512|P13639_598|P13639_605|P13639_318|P13639_239|P13639_272|P13639_275|P13639_594|P13639_629|P13639_259|P13639_42|P13639_235|P13639_252|P13639_314|P13639_328|P13639_333|P13639_391|P13639_407|P13639_426|P13639_571|P13639_619|P13639_648|P13639_676|P13639_845|P13639_322|P13639_330|P13639_438|P13639_572|P13639_638|	EEF2	DB02059; DB03223; DB04315; DB08348
P11586_245|P11586_262|P11586_10|P11586_66|P11586_543|P11586_553|P11586_246|P11586_878|	MTHFD1	DB00116; DB00157; DB02358; DB03461; DB04322
P40763_177|	STAT3	DB05959
P78417_11|P78417_136|P78417_143|P78417_198|P78417_220|P78417_110|	GSTO1	DB00143
P04181_405|	OAT	DB00114; DB00129; DB02054; DB02821
P49591_12|	SARS	DB00133

P23743_260|P23743_671|	DGKA	DB00163; DB14001; DB14002
P15880_211|P15880_212|P15880_257|P15880_263|P15880_275|P15880_71|	RPS2	DB09130
P46459_586|	NSF	DB01902
P21912_126|P21912_261|	SDHB	DB00139; DB04141; DB08689
P46940_368|P46940_1445|P46940_939|P46940_1558|	IQGAP1	DB11638
P49411_79|P49411_88|P49411_91|P49411_234|P49411_238|P49411_286|P49411_342|P49411_361|P49411_447|	TUFM	DB01593; DB04315
P62316_118|P62316_71|P62316_88|	SNRPD2	DB11638
P55809_176|P55809_185|P55809_296|P55809_418|P55809_421|P55809_481|P55809_271|	OXCT1	DB00139; DB02731
Q13423_394|Q13423_1059|Q13423_70|	NNT	DB00157; DB01763; DB03461; DB09092
Q9P289_233|	STK26	DB07853; DB12010

P00505_59|P00505_82|P00505_90|P00505_159|P00505_309|P00505_338|P00505_363|P00505_73|P00505_94|P00505_234|P00505_227|	GOT2	DB00114; DB00128; DB00142; DB02783
Q15031_79|Q15031_81|	LARS2	DB00149
P07437_19|P07437_58|P07437_122|P07437_154|P07437_216|P07437_252|P07437_297|P07437_324|P07437_336|P07437_350|P07437_379|P07437_103|	TUBB	DB00361; DB00541; DB00570; DB01179; DB01394; DB01873; DB03010; DB05147; DB05284; DB06042; DB09130; DB11638; DB11641; DB11731; DB12334
O60664_262|	PLIN3	DB01271; DB01279
P39748_200|P39748_267|P39748_80|	FEN1	DB01592
P22314_671|P22314_627|P22314_802|P22314_806|P22314_838|P22314_68|P22314_604|P22314_884|	UBA1	DB04119; DB04216
P30101_129|P30101_218|P30101_332|P30101_226|	PDIA3	DB01593; DB09130
P27797_41|P27797_48|P27797_62|P27797_151|P27797_153|P27797_207|P27797_209|P27797_276|	CALR	DB00025; DB00031; DB01065; DB06245; DB09130; DB11093; DB11348; DB13998; DB13999

P41250_82|P41250_219|P41250_646|P41250_99|P41250_108|P41250_501|P41250_204|	GARS	DB00145
P35219_192|	CA8	DB00909
P49773_21|P49773_83|P49773_30|P49773_82|	HINT1	DB00131; DB01972; DB02162; DB02183; DB03349
Q9Y6K9_309|	IKBKG	DB04998; DB05289
P78527_310|P78527_1407|P78527_2683|P78527_2829|P78527_3260|P78527_700|P78527_2366|P78527_3550|P78527_3603|P78527_4019|P78527_2746|P78527_357|P78527_3264|P78527_963|	PRKDC	DB00201; DB05210
P30038_487|	ALDH4A1	DB00157
P62993_76|	GRB2	DB00061; DB03276
P48735_45|P48735_48|P48735_69|P48735_80|P48735_106|P48735_130|P48735_133|P48735_155|P48735_166|P48735_180|P48735_193|P48735_199|P48735_272|P48735_275|P48735_280|P48735_282|P48735_384|P48735_413|P48735_426|P48735_127|P48735_360|P48735_243|P48735_256|	IDH2	DB01727; DB13874
P27708_964|	CAD	DB00128; DB03459

P09884_829|	POLA1	DB00242; DB00631; DB01073; DB01280
Q16775_229|	HAGH	DB00143; DB03889
P10768_64|P10768_186|P10768_200|P10768_10|	ESD	DB00143
P30049_165|	ATP5D	DB00228; DB00753; DB01028; DB01159; DB01189; DB01236
P12235_23|	SLC25A4	DB00171; DB00720; DB01736; DB02426; DB03429; DB04178
P84098_146|P84098_153|P84098_190|P84098_196|P84098_144|	RPL19	DB02494; DB07374; DB08437
P31153_303|P31153_234|	MAT2A	DB00118
O15067_25|O15067_279|	PFAS	DB00142
O95747_42|	OXSR1	DB12010
P55786_222|P55786_712|P55786_853|P55786_279|P55786_753|P55786_821|P55786_293|	NPEPPS	DB11638; DB11781
P00846_51|	MT-ATP6	DB00783; DB13952; DB13953; DB13954; DB13955; DB13956
P69905_17|P69905_41|	HBA1	DB00358; DB00893; DB01592; DB01593; DB02126; DB06154; DB07427; DB07428; DB07645; DB08077; DB08262; DB08486; DB08632; DB09112; DB09130; DB09140; DB09146; DB09147; DB09517; DB13995

P30519_168|P30519_199|	HMOX2	DB00157; DB04912
Q02224_1444|	CENPE	DB06097
Q9UJS0_408|	SLC25A13	DB00128
P0CG47_48|P0CG47_87|P0CG47_200|P0CG47_215|P0CG47_11|P0CG47_63|P0CG47_124|P0CG47_163|	UBB	DB02542
P05141_23|P05141_33|P05141_43|P05141_63|P05141_92|P05141_147|P05141_166|P05141_245|P05141_272|P05141_199|P05141_96|	SLC25A5	DB00720
P22033_621|	MUT	DB00115; DB00200
P25705_123|P25705_126|P25705_161|P25705_167|P25705_230|P25705_305|P25705_427|P25705_506|P25705_531|P25705_132|P25705_539|	ATP5A1	DB04216; DB07384; DB07394; DB08399; DB08629; DB11638
P12814_89|P12814_157|P12814_682|	ACTN1	DB06773; DB09130
P55072_754|P55072_663|	VCP	DB04395; DB12695

P08670_129|P08670_439|	VIM	DB11638; DB12695
P49189_366|	ALDH9A1	DB00157
Q9HAN9_56|	NMNAT1	DB03227; DB04099
P61313_83|	RPL15	DB02494; DB07374; DB08437
P15153_133|	RAC2	DB00514
P14866_97|P14866_229|P14866_269|P14866_493|P14866_533|P14866_418|	HNRNPL	DB09130
P48507_90|	GCLM	DB00142; DB00151
P14868_9|	DARS	DB00128
P63104_9|P63104_11|P63104_49|P63104_68|P63104_120|P63104_138|P63104_158|P63104_212|P63104_74|P63104_75|P63104_115|P63104_139|	YWHAZ	DB12695
P13073_53|P13073_60|P13073_65|	COX4I1	DB02659; DB04464
Q9Y617_116|Q9Y617_323|Q9Y617_127|Q9Y617_333|	PSAT1	DB00114; DB00142
P09936_4|P09936_65|P09936_71|P09936_123|P09936_221|P09936_15|P09936_78|P09936_131|P09936_157|	UCHL1	DB12695
Q9H1K4_82|Q9H1K4_79|	SLC25A18	DB00142
P01130_830|	LDLR	DB00707
P61160_217|	ACTR2	DB08235; DB08236

P22626_17|P22626_22|P22626_59|P22626_104|P22626_112|P22626_113|P22626_173|P22626_151|	HNRNPA2B1	DB09130; DB11638
P18669_106|P18669_176|P18669_39|P18669_100|P18669_113|P18669_228|P18669_241|P18669_251|P18669_138|P18669_225|P18669_157|	PGAM1	DB09130; DB11638
P22061_206|P22061_219|	PCMT1	DB01752
P04406_107|P04406_117|P04406_139|P04406_145|P04406_194|P04406_215|P04406_219|P04406_227|P04406_254|P04406_263|P04406_271|P04406_61|P04406_251|P04406_259|P04406_84|P04406_186|P04406_5|P04406_66|P04406_86|	GAPDH	DB00157; DB02059; DB03893; DB07347; DB09092; DB09130; DB11638
P35080_116|	PFN2	DB02078; DB02580
P11177_336|	PDHB	DB00119; DB00157
P08708_72|	RPS17	DB11638
P61769_111|	B2M	DB00254; DB02740; DB04464; DB09130
P54819_93|P54819_147|	AK2	DB01717; DB03366

Q06830_16|Q06830_93|Q06830_109|Q06830_178|Q06830_35|Q06830_67|Q06830_68|Q06830_168|Q06830_185|Q06830_190|Q06830_192|Q06830_197|Q06830_27|Q06830_136|	PRDX1	DB01593; DB09130; DB11638
P10606_57|	COX5B	DB02659; DB04464
O75390_76|O75390_103|O75390_382|O75390_459|O75390_43|O75390_352|O75390_215|O75390_321|	CS	DB01969; DB01992; DB02637; DB03182; DB03499; DB04230; DB04272
P30520_157|P30520_164|P30520_173|P30520_403|P30520_419|P30520_163|P30520_203|	ADSS	DB00128; DB05540
Q14181_232|	POLA2	DB00851
O95831_593|	AIFM1	DB03147; DB05282
P11021_185|P11021_447|P11021_122|P11021_125|P11021_340|P11021_370|P11021_113|P11021_213|	HSPA5	DB00025; DB00945; DB09130; DB13998; DB13999
P49588_766|P49588_625|P49588_366|	AARS	DB00160
P49589_49|	CARS	DB00151
P27695_125|	APEX1	DB04967

P62277_27|P62277_39|P62277_43|P62277_78|P62277_93|P62277_34|P62277_100|P62277_130|	RPS13	DB11638
P60842_54|P60842_146|P60842_174|P60842_193|P60842_291|P60842_369|P60842_68|P60842_226|P60842_238|P60842_309|	EIF4A1	DB09130
P37108_55|P37108_32|P37108_38|	SRP14	DB11638
Q99497_130|Q99497_182|	PARK7	DB09130
P06733_54|P06733_64|P06733_71|P06733_80|P06733_81|P06733_89|P06733_92|P06733_193|P06733_197|P06733_199|P06733_202|P06733_221|P06733_233|P06733_256|P06733_281|P06733_326|P06733_330|P06733_335|P06733_358|P06733_420|P06733_434|P06733_28|P06733_60|P06733_228|P06733_105|P06733_239|P06733_422|	ENO1	DB01593; DB09130; DB11638
P06730_184|	EIF4E	DB01649; DB01960; DB02716; DB05165; DB08217

P14174_78|	MIF	DB01880; DB02728; DB04272; DB07718; DB07888; DB08333; DB08334; DB08335; DB08765
Q04760_88|Q04760_157|Q04760_44|Q04760_140|Q04760_151|	GLO1	DB00143; DB00328; DB03130; DB03330; DB03345; DB03602; DB04132; DB08179
P06737_29|P06737_295|P06737_804|P06737_819|	PYGL	DB00114; DB00131; DB02089; DB02320; DB02379; DB03288; DB03496; DB03744; DB04522; DB05044; DB07315; DB07395; DB07396; DB07968; DB08844
P08559_385|	PDHA1	DB00157
P62837_8|P62837_128|	UBE2D2	DB02418
Q01082_842|Q01082_1354|Q01082_2269|Q01082_1312|Q01082_1878|Q01082_1991|Q01082_2054|Q01082_1981|Q01082_1824|	SPTBN1	DB01373; DB03401
P46782_191|P46782_201|P46782_44|	RPS5	DB11638
P46781_30|P46781_91|P46781_121|P46781_139|P46781_155|	RPS9	DB11638
Q9P2R7_205|	SUCLA2	DB00139
P31040_182|P31040_335|P31040_538|P31040_608|	SDHA	DB00139; DB04141; DB04657; DB04795; DB08689; DB09270
Q9H936_80|Q9H936_83|	SLC25A22	DB00142

P07384_84|P07384_86|	CAPN1	DB04276; DB04653; DB07627
P51151_112|	RAB9A	DB03793; DB04315
P51659_184|P51659_415|	HSD17B4	DB00157; DB03192
Q02218_970|Q02218_561|	OGDH	DB00157; DB00313; DB09092
P21796_20|P21796_109|P21796_201|P21796_236|P21796_252|P21796_266|	VDAC1	DB01375; DB09061; DB14009; DB14011
O60488_49|	ACSL4	DB00159; DB00197; DB00412
P25788_174|	PSMA3	DB08515; DB12695
P49841_292|	GSK3B	DB01356; DB01772; DB01793; DB01950; DB02010; DB02052; DB03444; DB04014; DB04395; DB07014; DB07058; DB07149; DB07584; DB07585; DB07676; DB07812; DB07859; DB07947; DB08073; DB12010; DB12129
P55263_224|	ADK	DB00131; DB00811; DB07173; DB07280
P23246_314|P23246_338|P23246_421|P23246_518|P23246_279|P23246_330|P23246_472|P23246_208|	SFPQ	DB09130; DB11638
P07737_38|P07737_54|P07737_70|P07737_91|P07737_105|P07737_108|P07737_116|P07737_126|P07737_127|	PFN1	DB07908; DB11638

P40939_60|P40939_214|P40939_255|P40939_259|P40939_289|P40939_295|P40939_303|P40939_415|P40939_460|P40939_728|P40939_129|P40939_411|P40939_631|P40939_334|	HADHA	DB00157
O14832_120|	PHYH	DB00025; DB00126; DB13998; DB13999
P62857_10|P62857_16|	RPS28	DB11638
P52597_224|	HNRNPF	DB12695
O43447_153|	PPIH	DB00172
P20674_72|	COX5A	DB02659; DB04464
P09211_55|P09211_128|P09211_189|P09211_116|P09211_191|P09211_209|	GSTP1	DB00143; DB00197; DB00316; DB00363; DB00903; DB01015; DB01242; DB01834; DB01915; DB02633; DB03003; DB03619; DB03686; DB03814; DB04132; DB04339; DB04972; DB05460; DB06246; DB07849; DB08370; DB09462; DB11672; DB11831; DB13014
P62913_38|P62913_52|P62913_67|	RPL11	DB02494; DB07374; DB08437
P62917_93|P62917_144|P62917_155|P62917_149|	RPL8	DB02494; DB07374; DB08437
P31943_349|P31943_173|	HNRNPH1	DB09130

P31946_13|P31946_51|P31946_122|P31946_160|P31946_11|P31946_77|P31946_70|P31946_214|	YWHAB	DB09130; DB12695
P31948_50|P31948_123|P31948_252|P31948_434|P31948_486|P31948_513|P31948_63|P31948_73|P31948_109|P31948_169|P31948_207|P31948_250|P31948_337|P31948_347|P31948_364|P31948_388|P31948_32|P31948_210|P31948_317|P31948_453|P31948_13|P31948_162|P31948_429|P31948_523|P31948_227|P31948_381|P31948_442|P31948_366|P31948_462|	STIP1	DB09130
P35914_179|	HMGCL	DB04594
P61604_28|P61604_40|P61604_80|P61604_56|	HSPE1	DB12695
Q9Y277_15|Q9Y277_20|Q9Y277_109|Q9Y277_115|	VDAC3	DB01375; DB06098

P05023_487|	ATP1A1	DB00390; DB00511; DB00774; DB00903; DB01021; DB01078; DB01092; DB01119; DB01158; DB01188; DB01244; DB01345; DB01370; DB01378; DB01396; DB01430; DB06157; DB13996
P04083_90|P04083_245|P04083_214|	ANXA1	DB00288; DB00741; DB01234
P33316_155|P33316_179|	DUT	DB03413; DB04685
P00491_265|	PNP	DB00242; DB00900; DB01667; DB02222; DB02230; DB02377; DB02391; DB02568; DB02796; DB02857; DB03101; DB03551; DB03609; DB03881; DB04076; DB04260; DB04335; DB04753; DB04754; DB04757; DB06185
Q13907_180|	IDI1	DB01785
P60953_133|P60953_131|	CDC42	DB02623; DB04315
O14727_142|	APAF1	DB00171
Q9UHY7_111|Q9UHY7_106|	ENOPH1	DB07912
P48047_54|P48047_70|P48047_73|P48047_162|P48047_60|P48047_84|	ATP5O	DB11638
P17812_557|P17812_109|	CTPS1	DB00130
P00367_183|P00367_258|P00367_365|P00367_480|	GLUD1	DB00142; DB00157; DB00756; DB04137; DB11081

P38606_580|	ATP6V1A	DB00630; DB01077; DB01133; DB06733; DB06734
P00813_23|P00813_273|P00813_170|P00813_164|P00813_225|P00813_232|P00813_323|P00813_331|	ADA	DB00552; DB00975; DB02096; DB02472; DB02616; DB02830; DB03015; DB03220; DB03370; DB03572; DB04218; DB04440; DB07711; DB07783; DB07785; DB07786
P31937_297|	HIBADH	DB00157
P49327_436|P49327_673|P49327_235|P49327_786|P49327_787|P49327_1116|P49327_1142|P49327_1151|P49327_1158|P49327_1239|P49327_1591|P49327_1866|P49327_1878|P49327_1911|P49327_1993|P49327_1523|	FASN	DB01034; DB01083
P31930_111|P31930_134|	UQCRC1	DB04141; DB04741; DB04799; DB07401; DB07763; DB07778; DB08330; DB08453; DB08690
Q13526_63|Q13526_82|	PIN1	DB01766; DB06867
P31939_14|P31939_266|P31939_199|P31939_66|P31939_137|P31939_389|P31939_357|	ATIC	DB00116; DB00642; DB01700; DB01972; DB02309; DB03442; DB04057
Q99623_89|Q99623_216|	PHB2	DB06774
Q13177_136|Q13177_246|	PAK2	DB12010

P22234_47|P22234_116|P22234_226|P22234_304|P22234_235|P22234_110|P22234_286|P22234_30|P22234_36|P22234_80|	PAICS	DB00128
P21333_865|P21333_1538|P21333_1071|P21333_1294|P21333_2513|P21333_2417|P21333_771|	FLNA	DB11638
P24752_66|P24752_174|P24752_190|P24752_230|P24752_251|P24752_266|P24752_223|	ACAT1	DB00795
O94925_164|	GLS	DB00142
P27348_9|P27348_49|P27348_68|P27348_85|P27348_11|P27348_139|P27348_115|P27348_212|P27348_158|	YWHAQ	DB12695
O15460_57|	P4HA2	DB00139; DB00172
P51617_397|	IRAK1	DB12010

P14625_95|P14625_269|P14625_340|P14625_404|P14625_458|P14625_534|P14625_547|P14625_561|P14625_593|P14625_597|P14625_630|P14625_633|P14625_663|P14625_671|P14625_682|P14625_137|P14625_168|P14625_467|P14625_683|P14625_532|P14625_628|P14625_623|	HSP90B1	DB00615; DB02103; DB02424; DB02935; DB03719; DB03758; DB08464; DB08465; DB09130
Q9Y285_315|Q9Y285_342|	FARSA	DB00120
P53597_308|	SUCLG1	DB00139
Q99714_99|Q99714_104|Q99714_105|	HSD17B10	DB00157; DB02820; DB09568
O00264_105|	PGRMC1	DB00514
O00264_105|	PGRMC1	DB00540; DB01104
P08865_89|P08865_212|	RPSA	DB04985; DB09130
O75330_589|	HMMR	DB08818
P11310_175|P11310_212|P11310_271|P11310_279|P11310_301|	ACADM	DB02910; DB03147; DB03415
Q07020_119|	RPL18	DB11638
Q07021_91|Q07021_104|Q07021_123|	C1QBP	DB08818; DB09130
Q9NSE4_241|Q9NSE4_500|	IARS2	DB00167
O95573_58|O95573_706|	ACSL3	DB00159

P10809_31|P10809_58|P10809_72|P10809_75|P10809_82|P10809_89|P10809_87|P10809_91|P10809_96|P10809_125|P10809_130|P10809_133|P10809_156|P10809_160|P10809_180|P10809_191|P10809_196|P10809_202|P10809_205|P10809_233|P10809_236|P10809_249|P10809_250|P10809_269|P10809_292|P10809_301|P10809_310|P10809_352|P10809_359|P10809_361|P10809_364|P10809_387|P10809_389|P10809_396|P10809_469|P10809_473|P10809_481|P10809_369|	HSPD1	DB09130
O14874_233|	BCKDK	DB02930
P07237_271|P07237_328|P07237_326|	P4HB	DB01593; DB03615; DB09130; DB11638
Q15067_260|	ACOX1	DB03147; DB07930
O95470_155|	SGPL1	DB00114
Q04917_69|	YWHAH	DB12695

P60174_92|P60174_225|P60174_231|P60174_106|P60174_212|P60174_122|P60174_193|P60174_43|P60174_179|P60174_275|	TPI1	DB01593; DB01695; DB02726; DB03026; DB03132; DB03135; DB03314; DB03379; DB03900; DB04326; DB04447; DB04510; DB07387; DB11638
P49368_248|P49368_78|P49368_21|P49368_222|P49368_381|P49368_138|	CCT3	DB04395; DB11638
P10515_362|P10515_368|P10515_386|P10515_363|P10515_376|P10515_396|	DLAT	DB00157; DB03758; DB03760
Q00534_26|	CDK6	DB03496; DB07379; DB07795; DB09073; DB11730; DB12001
P11387_148|P11387_669|P11387_174|	TOP1	DB00762; DB01030; DB04690; DB04882; DB04967; DB05129; DB05482; DB05630; DB05806; DB06069; DB06159; DB07354; DB08159; DB11254
P45880_247|P45880_120|	VDAC2	DB01375; DB06098
P26196_482|	DDX6	DB01694
P06493_33|P06493_20|	CDK1	DB02052; DB02116; DB02950; DB03428; DB03496; DB04014; DB05037; DB06195; DB12010

P08238_53|P08238_107|P08238_180|P08238_186|P08238_204|P08238_275|P08238_284|P08238_286|P08238_350|P08238_399|P08238_406|P08238_435|P08238_477|P08238_481|P08238_526|P08238_550|P08238_577|P08238_607|P08238_624|P08238_641|P08238_646|P08238_69|P08238_402|P08238_410|P08238_428|P08238_531|P08238_538|P08238_557|P08238_568|P08238_623|P08238_649|P08238_354|P08238_64|P08238_552|P08238_559|P08238_565|P08238_573|P08238_574|P08238_685|P08238_347|P08238_411|P08238_491|P08238_273|	HSP90AB1	DB02424; DB02754; DB03758; DB05134; DB06070; DB07594; DB07877; DB08045; DB08153; DB08292; DB08293; DB08346; DB08464; DB08465; DB09221
Q06203_442|Q06203_372|Q06203_349|Q06203_371|	PPAT	DB00130; DB01033; DB01254
P28331_467|	NDUFS1	DB00157
P62829_113|P62829_123|	RPL23	DB02494; DB07374; DB08437

P62826_38|P62826_60|P62826_71|P62826_134|P62826_142|P62826_152|P62826_159|P62826_99|P62826_127|P62826_37|P62826_141|	RAN	DB04315
P00918_24|P00918_39|P00918_45|P00918_76|P00918_167|P00918_80|P00918_256|	CA2	DB00232; DB00273; DB00311; DB00391; DB00436; DB00482; DB00562; DB00580; DB00606; DB00695; DB00703; DB00774; DB00819; DB00869; DB00880; DB00909; DB00999; DB01021; DB01031; DB01119; DB01144; DB01194; DB01325; DB01671; DB01748; DB01784; DB01942; DB01964; DB02069; DB02087; DB02220; DB02221; DB02292; DB02429; DB02479; DB02535; DB02602; DB02610; DB02679; DB02861; DB02866; DB02894; DB02986; DB03039; DB03221; DB03262; DB03270; DB03294; DB03333; DB03385; DB03526; DB03594; DB03596; DB03598; DB03697; DB03844; DB03877; DB03904; DB03950; DB03975; DB04002; DB04081; DB04089; DB04180; DB04203; DB04371; DB04394; DB04549; DB04600; DB04601; DB04763; DB06891; DB06954; DB07048; DB07050; DB07363; DB07467; DB07476; DB07596; DB07632; DB07710; DB07742; DB08046; DB08083; DB08155; DB08156; DB08157; DB08165; DB08202; DB08301; DB08329; DB08416; DB08418; DB08645; DB08659; DB08765; DB08782; DB08846; DB09460; DB09472
P50213_77|P50213_116|	IDH3A	DB00157; DB06757; DB09092; DB09130
P19784_103|	CSNK2A2	DB07546; DB12010
Q9Y4W6_508|Q9Y4W6_785|	AFG3L2	DB00171

P13612_189|	ITGA4	DB00108; DB04997; DB05092; DB05122; DB05468; DB06822; DB09033
Q9P2J5_464|Q9P2J5_719|Q9P2J5_350|	LARS	DB00149
P63208_130|	SKP1	DB01750; DB06980; DB06981; DB06982; DB07950
Q92598_185|Q92598_221|Q92598_272|Q92598_275|Q92598_430|Q92598_772|Q92598_790|Q92598_316|	HSPH1	DB12695
P12081_22|	HARS	DB00117
P50914_85|P50914_164|P50914_165|P50914_171|P50914_128|P50914_141|P50914_142|P50914_79|P50914_177|	RPL14	DB11638
P43490_189|	NAMPT	DB05217; DB12731
P62937_28|P62937_31|P62937_44|P62937_49|P62937_76|P62937_82|P62937_91|P62937_118|P62937_125|P62937_131|P62937_133|P62937_151|P62937_155|	PPIA	DB00091; DB00172; DB01742; DB02419; DB03393; DB09130; DB11638
Q9UDR5_584|	AASS	DB00142; DB00157; DB02338; DB04207
O75489_260|O75489_259|	NDUFS3	DB00157

P14324_295|P14324_123|P14324_413|	FDPS	DB00282; DB00399; DB00630; DB00710; DB00884; DB01785; DB02508; DB02552; DB04714; DB06548; DB07780; DB07841
P00390_401|	GSR	DB00143; DB00157; DB00262; DB01644; DB02153; DB02553; DB02895; DB03147; DB03310; DB03867; DB07393; DB07714; DB09130
P22830_118|P22830_133|	FECH	DB02659
P62241_128|P62241_139|P62241_157|P62241_170|P62241_37|	RPS8	DB11638
P17980_125|	PSMC3	DB12695
P06239_130|	LCK	DB01254; DB01830; DB02010; DB03023; DB04003; DB04395; DB06925; DB07146; DB07297; DB08055; DB08056; DB08057; DB08901; DB09079; DB12010
O75964_54|	ATP5L	DB11638; DB12695
P12236_23|P12236_147|P12236_166|P12236_105|	SLC25A6	DB00720
O75746_406|	SLC25A12	DB00128
P42766_71|P42766_79|P42766_118|P42766_43|P42766_74|P42766_77|	RPL35	DB11638

P68371_58|P68371_379|	TUBB4B	DB00518; DB00643; DB01873; DB03010; DB04910; DB05147; DB12695
P53611_34|	RABGGTB	DB04464; DB07780; DB07841
P30626_68|	SRI	DB11093; DB11348
P23368_26|	ME2	DB00157; DB01677; DB03499; DB03589; DB03680
P26440_146|	IVD	DB03147; DB04036
P34932_185|P34932_332|P34932_674|P34932_719|P34932_430|P34932_53|P34932_679|P34932_754|P34932_766|P34932_356|P34932_388|P34932_437|P34932_668|P34932_353|P34932_477|	HSPA4	DB12695
P09110_198|	ACAA1	DB09069

P10412_46|P10412_52|P10412_63|P10412_64|P10412_85|P10412_90|P10412_97|P10412_106|P10412_110|P10412_117|P10412_119|P10412_127|P10412_136|P10412_148|P10412_156|P10412_168|P10412_186|P10412_197|P10412_213|P10412_81|P10412_122|P10412_153|P10412_180|P10412_190|P10412_195|P10412_200|P10412_210|P10412_129|P10412_130|	HIST1H1E	DB09130
P32119_10|P32119_26|P32119_177|P32119_16|P32119_92|P32119_135|P32119_34|P32119_67|	PRDX2	DB02153; DB04048; DB09130

P07900_414|P07900_631|P07900_632|P07900_418|P07900_443|P07900_489|P07900_539|P07900_585|P07900_576|P07900_74|P07900_84|P07900_208|P07900_436|P07900_458|P07900_513|P07900_534|P07900_546|P07900_559|P07900_204|P07900_485|P07900_209|P07900_478|P07900_657|P07900_693|P07900_314|P07900_419|P07900_58|P07900_560|P07900_558|	HSP90AA1	DB00615; DB00716; DB02359; DB02424; DB02550; DB02754; DB02840; DB03093; DB03137; DB03504; DB03749; DB03809; DB03899; DB04054; DB04216; DB04254; DB04505; DB04588; DB05134; DB06070; DB06956; DB06957; DB06958; DB06961; DB06964; DB06969; DB07100; DB07317; DB07319; DB07324; DB07325; DB07495; DB07502; DB07594; DB07601; DB07877; DB08194; DB08197; DB08436; DB08442; DB08443; DB08557; DB08786; DB08787; DB08788; DB08789; DB09130; DB09221; DB12442
P14618_62|P14618_66|P14618_115|P14618_247|P14618_261|P14618_305|P14618_89|P14618_135|P14618_141|P14618_188|P14618_136|P14618_256|P14618_125|P14618_206|P14618_224|P14618_336|P14618_504|P14618_166|P14618_162|P14618_186|P14618_367|P14618_230|	PKM	DB00119; DB01733; DB02726; DB07628; DB07692; DB07697; DB09130; DB11638

P27824_118|P27824_127|P27824_170|P27824_182|P27824_398|P27824_515|P27824_99|P27824_199|P27824_210|	CANX	DB00025; DB00031; DB06245; DB11093; DB11348; DB13998; DB13999
Q08257_116|	CRYZ	DB00266; DB03461
P35754_20|	GLRX	DB00143
P40925_110|P40925_236|P40925_107|P40925_205|P40925_214|P40925_220|P40925_298|	MDH1	DB00157; DB03461; DB11638
P40926_74|P40926_78|P40926_91|P40926_157|P40926_165|P40926_185|P40926_203|P40926_215|P40926_239|P40926_297|P40926_301|P40926_307|P40926_314|P40926_324|P40926_329|P40926_105|P40926_335|P40926_328|	MDH2	DB00157; DB04272; DB09092
P63244_12|P63244_185|P63244_264|P63244_271|P63244_183|	RACK1	DB09130
O15382_156|O15382_377|O15382_111|	BCAT2	DB00114; DB00142; DB00149; DB00167; DB02142; DB02635; DB04074
O95865_51|	DDAH2	DB00155
O15144_295|	ARPC2	DB08235; DB08236
P26639_279|P26639_273|P26639_222|P26639_319|	TARS	DB00156

P39019_23|P39019_29|P39019_143|P39019_122|P39019_111|	RPS19	DB11638
O75521_92|O75521_51|O75521_62|O75521_335|O75521_177|	ECI2	DB08231
P61024_11|	CKS1B	DB00472; DB02681
Q9NVS9_100|Q9NVS9_186|	PNPO	DB00114; DB03247; DB03345
P00558_41|P00558_75|P00558_91|P00558_131|P00558_139|P00558_141|P00558_156|P00558_191|P00558_199|P00558_267|P00558_279|P00558_291|P00558_323|P00558_11|P00558_15|P00558_30|P00558_48|P00558_56|P00558_133|P00558_146|P00558_192|P00558_353|P00558_361|P00558_382|P00558_97|P00558_106|P00558_264|P00558_297|P00558_388|	PGK1	DB03909; DB04510; DB09130; DB11638
P41091_275|	EIF2S3	DB04315
Q96AE4_248|Q96AE4_591|Q96AE4_400|Q96AE4_233|	FUBP1	DB05786

Q92945_627|Q92945_628|Q92945_653|Q92945_281|Q92945_203|Q92945_473|Q92945_448|Q92945_291|Q92945_646|	KHSRP	DB02709; DB11638
Q99798_144|Q99798_409|Q99798_605|Q99798_730|Q99798_520|Q99798_689|Q99798_739|	ACO2	DB01727; DB03964; DB04072; DB04351; DB04562
P12277_304|P12277_101|P12277_242|P12277_267|P12277_298|P12277_307|P12277_313|P12277_265|	CKB	DB00148; DB13191
P09012_60|P09012_80|P09012_114|	SNRPA	DB02175
P48637_172|	GSS	DB00143; DB00145; DB00151; DB03408; DB04395; DB06151; DB09130
Q9Y266_53|Q9Y266_93|Q9Y266_268|Q9Y266_123|Q9Y266_160|Q9Y266_297|Q9Y266_315|Q9Y266_96|	NUDC	DB12695

P35579_30|P35579_29|P35579_910|P35579_1129|P35579_1445|P35579_1862|P35579_403|P35579_909|P35579_1024|P35579_1212|P35579_1240|P35579_1249|P35579_1775|P35579_1793|P35579_1806|P35579_1918|P35579_1802|P35579_79|P35579_299|P35579_637|P35579_682|P35579_860|P35579_938|P35579_1132|P35579_1404|P35579_1441|P35579_1477|P35579_1716|P35579_1754|P35579_102|P35579_186|P35579_560|P35579_1081|P35579_1193|P35579_1234|P35579_63|P35579_355|P35579_821|P35579_992|	MYH9	DB11638
P49720_77|	PSMB3	DB08515
Q14571_1662|	ITPR2	DB00201
Q06323_13|Q06323_190|Q06323_35|	PSME1	DB09130
O43175_289|O43175_394|O43175_21|O43175_351|O43175_58|O43175_384|	PHGDH	DB00157
P10599_94|P10599_39|P10599_8|P10599_96|	TXN	DB12695

P30405_67|P30405_91|P30405_183|	PPIF	DB00091; DB00172; DB02078; DB08168
O00182_88|	LGALS9	DB04472
Q13564_381|	NAE1	DB00171
Q9H4G4_53|	GLIPR2	DB03661
P23381_27|P23381_47|	WARS	DB00150; DB01831; DB04537
Q9NSD9_560|	FARSB	DB00120
P14927_96|	UQCRB	DB04141; DB04799; DB07401; DB07636; DB07763; DB07778; DB08330; DB08453; DB08690
P62942_53|P62942_45|P62942_35|P62942_48|	FKBP1A	DB00337; DB00864; DB00877; DB01712; DB01723; DB01951; DB02311; DB02888; DB03338; DB03621; DB04012; DB04094; DB05814; DB08231; DB08520; DB08597
P23526_389|P23526_20|P23526_43|P23526_46|	AHCY	DB02325; DB03216; DB03273; DB03769; DB09130
P09874_23|P09874_196|P09874_621|P09874_97|P09874_108|P09874_192|P09874_249|P09874_683|P09874_653|P09874_87|P09874_940|	PARP1	DB00277; DB01593; DB02498; DB02690; DB02701; DB03072; DB03073; DB03509; DB03722; DB04010; DB07096; DB07232; DB07330; DB07787; DB09074; DB11793; DB12332; DB13877

P23528_19|P23528_30|P23528_44|P23528_45|P23528_73|P23528_92|P23528_112|P23528_114|P23528_127|P23528_144|P23528_22|P23528_78|P23528_121|P23528_132|P23528_152|P23528_95|	CFL1	DB04147; DB09130; DB11638
P15170_247|P15170_103|P15170_208|P15170_490|P15170_72|P15170_138|P15170_254|P15170_238|	GSPT1	DB04315
O14949_82|	UQCRQ	DB04141; DB04799; DB07401; DB07763; DB07778; DB08330; DB08453; DB08690
Q12874_92|	SF3A3	DB12695
P22695_21|P22695_42|	UQCRC2	DB04141; DB04799; DB07401; DB07763; DB07778; DB08330; DB08453; DB08690
P49257_87|P49257_346|	LMAN1	DB00025; DB13998; DB13999
P16615_400|P16615_120|P16615_510|P16615_502|	ATP2A2	DB06157
Q14697_472|	GANAB	DB00491
P62269_91|P62269_150|	RPS18	DB11638
P08758_309|P08758_97|P08758_101|P08758_290|P08758_301|P08758_70|	ANXA5	DB02497; DB02846; DB02929; DB03484; DB03935; DB03959; DB03981; DB09130

P36507_88|	MAP2K2	DB06616; DB08911; DB11967; DB12010
Q02880_1327|	TOP2B	DB00380; DB00694; DB00773; DB04395; DB05022; DB05488; DB06042; DB06362; DB06421; DB08651
Q02880_1327|	TOP2B	DB00970
P23284_89|	PPIB	DB00172; DB04447
Q9BWD1_180|Q9BWD1_235|Q9BWD1_136|	ACAT2	DB01915; DB01992
O14818_115|	PSMA7	DB07558; DB08515
P09622_430|P09622_146|P09622_155|P09622_159|P09622_166|P09622_277|	DLD	DB00157; DB03147
P08243_379|P08243_385|	ASNS	DB00128; DB00142; DB00171; DB00174
P09429_29|P09429_30|P09429_55|P09429_59|P09429_88|P09429_114|P09429_127|P09429_128|P09429_157|P09429_165|P09429_167|P09429_172|P09429_177|P09429_12|P09429_43|P09429_65|P09429_82|P09429_90|P09429_154|P09429_180|P09429_7|P09429_50|P09429_146|P09429_112|P09429_150|P09429_68|P09429_147|P09429_44|	HMGB1	DB05869

P36578_29|P36578_364|P36578_368|P36578_374|P36578_375|P36578_380|P36578_399|P36578_412|P36578_411|P36578_423|P36578_348|P36578_390|P36578_405|	RPL4	DB11638
P17252_197|P17252_209|P17252_35|	PRKCA	DB00144; DB00163; DB05013; DB06451; DB06595; DB06641; DB08846; DB14001; DB14002
P17252_197|P17252_209|P17252_35|	PRKCA	DB00675
P49840_355|	GSK3A	DB12010
P30086_47|P30086_80|P30086_132|	PEBP1	DB09130
P12004_80|P12004_77|P12004_168|	PCNA	DB00279
P43487_179|P43487_111|P43487_50|P43487_68|P43487_150|P43487_190|P43487_76|	RANBP1	DB09130; DB12695
P11766_366|P11766_120|P11766_357|	ADH5	DB00157; DB03017; DB03704; DB04153
P13929_60|	ENO3	DB01709; DB01819; DB02726; DB03645

P06576_124|P06576_133|P06576_161|P06576_159|P06576_259|P06576_350|P06576_351|P06576_480|P06576_485|P06576_522|P06576_264|P06576_432|	ATP5B	DB04216; DB07384; DB07394; DB08399; DB08629; DB12695
P60900_102|	PSMA6	DB08515
P47985_168|	UQCRFS1	DB04141; DB04799; DB07401; DB07636; DB07763; DB07778; DB08330; DB08453; DB08690
P62258_69|P62258_215|P62258_123|P62258_50|P62258_73|P62258_142|P62258_118|P62258_153|P62258_78|P62258_125|	YWHAE	DB01780; DB12695
Q969G3_123|	SMARCE1	DB12695

Table 4.7. non-DBP domain enrichment.

ProRule Domain	Number Liganded	Number in Database	Database Frequency	P-Value	Description	BH Corrected Q-Value
PRU00691	6	37	0.00259267	2.45E-07	thioredoxin domain	1.37E-05
PRU00156	4	26	0.00182188	3.33E-05	PPIase cyclophilin-type domain	0.000933626
PRU00531	2	2	0.00014014	9.06E-05	WHEP-TRS domain	0.001463421
PRU01059	3	13	0.00091094	0.000105	Translational (tr)-type guanine nucleotide-binding (G) domain	0.001463421
PRU00282	2	3	0.00021022	0.000203	Solute carrier (Solcar) repeat	0.002273982

PRU00159	12	539	0.0377689	0.000304	Protein kinase domain	0.002833847
PRU00176	7	244	0.01709761	0.001436	RNA recognition motif (RRM) domain	0.011484922
PRU00117	3	39	0.00273282	0.002484	KH domain	0.017391087
PRU00599	2	12	0.00084087	0.003122	ADF-H domain	0.019424682
PRU01134	2	17	0.00119123	0.006129	Alpha-carbonic anhydrase domain	0.034321463
PRU00264	1	2	0.00014014	0.013503	Zinc finger PARP-type	0.050411052
PRU00209	1	2	0.00014014	0.013503	tRNA-binding domain	0.050411052
PRU00182	1	2	0.00014014	0.013503	S4 RNA-binding	0.050411052
PRU01151	1	2	0.00014014	0.013503	Pyruvate carboxyltransferase domain	0.050411052
PRU00666	1	2	0.00014014	0.013503	B12-binding domain	0.050411052
PRU01133	1	3	0.00021022	0.020187	Translationally controlled tumor protein (TCTP) domain	0.056522515
PRU01170	1	3	0.00021022	0.020187	Peripheral subunit-binding (PSBD) domain	0.056522515
PRU00278	1	3	0.00021022	0.020187	PpiC domain	0.056522515
PRU00605	1	3	0.00021022	0.020187	Glutamine amidotransferase (GATase) type 1 domain	0.056522515
PRU01202	1	3	0.00021022	0.020187	MGS-like domain	0.056522515
PRU00280	1	4	0.00028029	0.026825	Heavy-metal-associated domain	0.065314128
PRU00843	1	4	0.00028029	0.026825	Phosphagen kinase C-terminal domain	0.065314128
PRU00398	1	4	0.00028029	0.026825	PARP alpha-helical domain	0.065314128
PRU01138	1	5	0.00035036	0.03342	CoA carboxyltransferase domain	0.071981015
PRU00658	1	5	0.00035036	0.03342	L-type lectin-like (leguminous) domain	0.071981015
PRU00107	1	5	0.00035036	0.03342	Histidine kinase core domain	0.071981015
PRU00782	2	46	0.00322332	0.039537	Myosin motor domain	0.079939685
PRU01163	1	6	0.00042043	0.03997	Vicinal oxygen chelate (VOC) domain	0.079939685
PRU00542	3	117	0.00819844	0.046032	Helicase C-terminal domain	0.081332992

PRU00465	1	7	0.00049051	0.046476	2Fe-2S ferredoxin-type domain	0.081332992
PRU00464	1	7	0.00049051	0.046476	HIT	0.081332992
PRU00534	1	7	0.00049051	0.046476	FAT domain	0.081332992
PRU00541	3	123	0.00861888	0.051977	Helicase ATP-binding domain	0.088203823
PRU00267	2	59	0.00413426	0.061492	HMG boxes A and B DNA-binding domains	0.101281112
PRU00573	1	10	0.00070072	0.065734	Acyl-CoA-binding (ACB) domain	0.103480944
PRU00409	1	11	0.00077079	0.072067	ATP-grasp domain	0.103480944
PRU00164	1	11	0.00077079	0.072067	RanBD1	0.103480944
PRU00686	1	11	0.00077079	0.072067	Glutaredoxin domain	0.103480944
PRU00130	1	11	0.00077079	0.072067	Zinc finger matrin-type	0.103480944
PRU00214	2	67	0.00469484	0.076622	Ubiquitin-like	0.107270586
PRU00837	1	16	0.00112116	0.103102	Linker histone H1/H5 globular (H15) domain	0.1374692
PRU00239	1	16	0.00112116	0.103102	Cysteine proteinase calpain-type catalytic domain	0.1374692
PRU00397	1	17	0.00119123	0.109184	PARP catalytic domain	0.138962033
PRU00277	1	17	0.00119123	0.109184	PPIase FKBP-type domain	0.138962033
PRU00547	1	18	0.0012613	0.115226	CS domain	0.143392581
PRU00639	1	19	0.00133137	0.121227	Galactoside-binding lectin (galectin) domain	0.147581123
PRU01190	1	22	0.00154159	0.13899	Myosin N-terminal SH3-like domain	0.165605351
PRU00803	1	23	0.00161166	0.144832	FG-GAP repeat	0.168970462
PRU00044	2	109	0.00763787	0.169776	Calponin-homology (CH) domain	0.194029976
PRU00794	1	28	0.00196202	0.173457	Nudix hydrolase domain	0.194271503
PRU00441	1	31	0.00217224	0.190174	ABC transporter integral membrane type-1 domain	0.204803069
PRU00162	1	31	0.00217224	0.190174	PWWP	0.204803069
PRU01188	1	81	0.00567585	0.424275	Intermediate filament (IF) rod domain	0.448290741

PRU00191	1	108	0.0075678	0.521389	SH2 domain	0.540700071
PRU00041	1	139	0.00974003	0.613032	C2 domain	0.624178452
PRU00145	1	293	0.02053115	0.726505	PH	0.726505089

Table 4.8. DBP

ProRule Domain	Number Liganded	Number in Database	Database Frequency	P-Value	Description	BH Corrected Q-Value
PRU00176	32	244	0.017097611	1.08E-21	RNA recognition motif (RRM) domain	1.10E-19
PRU01185	8	26	0.001821877	4.19E-09	PCI domain	2.13E-07
PRU00117	5	39	0.002732815	0.000226	KH domain	0.005773005
PRU00042	1	811	0.056828533	0.000276	Zinc finger C2H2-type	0.005773005
PRU01040	3	9	0.00063065	0.000283	DZF domain	0.005773005
PRU00410	3	11	0.000770794	0.000506	WH1 domain	0.008608284
PRU00599	3	12	0.000840866	0.000651	ADF-H domain	0.009483363
PRU00998	2	4	0.000280289	0.001448	Stathmin-like (SLD) domain	0.018461742
PRU00691	4	37	0.00259267	0.001815	thioredoxin domain	0.020565021
PRU00526	2	6	0.000420433	0.0032	BRO1 domain	0.032637449
PRU00532	3	23	0.00161166	0.004104	Gcn5-related N-acetyltransferase (GNAT) domain	0.036687702
PRU00507	2	7	0.000490505	0.004316	NAC-A/B (NAC-alpha/beta) domain	0.036687702
PRU00542	6	117	0.008198444	0.005915	Helicase C-terminal domain	0.046412415
PRU00813	1	1	7.01E-05	0.013641	DhaL domain	0.073229224
PRU01006	1	1	7.01E-05	0.013641	Clathrin heavy-chain (CHCR) repeat	0.073229224
PRU01145	1	1	7.01E-05	0.013641	Zinc finger C2HC LYAR-type	0.073229224
PRU00272	1	1	7.01E-05	0.013641	Thermonuclease domain	0.073229224
PRU00519	1	1	7.01E-05	0.013641	Elongation factor 1 (EF-1) gamma C-terminal domain	0.073229224

PRU00118	1	1	7.01E-05	0.013641	KH type-2 domain	0.073229224
PRU00984	2	14	0.00098101	0.016215	DHR-2 domain	0.082698347
PRU00044	5	109	0.007637867	0.017988	Calponin-homology (CH) domain	0.087372215
PRU00115	2	16	0.001121155	0.020805	Importin N-terminal	0.096459698
PRU00277	2	17	0.001191227	0.023279	PPIase FKBP-type domain	0.099141488
PRU00160	3	44	0.003083176	0.023327	Protein-tyrosine phosphatase domain	0.099141488
PRU00547	2	18	0.001261299	0.025867	CS domain	0.100560057
PRU00386	1	2	0.000140144	0.027096	SGS domain	0.100560057
PRU00734	1	2	0.000140144	0.027096	CHORD domain	0.100560057
PRU00286	3	47	0.003293392	0.027605	dnaJ domain	0.100560057
PRU00278	1	3	0.000210217	0.040369	PpiC domain	0.137255665
PRU01175	1	3	0.000210217	0.040369	HD domain	0.137255665
PRU00267	3	59	0.004134258	0.048557	HMG boxes A and B DNA-binding domains	0.159767925
PRU01094	1	4	0.000280289	0.053462	Letm1 ribosome-binding (RBD) domain	0.161254404
PRU00627	1	4	0.000280289	0.053462	PWI domain	0.161254404
PRU00266	2	27	0.001891949	0.053751	Double stranded RNA-binding domain	0.161254404
PRU00100	2	29	0.002032093	0.06093	Guanylate kinase-like domain	0.173601875
PRU00214	3	67	0.004694836	0.065793	Ubiquitin-like	0.173601875
PRU00711	1	5	0.000350361	0.066377	4Fe-4S ferredoxin-type domain	0.173601875
PRU00231	1	5	0.000350361	0.066377	Longin domain	0.173601875
PRU00972	1	5	0.000350361	0.066377	MRG domain	0.173601875
PRU00132	1	6	0.000420433	0.079117	MSP	0.183407416
PRU00369	1	6	0.000420433	0.079117	BAG domain	0.183407416
PRU00170	1	6	0.000420433	0.079117	Reticulon	0.183407416
PRU00378	1	6	0.000420433	0.079117	DDHD domain	0.183407416

PRU01187	1	6	0.000420433	0.079117	Lamin-tail (LTD) domain	0.183407416
PRU00541	4	123	0.008618877	0.090752	Helicase ATP-binding domain	0.198973129
PRU01047	1	7	0.000490505	0.091684	OBG-type guanine nucleotide-binding (G) domain	0.198973129
PRU01106	1	7	0.000490505	0.091684	HotDog acyl-CoA thioesterase (ACOT)-type domain	0.198973129
PRU00332	1	8	0.000560577	0.10408	La-type HTH domain	0.20815968
PRU00385	1	8	0.000560577	0.10408	KASH domain	0.20815968
PRU00698	1	8	0.000560577	0.10408	MI domain	0.20815968
PRU01228	1	8	0.000560577	0.10408	PRU01228	0.20815968
PRU00137	1	9	0.00063065	0.116308	NTF2	0.219692246
PRU00695	1	9	0.00063065	0.116308	W2 domain	0.219692246
PRU00240	1	9	0.00063065	0.116308	Adenosine to inosine editase domain	0.219692246
PRU00579	1	10	0.000700722	0.128369	Rho GTPase-binding/formin homology 3 (GBD/FH3) domain	0.229713717
PRU00573	1	10	0.000700722	0.128369	Acyl-CoA-binding (ACB) domain	0.229713717
PRU00781	1	10	0.000700722	0.128369	Phosphatidylinositol phosphate kinase (PIPK) domain	0.229713717
PRU00045	1	11	0.000770794	0.140267	CAP-Gly	0.238454571
PRU01015	1	11	0.000770794	0.140267	SAM-dependent methyltransferase PRMT-type domain	0.238454571
PRU00686	1	11	0.000770794	0.140267	Glutaredoxin domain	0.238454571
PRU00221	1	12	0.000840866	0.152004	WD repeat	0.250070712
PRU00370	1	12	0.000840866	0.152004	BAH domain	0.250070712
PRU00434	2	52	0.003643753	0.160564	ABC transporter family domain	0.255000636
PRU00649	1	13	0.000910938	0.163581	TFIIS N-terminal domain	0.255000636
PRU01059	1	13	0.000910938	0.163581	Translational (tr)-type guanine nucleotide-binding (G) domain	0.255000636
PRU00084	2	54	0.003783897	0.170229	FERM	0.255000636

PRU00983	1	14	0.00098101	0.175	DHR-1 domain	0.255000636
PRU00774	1	14	0.00098101	0.175	Formin homology-2 (FH2) domain	0.255000636
PRU00404	1	14	0.00098101	0.175	Mu homology domain (MHD)	0.255000636
PRU01056	1	14	0.00098101	0.175	Septin-type guanine nucleotide-binding (G) domain	0.255000636
PRU00568	1	15	0.001051083	0.186265	TTL domain	0.267591992
PRU01083	1	16	0.001121155	0.197377	Cytidine and deoxycytidylate deaminases domain	0.272059582
PRU00167	1	16	0.001121155	0.197377	Ras-GAP	0.272059582
PRU00837	1	16	0.001121155	0.197377	Linker histone H1/H5 globular (H15) domain	0.272059582
PRU00175	1	298	0.020881508	0.201164	Zinc finger RING-type	0.273583156
PRU01055	1	17	0.001191227	0.208337	Dynamin-type guanine nucleotide-binding (G) domain	0.279610372
PRU01082	1	18	0.001261299	0.219149	PPM-type phosphatase domain	0.286579196
PRU01182	1	18	0.001261299	0.219149	MPN (Mpr1 Pad1 N-terminal) domain	0.286579196
PRU00361	1	20	0.001401443	0.240333	BAR domain	0.310303838
PRU00186	1	25	0.001751804	0.290826	SAP	0.370803497
PRU00156	1	26	0.001821877	0.300517	PPIase cyclophilin-type domain	0.378428544
PRU01188	2	81	0.005675846	0.305649	Intermediate filament (IF) rod domain	0.38019734
PRU00322	1	29	0.002032093	0.328805	Zinc finger RanBP2-type	0.39926313
PRU01077	1	29	0.002032093	0.328805	F-BAR domain	0.39926313
PRU00162	1	31	0.002172237	0.347028	PWWP	0.416434068
PRU00047	1	33	0.002312382	0.36476	Zinc finger CCHC-type	0.432621761
PRU00316	1	221	0.015485951	0.38104	FN3 domain	0.446736752
PRU00127	1	36	0.002522598	0.390462	MAGE	0.452580919
PRU00145	2	293	0.020531147	0.448602	PH	0.511244822
PRU00124	1	44	0.003083176	0.454054	LDL-receptor class A	0.511244822

PRU00159	5	539	0.037768902	0.456111	Protein kinase domain	0.511244822
PRU00782	1	46	0.00322332	0.468893	Myosin motor domain	0.519859245
PRU00163	1	50	0.003503609	0.497376	Rab-GAP TBC	0.545509271
PRU00035	1	54	0.003783897	0.524339	Bromodomain	0.568963973
PRU00224	1	68	0.004764908	0.607867	WW/rsp5/WWP domain	0.652657136
PRU00143	1	177	0.012402775	0.738909	PDZ	0.785091104
PRU00548	1	108	0.007567795	1	B30.2/SPRY domain	1
PRU00448	3	230	0.0161166	1	EF-hand	1
PRU00041	1	139	0.009740032	1	C2 domain	1
PRU00125	1	87	0.006096279	1	LIM zinc-binding domain	1
PRU00024	1	86	0.006026207	1	Zinc finger B-box-type	1
PRU00192	3	258	0.018078621	1	Src homology 3 (SH3) domain	1

Table 4.9. Subcellular location of HHS-465 and HHS-475 probe modified lysines.

Protein	Compartment Code	Compartment
P54577	C	Cytosol
Q96I99	PM	Plasma Membrane
Q15691	SK	Cytoskeleton
O75643	NINT	Nuclear Lumen
P68363	SK	Cytoskeleton
Q9Y3U8	C	Cytosol
P54578	C	Cytosol
P40227	SK	Cytoskeleton
Q9HB71	C	Cytosol
P08575	PM	Plasma Membrane
P13693	C	Cytosol
P57737	C	Cytosol
O14832	C	Cytosol
Q8WZ42	C	Cytosol
P61970	C	Cytosol
P62753	C	Cytosol
P62750	C	Cytosol
P22392	C	Cytosol

Q5VYK3	ML2	Multiple Organelles
P04075	SK	Cytoskeleton
P61978	C	Cytosol
P08183	PM	Plasma Membrane
P07910	SK	Cytoskeleton
P84077	C	Cytosol
P13995	M	Mitochondria
P20073	C	Cytosol
Q14247	SK	Cytoskeleton
P78371	SK	Cytoskeleton
Q8N5F7	C	Cytosol
P19623	C	Cytosol
P52209	C	Cytosol
P78406	C	Cytosol
Q9Y2R5	MINT	Mitochondria Lumen
P50213	M	Mitochondria
Q00535	SK	Cytoskeleton
Q9NXR1	SK	Cytoskeleton
Q9Y2R9	MINT	Mitochondria Lumen
P60900	C	Cytosol
P30049	M	Mitochondria
P30048	C	Cytosol
Q9UHB9	C	Cytosol
Q8N8S7	SK	Cytoskeleton
P0C0S8	NINT	Nuclear Lumen
O43283	C	Cytosol
P41250	C	Cytosol
P30040	PM	Plasma Membrane
P41252	C	Cytosol
P30042	M	Mitochondria
O75190	C	Cytosol
Q12931	M	Mitochondria
Q9Y678	C	Cytosol
Q13011	C	Cytosol
P40429	C	Cytosol
Q9BV20	C	Cytosol
Q9C0D2	SK	Cytoskeleton
Q13838	C	Cytosol
P08574	M	Mitochondria
O75351	C	Cytosol
Q8N163	C	Cytosol
P62258	C	Cytosol
Q14790	SK	Cytoskeleton
Q6ZMR3	C	Cytosol
P09110	C	Cytosol
Q9Y696	SK	Cytoskeleton

Q93009	C	Cytosol
P19784	C	Cytosol
Q5K651	C	Cytosol
P62873	C	Cytosol
P05388	C	Cytosol
P62979	C	Cytosol
Q9GZR7	C	Cytosol
Q15003	C	Cytosol
Q07002	C	Cytosol
P15121	C	Cytosol
O95456	C	Cytosol
P20618	C	Cytosol
P52272	NINT	Nuclear Lumen
O95453	C	Cytosol
P67809	C	Cytosol
Q9H444	C	Cytosol
Q99426	SK	Cytoskeleton
P25786	C	Cytosol
P25787	C	Cytosol
Q15366	C	Cytosol
P25789	C	Cytosol
Q8TDX7	SK	Cytoskeleton
Q15365	C	Cytosol
P07766	PM	Plasma Membrane
O75794	C	Cytosol
P29401	C	Cytosol
Q9UMS4	C	Cytosol
P14735	C	Cytosol
Q9P2J5	C	Cytosol
Q9Y520	C	Cytosol
Q9Y487	PM	Plasma Membrane
P39023	C	Cytosol
O75436	C	Cytosol
P35241	PM	Plasma Membrane
O75533	NINT	Nuclear Lumen
P61158	SK	Cytoskeleton
O75821	C	Cytosol
O00571	C	Cytosol
Q96AC1	C	Cytosol
O95817	C	Cytosol
P09651	C	Cytosol
Q9UFN0	C	Cytosol
Q96CS3	ER	Endoplasmic Reticulum
Q15024	C	Cytosol
A6NDG6	C	Cytosol
P49643	NINT	Nuclear Lumen

P62807	C	Cytosol
P62805	NINT	Nuclear Lumen
O60610	SK	Cytoskeleton
Q14103	C	Cytosol
O94776	NINT	Nuclear Lumen
P31946	C	Cytosol
Q06203	C	Cytosol
P67936	SK	Cytoskeleton
P23526	C	Cytosol
P68104	C	Cytosol
P27635	C	Cytosol
Q9BXW7	M	Mitochondria
O60814	C	Cytosol
O14980	C	Cytosol
P36542	M	Mitochondria
Q9BUT1	C	Cytosol
Q9Y450	C	Cytosol
P63220	C	Cytosol
P11142	C	Cytosol
O43837	M	Mitochondria
Q96PU8	C	Cytosol
Q92930	C	Cytosol
P12268	C	Cytosol
P48643	SK	Cytoskeleton
Q96EK6	C	Cytosol
Q09161	C	Cytosol
Q8NFH4	C	Cytosol
Q13151	NINT	Nuclear Lumen
P25325	C	Cytosol
P50502	C	Cytosol
P34897	SK	Cytoskeleton
Q9H300	MINT	Mitochondria Lumen
A6NHG4	C	Cytosol
P49736	SK	Cytoskeleton
P13796	SK	Cytoskeleton
O95071	C	Cytosol
Q13601	C	Cytosol
O75899	C	Cytosol
Q9Y2L1	C	Cytosol
P06400	ML4	Multiple Organelle Lumens
Q14203	SK	Cytoskeleton
P17252	C	Cytosol
Q14204	SK	Cytoskeleton
Q9UII2	PM	Plasma Membrane
P09496	C	Cytosol
O60762	ER	Endoplasmic Reticulum

P62899	C	Cytosol
Q14566	NINT	Nuclear Lumen
P62841	C	Cytosol
Q9BUJ2	NINT	Nuclear Lumen
P00338	C	Cytosol
Q15185	C	Cytosol
P37268	ER	Endoplasmic Reticulum
O75947	M	Mitochondria
P09960	C	Cytosol
Q92841	C	Cytosol
P17844	C	Cytosol
P50570	SK	Cytoskeleton
P62269	C	Cytosol
P07814	C	Cytosol
Q86VP6	C	Cytosol
Q6UB35	M	Mitochondria
P30084	M	Mitochondria
P30086	C	Cytosol
O94903	C	Cytosol
P31146	C	Cytosol
Q2TAY7	C	Cytosol
P49257	ML2	Multiple Organelles
P22102	C	Cytosol
Q96IX5	M	Mitochondria
P06744	C	Cytosol
Q8NFC6	NINT	Nuclear Lumen
Q92522	NINT	Nuclear Lumen
Q13126	C	Cytosol
O43242	C	Cytosol
Q13033	C	Cytosol
Q8NEV1	NINT	Nuclear Lumen
P06748	C	Cytosol
Q9UPN3	SK	Cytoskeleton
P38432	NINT	Nuclear Lumen
P32322	M	Mitochondria
P46782	C	Cytosol
P32321	C	Cytosol
Q13085	SK	Cytoskeleton
Q9NQW7	C	Cytosol
Q13616	C	Cytosol
P26583	C	Cytosol
O43765	C	Cytosol
Q9H0A0	NINT	Nuclear Lumen
Q96C36	M	Mitochondria
Q9UBF2	C	Cytosol
Q02878	C	Cytosol

O00299	C	Cytosol
P07195	C	Cytosol
Q01844	C	Cytosol
Q7Z333	C	Cytosol
Q02750	SK	Cytoskeleton
Q96F07	C	Cytosol
O00244	C	Cytosol
Q07955	C	Cytosol
P16152	C	Cytosol
Q9BTT0	V	Vesicle
P35232	C	Cytosol
O14950	C	Cytosol
P33316	M	Mitochondria
P15927	ML4	Multiple Organelle Lumens
O95202	M	Mitochondria
Q02543	C	Cytosol
P30038	MINT	Mitochondria Lumen
P31689	SK	Cytoskeleton
Q9HAV4	C	Cytosol
Q15046	C	Cytosol
Q12802	C	Cytosol
P13073	M	Mitochondria
Q96P70	C	Cytosol
P26640	C	Cytosol
P46940	SK	Cytoskeleton
Q99460	C	Cytosol
Q9NTJ3	C	Cytosol
P0DN79	C	Cytosol
O95163	C	Cytosol
Q8WWV3	M	Mitochondria
O75369	SK	Cytoskeleton
P04083	C	Cytosol
P60709	SK	Cytoskeleton
Q00534	C	Cytosol
Q12965	SK	Cytoskeleton
P60866	C	Cytosol
P49915	C	Cytosol
Q96EY7	C	Cytosol
P13639	C	Cytosol
Q96EY1	C	Cytosol
P52907	SK	Cytoskeleton
O75131	C	Cytosol
P12277	C	Cytosol
P11586	C	Cytosol
P61353	C	Cytosol
P62847	C	Cytosol

P41567	C	Cytosol
P40763	C	Cytosol
P78417	C	Cytosol
P04181	M	Mitochondria
Q7KZ85	NINT	Nuclear Lumen
P14324	C	Cytosol
P60953	SK	Cytoskeleton
P23743	C	Cytosol
P38919	C	Cytosol
Q96SN8	SK	Cytoskeleton
P15880	C	Cytosol
Q8TCG1	C	Cytosol
P21912	PM	Plasma Membrane
P11940	C	Cytosol
P26641	C	Cytosol
Q6FI13	NINT	Nuclear Lumen
Q8WYP5	C	Cytosol
Q6P4I2	C	Cytosol
P05198	C	Cytosol
P62316	C	Cytosol
P55809	M	Mitochondria
Q13423	M	Mitochondria
P35268	C	Cytosol
P00505	PM	Plasma Membrane
Q15031	M	Mitochondria
P07437	SK	Cytoskeleton
P61758	C	Cytosol
P46779	C	Cytosol
Q6UB98	C	Cytosol
Q9Y490	SK	Cytoskeleton
Q9NVE7	C	Cytosol
P39748	M	Mitochondria
Q9NYU2	ML2	Multiple Organelles
Q13206	C	Cytosol
P23381	C	Cytosol
Q9GZM8	SK	Cytoskeleton
P22314	C	Cytosol
Q86SR1	GM	Golgi Apparatus Membrane
P50395	C	Cytosol
Q14847	C	Cytosol
P23528	C	Cytosol
P30101	PM	Plasma Membrane
P27797	C	Cytosol
P30041	C	Cytosol
P35606	C	Cytosol
O14737	C	Cytosol

P83111	C	Cytosol
P51532	NINT	Nuclear Lumen
P35219	C	Cytosol
P21675	NINT	Nuclear Lumen
P49773	SK	Cytoskeleton
Q9Y6K9	C	Cytosol
P62081	SK	Cytoskeleton
P78527	C	Cytosol
P25205	C	Cytosol
Q14320	NINT	Nuclear Lumen
P62993	C	Cytosol
P27707	C	Cytosol
Q16181	C	Cytosol
Q96SI9	SK	Cytoskeleton
P48739	ML3	Multiple Organelle Membranes
P27708	C	Cytosol
P16949	SK	Cytoskeleton
P30044	C	Cytosol
P09884	C	Cytosol
P17980	C	Cytosol
Q16775	C	Cytosol
Q96AG4	ML2	Multiple Organelles
O60884	C	Cytosol
Q16778	C	Cytosol
P17987	SK	Cytoskeleton
Q9Y4L1	ER	Endoplasmic Reticulum
Q92804	C	Cytosol
Q15813	SK	Cytoskeleton
Q9NR45	C	Cytosol
P00390	C	Cytosol
Q13283	C	Cytosol
P10768	V	Vesicle
Q9H0B6	SK	Cytoskeleton
Q9Y3Z3	PM	Plasma Membrane
P84098	C	Cytosol
Q709C8	C	Cytosol
P63173	C	Cytosol
Q13045	SK	Cytoskeleton
O00154	C	Cytosol
Q15269	NINT	Nuclear Lumen
P84095	C	Cytosol
P61221	C	Cytosol
P52566	SK	Cytoskeleton
O95747	C	Cytosol
P39019	C	Cytosol
P52565	SK	Cytoskeleton

Q14554	ERM	Endoplasmic Resticulum Membrane
Q6ZUM4	C	Cytosol
P61981	C	Cytosol
P55060	C	Cytosol
Q14258	C	Cytosol
P55786	C	Cytosol
P22626	C	Cytosol
P69905	C	Cytosol
P30519	PM	Plasma Membrane
O43502	C	Cytosol
Q02224	SK	Cytoskeleton
Q8NC51	C	Cytosol
P18669	C	Cytosol
O14776	NINT	Nuclear Lumen
Q96H79	C	Cytosol
P05141	PM	Plasma Membrane
Q9UQ80	C	Cytosol
P63241	C	Cytosol
P22033	M	Mitochondria
Q9UHD8	SK	Cytoskeleton
P37837	C	Cytosol
Q8IZP2	C	Cytosol
O75044	C	Cytosol
Q05209	C	Cytosol
P25705	PM	Plasma Membrane
Q96CW1	C	Cytosol
P12814	C	Cytosol
Q7Z4S6	SK	Cytoskeleton
Q9BRT2	M	Mitochondria
P31937	MINT	Mitochondria Lumen
O75323	M	Mitochondria
Q04837	M	Mitochondria
P48426	C	Cytosol
Q01813	C	Cytosol
P49792	C	Cytosol
Q53FA7	C	Cytosol
O43592	C	Cytosol
P40121	C	Cytosol
Q00341	C	Cytosol
Q00610	C	Cytosol
Q2KHM9	C	Cytosol
Q5SRE5	N	Nucleus
Q9C0B1	NINT	Nuclear Lumen
P14866	C	Cytosol
P09012	NINT	Nuclear Lumen
Q8N4J0	C	Cytosol

Q9UQ13	C	Cytosol
Q16543	C	Cytosol
Q52LJ0	C	Cytosol
P14868	C	Cytosol
P63104	C	Cytosol
P49321	C	Cytosol
P49458	C	Cytosol
Q9HBG6	C	Cytosol
Q13263	NINT	Nuclear Lumen
Q13303	SK	Cytoskeleton
P18124	C	Cytosol
P49454	C	Cytosol
Q9P0L0	SK	Cytoskeleton
Q14671	C	Cytosol
Q969G3	NINT	Nuclear Lumen
Q969T7	C	Cytosol
Q02790	SK	Cytoskeleton
Q9Y617	C	Cytosol
P31939	C	Cytosol
Q8N3U4	C	Cytosol
Q9UHV9	C	Cytosol
Q01105	C	Cytosol
P29350	C	Cytosol
Q9H1K4	MINT	Mitochondria Lumen
Q8IYB3	C	Cytosol
Q99961	C	Cytosol
P01130	PM	Plasma Membrane
P61160	SK	Cytoskeleton
Q9H773	C	Cytosol
P42766	C	Cytosol
P61163	SK	Cytoskeleton
P00846	MINT	Mitochondria Lumen
Q13094	C	Cytosol
Q9UNF1	C	Cytosol
Q99623	C	Cytosol
P36957	M	Mitochondria
Q9H9P8	M	Mitochondria
P31948	C	Cytosol
P18206	SK	Cytoskeleton
Q9UKM9	NINT	Nuclear Lumen
P04406	SK	Cytoskeleton
P46109	C	Cytosol
P35080	SK	Cytoskeleton
Q99613	C	Cytosol
P36551	C	Cytosol
P24539	M	Mitochondria

P11177	M	Mitochondria
P63218	PM	Plasma Membrane
P14550	C	Cytosol
P61769	C	Cytosol
P29692	C	Cytosol
O43847	C	Cytosol
P54819	MINT	Mitochondria Lumen
Q06830	C	Cytosol
Q06787	C	Cytosol
Q8WXH0	C	Cytosol
Q9H1E3	C	Cytosol
Q9NRN7	C	Cytosol
O75390	M	Mitochondria
Q92608	SK	Cytoskeleton
O75396	ML2	Multiple Organelles
P30520	C	Cytosol
Q14181	C	Cytosol
Q9BZD4	C	Cytosol
Q8TCC3	MINT	Mitochondria Lumen
Q14185	C	Cytosol
P08686	ERM	Endoplasmic Resticulum Membrane
Q9UPV0	C	Cytosol
O75886	C	Cytosol
P49748	C	Cytosol
Q9NZI8	C	Cytosol
P08133	C	Cytosol
Q9UL46	C	Cytosol
Q15428	NINT	Nuclear Lumen
Q99986	C	Cytosol
Q15785	C	Cytosol
P62701	C	Cytosol
P24534	C	Cytosol
P49411	M	Mitochondria
P49588	C	Cytosol
P49589	C	Cytosol
Q13573	NINT	Nuclear Lumen
P27694	NINT	Nuclear Lumen
O60508	NINT	Nuclear Lumen
P62277	C	Cytosol
P17858	C	Cytosol
Q9NZZ3	C	Cytosol
P09972	SK	Cytoskeleton
Q9H3K6	C	Cytosol
Q8NE71	C	Cytosol
P60842	C	Cytosol
Q15181	C	Cytosol

O75083	C	Cytosol
O00231	C	Cytosol
O00232	C	Cytosol
Q09028	C	Cytosol
P23588	C	Cytosol
P98171	SK	Cytoskeleton
P37108	C	Cytosol
P48507	C	Cytosol
P06733	C	Cytosol
P06730	C	Cytosol
P14174	C	Cytosol
Q04760	C	Cytosol
P06737	C	Cytosol
P22234	C	Cytosol
P55735	C	Cytosol
P55327	C	Cytosol
Q15555	SK	Cytoskeleton
Q01082	C	Cytosol
Q9UI08	SK	Cytoskeleton
P50991	SK	Cytoskeleton
P50990	SK	Cytoskeleton
P10606	M	Mitochondria
P50995	C	Cytosol
Q15257	C	Cytosol
P46781	C	Cytosol
A0AVT1	C	Cytosol
P42704	SK	Cytoskeleton
O43719	NINT	Nuclear Lumen
Q96C23	C	Cytosol
O75489	M	Mitochondria
Q9P2R7	M	Mitochondria
P40424	C	Cytosol
P31040	M	Mitochondria
P05114	C	Cytosol
O43707	C	Cytosol
P62888	C	Cytosol
Q9H3P7	ML2	Multiple Organelles
P51659	C	Cytosol
Q5SY16	NINT	Nuclear Lumen
Q9P260	V	Vesicle
Q8WVM8	C	Cytosol
P63261	SK	Cytoskeleton
Q02218	M	Mitochondria
O95373	C	Cytosol
P20700	N	Nucleus
P55884	C	Cytosol

P21796	PM	Plasma Membrane
Q9NVG8	C	Cytosol
Q7Z6Z7	C	Cytosol
Q86XL3	ER	Endoplasmic Reticulum
P46977	ERM	Endoplasmic Resticulum Membrane
P46821	SK	Cytoskeleton
Q9C0C9	C	Cytosol
P25788	C	Cytosol
Q71UI9	NINT	Nuclear Lumen
P49841	C	Cytosol
P43243	NINT	Nuclear Lumen
Q15459	NINT	Nuclear Lumen
Q14008	C	Cytosol
Q13813	SK	Cytoskeleton
Q9HAN9	NINT	Nuclear Lumen
P07737	SK	Cytoskeleton
Q86WX3	C	Cytosol
P62851	C	Cytosol
P0DMV8	C	Cytosol
P18621	C	Cytosol
P40939	M	Mitochondria
Q8NCW5	C	Cytosol
Q9BZJ0	NINT	Nuclear Lumen
P62857	C	Cytosol
Q93077	NINT	Nuclear Lumen
Q93079	C	Cytosol
P35221	SK	Cytoskeleton
P28062	C	Cytosol
P57076	SK	Cytoskeleton
O43447	C	Cytosol
P20674	MINT	Mitochondria Lumen
Q9NQC3	PM	Plasma Membrane
P52292	C	Cytosol
P35579	SK	Cytoskeleton
Q8WUA2	C	Cytosol
P09211	C	Cytosol
Q92888	C	Cytosol
P62913	C	Cytosol
O76003	C	Cytosol
P62917	C	Cytosol
Q10570	NINT	Nuclear Lumen
O15372	C	Cytosol
O15371	C	Cytosol
P49406	ML2	Multiple Organelles
Q15029	C	Cytosol
P62308	C	Cytosol

Q8N1F7	N	Nucleus
P62304	C	Cytosol
Q15027	V	Vesicle
Q13451	C	Cytosol
Q9BPW8	M	Mitochondria
P35914	C	Cytosol
P50552	SK	Cytoskeleton
Q86V81	C	Cytosol
P61604	M	Mitochondria
Q6IPU0	C	Cytosol
Q9Y277	M	Mitochondria
Q7Z7F7	MINT	Mitochondria Lumen
P63151	C	Cytosol
Q08AE8	SK	Cytoskeleton
Q9NTJ5	ML2	Multiple Organelles
P04080	C	Cytosol
Q8NI27	NINT	Nuclear Lumen
P22307	C	Cytosol
P23396	C	Cytosol
P00491	SK	Cytoskeleton
Q12849	C	Cytosol
Q9UJU6	C	Cytosol
O95831	C	Cytosol
P46459	C	Cytosol
P35611	C	Cytosol
Q16531	C	Cytosol
O14727	C	Cytosol
P53804	C	Cytosol
Q9NYZ3	C	Cytosol
Q9UHY7	C	Cytosol
O95433	C	Cytosol
Q01130	C	Cytosol
Q10713	M	Mitochondria
O00151	SK	Cytoskeleton
P48047	PM	Plasma Membrane
P17812	C	Cytosol
Q9UJZ1	SK	Cytoskeleton
O95260	C	Cytosol
P62987	C	Cytosol
P14314	ER	Endoplasmic Reticulum
P00367	C	Cytosol
P38606	C	Cytosol
P00813	C	Cytosol
P61088	C	Cytosol
P08670	SK	Cytoskeleton
P49327	C	Cytosol

P32969	C	Cytosol
P31930	C	Cytosol
Q9BSJ2	SK	Cytoskeleton
Q5JTV8	N	Nucleus
Q4VCS5	C	Cytosol
P04844	ERM	Endoplasmic Resticulum Membrane
Q16763	C	Cytosol
P04843	C	Cytosol
P09936	C	Cytosol
P35244	NINT	Nuclear Lumen
Q7L2H7	C	Cytosol
Q92499	C	Cytosol
Q9NUI1	C	Cytosol
Q13177	C	Cytosol
Q99536	M	Mitochondria
Q8IZX4	NINT	Nuclear Lumen
Q9BPX3	C	Cytosol
Q14019	SK	Cytoskeleton
Q5TCZ1	C	Cytosol
Q9Y3A2	C	Cytosol
P62424	C	Cytosol
Q96DT5	SK	Cytoskeleton
P08559	M	Mitochondria
Q9Y2T4	C	Cytosol
P07900	C	Cytosol
P61254	C	Cytosol
P68431	NINT	Nuclear Lumen
O95757	C	Cytosol
P21333	SK	Cytoskeleton
P27695	C	Cytosol
Q13625	C	Cytosol
P23246	C	Cytosol
Q00013	C	Cytosol
P49711	NINT	Nuclear Lumen
P31943	C	Cytosol
Q9P289	C	Cytosol
Q9H9T3	C	Cytosol
P55072	C	Cytosol
P30566	C	Cytosol
P84243	NINT	Nuclear Lumen
P24752	M	Mitochondria
Q9UNL2	ERM	Endoplasmic Resticulum Membrane
P51572	C	Cytosol
Q9H082	G	Golgi Apparatus
O94925	C	Cytosol
P52888	C	Cytosol

P27348	C	Cytosol
P38159	NINT	Nuclear Lumen
P47985	M	Mitochondria
Q14765	C	Cytosol
P52597	C	Cytosol
Q14152	SK	Cytoskeleton
Q5VTE0	C	Cytosol
P14625	C	Cytosol
Q9BXT5	C	Cytosol
Q9Y285	C	Cytosol
P51617	C	Cytosol
Q99714	C	Cytosol
O00267	NINT	Nuclear Lumen
Q5TCQ9	PM	Plasma Membrane
O00264	PM	Plasma Membrane
Q9UJV9	C	Cytosol
P48735	C	Cytosol
Q5THR3	NINT	Nuclear Lumen
O75431	M	Mitochondria
Q9NVP1	C	Cytosol
O75330	SK	Cytoskeleton
P11310	M	Mitochondria
Q07020	C	Cytosol
Q00059	C	Cytosol
Q12905	ML4	Multiple Organelle Lumens
Q9NSE4	C	Cytosol
Q6FI81	C	Cytosol
Q3LXA3	C	Cytosol
Q13325	SK	Cytoskeleton
Q9H0X9	C	Cytosol
O95573	C	Cytosol
Q86VS8	SK	Cytoskeleton
P13010	C	Cytosol
P10809	C	Cytosol
Q9NRX4	C	Cytosol
Q8WUM4	SK	Cytoskeleton
O14979	C	Cytosol
Q15631	C	Cytosol
O14874	M	Mitochondria
Q9Y2W1	NINT	Nuclear Lumen
Q96G03	C	Cytosol
P07237	PM	Plasma Membrane
O95347	C	Cytosol
Q15067	C	Cytosol
O95470	ER	Endoplasmic Reticulum
Q7L5N1	C	Cytosol

Q96LB3	V	Vesicle
P47756	SK	Cytoskeleton
Q04917	C	Cytosol
Q9Y237	C	Cytosol
P60174	C	Cytosol
Q93084	ML2	Multiple Organelles
Q13257	C	Cytosol
P49368	SK	Cytoskeleton
Q13310	C	Cytosol
P10515	M	Mitochondria
Q2M2Z5	C	Cytosol
Q14697	G	Golgi Apparatus
P05023	PM	Plasma Membrane
P11387	NINT	Nuclear Lumen
P45880	PM	Plasma Membrane
P78344	C	Cytosol
Q9NYF8	C	Cytosol
Q3L8U1	C	Cytosol
Q99497	C	Cytosol
Q14683	C	Cytosol
P26196	C	Cytosol
P52815	M	Mitochondria
P06493	C	Cytosol
Q96M27	G	Golgi Apparatus
P08237	C	Cytosol
P08865	C	Cytosol
P05455	C	Cytosol
P08238	C	Cytosol
Q14151	C	Cytosol
P08621	C	Cytosol
P28331	M	Mitochondria
P62829	C	Cytosol
Q9NZW5	PM	Plasma Membrane
P62820	C	Cytosol
Q15233	NINT	Nuclear Lumen
P06454	C	Cytosol
O14617	ML2	Multiple Organelles
P62826	C	Cytosol
P00918	C	Cytosol
Q13404	C	Cytosol
P51858	C	Cytosol
Q9Y4W2	C	Cytosol
Q9NY27	C	Cytosol
P52701	C	Cytosol
Q9Y4W6	M	Mitochondria
Q93034	C	Cytosol

P63167	SK	Cytoskeleton
Q9Y6G9	SK	Cytoskeleton
P63208	C	Cytosol
Q8NBS9	ER	Endoplasmic Reticulum
P14678	C	Cytosol
P28340	C	Cytosol
Q9H845	M	Mitochondria
Q92598	SK	Cytoskeleton
P33993	C	Cytosol
P33991	NINT	Nuclear Lumen
P12081	C	Cytosol
P50914	C	Cytosol
P47914	C	Cytosol
Q9UN37	C	Cytosol
Q6P996	G	Golgi Apparatus
P43490	C	Cytosol
P42677	C	Cytosol
O14656	SK	Cytoskeleton
P62633	C	Cytosol
P60981	SK	Cytoskeleton
P50851	PM	Plasma Membrane
P61513	C	Cytosol
P15924	SK	Cytoskeleton
Q9UBQ0	C	Cytosol
P49593	C	Cytosol
O15320	ERM	Endoplasmic Resticulum Membrane
P49591	C	Cytosol
P08243	C	Cytosol
Q99996	SK	Cytoskeleton
Q6UB99	C	Cytosol
O60664	C	Cytosol
P22830	M	Mitochondria
Q9UK45	C	Cytosol
Q9Y3F4	C	Cytosol
Q9NRV9	C	Cytosol
Q16204	SK	Cytoskeleton
P46063	C	Cytosol
Q07021	C	Cytosol
Q92688	C	Cytosol
Q9BXJ9	C	Cytosol
O75964	M	Mitochondria
P62249	C	Cytosol
Q8N183	M	Mitochondria
Q96A33	ER	Endoplasmic Reticulum
Q9UNH7	C	Cytosol
P12236	M	Mitochondria

O75746	M	Mitochondria
P12235	PM	Plasma Membrane
Q9H0D6	NINT	Nuclear Lumen
P68371	SK	Cytoskeleton
O43143	C	Cytosol
Q96RE9	NINT	Nuclear Lumen
O94966	C	Cytosol
P53611	C	Cytosol
Q32MZ4	SK	Cytoskeleton
P05408	V	Vesicle
Q8N0V3	M	Mitochondria
O15347	C	Cytosol
P55084	ML2	Multiple Organelles
Q99615	SK	Cytoskeleton
O75663	C	Cytosol
Q8IYB8	M	Mitochondria
P53597	C	Cytosol
Q96I24	C	Cytosol
P26368	NINT	Nuclear Lumen
P16401	NINT	Nuclear Lumen
Q14C86	C	Cytosol
P16403	NINT	Nuclear Lumen
P16402	NINT	Nuclear Lumen
Q9Y2A7	C	Cytosol
P23368	M	Mitochondria
Q14161	NINT	Nuclear Lumen
Q9H936	MINT	Mitochondria Lumen
Q8TEX9	C	Cytosol
P34932	C	Cytosol
P58876	C	Cytosol
P25398	C	Cytosol
Q96DI7	C	Cytosol
Q14651	C	Cytosol
P46783	C	Cytosol
Q96HC4	SK	Cytoskeleton
Q9BRX5	NINT	Nuclear Lumen
Q9NUJ1	C	Cytosol
P55263	C	Cytosol
P55265	C	Cytosol
P30626	C	Cytosol
P32119	C	Cytosol
O60841	C	Cytosol
P30050	C	Cytosol
P26373	C	Cytosol
P48556	C	Cytosol
O95149	C	Cytosol

Q99729	C	Cytosol
P14618	C	Cytosol
O75347	SK	Cytoskeleton
O15067	C	Cytosol
P27824	ER	Endoplasmic Reticulum
P25685	C	Cytosol
Q9UNS2	C	Cytosol
Q9H8S9	C	Cytosol
Q9Y5A7	C	Cytosol
P36578	C	Cytosol
P38117	C	Cytosol
Q9Y2X7	C	Cytosol
P51580	C	Cytosol
Q9Y6Y8	C	Cytosol
P13612	PM	Plasma Membrane
P62906	C	Cytosol
Q9UDR5	M	Mitochondria
Q9UIF9	C	Cytosol
P35754	C	Cytosol
P26038	SK	Cytoskeleton
Q9H2W6	M	Mitochondria
P40925	C	Cytosol
P62861	C	Cytosol
P40926	M	Mitochondria
P19338	NINT	Nuclear Lumen
O14929	C	Cytosol
P51991	C	Cytosol
P83731	C	Cytosol
Q96HS1	M	Mitochondria
Q00325	PM	Plasma Membrane
O00410	C	Cytosol
Q13362	C	Cytosol
Q96FJ2	SK	Cytoskeleton
P63244	C	Cytosol
O60563	NINT	Nuclear Lumen
P62333	C	Cytosol
O15382	M	Mitochondria
Q9NZ45	M	Mitochondria
O95865	SK	Cytoskeleton
O60234	VINT	Vesicle Lumen
P41091	C	Cytosol
O15144	SK	Cytoskeleton
Q9UIA9	C	Cytosol
Q96PK6	C	Cytosol
A8MWD9	NINT	Nuclear Lumen
Q14980	C	Cytosol

Q9Y265	SK	Cytoskeleton
P61956	NINT	Nuclear Lumen
P26639	SK	Cytoskeleton
Q13907	C	Cytosol
O14497	NINT	Nuclear Lumen
P13797	C	Cytosol
Q08211	SK	Cytoskeleton
Q13442	C	Cytosol
Q96KK5	NINT	Nuclear Lumen
P53004	C	Cytosol
P35580	C	Cytosol
P62263	C	Cytosol
Q9UBU8	NINT	Nuclear Lumen
P47813	C	Cytosol
Q01518	PM	Plasma Membrane
O75521	C	Cytosol
Q9BQE5	ERM	Endoplasmic Resticulum Membrane
P18077	C	Cytosol
P60228	C	Cytosol
Q00688	C	Cytosol
Q4G176	M	Mitochondria
Q13765	C	Cytosol
P61024	NINT	Nuclear Lumen
Q8N6H7	C	Cytosol
P51784	C	Cytosol
Q9NVS9	C	Cytosol
Q9UHX1	NINT	Nuclear Lumen
Q96A72	NINT	Nuclear Lumen
Q9UBT2	C	Cytosol
P56381	MINT	Mitochondria Lumen
Q16658	SK	Cytoskeleton
Q12874	NINT	Nuclear Lumen
P00558	C	Cytosol
Q99832	SK	Cytoskeleton
Q16891	M	Mitochondria
Q96AE4	NINT	Nuclear Lumen
P46108	SK	Cytoskeleton
Q92945	C	Cytosol
Q15084	C	Cytosol
O15318	C	Cytosol
Q99798	M	Mitochondria
Q9BX67	PM	Plasma Membrane
Q03001	SK	Cytoskeleton
P08708	C	Cytosol
Q9UQE7	C	Cytosol
Q99879	C	Cytosol

Q92785	C	Cytosol
Q16576	C	Cytosol
Q9UIG0	NINT	Nuclear Lumen
Q16352	N	Nucleus
P48637	C	Cytosol
Q9Y266	SK	Cytoskeleton
Q01469	C	Cytosol
O60306	NINT	Nuclear Lumen
Q92621	N	Nucleus
P61247	C	Cytosol
Q00839	PM	Plasma Membrane
O14744	C	Cytosol
P13984	SK	Cytoskeleton
Q9NQ75	SK	Cytoskeleton
Q7KZF4	C	Cytosol
P56192	C	Cytosol
P49720	C	Cytosol
P35573	C	Cytosol
P13804	M	Mitochondria
P0CG47	C	Cytosol
Q9HAV7	M	Mitochondria
Q14571	PM	Plasma Membrane
Q13526	C	Cytosol
Q13617	C	Cytosol
O75937	C	Cytosol
P15311	SK	Cytoskeleton
O75935	SK	Cytoskeleton
P53396	C	Cytosol
Q7L1Q6	C	Cytosol
P55160	C	Cytosol
O76021	NINT	Nuclear Lumen
Q06323	C	Cytosol
P07954	C	Cytosol
Q8TAQ2	NINT	Nuclear Lumen
O94913	C	Cytosol
Q9Y2Z0	C	Cytosol
P41227	C	Cytosol
O43175	C	Cytosol
P10599	C	Cytosol
Q8TDB6	C	Cytosol
P30405	M	Mitochondria
P31150	C	Cytosol
P83881	C	Cytosol
P31153	C	Cytosol
Q9H074	C	Cytosol
P49207	C	Cytosol

Q8WVJ2	SK	Cytoskeleton
P48444	C	Cytosol
Q8N5K1	ML2	Multiple Organelles
P53007	MINT	Mitochondria Lumen
Q9HC36	M	Mitochondria
Q13098	C	Cytosol
Q9HC35	SK	Cytoskeleton
Q9NTK5	C	Cytosol
Q9H3S7	C	Cytosol
O00182	C	Cytosol
Q13564	C	Cytosol
P53621	C	Cytosol
O00186	C	Cytosol
Q12906	C	Cytosol
Q9HC38	M	Mitochondria
Q99459	C	Cytosol
Q9NX58	C	Cytosol
P09429	PM	Plasma Membrane
Q9NSD9	C	Cytosol
P26599	NINT	Nuclear Lumen
P78316	NINT	Nuclear Lumen
P38646	C	Cytosol
Q969Q0	C	Cytosol
Q96ST8	C	Cytosol
P14927	MINT	Mitochondria Lumen
Q9P035	C	Cytosol
P14921	C	Cytosol
Q07666	C	Cytosol
Q5TBB1	NINT	Nuclear Lumen
P03928	MINT	Mitochondria Lumen
O75832	C	Cytosol
Q96ST2	NINT	Nuclear Lumen
Q9Y512	M	Mitochondria
Q9H583	M	Mitochondria
O43390	ER	Endoplasmic Reticulum
P42167	C	Cytosol
P12956	C	Cytosol
O60832	C	Cytosol
P07951	SK	Cytoskeleton
Q13435	NINT	Nuclear Lumen
P09874	ML2	Multiple Organelles
P13929	C	Cytosol
Q9UQ35	NINT	Nuclear Lumen
Q9H4A4	PM	Plasma Membrane
P07384	C	Cytosol
Q9NZ01	ER	Endoplasmic Reticulum

Q15052	C	Cytosol
O14949	M	Mitochondria
P22061	C	Cytosol
P68036	C	Cytosol
P06576	PM	Plasma Membrane
Q13247	NINT	Nuclear Lumen
O75150	C	Cytosol
Q99471	C	Cytosol
Q13243	C	Cytosol
Q13242	NINT	Nuclear Lumen
P39687	C	Cytosol
Q9UJA5	NINT	Nuclear Lumen
P37802	C	Cytosol
Q14694	C	Cytosol
O43488	C	Cytosol
O60271	SK	Cytoskeleton
P62837	C	Cytosol
P62942	C	Cytosol
P29144	C	Cytosol
P62834	C	Cytosol
Q86V21	C	Cytosol
P08758	C	Cytosol
Q04446	C	Cytosol
P36507	SK	Cytoskeleton
Q6IBN1	C	Cytosol
Q02880	C	Cytosol
P23284	C	Cytosol
Q1KMD3	NINT	Nuclear Lumen
Q8WXX5	C	Cytosol
Q56VL3	V	Vesicle
O14818	C	Cytosol
Q13505	M	Mitochondria
P62937	C	Cytosol
P09622	M	Mitochondria
P19525	C	Cytosol
Q96CT7	SK	Cytoskeleton
P61077	C	Cytosol
Q9UKK9	C	Cytosol
O43865	C	Cytosol
Q9BZZ5	C	Cytosol
P53999	NINT	Nuclear Lumen
Q92905	C	Cytosol
Q92925	NINT	Nuclear Lumen
Q86U86	NINT	Nuclear Lumen
Q96DG6	C	Cytosol
Q9NY12	NINT	Nuclear Lumen

P18754	C	Cytosol
P53990	C	Cytosol
P68032	C	Cytosol
Q15126	C	Cytosol
O15460	C	Cytosol
Q96FW1	C	Cytosol
P26440	MINT	Mitochondria Lumen
P63279	C	Cytosol
Q7Z7H5	ERM	Endoplasmic Resticulum Membrane
O60488	C	Cytosol
Q4LE39	C	Cytosol
Q6DD88	ER	Endoplasmic Reticulum
Q9NXF7	NINT	Nuclear Lumen
Q9Y312	NINT	Nuclear Lumen
P49840	SK	Cytoskeleton
Q9UJS0	PM	Plasma Membrane
P46776	C	Cytosol
P46777	C	Cytosol
P15170	C	Cytosol
Q9NXG2	NINT	Nuclear Lumen
P46778	C	Cytosol
P11021	PM	Plasma Membrane
P16615	C	Cytosol
Q8WXF1	C	Cytosol
Q9Y262	C	Cytosol
Q15056	C	Cytosol
O95721	C	Cytosol
Q9BZH6	SK	Cytoskeleton
Q9BRA2	C	Cytosol
P43487	C	Cytosol
O75477	ER	Endoplasmic Reticulum
P11766	C	Cytosol
Q14974	C	Cytosol
Q92900	C	Cytosol
Q9UK58	NINT	Nuclear Lumen
Q07866	SK	Cytoskeleton
Q9BWD1	C	Cytosol
Q9Y6N5	MINT	Mitochondria Lumen
P22695	M	Mitochondria
Q6P2Q9	NINT	Nuclear Lumen
P35637	C	Cytosol
Q8WU39	C	Cytosol
P27701	PM	Plasma Membrane
P33992	C	Cytosol
Q08257	C	Cytosol
Q3ZCM7	SK	Cytoskeleton

Q92973	C	Cytosol
Q9H2P0	C	Cytosol
P49189	C	Cytosol
P84103	C	Cytosol
P12004	NINT	Nuclear Lumen
Q9BTE3	C	Cytosol
Q96A26	C	Cytosol
Q9UJX3	C	Cytosol

Table 4.11. Enrichment STP-alkyne

ProRule Domain	Number Liganded	Number in Database	Database Frequency	P-Value	Description	BH Corrected Q-Value
PRU00531	2	2	6.58E-05	9.54E-06	WHEP-TRS domain	0.000448587
PRU00176	7	378	0.012435438	2.08E-05	RNA recognition motif (RRM) domain	0.000489196
PRU00526	2	6	0.000197388	8.54E-05	BRO1 domain	0.001338115
PRU00599	2	12	0.000394776	0.000339	ADF-H domain	0.003731654
PRU01084	2	13	0.000427674	0.000397	Hexokinase domain	0.003731654
PRU00547	2	17	0.000559266	0.000675	CS domain	0.005287623
PRU00159	6	512	0.016843767	0.000947	Protein kinase domain	0.006356675
PRU00717	1	1	3.29E-05	0.002202	RINT1/TIP20 domain	0.010348336
PRU00518	1	1	3.29E-05	0.002202	YrdC-like domain	0.010348336
PRU00257	1	1	3.29E-05	0.002202	Cro/C1-type HTH domain	0.010348336
PRU00958	1	2	6.58E-05	0.004399	tRNA (guanine(26)-N(2))-dimethyltransferase (EC 2.1.1.216)	0.015903252
PRU00467	1	2	6.58E-05	0.004399	AMMECR1 domain	0.015903252
PRU00073	1	2	6.58E-05	0.004399	DRADA	0.015903252
PRU00084	2	50	0.001644899	0.005572	FERM	0.018706855
PRU01133	1	3	9.87E-05	0.006591	Translationally controlled tumor protein (TCTP) domain	0.019361075
PRU00690	1	3	9.87E-05	0.006591	Nop domain	0.019361075
PRU00170	1	4	0.000131592	0.008778	Reticulon	0.02426992

PRU00267	2	66	0.002171267	0.009492	HMG boxes A and B DNA-binding domains	0.024784926
PRU01040	1	5	0.00016449	0.010961	DZF domain	0.025758853
PRU00641	1	5	0.00016449	0.010961	Poly(A)-binding protein C-terminal (PABC) domain	0.025758853
PRU00695	1	7	0.000230286	0.015312	W2 domain	0.031290729
PRU01047	1	7	0.000230286	0.015312	OBG-type guanine nucleotide-binding (G) domain	0.031290729
PRU00573	1	7	0.000230286	0.015312	Acyl-CoA-binding (ACB) domain	0.031290729
PRU00810	1	8	0.000263184	0.017481	PAH domain	0.034233708
PRU01015	1	11	0.000361878	0.023959	SAM-dependent methyltransferase PRMT-type domain	0.045042033
PRU00167	1	15	0.00049347	0.03253	Ras-GAP	0.05818093
PRU00837	1	16	0.000526368	0.034661	Linker histone H1/H5 globular (H15) domain	0.05818093
PRU00439	1	16	0.000526368	0.034661	MAD homology domain 2 (MH2)	0.05818093
PRU00096	1	18	0.000592164	0.03891	GOLD	0.063060252
PRU01059	1	22	0.000723756	0.047351	Translational (tr)-type guanine nucleotide-binding (G) domain	0.074183875
PRU00277	1	24	0.000789552	0.051545	PPIase FKBP-type domain	0.075706604
PRU00156	1	24	0.000789552	0.051545	PPIase cyclophilin-type domain	0.075706604
PRU00794	1	27	0.000888246	0.057801	Nudix hydrolase domain	0.082322803
PRU00415	1	28	0.000921144	0.059877	Saposin B-type domain	0.082771794
PRU00288	1	30	0.00098694	0.064017	ARF GTPase-activating proteins domain	0.085965225
PRU00266	1	33	0.001085633	0.070192	Double stranded RNA-binding domain	0.091639297
PRU00691	1	51	0.001677797	0.106409	thioredoxin domain	0.135167865
PRU00448	3	576	0.018949238	0.134346	EF-hand	0.165623958
PRU00214	1	67	0.002204165	0.137433	Ubiquitin-like	0.165623958
PRU00434	1	80	0.002631839	0.161856	ABC transporter family domain	0.190181079
PRU00542	1	108	0.003552982	0.212171	Helicase C-terminal domain	0.243219952

PRU00044	1	114	0.00375037	0.222559	Calponin-homology (CH) domain	0.249053808
PRU00125	1	160	0.005263677	0.297843	LIM zinc-binding domain	0.325548987
PRU00274	1	166	0.005461065	0.307117	Serine proteases, trypsin domain	0.328056778
PRU00114	1	1464	0.048162648	0.381453	Ig-like domain	0.398406242
PRU00145	1	290	0.009540415	0.473907	PH	0.484208911
PRU00521	1	592	0.019475606	1	G-protein coupled receptors family 1	1

Table 4.12. Enrichment SuTEx hyper-reactive

ProRule Domain	Number Liganded	Number in Database	Database Frequency	P-Value	Description	BH Corrected Q-Value
PRU01188	5	74	0.00243445	1.16E-08	Intermediate filament (IF) rod domain	2.32E-07
PRU00044	4	114	0.00375037	5.01E-06	Calponin-homology (CH) domain	5.01E-05
PRU01055	2	28	0.00092114	0.000363	Dynamin-type guanine nucleotide-binding (G) domain	0.002418747
PRU00966	1	1	3.29E-05	0.000986	NF-YA/HAP2 family	0.004932344
PRU00719	1	2	6.58E-05	0.001972	YjeF N-terminal domain	0.006573323
PRU01202	1	3	9.87E-05	0.002957	MGS-like domain	0.006573323
PRU00109	1	4	0.00013159	0.00394	HORMA	0.008447387
PRU00176	3	378	0.01243544	0.006075	RNA recognition motif (RRM) domain	0.009850586
PRU01015	1	11	0.00036188	0.0108	SAM-dependent methyltransferase PRMT-type domain	0.013500096
PRU00534	1	12	0.00039478	0.011776	FAT domain	0.013771115
PRU00466	1	16	0.00052637	0.015671	Laminin N-terminal domain	0.019626215
PRU01059	1	22	0.00072376	0.021486	Translational (tr)-type guanine nucleotide-binding (G) domain	0.019626215
PRU00100	1	23	0.00075665	0.022452	Guanylate kinase-like domain	0.024109384
PRU01185	1	24	0.00078955	0.023417	PCI domain	0.027549836
PRU00277	1	24	0.00078955	0.023417	PPIase FKBP-type domain	0.027549836
PRU00089	1	48	0.0015791	0.046304	Fork-head DNA-binding domain	0.027549836
PRU00191	1	117	0.00384906	0.109253	SH2 domain	0.027549836

PRU00723	1	132	0.00434253	0.122396	Zinc finger C3H1-type	0.051449125

Table 4.13. Activated Ester Ligands Enrichment

ProRule Domain	Number Liganded	Number in Database	Database Frequency	P-Value	Description	BH Corrected Q-Value
PRU00170	2	4	0.000131592	3.99E-06	Reticulon	7.19E-05
PRU00717	1	1	3.29E-05	0.000724	RINT1/TIP20 domain	0.006511551
PRU01012	1	3	9.87E-05	0.002169	SAM-dependent methyltransferase TRM10-type domain	0.01301411
PRU00573	1	7	0.000230286	0.005054	Acyl-CoA-binding (ACB) domain	0.014891254
PRU01047	1	7	0.000230286	0.005054	OBG-type guanine nucleotide-binding (G) domain	0.014891254
PRU00810	1	8	0.000263184	0.005774	PAH domain	0.014891254
PRU00159	3	512	0.016843767	0.005791	Protein kinase domain	0.014891254
PRU01084	1	13	0.000427674	0.009367	Hexokinase domain	0.021075058
PRU00186	1	22	0.000723756	0.015802	SAP	0.028443965
PRU01059	1	22	0.000723756	0.015802	Translational (tr)-type guanine nucleotide-binding (G) domain	0.028443965
PRU00794	1	27	0.000888246	0.01936	Nudix hydrolase domain	0.02975419
PRU00415	1	28	0.000921144	0.02007	Saposin B-type domain	0.02975419
PRU00288	1	30	0.00098694	0.021489	ARF GTPase-activating proteins domain	0.02975419
PRU00176	2	378	0.012435438	0.030294	RNA recognition motif (RRM) domain	0.038949126
PRU01188	1	74	0.002434451	0.052211	Intermediate filament (IF) rod domain	0.062653018
PRU00434	1	80	0.002631839	0.056328	ABC transporter family domain	0.063369155
PRU00117	1	87	0.002862125	0.06111	KH domain	0.064704775
PRU00448	1	576	0.018949238	0.343534	EF-hand	0.343533538

Table 4.14. SuTEx 1,2,4 Ligand Enrichment

ProRule Domain	Number Liganded	Number in Database	Database Frequency	P-Value	Description	BH Corrected Q-Value
PRU00691	3	37	0.002593	0.0002937	thioredoxin domain	0.0108657
PRU01059	2	13	0.000911	0.0009484	Translational (tr)-type guanine nucleotide-binding (G) domain	0.01392867

PRU00267	3	59	0.004134	0.0011294	HMG boxes A and B DNA-binding domains	0.01392867
PRU00277	2	17	0.001191	0.0016077	PPIase FKBP-type domain	0.01487163
PRU00519	1	1	7.01E-05	0.0034278	Elongation factor 1 (EF-1) gamma C-terminal domain	0.01949077
PRU01185	2	26	0.001822	0.0036874	PCI domain	0.01949077
PRU00156	2	26	0.001822	0.0036874	PPIase cyclophilin-type domain	0.01949077
PRU00191	3	108	0.007568	0.0061599	SH2 domain	0.02813655
PRU00386	1	2	0.00014	0.006844	SGS domain	0.02813655
PRU00117	2	39	0.002733	0.008065	KH domain	0.02984037
PRU00797	1	3	0.00021	0.0102488	SIS domain	0.0316005
PRU01202	1	3	0.00021	0.0102488	MGS-like domain	0.0316005
PRU01138	1	5	0.00035	0.0170241	CoA carboxyltransferase domain	0.04716276
PRU01163	1	6	0.00042	0.0203947	Vicinal oxygen chelate (VOC) domain	0.04716276

Table 4.15.

PDB_Structure	Residue	Amino.Acid.No	Chain	pKa	Buried	Liganded
6S8L	TYR	24	A	13.37	100	Liganded
6S8L	TYR	83	A	12.89	50	Not Liganded
6S8L	TYR	103	A	14.2	100	Not Liganded
6S8L	TYR	108	A	13.15	48	Not Liganded
6S8L	TYR	161	A	11.78	45	Not Liganded
6S8L	TYR	172	A	13.08	95	Not Liganded
6S8L	TYR	185	A	15.01	100	Not Liganded
6S8L	TYR	210	A	10.58	43	Not Liganded
6S8L	TYR	224	A	14.06	97	Not Liganded
6S8L	TYR	262	A	10.6	0	Not Liganded
6S8L	TYR	272	A	12.73	100	Not Liganded
6S8L	TYR	282	A	10.04	0	Not Liganded
6S8L	TYR	312	A	13.16	77	Not Liganded
6S8L	TYR	319	A	12.55	74	Not Liganded
6S8L	TYR	357	A	10.41	0	Not Liganded
6S8L	TYR	399	A	11.16	30	Not Liganded
6S8L	TYR	408	A	14.51	100	Not Liganded
6S8L	TYR	432	A	13.31	100	Not Liganded
6S8L	TYR	36	B	11.02	0	Not Liganded
6S8L	TYR	52	B	13.7	100	Not Liganded
6S8L	TYR	53	B	13.05	100	Not Liganded

6S8L	TYR	61	B	11.43	17	Not Liganded
6S8L	TYR	108	B	12.93	50	Not Liganded
6S8L	TYR	161	B	13.57	35	Not Liganded
6S8L	TYR	185	B	14.54	100	Not Liganded
6S8L	TYR	202	B	16.6	100	Not Liganded
6S8L	TYR	210	B	11.06	25	Not Liganded
6S8L	TYR	224	B	12.01	58	Not Liganded
6S8L	TYR	312	B	12.08	93	Not Liganded
6S8L	TYR	342	B	10.14	0	Not Liganded
6S8L	TYR	408	B	14.56	100	Not Liganded
6S8L	TYR	432	B	14.78	100	Not Liganded
6S8L	TYR	435	B	11.92	56	Not Liganded
6S8L	TYR	57	F	11.14	60	Not Liganded
6LPF	TYR	46	A	13.57	93	Not Liganded
6LPF	TYR	52	A	21.53	100	Not Liganded
6LPF	TYR	54	A	14.23	100	Not Liganded
6LPF	TYR	76	A	13.79	53	Not Liganded
6LPF	TYR	111	A	10.49	0	Not Liganded
6LPF	TYR	156	A	10.33	0	Not Liganded
6LPF	TYR	183	A	10.96	33	Not Liganded
6LPF	TYR	213	A	11.69	46	Not Liganded
6LPF	TYR	214	A	16.03	100	Not Liganded
6LPF	TYR	237	A	11.52	48	Not Liganded
6LPF	TYR	240	A	12.15	57	Not Liganded
6LPF	TYR	264	A	11.89	47	Not Liganded
6LPF	TYR	275	A	11.14	15	Not Liganded
6LPF	TYR	313	A	13.05	82	Not Liganded
6LPF	TYR	336	A	10.88	33	Not Liganded
6LPF	TYR	369	A	10.49	30	Not Liganded
6LPF	TYR	373	A	10.64	16	Not Liganded
6LPF	TYR	416	A	10.92	18	Not Liganded
6LPF	TYR	468	A	9.79	7	Not Liganded
6LPF	TYR	473	A	10.25	0	Liganded
6LPF	TYR	507	A	16.43	100	Not Liganded
6LPF	TYR	531	A	11.36	24	Not Liganded
6LPF	TYR	534	A	14.38	100	Not Liganded
6LPF	TYR	577	A	12.67	40	Not Liganded
6LPF	TYR	600	A	11.6	100	Not Liganded
6LPF	TYR	604	A	14.61	100	Not Liganded
6LPF	TYR	637	A	11.46	19	Not Liganded
6LPF	TYR	666	A	15.1	100	Not Liganded
6LPF	TYR	684	A	15.87	100	Not Liganded
6LPF	TYR	685	A	13.59	100	Not Liganded
6LPF	TYR	687	A	12.68	72	Not Liganded
6LPF	TYR	768	A	10.61	0	Not Liganded
6LPF	TYR	812	A	14.92	100	Not Liganded

6LPF	TYR	835	A	12.88	63	Not Liganded
6LPF	TYR	901	A	16	88	Not Liganded
6LPF	TYR	916	A	10.06	0	Not Liganded
6LPF	TYR	939	A	10.56	2	Not Liganded
6LPF	TYR	944	A	12.58	75	Not Liganded
6LPF	TYR	46	B	13.82	98	Not Liganded
6LPF	TYR	52	B	21.43	100	Not Liganded
6LPF	TYR	54	B	14.09	100	Not Liganded
6LPF	TYR	76	B	13.99	55	Not Liganded
6LPF	TYR	111	B	10.34	0	Not Liganded
6LPF	TYR	156	B	10.14	0	Not Liganded
6LPF	TYR	183	B	10.94	37	Not Liganded
6LPF	TYR	213	B	11.75	45	Not Liganded
6LPF	TYR	214	B	15.96	100	Not Liganded
6LPF	TYR	237	B	11.62	56	Not Liganded
6LPF	TYR	240	B	12.17	61	Not Liganded
6LPF	TYR	264	B	11.8	62	Not Liganded
6LPF	TYR	275	B	11.16	13	Not Liganded
6LPF	TYR	313	B	13.16	94	Not Liganded
6LPF	TYR	336	B	11.04	37	Not Liganded
6LPF	TYR	369	B	10.61	31	Not Liganded
6LPF	TYR	373	B	10.52	15	Not Liganded
6LPF	TYR	416	B	10.11	17	Not Liganded
6LPF	TYR	468	B	10	50	Not Liganded
6LPF	TYR	473	B	10.24	0	Liganded
6LPF	TYR	507	B	16.69	100	Not Liganded
6LPF	TYR	531	B	10.99	23	Not Liganded
6LPF	TYR	534	B	14.47	100	Not Liganded
6LPF	TYR	577	B	12.81	42	Not Liganded
6LPF	TYR	600	B	11.26	100	Not Liganded
6LPF	TYR	604	B	15.12	100	Not Liganded
6LPF	TYR	637	B	11.05	11	Not Liganded
6LPF	TYR	666	B	15.19	100	Not Liganded
6LPF	TYR	684	B	15.69	100	Not Liganded
6LPF	TYR	685	B	13.71	100	Not Liganded
6LPF	TYR	687	B	13.11	72	Not Liganded
6LPF	TYR	768	B	12.24	32	Not Liganded
6LPF	TYR	812	B	15.17	100	Not Liganded
6LPF	TYR	835	B	13.14	68	Not Liganded
6LPF	TYR	901	B	17.92	100	Not Liganded
6LPF	TYR	916	B	10.31	0	Not Liganded
6LPF	TYR	939	B	10.66	8	Not Liganded
6LPF	TYR	944	B	12.8	80	Not Liganded
6LPF	TYR	985	B	10.59	0	Not Liganded
6IIK	TYR	115	A	14.14	89	Not Liganded
6IIK	TYR	136	A	10.7	34	Not Liganded

6IIK	TYR	151	A	11.99	64	Not Liganded
6IIK	TYR	195	A	11.29	67	Not Liganded
6IIK	TYR	285	A	10.02	0	Liganded
6IIK	TYR	311	A	11.91	0	Not Liganded
6IIK	TYR	323	A	14.2	80	Not Liganded
6IIK	TYR	356	A	10.48	0	Not Liganded
6IIK	TYR	401	A	9.98	0	Not Liganded
6IIK	TYR	417	A	10.76	20	Not Liganded
6IIK	TYR	418	A	14.66	100	Not Liganded
6IIK	TYR	436	A	15.65	94	Not Liganded
6IIK	TYR	476	A	16.71	90	Not Liganded
6IIK	TYR	480	A	14.11	100	Not Liganded
6IIK	TYR	115	B	14.07	88	Not Liganded
6IIK	TYR	136	B	11.21	32	Not Liganded
6IIK	TYR	151	B	11.43	65	Not Liganded
6IIK	TYR	195	B	10.75	67	Not Liganded
6IIK	TYR	285	B	9.94	0	Liganded
6IIK	TYR	311	B	11.57	0	Not Liganded
6IIK	TYR	323	B	14.31	80	Not Liganded
6IIK	TYR	356	B	10.43	0	Not Liganded
6IIK	TYR	401	B	10.23	0	Not Liganded
6IIK	TYR	417	B	10.28	15	Not Liganded
6IIK	TYR	418	B	14.51	100	Not Liganded
6IIK	TYR	436	B	15.85	90	Not Liganded
6IIK	TYR	476	B	14.72	84	Not Liganded
6IIK	TYR	480	B	14.08	100	Not Liganded
6GZL	TYR	32	A	9.6	0	Liganded
6GZL	TYR	50	A	12.13	16	Not Liganded
6GZL	TYR	65	A	11.22	0	Not Liganded
6GZL	TYR	75	A	12.85	28	Not Liganded
6GZL	TYR	77	A	9.86	3	Not Liganded
6GZL	TYR	611	B	10.18	0	Not Liganded
6.00E+07	TYR	49	L	13.47	100	Not Liganded
6.00E+07	TYR	70	L	12.47	51	Not Liganded
6.00E+07	TYR	107	L	12.15	40	Not Liganded
6.00E+07	TYR	112	L	11.25	57	Liganded
6.00E+07	TYR	118	L	13.96	68	Not Liganded
6.00E+07	TYR	139	L	18.46	100	Not Liganded
6.00E+07	TYR	147	L	13.38	88	Not Liganded
6.00E+07	TYR	197	L	11.92	70	Not Liganded
6.00E+07	TYR	202	L	13.36	90	Not Liganded
6.00E+07	TYR	249	L	9.97	0	Not Liganded
6.00E+07	TYR	308	L	11.54	72	Not Liganded
6.00E+07	TYR	322	L	15.02	75	Not Liganded
6.00E+07	TYR	343	L	11.36	50	Not Liganded
6.00E+07	TYR	401	L	14.89	100	Not Liganded

6.00E+07	TYR	424	L	14.9	100	Not Liganded
6.00E+07	TYR	428	L	12.75	95	Not Liganded
6.00E+07	TYR	437	L	15.14	90	Not Liganded
6.00E+07	TYR	482	L	14.08	100	Not Liganded
6.00E+07	TYR	484	L	11.13	30	Not Liganded
6.00E+07	TYR	503	L	11.11	19	Not Liganded
6.00E+07	TYR	507	L	18.46	95	Not Liganded
6.00E+07	TYR	49	C	13.5	100	Not Liganded
6.00E+07	TYR	70	C	12.45	51	Not Liganded
6.00E+07	TYR	107	C	12.15	40	Not Liganded
6.00E+07	TYR	112	C	11.41	58	Liganded
6.00E+07	TYR	118	C	14.1	68	Not Liganded
6.00E+07	TYR	139	C	18.55	100	Not Liganded
6.00E+07	TYR	147	C	12.84	92	Not Liganded
6.00E+07	TYR	197	C	11.89	69	Not Liganded
6.00E+07	TYR	202	C	13.42	90	Not Liganded
6.00E+07	TYR	249	C	9.95	0	Not Liganded
6.00E+07	TYR	308	C	11.42	67	Not Liganded
6.00E+07	TYR	322	C	14.26	57	Not Liganded
6.00E+07	TYR	343	C	11.35	47	Not Liganded
6.00E+07	TYR	401	C	15.15	100	Not Liganded
6.00E+07	TYR	424	C	14.62	100	Not Liganded
6.00E+07	TYR	428	C	12.52	92	Not Liganded
6.00E+07	TYR	437	C	15.6	90	Not Liganded
6.00E+07	TYR	482	C	13.96	100	Not Liganded
6.00E+07	TYR	484	C	11.14	29	Not Liganded
6.00E+07	TYR	503	C	11.19	22	Not Liganded
6.00E+07	TYR	507	C	18.6	97	Not Liganded
6.00E+07	TYR	49	F	13.48	100	Not Liganded
6.00E+07	TYR	70	F	12.59	54	Not Liganded
6.00E+07	TYR	107	F	12.22	42	Not Liganded
6.00E+07	TYR	112	F	11.31	57	Liganded
6.00E+07	TYR	118	F	14.13	69	Not Liganded
6.00E+07	TYR	139	F	18	100	Not Liganded
6.00E+07	TYR	147	F	12.92	93	Not Liganded
6.00E+07	TYR	197	F	11.87	71	Not Liganded
6.00E+07	TYR	202	F	13.3	89	Not Liganded
6.00E+07	TYR	249	F	10.01	0	Not Liganded
6.00E+07	TYR	308	F	11.44	69	Not Liganded
6.00E+07	TYR	322	F	14.29	59	Not Liganded
6.00E+07	TYR	343	F	11.32	48	Not Liganded
6.00E+07	TYR	401	F	16.21	100	Not Liganded
6.00E+07	TYR	424	F	14.49	100	Not Liganded
6.00E+07	TYR	428	F	12.42	90	Not Liganded
6.00E+07	TYR	437	F	15.43	88	Not Liganded
6.00E+07	TYR	482	F	13.95	99	Not Liganded

6.00E+07	TYR	484	F	11.15	28	Not Liganded
6.00E+07	TYR	503	F	11.12	22	Not Liganded
6.00E+07	TYR	507	F	18.38	91	Not Liganded
6.00E+07	TYR	49	N	13.51	100	Not Liganded
6.00E+07	TYR	70	N	12.49	53	Not Liganded
6.00E+07	TYR	107	N	12.18	42	Not Liganded
6.00E+07	TYR	112	N	11.59	61	Liganded
6.00E+07	TYR	118	N	14.16	71	Not Liganded
6.00E+07	TYR	139	N	18.25	100	Not Liganded
6.00E+07	TYR	147	N	12.91	95	Not Liganded
6.00E+07	TYR	197	N	11.86	68	Not Liganded
6.00E+07	TYR	202	N	13.27	89	Not Liganded
6.00E+07	TYR	249	N	10.03	0	Not Liganded
6.00E+07	TYR	308	N	11.42	67	Not Liganded
6.00E+07	TYR	322	N	14.23	58	Not Liganded
6.00E+07	TYR	343	N	10.84	52	Not Liganded
6.00E+07	TYR	401	N	16.42	100	Not Liganded
6.00E+07	TYR	424	N	14.77	100	Not Liganded
6.00E+07	TYR	428	N	12.38	89	Not Liganded
6.00E+07	TYR	437	N	15.62	90	Not Liganded
6.00E+07	TYR	482	N	13.99	100	Not Liganded
6.00E+07	TYR	484	N	11.11	28	Not Liganded
6.00E+07	TYR	503	N	11.14	16	Not Liganded
6.00E+07	TYR	507	N	18.46	93	Not Liganded
6.00E+07	TYR	49	Q	13.45	100	Not Liganded
6.00E+07	TYR	70	Q	12.43	51	Not Liganded
6.00E+07	TYR	107	Q	12.19	40	Not Liganded
6.00E+07	TYR	112	Q	11.44	58	Liganded
6.00E+07	TYR	118	Q	13.61	68	Not Liganded
6.00E+07	TYR	139	Q	18.58	100	Not Liganded
6.00E+07	TYR	147	Q	12.97	95	Not Liganded
6.00E+07	TYR	197	Q	11.89	71	Not Liganded
6.00E+07	TYR	202	Q	13.35	90	Not Liganded
6.00E+07	TYR	249	Q	10.03	0	Not Liganded
6.00E+07	TYR	308	Q	11.26	69	Not Liganded
6.00E+07	TYR	322	Q	14.74	68	Not Liganded
6.00E+07	TYR	343	Q	11.11	47	Not Liganded
6.00E+07	TYR	401	Q	15.22	100	Not Liganded
6.00E+07	TYR	424	Q	14.58	100	Not Liganded
6.00E+07	TYR	428	Q	12.59	92	Not Liganded
6.00E+07	TYR	437	Q	15.69	92	Not Liganded
6.00E+07	TYR	482	Q	14.02	100	Not Liganded
6.00E+07	TYR	484	Q	10.86	28	Not Liganded
6.00E+07	TYR	503	Q	11.28	22	Not Liganded
6.00E+07	TYR	507	Q	18.39	93	Not Liganded
6.00E+07	TYR	49	T	13.48	100	Not Liganded

6.00E+07	TYR	70	T	12.43	50	Not Liganded
6.00E+07	TYR	107	T	12.17	41	Not Liganded
6.00E+07	TYR	112	T	11.37	56	Liganded
6.00E+07	TYR	118	T	14.03	68	Not Liganded
6.00E+07	TYR	139	T	18.64	100	Not Liganded
6.00E+07	TYR	147	T	12.9	95	Not Liganded
6.00E+07	TYR	197	T	11.84	67	Not Liganded
6.00E+07	TYR	202	T	13.5	92	Not Liganded
6.00E+07	TYR	249	T	11.01	64	Not Liganded
6.00E+07	TYR	308	T	11.49	70	Not Liganded
6.00E+07	TYR	322	T	14.3	59	Not Liganded
6.00E+07	TYR	343	T	11.17	44	Not Liganded
6.00E+07	TYR	401	T	14.89	100	Not Liganded
6.00E+07	TYR	424	T	14.79	100	Not Liganded
6.00E+07	TYR	428	T	12.52	92	Not Liganded
6.00E+07	TYR	437	T	16.04	94	Not Liganded
6.00E+07	TYR	482	T	13.98	100	Not Liganded
6.00E+07	TYR	484	T	11.16	29	Not Liganded
6.00E+07	TYR	503	T	11.22	22	Not Liganded
6.00E+07	TYR	507	T	18.18	93	Not Liganded
6.00E+07	TYR	49	W	13.47	100	Not Liganded
6.00E+07	TYR	70	W	12.51	52	Not Liganded
6.00E+07	TYR	107	W	12.14	41	Not Liganded
6.00E+07	TYR	112	W	10.95	59	Liganded
6.00E+07	TYR	118	W	14.06	69	Not Liganded
6.00E+07	TYR	139	W	18.64	100	Not Liganded
6.00E+07	TYR	147	W	12.83	94	Not Liganded
6.00E+07	TYR	197	W	11.82	67	Not Liganded
6.00E+07	TYR	202	W	13.35	90	Not Liganded
6.00E+07	TYR	249	W	9.97	0	Not Liganded
6.00E+07	TYR	308	W	11.16	68	Not Liganded
6.00E+07	TYR	322	W	14.35	60	Not Liganded
6.00E+07	TYR	343	W	11.25	45	Not Liganded
6.00E+07	TYR	401	W	16.62	100	Not Liganded
6.00E+07	TYR	424	W	14.61	100	Not Liganded
6.00E+07	TYR	428	W	12.48	92	Not Liganded
6.00E+07	TYR	437	W	15.74	91	Not Liganded
6.00E+07	TYR	482	W	13.94	99	Not Liganded
6.00E+07	TYR	484	W	11.38	29	Not Liganded
6.00E+07	TYR	503	W	11.17	21	Not Liganded
6.00E+07	TYR	507	W	18.76	93	Not Liganded
6.00E+07	TYR	49	B	13.45	100	Not Liganded
6.00E+07	TYR	70	B	12.49	52	Not Liganded
6.00E+07	TYR	107	B	12.17	40	Not Liganded
6.00E+07	TYR	112	B	10.8	59	Liganded
6.00E+07	TYR	118	B	14.04	68	Not Liganded

6.00E+07	TYR	139	B	18.6	100	Not Liganded
6.00E+07	TYR	147	B	12.89	93	Not Liganded
6.00E+07	TYR	197	B	11.9	70	Not Liganded
6.00E+07	TYR	202	B	13.26	88	Not Liganded
6.00E+07	TYR	249	B	9.92	0	Not Liganded
6.00E+07	TYR	308	B	11.4	67	Not Liganded
6.00E+07	TYR	322	B	14.27	58	Not Liganded
6.00E+07	TYR	343	B	11.2	46	Not Liganded
6.00E+07	TYR	401	B	14.81	100	Not Liganded
6.00E+07	TYR	424	B	14.63	100	Not Liganded
6.00E+07	TYR	428	B	12.62	91	Not Liganded
6.00E+07	TYR	437	B	15.49	89	Not Liganded
6.00E+07	TYR	482	B	13.92	99	Not Liganded
6.00E+07	TYR	484	B	11.08	27	Not Liganded
6.00E+07	TYR	503	B	11.35	22	Not Liganded
6.00E+07	TYR	507	B	17.81	90	Not Liganded
6ASY	TYR	39	A	10.03	97	Not Liganded
6ASY	TYR	65	A	12.24	100	Not Liganded
6ASY	TYR	127	A	12.19	58	Liganded
6ASY	TYR	160	A	11.71	39	Not Liganded
6ASY	TYR	175	A	12.24	82	Not Liganded
6ASY	TYR	209	A	13.89	66	Not Liganded
6ASY	TYR	270	A	11.2	15	Not Liganded
6ASY	TYR	313	A	10.57	0	Not Liganded
6ASY	TYR	396	A	11.88	90	Not Liganded
6ASY	TYR	462	A	11.95	19	Not Liganded
6ASY	TYR	564	A	11.36	32	Not Liganded
6ASY	TYR	566	A	10.57	0	Not Liganded
6ASY	TYR	39	B	10.1	96	Not Liganded
6ASY	TYR	65	B	12.1	100	Not Liganded
6ASY	TYR	127	B	12.5	58	Liganded
6ASY	TYR	160	B	11.75	40	Not Liganded
6ASY	TYR	175	B	12.21	81	Not Liganded
6ASY	TYR	209	B	13.72	64	Not Liganded
6ASY	TYR	270	B	11.25	18	Not Liganded
6ASY	TYR	313	B	10.55	0	Not Liganded
6ASY	TYR	396	B	11.22	91	Not Liganded
6ASY	TYR	462	B	10.64	17	Not Liganded
6ASY	TYR	564	B	11.74	32	Not Liganded
6ASY	TYR	566	B	10.63	0	Not Liganded
5XIX	TYR	123	A	10.12	0	Not Liganded
5XIX	TYR	155	A	11.36	60	Not Liganded
5XIX	TYR	168	A	9.65	0	Not Liganded
5XIX	TYR	182	A	11.12	8	Not Liganded
5XIX	TYR	265	A	17.1	100	Not Liganded
5XIX	TYR	266	A	12.19	84	Not Liganded

5XIX	TYR	289	A	13.81	77	Not Liganded
5XIX	TYR	303	A	15.83	100	Not Liganded
5XIX	TYR	321	A	17.42	100	Not Liganded
5XIX	TYR	335	A	12.77	89	Not Liganded
5XIX	TYR	393	A	11.66	36	Not Liganded
5XIX	TYR	413	A	10.53	7	Not Liganded
5XIX	TYR	448	A	10.98	100	Not Liganded
5XIX	TYR	489	A	11.96	71	Liganded
5XIX	TYR	499	A	12.32	72	Not Liganded
5XIX	TYR	500	A	12.14	58	Not Liganded
5XIX	TYR	502	A	15.76	100	Not Liganded
5XIX	TYR	508	A	10.75	21	Not Liganded
5XIX	TYR	516	A	14.22	100	Not Liganded
5XIX	TYR	531	A	10.08	0	Not Liganded
5XIX	TYR	539	A	14.08	100	Not Liganded
5XIX	TYR	123	B	10.1	0	Not Liganded
5XIX	TYR	155	B	11.36	62	Not Liganded
5XIX	TYR	168	B	9.77	0	Not Liganded
5XIX	TYR	182	B	10.78	11	Not Liganded
5XIX	TYR	265	B	17.57	100	Not Liganded
5XIX	TYR	266	B	11.86	86	Not Liganded
5XIX	TYR	289	B	13.73	74	Not Liganded
5XIX	TYR	303	B	15.69	100	Not Liganded
5XIX	TYR	321	B	17.63	100	Not Liganded
5XIX	TYR	335	B	12.85	91	Not Liganded
5XIX	TYR	393	B	11.52	33	Not Liganded
5XIX	TYR	413	B	10.73	9	Not Liganded
5XIX	TYR	448	B	11.16	100	Not Liganded
5XIX	TYR	489	B	11.89	70	Liganded
5XIX	TYR	499	B	12.3	68	Not Liganded
5XIX	TYR	500	B	12.17	59	Not Liganded
5XIX	TYR	502	B	15.54	100	Not Liganded
5XIX	TYR	508	B	10.8	23	Not Liganded
5XIX	TYR	516	B	14.24	100	Not Liganded
5XIX	TYR	531	B	9.78	0	Not Liganded
5XIX	TYR	539	B	14.1	100	Not Liganded
5XIX	TYR	123	C	10.14	0	Not Liganded
5XIX	TYR	155	C	11.16	63	Not Liganded
5XIX	TYR	168	C	9.59	0	Not Liganded
5XIX	TYR	182	C	11.18	8	Not Liganded
5XIX	TYR	265	C	18.21	100	Not Liganded
5XIX	TYR	266	C	12.37	86	Not Liganded
5XIX	TYR	289	C	13.52	71	Not Liganded
5XIX	TYR	303	C	15.35	100	Not Liganded
5XIX	TYR	321	C	14.11	100	Not Liganded
5XIX	TYR	335	C	12.9	88	Not Liganded

5XIX	TYR	393	C	11.36	35	Not Liganded
5XIX	TYR	413	C	10.73	3	Not Liganded
5XIX	TYR	448	C	15.71	83	Not Liganded
5XIX	TYR	489	C	13.62	71	Liganded
5XIX	TYR	499	C	11.49	60	Not Liganded
5XIX	TYR	500	C	12.05	57	Not Liganded
5XIX	TYR	502	C	15.25	100	Not Liganded
5XIX	TYR	508	C	10.74	19	Not Liganded
5XIX	TYR	516	C	14.05	100	Not Liganded
5XIX	TYR	531	C	9.73	0	Not Liganded
5XIX	TYR	539	C	14.22	100	Not Liganded
5XIX	TYR	123	D	10.12	0	Not Liganded
5XIX	TYR	155	D	11.15	62	Not Liganded
5XIX	TYR	168	D	10.16	0	Not Liganded
5XIX	TYR	182	D	11.08	10	Not Liganded
5XIX	TYR	265	D	18.49	100	Not Liganded
5XIX	TYR	266	D	12.27	85	Not Liganded
5XIX	TYR	289	D	13.53	69	Not Liganded
5XIX	TYR	303	D	15.48	100	Not Liganded
5XIX	TYR	321	D	14.24	100	Not Liganded
5XIX	TYR	335	D	12.98	88	Not Liganded
5XIX	TYR	393	D	11.27	36	Not Liganded
5XIX	TYR	413	D	10.88	7	Not Liganded
5XIX	TYR	448	D	15.8	80	Not Liganded
5XIX	TYR	489	D	13.76	70	Liganded
5XIX	TYR	499	D	11.38	60	Not Liganded
5XIX	TYR	500	D	12.04	57	Not Liganded
5XIX	TYR	502	D	15.14	100	Not Liganded
5XIX	TYR	508	D	10.77	20	Not Liganded
5XIX	TYR	516	D	14.16	100	Not Liganded
5XIX	TYR	531	D	9.83	0	Not Liganded
5XIX	TYR	539	D	14.17	100	Not Liganded
5XDR	TYR	127	A	10.94	38	Not Liganded
5XDR	TYR	128	A	10.56	0	Not Liganded
5XDR	TYR	142	A	10.46	0	Not Liganded
5XDR	TYR	177	A	11.22	33	Not Liganded
5XDR	TYR	219	A	11.95	50	Not Liganded
5XDR	TYR	235	A	16.31	100	Not Liganded
5XDR	TYR	254	A	11.78	84	Not Liganded
5XDR	TYR	303	A	13.32	72	Not Liganded
5XDR	TYR	323	A	10.8	27	Not Liganded
5XDR	TYR	331	A	12.17	48	Not Liganded
5XDR	TYR	389	A	12.21	57	Not Liganded
5XDR	TYR	447	A	12.08	66	Not Liganded
5XDR	TYR	485	A	15.87	90	Not Liganded
5XDR	TYR	490	A	9.19	30	Not Liganded

5XDR	TYR	499	A	10.13	0	Liganded
5XDR	TYR	545	A	11.06	39	Not Liganded
5XDR	TYR	581	A	11.26	41	Not Liganded
5XDR	TYR	631	A	13.13	58	Not Liganded
5XDR	TYR	645	A	10.11	0	Not Liganded
5XDR	TYR	651	A	10.58	4	Not Liganded
5XDR	TYR	685	A	12.77	51	Not Liganded
5XDR	TYR	686	A	11.34	41	Not Liganded
5XDR	TYR	697	A	13.98	100	Not Liganded
5XDR	TYR	710	A	13.51	63	Not Liganded
5XDR	TYR	736	A	13.29	100	Not Liganded
5XDR	TYR	746	A	10.21	0	Not Liganded
5XDR	TYR	765	A	13.87	93	Not Liganded
5XDR	TYR	766	A	15.38	100	Not Liganded
5XDR	TYR	792	A	10.31	0	Not Liganded
5UZQ	TYR	69	A	9.57	0	Not Liganded
5UZQ	TYR	80	A	15.3	100	Not Liganded
5UZQ	TYR	185	A	10.2	0	Not Liganded
5UZQ	TYR	194	A	10.71	1	Not Liganded
5UZQ	TYR	199	A	13.14	83	Not Liganded
5UZQ	TYR	217	A	15.14	57	Not Liganded
5UZQ	TYR	221	A	11.8	47	Not Liganded
5UZQ	TYR	246	A	11.25	59	Not Liganded
5UZQ	TYR	258	A	13.91	100	Not Liganded
5UZQ	TYR	286	A	14.48	82	Not Liganded
5UZQ	TYR	331	A	10.84	25	Not Liganded
5UZQ	TYR	345	A	15.74	100	Liganded
5UZQ	TYR	357	A	12.89	88	Not Liganded
5UZQ	TYR	381	A	10.03	40	Not Liganded
5UZQ	TYR	411	A	10.54	2	Not Liganded
5UZQ	TYR	412	A	12.59	48	Not Liganded
5UZQ	TYR	419	A	14.44	100	Not Liganded
5UZQ	TYR	420	A	12.82	67	Not Liganded
5OF9	TYR	6	A	12.17	16	Not Liganded
5OF9	TYR	18	A	13.93	100	Not Liganded
5OF9	TYR	51	A	13.69	69	Not Liganded
5OF9	TYR	100	A	14.86	100	Not Liganded
5OF9	TYR	173	A	12.2	43	Not Liganded
5OF9	TYR	175	A	12.77	23	Not Liganded
5OF9	TYR	243	A	11.45	100	Not Liganded
5OF9	TYR	248	A	16.33	100	Not Liganded
5OF9	TYR	272	A	11.36	46	Not Liganded
5OF9	TYR	277	A	12.68	47	Not Liganded
5OF9	TYR	279	A	11.35	46	Not Liganded
5OF9	TYR	385	A	14.04	100	Not Liganded
5OF9	TYR	394	A	15.18	83	Not Liganded

5OF9	TYR	418	A	15.92	93	Liganded
5OF9	TYR	436	A	14.37	81	Not Liganded
5OF9	TYR	450	A	14.19	95	Not Liganded
5OF9	TYR	470	A	12.53	73	Not Liganded
5OF9	TYR	485	A	10.25	0	Not Liganded
5OF9	TYR	519	A	9.54	1	Not Liganded
5OF9	TYR	6	B	13.11	30	Not Liganded
5OF9	TYR	18	B	16.37	100	Not Liganded
5OF9	TYR	51	B	13.68	67	Not Liganded
5OF9	TYR	100	B	15.64	100	Not Liganded
5OF9	TYR	173	B	12.53	44	Not Liganded
5OF9	TYR	175	B	12.44	10	Not Liganded
5OF9	TYR	243	B	11.21	100	Not Liganded
5OF9	TYR	248	B	16.23	100	Not Liganded
5OF9	TYR	272	B	11.7	51	Not Liganded
5OF9	TYR	277	B	12.83	51	Not Liganded
5OF9	TYR	279	B	11.32	45	Not Liganded
5OF9	TYR	385	B	14.01	100	Not Liganded
5OF9	TYR	394	B	15.13	81	Not Liganded
5OF9	TYR	418	B	14.99	100	Liganded
5OF9	TYR	436	B	14.36	84	Not Liganded
5OF9	TYR	450	B	14.35	100	Not Liganded
5OF9	TYR	470	B	12.37	70	Not Liganded
5OF9	TYR	485	B	9.74	0	Not Liganded
5OF9	TYR	519	B	10.07	0	Not Liganded
5NQR	TYR	16	A	10.16	0	Not Liganded
5NQR	TYR	36	A	11.9	61	Not Liganded
5NQR	TYR	74	A	10.08	0	Liganded
5NQR	TYR	90	A	10.74	31	Not Liganded
5NQR	TYR	119	A	10.99	49	Not Liganded
5NQR	TYR	198	A	14.66	76	Not Liganded
5NQR	TYR	200	A	14.23	100	Not Liganded
5NQR	TYR	16	B	10.29	0	Not Liganded
5NQR	TYR	36	B	11.94	64	Not Liganded
5NQR	TYR	74	B	10.13	0	Liganded
5NQR	TYR	90	B	10.99	33	Not Liganded
5NQR	TYR	119	B	11.03	48	Not Liganded
5NQR	TYR	198	B	13.11	73	Not Liganded
5NQR	TYR	200	B	14.02	100	Not Liganded
5KY6	TYR	2	A	10.43	3	Not Liganded
5KY6	TYR	4	A	11.44	17	Not Liganded
5KY6	TYR	58	A	12.39	64	Not Liganded
5KY6	TYR	84	A	12.53	19	Not Liganded
5KY6	TYR	137	A	10.8	58	Not Liganded
5KY6	TYR	173	A	16.91	100	Not Liganded
5KY6	TYR	203	A	12.76	86	Not Liganded

5KY6	TYR	213	A	13.63	100	Not Liganded
5KY6	TYR	222	A	13.89	86	Not Liganded
5KY6	TYR	301	A	13.8	100	Liganded
5KY6	TYR	327	A	13.42	100	Not Liganded
5KY6	TYR	342	A	10.86	16	Not Liganded
5KY6	TYR	2	B	10.18	6	Not Liganded
5KY6	TYR	4	B	11.38	20	Not Liganded
5KY6	TYR	58	B	12.08	64	Not Liganded
5KY6	TYR	84	B	12.7	23	Not Liganded
5KY6	TYR	137	B	10.7	58	Not Liganded
5KY6	TYR	173	B	16.74	100	Not Liganded
5KY6	TYR	203	B	13	91	Not Liganded
5KY6	TYR	213	B	13.77	100	Not Liganded
5KY6	TYR	222	B	12.17	63	Not Liganded
5KY6	TYR	301	B	13.75	100	Liganded
5KY6	TYR	327	B	13.29	100	Not Liganded
5KY6	TYR	342	B	11.18	20	Not Liganded
5KY6	TYR	363	B	12.09	42	Not Liganded
5KY6	TYR	2	C	10.19	2	Not Liganded
5KY6	TYR	4	C	11.25	16	Not Liganded
5KY6	TYR	58	C	12.19	65	Not Liganded
5KY6	TYR	84	C	12.65	21	Not Liganded
5KY6	TYR	137	C	11.38	59	Not Liganded
5KY6	TYR	173	C	16.96	100	Not Liganded
5KY6	TYR	203	C	13.05	91	Not Liganded
5KY6	TYR	213	C	13.68	100	Not Liganded
5KY6	TYR	222	C	12.29	64	Not Liganded
5KY6	TYR	301	C	13.67	100	Liganded
5KY6	TYR	327	C	13.37	100	Not Liganded
5KY6	TYR	342	C	11.17	18	Not Liganded
5KY6	TYR	363	C	12	39	Not Liganded
5KY6	TYR	2	D	10.43	6	Not Liganded
5KY6	TYR	4	D	11.31	16	Not Liganded
5KY6	TYR	58	D	12.37	66	Not Liganded
5KY6	TYR	84	D	12.51	18	Not Liganded
5KY6	TYR	137	D	10.72	58	Not Liganded
5KY6	TYR	173	D	17.11	100	Not Liganded
5KY6	TYR	203	D	12.8	87	Not Liganded
5KY6	TYR	213	D	13.62	100	Not Liganded
5KY6	TYR	222	D	14.05	89	Not Liganded
5KY6	TYR	301	D	13.72	100	Liganded
5KY6	TYR	327	D	13.43	100	Not Liganded
5KY6	TYR	342	D	11.02	16	Not Liganded
5J0A	TYR	47	A	10.16	0	Not Liganded
5J0A	TYR	74	A	14.99	90	Not Liganded
5J0A	TYR	78	A	12.93	88	Not Liganded

5J0A	TYR	100	A	14.12	100	Not Liganded
5J0A	TYR	117	A	13.77	55	Not Liganded
5J0A	TYR	131	A	10.95	35	Not Liganded
5J0A	TYR	156	A	10.07	23	Liganded
5J0A	TYR	206	A	14.78	100	Not Liganded
5J0A	TYR	271	A	15.23	65	Not Liganded
5J0A	TYR	272	A	10.14	1	Not Liganded
5J0A	TYR	290	A	11.47	33	Not Liganded
5J0A	TYR	47	B	10.65	0	Not Liganded
5J0A	TYR	74	B	14.46	93	Not Liganded
5J0A	TYR	78	B	15.99	89	Not Liganded
5J0A	TYR	100	B	13.93	99	Not Liganded
5J0A	TYR	117	B	13.54	52	Not Liganded
5J0A	TYR	131	B	10.47	32	Not Liganded
5J0A	TYR	156	B	10.01	20	Liganded
5J0A	TYR	206	B	14.85	100	Not Liganded
5J0A	TYR	271	B	15.1	65	Not Liganded
5J0A	TYR	272	B	10.41	0	Not Liganded
5J0A	TYR	290	B	11.74	40	Not Liganded
5IQP	TYR	19	A	10.9	10	Not Liganded
5IQP	TYR	48	A	12.26	66	Not Liganded
5IQP	TYR	82	A	13.15	68	Not Liganded
5IQP	TYR	104	A	10.27	0	Not Liganded
5IQP	TYR	118	A	12.52	67	Not Liganded
5IQP	TYR	125	A	15.47	98	Not Liganded
5IQP	TYR	128	A	12.14	95	Liganded
5IQP	TYR	149	A	15.37	100	Not Liganded
5IQP	TYR	178	A	10.54	26	Not Liganded
5IQP	TYR	179	A	10.48	0	Not Liganded
5IQP	TYR	211	A	10.19	0	Not Liganded
5IQP	TYR	19	B	10.94	11	Not Liganded
5IQP	TYR	48	B	12.5	68	Not Liganded
5IQP	TYR	82	B	13.06	66	Not Liganded
5IQP	TYR	104	B	10.05	0	Not Liganded
5IQP	TYR	118	B	11.73	65	Not Liganded
5IQP	TYR	125	B	15.07	95	Not Liganded
5IQP	TYR	128	B	12.19	96	Liganded
5IQP	TYR	149	B	15.27	100	Not Liganded
5IQP	TYR	178	B	10.72	29	Not Liganded
5IQP	TYR	179	B	10.47	0	Not Liganded
5IQP	TYR	211	B	10.31	0	Not Liganded
5IKO	TYR	51	A	10.05	12	Not Liganded
5IKO	TYR	74	A	14.17	100	Not Liganded
5IKO	TYR	75	A	10.25	0	Not Liganded
5IKO	TYR	83	A	11.9	100	Not Liganded
5IKO	TYR	84	A	15.24	100	Not Liganded

5IKO	TYR	90	A	13.5	100	Not Liganded
5IKO	TYR	113	A	10.22	0	Not Liganded
5IKO	TYR	155	A	9.29	100	Not Liganded
5IKO	TYR	157	A	14.54	100	Not Liganded
5IKO	TYR	161	A	14.26	100	Not Liganded
5IKO	TYR	185	A	9.8	0	Not Liganded
5IKO	TYR	196	A	10.41	15	Not Liganded
5IKO	TYR	203	A	13.42	54	Not Liganded
5IKO	TYR	226	A	10.51	45	Not Liganded
5IKO	TYR	233	A	11.65	53	Not Liganded
5IKO	TYR	262	A	10.08	0	Not Liganded
5IKO	TYR	280	A	16.74	100	Not Liganded
5IKO	TYR	297	A	15.14	100	Not Liganded
5IKO	TYR	374	A	15.16	100	Not Liganded
5IKO	TYR	404	A	10.15	22	Not Liganded
5IKO	TYR	472	A	10.13	0	Not Liganded
5IKO	TYR	553	A	12.47	78	Not Liganded
5IKO	TYR	573	A	10.76	83	Not Liganded
5IKO	TYR	587	A	12.6	30	Not Liganded
5IKO	TYR	613	A	12.66	47	Not Liganded
5IKO	TYR	648	A	14.27	100	Not Liganded
5IKO	TYR	726	A	13.98	90	Not Liganded
5IKO	TYR	731	A	11.11	40	Not Liganded
5IKO	TYR	732	A	11.24	10	Liganded
5IKO	TYR	777	A	12.28	75	Not Liganded
5IKO	TYR	780	A	14.22	100	Not Liganded
5IKO	TYR	791	A	14.64	86	Not Liganded
5IKO	TYR	820	A	12.22	100	Not Liganded
5IA7	TYR	18	A	9.9	0	Liganded
5IA7	TYR	18	B	9.9	0	Liganded
5FV7	TYR	26	A	13.47	40	Not Liganded
5FV7	TYR	40	A	10.36	0	Not Liganded
5FV7	TYR	69	A	10.77	26	Not Liganded
5FV7	TYR	83	A	12.62	100	Not Liganded
5FV7	TYR	152	A	10.68	24	Not Liganded
5FV7	TYR	173	A	12.42	48	Not Liganded
5FV7	TYR	234	A	14.43	77	Not Liganded
5FV7	TYR	268	A	10.25	0	Liganded
5FV7	TYR	26	B	11.58	25	Not Liganded
5FV7	TYR	40	B	10.24	0	Not Liganded
5FV7	TYR	69	B	10.56	18	Not Liganded
5FV7	TYR	83	B	12.52	100	Not Liganded
5FV7	TYR	152	B	10.38	22	Not Liganded
5FV7	TYR	173	B	12.3	33	Not Liganded
5FV7	TYR	234	B	14.35	66	Not Liganded
5FV7	TYR	268	B	10	0	Liganded

5EPC	TYR	12	A	10.81	8	Liganded
5EPC	TYR	35	A	13.26	50	Not Liganded
5EPC	TYR	66	A	12.88	71	Not Liganded
5EPC	TYR	157	A	12.08	41	Not Liganded
5EPC	TYR	195	A	17.56	100	Not Liganded
5EPC	TYR	232	A	12.93	100	Not Liganded
5EPC	TYR	268	A	11.04	28	Not Liganded
5EPC	TYR	322	A	13.76	91	Not Liganded
5EPC	TYR	353	A	10.48	29	Not Liganded
5EPC	TYR	420	A	10.64	60	Not Liganded
5EPC	TYR	428	A	11.41	42	Not Liganded
5EPC	TYR	430	A	12.75	64	Not Liganded
5EPC	TYR	466	A	11.61	68	Not Liganded
5EPC	TYR	476	A	12.22	46	Not Liganded
5EPC	TYR	517	A	10.88	96	Not Liganded
5EPC	TYR	521	A	10.94	36	Not Liganded
5EPC	TYR	12	B	10.79	5	Liganded
5EPC	TYR	35	B	13.13	44	Not Liganded
5EPC	TYR	66	B	12.84	69	Not Liganded
5EPC	TYR	157	B	12.05	36	Not Liganded
5EPC	TYR	195	B	17.58	100	Not Liganded
5EPC	TYR	232	B	13	100	Not Liganded
5EPC	TYR	268	B	10.95	22	Not Liganded
5EPC	TYR	322	B	13.56	91	Not Liganded
5EPC	TYR	353	B	10.56	25	Not Liganded
5EPC	TYR	420	B	10.65	57	Not Liganded
5EPC	TYR	428	B	11.15	40	Not Liganded
5EPC	TYR	430	B	12.4	55	Not Liganded
5EPC	TYR	466	B	11.55	60	Not Liganded
5EPC	TYR	476	B	12.19	45	Not Liganded
5EPC	TYR	517	B	11.98	93	Not Liganded
5EPC	TYR	521	B	10.6	30	Not Liganded
5CYO	TYR	112	A	13.4	98	Not Liganded
5CYO	TYR	115	A	11	36	Not Liganded
5CYO	TYR	138	A	18.01	100	Not Liganded
5CYO	TYR	198	A	13.39	82	Not Liganded
5CYO	TYR	231	A	10.96	11	Liganded
5CYO	TYR	260	A	10.16	2	Not Liganded
5CYO	TYR	285	A	12.41	24	Not Liganded
5CYO	TYR	112	B	13.69	100	Not Liganded
5CYO	TYR	115	B	10.95	36	Not Liganded
5CYO	TYR	138	B	16.72	100	Not Liganded
5CYO	TYR	198	B	12.92	73	Not Liganded
5CYO	TYR	231	B	10.57	0	Liganded
5CYO	TYR	260	B	9.89	0	Not Liganded
5CYO	TYR	285	B	12.26	25	Not Liganded

4XW3	TYR	96	A	10.53	0	Liganded
4XW3	TYR	134	A	17.49	98	Not Liganded
4XW3	TYR	135	A	16.92	100	Not Liganded
4XW3	TYR	182	A	12.84	65	Not Liganded
4XW3	TYR	195	A	12.92	90	Not Liganded
4XW3	TYR	265	A	10.4	19	Not Liganded
4XW3	TYR	96	B	10.21	0	Liganded
4XW3	TYR	134	B	15.04	68	Not Liganded
4XW3	TYR	135	B	16.91	100	Not Liganded
4XW3	TYR	182	B	14.14	100	Not Liganded
4XW3	TYR	195	B	11.14	44	Not Liganded
4XW3	TYR	265	B	10.13	0	Not Liganded
4XOS	TYR	131	A	13.97	57	Liganded
4XOS	TYR	144	A	9.93	7	Not Liganded
4XOS	TYR	148	A	9.96	0	Not Liganded
4XOS	TYR	131	B	13.84	56	Liganded
4XOS	TYR	144	B	10.02	0	Not Liganded
4XOS	TYR	148	B	10.13	0	Not Liganded
4RJT	TYR	14	A	14.02	70	Not Liganded
4RJT	TYR	53	A	10.14	0	Not Liganded
4RJT	TYR	96	A	10.6	28	Liganded
4RJT	TYR	108	A	9.84	3	Not Liganded
4RJT	TYR	123	A	11.41	40	Not Liganded
4RJT	TYR	199	A	13.47	100	Not Liganded
4RJT	TYR	286	A	11.33	60	Not Liganded
4RJT	TYR	299	A	9.52	0	Not Liganded
4RJT	TYR	309	A	10.38	28	Not Liganded
4RJT	TYR	352	A	12.62	63	Not Liganded
4RJT	TYR	356	A	10.3	36	Not Liganded
4RJT	TYR	367	A	11.4	34	Not Liganded
4RJT	TYR	402	A	10.23	17	Not Liganded
4RJT	TYR	425	A	13.62	86	Not Liganded
4RJT	TYR	14	B	15.22	80	Not Liganded
4RJT	TYR	53	B	10.14	0	Not Liganded
4RJT	TYR	96	B	10.6	27	Liganded
4RJT	TYR	108	B	9.9	9	Not Liganded
4RJT	TYR	123	B	11.38	41	Not Liganded
4RJT	TYR	199	B	13.74	100	Not Liganded
4RJT	TYR	286	B	11.42	61	Not Liganded
4RJT	TYR	299	B	9.58	0	Not Liganded
4RJT	TYR	309	B	10.34	27	Not Liganded
4RJT	TYR	352	B	12.73	68	Not Liganded
4RJT	TYR	356	B	10.54	37	Not Liganded
4RJT	TYR	367	B	11.36	33	Not Liganded
4RJT	TYR	402	B	10.12	15	Not Liganded
4RJT	TYR	425	B	13.54	84	Not Liganded

4RJT	TYR	14	C	14.8	76	Not Liganded
4RJT	TYR	53	C	10.17	0	Not Liganded
4RJT	TYR	96	C	10.03	27	Liganded
4RJT	TYR	108	C	9.88	6	Not Liganded
4RJT	TYR	123	C	11.45	44	Not Liganded
4RJT	TYR	199	C	13.69	100	Not Liganded
4RJT	TYR	286	C	11	60	Not Liganded
4RJT	TYR	299	C	9.5	0	Not Liganded
4RJT	TYR	309	C	10.33	26	Not Liganded
4RJT	TYR	352	C	12.71	65	Not Liganded
4RJT	TYR	356	C	10.47	37	Not Liganded
4RJT	TYR	367	C	11.43	33	Not Liganded
4RJT	TYR	402	C	10.35	18	Not Liganded
4RJT	TYR	425	C	14	88	Not Liganded
4P22	TYR	55	A	11.58	83	Not Liganded
4P22	TYR	60	A	15.45	100	Not Liganded
4P22	TYR	117	A	14.09	100	Not Liganded
4P22	TYR	141	A	11.47	70	Not Liganded
4P22	TYR	147	A	10.66	0	Not Liganded
4P22	TYR	273	A	9.6	0	Liganded
4P22	TYR	286	A	11.46	21	Not Liganded
4P22	TYR	388	A	13.17	80	Not Liganded
4P22	TYR	425	A	13.93	100	Not Liganded
4P22	TYR	55	B	11.89	86	Not Liganded
4P22	TYR	60	B	15.12	94	Not Liganded
4P22	TYR	117	B	13.25	100	Not Liganded
4P22	TYR	141	B	10.09	0	Not Liganded
4P22	TYR	147	B	10.64	0	Not Liganded
4P22	TYR	273	B	9.86	0	Liganded
4P22	TYR	286	B	11.21	19	Not Liganded
4P22	TYR	388	B	13.2	77	Not Liganded
4P22	TYR	425	B	14.01	100	Not Liganded
4NUA	TYR	10	A	12.33	88	Not Liganded
4NUA	TYR	51	A	11.46	21	Not Liganded
4NUA	TYR	58	A	10.92	45	Not Liganded
4NUA	TYR	119	A	11.85	31	Not Liganded
4NUA	TYR	140	A	12.84	64	Not Liganded
4NUA	TYR	146	A	10.81	32	Not Liganded
4NUA	TYR	152	A	12.7	67	Not Liganded
4NUA	TYR	153	A	10.11	3	Not Liganded
4NUA	TYR	165	A	10.29	0	Not Liganded
4NUA	TYR	193	A	19.16	100	Not Liganded
4NUA	TYR	199	A	9.93	7	Not Liganded
4NUA	TYR	204	A	10.67	100	Not Liganded
4NUA	TYR	207	A	13.23	75	Not Liganded
4NUA	TYR	215	A	11.17	37	Not Liganded

4NUA	TYR	245	A	11.02	30	Not Liganded
4NUA	TYR	283	A	10.24	2	Not Liganded
4NUA	TYR	290	A	16.73	100	Not Liganded
4NUA	TYR	305	A	15.83	100	Not Liganded
4NUA	TYR	317	A	12.36	79	Not Liganded
4NUA	TYR	322	A	10.25	1	Not Liganded
4NUA	TYR	332	A	9.95	0	Not Liganded
4NUA	TYR	349	A	12.9	73	Liganded
4KXV	TYR	4	A	11.91	26	Not Liganded
4KXV	TYR	58	A	13.73	99	Not Liganded
4KXV	TYR	83	A	13.47	98	Not Liganded
4KXV	TYR	137	A	13.23	75	Not Liganded
4KXV	TYR	141	A	10.76	35	Not Liganded
4KXV	TYR	147	A	13.01	97	Not Liganded
4KXV	TYR	150	A	11.64	100	Not Liganded
4KXV	TYR	173	A	13.76	60	Not Liganded
4KXV	TYR	202	A	12.15	76	Not Liganded
4KXV	TYR	275	A	9.62	9	Not Liganded
4KXV	TYR	309	A	12.93	75	Liganded
4KXV	TYR	321	A	15.87	100	Not Liganded
4KXV	TYR	363	A	10.53	6	Not Liganded
4KXV	TYR	447	A	15.13	100	Not Liganded
4KXV	TYR	481	A	17.26	93	Not Liganded
4KXV	TYR	563	A	11.69	35	Not Liganded
4KXV	TYR	564	A	9.13	38	Not Liganded
4KBO	TYR	118	A	12	73	Not Liganded
4KBO	TYR	128	A	10.23	0	Liganded
4KBO	TYR	161	A	10.82	13	Not Liganded
4KBO	TYR	181	A	10.96	0	Not Liganded
4KBO	TYR	196	A	13.54	92	Not Liganded
4KBO	TYR	230	A	11.87	55	Not Liganded
4KBO	TYR	243	A	13.39	90	Not Liganded
4KBO	TYR	331	A	10.14	0	Not Liganded
4H5R	TYR	15	A	16.92	100	Not Liganded
4H5R	TYR	41	A	11.75	95	Liganded
4H5R	TYR	107	A	10.21	11	Not Liganded
4H5R	TYR	115	A	11.63	0	Not Liganded
4H5R	TYR	134	A	12.44	43	Not Liganded
4H5R	TYR	149	A	13.17	89	Not Liganded
4H5R	TYR	183	A	11.39	53	Not Liganded
4H5R	TYR	288	A	10.68	0	Not Liganded
4H5R	TYR	294	A	13.61	70	Not Liganded
4H5R	TYR	371	A	10.65	29	Not Liganded
4H5R	TYR	15	B	16.97	100	Not Liganded
4H5R	TYR	41	B	12.02	97	Liganded
4H5R	TYR	107	B	10.19	10	Not Liganded

4H5R	TYR	115	B	11.64	0	Not Liganded
4H5R	TYR	134	B	12.5	42	Not Liganded
4H5R	TYR	149	B	13.12	87	Not Liganded
4H5R	TYR	183	B	11.39	55	Not Liganded
4H5R	TYR	288	B	10.81	0	Not Liganded
4H5R	TYR	294	B	13.68	71	Not Liganded
4H5R	TYR	371	B	10.66	31	Not Liganded
4FCJ	TYR	19	A	21.67	100	Not Liganded
4FCJ	TYR	20	A	15.52	100	Not Liganded
4FCJ	TYR	34	A	17.7	100	Not Liganded
4FCJ	TYR	40	A	14.91	100	Not Liganded
4FCJ	TYR	56	A	10.64	30	Liganded
4FCJ	TYR	125	A	11.36	40	Not Liganded
4FCJ	TYR	133	A	11.64	57	Not Liganded
4FCJ	TYR	19	B	21.95	100	Not Liganded
4FCJ	TYR	20	B	15.55	100	Not Liganded
4FCJ	TYR	34	B	17.58	100	Not Liganded
4FCJ	TYR	40	B	14.78	100	Not Liganded
4FCJ	TYR	56	B	11.02	42	Liganded
4FCJ	TYR	125	B	10.74	18	Not Liganded
4FCJ	TYR	133	B	12.18	71	Not Liganded
4CET	TYR	20	A	10.1	6	Not Liganded
4CET	TYR	43	A	10.62	27	Liganded
4CET	TYR	68	A	13.79	60	Not Liganded
4CET	TYR	76	A	10.95	28	Not Liganded
4CET	TYR	127	A	11.28	37	Not Liganded
4CET	TYR	129	A	10.21	0	Not Liganded
4CET	TYR	133	A	10.44	4	Not Liganded
4CET	TYR	156	A	10.81	34	Not Liganded
4CET	TYR	191	A	11.71	46	Not Liganded
4CET	TYR	222	A	10.15	0	Not Liganded
4BSM	TYR	36	A	10.12	0	Liganded
4BSM	TYR	78	A	12.6	58	Not Liganded
4BSM	TYR	105	A	12.91	35	Not Liganded
4BSM	TYR	126	A	11.61	55	Not Liganded
4BSM	TYR	240	A	9.46	0	Not Liganded
4BSM	TYR	252	A	10.26	0	Not Liganded
4BSM	TYR	279	A	10.84	0	Not Liganded
4BSM	TYR	308	A	11.27	20	Not Liganded
4BSM	TYR	353	A	12.04	41	Not Liganded
4BSM	TYR	372	A	14.39	100	Not Liganded
4BSM	TYR	381	A	10.3	5	Not Liganded
4BSM	TYR	409	A	17.76	91	Not Liganded
4BSM	TYR	454	A	12.22	70	Not Liganded
4BSM	TYR	463	A	11.56	11	Not Liganded
4BSM	TYR	469	A	11	6	Not Liganded

4BSM	TYR	546	A	15.59	81	Not Liganded
4BSM	TYR	551	A	13.76	96	Not Liganded
4BSM	TYR	634	A	10.95	53	Not Liganded
4BSM	TYR	639	A	10.14	15	Not Liganded
4BSM	TYR	657	A	12.92	87	Not Liganded
4BSM	TYR	714	A	11.75	51	Not Liganded
4BSM	TYR	721	A	13.17	53	Not Liganded
4BSM	TYR	788	A	10.6	23	Not Liganded
4BSM	TYR	915	A	10.35	0	Not Liganded
4BSM	TYR	918	A	10.31	0	Not Liganded
4BEX	TYR	68	1	12.83	82	Not Liganded
4BEX	TYR	82	1	13.53	73	Not Liganded
4BEX	TYR	85	1	16.58	91	Not Liganded
4BEX	TYR	89	1	12.42	22	Liganded
4BEX	TYR	117	1	11.82	64	Not Liganded
3SRH	TYR	82	A	10.34	10	Not Liganded
3SRH	TYR	104	A	13.11	60	Not Liganded
3SRH	TYR	147	A	10.23	0	Not Liganded
3SRH	TYR	160	A	12.47	43	Not Liganded
3SRH	TYR	174	A	11.31	51	Not Liganded
3SRH	TYR	369	A	10.53	0	Not Liganded
3SRH	TYR	389	A	13.31	78	Liganded
3SRH	TYR	443	A	13.94	80	Not Liganded
3SRH	TYR	465	A	13.08	93	Not Liganded
3SRH	TYR	82	B	10.25	12	Not Liganded
3SRH	TYR	104	B	12.55	58	Not Liganded
3SRH	TYR	147	B	10.23	0	Not Liganded
3SRH	TYR	160	B	12.25	35	Not Liganded
3SRH	TYR	174	B	10.71	49	Not Liganded
3SRH	TYR	369	B	10.45	0	Not Liganded
3SRH	TYR	389	B	13.1	76	Liganded
3SRH	TYR	443	B	13.87	83	Not Liganded
3SRH	TYR	465	B	12.71	90	Not Liganded
3SRH	TYR	82	C	10.29	9	Not Liganded
3SRH	TYR	104	C	12.25	58	Not Liganded
3SRH	TYR	147	C	10.14	0	Not Liganded
3SRH	TYR	160	C	12.49	41	Not Liganded
3SRH	TYR	174	C	10.22	47	Not Liganded
3SRH	TYR	369	C	10.4	0	Not Liganded
3SRH	TYR	389	C	13.23	80	Liganded
3SRH	TYR	443	C	14.06	84	Not Liganded
3SRH	TYR	465	C	13.18	95	Not Liganded
3SRH	TYR	82	D	10.55	28	Not Liganded
3SRH	TYR	104	D	12.73	58	Not Liganded
3SRH	TYR	147	D	10.19	0	Not Liganded
3SRH	TYR	160	D	12.62	41	Not Liganded

3SRH	TYR	174	D	10.85	47	Not Liganded
3SRH	TYR	369	D	10.51	0	Not Liganded
3SRH	TYR	389	D	13.02	75	Liganded
3SRH	TYR	443	D	13.37	86	Not Liganded
3SRH	TYR	465	D	13.35	100	Not Liganded
3Q6M	TYR	309	A	11.8	33	Not Liganded
3Q6M	TYR	313	A	12.37	47	Not Liganded
3Q6M	TYR	364	A	10.86	20	Not Liganded
3Q6M	TYR	381	A	14.09	73	Not Liganded
3Q6M	TYR	434	A	13.71	88	Not Liganded
3Q6M	TYR	438	A	13.83	100	Not Liganded
3Q6M	TYR	465	A	18.06	100	Liganded
3Q6M	TYR	466	A	10.48	10	Not Liganded
3Q6M	TYR	480	A	13.04	87	Not Liganded
3Q6M	TYR	492	A	12.4	61	Not Liganded
3Q6M	TYR	493	A	12.35	82	Not Liganded
3Q6M	TYR	520	A	11.42	53	Not Liganded
3Q6M	TYR	528	A	11.2	9	Not Liganded
3Q6M	TYR	604	A	9.94	0	Not Liganded
3Q6M	TYR	667	A	12.19	52	Not Liganded
3Q6M	TYR	689	A	14.94	100	Not Liganded
3Q6M	TYR	309	B	11.74	35	Not Liganded
3Q6M	TYR	313	B	13.78	70	Not Liganded
3Q6M	TYR	364	B	10.83	21	Not Liganded
3Q6M	TYR	381	B	14.31	71	Not Liganded
3Q6M	TYR	434	B	13.31	85	Not Liganded
3Q6M	TYR	438	B	12.1	100	Not Liganded
3Q6M	TYR	465	B	17.93	100	Liganded
3Q6M	TYR	466	B	10.63	11	Not Liganded
3Q6M	TYR	480	B	13.4	91	Not Liganded
3Q6M	TYR	492	B	12.73	61	Not Liganded
3Q6M	TYR	493	B	12.49	83	Not Liganded
3Q6M	TYR	520	B	11.38	49	Not Liganded
3Q6M	TYR	528	B	10.31	0	Not Liganded
3Q6M	TYR	604	B	10.07	0	Not Liganded
3Q6M	TYR	667	B	12.69	56	Not Liganded
3Q6M	TYR	689	B	15.23	100	Not Liganded
3Q6M	TYR	309	C	11.81	35	Not Liganded
3Q6M	TYR	313	C	12.59	43	Not Liganded
3Q6M	TYR	364	C	12.51	73	Not Liganded
3Q6M	TYR	381	C	13.74	62	Not Liganded
3Q6M	TYR	434	C	13.16	81	Not Liganded
3Q6M	TYR	438	C	13.36	100	Not Liganded
3Q6M	TYR	465	C	17.85	100	Liganded
3Q6M	TYR	466	C	10.4	10	Not Liganded
3Q6M	TYR	480	C	12.84	88	Not Liganded

3Q6M	TYR	492	C	12.23	57	Not Liganded
3Q6M	TYR	493	C	12.14	82	Not Liganded
3Q6M	TYR	520	C	11.3	45	Not Liganded
3Q6M	TYR	528	C	10.32	8	Not Liganded
3Q6M	TYR	604	C	10.09	0	Not Liganded
3Q6M	TYR	667	C	10.4	45	Not Liganded
3Q6M	TYR	689	C	10.14	0	Not Liganded
3PFF	TYR	16	A	12.47	98	Not Liganded
3PFF	TYR	31	A	13.52	51	Not Liganded
3PFF	TYR	120	A	16.69	70	Not Liganded
3PFF	TYR	124	A	11.23	25	Not Liganded
3PFF	TYR	131	A	11.71	0	Not Liganded
3PFF	TYR	192	A	15.9	95	Not Liganded
3PFF	TYR	196	A	12.46	65	Not Liganded
3PFF	TYR	199	A	14.1	71	Not Liganded
3PFF	TYR	213	A	10.71	28	Not Liganded
3PFF	TYR	227	A	11.6	36	Not Liganded
3PFF	TYR	247	A	10.24	9	Not Liganded
3PFF	TYR	252	A	10.4	18	Not Liganded
3PFF	TYR	288	A	12.89	100	Not Liganded
3PFF	TYR	304	A	10.26	47	Not Liganded
3PFF	TYR	307	A	11.87	100	Not Liganded
3PFF	TYR	317	A	11.72	0	Not Liganded
3PFF	TYR	319	A	13.59	100	Not Liganded
3PFF	TYR	364	A	10.47	18	Not Liganded
3PFF	TYR	384	A	10.96	45	Not Liganded
3PFF	TYR	517	A	10.18	0	Not Liganded
3PFF	TYR	531	A	10.35	0	Not Liganded
3PFF	TYR	542	A	11.36	0	Not Liganded
3PFF	TYR	579	A	11.5	39	Not Liganded
3PFF	TYR	588	A	10.8	8	Not Liganded
3PFF	TYR	652	A	9.86	0	Not Liganded
3PFF	TYR	659	A	13.24	100	Not Liganded
3PFF	TYR	682	A	10.75	48	Liganded
3PFF	TYR	692	A	12.09	67	Not Liganded
3PFF	TYR	704	A	14.53	100	Not Liganded
3PFF	TYR	725	A	11.25	12	Not Liganded
3PFF	TYR	801	A	11.47	17	Not Liganded
3PBH	TYR	16	A	9.27	0	Not Liganded
3PBH	TYR	31	A	10.69	17	Not Liganded
3PBH	TYR	37	A	14.4	100	Not Liganded
3PBH	TYR	75	A	10.32	0	Not Liganded
3PBH	TYR	94	A	10.51	0	Not Liganded
3PBH	TYR	103	A	14.25	100	Not Liganded
3PBH	TYR	136	A	11.54	25	Not Liganded
3PBH	TYR	140	A	13.32	48	Not Liganded

3PBH	TYR	146	A	10.22	13	Not Liganded
3PBH	TYR	148	A	10.14	0	Not Liganded
3PBH	TYR	151	A	12.24	80	Not Liganded
3PBH	TYR	165	A	10.25	0	Not Liganded
3PBH	TYR	177	A	10.58	0	Liganded
3PBH	TYR	183	A	13.32	82	Not Liganded
3PBH	TYR	188	A	16.88	96	Not Liganded
3PBH	TYR	214	A	11.3	37	Not Liganded
3GJ0	TYR	39	A	11.62	64	Not Liganded
3GJ0	TYR	79	A	14.99	100	Not Liganded
3GJ0	TYR	80	A	13.26	77	Not Liganded
3GJ0	TYR	98	A	10.06	45	Not Liganded
3GJ0	TYR	146	A	16.05	100	Liganded
3GJ0	TYR	147	A	11.82	58	Not Liganded
3GJ0	TYR	155	A	13.67	55	Not Liganded
3GJ0	TYR	197	A	10.89	31	Not Liganded
3GJ0	TYR	39	B	10.25	0	Not Liganded
3GJ0	TYR	79	B	14.56	100	Not Liganded
3GJ0	TYR	80	B	12.45	56	Not Liganded
3GJ0	TYR	98	B	10.17	45	Not Liganded
3GJ0	TYR	146	B	15.99	100	Liganded
3GJ0	TYR	147	B	11.9	57	Not Liganded
3GJ0	TYR	155	B	11.95	52	Not Liganded
3GJ0	TYR	197	B	11.12	31	Not Liganded
3FRR	TYR	43	A	9.01	0	Liganded
3FRR	TYR	64	A	10.51	12	Not Liganded
3FRR	TYR	75	A	12.25	37	Not Liganded
3FRR	TYR	128	A	11.93	47	Not Liganded
3FRR	TYR	132	A	13.34	57	Not Liganded
3FRR	TYR	165	A	12.72	47	Not Liganded
3FRR	TYR	173	A	10.4	0	Not Liganded
3FRR	TYR	177	A	13.01	39	Not Liganded
3FCX	TYR	35	A	11.56	43	Not Liganded
3FCX	TYR	49	A	13.74	100	Not Liganded
3FCX	TYR	67	A	13.99	100	Not Liganded
3FCX	TYR	106	A	15.26	100	Not Liganded
3FCX	TYR	118	A	13.68	100	Not Liganded
3FCX	TYR	121	A	15.62	100	Not Liganded
3FCX	TYR	123	A	14.83	100	Not Liganded
3FCX	TYR	166	A	16.19	100	Not Liganded
3FCX	TYR	191	A	12.49	60	Not Liganded
3FCX	TYR	202	A	13.06	100	Liganded
3FCX	TYR	211	A	11.83	77	Not Liganded
3FCX	TYR	258	A	10.15	0	Not Liganded
3FCX	TYR	262	A	13.77	88	Not Liganded
3FCX	TYR	263	A	10.01	0	Not Liganded

3FCX	TYR	279	A	10.58	6	Not Liganded
3FCX	TYR	35	B	11.2	35	Not Liganded
3FCX	TYR	49	B	13.69	100	Not Liganded
3FCX	TYR	67	B	13.94	100	Not Liganded
3FCX	TYR	106	B	14.54	100	Not Liganded
3FCX	TYR	118	B	14.99	71	Not Liganded
3FCX	TYR	121	B	15.11	100	Not Liganded
3FCX	TYR	123	B	14.72	100	Not Liganded
3FCX	TYR	166	B	16.28	100	Not Liganded
3FCX	TYR	191	B	11.7	100	Not Liganded
3FCX	TYR	202	B	13.3	100	Liganded
3FCX	TYR	211	B	12.03	56	Not Liganded
3FCX	TYR	258	B	10.04	0	Not Liganded
3FCX	TYR	262	B	14.21	100	Not Liganded
3FCX	TYR	263	B	10.02	0	Not Liganded
3FCX	TYR	279	B	11.98	8	Not Liganded
3F8U	TYR	67	A	15.22	100	Liganded
3F8U	TYR	95	A	12.63	36	Not Liganded
3F8U	TYR	100	A	13.82	63	Not Liganded
3F8U	TYR	115	A	12.29	55	Not Liganded
3F8U	TYR	182	A	11.53	51	Not Liganded
3F8U	TYR	196	A	11.61	34	Not Liganded
3F8U	TYR	222	A	11.8	27	Not Liganded
3F8U	TYR	264	A	13.61	82	Not Liganded
3F8U	TYR	265	A	14.52	88	Not Liganded
3F8U	TYR	269	A	11.9	69	Not Liganded
3F8U	TYR	278	A	8.95	0	Not Liganded
3F8U	TYR	356	A	12.03	38	Not Liganded
3F8U	TYR	364	A	11.23	29	Not Liganded
3F8U	TYR	402	A	12.58	63	Not Liganded
3F8U	TYR	416	A	14.96	100	Not Liganded
3F8U	TYR	445	A	12.02	72	Not Liganded
3F8U	TYR	454	A	9.33	25	Not Liganded
3F8U	TYR	467	A	12.04	37	Not Liganded
3F8U	TYR	479	A	12.38	49	Not Liganded
3F8U	TYR	45	B	10.89	7	Not Liganded
3F8U	TYR	62	B	10.46	20	Not Liganded
3F8U	TYR	164	B	12.53	100	Not Liganded
3F8U	TYR	249	B	12.12	75	Not Liganded
3F8U	TYR	257	B	11.9	46	Not Liganded
3F8U	TYR	269	B	9.69	4	Not Liganded
3F8U	TYR	301	B	12.29	30	Not Liganded
3F8U	TYR	360	B	11.92	57	Not Liganded
3F8U	TYR	67	C	15.18	100	Liganded
3F8U	TYR	95	C	12.31	25	Not Liganded
3F8U	TYR	100	C	14.04	57	Not Liganded

3F8U	TYR	115	C	12.54	58	Not Liganded
3F8U	TYR	182	C	11.33	48	Not Liganded
3F8U	TYR	196	C	11.63	35	Not Liganded
3F8U	TYR	222	C	11.85	29	Not Liganded
3F8U	TYR	264	C	13.91	85	Not Liganded
3F8U	TYR	265	C	14.28	87	Not Liganded
3F8U	TYR	269	C	11.75	66	Not Liganded
3F8U	TYR	278	C	8.9	0	Not Liganded
3F8U	TYR	356	C	12.04	39	Not Liganded
3F8U	TYR	364	C	10.99	25	Not Liganded
3F8U	TYR	402	C	12.71	66	Not Liganded
3F8U	TYR	416	C	14.94	100	Not Liganded
3F8U	TYR	445	C	12.01	72	Not Liganded
3F8U	TYR	454	C	9.37	26	Not Liganded
3F8U	TYR	467	C	11.98	36	Not Liganded
3F8U	TYR	479	C	12.38	49	Not Liganded
3F8U	TYR	45	D	10.9	11	Not Liganded
3F8U	TYR	62	D	10.42	19	Not Liganded
3F8U	TYR	164	D	12.78	96	Not Liganded
3F8U	TYR	249	D	12.11	74	Not Liganded
3F8U	TYR	257	D	12.07	48	Not Liganded
3F8U	TYR	269	D	9.68	6	Not Liganded
3F8U	TYR	301	D	11.77	26	Not Liganded
3F8U	TYR	360	D	11.73	48	Not Liganded
3.00E+77	TYR	12	A	11.41	40	Not Liganded
3.00E+77	TYR	32	A	11.74	42	Not Liganded
3.00E+77	TYR	70	A	11.72	37	Not Liganded
3.00E+77	TYR	101	A	13.59	100	Not Liganded
3.00E+77	TYR	131	A	11.29	40	Not Liganded
3.00E+77	TYR	148	A	17.21	100	Not Liganded
3.00E+77	TYR	150	A	19.38	100	Not Liganded
3.00E+77	TYR	151	A	16.16	97	Not Liganded
3.00E+77	TYR	230	A	14.37	100	Not Liganded
3.00E+77	TYR	240	A	12.25	61	Not Liganded
3.00E+77	TYR	249	A	14.3	89	Not Liganded
3.00E+77	TYR	279	A	14.96	98	Not Liganded
3.00E+77	TYR	289	A	13.99	83	Liganded
3.00E+77	TYR	346	A	10.05	100	Not Liganded
3.00E+77	TYR	12	B	10.7	29	Not Liganded
3.00E+77	TYR	32	B	10.96	40	Not Liganded
3.00E+77	TYR	70	B	11.71	37	Not Liganded
3.00E+77	TYR	101	B	13.36	100	Not Liganded
3.00E+77	TYR	131	B	11.13	36	Not Liganded
3.00E+77	TYR	148	B	17.42	100	Not Liganded
3.00E+77	TYR	150	B	19.24	100	Not Liganded
3.00E+77	TYR	151	B	16.45	100	Not Liganded

3.00E+77	TYR	230	B	14.29	100	Not Liganded
3.00E+77	TYR	240	B	12.45	65	Not Liganded
3.00E+77	TYR	249	B	13.64	81	Not Liganded
3.00E+77	TYR	279	B	14.92	100	Not Liganded
3.00E+77	TYR	289	B	13.79	77	Liganded
3.00E+77	TYR	346	B	10.13	100	Not Liganded
3.00E+77	TYR	12	C	9.75	0	Not Liganded
3.00E+77	TYR	32	C	10.2	36	Not Liganded
3.00E+77	TYR	70	C	11.34	35	Not Liganded
3.00E+77	TYR	101	C	13.32	100	Not Liganded
3.00E+77	TYR	131	C	10.99	32	Not Liganded
3.00E+77	TYR	148	C	17.35	100	Not Liganded
3.00E+77	TYR	150	C	18.9	100	Not Liganded
3.00E+77	TYR	151	C	16.19	96	Not Liganded
3.00E+77	TYR	230	C	13.84	100	Not Liganded
3.00E+77	TYR	240	C	9.64	0	Not Liganded
3.00E+77	TYR	249	C	12.97	47	Not Liganded
3.00E+77	TYR	279	C	14.68	96	Not Liganded
3.00E+77	TYR	289	C	13.82	83	Liganded
3.00E+77	TYR	346	C	10.78	93	Not Liganded
3CU8	TYR	19	A	11.59	25	Liganded
3CU8	TYR	48	A	13.82	68	Not Liganded
3CU8	TYR	82	A	13.38	68	Not Liganded
3CU8	TYR	118	A	12.5	74	Not Liganded
3CU8	TYR	125	A	13.79	100	Not Liganded
3CU8	TYR	126	A	10.92	41	Not Liganded
3CU8	TYR	128	A	15.07	100	Not Liganded
3CU8	TYR	149	A	16.03	100	Not Liganded
3CU8	TYR	178	A	11.31	37	Not Liganded
3CU8	TYR	179	A	10.52	0	Not Liganded
3CU8	TYR	211	A	10.13	0	Not Liganded
3CU8	TYR	19	B	11.19	23	Liganded
3CU8	TYR	48	B	13.4	67	Not Liganded
3CU8	TYR	82	B	13.22	61	Not Liganded
3CU8	TYR	118	B	12.4	69	Not Liganded
3CU8	TYR	125	B	14.29	100	Not Liganded
3CU8	TYR	126	B	10.91	39	Not Liganded
3CU8	TYR	128	B	15.49	100	Not Liganded
3CU8	TYR	149	B	14.56	100	Not Liganded
3CU8	TYR	178	B	11.15	33	Not Liganded
3CU8	TYR	179	B	10.57	0	Not Liganded
3CU8	TYR	211	B	10.1	0	Not Liganded
3CTZ	TYR	22	A	10.26	0	Not Liganded
3CTZ	TYR	30	A	13.48	100	Not Liganded
3CTZ	TYR	42	A	13.02	70	Not Liganded
3CTZ	TYR	78	A	9.25	38	Not Liganded

3CTZ	TYR	128	A	13.42	98	Liganded
3CTZ	TYR	173	A	11.14	15	Not Liganded
3CTZ	TYR	225	A	13.2	100	Not Liganded
3CTZ	TYR	261	A	10.68	9	Not Liganded
3CTZ	TYR	268	A	15.31	100	Not Liganded
3CTZ	TYR	296	A	11.72	36	Not Liganded
3CTZ	TYR	312	A	10.57	23	Not Liganded
3CTZ	TYR	396	A	11.09	24	Not Liganded
3CTZ	TYR	412	A	13.17	100	Not Liganded
3CTZ	TYR	420	A	15.66	100	Not Liganded
3CTZ	TYR	439	A	14.55	13	Not Liganded
3CTZ	TYR	446	A	11.51	8	Not Liganded
3CTZ	TYR	483	A	13.88	94	Not Liganded
3CTZ	TYR	506	A	10.55	17	Not Liganded
3CTZ	TYR	526	A	11.87	21	Not Liganded
3CTZ	TYR	527	A	11.84	100	Not Liganded
3CTZ	TYR	549	A	9.9	0	Not Liganded
3CTZ	TYR	588	A	13.13	100	Not Liganded
2ZJ3	TYR	348	A	10.08	0	Not Liganded
2ZJ3	TYR	377	A	11.19	50	Not Liganded
2ZJ3	TYR	434	A	10.62	8	Not Liganded
2ZJ3	TYR	477	A	14.18	100	Not Liganded
2ZJ3	TYR	534	A	10.22	0	Liganded
2ZJ3	TYR	546	A	13.38	65	Not Liganded
2ZJ3	TYR	548	A	11.18	37	Not Liganded
2ZJ3	TYR	563	A	10.14	10	Not Liganded
2ZJ3	TYR	598	A	12.38	19	Not Liganded
2ZJ3	TYR	665	A	9.84	0	Not Liganded
2ZB4	TYR	29	A	10.2	0	Not Liganded
2ZB4	TYR	45	A	11.67	42	Not Liganded
2ZB4	TYR	51	A	14.46	100	Not Liganded
2ZB4	TYR	64	A	10.25	0	Not Liganded
2ZB4	TYR	100	A	11.77	30	Not Liganded
2ZB4	TYR	128	A	11.73	41	Not Liganded
2ZB4	TYR	208	A	14.67	62	Not Liganded
2ZB4	TYR	228	A	15.35	100	Not Liganded
2ZB4	TYR	259	A	12.7	100	Not Liganded
2ZB4	TYR	265	A	15.17	100	Liganded
2ZB4	TYR	292	A	10.65	20	Not Liganded
2YRQ	TYR	23	A	10.89	3	Liganded
2YRQ	TYR	78	A	10.52	1	Not Liganded
2YRQ	TYR	85	A	10.44	0	Not Liganded
2YRQ	TYR	116	A	10.37	1	Not Liganded
2YRQ	TYR	151	A	11.54	4	Not Liganded
2YRQ	TYR	162	A	10.35	5	Not Liganded
2YRQ	TYR	169	A	10.67	0	Not Liganded

2XQQ	TYR	32	A	9.7	0	Liganded
2XQQ	TYR	41	A	10.92	1	Not Liganded
2XQQ	TYR	50	A	12.14	16	Not Liganded
2XQQ	TYR	65	A	11.61	66	Not Liganded
2XQQ	TYR	75	A	14.71	91	Not Liganded
2XQQ	TYR	77	A	12.04	60	Not Liganded
2XQQ	TYR	32	B	10.02	0	Liganded
2XQQ	TYR	41	B	11.05	1	Not Liganded
2XQQ	TYR	50	B	12.55	17	Not Liganded
2XQQ	TYR	65	B	10.28	0	Not Liganded
2XQQ	TYR	75	B	12.16	31	Not Liganded
2XQQ	TYR	77	B	9.75	0	Not Liganded
2XQQ	TYR	32	C	13.25	55	Liganded
2XQQ	TYR	41	C	11.49	26	Not Liganded
2XQQ	TYR	50	C	11.88	11	Not Liganded
2XQQ	TYR	65	C	9.83	18	Not Liganded
2XQQ	TYR	75	C	13.95	65	Not Liganded
2XQQ	TYR	77	C	10.07	26	Not Liganded
2XQQ	TYR	32	D	10.2	0	Liganded
2XQQ	TYR	41	D	12.11	35	Not Liganded
2XQQ	TYR	50	D	14.81	71	Not Liganded
2XQQ	TYR	65	D	10.18	0	Not Liganded
2XQQ	TYR	75	D	12.1	21	Not Liganded
2XQQ	TYR	77	D	9.91	0	Not Liganded
2VYI	TYR	114	A	12.13	56	Not Liganded
2VYI	TYR	127	A	12.51	27	Not Liganded
2VYI	TYR	135	A	10.67	37	Not Liganded
2VYI	TYR	141	A	9.97	0	Liganded
2VYI	TYR	158	A	13.36	54	Not Liganded
2VYI	TYR	162	A	10.68	9	Not Liganded
2VYI	TYR	181	A	11.31	28	Not Liganded
2VYI	TYR	182	A	12.46	56	Not Liganded
2VYI	TYR	195	A	11.65	41	Not Liganded
2VYI	TYR	114	B	12.38	56	Not Liganded
2VYI	TYR	127	B	12.37	17	Not Liganded
2VYI	TYR	135	B	10.64	33	Not Liganded
2VYI	TYR	141	B	9.87	0	Liganded
2VYI	TYR	158	B	12.74	48	Not Liganded
2VYI	TYR	162	B	10.08	6	Not Liganded
2VYI	TYR	181	B	10.89	29	Not Liganded
2VYI	TYR	182	B	12.43	57	Not Liganded
2VYI	TYR	195	B	11.48	36	Not Liganded
2V40	TYR	77	A	10.01	0	Not Liganded
2V40	TYR	170	A	12.54	95	Not Liganded
2V40	TYR	202	A	11.19	56	Liganded
2V40	TYR	206	A	9.82	4	Not Liganded

2V40	TYR	223	A	10.87	23	Not Liganded
2V40	TYR	236	A	10.61	0	Not Liganded
2V40	TYR	239	A	10.3	0	Not Liganded
2V40	TYR	266	A	10.15	0	Not Liganded
2V40	TYR	294	A	12.08	46	Not Liganded
2V40	TYR	300	A	17.6	100	Not Liganded
2V40	TYR	348	A	11.74	48	Not Liganded
2V40	TYR	378	A	17.06	95	Not Liganded
2V40	TYR	402	A	12.46	60	Not Liganded
2V40	TYR	428	A	13.71	100	Not Liganded
2QUH	TYR	100	A	11.66	63	Not Liganded
2QUH	TYR	150	A	11.09	36	Not Liganded
2QUH	TYR	157	A	17.11	100	Not Liganded
2QUH	TYR	159	A	16.59	100	Not Liganded
2QUH	TYR	201	A	12.5	70	Not Liganded
2QUH	TYR	212	A	13.03	60	Not Liganded
2QUH	TYR	214	A	10.53	5	Not Liganded
2QUH	TYR	240	A	12.75	100	Not Liganded
2QUH	TYR	248	A	16.32	100	Not Liganded
2QUH	TYR	316	A	15.21	88	Liganded
2QUH	TYR	329	A	12.05	76	Not Liganded
2QUH	TYR	402	A	12.97	100	Not Liganded
2QUH	TYR	420	A	12.96	54	Not Liganded
2QUH	TYR	100	B	11.97	77	Not Liganded
2QUH	TYR	150	B	10.5	22	Not Liganded
2QUH	TYR	157	B	17.16	100	Not Liganded
2QUH	TYR	159	B	16.76	100	Not Liganded
2QUH	TYR	201	B	12.22	67	Not Liganded
2QUH	TYR	212	B	12.32	50	Not Liganded
2QUH	TYR	214	B	10.55	0	Not Liganded
2QUH	TYR	240	B	13.18	98	Not Liganded
2QUH	TYR	248	B	16.77	100	Not Liganded
2QUH	TYR	316	B	15.16	92	Liganded
2QUH	TYR	329	B	10.31	72	Not Liganded
2QUH	TYR	402	B	14.25	100	Not Liganded
2QUH	TYR	420	B	13.68	58	Not Liganded
2QC7	TYR	47	A	10.73	10	Not Liganded
2QC7	TYR	64	A	10.17	0	Liganded
2QC7	TYR	66	A	10.14	0	Not Liganded
2QC7	TYR	96	A	11.18	43	Not Liganded
2QC7	TYR	108	A	12.42	42	Not Liganded
2QC7	TYR	115	A	11.13	35	Not Liganded
2QC7	TYR	119	A	11.18	36	Not Liganded
2QC7	TYR	132	A	10.81	14	Not Liganded
2QC7	TYR	151	A	10.58	0	Not Liganded
2QC7	TYR	161	A	11.5	22	Not Liganded

2QC7	TYR	202	A	14.67	70	Not Liganded
2QC7	TYR	47	B	10.65	11	Not Liganded
2QC7	TYR	64	B	10.18	0	Liganded
2QC7	TYR	66	B	10.32	0	Not Liganded
2QC7	TYR	96	B	10.65	0	Not Liganded
2QC7	TYR	108	B	12.29	42	Not Liganded
2QC7	TYR	115	B	11.28	37	Not Liganded
2QC7	TYR	119	B	11.24	37	Not Liganded
2QC7	TYR	132	B	10.8	16	Not Liganded
2QC7	TYR	151	B	10.6	0	Not Liganded
2QC7	TYR	161	B	11.5	22	Not Liganded
2QC7	TYR	202	B	14.82	73	Not Liganded
2Q5H	TYR	80	A	13.74	92	Not Liganded
2Q5H	TYR	87	A	10.04	0	Not Liganded
2Q5H	TYR	94	A	11.38	48	Not Liganded
2Q5H	TYR	195	A	11.07	12	Not Liganded
2Q5H	TYR	207	A	11.7	18	Not Liganded
2Q5H	TYR	241	A	12.09	14	Not Liganded
2Q5H	TYR	320	A	10.03	0	Not Liganded
2Q5H	TYR	322	A	10.23	10	Not Liganded
2Q5H	TYR	354	A	13.54	52	Not Liganded
2Q5H	TYR	360	A	10.65	36	Not Liganded
2Q5H	TYR	362	A	14.04	100	Not Liganded
2Q5H	TYR	386	A	11.36	0	Not Liganded
2Q5H	TYR	399	A	11.14	43	Not Liganded
2Q5H	TYR	413	A	14.54	91	Liganded
2Q5H	TYR	512	A	10.35	0	Not Liganded
2Q5H	TYR	532	A	15.62	66	Not Liganded
2Q5H	TYR	604	A	13.02	100	Not Liganded
2Q5H	TYR	669	A	11.29	14	Not Liganded
2PD6	TYR	169	A	13.35	100	Liganded
2PD6	TYR	247	A	12.51	58	Not Liganded
2PD6	TYR	169	B	13.55	100	Liganded
2PD6	TYR	247	B	12.15	45	Not Liganded
2PD6	TYR	169	C	13.41	100	Liganded
2PD6	TYR	247	C	12.42	53	Not Liganded
2PD6	TYR	169	D	13.6	100	Liganded
2PD6	TYR	247	D	12.89	67	Not Liganded
2OK3	TYR	36	A	10.17	30	Not Liganded
2OK3	TYR	37	A	15.41	100	Not Liganded
2OK3	TYR	75	A	11.84	20	Not Liganded
2OK3	TYR	78	A	9.76	0	Not Liganded
2OK3	TYR	105	A	13.76	79	Not Liganded
2OK3	TYR	115	A	10.63	33	Liganded
2OK3	TYR	141	A	10.19	0	Not Liganded
2LQN	TYR	15	A	12.12	24	Not Liganded

2LQN	TYR	48	A	10.35	25	Not Liganded
2LQN	TYR	61	A	16.91	100	Not Liganded
2LQN	TYR	88	A	13.7	97	Not Liganded
2LQN	TYR	92	A	10.22	3	Liganded
2LQN	TYR	105	A	9.94	0	Not Liganded
2LQN	TYR	127	A	10.4	17	Not Liganded
2LQN	TYR	132	A	10.11	0	Not Liganded
2LQN	TYR	177	A	10.75	0	Not Liganded
2LQN	TYR	198	A	10.23	1	Not Liganded
2LQN	TYR	207	A	10.09	0	Not Liganded
2LQN	TYR	251	A	10.62	0	Not Liganded
2IF1	TYR	43	A	10.74	0	Not Liganded
2IF1	TYR	67	A	10.66	16	Not Liganded
2IF1	TYR	92	A	10.38	8	Liganded
2IE4	TYR	11	A	10.26	0	Not Liganded
2IE4	TYR	60	A	11.87	0	Not Liganded
2IE4	TYR	85	A	10.05	0	Not Liganded
2IE4	TYR	155	A	12.33	35	Not Liganded
2IE4	TYR	169	A	10.36	11	Not Liganded
2IE4	TYR	261	A	10.68	18	Liganded
2IE4	TYR	426	A	11.28	59	Not Liganded
2IE4	TYR	456	A	11.53	72	Not Liganded
2IE4	TYR	495	A	13.37	100	Not Liganded
2IE4	TYR	577	A	10.9	25	Not Liganded
2IE4	TYR	80	C	15.57	100	Not Liganded
2IE4	TYR	86	C	15.51	100	Not Liganded
2IE4	TYR	91	C	9.96	0	Not Liganded
2IE4	TYR	92	C	10.87	9	Not Liganded
2IE4	TYR	107	C	12.56	73	Not Liganded
2IE4	TYR	127	C	10.93	25	Not Liganded
2IE4	TYR	130	C	10.44	0	Not Liganded
2IE4	TYR	137	C	13.28	69	Not Liganded
2IE4	TYR	145	C	9.63	0	Not Liganded
2IE4	TYR	152	C	10.31	8	Not Liganded
2IE4	TYR	218	C	10.62	0	Not Liganded
2IE4	TYR	248	C	10.59	15	Not Liganded
2IE4	TYR	265	C	11.71	98	Not Liganded
2IE4	TYR	267	C	11.84	59	Not Liganded
2IE4	TYR	284	C	9.67	5	Not Liganded
2H31	TYR	14	A	13.2	72	Not Liganded
2H31	TYR	22	A	11.32	0	Liganded
2H31	TYR	119	A	10.17	0	Not Liganded
2H31	TYR	122	A	10	0	Not Liganded
2H31	TYR	316	A	11.44	30	Not Liganded
2H31	TYR	345	A	10.48	1	Not Liganded
2GSE	TYR	32	A	10.09	2	Not Liganded

2GSE	TYR	36	A	11.42	0	Not Liganded
2GSE	TYR	135	A	13.85	70	Not Liganded
2GSE	TYR	167	A	13.99	100	Not Liganded
2GSE	TYR	182	A	13.45	63	Not Liganded
2GSE	TYR	251	A	17.68	100	Not Liganded
2GSE	TYR	275	A	11.07	100	Not Liganded
2GSE	TYR	290	A	13.6	100	Not Liganded
2GSE	TYR	395	A	16.1	99	Not Liganded
2GSE	TYR	431	A	9.63	3	Liganded
2GSE	TYR	468	A	11.72	94	Not Liganded
2GSE	TYR	479	A	15.21	93	Not Liganded
2GSE	TYR	32	B	10.17	6	Not Liganded
2GSE	TYR	36	B	11.49	0	Not Liganded
2GSE	TYR	135	B	14.08	71	Not Liganded
2GSE	TYR	167	B	14	100	Not Liganded
2GSE	TYR	182	B	13.31	60	Not Liganded
2GSE	TYR	251	B	17.89	100	Not Liganded
2GSE	TYR	275	B	10.58	100	Not Liganded
2GSE	TYR	290	B	13.51	100	Not Liganded
2GSE	TYR	395	B	16.57	98	Not Liganded
2GSE	TYR	431	B	9.69	4	Liganded
2GSE	TYR	468	B	11.94	90	Not Liganded
2GSE	TYR	479	B	15.28	97	Not Liganded
2GSE	TYR	32	C	10.12	6	Not Liganded
2GSE	TYR	36	C	10.66	0	Not Liganded
2GSE	TYR	135	C	13.73	71	Not Liganded
2GSE	TYR	167	C	13.88	100	Not Liganded
2GSE	TYR	182	C	13.37	61	Not Liganded
2GSE	TYR	251	C	17.72	100	Not Liganded
2GSE	TYR	275	C	11.14	100	Not Liganded
2GSE	TYR	290	C	13.63	100	Not Liganded
2GSE	TYR	395	C	15.76	99	Not Liganded
2GSE	TYR	431	C	9.7	5	Liganded
2GSE	TYR	468	C	11.99	93	Not Liganded
2GSE	TYR	479	C	15.32	95	Not Liganded
2GSE	TYR	32	D	10.11	7	Not Liganded
2GSE	TYR	36	D	11.12	0	Not Liganded
2GSE	TYR	135	D	14.09	71	Not Liganded
2GSE	TYR	167	D	13.96	100	Not Liganded
2GSE	TYR	182	D	13.61	65	Not Liganded
2GSE	TYR	251	D	17.71	100	Not Liganded
2GSE	TYR	275	D	10.86	100	Not Liganded
2GSE	TYR	290	D	13.48	100	Not Liganded
2GSE	TYR	395	D	16.63	99	Not Liganded
2GSE	TYR	431	D	9.62	4	Liganded
2GSE	TYR	468	D	11.66	95	Not Liganded

2GSE	TYR	479	D	15.15	95	Not Liganded
2GRN	TYR	68	A	13.35	66	Liganded
2GRN	TYR	87	A	13.3	52	Not Liganded
2GRN	TYR	134	A	12.5	41	Not Liganded
2GRN	TYR	137	A	10.56	19	Not Liganded
2GRN	TYR	144	A	13.34	79	Not Liganded
2GRN	TYR	536	B	11.02	13	Not Liganded
2GRN	TYR	550	B	14.65	71	Not Liganded
2GRN	TYR	585	B	10.29	0	Not Liganded
2EYZ	TYR	14	A	12.4	70	Not Liganded
2EYZ	TYR	47	A	11.67	46	Not Liganded
2EYZ	TYR	60	A	11.45	31	Not Liganded
2EYZ	TYR	104	A	16.26	100	Not Liganded
2EYZ	TYR	108	A	10.13	0	Liganded
2EYZ	TYR	136	A	10.41	0	Not Liganded
2EYZ	TYR	186	A	10.72	31	Not Liganded
2EYZ	TYR	190	A	9.71	0	Not Liganded
2EYZ	TYR	221	A	10.16	0	Not Liganded
2EYZ	TYR	239	A	11.2	58	Not Liganded
2EYZ	TYR	251	A	10.43	0	Not Liganded
2E5B	TYR	18	A	12.57	100	Not Liganded
2E5B	TYR	23	A	12.54	71	Not Liganded
2E5B	TYR	26	A	15.34	100	Not Liganded
2E5B	TYR	34	A	12.75	95	Not Liganded
2E5B	TYR	36	A	16	100	Not Liganded
2E5B	TYR	54	A	12.09	61	Not Liganded
2E5B	TYR	60	A	13.94	100	Not Liganded
2E5B	TYR	64	A	17.01	100	Not Liganded
2E5B	TYR	69	A	18.97	100	Not Liganded
2E5B	TYR	87	A	14.36	100	Not Liganded
2E5B	TYR	103	A	11.03	0	Not Liganded
2E5B	TYR	108	A	12.76	12	Not Liganded
2E5B	TYR	142	A	11.99	71	Not Liganded
2E5B	TYR	157	A	14.3	100	Not Liganded
2E5B	TYR	175	A	11.34	13	Not Liganded
2E5B	TYR	188	A	11.71	51	Not Liganded
2E5B	TYR	195	A	13.92	100	Not Liganded
2E5B	TYR	230	A	11.81	49	Not Liganded
2E5B	TYR	231	A	18.35	100	Not Liganded
2E5B	TYR	240	A	11.08	25	Not Liganded
2E5B	TYR	281	A	13.42	82	Not Liganded
2E5B	TYR	284	A	10.52	41	Not Liganded
2E5B	TYR	341	A	10.62	5	Not Liganded
2E5B	TYR	347	A	11.15	24	Not Liganded
2E5B	TYR	403	A	10.41	23	Not Liganded
2E5B	TYR	453	A	10.34	0	Not Liganded

2E5B	TYR	471	A	10.79	47	Liganded
2E5B	TYR	18	B	14.34	100	Not Liganded
2E5B	TYR	23	B	12.36	67	Not Liganded
2E5B	TYR	26	B	15.25	100	Not Liganded
2E5B	TYR	34	B	12.64	93	Not Liganded
2E5B	TYR	36	B	16.13	100	Not Liganded
2E5B	TYR	54	B	12.13	61	Not Liganded
2E5B	TYR	60	B	13.84	100	Not Liganded
2E5B	TYR	64	B	19.2	100	Not Liganded
2E5B	TYR	69	B	17.02	100	Not Liganded
2E5B	TYR	87	B	14.43	100	Not Liganded
2E5B	TYR	103	B	12.35	0	Not Liganded
2E5B	TYR	108	B	12.67	13	Not Liganded
2E5B	TYR	142	B	12.05	73	Not Liganded
2E5B	TYR	157	B	14.22	100	Not Liganded
2E5B	TYR	175	B	12.23	12	Not Liganded
2E5B	TYR	188	B	11.92	52	Not Liganded
2E5B	TYR	195	B	13.86	100	Not Liganded
2E5B	TYR	230	B	11.73	49	Not Liganded
2E5B	TYR	231	B	18.51	100	Not Liganded
2E5B	TYR	240	B	11.18	28	Not Liganded
2E5B	TYR	281	B	13.45	83	Not Liganded
2E5B	TYR	284	B	10.39	37	Not Liganded
2E5B	TYR	341	B	10.59	5	Not Liganded
2E5B	TYR	347	B	11.17	25	Not Liganded
2E5B	TYR	403	B	10.46	22	Not Liganded
2E5B	TYR	453	B	10.33	0	Not Liganded
2E5B	TYR	471	B	12.44	48	Liganded
2DUD	TYR	83	A	10.22	0	Not Liganded
2DUD	TYR	85	A	9.67	0	Not Liganded
2DUD	TYR	93	A	11.97	14	Not Liganded
2DUD	TYR	100	A	12.77	99	Not Liganded
2DUD	TYR	103	A	10.27	0	Liganded
2DUD	TYR	83	B	10.19	0	Not Liganded
2DUD	TYR	85	B	10.08	0	Not Liganded
2DUD	TYR	93	B	11.42	10	Not Liganded
2DUD	TYR	100	B	13.36	98	Not Liganded
2DUD	TYR	103	B	9.85	0	Liganded
2DFD	TYR	38	A	12.35	41	Not Liganded
2DFD	TYR	62	A	11.43	28	Liganded
2DFD	TYR	143	A	12.57	69	Not Liganded
2DFD	TYR	235	A	14.58	91	Not Liganded
2DFD	TYR	269	A	14.01	72	Not Liganded
2DFD	TYR	38	B	12.35	46	Not Liganded
2DFD	TYR	62	B	11.03	22	Liganded
2DFD	TYR	143	B	12.12	64	Not Liganded

2DFD	TYR	235	B	14.4	87	Not Liganded
2DFD	TYR	269	B	13.88	69	Not Liganded
2DFD	TYR	38	C	11.98	39	Not Liganded
2DFD	TYR	62	C	11.17	25	Liganded
2DFD	TYR	143	C	12.45	69	Not Liganded
2DFD	TYR	235	C	14.56	90	Not Liganded
2DFD	TYR	269	C	13.99	70	Not Liganded
2DFD	TYR	38	D	12.25	43	Not Liganded
2DFD	TYR	62	D	11.33	27	Liganded
2DFD	TYR	143	D	12.26	71	Not Liganded
2DFD	TYR	235	D	13.99	87	Not Liganded
2DFD	TYR	269	D	14.08	70	Not Liganded
2D2Z	TYR	104	A	10.34	0	Not Liganded
2D2Z	TYR	128	A	12.6	45	Not Liganded
2D2Z	TYR	154	A	12.45	76	Not Liganded
2D2Z	TYR	205	A	11.26	19	Not Liganded
2D2Z	TYR	220	A	17.41	100	Not Liganded
2D2Z	TYR	225	A	13.45	76	Not Liganded
2D2Z	TYR	244	A	13.04	90	Liganded
2D2Z	TYR	104	B	11.23	51	Not Liganded
2D2Z	TYR	128	B	12.86	56	Not Liganded
2D2Z	TYR	154	B	11.21	41	Not Liganded
2D2Z	TYR	205	B	10.99	16	Not Liganded
2D2Z	TYR	220	B	17.48	100	Not Liganded
2D2Z	TYR	225	B	13.7	81	Not Liganded
2D2Z	TYR	244	B	11.97	68	Liganded
2D2Z	TYR	104	C	10.37	0	Not Liganded
2D2Z	TYR	128	C	13.78	75	Not Liganded
2D2Z	TYR	154	C	10.98	34	Not Liganded
2D2Z	TYR	205	C	12.5	57	Not Liganded
2D2Z	TYR	220	C	17.42	100	Not Liganded
2D2Z	TYR	225	C	14.69	100	Not Liganded
2D2Z	TYR	244	C	11.84	65	Liganded
2CPL	TYR	48	A	14.32	100	Liganded
2CPL	TYR	79	A	12.07	35	Not Liganded
2BR9	TYR	9	A	10.13	0	Not Liganded
2BR9	TYR	20	A	10.87	0	Not Liganded
2BR9	TYR	49	A	14.71	73	Liganded
2BR9	TYR	85	A	10.23	0	Not Liganded
2BR9	TYR	121	A	12.67	70	Not Liganded
2BR9	TYR	122	A	10.49	23	Not Liganded
2BR9	TYR	128	A	14.66	100	Not Liganded
2BR9	TYR	131	A	18.13	100	Not Liganded
2BR9	TYR	152	A	15.43	100	Not Liganded
2BR9	TYR	181	A	10.39	26	Not Liganded
2BR9	TYR	182	A	10.46	0	Not Liganded

2BR9	TYR	214	A	10.1	0	Not Liganded
2AI6	TYR	22	A	13.06	94	Not Liganded
2AI6	TYR	47	A	12.33	43	Not Liganded
2AI6	TYR	52	A	10.48	0	Not Liganded
2AI6	TYR	57	A	11.17	15	Not Liganded
2AI6	TYR	91	A	9.59	15	Not Liganded
2AI6	TYR	93	A	10.37	0	Liganded
2AI6	TYR	97	A	11.34	8	Not Liganded
2AI6	TYR	113	A	10.31	0	Not Liganded
2AI6	TYR	116	A	10.24	2	Not Liganded
2AI6	TYR	125	A	10.22	0	Not Liganded
2A2R	TYR	3	A	11.28	46	Not Liganded
2A2R	TYR	7	A	11.82	100	Liganded
2A2R	TYR	49	A	14.5	100	Not Liganded
2A2R	TYR	63	A	12.23	58	Not Liganded
2A2R	TYR	79	A	11.98	100	Not Liganded
2A2R	TYR	103	A	13.58	76	Not Liganded
2A2R	TYR	108	A	10.52	52	Not Liganded
2A2R	TYR	111	A	10.75	5	Not Liganded
2A2R	TYR	118	A	13.2	74	Not Liganded
2A2R	TYR	153	A	14.51	80	Not Liganded
2A2R	TYR	179	A	17.08	100	Not Liganded
2A2R	TYR	198	A	12.23	77	Not Liganded
2A2R	TYR	3	B	11.87	42	Not Liganded
2A2R	TYR	7	B	11.85	100	Liganded
2A2R	TYR	49	B	14.51	100	Not Liganded
2A2R	TYR	63	B	12.09	54	Not Liganded
2A2R	TYR	79	B	14.76	100	Not Liganded
2A2R	TYR	103	B	13.55	77	Not Liganded
2A2R	TYR	108	B	10.44	51	Not Liganded
2A2R	TYR	111	B	10.74	5	Not Liganded
2A2R	TYR	118	B	13.12	72	Not Liganded
2A2R	TYR	153	B	14.76	82	Not Liganded
2A2R	TYR	179	B	17.1	100	Not Liganded
2A2R	TYR	198	B	12.32	79	Not Liganded
1YZ1	TYR	4	A	11.25	31	Not Liganded
1YZ1	TYR	18	A	11.94	46	Not Liganded
1YZ1	TYR	88	A	13.57	97	Not Liganded
1YZ1	TYR	91	A	14.82	93	Liganded
1YZ1	TYR	95	A	15.88	100	Not Liganded
1YZ1	TYR	132	A	12.2	51	Not Liganded
1YZ1	TYR	151	A	11.32	45	Not Liganded
1YZ1	TYR	159	A	11.61	38	Not Liganded
1YZ1	TYR	4	B	11.42	31	Not Liganded
1YZ1	TYR	18	B	12.02	47	Not Liganded
1YZ1	TYR	88	B	13.26	96	Not Liganded

1YZ1	TYR	91	B	14.95	93	Liganded
1YZ1	TYR	95	B	16.26	100	Not Liganded
1YZ1	TYR	132	B	12.14	51	Not Liganded
1YZ1	TYR	151	B	11.11	38	Not Liganded
1YZ1	TYR	159	B	11.75	35	Not Liganded
1YZ1	TYR	4	C	11.05	30	Not Liganded
1YZ1	TYR	18	C	11.91	46	Not Liganded
1YZ1	TYR	88	C	13.56	96	Not Liganded
1YZ1	TYR	91	C	16.52	100	Liganded
1YZ1	TYR	95	C	15.15	100	Not Liganded
1YZ1	TYR	132	C	11.15	52	Not Liganded
1YZ1	TYR	151	C	11.3	42	Not Liganded
1YZ1	TYR	159	C	11.33	0	Not Liganded
1YZ1	TYR	4	D	11.13	29	Not Liganded
1YZ1	TYR	18	D	11.89	47	Not Liganded
1YZ1	TYR	88	D	13.03	92	Not Liganded
1YZ1	TYR	91	D	14.88	94	Liganded
1YZ1	TYR	95	D	15.92	100	Not Liganded
1YZ1	TYR	132	D	12.18	50	Not Liganded
1YZ1	TYR	151	D	11.22	41	Not Liganded
1YZ1	TYR	159	D	11.44	36	Not Liganded
1YFK	TYR	4	A	10.03	0	Not Liganded
1YFK	TYR	26	A	11.02	42	Not Liganded
1YFK	TYR	50	A	9.84	29	Not Liganded
1YFK	TYR	92	A	13.35	100	Not Liganded
1YFK	TYR	119	A	11.27	23	Not Liganded
1YFK	TYR	133	A	10.12	0	Liganded
1YFK	TYR	142	A	12.67	100	Not Liganded
1YFK	TYR	218	A	14.04	66	Not Liganded
1YFK	TYR	4	B	10.32	0	Not Liganded
1YFK	TYR	26	B	11.08	44	Not Liganded
1YFK	TYR	50	B	9.96	30	Not Liganded
1YFK	TYR	92	B	13.52	100	Not Liganded
1YFK	TYR	119	B	11.16	18	Not Liganded
1YFK	TYR	133	B	10.08	0	Liganded
1YFK	TYR	142	B	12.52	100	Not Liganded
1YFK	TYR	218	B	14.06	65	Not Liganded
1XQ8	TYR	39	A	10.04	0	Liganded
1XQ8	TYR	125	A	10.04	0	Not Liganded
1XQ8	TYR	133	A	10.05	0	Not Liganded
1XQ8	TYR	136	A	10.16	0	Not Liganded
1WZY	TYR	25	A	13.2	47	Not Liganded
1WZY	TYR	30	A	10.93	0	Not Liganded
1WZY	TYR	36	A	12.19	67	Not Liganded
1WZY	TYR	43	A	10.35	0	Not Liganded
1WZY	TYR	64	A	10.31	0	Not Liganded

1WZY	TYR	102	A	12.36	53	Not Liganded
1WZY	TYR	113	A	10.05	10	Liganded
1WZY	TYR	128	A	10.39	0	Not Liganded
1WZY	TYR	131	A	13.25	38	Not Liganded
1WZY	TYR	139	A	10.86	30	Not Liganded
1WZY	TYR	187	A	9.05	76	Not Liganded
1WZY	TYR	193	A	14.95	72	Not Liganded
1WZY	TYR	205	A	10.43	40	Not Liganded
1WZY	TYR	233	A	10.33	12	Not Liganded
1WZY	TYR	263	A	10.98	26	Not Liganded
1WZY	TYR	312	A	13.31	65	Not Liganded
1WZY	TYR	316	A	12.03	18	Not Liganded
1WZY	TYR	317	A	11	1	Not Liganded
1WYM	TYR	14	A	11.01	19	Not Liganded
1WYM	TYR	62	A	10.74	26	Not Liganded
1WYM	TYR	95	A	12.24	56	Liganded
1WOU	TYR	4	A	10.48	1	Not Liganded
1WOU	TYR	30	A	13.28	70	Not Liganded
1WOU	TYR	68	A	12.77	48	Not Liganded
1WOU	TYR	76	A	11.16	16	Not Liganded
1WOU	TYR	99	A	10.78	27	Liganded
1W7B	TYR	24	A	9.83	0	Not Liganded
1W7B	TYR	30	A	9.92	0	Not Liganded
1W7B	TYR	75	A	11.44	34	Not Liganded
1W7B	TYR	109	A	14.58	100	Not Liganded
1W7B	TYR	147	A	14.1	53	Not Liganded
1W7B	TYR	151	A	11.53	36	Not Liganded
1W7B	TYR	188	A	10.12	0	Not Liganded
1W7B	TYR	199	A	10.37	0	Not Liganded
1W7B	TYR	232	A	11.36	66	Not Liganded
1W7B	TYR	235	A	9.79	0	Not Liganded
1W7B	TYR	238	A	9.18	0	Not Liganded
1W7B	TYR	269	A	15.59	100	Not Liganded
1W7B	TYR	275	A	10.02	0	Not Liganded
1W7B	TYR	311	A	13.51	31	Not Liganded
1W7B	TYR	316	A	10.78	11	Not Liganded
1W7B	TYR	317	A	10.11	0	Liganded
1W7B	TYR	318	A	11.23	1	Not Liganded
1W7B	TYR	327	A	14.22	64	Not Liganded
1W7B	TYR	333	A	10.26	7	Not Liganded
1U8F	TYR	42	O	11.66	60	Not Liganded
1U8F	TYR	45	O	12.72	94	Not Liganded
1U8F	TYR	49	O	12.5	66	Not Liganded
1U8F	TYR	94	O	13.75	48	Liganded
1U8F	TYR	140	O	11.92	41	Not Liganded
1U8F	TYR	255	O	13.34	85	Not Liganded

1U8F	TYR	276	O	12.71	23	Not Liganded
1U8F	TYR	314	O	14.05	100	Not Liganded
1U8F	TYR	320	O	14.4	100	Not Liganded
1U8F	TYR	42	P	12.01	71	Not Liganded
1U8F	TYR	45	P	12.94	98	Not Liganded
1U8F	TYR	49	P	12.53	66	Not Liganded
1U8F	TYR	94	P	13.98	51	Liganded
1U8F	TYR	140	P	12.07	42	Not Liganded
1U8F	TYR	255	P	13.35	85	Not Liganded
1U8F	TYR	276	P	12.81	23	Not Liganded
1U8F	TYR	314	P	14.62	100	Not Liganded
1U8F	TYR	320	P	14.56	100	Not Liganded
1U8F	TYR	42	Q	11.92	68	Not Liganded
1U8F	TYR	45	Q	12.93	97	Not Liganded
1U8F	TYR	49	Q	12.66	68	Not Liganded
1U8F	TYR	94	Q	13.73	47	Liganded
1U8F	TYR	140	Q	12.03	42	Not Liganded
1U8F	TYR	255	Q	13.3	84	Not Liganded
1U8F	TYR	276	Q	12.73	21	Not Liganded
1U8F	TYR	314	Q	14.64	100	Not Liganded
1U8F	TYR	320	Q	14.56	100	Not Liganded
1U8F	TYR	42	R	11.82	65	Not Liganded
1U8F	TYR	45	R	12.82	93	Not Liganded
1U8F	TYR	49	R	12.59	70	Not Liganded
1U8F	TYR	94	R	14.08	50	Liganded
1U8F	TYR	140	R	11.93	41	Not Liganded
1U8F	TYR	255	R	13.37	84	Not Liganded
1U8F	TYR	276	R	12.88	24	Not Liganded
1U8F	TYR	314	R	14.61	100	Not Liganded
1U8F	TYR	320	R	14.49	100	Not Liganded
1T09	TYR	34	A	11.03	33	Not Liganded
1T09	TYR	42	A	10.91	17	Not Liganded
1T09	TYR	135	A	16.59	100	Not Liganded
1T09	TYR	139	A	12.58	79	Not Liganded
1T09	TYR	156	A	10.9	13	Not Liganded
1T09	TYR	167	A	10.44	19	Not Liganded
1T09	TYR	183	A	11.6	62	Not Liganded
1T09	TYR	208	A	10.31	43	Not Liganded
1T09	TYR	219	A	13.73	100	Not Liganded
1T09	TYR	231	A	11.47	33	Not Liganded
1T09	TYR	235	A	11.07	50	Not Liganded
1T09	TYR	246	A	14.07	99	Liganded
1T09	TYR	272	A	12.43	80	Not Liganded
1T09	TYR	285	A	12.16	60	Not Liganded
1T09	TYR	316	A	10.92	27	Not Liganded
1T09	TYR	319	A	10.46	13	Not Liganded

1T09	TYR	391	A	10.5	16	Not Liganded
1T09	TYR	34	B	11.16	37	Not Liganded
1T09	TYR	42	B	10.96	18	Not Liganded
1T09	TYR	135	B	16.35	100	Not Liganded
1T09	TYR	139	B	18.61	95	Not Liganded
1T09	TYR	156	B	11.26	14	Not Liganded
1T09	TYR	167	B	10.93	27	Not Liganded
1T09	TYR	183	B	11.27	48	Not Liganded
1T09	TYR	208	B	11.74	47	Not Liganded
1T09	TYR	219	B	14.08	100	Not Liganded
1T09	TYR	231	B	11.92	33	Not Liganded
1T09	TYR	235	B	11.11	50	Not Liganded
1T09	TYR	246	B	13.91	96	Liganded
1T09	TYR	272	B	22.95	100	Not Liganded
1T09	TYR	285	B	11.25	60	Not Liganded
1T09	TYR	316	B	10.05	25	Not Liganded
1T09	TYR	319	B	10.35	10	Not Liganded
1T09	TYR	391	B	10.23	14	Not Liganded
1QZ2	TYR	161	A	10.26	0	Not Liganded
1QZ2	TYR	177	A	10.45	0	Not Liganded
1QZ2	TYR	178	A	10.1	0	Not Liganded
1QZ2	TYR	202	A	9.63	3	Liganded
1QZ2	TYR	220	A	10.07	0	Not Liganded
1QZ2	TYR	225	A	10.49	0	Not Liganded
1QZ2	TYR	245	A	14	87	Not Liganded
1QZ2	TYR	280	A	12.69	43	Not Liganded
1QZ2	TYR	286	A	10.25	3	Not Liganded
1QZ2	TYR	293	A	12.04	59	Not Liganded
1QZ2	TYR	302	A	10.43	0	Not Liganded
1QZ2	TYR	383	A	10.93	4	Not Liganded
1QZ2	TYR	411	A	11.95	11	Not Liganded
1QZ2	TYR	161	B	10.06	0	Not Liganded
1QZ2	TYR	177	B	11.28	1	Not Liganded
1QZ2	TYR	178	B	9.82	0	Not Liganded
1QZ2	TYR	202	B	9.64	0	Liganded
1QZ2	TYR	220	B	9.86	0	Not Liganded
1QZ2	TYR	225	B	10.54	0	Not Liganded
1QZ2	TYR	245	B	13.76	91	Not Liganded
1QZ2	TYR	280	B	12.06	44	Not Liganded
1QZ2	TYR	286	B	9.36	0	Not Liganded
1QZ2	TYR	293	B	11.97	55	Not Liganded
1QZ2	TYR	302	B	11.04	3	Not Liganded
1QZ2	TYR	383	B	11.48	20	Not Liganded
1QZ2	TYR	411	B	10.9	14	Not Liganded
1QZ2	TYR	161	C	8.98	0	Not Liganded
1QZ2	TYR	177	C	11.65	0	Not Liganded

1QZ2	TYR	178	C	11.4	32	Not Liganded
1QZ2	TYR	202	C	9.81	0	Liganded
1QZ2	TYR	220	C	9.62	13	Not Liganded
1QZ2	TYR	225	C	10.4	10	Not Liganded
1QZ2	TYR	245	C	13.93	93	Not Liganded
1QZ2	TYR	280	C	12.83	47	Not Liganded
1QZ2	TYR	286	C	10.28	0	Not Liganded
1QZ2	TYR	293	C	12.09	47	Not Liganded
1QZ2	TYR	302	C	10.86	0	Not Liganded
1QZ2	TYR	383	C	10.9	6	Not Liganded
1QZ2	TYR	411	C	10.92	0	Not Liganded
1PBU	TYR	297	A	14.1	100	Not Liganded
1PBU	TYR	309	A	10.82	14	Not Liganded
1PBU	TYR	323	A	12.26	44	Not Liganded
1PBU	TYR	326	A	11.69	37	Not Liganded
1PBU	TYR	394	A	10.62	0	Not Liganded
1PBU	TYR	397	A	13.92	75	Not Liganded
1PBU	TYR	416	A	13.12	83	Liganded
1M9I	TYR	10	A	11.95	33	Not Liganded
1M9I	TYR	30	A	9.86	0	Liganded
1M9I	TYR	62	A	13.34	36	Not Liganded
1M9I	TYR	66	A	11.17	1	Not Liganded
1M9I	TYR	76	A	10.04	0	Not Liganded
1M9I	TYR	95	A	9.9	22	Not Liganded
1M9I	TYR	134	A	13.05	40	Not Liganded
1M9I	TYR	138	A	11.89	35	Not Liganded
1M9I	TYR	185	A	10.44	0	Not Liganded
1M9I	TYR	201	A	9.4	6	Not Liganded
1M9I	TYR	218	A	12.03	60	Not Liganded
1M9I	TYR	255	A	14.09	100	Not Liganded
1M9I	TYR	297	A	14.96	100	Not Liganded
1M9I	TYR	302	A	10.23	7	Not Liganded
1M9I	TYR	313	A	13.8	64	Not Liganded
1M9I	TYR	340	A	10.41	33	Not Liganded
1M9I	TYR	439	A	11.26	100	Not Liganded
1M9I	TYR	477	A	11.94	45	Not Liganded
1M9I	TYR	481	A	12.14	43	Not Liganded
1M9I	TYR	556	A	9.09	100	Not Liganded
1M9I	TYR	572	A	11.12	28	Not Liganded
1M9I	TYR	609	A	11.55	62	Not Liganded
1M9I	TYR	645	A	16.67	92	Not Liganded
1JLH	TYR	16	A	10.98	34	Not Liganded
1JLH	TYR	54	A	12.73	82	Not Liganded
1JLH	TYR	91	A	14.65	93	Not Liganded
1JLH	TYR	143	A	10.85	4	Not Liganded
1JLH	TYR	173	A	11.24	64	Not Liganded

1JLH	TYR	182	A	12.96	100	Liganded
1JLH	TYR	273	A	12.57	100	Not Liganded
1JLH	TYR	326	A	14.06	100	Not Liganded
1JLH	TYR	340	A	13.22	100	Not Liganded
1JLH	TYR	343	A	13	66	Not Liganded
1JLH	TYR	350	A	14.38	100	Not Liganded
1JLH	TYR	362	A	12.76	83	Not Liganded
1JLH	TYR	391	A	17.82	100	Not Liganded
1JLH	TYR	493	A	16.69	100	Not Liganded
1JLH	TYR	16	B	11.49	34	Not Liganded
1JLH	TYR	54	B	12.53	83	Not Liganded
1JLH	TYR	91	B	14.57	93	Not Liganded
1JLH	TYR	143	B	10.88	5	Not Liganded
1JLH	TYR	173	B	11.3	64	Not Liganded
1JLH	TYR	182	B	13.11	100	Liganded
1JLH	TYR	273	B	12.61	100	Not Liganded
1JLH	TYR	326	B	14.07	100	Not Liganded
1JLH	TYR	340	B	13.2	100	Not Liganded
1JLH	TYR	343	B	13.09	68	Not Liganded
1JLH	TYR	350	B	14.5	100	Not Liganded
1JLH	TYR	362	B	12.85	82	Not Liganded
1JLH	TYR	391	B	17.82	100	Not Liganded
1JLH	TYR	493	B	16.68	100	Not Liganded
1JLH	TYR	16	C	11.43	36	Not Liganded
1JLH	TYR	54	C	12.68	85	Not Liganded
1JLH	TYR	91	C	14.58	91	Not Liganded
1JLH	TYR	143	C	11.07	7	Not Liganded
1JLH	TYR	173	C	11.21	63	Not Liganded
1JLH	TYR	182	C	13.07	100	Liganded
1JLH	TYR	273	C	12.57	100	Not Liganded
1JLH	TYR	326	C	14.07	100	Not Liganded
1JLH	TYR	340	C	13.26	100	Not Liganded
1JLH	TYR	343	C	12.98	66	Not Liganded
1JLH	TYR	350	C	14.58	100	Not Liganded
1JLH	TYR	362	C	12.69	82	Not Liganded
1JLH	TYR	391	C	17.81	100	Not Liganded
1JLH	TYR	493	C	16.42	100	Not Liganded
1JLH	TYR	16	D	11.34	36	Not Liganded
1JLH	TYR	54	D	12.69	83	Not Liganded
1JLH	TYR	91	D	14.54	92	Not Liganded
1JLH	TYR	143	D	11.92	1	Not Liganded
1JLH	TYR	173	D	11.29	62	Not Liganded
1JLH	TYR	182	D	13	100	Liganded
1JLH	TYR	273	D	12.57	100	Not Liganded
1JLH	TYR	326	D	14.06	100	Not Liganded
1JLH	TYR	340	D	13.18	100	Not Liganded

1JLH	TYR	343	D	13.11	67	Not Liganded
1JLH	TYR	350	D	14.4	100	Not Liganded
1JLH	TYR	362	D	12.73	81	Not Liganded
1JLH	TYR	391	D	17.73	100	Not Liganded
1JLH	TYR	493	D	16.45	100	Not Liganded
1J1B	TYR	56	A	11.56	56	Not Liganded
1J1B	TYR	71	A	10.65	23	Not Liganded
1J1B	TYR	114	A	10.5	21	Not Liganded
1J1B	TYR	117	A	9.77	36	Not Liganded
1J1B	TYR	127	A	11.19	16	Not Liganded
1J1B	TYR	134	A	10.68	31	Not Liganded
1J1B	TYR	140	A	10.03	21	Not Liganded
1J1B	TYR	146	A	10.67	20	Not Liganded
1J1B	TYR	157	A	11.14	20	Not Liganded
1J1B	TYR	161	A	12.83	79	Not Liganded
1J1B	TYR	163	A	14.3	97	Not Liganded
1J1B	TYR	171	A	11.14	42	Not Liganded
1J1B	TYR	216	A	16.37	92	Not Liganded
1J1B	TYR	221	A	10.88	45	Not Liganded
1J1B	TYR	222	A	15.79	92	Not Liganded
1J1B	TYR	234	A	12.44	97	Not Liganded
1J1B	TYR	288	A	13.15	100	Liganded
1J1B	TYR	323	A	13.5	81	Not Liganded
1J1B	TYR	556	B	12.07	73	Not Liganded
1J1B	TYR	571	B	10.59	30	Not Liganded
1J1B	TYR	614	B	10.86	47	Not Liganded
1J1B	TYR	617	B	11	41	Not Liganded
1J1B	TYR	627	B	12.01	21	Not Liganded
1J1B	TYR	634	B	10.73	36	Not Liganded
1J1B	TYR	640	B	10.19	21	Not Liganded
1J1B	TYR	646	B	10.58	18	Not Liganded
1J1B	TYR	657	B	11.01	18	Not Liganded
1J1B	TYR	661	B	12.82	78	Not Liganded
1J1B	TYR	663	B	14.24	98	Not Liganded
1J1B	TYR	671	B	11.19	42	Not Liganded
1J1B	TYR	716	B	14.64	98	Not Liganded
1J1B	TYR	721	B	10.74	45	Not Liganded
1J1B	TYR	722	B	15.95	93	Not Liganded
1J1B	TYR	734	B	12.54	99	Not Liganded
1J1B	TYR	788	B	11.69	88	Not Liganded
1J1B	TYR	823	B	13.51	82	Not Liganded
1I0Z	TYR	83	A	13.13	83	Not Liganded
1I0Z	TYR	127	A	10.24	0	Not Liganded
1I0Z	TYR	145	A	10.91	33	Not Liganded
1I0Z	TYR	172	A	12.67	68	Not Liganded
1I0Z	TYR	239	A	12.63	46	Not Liganded

1I0Z	TYR	247	A	10.93	96	Not Liganded
1I0Z	TYR	281	A	10.77	37	Liganded
1I0Z	TYR	83	B	13.7	88	Not Liganded
1I0Z	TYR	127	B	10.09	0	Not Liganded
1I0Z	TYR	145	B	11.11	37	Not Liganded
1I0Z	TYR	172	B	12.72	70	Not Liganded
1I0Z	TYR	239	B	11.81	42	Not Liganded
1I0Z	TYR	247	B	13.46	98	Not Liganded
1I0Z	TYR	281	B	10.77	35	Liganded
1GZK	TYR	154	A	10.36	0	Not Liganded
1GZK	TYR	177	A	10.21	13	Not Liganded
1GZK	TYR	178	A	11.27	28	Not Liganded
1GZK	TYR	217	A	10.58	0	Not Liganded
1GZK	TYR	231	A	13.29	89	Not Liganded
1GZK	TYR	255	A	12.42	79	Not Liganded
1GZK	TYR	265	A	10	0	Not Liganded
1GZK	TYR	273	A	15.53	100	Not Liganded
1GZK	TYR	316	A	12.07	54	Not Liganded
1GZK	TYR	327	A	10.54	10	Liganded
1GZK	TYR	341	A	12.23	54	Not Liganded
1GZK	TYR	351	A	9.95	0	Not Liganded
1GZK	TYR	438	A	10.31	25	Not Liganded
1GIF	TYR	37	A	10.23	0	Not Liganded
1GIF	TYR	76	A	11.76	48	Not Liganded
1GIF	TYR	96	A	13.42	87	Liganded
1GIF	TYR	99	A	13.82	90	Not Liganded
1GIF	TYR	100	A	14.25	100	Not Liganded
1GIF	TYR	37	B	10.26	0	Not Liganded
1GIF	TYR	76	B	11.66	43	Not Liganded
1GIF	TYR	96	B	13.21	85	Liganded
1GIF	TYR	99	B	13.75	91	Not Liganded
1GIF	TYR	100	B	13.49	100	Not Liganded
1GIF	TYR	37	C	10.27	0	Not Liganded
1GIF	TYR	76	C	11.82	43	Not Liganded
1GIF	TYR	96	C	13.18	84	Liganded
1GIF	TYR	99	C	13.71	91	Not Liganded
1GIF	TYR	100	C	12.32	100	Not Liganded
1EGX	TYR	16	A	10.42	0	Not Liganded
1EGX	TYR	39	A	10.32	2	Liganded
1EGX	TYR	72	A	15.52	100	Not Liganded
1EF7	TYR	15	A	10.52	0	Liganded
1EF7	TYR	27	A	10.66	17	Not Liganded
1EF7	TYR	82	A	12.8	77	Not Liganded
1EF7	TYR	96	A	11.91	58	Not Liganded
1EF7	TYR	124	A	10.88	22	Not Liganded
1EF7	TYR	132	A	14.17	82	Not Liganded

1EF7	TYR	146	A	10.27	0	Not Liganded
1EF7	TYR	164	A	12.03	52	Not Liganded
1EF7	TYR	169	A	12.61	40	Not Liganded
1EF7	TYR	172	A	10.37	0	Not Liganded
1EF7	TYR	177	A	10.21	0	Not Liganded
1EF7	TYR	195	A	10.12	25	Not Liganded
1EF7	TYR	219	A	10.27	4	Not Liganded
1EF7	TYR	227	A	9.11	0	Not Liganded
1EF7	TYR	15	B	10.41	0	Liganded
1EF7	TYR	27	B	10.44	8	Not Liganded
1EF7	TYR	82	B	12.99	76	Not Liganded
1EF7	TYR	96	B	11.76	56	Not Liganded
1EF7	TYR	124	B	10.85	23	Not Liganded
1EF7	TYR	132	B	14.06	83	Not Liganded
1EF7	TYR	146	B	10.25	0	Not Liganded
1EF7	TYR	164	B	12.67	51	Not Liganded
1EF7	TYR	169	B	12.46	41	Not Liganded
1EF7	TYR	172	B	10.45	0	Not Liganded
1EF7	TYR	177	B	10.17	0	Not Liganded
1EF7	TYR	195	B	10.1	27	Not Liganded
1EF7	TYR	219	B	10.26	6	Not Liganded
1EF7	TYR	227	B	9.69	0	Not Liganded
1BD9	TYR	29	A	13.18	96	Not Liganded
1BD9	TYR	64	A	11.32	27	Not Liganded
1BD9	TYR	81	A	9.93	0	Not Liganded
1BD9	TYR	106	A	15.3	100	Not Liganded
1BD9	TYR	120	A	16.31	100	Liganded
1BD9	TYR	125	A	15.93	97	Not Liganded
1BD9	TYR	158	A	13.08	26	Not Liganded
1BD9	TYR	169	A	17.98	100	Not Liganded
1BD9	TYR	176	A	11.39	41	Not Liganded
1BD9	TYR	181	A	11.85	67	Not Liganded
1BD9	TYR	29	B	13.4	99	Not Liganded
1BD9	TYR	64	B	11.35	28	Not Liganded
1BD9	TYR	81	B	9.98	0	Not Liganded
1BD9	TYR	106	B	15.29	100	Not Liganded
1BD9	TYR	120	B	16.36	100	Liganded
1BD9	TYR	125	B	16.03	99	Not Liganded
1BD9	TYR	158	B	13.09	30	Not Liganded
1BD9	TYR	169	B	17.92	100	Not Liganded
1BD9	TYR	176	B	11.28	41	Not Liganded
1BD9	TYR	181	B	12.09	76	Not Liganded
1AVH	TYR	91	A	15.45	98	Not Liganded
1AVH	TYR	94	A	11.27	47	Not Liganded
1AVH	TYR	129	A	13.22	48	Liganded
1AVH	TYR	133	A	11.84	36	Not Liganded

1AVH	TYR	148	A	10.41	0	Not Liganded
1AVH	TYR	149	A	12.88	84	Not Liganded
1AVH	TYR	213	A	11.61	43	Not Liganded
1AVH	TYR	250	A	13.31	100	Not Liganded
1AVH	TYR	256	A	9.21	0	Not Liganded
1AVH	TYR	257	A	10.6	19	Not Liganded
1AVH	TYR	297	A	11.45	0	Not Liganded
1AVH	TYR	308	A	14.14	61	Not Liganded
1AVH	TYR	91	B	15.04	98	Not Liganded
1AVH	TYR	94	B	11.26	46	Not Liganded
1AVH	TYR	129	B	13.09	43	Liganded
1AVH	TYR	133	B	11.6	26	Not Liganded
1AVH	TYR	148	B	10.44	0	Not Liganded
1AVH	TYR	149	B	12.61	71	Not Liganded
1AVH	TYR	213	B	12.02	45	Not Liganded
1AVH	TYR	250	B	13.75	100	Not Liganded
1AVH	TYR	256	B	10.06	0	Not Liganded
1AVH	TYR	257	B	10.87	24	Not Liganded
1AVH	TYR	297	B	10.16	0	Not Liganded
1AVH	TYR	308	B	14.13	63	Not Liganded

Table 4.16. GSTP1 Dual Screen Results

JWB Inhibitor	Normalized Lane Intenstiy (Inhibitor/DMSO)	Normalized Band Intenstiy (Inhibitor/DMSO)	AutoDock Affinity (Kcal/mol)
101	0.851323804	0.980038463	-6.3
102	0.832815888	1.039534624	-7.3
104	0.647433928	0.84259362	-7.2
105	0.616319988	0.760287272	-7.4
106	0.623118331	0.801085239	-7.1
107	0.317456275	0.567487844	-7.1
108	0.605849451	0.720539571	-7.8
109	0.789692247	0.906217355	-7.7
111	0.388242998	0.692272141	-7.1
112	0.797539467	0.914800343	-8.2
116	0.867812369	0.980425258	-6.5
117	0.891484649	1.004864963	-7.4
119	0.653501906	0.737698314	-7.4
120	0.568354562	0.61285215	-7.4
121	0.353392955	0.504103101	-7.2
122	0.375893597	0.547263178	-7.3
123	0.62348918	0.688955484	-8.2
124	0.436866278	0.499510367	-7.8
126	0.509179936	0.690414172	-7.2
127	0.75240169	0.781729966	-8.4
131	0.831321354	0.963604238	-6.5

132	0.52179896	0.685022564	-7.4
134	0.421715528	0.591223332	-7.2
135	0.454385607	0.538563496	-7.4
136	0.561319588	0.648866634	-7.3
137	0.201618519	0.346087087	-7.3
138	0.580692711	0.693478956	-8.2
139	0.346944498	0.416323954	-7.8
141	0.341612819	0.593841225	-7.3
142	0.869720417	0.946186447	-8.3
146	0.94447896	0.991921515	-7
147	0.555704281	0.626683617	-8
149	0.313737428	0.37089193	-7.9
150	0.410908983	0.464818734	-8
151	0.404204329	0.478076002	-8
152	0.175593828	0.310696363	-7.8
153	0.418268534	0.458295264	-8.9
154	0.578889646	0.635237414	-7.9
156	0.473175604	0.650987635	-7.8
157	0.717279589	0.754766215	-8.9
161	0.952875039	1.115736611	-6.6
162	0.933652947	1.026605297	-7.5
164	1	0.993424495	-7.3
165	0.833233131	0.909356008	-7.5
166	0.86400632	1.181308054	-7.3
167	0.337411256	0.411264138	-7.3
168	0.459469663	0.501407869	-8.5
169	0.661004896	0.731236843	-7.8
171	0.436909209	0.722856531	-7.4
172	0.646446428	0.77770171	-8.4
176	0.851282529	0.945077515	-6.2
177	0.599252941	0.774178322	-7.3
179	0.217765469	0.44033655	-7.1
180	0.387672882	0.670710386	-7.1
181	0.424057417	0.618528562	-7.1
182	0.384818077	0.543469987	-7.1
183	0.280372055	0.359865784	-7.8
184	0.303260916	0.443129244	-7.6
186	0.392478728	0.63988966	-7.1
187	0.77864146	0.967959468	-8.2
191	0.971335025	1.014629827	-6.3
192	0.400448515	0.656033837	-7.2
194	0.179500317	0.354995588	-7.1
195	0.459250794	0.685762712	-7.1
196	0.342944749	0.494466117	-7.1
197	0.46639318	0.63583909	-7.1
198	0.706188554	0.791481605	-7.9

201	0.355199389	0.624526671	-7
202	0.694991582	0.877325868	-8.2
206	0.997643819	1.056541399	-6
207	0.536866391	0.691784728	-7
209	0.781986539	0.880453074	-6.9
210	0.571298922	0.683583523	-6.9
211	0.816220185	0.976213088	-6.9
212	0.476072427	0.608017896	-6.9
213	0.520783726	0.633994382	-7.9
214	0.362997788	0.44739781	-7.2
216	0.360337323	0.68822907	-6.7
217	0.701411456	0.798769468	-8
221	0.559916589	0.729590752	-7.6
222	0.489124758	0.629676547	-7.8
223	0.751260691	0.725219431	-8.6
224	0.811211228	0.82297362	-7.8
226	0.324441512	0.531034583	-7.4
227	0.331641784	0.526513243	-7.3
228	0.275137908	0.495017801	-7.7
229	0.253386522	0.524366729	-7.1
230	0.262883384	0.529237126	-7.4
231	0.236797891	0.459255393	-7.4
232	0.424160869	0.593429627	-7.5
233	0.339726489	0.474758584	-7.9
234	0.368570634	0.559593867	-7.6
235	0.576860541	0.666293054	-7.5
237	0.59856862	0.720363978	-7.3
238	0.666828062	0.739153226	-7.3
239	0.730542905	0.764412566	-7.2
241	0.641955486	0.701610357	-7.9

Table 4.17. DPP3 Dual Screen Results

JWB Inhibitor	Normalized Lane Intenstiy (Inhibitor/DMSO)	Normalized Band Intenstiy (Inhibitor/DMSO)	AutoDock Affinity (Kcal/mol)
101	0.733567146	1.03228334	-7.2
102	0.828713655	0.8563548	-7.8
104	0.908360674	0.94071985	-7.3
105	0.930535128	0.82425952	-7.9
106	0.963118	0.81906702	-7.4
107	0.871252404	0.78153894	-7.1
108	0.909378889	0.77798673	-8.9
109	0.870234189	0.93414825	-7.9
111	0.840253422	0.71747375	-7.4
112	0.822038692	0.92389908	-8.8
116	0.732096391	1.04231312	-6.8

117	0.745446317	0.75228543	-7.8
119	0.756307275	0.65159066	-7.5
120	0.801221858	0.75934806	-7.6
121	0.758343704	0.60501489	-7.5
122	0.763774183	0.76450922	-7.4
123	0.413508315	0.6403385	-8.9
124	0.808236226	0.71960508	-7.8
126	1	0.80227759	-7.6
127	0.806426066	0.85100559	-8.9
131	0.714428135	1.04994365	-6.8
132	0.508279896	0.76589856	-7.7
134	0.553082795	0.7466356	-7.5
135	0.554976975	0.74140379	-7.6
136	0.609971245	0.66257297	-7.6
137	0.391460196	0.57185169	-7.4
138	0.726261385	0.79315877	-9.1
139	0.492977579	0.59791241	-8
141	0.462137819	0.70792048	-7.5
142	0.775067941	0.88696936	-8.8
146	0.909635732	1.04850966	-7.7
147	0.748435601	0.87005417	-8.8
149	0.718001146	0.81164628	-8.2
150	0.464842378	0.57595525	-8.9
151	0.524482823	0.61860109	-8.2
152	0.41550891	0.50856136	-8
153	0.63940743	0.75695911	-9.5
154	0.594916291	0.72807762	-8.3
156	0.61019797	0.73097332	-8.6
157	0.695945132	0.85184678	-9.1
161	0.779559633	0.82988108	-7.1
162	0.824047487	0.82923784	-8.1
164	0.656327837	0.68577008	-7.6
165	0.599604246	0.66406216	-7.9
166	0.582480406	0.61239507	-7.6
167	0.602786562	0.66835185	-7.5
168	0.566109753	0.59099616	-9.1
169	0.65233567	0.65533584	-8.3
171	0.739484937	0.78428891	-7.6
172	0.644670914	0.69429675	-8.8
176	0.755772054	0.83691459	-6.8
177	0.730172867	0.83217033	-7.4
179	0.546678393	0.63227666	-7.2
180	0.631568068	0.68677273	-7.3
181	0.747566175	0.7402063	-7.3
182	0.523949275	0.65512682	-6.9
183	0.644506195	0.58764108	-8.8
184	0.682805673	0.59610025	-7.8
186	0.609095956	0.63424489	-7
187	0.548405074	0.53531557	-8
191	0.758298318	0.87406981	-6.5
192	0.75722618	0.84868068	-7.5

194	0.184285573	0.30547525	-7.2
195	0.692363961	0.80413271	-7.4
196	0.740382927	0.80712016	-7.3
197	0.720090802	0.84895015	-6.9
198	0.438788876	0.50724189	-8.8
201	0.715746797	0.82350082	-7
202	0.523523487	0.60812455	-8.7
206	0.740705342	0.78147704	-6.4
207	0.744144282	0.75426404	-7.3
209	0.590502737	0.71734163	-6.8
210	0.542887244	0.60495446	-7
211	0.675362155	0.71546291	-7
212	0.651724085	0.63076268	-6.9
213	0.344310552	0.46468035	-8.3
214	0.389157851	0.49984955	-7.5
216	0.465853535	0.56622314	-6.7
217	0.652275375	0.76665107	-8.2
221	0.739229635	0.94264141	-7.6
222	0.695700494	0.98577325	-8
223	0.843657829	1.03164869	-8.3
224	1	1.15782133	-7.9
226	0.598859889	1.01613577	-7.3
227	0.590343471	0.97228169	-7.2
228	0.364827414	0.94607175	-8.9
229	0.399907285	0.94621259	-7.7
230	0.388204548	0.9440252	-7.7
231	0.501533441	0.8400396	-7.3
232	0.530491693	0.81606828	-7.3
233	0.578837095	0.68988821	-9.2
234	0.52833779	0.83831604	-8.1
235	0.620459648	0.87831285	-7.7
237	0.72345831	1.05515825	-7
238	0.464360398	0.85217437	-7.1
239	0.492895562	0.71663136	-6.9
241	0.595301091	0.72560233	-8.9

Works Cited

1. Downard, K. *Mass Spectrometry*. (2004). doi:10.1039/9781847551306.
2. Kinter, M. & Sherman, N. E. Protein Sequencing and Identification Using Tandem Mass Spectrometry. (2000) doi:10.1002/0471721980.
3. Mitchell Wells, J. & McLuckey, S. A. Collision-Induced Dissociation (CID) of Peptides and Proteins. in *Methods in Enzymology* vol. 402 148–185 (Academic Press, 2005).
4. Sleno, L. & Volmer, D. A. Ion activation methods for tandem mass spectrometry. *J. Mass Spectrom.* **39**, 1091–1112 (2004).
5. Olsen, J. V. *et al.* Higher-energy C-trap dissociation for peptide modification analysis. *Nat. Methods* **4**, 709–712 (2007).
6. Zubarev, R. A. & Makarov, A. Orbitrap Mass Spectrometry. *Anal. Chem.* **85**, 5288–5296 (2013).
7. Chowdhury, S. K., Katta, V. & Chait, B. T. Electrospray ionization mass spectrometric peptide mapping: A rapid, sensitive technique for protein structure analysis. *Biochem. Biophys. Res. Commun.* **167**, 686–692 (1990).
8. Pitt, J. J. Principles and Applications of Liquid Chromatography-Mass Spectrometry in Clinical Biochemistry. *Clin. Biochem. Rev.* **30**, 19–34 (2009).
9. Gama, M. R., Collins, C. H. & Bottoli, C. B. G. Nano-Liquid Chromatography in Pharmaceutical and Biomedical Research. *J. Chromatogr. Sci.* **51**, 694–703 (2013).
10. McDonald, W. H. & Yates, J. R. Shotgun Proteomics and Biomarker Discovery. *Dis. Markers* **18**, 99–105 (2002).
11. Eng, J. K., McCormack, A. L. & Yates, J. R. An approach to correlate tandem mass spectral data of peptides with amino acid sequences in a protein database. *J. Am. Soc. Mass Spectrom.* **5**, 976–989 (1994).
12. Meier, F., Geyer, P. E., Virreira Winter, S., Cox, J. & Mann, M. BoxCar acquisition method enables single-shot proteomics at a depth of 10,000 proteins in 100 minutes. *Nat. Methods* **15**, 440–448 (2018).
13. Hood, L. & Rowen, L. The Human Genome Project: big science transforms biology and medicine. *Genome Med.* **5**, 79 (2013).
14. Hubler, S. L. *et al.* Challenges in Peptide-Spectrum Matching: A Robust and Reproducible Statistical Framework for Removing Low-Accuracy, High-Scoring Hits. *J. Proteome Res.* **19**, 161–173 (2020).
15. Hoopmann, M. R. & Moritz, R. L. Current algorithmic solutions for peptide-based proteomics data generation and identification. *Curr. Opin. Biotechnol.* **24**, (2013).
16. Verheggen, K. *et al.* Anatomy and evolution of database search engines—a central component of mass spectrometry based proteomic workflows. *Mass Spectrom. Rev.* **39**, 292–306 (2020).
17. Bern, M., Kil, Y. J. & Becker, C. Byonic: Advanced Peptide and Protein Identification Software. *Curr. Protoc. Bioinforma.* **40**, (2012).
18. Seidler, J., Zinn, N., Boehm, M. E. & Lehmann, W. D. De novo sequencing of peptides by MS/MS. *PROTEOMICS* **10**, 634–649 (2010).
19. Cravatt, B. F., Wright, A. T. & Kozarich, J. W. Activity-Based Protein Profiling: From Enzyme Chemistry to Proteomic Chemistry. *Annu. Rev. Biochem.* **77**, 383–414

(2008).
20. Roberts, A. M., Ward, C. C. & Nomura, D. K. Activity-based protein profiling for mapping and pharmacologically interrogating proteome-wide ligandable hotspots. *Curr. Opin. Biotechnol.* **43**, 25–33 (2017).
21. *Activity-Based Protein Profiling*. vol. 420 (Springer International Publishing, 2019).
22. Liu, Y., Patricelli, M. P. & Cravatt, B. F. Activity-based protein profiling: The serine hydrolases. *Proc. Natl. Acad. Sci.* **96**, 14694–14699 (1999).
23. Nordin, B. E. *et al.* ATP Acyl Phosphate Reactivity Reveals Native Conformations of Hsp90 Paralogs and Inhibitor Target Engagement. *Biochemistry* **54**, 3024–3036 (2015).
24. Patricelli, M. P. *et al.* Functional Interrogation of the Kinome Using Nucleotide Acyl Phosphates. *Biochemistry* **46**, 350–358 (2007).
25. De Cesco, S., Kurian, J., Dufresne, C., Mittermaier, A. K. & Moitessier, N. Covalent inhibitors design and discovery. *Eur. J. Med. Chem.* **138**, 96–114 (2017).
26. Liu, R., Yue, Z., Tsai, C.-C. & Shen, J. Assessing Lysine and Cysteine Reactivities for Designing Targeted Covalent Kinase Inhibitors. *J. Am. Chem. Soc.* **141**, 6553–6560 (2019).
27. Hacker, S. M. *et al.* Global profiling of lysine reactivity and ligandability in the human proteome. *Nat. Chem.* **9**, 1181–1190 (2017).
28. Kathman, S. G., Xu, Z. & Statsyuk, A. V. A Fragment-Based Method to Discover Irreversible Covalent Inhibitors of Cysteine Proteases. *J. Med. Chem.* **57**, 4969–4974 (2014).
29. Kuljanin, M. *et al.* Reimagining high-throughput profiling of reactive cysteines for cell-based screening of large electrophile libraries. *Nat. Biotechnol.* **39**, 630–641 (2021).
30. Abo, M., Li, C. & Weerapana, E. Isotopically-Labeled Iodoacetamide-Alkyne Probes for Quantitative Cysteine-Reactivity Profiling. *Mol. Pharm.* **15**, 743–749 (2018).
31. Fonović, M. & Bogyo, M. Activity-based probes as a tool for functional proteomic analysis of proteases. *Expert Rev. Proteomics* **5**, 721–730 (2008).
32. Drewes, G. & Knapp, S. Chemoproteomics and Chemical Probes for Target Discovery. *Trends Biotechnol.* **36**, 1275–1286 (2018).
33. Speers, A. E., Adam, G. C. & Cravatt, B. F. Activity-Based Protein Profiling in Vivo Using a Copper(I)-Catalyzed Azide-Alkyne [3 + 2] Cycloaddition. *J. Am. Chem. Soc.* **125**, 4686–4687 (2003).
34. Rostovtsev, V. V., Green, L. G., Fokin, V. V. & Sharpless, K. B. A Stepwise Huisgen Cycloaddition Process: Copper(I)-Catalyzed Regioselective "Ligation" of Azides and Terminal Alkynes. *Angew. Chem. Int. Ed.* **41**, 2596–2599 (2002).
35. Hirsch, J. D. *et al.* Easily reversible desthiobiotin binding to streptavidin, avidin, and other biotin-binding proteins: uses for protein labeling, detection, and isolation. *Anal. Biochem.* **308**, 343–357 (2002).
36. Franks, C. E., Campbell, S. T., Purow, B. W., Harris, T. E. & Hsu, K.-L. The Ligand Binding Landscape of Diacylglycerol Kinases. *Cell Chem. Biol.* **24**, 870-880.e5 (2017).

37. Hsu, K.-L. *et al.* DAGLβ inhibition perturbs a lipid network involved in macrophage inflammatory responses. *Nat. Chem. Biol.* **8**, 999–1007 (2012).
38. Hsu, K.-L. *et al.* Discovery and Optimization of Piperidyl-1,2,3-Triazole Ureas as Potent, Selective, and in Vivo-Active Inhibitors of α/β-Hydrolase Domain Containing 6 (ABHD6). *J. Med. Chem.* **56**, 8270–8279 (2013).
39. Wolf, E. V. *et al.* A New Class of Rhomboid Protease Inhibitors Discovered by Activity-Based Fluorescence Polarization. *PLOS ONE* **8**, e72307 (2013).
40. Lichtman, J. W. & Conchello, J.-A. Fluorescence microscopy. *Nat. Methods* **2**, 910–919 (2005).
41. Aaltonen, N. *et al.* Tissue-ABPP enables high-resolution confocal fluorescence imaging of serine hydrolase activity in cryosections – Application to glioma brain unveils activity hotspots originating from tumor-associated neutrophils. *bioRxiv* 783704 (2019) doi:10.1101/783704.
42. Speers, A. E. & Cravatt, B. F. Activity-Based Protein Profiling (ABPP) and Click Chemistry (CC)-ABPP by MudPIT Mass Spectrometry. *Curr. Protoc. Chem. Biol.* **1**, 29–41 (2009).
43. Holderfield, M., Deuker, M. M., McCormick, F. & McMahon, M. Targeting RAF kinases for cancer therapy: BRAF-mutated melanoma and beyond. *Nat. Rev. Cancer* **14**, 455–467 (2014).
44. Lu, T. *et al.* Discovery of a subtype-selective, covalent inhibitor against palmitoylation pocket of TEAD3. *Acta Pharm. Sin. B* (2021) doi:10.1016/j.apsb.2021.04.015.
45. Klaeger, S. *et al.* The target landscape of clinical kinase drugs. *Science* **358**, eaan4368 (2017).
46. Médard, G. *et al.* Optimized Chemical Proteomics Assay for Kinase Inhibitor Profiling. *J. Proteome Res.* **14**, 1574–1586 (2015).
47. Jameson, D. M. & Ross, J. A. Fluorescence Polarization/Anisotropy in Diagnostics and Imaging. *Chem. Rev.* **110**, 2685–2708 (2010).
48. Mann, M. Functional and quantitative proteomics using SILAC. *Nat. Rev. Mol. Cell Biol.* **7**, 952–958 (2006).
49. Navarrete-Perea, J., Yu, Q., Gygi, S. P. & Paulo, J. A. Streamlined Tandem Mass Tag (SL-TMT) Protocol: An Efficient Strategy for Quantitative (Phospho)proteome Profiling Using Tandem Mass Tag-Synchronous Precursor Selection-MS3. *J. Proteome Res.* **17**, 2226–2236 (2018).
50. Aggarwal, K., Choe, L. H. & Lee, K. H. Shotgun proteomics using the iTRAQ isobaric tags. *Brief. Funct. Genomics* **5**, 112–120 (2006).
51. Zanon, P. R. A., Lewald, L. & Hacker, S. M. Isotopically Labeled Desthiobiotin Azide (isoDTB) Tags Enable Global Profiling of the Bacterial Cysteinome. *Angew. Chem.* **132**, 2851–2858 (2020).
52. Long, J. Z. & Cravatt, B. F. The Metabolic Serine Hydrolases and Their Functions in Mammalian Physiology and Disease. *Chem. Rev.* **111**, 6022–6063 (2011).
53. Bachovchin, D. A. & Cravatt, B. F. The pharmacological landscape and therapeutic potential of serine hydrolases. *Nat. Rev. Drug Discov.* **11**, 52–68 (2012).
54. Shin, M. *et al.* Liposomal Delivery of Diacylglycerol Lipase-Beta Inhibitors to

Macrophages Dramatically Enhances Selectivity and Efficacy in Vivo. *Mol. Pharm.* **15**, 721–728 (2018).
55. Adams, J. A. Kinetic and Catalytic Mechanisms of Protein Kinases. *Chem. Rev.* **101**, 2271–2290 (2001).
56. Bhullar, K. S. *et al.* Kinase-targeted cancer therapies: progress, challenges and future directions. *Mol. Cancer* **17**, (2018).
57. Golkowski, M. *et al.* Kinobead and Single-Shot LC-MS Profiling Identifies Selective PKD Inhibitors. *J. Proteome Res.* **16**, 1216–1227 (2017).
58. Reinecke, M. *et al.* Kinobeads: A Chemical Proteomic Approach for Kinase Inhibitor Selectivity Profiling and Target Discovery. in *Target Discovery and Validation* 97–130 (John Wiley & Sons, Ltd, 2019). doi:10.1002/9783527818242.ch4.
59. Cooper, M. J. *et al.* Application of Multiplexed Kinase Inhibitor Beads to Study Kinome Adaptations in Drug-Resistant Leukemia. *PLOS ONE* **8**, e66755 (2013).
60. Kuenzi, B. M. *et al.* Polypharmacology-based ceritinib repurposing using integrated functional proteomics. *Nat. Chem. Biol.* **13**, 1222–1231 (2017).
61. MacKinnon, A. L. & Taunton, J. Target Identification by Diazirine Photo-Cross-linking and Click Chemistry. *Curr. Protoc. Chem. Biol.* **1**, 55–73 (2009).
62. Ward, C. C., Kleinman, J. I. & Nomura, D. K. NHS-Esters As Versatile Reactivity-Based Probes for Mapping Proteome-Wide Ligandable Hotspots. *ACS Chem. Biol.* **12**, 1478–1483 (2017).
63. Nguyen, D.-T. *et al.* Pharos: Collating protein information to shed light on the druggable genome. *Nucleic Acids Res.* **45**, D995–D1002 (2017).
64. Overington, J. P., Al-Lazikani, B. & Hopkins, A. L. How many drug targets are there? *Nat. Rev. Drug Discov.* **5**, 993–996 (2006).
65. Koresawa, M. & Okabe, T. High-Throughput Screening with Quantitation of ATP Consumption: A Universal Non-Radioisotope, Homogeneous Assay for Protein Kinase. *ASSAY Drug Dev. Technol.* **2**, 153–160 (2004).
66. Eder, J., Sedrani, R. & Wiesmann, C. The discovery of first-in-class drugs: origins and evolution. *Nat. Rev. Drug Discov.* **13**, 577–587 (2014).
67. Moffat, J. G., Vincent, F., Lee, J. A., Eder, J. & Prunotto, M. Opportunities and challenges in phenotypic drug discovery: an industry perspective. *Nat. Rev. Drug Discov.* **16**, 531–543 (2017).
68. Knight, Z. A., Lin, H. & Shokat, K. M. Targeting the cancer kinome through polypharmacology. *Nat. Rev. Cancer* **10**, 130–137 (2010).
69. Drewes, G. Chemical Proteomics in Drug Discovery. *Methods Mol. Biol.* 15–21 (2011) doi:10.1007/978-1-61779-364-6_2.
70. Roskoski, R. Orally effective FDA-approved protein kinase targeted covalent inhibitors (TCIs). *Pharmacol. Res.* **165**, 105422 (2021).
71. Ni, D., Lu, S. & Zhang, J. Emerging roles of allosteric modulators in the regulation of protein-protein interactions (PPIs): A new paradigm for PPI drug discovery. *Med. Res. Rev.* **39**, 2314–2342 (2019).
72. Baillie, T. A. Targeted Covalent Inhibitors for Drug Design. *Angew. Chem. Int. Ed.* **55**, 13408–13421 (2016).
73. Chatterjee, P. *et al.* Can Relative Binding Free Energy Predict Selectivity of

Reversible Covalent Inhibitors? *J. Am. Chem. Soc.* **139**, 17945–17952 (2017).
74. Baillie, T. A. Approaches to mitigate the risk of serious adverse reactions in covalent drug design. *Expert Opin. Drug Discov.* **16**, 275–287 (2021).
75. Thibaudeau, T. A. & Smith, D. M. A Practical Review of Proteasome Pharmacology. *Pharmacol. Rev.* **71**, 170–197 (2019).
76. Kennedy, S. P., Hastings, J. F., Han, J. Z. R. & Croucher, D. R. The Under-Appreciated Promiscuity of the Epidermal Growth Factor Receptor Family. *Front. Cell Dev. Biol.* **4**, (2016).
77. Lu, S., Jang, H., Gu, S., Zhang, J. & Nussinov, R. Drugging Ras GTPase: a comprehensive mechanistic and signaling structural view. *Chem. Soc. Rev.* **45**, 4929–4952 (2016).
78. Canon, J. *et al.* The clinical KRAS(G12C) inhibitor AMG 510 drives anti-tumour immunity. *Nature* **575**, 217–223 (2019).
79. Commissioner, O. of the. FDA Approves First Targeted Therapy for Lung Cancer Mutation Previously Considered Resistant to Drug Therapy. *FDA* https://www.fda.gov/news-events/press-announcements/fda-approves-first-targeted-therapy-lung-cancer-mutation-previously-considered-resistant-drug (2021).
80. Ehmann, D. E. *et al.* Avibactam is a covalent, reversible, non–β-lactam β-lactamase inhibitor. *Proc. Natl. Acad. Sci.* **109**, 11663–11668 (2012).
81. H. Jones, L. & W. Kelly, J. Structure-based design and analysis of SuFEx chemical probes. *RSC Med. Chem.* **11**, 10–17 (2020).
82. Liu, Z. *et al.* SuFEx Click Chemistry Enabled Late-Stage Drug Functionalization. *J. Am. Chem. Soc.* **140**, 2919–2925 (2018).
83. Zheng, Q. *et al.* SuFEx-enabled, agnostic discovery of covalent inhibitors of human neutrophil elastase. *Proc. Natl. Acad. Sci.* **116**, 18808–18814 (2019).
84. Dong, J., Krasnova, L., Finn, M. G. & Sharpless, K. B. Sulfur(VI) Fluoride Exchange (SuFEx): Another Good Reaction for Click Chemistry. *Angew. Chem. Int. Ed.* **53**, 9430–9448 (2014).
85. Zhao, Q. *et al.* Broad-Spectrum Kinase Profiling in Live Cells with Lysine-Targeted Sulfonyl Fluoride Probes. *J. Am. Chem. Soc.* **139**, 680–685 (2017).
86. MacLean, B. *et al.* Skyline: an open source document editor for creating and analyzing targeted proteomics experiments. *Bioinforma. Oxf. Engl.* **26**, 966–968 (2010).
87. Yu, F., Li, N. & Yu, W. PIPI: PTM-Invariant Peptide Identification Using Coding Method. *J. Proteome Res.* **15**, 4423–4435 (2016).
88. Marx, H. *et al.* A large synthetic peptide and phosphopeptide reference library for mass spectrometry–based proteomics. *Nat. Biotechnol.* **31**, 557–564 (2013).
89. Shteynberg, D. D. *et al.* PTMProphet: Fast and Accurate Mass Modification Localization for the Trans-Proteomic Pipeline. *J. Proteome Res.* **18**, 4262–4272 (2019).
90. Palafox, M. F., Desai, H. S., Arboleda, V. A. & Backus, K. M. From chemoproteomic-detected amino acids to genomic coordinates: insights into precise multi-omic data integration. *Mol. Syst. Biol.* **17**, e9840 (2021).
91. Mi, H., Muruganujan, A., Casagrande, J. T. & Thomas, P. D. Large-scale gene function analysis with the PANTHER classification system. *Nat. Protoc.* **8**, 1551–1566 (2013).

92. Counihan, J. L., Ford, B. & Nomura, D. K. Mapping proteome-wide interactions of reactive chemicals using chemoproteomic platforms. *Curr. Opin. Chem. Biol.* **30**, 68–76 (2016).
93. London, N. *et al.* Covalent docking of large libraries for the discovery of chemical probes. *Nat. Chem. Biol.* **10**, 1066–1072 (2014).
94. Bensinger, D. *et al.* Virtual Screening Identifies Irreversible FMS-like Tyrosine Kinase 3 Inhibitors with Activity toward Resistance-Conferring Mutations. *J. Med. Chem.* **62**, 2428–2446 (2019).
95. Morris, G. M. *et al.* AutoDock4 and AutoDockTools4: Automated docking with selective receptor flexibility. *J. Comput. Chem.* **30**, 2785–2791 (2009).
96. Peng, Y. *et al.* 5-HT2C Receptor Structures Reveal the Structural Basis of GPCR Polypharmacology. *Cell* **172**, 719-730.e14 (2018).
97. Barone, J. A. *et al.* Safety Evaluation of Ritanserin—An Investigational Serotonin Antagonist. *Drug Intell. Clin. Pharm.* **20**, 770–775 (1986).
98. Purow, B. Molecular Pathways: Targeting Diacylglycerol Kinase Alpha in Cancer. *Clin. Cancer Res.* **21**, 5008–5012 (2015).
99. Boroda, S., Niccum, M., Raje, V., Purow, B. W. & Harris, T. E. Dual activities of ritanserin and R59022 as DGKα inhibitors and serotonin receptor antagonists. *Biochem. Pharmacol.* **123**, 29–39 (2017).
100. McCloud, R. L. *et al.* Deconstructing Lipid Kinase Inhibitors by Chemical Proteomics. *Biochemistry* **57**, 231–236 (2017).
101. Sakane, F., Imai, S., Kai, M., Yasuda, S. & Kanoh, H. Diacylglycerol kinases: Why so many of them? *Biochim. Biophys. Acta BBA - Mol. Cell Biol. Lipids* **1771**, 793–806 (2007).
102. Greer, P. Closing in on the biological functions of fps/fes and fer. *Nat. Rev. Mol. Cell Biol.* **3**, 278–289 (2002).
103. Dominguez, C. L. *et al.* Diacylglycerol Kinase α Is a Critical Signaling Node and Novel Therapeutic Target in Glioblastoma and Other Cancers. *Cancer Discov.* **3**, 782–797 (2013).
104. Olmez, I. *et al.* Targeting the mesenchymal subtype in glioblastoma and other cancers via inhibition of diacylglycerol kinase alpha. *Neuro-Oncol.* **20**, 192–202 (2017).
105. Schilling, B. *et al.* Platform-independent and Label-free Quantitation of Proteomic Data Using MS1 Extracted Ion Chromatograms in Skyline. *Mol. Cell. Proteomics* **11**, 202–214 (2012).
106. Edgar, R. C. MUSCLE: a multiple sequence alignment method with reduced time and space complexity. *BMC Bioinformatics* **5**, 113 (2004).
107. Rice, P., Longden, I. & Bleasby, A. EMBOSS: The European Molecular Biology Open Software Suite. *Trends Genet.* **16**, 276–277 (2000).
108. Kepp, O., Galluzzi, L., Lipinski, M., Yuan, J. & Kroemer, G. Cell death assays for drug discovery. *Nat. Rev. Drug Discov.* **10**, 221–237 (2011).
109. Bartling, B. RasGTPase-activating protein is a target of caspases in spontaneous apoptosis of lung carcinoma cells and in response to etoposide. *Carcinogenesis* **25**, 909–921 (2004).
110. Wang, Y., Yang, H., Liu, H., Huang, J. & Song, X. Effect of staurosporine on the

mobility and invasiveness of lung adenocarcinoma A549 cells: an in vitro study. *BMC Cancer* **9**, (2009).
111. Patricelli, M. P. *et al.* In Situ Kinase Profiling Reveals Functionally Relevant Properties of Native Kinases. *Chem. Biol.* **18**, 699–710 (2011).
112. Shin, M., Franks, C. E. & Hsu, K.-L. Isoform-selective activity-based profiling of ERK signaling. *Chem. Sci.* **9**, 2419–2431 (2018).
113. Chang, J. W. *et al.* Selective Inhibitor of Platelet-Activating Factor Acetylhydrolases 1b2 and 1b3 That Impairs Cancer Cell Survival. *ACS Chem. Biol.* **10**, 925–932 (2015).
114. Nagano, J. M. G. *et al.* Selective inhibitors and tailored activity probes for lipoprotein-associated phospholipase A2. *Bioorg. Med. Chem. Lett.* **23**, 839–843 (2013).
115. Agarwal, A. *et al.* The AKT/IκB kinase pathway promotes angiogenic/metastatic gene expression in colorectal cancer by activating nuclear factor-κB and β-catenin. *Oncogene* **24**, 1021–1031 (2004).
116. Castellano, E. *et al.* Requirement for Interaction of PI3-Kinase p110α with RAS in Lung Tumor Maintenance. *Cancer Cell* **24**, 617–630 (2013).
117. Sanclemente, M. *et al.* c-RAF Ablation Induces Regression of Advanced Kras/Trp53 Mutant Lung Adenocarcinomas by a Mechanism Independent of MAPK Signaling. *Cancer Cell* **33**, 217-228.e4 (2018).
118. Blackford, A. N. & Jackson, S. P. ATM, ATR, and DNA-PK: The Trinity at the Heart of the DNA Damage Response. *Mol. Cell* **66**, 801–817 (2017).
119. Graziano, S. L. *et al.* Involvement of theRAFI locus, at band 3p25, in the 3p deletion of small-cell lung cancer. *Genes. Chromosomes Cancer* **3**, 283–293 (1991).
120. Morrow, A. A. *et al.* The Lipid Kinase PI4KIIIβ Is Highly Expressed in Breast Tumors and Activates Akt in Cooperation with Rab11a. *Mol. Cancer Res.* **12**, 1492–1508 (2014).
121. Cheng, Y. *et al.* eEF-2 kinase is a critical regulator of Warburg effect through controlling PP2A-A synthesis. *Oncogene* **35**, 6293–6308 (2016).
122. Ye, J. *et al.* The GCN2-ATF4 pathway is critical for tumour cell survival and proliferation in response to nutrient deprivation. *EMBO J.* **29**, 2082–2096 (2010).
123. Kim, J.-A. *et al.* Amplification of TLK2 Induces Genomic Instability via Impairing the G2–M Checkpoint. *Mol. Cancer Res.* **14**, 920–927 (2016).
124. Lewis, T. S., Shapiro, P. S. & Ahn, N. G. Signal Transduction through MAP Kinase Cascades. *Adv. Cancer Res.* 49–139 (1998) doi:10.1016/s0065-230x(08)60765-4.
125. Pearson, G. *et al.* Mitogen-Activated Protein (MAP) Kinase Pathways: Regulation and Physiological Functions*. *Endocr. Rev.* **22**, 153–183 (2001).
126. Seger, R. & Krebs, E. G. The MAPK signaling cascade. *FASEB J.* **9**, 726–735 (1995).
127. Simanshu, D. K., Nissley, D. V. & McCormick, F. RAS Proteins and Their Regulators in Human Disease. *Cell* **170**, 17–33 (2017).
128. Dhillon, A. S., Hagan, S., Rath, O. & Kolch, W. MAP kinase signalling pathways in cancer. *Oncogene* **26**, 3279–3290 (2007).
129. Griner, E. M. & Kazanietz, M. G. Protein kinase C and other diacylglycerol effectors in cancer. *Nat. Rev. Cancer* **7**, 281–294 (2007).

130. Wu, P., Nielsen, T. E. & Clausen, M. H. FDA-approved small-molecule kinase inhibitors. *Trends Pharmacol. Sci.* **36**, 422–439 (2015).
131. Sadaghiani, A. M., Verhelst, S. H. & Bogyo, M. Tagging and detection strategies for activity-based proteomics. *Curr. Opin. Chem. Biol.* **11**, 20–28 (2007).
132. Niphakis, M. J. & Cravatt, B. F. Enzyme Inhibitor Discovery by Activity-Based Protein Profiling. *Annu. Rev. Biochem.* **83**, 341–377 (2014).
133. Deu, E., Verdoes, M. & Bogyo, M. New approaches for dissecting protease functions to improve probe development and drug discovery. *Nat. Struct. Mol. Biol.* **19**, 9–16 (2012).
134. Kumar, S. *et al.* Activity-based probes for protein tyrosine phosphatases. *Proc. Natl. Acad. Sci.* **101**, 7943–7948 (2004).
135. Vocadlo, D. J. & Bertozzi, C. R. A Strategy for Functional Proteomic Analysis of Glycosidase Activity from Cell Lysates. *Angew. Chem. Int. Ed.* **43**, 5338–5342 (2004).
136. Weerapana, E. *et al.* Quantitative reactivity profiling predicts functional cysteines in proteomes. *Nature* **468**, 790–795 (2010).
137. Lin, S. *et al.* Redox-based reagents for chemoselective methionine bioconjugation. *Science* **355**, 597–602 (2017).
138. Matthews, M. L. *et al.* Chemoproteomic profiling and discovery of protein electrophiles in human cells. *Nat. Chem.* **9**, 234–243 (2016).
139. Parker, C. G. *et al.* Ligand and Target Discovery by Fragment-Based Screening in Human Cells. *Cell* **168**, 527-541.e29 (2017).
140. Narayanan, A. & Jones, L. H. Sulfonyl fluorides as privileged warheads in chemical biology. *Chem. Sci.* **6**, 2650–2659 (2015).
141. Gao, B. *et al.* Bifluoride-catalysed sulfur(VI) fluoride exchange reaction for the synthesis of polysulfates and polysulfonates. *Nat. Chem.* **9**, 1083–1088 (2017).
142. Dong, J., Sharpless, K. B., Kwisnek, L., Oakdale, J. S. & Fokin, V. V. SuFEx-Based Synthesis of Polysulfates. *Angew. Chem. Int. Ed.* **53**, 9466–9470 (2014).
143. Fahrney, D. E. & Gold, A. M. Sulfonyl Fluorides as Inhibitors of Esterases. I. Rates of Reaction with Acetylcholinesterase, α-Chymotrypsin, and Trypsin. *J. Am. Chem. Soc.* **85**, 997–1000 (1963).
144. Shannon, D. A. *et al.* Sulfonyl Fluoride Analogues as Activity-Based Probes for Serine Proteases. *ChemBioChem* **13**, 2327–2330 (2012).
145. Gu, C. *et al.* Chemical Proteomics with Sulfonyl Fluoride Probes Reveals Selective Labeling of Functional Tyrosines in Glutathione Transferases. *Chem. Biol.* **20**, 541–548 (2013).
146. Yang, B. *et al.* Proximity-enhanced SuFEx chemical cross-linker for specific and multitargeting cross-linking mass spectrometry. *Proc. Natl. Acad. Sci.* **115**, 11162–11167 (2018).
147. Yang, X. *et al.* An Affinity-Based Probe for the Human Adenosine A2A Receptor. *J. Med. Chem.* **61**, 7892–7901 (2018).
148. Chen, W. *et al.* Arylfluorosulfates Inactivate Intracellular Lipid Binding Protein(s) through Chemoselective SuFEx Reaction with a Binding Site Tyr Residue. *J. Am. Chem. Soc.* **138**, 7353–7364 (2016).
149. Fadeyi, O. O. *et al.* Covalent Enzyme Inhibition through Fluorosulfate

Modification of a Noncatalytic Serine Residue. *ACS Chem. Biol.* **12**, 2015–2020 (2017).
150. Mortenson, D. E. *et al.* "Inverse Drug Discovery" Strategy To Identify Proteins That Are Targeted by Latent Electrophiles As Exemplified by Aryl Fluorosulfates. *J. Am. Chem. Soc.* **140**, 200–210 (2017).
151. Chen, H. & Boutros, P. C. VennDiagram: a package for the generation of highly-customizable Venn and Euler diagrams in R. *BMC Bioinformatics* **12**, (2011).
152. Wishart, D. S. *et al.* DrugBank 5.0: a major update to the DrugBank database for 2018. *Nucleic Acids Res.* **46**, D1074–D1082 (2017).
153. Hornbeck, P. V. *et al.* PhosphoSitePlus, 2014: mutations, PTMs and recalibrations. *Nucleic Acids Res.* **43**, D512–D520 (2014).
154. Bereman, M. S. *et al.* An Automated Pipeline to Monitor System Performance in Liquid Chromatography–Tandem Mass Spectrometry Proteomic Experiments. *J. Proteome Res.* **15**, 4763–4769 (2016).
155. Adibekian, A. *et al.* Click-generated triazole ureas as ultrapotent in vivo–active serine hydrolase inhibitors. *Nat. Chem. Biol.* **7**, 469–478 (2011).
156. Ahn, K. *et al.* Discovery of a Selective Covalent Inhibitor of Lysophospholipase-like 1 (LYPLAL1) as a Tool to Evaluate the Role of this Serine Hydrolase in Metabolism. *ACS Chem. Biol.* **11**, 2529–2540 (2016).
157. Hentze, M. W., Castello, A., Schwarzl, T. & Preiss, T. A brave new world of RNA-binding proteins. *Nat. Rev. Mol. Cell Biol.* **19**, 327–341 (2018).
158. Yaffe, M. B. Phosphotyrosine-binding domains in signal transduction. *Nat. Rev. Mol. Cell Biol.* **3**, 177–186 (2002).
159. Shannon, D. A. *et al.* Investigating the Proteome Reactivity and Selectivity of Aryl Halides. *J. Am. Chem. Soc.* **136**, 3330–3333 (2014).
160. Humphrey, S. J. *et al.* Dynamic Adipocyte Phosphoproteome Reveals that Akt Directly Regulates mTORC2. *Cell Metab.* **17**, 1009–1020 (2013).
161. Lundby, A. *et al.* Quantitative maps of protein phosphorylation sites across 14 different rat organs and tissues. *Nat. Commun.* **3**, (2012).
162. Song, G. *et al.* Proteome-wide Tyrosine Phosphorylation Analysis Reveals Dysregulated Signaling Pathways in Ovarian Tumors. *Mol. Cell. Proteomics* **18**, 448–460 (2019).
163. Hitosugi, T. *et al.* Tyrosine Phosphorylation Inhibits PKM2 to Promote the Warburg Effect and Tumor Growth. *Sci. Signal.* **2**, ra73–ra73 (2009).
164. Weerapana, E., Simon, G. M. & Cravatt, B. F. Disparate proteome reactivity profiles of carbon electrophiles. *Nat. Chem. Biol.* **4**, 405–407 (2008).
165. Harris, T. K. & Turner, G. J. Structural Basis of Perturbed pKa Values of Catalytic Groups in Enzyme Active Sites. *IUBMB Life Int. Union Biochem. Mol. Biol. Life* **53**, 85–98 (2002).
166. Decker, C. J. & Parker, R. P-Bodies and Stress Granules: Possible Roles in the Control of Translation and mRNA Degradation. *Cold Spring Harb. Perspect. Biol.* **4**, a012286–a012286 (2012).
167. Song, L., Turkson, J., Karras, J. G., Jove, R. & Haura, E. B. Activation of Stat3 by receptor tyrosine kinases and cytokines regulates survival in human non-small cell carcinoma cells. *Oncogene* **22**, 4150–4165 (2003).

168. Hong, J. Y., Oh, I.-H. & McCrea, P. D. Phosphorylation and isoform use in p120-catenin during development and tumorigenesis. *Biochim. Biophys. Acta BBA - Mol. Cell Res.* **1863**, 102–114 (2016).
169. Subramanian, A. *et al.* Gene set enrichment analysis: A knowledge-based approach for interpreting genome-wide expression profiles. *Proc. Natl. Acad. Sci. U. S. A.* **102**, 15545–15550 (2005).
170. Bai, J. *et al.* BioContainers Registry: Searching Bioinformatics and Proteomics Tools, Packages, and Containers. *J. Proteome Res.* **20**, 2056–2061 (2021).
171. Jalili, V. *et al.* The Galaxy platform for accessible, reproducible and collaborative biomedical analyses: 2020 update. *Nucleic Acids Res.* **48**, W395–W402 (2020).
172. Hahm, H. S. *et al.* Global targeting of functional tyrosines using sulfur-triazole exchange chemistry. *Nat. Chem. Biol.* **16**, 150–159 (2019).
173. Maik-Rachline, G., Hacohen-Lev-Ran, A. & Seger, R. Nuclear ERK: Mechanism of Translocation, Substrates, and Role in Cancer. *Int. J. Mol. Sci.* **20**, 1194 (2019).
174. Søndergaard, C. R., Olsson, M. H. M., Rostkowski, M. & Jensen, J. H. Improved Treatment of Ligands and Coupling Effects in Empirical Calculation and Rationalization of pKa Values. *J. Chem. Theory Comput.* **7**, 2284–2295 (2011).
175. Bailey, T. L. *et al.* MEME Suite: tools for motif discovery and searching. *Nucleic Acids Res.* **37**, W202–W208 (2009).
176. Quirós, M., Gražulis, S., Girdzijauskaitė, S., Merkys, A. & Vaitkus, A. Using SMILES strings for the description of chemical connectivity in the Crystallography Open Database. *J. Cheminformatics* **10**, 23 (2018).
177. Trott, O. & Olson, A. J. AutoDock Vina: Improving the speed and accuracy of docking with a new scoring function, efficient optimization, and multithreading. *J. Comput. Chem.* **31**, 455–461 (2010).
178. Schrödinger, LLC. The PyMOL Molecular Graphics System, Version 1.8. (2015).
179. Campbell, S. T. *et al.* Chemoproteomic Discovery of a Ritanserin-Targeted Kinase Network Mediating Apoptotic Cell Death of Lung Tumor Cells. *Mol. Pharmacol.* **94**, 1246–1255 (2018).
180. Sigrist, C. J. A. *et al.* ProRule: a new database containing functional and structural information on PROSITE profiles. *Bioinformatics* **21**, 4060–4066 (2005).
181. Raje, S. & Thorpe, C. Inter-Domain Redox Communication in Flavoenzymes of the Quiescin/Sulfhydryl Oxidase Family: Role of a Thioredoxin Domain in Disulfide Bond Formation,. *Biochemistry* **42**, 4560–4568 (2003).
182. Khoshnevis, S. *et al.* Structural integrity of the PCI domain of eIF3a/TIF32 is required for mRNA recruitment to the 43S pre-initiation complexes. *Nucleic Acids Res.* **42**, 4123–4139 (2014).
183. Wolkowicz, U. M. & Cook, A. G. NF45 dimerizes with NF90, Zfr and SPNR via a conserved domain that has a nucleotidyltransferase fold. *Nucleic Acids Res.* **40**, 9356–9368 (2012).
184. Charton, M. Electrical Effect Substituent Constants for Correlation Analysis. *Prog. Phys. Org. Chem.* 119–251 (2007) doi:10.1002/9780470171929.ch3.
185. Backus, K. M. *et al.* Proteome-wide covalent ligand discovery in native biological systems. *Nature* **534**, 570–574 (2016).

186. Fox, P. L. & Jia, J. Identification of EPRS domains required for formation of the GAIT mRNP: Key roles of WHEP-TRS repeats. *FASEB J.* **20**, A1372–A1372 (2006).
187. Wu, K. C. *et al.* Coiled-Coil Trigger Motifs in the 1B and 2B Rod Domain Segments Are Required for the Stability of Keratin Intermediate Filaments. *Mol. Biol. Cell* **11**, 3539–3558 (2000).
188. Korenbaum, E. & Rivero, F. Calponin homology domains at a glance. *J. Cell Sci.* **115**, 3543–3545 (2002).
189. Brulet, J. W., Borne, A. L., Yuan, K., Libby, A. H. & Hsu, K.-L. Liganding Functional Tyrosine Sites on Proteins Using Sulfur–Triazole Exchange Chemistry. *J. Am. Chem. Soc.* **142**, 8270–8280 (2020).
190. Azevedo, C. & Saiardi, A. Why always lysine? The ongoing tale of one of the most modified amino acids. *Adv. Biol. Regul.* **60**, 144–150 (2016).
191. Callebaut, I. An EVH1/WH1 domain as a key actor in TGFβ signalling. *FEBS Lett.* **519**, 178–180 (2002).
192. Huang, T. *et al.* Chemoproteomic profiling of kinases in live cells using electrophilic sulfonyl triazole probes. *Chem. Sci.* **12**, 3295–3307 (2021).
193. Brewer, F. K., Follit, C. A., Vogel, P. D. & Wise, J. G. In Silico Screening for Inhibitors of P-Glycoprotein That Target the Nucleotide Binding Domains. *Mol. Pharmacol.* **86**, 716–726 (2014).
194. al-Shawi, M. K., Urbatsch, I. L. & Senior, A. E. Covalent inhibitors of P-glycoprotein ATPase activity. *J. Biol. Chem.* **269**, 8986–8992 (1994).